



HAL
open science

Seabirds as bioindicators of past and current mercury contamination : a global approach

Fanny Cusset

► **To cite this version:**

Fanny Cusset. Seabirds as bioindicators of past and current mercury contamination : a global approach. Animal biology. Université de La Rochelle, 2023. English. NNT : 2023LAROS025 . tel-04516268

HAL Id: tel-04516268

<https://theses.hal.science/tel-04516268>

Submitted on 22 Mar 2024

HAL is a multi-disciplinary open access archive for the deposit and dissemination of scientific research documents, whether they are published or not. The documents may come from teaching and research institutions in France or abroad, or from public or private research centers.

L'archive ouverte pluridisciplinaire **HAL**, est destinée au dépôt et à la diffusion de documents scientifiques de niveau recherche, publiés ou non, émanant des établissements d'enseignement et de recherche français ou étrangers, des laboratoires publics ou privés.



ÉCOLE DOCTORALE - 618

Laboratories :

Littoral, Environnement et Sociétés (LIENSS)

Centre d'Études Biologiques de Chizé (CEBC)

Fanny CUSSET

PhD THESIS

**SEABIRDS AS BIOINDICATORS
OF PAST AND CURRENT MERCURY
CONTAMINATION: A GLOBAL APPROACH**

Defended on September, 18th 2023

For the Degree of Doctor of Philosophy from La Rochelle University

Discipline: Environmental and Populational Biology, Ecology

COMMITTEE MEMBERS:

Florence CAURANT	Professor, La Rochelle Université, <u>President of the committee</u>
Aurélie GOUTTE	Lecturer, École Pratique des Hautes Études, <u>Reviewer</u>
Alexander BOND	Senior Curator, Bird Group Tring-Natural History Museum, <u>Reviewer</u>
Paco BUSTAMANTE	Professor, La Rochelle University, <u>Thesis supervisor</u>
Yves CHEREL	Research director, CEBC, <u>Thesis supervisor</u>
Jérôme FORT	CNRS Researcher, LIENSS, <u>Thesis co-supervisor</u>
Anne LORRAIN	Research director, LEMAR, UBO, <u>Examiner</u>
Sophie LANCO-BERTRAND	Research director, MARBEC, IRD, <u>Examiner</u>



ÉCOLE DOCTORALE - 618

Laboratoires :

Littoral, Environnement et Sociétés (LIENSs)

Centre d'Études Biologiques de Chizé (CEBC)

Fanny CUSSET
THÈSE DE DOCTORAT

**LES OISEAUX MARINS, BIOINDICATEURS DE
LA CONTAMINATION PASSÉE ET ACTUELLE
PAR LE MERCURE : UNE APPROCHE
GLOBALE**

Soutenue le 18 Septembre 2023

Pour l'obtention du grade de Docteur de La Rochelle Université
Discipline: Biologie de l'Environnement, des Populations, Écologie

MEMBRES DU JURY:

Florence CAURANT
Aurélie GOUTTE

Alexander BOND

Paco BUSTAMANTE

Yves CHEREL

Jérôme FORT

Anne LORRAIN

Sophie LANCO-BERTRAND

Professeur à La Rochelle Université, Présidente du jury
Maître de Conférences à l'École Pratique des Hautes Études,
Rapporteuse

Conservateur Principal au Muséum d'Histoire Naturelle-Bird Group
Tring, Rapporteur

Professeur à La Rochelle University, Directeur de thèse

Directeur de recherche au CEBC, Directeur de thèse

Chargé de recherche au LIENSs, Encadrant de thèse

Directrice de recherche, LEMAR, UBO, Examinatrice

Directrice de recherche, MARBEC, IRD, Examinatrice



Ce travail de thèse a été réalisé au sein des équipes :

Littoral Environnement et Sociétés (LIENSs)

UMR 7266 CNRS-La Rochelle Université

Équipe AMARE

Centre d'Études Biologiques de Chizé (CEBC)

UMR 7372 CNRS-La Rochelle Université

Équipe Prédateurs Marins

En collaboration avec :

Institut de Sciences Analytiques et de Physico-Chimique pour l'Environnement et les Matériaux (IPREM)

UMR 5254 CNRS-Université de Pau et des Pays de l'Adour

Grâce au soutien financier, technique et logistique de :

La Rochelle Université

EU-SYNTHESYS+

Comité National Français de la Recherche Arctique et Antarctique (CNFRAA)

«Fais de ta vie un rêve, et d'un rêve une réalité.»

Antoine de St Exupéry

Table of content

Preface

Acknowledgments.....	i
Communication.....	iv
Field work.....	vi
Contributions, supervision, teaching.....	vii
Abbreviations.....	ix
Credits.....	x

Chapter 1: Introduction

1. Mercury, a global pollutant of major concern.....	2
1.1. Sources of Hg in the environment.....	2
1.2. Long-range transport of Hg.....	3
1.3. Mercury cycle and fate in marine food webs.....	3
1.4. A chemical of major public health concern.....	6
2. Oceans, a grey zone for the environmental monitoring of Hg.....	8
2.1. Role of the oceans in the Hg cycle and transfer.....	8
2.2. Monitoring Hg in the oceans.....	10
2.3. A focus on remote oceanic regions.....	11
Tropical oceans.....	11
Polar oceans.....	12
3. Seabirds as bioindicators of Hg contamination in marine food webs.....	12
4. Main objectives and outline of the thesis.....	16

Chapter 2: Methodological approach

1. Description of bioindicator seabird species.....	22
2. Feathers, valuable archives for Hg biomonitoring in the oceans.....	25
2.1. Mercury exposure, distribution and excretion routes in seabirds.....	25
2.2. A powerful tool for Hg biomonitoring across space and time.....	26
2.2.1. Different tissues, different scales.....	27
2.2.2. Different ages, different scales.....	30
2.2.3. Feathers as a time-machine.....	31

2.3. Feather sampling	32
3. Laboratory analyses.....	32
3.1. Sample preparation.....	33
3.2. Mercury analyses.....	33
3.2.1. Total mercury analyses	33
3.2.2. Mercury speciation analyses.....	33
3.3. Stable isotope analyses	36
3.3.1. Bulk analyses.....	36
3.3.2. Compound-Specific Stable Isotope Analyses of Amino-Acids	39
4. Combining Hg and stable isotopes in feathers.....	42
Adults	42
Chicks.....	43
5. Data analyses.....	44

Chapter 3: Spatial monitoring of Hg contamination in tropical and polar ecosystems

1. Arctic marine ecosystems

1.1. Context	50
1.2. Main findings and discussion	52
a) Does Hg contamination during the breeding season vary across the Arctic?.....	52
b) Are Brünnich's guillemots at risk in the Arctic?	55
1.3. Conclusion.....	57
1.4. Summary	58

2. Tropical marine ecosystems

2.1. Context	60
2.2. Aim and predictions	60
2.3. Results and discussion.....	61
a) What are the spatial patterns of Hg contamination in tropical marine food webs ?.....	611
b) What are the drivers of Hg contamination and its spatial patterns ?	69
c) What about temporal patterns in tropical ecosystems ?	73
2.4. Conclusions and perspectives.....	75
2.5. Summary	77

3. Antarctic marine ecosystems

3.1. Context	79
3.2. Aims and predictions	80
3.3. Results and discussion	81
a) Circumpolar assessment of Hg contamination in Adélie penguins	81
b) Does the trophic ecology of Adélie penguins drive spatial variation in Hg contamination?	86
c) Are environmental drivers involved in the circumpolar variation of Hg contamination?	88
d) Could spatial patterns result from temporal patterns of Hg contamination?	89
e) Was Hg contamination different between the sexes in adult Adélie penguins?	90
3.4. Conclusions and perspectives	92
3.5. Summary	93

4. Discussion

4.1. Highlights	95
4.2. Can we associate feather Hg concentrations of seabirds with geographical areas?	97

Chapter 4: Long-term monitoring of Hg contamination in tropical and polar ecosystems

1. Arctic marine ecosystems

1.1. Context	1066
1.2. Aims and predictions	106
1.3. Results and discussion	107
a) Long-term trends of Hg contamination and trophic ecology in Brünnich's guillemots	108
b) What is the influence of trophic ecology on the temporal trend of Hg contamination?	112
c) Which unknown factors?	113
1.4. Conclusions and perspectives	116
1.5. Summary	118

2. Tropical marine ecosystems

Part 1: Retrospective investigation of Hg contamination: century time series	120
2.1. Context and objectives	120
2.2. Result and discussion	121
a) Long-term trend in foraging ecology: an update	124
b) Long-term trend in Hg contamination	124
c) Drivers of Hg contamination over time	126
d) Influence of climate change and fisheries on tropical Hg contamination	127

e) Was Hg contamination involved in the population decline of sooty terns in Ascension Island?.....	128
2.3. Conclusions	132
Part 2: Retrospective investigation of Hg contamination: epoch comparison	132
2.4. Context	132
2.5. Results and Discussion.....	133
2.6. Summary	136
3. Antarctic marine ecosystems	
3.1. Context	138
3.2. Results and Discussion.....	139
3.3. Conclusion.....	142
4. Discussion	143
Chapter 5: Conclusions, critical evaluation and perspectives	
5.1. Highlights of the doctoral work.....	150
5.2. Critical evaluation	154
5.2.1. Are seabirds <i>really</i> good bioindicators of Hg contamination in marine food webs?	154
5.2.2. Are feathers <i>really</i> relevant for Hg biomonitoring?	156
5.2.3. Are stable isotopes <i>really</i> informative when monitoring Hg contamination at large-spatial scale?	158
5.3. Perspectives: what's next?.....	159
5.4. Conclusion.....	162
Bibliography	163
Annexes	187
Papers	213
Paper 1 : Sooty terns as bioindicators of mercury contamination in marine ecosystems: a pantropical approach.....	214
Paper 2: Circumpolar assessment of mercury contamination: the Adélie penguin as a bioindicator of Antarctic marine ecosystems.....	251
Paper 3: Long-term mercury contamination in Arctic marine ecosystems: the Brünnich's guillemot as bioindicator species.....	291
Paper 4: A century of mercury: ecosystem-wide changes drive increasing contamination in a tropical seabird species in the South Atlantic Ocean.....	301

PREFACE

Acknowledgments

Quatre ans, une pandémie, un bébé et une thèse plus tard, il est temps pour moi de remercier toutes les personnes qui m'ont accompagné, de près ou de loin, tout au long de cette aventure.

Mes premiers remerciements vont évidemment à mes directeurs de thèse. Pendant ces quatre années où vous m'avez accompagné, j'avais l'habitude de dire à tout le monde, et non sans fierté, que j'avais une réunion avec mon « Conseil du Soleil ». Non, cela ne faisait pas référence au cirque du même nom. Alors, pourquoi ce nom ? Tout simplement parce que ces moments d'échange tous les quatre constituaient des moments clés pour moi, de véritables réunions au sommet, d'une importance au moins aussi grande que le soleil. Ce n'était en fait que le signe de ma grande estime pour vous trois. Merci pour ces échanges enrichissants, pour vos conseils avisés, toujours dans la bonne humeur. Merci Yves pour ta rigueur et ton œil de lynx; grâce à toi aujourd'hui dès que je lis ou que je rédige une discussion, je ne peux m'empêcher de voir ton commentaire : « 8 pages, c'est trop long ! Il ne faut pas dépasser 7 ». Merci Paco pour ton accompagnement au quotidien, ta réactivité à toute épreuve et ton soutien; tu as tout mis en œuvre durant ma grossesse et mon congé maternité, pour que cette thèse se passe au mieux et que mes ambitions initiales puissent se concrétiser. Merci Jérôme d'avoir oublié quelques rendez-vous en chemin; un très bon moyen pour moi, gourmande comme je suis, d'avoir des chocolatinnes gratuites (et oui, tu sais bien que je n'ai pas fini de te charrier avec ça). Merci à vous trois pour votre bienveillance, lorsque ma vie a été chamboulée avec l'arrivée d'un petit être humain. Je vous dois beaucoup et je sais que ceci n'est que le début d'une plus grande histoire.

Les prochains sur la liste sont les piliers des plateformes analytiques, sans qui les analyses en laboratoire ne seraient pas possible : Gaël, Maud et Carine, à qui j'ai dit à maintes reprises (après trois fois, j'ai arrêté de compter) : « C'est les dernières plumes que j'analyse », et puis ensuite « Non, mais j'en ai juste 15 de plus ». Merci à vous pour ces moments de partage. Un merci particulier à Pierre Richard, qui a partagé son expérience et une infime partie de son savoir sur les CSIA avec moi, alors qu'il n'était qu'à quelques mois de la fin de son (deuxième) éméritat. Merci à Manu et Océane, à Pau, pour votre soutien et votre aide avec ces satanés analyses de plumes (Quelle idée de bosser sur des plumes aussi!). Ça a été un vrai plaisir de travailler avec vous et j'espère que nos chemins se recroiseront.

Aux collègues piafologues permanents : Marta, Julie (alias la Juls), Gauthier, Céline, Prescillia; et intermittents : Miguel, Ivo, Nico, Laura ; merci pour nos échanges, nos moments d'entraide, nos apéros, et puis pour votre écoute lorsqu'il fallait vider son sac. Alice, un merci tout particulier pour toi, mon « soldat de l'ombre », toi mon mentor scientifique et statistique, figure de rigueur et d'excellence. Merci à mes propres stagiaires pour leur contribution à ce grand projet de thèse : Pierre, Mickaël, Olga ; et aux stagiaires de collègues que j'ai mis à contribution sur mes analyses de laboratoire : Margaux, Louis. Merci aux membres de l'équipe Écotox (Axe 3) et de l'équipe AMARE pour votre accueil.

Aux gestionnaires à qui j'ai causé de sacrés maux de tête : Johan, merci pour ta patience dans mes démarches à répétition, de permis et d'envois qui ne se ressemblaient pas les uns les autres, mais surtout dans les démarches d'ordre de mission avec un système en pleine restructuration. Merci à Lucia et les autres gestionnaires, que j'ai moins côtoyés au quotidien mais qui font tourner le laboratoire. Merci à Eva et Armelle pour votre soutien respectif pour l'administratif ou les activités de vulgarisation en tout genre; merci pour votre bienveillance et votre gentillesse. Merci à tous mes collaborateurs de par le monde, sans qui je n'aurais pas pu mener la science que je voulais, tel que je le voulais.

Merci à La Rochelle Université et l'École Doctorale Euclide, pour son accueil et son soutien, particulièrement durant cette période troublée causée par une certaine pandémie. Je vous suis très reconnaissante pour cette extension de thèse de 8 mois, qui m'a permis de ne pas revoir mes plans à la baisse. Merci à l'ADOCS pour toutes les activités mises en place afin de réunir les jeunes chercheurs et chercheuses de la Rochelle, et plus particulièrement pour l'organisation du Festival du Film Pas Trop Scientifique, auquel j'ai eu la chance de participer.

Aux collègues du Bureau de l'Ambiance, Ophélia (alias Niort J'Adore), Margot (alias Fleur de Sel) et Clément (alias Princesse en Feu), frères et sœurs d'armes avec qui j'ai passé toutes les étapes de ce doctorat, parce qu'évidemment je suis la dernière. Merci pour les moments de craquage, de musique nulle beaucoup trop forte, de blagues vaseuses (de Margot), lourdes (de Clément) et tendancieuses (d'Ophélia), les moments de confiance et de soutien. C'est une étape importante dans une vie et je suis heureuse et fière de l'avoir passé à vos côtés.

Aux copains, au travail et à la vie. Antoine (alias Minepito) et Dimitri (alias Monsieur K). À la base, vous étiez des collègues de travail, mais très vite vous êtes devenus plus que ça (évidemment, seulement pour Renaud, pas pour moi je le sais bien). Merci Carole (alias

Carlota), Laura et Diane d'avoir équilibré la folie de ces deux boulets (qu'aurais-je fait sans vous !). Merci de faire partie de notre famille de cœur.

À ma famille de sang maintenant. Merci pour votre soutien, vous qui m'avez vu regarder, en boucle, « Sauver Willy » dès l'âge de 3 ans. Aujourd'hui, je réalise un rêve et c'est grâce à moi certes, mais à vous aussi évidemment; vous qui m'avez soutenu dans mon choix d'études et mon exil canadien, qui m'ont mené ici, aujourd'hui. Merci à ma belle-famille (François et Béa particulièrement), qui nous a accueilli pour le dernier mois de ma rédaction : vous avez grandement facilité ma vie sur cette période intense de travail acharné et je vous en suis grandement reconnaissante. Merci à mon fils, ce petit ange aux yeux bleus, de m'avoir appris que, même lorsque l'on pense être exténué, avec les batteries complètement à plat, on arrive quand même à dépasser ses limites (parce qu'on n'a pas le choix, finalement). A toi, Renaud, mon amour, merci de m'accompagner dans ces péripéties de chercheuse depuis 9 ans maintenant. Depuis le Québec, tu as vécu toutes les phases avec moi, les bonnes et les moins bonnes, les succès et les remises en question existentielles. Merci d'être à mes côtés, dans ma quête d'épanouissement professionnel et personnel (puisque les deux sont étroitement liés dans ce métier). Aujourd'hui, tu arrives à expliquer mon travail presque mieux que moi, et j'en suis assez fière !

« La thèse, c'est un marathon, avec un sprint à la fin » (Yves Cherel, 2019).

Grâce à vous tous, ce marathon a été « moins pire » comme on dirait au Québec, et bien plus facile et agréable à surmonter. Vous serez toujours associés à ce souvenir et à cette étape clé de ma vie. Et maintenant ? Rendez-vous au prochain épisode !

Communication

Papers included in the doctoral dissertation

- Paper 1** **Cusset, F.**, Richard, P., Fort, J., Bost, C., Bugoni, L., Carlisle, N., Charriot, M., Cupidon, A., Darocha, B., Dunlop, N., Feare, C., Quintas, A.G., Gestemme, T., Guillou, G., Matilde, E., Morgan, M., O'Dwyer, T., Pimm, S., Costa Neves, V.R., Rocamora, G., Shearer, L., Soanes, L., Ventosa, E., Withers, T., Cherel, Y., Bustamante, P. (*In preparation*) Sooty terns as bioindicators of mercury contamination in marine ecosystems: a pantropical approach.
- Paper 2** **Cusset, F.**, Bustamante, P., Carravieri, A., Bertin, C., Brasso, R., Corsi, I., Dunn, M., Emmerson, L., Guillou, G., Hart, T., Juárez, M., Kato A., Machado, A.L., Michelor, C., Olmastroni, S., Polito, M., Raclot, T., Santos, M., Schmidt, A., Southwell, C., Soutullo, A., Thiébot, J.B., Trathan, P., Vivion, P., Waluda, C., Fort, J., Cherel, Y. (2023) Circumpolar assessment of mercury contamination: spatial variations in Adélie penguins as bioindicator of Antarctic marine ecosystems. *Ecotoxicology*, 32: 1024-1049. DOI: <https://doi.org/10.1007/s10646-023-02709-9>
- Paper 3** **Cusset, F.**, Bustamante, P., Albert, C., Amouroux, D., Asensio, O., Brault-Favrou, M., Guillou, G., Linnebjerg, J., Merkel, F., Tessier, E., Cherel, Y., Fort, J. (*In preparation*) Long-term mercury contamination Arctic marine ecosystems : the Brünnich's guillemot as bioindicator.
- Paper 4** **Cusset, F.**, Reynolds, S. J., Carravieri, A., Amouroux, D., Asensio, O., Dickey, R., Fort, J., Hughes, J., Paiva, V. H., Ramos, J. R., Shearer, L., Tessier, E., Weran, C.P., Cherel, Y. (2023) A century of mercury: Ecosystem-wide changes drive increasing contamination in a tropical seabird species in the South Atlantic Ocean. *Environmental Pollution*, 323:121187. DOI: <https://doi.org/10.01016/j.envpol.2023.121187>

Other papers related to the doctoral work

- 1) Olmastroni, S., **Cusset, F.**, Bustamante, P., Cherel, Y., Corsi, I. (2024) Living in a challenging environment: monitoring stress ecology by non-destructive methods in Adélie penguins. *Accepted in Science of the Total Environment*.

Other papers not related to the doctoral work

- 1) Bruyant, F., Amiraux, R., Amyot, M.-P., Archambault, P., Artigue, L., Barbedo de Freitas, L., Bécu, G., Bélanger, S., Bourgain, P., Bricaud, A., Brouard, E., Brunet, C., Burgers, T., Caleb, D., Chalut, K., Claustre, H., Cornet-Barthaux, V., Coupel, P., Cusa, M., **Cusset, F.**, Dadaglio, L., Davelaar, M., Deslongchamps, G., Dimier, C., Dinasquet, J., Dumont, D., Else, B., Eulaers, I., Ferland, J., Filteau, G., Forget, M.-H., Fort, J., Fortier, L., Galí, M., Gallinari, M., Garbus, S.-E., Garcia, N., Gérikas Ribeiro, C., Gombault, C., Gourvil, P., Goyens, C., Grant, C.,

Grondin, P.-L., Guillot, P., Hillion, S., Husherr, R., Joux, F., Joy-Warren, H., Joyal, G., Kieber, D., Lafond, A., Lagunas, J., Lajeunesse, P., Lalande, C., Larivière, J., Le Gall, F., Leblanc, K., Leblanc, M., Legras, J., Lévesque, K., Lewis, K.-M., Leymarie, E., Leynaert, A., Linkowski, T., Lizotte, M., Lopes dos Santos, A., Marec, C., Marie, D., Massé, G., Massicotte, P., Matsuoka, A., Miller, L. A., Mirshak, S., Morata, N., Moriceau, B., Morin, P.-I., Morisset, S., Mosbech, A., Mucci, A., Nadaï, G., Nozais, C., Obernosterer, I., Paire, T., Panagiotopoulos, C., Parenteau, M., Pelletier, N., Picheral, M., Quéguiner, B., Raimbault, P., Ras, J., Rehm, E., Ribot Lacosta, L., Rontani, J.-F., Saint-Béat, B., Sansoulet, J., Sardet, N., Schmechtig, C., Sciandra, A., Sempéré, R., Sévigny, C., Toullec, J., Tragin, M., Tremblay, J.-É., Trotter, A.-P., Vaultot, D., Vladoiu, A., Xue, L., Yunda-Guarin, G., and Babin, M. (2022) The Green Edge cruise: investigating the marginal ice zone processes during late spring and early summer to understand the fate of the Arctic phytoplankton bloom, *Earth System Science Data*, 14: 4607–4642. DOI: <https://doi.org/10.5194/essd-14-4607-2022>

- 2) **Cusset, F.**, Charrier, J., Massé, G., Mallory, M., Braune, B., Provencher, J., Massicotte, P., Guillou, G., and Fort, F. (2023) The consumption of ice-derived resources is associated with higher mercury contamination. *Environmental Research*. 238, Part 1: 117066. DOI: <https://doi.org/10.1016/j.envres.2023.117066>

Contributions to conferences/workshops and awards

International:

2020: Arcticnet Annual Meeting (oral presentation; visio-conference)

2023: 11th International Penguin Congress; Viña del Mar, Chili (oral presentation; in-person)

National:

2021 : 17èmes Journées Scientifiques du CNFRA 2021 (oral presentation; in-person)

Roland Schlich Award (best oral communication)

2021 : Colloque des doctorants 2021 (oral presentation + poster; in-person)

Best Poster Award

2022: ILETOP Closing Meeting; La Rochelle, France (oral presentation; in-person)

2023 : Journées Prédateurs Marins du CEBC; La Rochelle, France (2023; in person)

2023: 19èmes Journées Scientifiques du CNFRAA; Paris, France (oral presentation; in person)

Outreach

- 1) « Pépites du LIENSs » (2020–2023): organising and managing the scientific seminars at the LIENSs

2) Content creation on social medias

- « Docs 122 » (Instagram) and « Docs de l'Environnement » (Facebook)
Sharing the daily life of PhD students in Environmental Sciences on social medias
- « LR Expeditioners » (Instagram)
Sharing the daily life on the AKMA 2-Ocean Senses campaign (2022) in the Arctic Ocean (2 weeks, Svalbard)

3) « Fête de la Science » (2020, 2021)

4) « Festival du Film Pas Trop Scientifique » : Presentation of a short movie entitled «*De l'encre à la plume : le récit du mercure*» (Available at: <https://www.youtube.com/watch?v=jKdEkBs6yTM>)

5) Cordées de la Réussite – Cap Sciences (2022)

Discussion on our research and study tracks, and how to become a PhD student.

6) « Projet Savanturier » (2021–2023): Scientific mentor for French pupils (CM1/CM2)

7) Radio interview with Radio Catholique de France (RCF; 2023), available at:

<https://www.rcf.fr/ecologie-et-solidarite/littoral-environnement-societes>

Field work

Related to the doctoral work

Thanks to funding from EU Synthesys+ program, I visited two Natural History Museums in Copenhagen (Denmark) and Tring (UK) in 2021 (2 weeks) and 2022 (1 week), respectively. After making the inventory of available specimens, I sampled body feathers of Brünnich's guillemots first and foremost, but also of sooty terns and Adélie penguins when sampling locations of museum specimens matched those of contemporary sampling (see Chapter 3).

Not related to the doctoral work

In 2020, I accompanied Gauthier Poiriez to help in seabird field work (2 weeks) on the Mediterranean coast (Marseille and surrounding islands, and Corsica), which consisted in catching chicks of Cory's shearwater (*Calonectris borealis*) to collect blood and feather samples across four different sites. This field work was part of a French project under the «Directive Cadre Stratégie pour le Milieu Marin» (DCSMM), led by Paco Bustamante and Gauthier Poiriez (LIENSs), that uses seabirds as bioindicators of good environmental status. In this project, 10 seabird species (both adults and chicks) are sampled for blood and feathers, in a total of 32 sites distributed along the entire French coastline (*i.e.*, Atlantic and Mediterranean coasts).

In 2021, I occasionally participated to fieldwork conducted on Ré Island for the PAMPAS project («Evolution de l’identité PATrimoniale des Marais des Pertuis Charentais en réponse à l’Aléa de Submersion marine»). My task mainly consisted in recovering the fishing nets and listing the captured species (*e.g.*, fish, invertebrates), without getting stuck in the mud.

In 2022, I participated to the AKMA 2-Ocean Senses research cruise (CAGE-2022 campaign) onboard the Kronprins Haakon in Svalbard (Barents Sea; 2 weeks), a scientific expedition that was led by Giuliana Panieri (CAGE, Arctic University of Norway). AKMA stands for «Advancing Knowledge on Methane in the Arctic». In addition to the science goals, both scientists and teachers on board worked together to also develop teaching tools to make young students discover the Arctic through their senses (*i.e.*, sight, smell, sound, touch and taste).

Contributions, supervision and teaching

Contributions in the doctoral work

For laboratory analyses conducted in la Rochelle (*i.e.*, Hg and bulk stable isotopes), six colleagues helped me with laboratory work during my PhD, especially during my pregnancy and maternity leave.

Table 0.1. Laboratory work and number of samples for each colleague and analytical step included in feather preparation (*i.e.*, preparation, cleaning and cutting) and analyses. AMA and SIA refer to total-Hg (using an Advanced Mercury Analyser) and stable isotope analyses.

Colleagues	Preparation	Cleaning	Cutting	AMA	SIA
Pierre Vivion	112	159	67	134	112
Margaux Mollier	0	73	6	24	0
Olga Krug	83	83	30	75	0
Mickael Charriot	86	86	30	138	86
Louis Trousse	80	80	20	0	0
Sandy Pascaud	302	641	413	0	267
Total					
Colleagues	663	1122	566	371	465
Thesis	2279	2279	2279	2279	2279
Percentage					
Colleagues	29,1	49,2	24,8	16,3	20,4
Me	70,9	50,8	75,2	83,7	79,6

Overall, the majority of laboratory work (72%) was conducted by me and the rest (28%) by my colleagues (Table 0.1).

Compound-Specific Stable Isotope Analyses were also performed in La Rochelle, with the help of Pierre Richard (PR). The majority of the chemical preparation of samples was conducted by me, whereas post-analyses data treatment (*e.g.*, peak integration, data correction) was mainly performed by PR.

For laboratory analyses conducted in Pau (*i.e.*, Hg speciation analyses), I participated actively to sample preparation for GC analyses (see methodological procedures in Chapter 2 and Paper 4), with the help of Emmanuel Tessier (ET) and Océane Asensio (OA). GC analyses were performed by ET and OA. Post-GC data treatment was performed by me, with deep verification by ET.

Interns supervised

Pierre Vivion (2021, 2 months) – Master 1 (*i.e.*, M.Sc.) : « Variabilité spatiale de la contamination par le mercure de trois espèces de manchots du genre *Pygoscelis* en Antarctique »

Mickael Charriot (2022, 2 months) – Master 1 (*i.e.*, M.Sc.): « La sterne fuligineuse, bioindicateur de la contamination au mercure des écosystèmes marins tropicaux »

Olga Krug (2022, 2 months) – Licence 3 (*i.e.*, B.Sc.): « Variabilité temporelle de la contamination au mercure chez les guillemots de Brünnich au Groenland »

Teaching activities

54h, Plant and animal biology (practical courses)

Abbreviations

AA	Amino-acid
ADPE	Adélie penguin
AMA	Advanced Mercury Analyzer
AMAP	Arctic Monitoring Assessment Program
ASGM	Artisanal small-scale gold mining
BF	Body feather
BNHM	British Natural History Museum
BRUG	Brünnich's guillemot
CCAMLR	Commission for the Conservation of Antarctic Marine Living Resources
CEBC	Centre d'Études Biologiques de Chizé
CO ₂	Carbon dioxide
CSIA	Compound-specific stable isotope analysis
dw	Dry weight
GAM	Generalized Additive Model
GBMS	Global Biotic Mercury Synthesis
GC	Gas chromatography
GLM	Generalized Linear Model
Glu/Glx	Glutamic Acid
GMA	Global Mercury Assessment
HF	Head feather
Hg	Mercury
ICP	Inductively Coupled Plasma
iHg	Inorganic mercury
IPCC	Intergovernmental Panel on Climate Change
IPREM	Institut des Sciences Analytiques et de Physico-Chimie pour l'Environnement et les Matériaux
IUCN	International Union for Conservation of Nature
LIENSs	Littoral, Environnement et Sociétés
MDF	Mass-dependent fractionation
MeHg	Methyl-mercury
MIF	Mass-independent fractionation
MS	Mass spectrometry
NH	Northern Hemisphere
Phe	Phenylalanine
SD	Standard deviation
SH	Southern Hemisphere
SOTE	Sooty tern
TP	Trophic position
UNEP	United Nations Environmental Program

Credits

Photos

Chapter 1

Alberto Pina Ortiz (Red-billed tropicbird, blue-footed booby)

Audran Morel (European shag, Lesser black-backed gull, Atlantic puffin, Common tern)

Céline Albert (Little auk)

Davide Oddone (Northern fulmar)

Prescillia Lemesle (Black-legged kittiwake)

Samuel Blanc (Empereur penguin)

Thomas Lacoue-Labarthe (Common eider)

Chapter 2

Coline Marciau (Adélie penguins)

Laura Shearer (Sooty terns)

Mark Mallory (Brünnich's guillemots)

Chapter 3

Coline Marciau (Adélie penguins in Dumont d'Urville, Terre Adélie)

Diane Espel (Breeding colony in the Chesterfield Islands, Pacific Ocean)

Mark Mallory (Breeding colony in Prince Leopold Island, Canadian Arctic)

Artwork

Julie Charrier (Illustration of bioindicator species)

Clément Bertin (Spatial representation of Hg hotspots)

Thierry Guyot (Clouds and shrimp drawings)

IconFinder & Flaticon (free images available online)

Chapter 4

Céline Albert (Breeding colony of little auks in Kap Hoegh, Greenland)

Coline Marciau (Adélie penguins on the icy coast, Dumont d'Urville, Adélie Land)

Fanny Cusset (Great Auk, kept at the Natural History Museum of Denmark, Copenhagen)

Laura Shearer (Breeding colony of sooty terns in Ascension Island)

Annexes

Céline Albert (Brünnich's guillemots, somewhere in the Arctic Ocean)

Chloé Pupier (Île aux Oiseaux, Atoll de Mataiva)

Coline Marciau (Adélie penguin in Dumont d'Urville)

Laura Shearer (Sooty terns in Ascension Island, South Atlantic Ocean)

Natalia Zaldúa (Chinstrap and Gentoo penguins, Ardley Island, South Shetland Islands)

Samuel Blanc (Emperor penguin)

Chapter 1

Introduction

1. Mercury, a global pollutant of major concern

1.1. Sources of Hg in the environment

Mercury (Hg) is a non-essential and toxic metal, and its impacts on human and environmental health are a major concern. Hg is primarily emitted in the atmosphere in its volatile form (Hg⁰) by both natural and human sources (Eagles-Smith et al., 2018). Natural sources include **volcanic** and **hydrothermal activities**, as well as **rock weathering** and **natural fires** (Mason, 2009; Schneider et al., 2023). In contrast, anthropogenic emissions largely exceed natural emissions and include numerous sources that contribute differently to the Hg cycle depending on the hemisphere (Fisher et al., 2023). First, **industrial sources** represent a major anthropogenic source of Hg. They include coal-fired power generation and incinerators, non-ferrous metals production, as well as municipal waste and e-waste dumps. Second, **industrial mining** and **artisanal small-scale gold mining** (ASGM) are substantial sources of anthropogenic Hg. Mercury amalgamation represents the most common method of gold recovery used by ASGMiners worldwide (Keane et al., 2023). During the various stages of the amalgamation process, Hg is released in the atmosphere, but also to aquatic environments through wash-off during rain and flood events. Third, **anthropogenic fires** and **deforestation**, which often go hand in hand, represent a significant source of global atmospheric Hg, releasing Hg sequestered in the vegetation and soil by volatilization (Fisher et al., 2023; Outridge et al., 2018). Together, they mobilize Hg sequestered in the terrestrial biosphere (*i.e.*, vegetation and soil) *via* direct emission to the air, soil leaching and erosion, as well as releases to water bodies and removal of vegetation that would otherwise serve as sink for atmospheric Hg (Amirbahman et al., 2004; Dittman et al., 2010). In addition to anthropogenic Hg emissions, land and ocean re-emissions play also a significant role in Hg cycling globally (Zhang et al., 2023).

Globally, the amount of Hg released into the environment has steadily increased since the Industrial Revolution, resulting in a three- to five-fold increase of Hg on land, in the atmosphere and the ocean (Lamborg et al., 2014; Selin, 2009). This considerable increase over the last centuries results from both current and legacy anthropogenic emissions. Legacy emissions are defined as «anthropogenic emissions and releases that took place in the past, either at the time when Hg was produced or employed in a manufacturing process or gradually (in the intervening years to the present) from historic end- or by-products containing Hg» (Fisher et al., 2023). Given the persistent nature of Hg in the environment, legacy Hg continues to contribute to the

current biogeochemical cycling of Hg, with re-emission from both ocean and terrestrial reservoirs (Amos et al., 2013).

Historical, political, cultural and socioeconomic differences between Northern and Southern countries have led to different anthropogenic perturbations to natural Hg cycling between the two hemispheres. For instance, ASGM, deforestation and fires are more prevalent in the Southern Hemisphere, whereas legacy Hg emissions and industrial sources are dominant in the Northern Hemisphere (Fisher et al., 2023).

1.2. Long-range transport of Hg

Both natural and anthropogenic Hg travel across oceans and continents, predominantly through the global atmospheric circulation (Driscoll et al., 2013). Considering its large residence time in the atmosphere, from several months to one year (Horowitz et al., 2017; Streets et al., 2019; Zhang and Zhang, 2022), Hg disperses widely before its deposition in all ecosystems of the world. The large-scale transport of Hg is also facilitated through two additional pathways: river run-offs and the global oceanic circulation, although their contributions are minor compared to the global atmospheric transport (Outridge et al., 2018). Thus, even the most remote oceanic regions (*i.e.*, oceanic regions that are not subject to the direct influence of anthropogenic emission sources) are affected by this global pollutant.

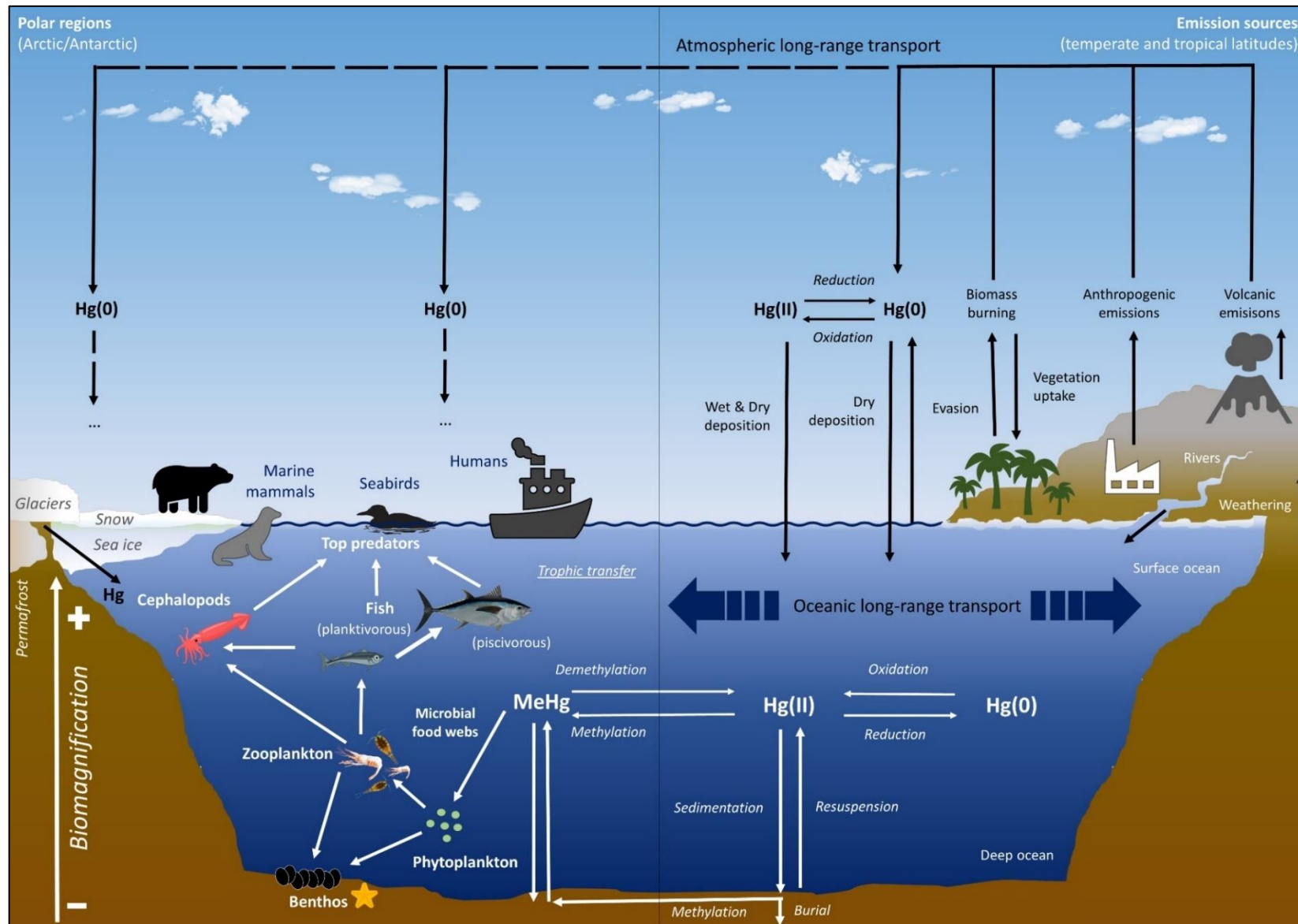
1.3. Mercury cycle and fate in marine food webs

The Hg cycle is complex and includes a multitude of physical, biogeochemical and ecological interactions, transformations and fluxes between the atmosphere, the land and the ocean, and is becoming more complex with ongoing climate change (Chételat et al., 2022; McKinney et al., 2022; Sonke et al., 2023). Besides, these processes can vary between oceanic regions. For example, Hg cycling and its underlying processes in tropical oceans differ from the one in polar oceans (see Section 2.3 for further details). For an example in Arctic marine ecosystems, the reader is referred to Braune et al. (2015), which provide an extensive review of major pathways and Hg transformations in the Canadian Arctic. A simplified representation of Hg sources, cycle and fate in the oceans is provided in [Figure 1.1](#). Briefly, Hg⁰ (*i.e.*, the dominant Hg species emitted in the atmosphere) will be transformed in different Hg species (*e.g.*, divalent inorganic Hg – Hg^{II}; methyl-Hg – MeHg) through chemical reactions (*e.g.*, oxidation, reduction,

methylation, photo-demethylation). Mercury, in its various forms, will then be deposited in the oceans through wet (*i.e.*, when Hg species, either gaseous or particulate, are deposited by rain, snow or fog) and dry deposition (*i.e.*, deposition of aerosol particles) (Figure 1.1). A global review of Hg species and deposition processes is provided in Li et al. (2020) for further information. In the ocean, Hg is methylated by naturally occurring microorganisms into methyl-Hg (MeHg), its most toxic and bioavailable form (Driscoll et al., 2013). Methylation mainly occurs in the mesopelagic ocean, associated with anoxic (*i.e.*, in the absence of oxygen) conditions, as well as ocean sediments (Bowman et al., 2020; Cossa, 2013; Gilmour et al., 2013; Mason, 2012), but may also occur in oxic subsurface waters (Villar et al., 2020).

Because of its high assimilation efficiency and strong affinity for proteins, MeHg bioaccumulates in marine organisms (*i.e.*, concentrations increase over time in their tissues). Bioaccumulation results from both the uptake of dissolved chemicals from water (*i.e.*, bioconcentration) and the uptake from ingested food and sediment residues (Burger and Gochfeld, 2004). For example, Hg concentrations in a seabird chick will be lower compared to an adult, because of its shorter life and hence shorter exposure to Hg. In marine food webs, MeHg is transferred from phytoplankton, at the base of the food web, to zooplankton, fish and cephalopods, up to top predators, such as marine mammals and seabirds (Figure 1.1). During this transfer, MeHg biomagnifies along the food web (*i.e.*, concentrations increase at each trophic level; Burger, 2002). Therefore, top predators present some of the highest Hg concentrations in wildlife, making them particularly sensitive to the toxicity of this global pollutant.

Figure 1.1. Conceptual, simplified representation of the Hg cycle from emission sources, in temperate and tropical latitudes, to polar oceans, including its major sources (anthropogenic and natural), long-range transport, major speciation processes and its trophic transfer in marine food webs. The Hg biogeochemical cycle is far more complex, with processes and interactions differing between oceanic regions worldwide. The reader is referred to AMAP (2021) for the Arctic, or to Chen and Evers (2023) for the Southern Hemisphere.



1.4. A chemical of major public health concern

Mercury belongs to the «10 chemicals of major public health concern», defined by the World Health Organization (WHO, 2020). It is a major threat for both wildlife and human populations worldwide. In wildlife, Hg causes a wide variety of deleterious effects, for example on vitamin metabolism, thyroid and steroid hormone balances, oxidative stress, tissue pathology (Dietz et al., 2019; Tan et al., 2009). As a neurotoxic, it can cause visual and sensory deficits (Wolfe et al., 1998), changes in behaviour and can impair the reproductive success (*i.e.*, reprotoxic; Evers et al., 2008; Scheuhammer et al., 2012; Whitney and Cristol, 2018). In addition, Hg can also affect the immune functioning (*i.e.*, immunotoxic), favoring the development of diseases, such as influenza in birds (Teitelbaum et al., 2022). In humans, it can cause severe physical and neurological harm, with growing evidence of impacts on the cardiovascular and immune systems too (Basu et al., 2023), and can even lead to death at sufficiently high concentrations, as is the case in the Minamata Disease (see [Box 1](#) for further details; Takeuchi et al., 1962). Mercury poisoning events during the mid-twentieth century have led to new regulations (Basu et al., 2023), such as the Minamata Convention on Mercury ([Box 1](#)), to protect human health and the environment, by controlling and reducing anthropogenic releases of Hg globally. Currently, the Minamata Convention Secretariat, with guidance from the United Nations Environmental Program (UNEP), is developing guidance for monitoring programs in member countries, to evaluate the effectiveness of the Minamata Convention. Scientific input is critical today and in the next years for guiding the policies related to effectiveness evaluation.

Box 1



**DID YOU
KNOW**



The Minamata Convention

Mercury is a toxic pollutant and its adverse effects on human health were first reported in the 1950s in Minamata, a small port city in Japan. For more than 30 years, Hg-tainted industrial wastewaters were released in Minamata Bay, poisoning the entire ecosystem locally, starting with small mammals (cats, rats and mice) and then impacting fishermen and their families. They all had one feature in common: they consumed marine resources from the bay (fish and shellfish). Since then, the disease resulting from Hg poisoning is known as the Minamata Disease. This incurable disease causes severe and permanent physical (limb flexion) and neurological (unsteadiness, convulsions, abnormal movements, brain atrophy, loss of neurones) damage and can even lead to death (Takeuchi et al., 1962). In 2009, more than 13,000 victims were officially recognised by the Japanese government, but several thousand people are still awaiting decision.

This terrible tragedy led to the creation of a global agreement on environment and health in 2013: the Minamata Convention. This international treaty was ratified by 140 countries, including France, and entered into force in 2017. Since then, parties have been working together to protect human health and the environment from the adverse effects of Hg worldwide, for instance by:

- ① controlling the Hg supply and trade,
- ① reducing the use, emission and release of Hg,
- ① raising public awareness,
- ① building the necessary institutional capacity for the implementation of the Minamata Convention.

More information available at:
<https://mercuryconvention.org/en>



**MINAMATA
CONVENTION
ON MERCURY**



Seafood represents the main source of protein for billions of people worldwide (FAO, 2020), but also the principal source of Hg for humans and wildlife. From a human perspective, socio-economic costs of Hg contamination were estimated in billions of dollars *per year* (Trasande et al., 2005). Mercury contamination thus constitutes a global threat, not only economically but also sanitarily and environmentally. Assessing the risks associated with the consumption of marine resources is crucial and can be achieved through environmental monitoring of Hg in the oceans.

2. Oceans, a grey zone for the environmental monitoring of Hg

2.1. Role of the oceans in the Hg cycle and transfer

Oceans represent a crucial compartment in Hg cycling, allowing for Hg storage over long periods of time and its subsequent, continuous reemissions. An updated budget of Hg fluxes and masses, from both natural and anthropogenic origins, for the oceans and its compartments was presented in the last Global Mercury Assessment ([Figure 1.2](#); UN Environment, 2018). For pelagic ocean regions, the dominant source of Hg is atmospheric deposition (Obrist et al., 2018). In fact, oceans receive 80% of total atmospheric Hg, as dry and wet depositions (Horowitz et al., 2017). In contrast, the sinks of Hg for the oceans are minor, including burial in coastal and deep ocean sediments, and re-emission from the ocean surface to the atmosphere. This leads to the build up of Hg in ocean waters, hence identifying oceans as a net sink for atmospheric Hg (Fisher et al., 2023).

Modelling efforts, that updated the global and ocean Hg budgets for the Global Mercury Assessment, revealed that two-thirds of all anthropogenic Hg in the oceans originated from mining since the 16th century and entered the oceans prior 1920 (Lamborg et al., 2014; Zhang et al., 2014). The remaining third has mainly originated from coal combustion and other industrial activities since 1920. Model estimations revealed that the removal of this anthropogenic Hg from the world's oceans will take many decades to centuries, varying substantially between different ocean basins (UN Environment, 2018).

Furthermore, due to the methylation that occurs specifically in their waters, and considering their huge surface and volume, oceans promote the bioavailability and the toxicity of MeHg, posing serious threats to both wildlife and humans that heavily rely on marine resources

worldwide. Most MeHg is likely produced *in situ* in oceanic waters rather than transported offshore by rivers, and is efficiently assimilated by small marine organisms (*i.e.*, procaryotes, unicellular eucaryotes such as phytoplankton) (*i.e.*, short lifetime; Liu et al., 2021). Oceans thus represent an effective factory of MeHg and hence a hotspot reservoir for both wildlife and humans.

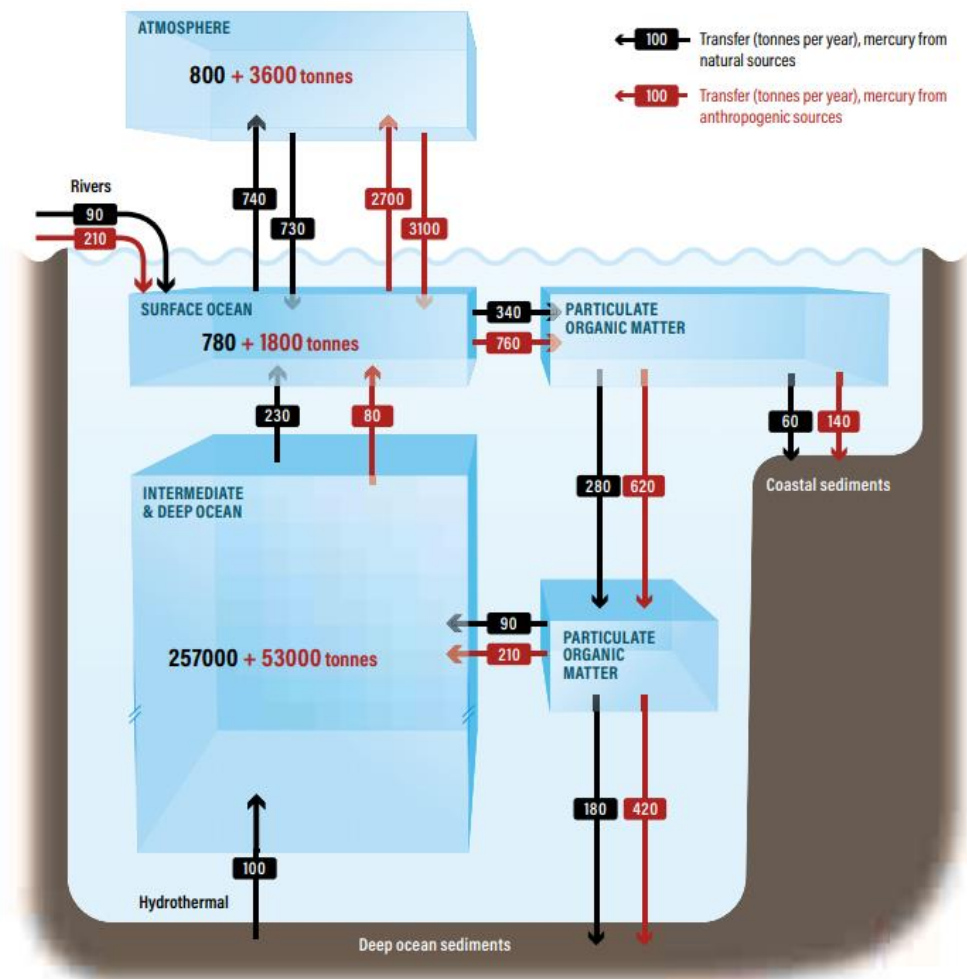


Figure 1.2. Natural and anthropogenic fluxes and masses of Hg in the world's oceans; extracted from the Global Mercury Assessment (UN Environment, 2018).

Yet, monitoring MeHg and Hg species in general in vast oceans, which represent 70% of the planet's surface, is challenging. This requires huge and expensive sampling efforts, with oceanographic campaigns on research vessels and an enormous number of sampling stations across various regions. Given these logistical and financial constraints, an alternative consists

in monitoring Hg using marine biota as bioindicators, since they reflect the Hg contamination of the food web and ecosystem on which they rely.

2.2. Monitoring Hg in the oceans

Monitoring Hg in biota enables to understand spatial gradients and temporal trends in MeHg availability, over local, regional and global scales, and to assess whether inputs of anthropogenic Hg in the oceans are safe or harmful for both wildlife and humans. In 2019, the Biodiversity Research Institute (BRI) published the Global Biotic Mercury Synthesis (GBMS), where all biotic (*i.e.*, in living organisms) Hg data were compiled from peer-reviewed published literature into one single database (Evers, 2019). The authors targeted bioindicator species as defined by the Article 19 of the Minamata Convention which states that: «In terms of bioindicator selection linked to human health or ecological health, the taxa of greatest interest for the Minamata Convention include freshwater and marine fish, sea turtles, birds and marine mammals». Their complete methodology is described in the Technical Information Report on Hg Monitoring in Biota (Evers, 2019). In total, the GBMS included around 1,095 peer-reviewed scientific publications, representing 458,840 Hg samples from about 375,677 individuals, collected in more than 2,781 unique locations in 119 countries (see [Table A1](#) in Annexes for further details).

Overall, the GBMS revealed that continents were much more documented than oceans, representing 77% and 23% of global Hg data, respectively ([Figure 1.3.A](#)). Oceans, when considered alone, also presented some disparities between ocean basins ([Figure 1.3.B](#)). The North Pacific and North Atlantic Oceans were the most monitored basins. In contrast, oceans from the Southern Hemisphere (*i.e.*, South Pacific, South Atlantic and Indian Oceans) were little explored, as well as polar oceans, with the number of Hg samples being higher in the Arctic compared to the Antarctic because of the Arctic Monitoring and Assessment Program and its long-term monitoring program of Hg across the Arctic (see AMAP, 2021). In general, these Hg data were mostly acquired in coastal environments. By comparison, Hg data for the open ocean are scarce, especially in remote oceanic regions.

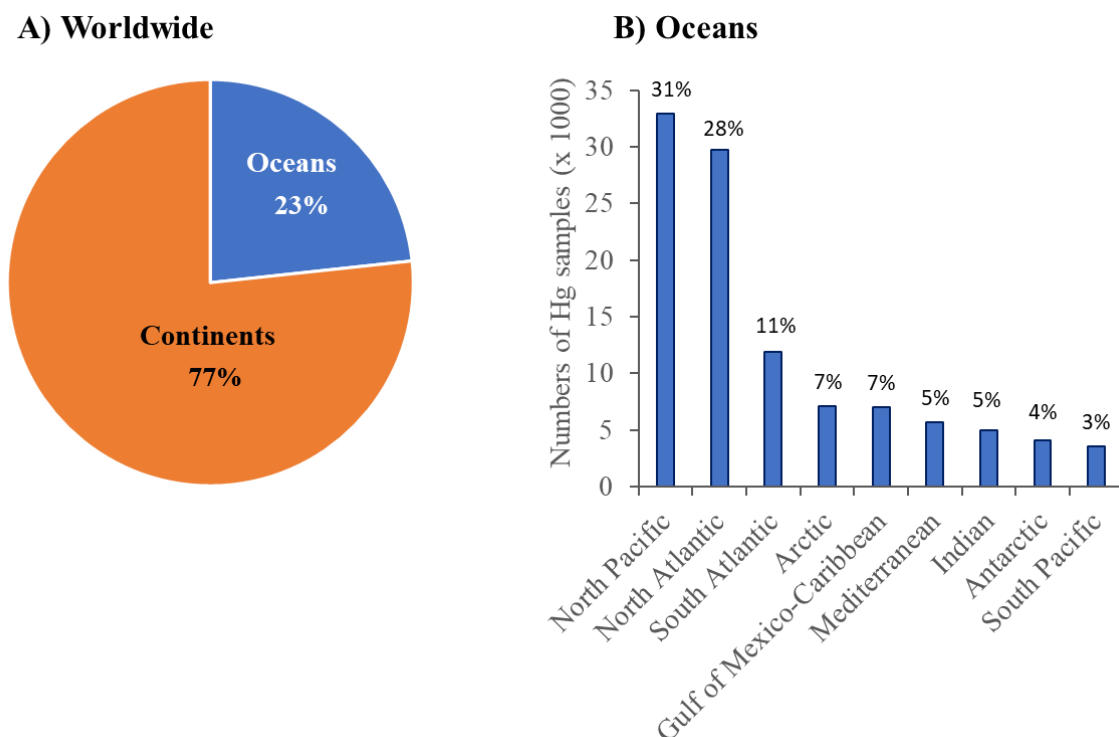


Figure 1.3. Summary of biotic Hg concentrations from the Global Biotic Mercury Synthesis (Evers, 2019): Comparison of biotic Hg concentrations **(A)** for continental (n=351,963) and oceanic (n=106,877) regions, and **(B)** between major ocean basins and seas.

2.3. A focus on remote oceanic regions

Considering their remoteness from any land masses and any direct anthropogenic sources of Hg, remote oceanic regions (*i.e.*, pelagic oceans) could be easily considered as pristine. But are they really? To answer this question, we identified, based on the GBMS, two main remote oceanic regions, lacking large-scale monitoring of biotic Hg: tropical and polar oceans.

Tropical oceans. Recently, the Global Mercury Impact Synthesis (see Chen and Evers, 2023 and references therein) specifically identified the vast open oceans from the Southern Hemisphere as regions where Hg data and scientific understanding were most lacking. Thus, little is known about the interactions between Hg and ecosystem functioning in the tropical oceans. Yet, this paucity of Hg data intersects with a large fraction of global Hg emissions (Selin et al., 2018). Of the total atmospheric deposition of Hg received by the oceans, 49% is limited to tropical regions (Horowitz et al., 2017). Besides, it is here that both deforestation of rainforest (Schneider et al., 2023) and ASGM occurs. Present in 80 countries, this latter activity produces up to 20% of the world's gold (Keane et al., 2023). ASGM is a widespread activity, which

employs 15 million miners and represent a source of livelihood for 100 million people globally (UN Environment, 2018; Fisher et al., 2023). Yet, gold mining is the dominant source of Hg inputs locally (*i.e.*, in tropical ecosystems) and globally (*i.e.*, impacting all countries; Eagles-Smith et al., 2018; Fisher et al., 2023). In addition, tropical oceans have recently experienced increased oxygen-depletion (Breitburg et al., 2018), creating favourable anoxic conditions for MeHg formation (Cossa, 2013; Mason et al., 2012; Sunderland et al., 2009 but see Villar et al., 2020). Therefore, quantifying Hg contamination in tropical oceans and wildlife, particularly its spatial and temporal trends, is urgently needed.

Polar oceans. Polar oceans are particularly sensitive to global change (*e.g.*, warming). Yet, this has led to profound perturbations of the polar marine ecosystems, with secondary effects on Hg cycling and exposure of polar wildlife. The effects of climate change on Hg cycling were especially documented in the Arctic (see Chételat et al., 2022 and McKinney et al., 2022 for a complete review). Overall, climate change may impact Hg deposition, abiotic cycling and uptake, as well as its transfer in marine food webs resulting from ecosystem changes (Braune et al., 2014b; Kozak et al., 2021; McKinney et al., 2017). For example, Hg exposure of Arctic marine wildlife may change according to the increased river transport of Hg through the melting of glaciers and permafrost, as well as the loss of sea ice, which alters Hg chemistry and food webs interactions, and hence Hg biomagnification and transfer in marine ecosystems. In contrast, such knowledge on Hg cycling and effects of climate change is scarce in the Antarctic, which plays a key role in the regulation of the world's climate and the production of attractive marine resources (*e.g.*, krill). Assessing Hg contamination in these rapidly changing ecosystems is critical to evaluate the effectiveness of established regulations on Hg emissions and the anthropogenic impacts on polar oceans and their marine ecosystems.

3. Seabirds as bioindicators of Hg contamination in marine food webs

Monitoring remote oceanic regions, such as tropical and polar oceans, is logistically challenging and expensive, but can be achieved through investigations of bioindicators that feed extensively across their waters. For more than 50 years, seabirds have been extensively used as bioindicators of marine ecosystems (Burger and Gochfeld, 2004; Furness, 1993), since they are highly sensitive to changes in oceanographic conditions, food supply or pollution (Cairns, 1988; Provencher et al., 2012; Vihtakari et al., 2018).

More specifically, using seabirds as bioindicators is advantageous for many reasons. First, they are meso- and top predators. They occupy high trophic position in marine food webs and thus exhibit high Hg concentrations resulting from biomagnification. Second, they are long-lived and bioaccumulate Hg throughout their life. Consequently, they integrate and reflect Hg contamination of marine food webs on which they rely (Fort et al., 2016; Furness and Camphuysen, 1997; Piatt et al., 2007). Third, they are philopatric: many species return to the same nest and colony for years, allowing long-term monitoring and resampling the same individuals from one year to the next (Burger, 1993). Fourth, they are colonial (*i.e.*, they concentrate in high numbers in breeding colonies on land), resulting in large sample sizes concentrated in one location. Thus, several individuals can be sampled simultaneously and repeatedly through time. Fifth, they are widely distributed and ubiquitous (*i.e.*, they are present in all marine ecosystems).



Box 2

What is a seabird ?

« *A bird that spend part or all of its life interacting with the ocean, particularly as a food source, and not just migrating over it.* »

(Harrison et al., 2021)

DID YOU KNOW ?

While oceans cover around 70% of the Earth, seabirds only represent 3-4% of the 9,000 bird species known to date (*i.e.*, > 400 species) and constitute the most threatened bird group (Croxall et al., 2012). In general, seabirds have a longer lifespan, start breeding older, produce a smaller number of offsprings and show a greater parental investment compared to the majority of terrestrial birds (Schreiber et Burger, 2001). Seabirds spend the majority of their time at sea and only come to land for breeding.

A few numbers

434

9

18

Recently, the new seabird identification guide has recognized a total of 25 seabird groups, including Seaducks, Grebes, Shearwaters, Phalaropes, Skimmers, Gulls, Noddies and **Terns**, Skuas and Jaegers, **Auks**, Tropicbirds, Loons, **Penguins**, Albatrosses, Storm- petrels, Petrels, Shearwaters and Diving Petrels, Frigatebirds, Gannets and Boobies, Cormorants and Shags and Pelicans (Harrison et al., 2021).

(Bioindicator species in this thesis belong to the groups indicated in bold.)

Box 2



DID YOU KNOW



(following)

What is a seabird ?

In seabirds, the diversity of form, size, distribution, ecology and behaviour amongst the different groups is considerable. For example, albatrosses are experts in aerodynamics and are capable of flying >1000 km in a single day. In contrast, penguins are flightless and spend most of their lives immersed in waters as expert submariners:

some are capable to submerge for more than 20 min at a time and reach depths >500 m. With a relatively limited foraging range when breeding, auks become pelagic outside the breeding season.

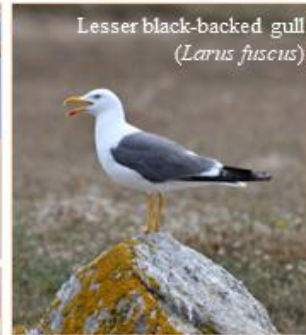
A few examples



Common eider
(*Somateria mollissima*)



Black-legged kittiwake
(*Rissa tridactyla*)



Lesser black-backed gull
(*Larus fuscus*)



Common tern (*Sterna hirundo*)



Emperor penguin
(*Aptenodytes forsteri*)



Northern fulmar
(*Fulmarus glacialis*)



Atlantic puffin (*Fratercula arctica*)



Red-billed tropicbird
(*Phaethon aethereus*)



European shag
(*Phalacrocorax aristotelis*)



Little auk
(*Alle alle*)



Blue-footed booby
(*Sula nebouxi*)

Seabirds have various life history strategies and cycles, behavior and physiology, diet and habitat uses. Thus, their vulnerability to contaminants and environmental changes varies (Burger et Gochfeld, 2001a).

As abundant consumers of marine resources, they play a key role in the functioning of marine ecosystems worldwide (Brooke, 2004; González-Bergonzoni Ivan et al., 2017; Welch et al., 1992). Many seabirds travel over substantial distances to feed, sampling prey from different regions. Seabirds thus represent bioindicators for local, regional and global scales. From a more practical point of view, they are large in size and conspicuous, and thus easily observed and monitored. Finally, they are emblematic and of particular interest to the public, so that people do care about the conservation of seabirds (see [Box 2](#)).

Seabirds were extensively studied to monitor Hg in oceans and marine ecosystems, for instance by sampling different tissues to obtain information at different temporal scales, from recent Hg uptake (*i.e.*, blood) to longer term contamination (*i.e.*, internal tissues, eggs and feathers; see Chapter 2 for a more extensive presentation) (Bearhop et al., 2000; Furness et al., 1986; Mallory et al., 2018; Mallory and Braune, 2012; Monteiro and Furness, 2001). In monitoring programs in general, particular attention is given to effective, non-destructive and non-invasive monitoring tools that do not jeopardize the health or the survival of the monitored species. For seabirds, this is the case with blood, eggs and feathers, which were identified in the GBMS as the tissues of interest for Hg biomonitoring and recommended for international monitoring programs (Evers et al., 2019).

According to the GBMS (see Section 2.2), Hg biomonitoring in the oceans is unequally distributed depending on the ocean basins. Seabirds were the second most monitored taxa, after fish, which represented 39% and 52% of all Hg samples, respectively ([Figure 1.4.A](#)). Similar to [Figure 1.3](#), spatial disparities were also observed when considering birds alone ([Figure 1.4.B](#)). Again, ocean basins that were the most monitored were the North Pacific and Atlantic Oceans, representing together almost 75% of all Hg data in seabirds. The remaining 25% is shared between tropical and subtropical oceans, as well as polar oceans.

Overall, seabirds represent useful bioindicators of the health of coastal ecosystems, providing essential information for human exposure (Burger and Gochfeld, 2001a) – since birds and humans exploit similar marine resources – but also in remote marine ecosystems that are usually hardly accessible to humans.

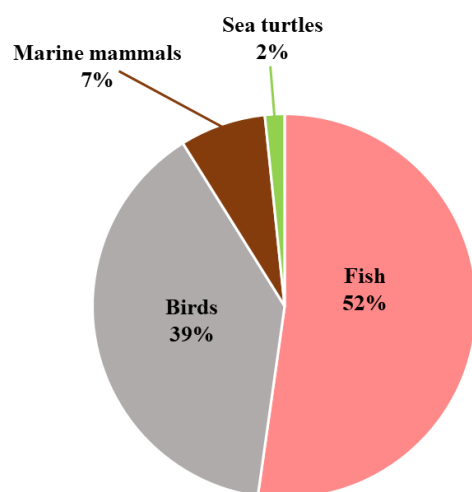
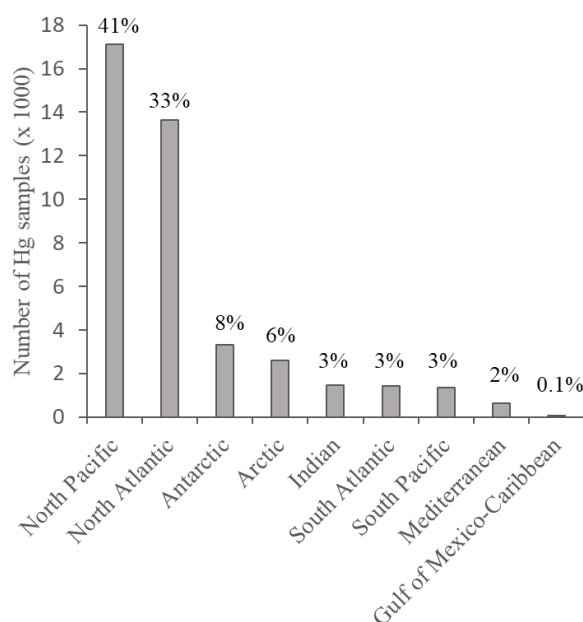
A) Major taxa for ocean monitoring**B) Birds**

Figure 1.4. Summary of biotic Hg concentrations from the Global Biotic Mercury Synthesis (Evers, 2019): Comparison of biotic Hg concentrations **(A)** across all major taxa ($n=106,877$) for ocean Hg monitoring, including fish ($n=55,828$), birds ($n=41,542$), marine mammals ($n=7,741$) and sea turtles ($n=1,766$) and **(B)** between major ocean basins and seas for birds only (in the descending order).

4. Main objectives and outline of the thesis

In this context, seabirds are ideal candidates to document both past and current Hg contamination in remote oceanic regions. Three regions were targeted in this doctoral work: (i) the Arctic Ocean, (ii) the intertropical zone, encompassing the three oceans (*i.e.*, Pacific, Atlantic and Indian Oceans) and (iii) the Southern Ocean. For each of these oceanic regions, one bioindicator seabird species was selected following recommendations of the GBMS and the Minamata Convention of Mercury, based on their wide spatial distribution and their high abundance in the selected region, and reflecting Hg contamination specifically in all three regions. This included the Brünnich guillemot (or thick-billed murre, *Uria lomvia*), the sooty tern (*Onychoprion fuscatus*) and the Adélie penguin (*Pygoscelis adeliae*), respectively. General information (*i.e.*, distribution and ecology) about each species is provided in the Annexes. For all species, feathers, which reflect longer term Hg contamination (*i.e.*, for several months up to

one year) across a large spatial scale in seabirds (see Chapter for an exhaustive explanation), were used as biomonitoring tool, to serve the following scientific objective:

Main objective:

Document past and current trends in environmental Hg contamination, in remote oceanic regions by using seabirds as bioindicators.

The present thesis presents the doctoral work, with this main objective as scientific target, in the form of a comprehensive synthesis, divided into five chapters. The main questions of these chapters will be briefly described here, and the hypotheses, predictions, main results and subsequent conclusions and discussions will be presented along the corresponding chapters. The methodological approach is presented in Chapter 2, to avoid redundancy along the thesis as much as possible, but complete methodology is provided in the corresponding scientific papers (*i.e.*, published, submitted and in preparation), which are available in Annexes. The general conclusion of this doctoral work, its critical evaluation and its perspectives are presented in a final chapter (Chapter 5).

The main objective was divided into two specific objectives, as follows:

Objective 1:

Document spatial variations of current Hg contamination in these remote oceanic regions and their marine ecosystems.

Chapter 3 is mostly dedicated to a large-scale spatial assessment of current Hg contamination in the intertropical region (pantropical assessment) and the Antarctic (circumpolar assessment). Scientific papers associated with this chapter include **Papers 1** (in preparation) and **2** (submitted), respectively. This chapter also includes spatial comparisons of Hg contamination in the Arctic, as a contribution to the ARCTOX program.

At such large spatial scales, we expected both intra- and inter-ocean differences in Hg contamination, in relation with differences in Hg sources and cycling between hemispheres, but also differences in environmental conditions at the base of marine food webs which drive its transfer along food webs towards seabirds.

Objective 2:

Document temporal trends of Hg contamination since the Industrial Era until the present day in these remote oceanic regions and their marine ecosystems.

Chapter 4 is mainly dedicated to a retrospective assessment (*i.e.*, multi-decadal/century time-series) of Hg contamination in the Arctic and the intertropical region (*i.e.*, South Atlantic Ocean). Scientific papers associated with this chapter include **Papers 3** (in preparation) and **4** (published), respectively. This chapter also includes temporal comparisons of Hg contamination (*i.e.*, comparison of two or several epochs, separated by extended periods of time with no Hg data) in the intertropical region and the Antarctic.

As a result of increasing anthropogenic emissions of Hg since the Industrial Revolution, we were expecting increasing trends in seabirds from all regions. However, since Hg sources and cycling differ across oceanic regions (see Section 2.3), as well as their respective evolution through time, we also expected a difference in temporal trends depending on the region (*e.g.*, different increase rates and patterns; Sonke et al., 2023).

Given the scientific structure of the doctoral work (*i.e.*, all oceanic regions are studied across both space and time), some redundancy was inevitable in the present thesis, particularly in the chapters' structure. **Figure 1.5** provides a conceptual summary of the structure of this doctoral work, associating each region with their corresponding objectives.

Chapter 2

Methodological approach

1. Description of bioindicator seabird species

Three seabird species were selected as bioindicator species of three remote oceanic regions (the Arctic, the intertropical region and the Antarctic). A general description is provided here for each species, but more information is available in the Annexes.

The **Brünnich's guillemot** (or thick-billed murre, *Uria lomvia*) is an ideal candidate to monitor Hg contamination in Arctic marine food webs. With a near circumpolar distribution, this species is amongst the most abundant seabird in the Arctic during the breeding season, with an estimated world population of 15-20 million birds (Gaston et Hipfner, 2020). Guillemots breed on rocky cliffs (Figure 2.1), in waters where sea ice occurs (Harrison et al., 2021). When ice conditions are favourable, they are closely tied to sea ice and its derived resources for feeding (Cusset et al., 2019). As pursuit-divers, they forage underwater to depths of > 100 m (Croll et al., 1992), mainly feeding on fish such as Arctic cod (*Boreogadus saida*), capelin (*Mallotus villosus*) and sandlance (*Ammodytes* sp.), as well as macrozooplankton including amphipods (Hyperiididae and Gammaridae) and copepods (*Calanus* spp.; Gaston et al., 2005; Gaston and Nettleship, 1981).



Figure 2.1. Adult Brünnich's guillemots nesting on Prince Leopold Island (Canadian Arctic)

As for all Alcids, guillemots molt twice a year, including a total, post-breeding molt and a partial, pre-breeding molt. Molt and implications for Hg monitoring will be discussed in Section 2.2.1. In the IUCN Red List of Threatened Species, Brünnich's guillemots are listed of «Least Concern».

The **sooty tern** (*Onychoprion fuscatus*) is the most abundant tropical seabird, widely distributed in all three ocean basins, with about 60-80 million birds in total worldwide (Schreiber et al., 2020). This species is therefore an ideal candidate to monitor Hg contamination in tropical food webs. Sooty terns nest on bare ground (Figure 2.2), on tropical islands and coral atolls (Harrison et al., 2021). They are highly aerial and spend only a very limited time on water (Jaeger et al., 2017). As epipelagic seabirds, sooty terns feed on small pelagic fish and squid caught at or near the ocean surface (Ashmole, 1963; Reynolds et al., 2019). They are heavily reliant on large schools of surface-swimming tunas, such as yellowfin (*Thunnus albacares*) and skipjack (*Katsuwonus pelamis*) tuna, to drive their common prey to the ocean surface, where many tropical seabirds forage in so-called «facilitated foraging» (Ashmole, 1963; Au and Pitman, 1986; Balance and Pitman, 1999; Maxwell and Morgan, 2013). Information about their molt and implications for Hg monitoring is provided in Section 2.2.1.



Figure 2.2. Adult sooty tern in the breeding colony of Ascension Island (South Atlantic Ocean).

Globally, sooty terns are listed of «Least Concern» in the IUCN Red List, even though some populations could be considered as «Critically Endangered» considering recent declines in population size, as in the case of Ascension Island in the South Atlantic Ocean (–84% between the 1940s and the 1990s ; Hughes et al., 2017).

The **Adélie penguin** (*Pygoscelis adeliae*) is an ideal candidate to monitor Hg contamination in Antarctic marine food webs. This species has been selected as an indicator species for the Commission for the Conservation of Antarctic Marine Living Resources (CCAMLR) for the Ecosystem Monitoring Program (Agnew, 1997), which aims to ensure that krill fisheries take account of the needs of krill-predators, such as seals and seabirds, and to distinguish between environmental variation/changes and fishing activities in the Southern Ocean. With its circumpolar distribution, it is the most common and abundant penguin species in Antarctica (Figure 2.3), with 3.5-4.1 million breeding pairs in total (Lynch and LaRue, 2014).



Figure 2.3. Adélie penguins (adult and moulting chick) in Dumont d’Urville (Adélie Land).

Adélie penguins forage in Antarctic waters year-round (Ballard et al., 2010; Takahashi et al., 2018; Thiebot et al., 2019) and are strongly associated with sea-ice environments, both during

the breeding (Emmerson and Southwell, 2008; Guen et al., 2018; Kokubun et al., 2021) and non-breeding seasons (Emmerson and Southwell, 2011). They feed preferentially in waters covered by 20 to 80% sea ice, but also in the open sea (Cottin et al., 2012; Guen et al., 2018; Michelot et al., 2020). In these habitats, their diet comprises different euphausiid crustaceans, a large component of the Antarctic krill (*Euphausia superba*) and smaller amounts of the ice krill (*Euphausia crystallophias*; Tierney et al., 2009). Their diet also includes fish species such as the Antarctic silverfish (*Pleuragramma antarcticum*) in different proportions according to colony location and season (Ainley et al., 1998; Ainley, 2002). As for all penguins, they present a unique moulting pattern, replacing their entire plumage simultaneously in a few weeks (Adams and Brown, 1990). Molt and implications for Hg monitoring will be further discussed in Section 2.2.1. Globally, they are listed of «Least Concern» in the IUCN Red List (Martínez et al., 2020).

2. Feathers, valuable archives for Hg biomonitoring in the oceans

When monitoring Hg in seabirds, different tissues can be collected, and the utility of a particular tissue varies with the contaminant and the research question. Internal tissues and eggs of seabirds have usually received particular attention, because they are useful for impact studies and risk assessments of Hg contamination for wildlife and humans that consume them (Albert et al., 2019; Furness, 1993). However, the sampling of internal tissues and eggs is destructive (i.e., implies to kill the individuals), except in the case of carcasses found in the environment. For large-scale and long-term monitoring, it is more appropriate to promote non-lethal sampling of blood and feathers, which incorporate Hg accumulated in the body and reflect the bird's contamination.

2.1. Mercury exposure, distribution and excretion routes in seabirds

In seabirds, exposure routes to Hg include inhalation (*i.e.*, air), food and water ingestion but the dominant route is through the diet (Burger and Gochfeld, 2001b; Gochfeld, 2000). Ingested Hg includes both MeHg, which represents the main bioavailable and assimilated form, and iHg that is hardly assimilated by the organism.

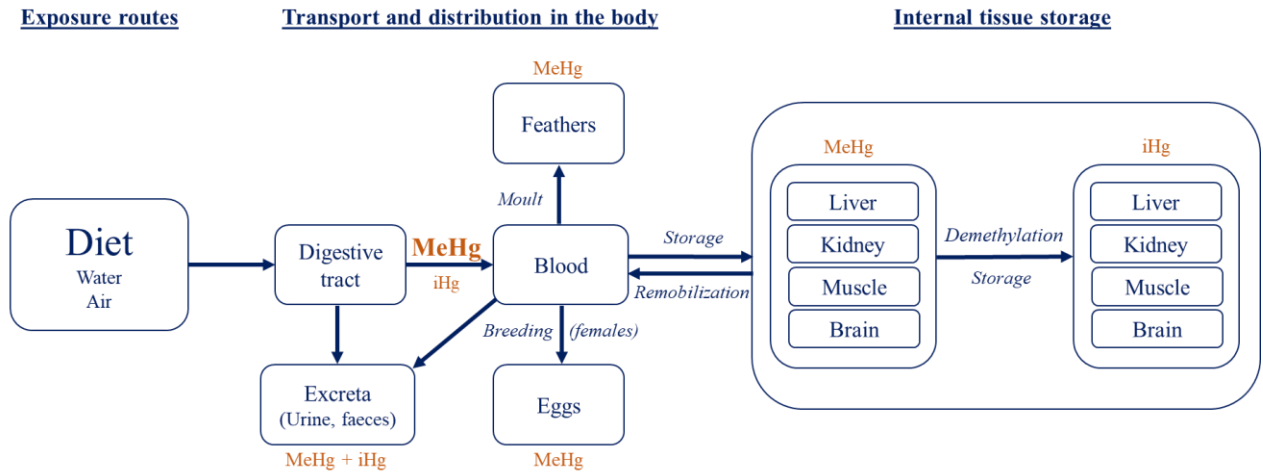


Figure 2.4. Simplified model of Hg dynamics in seabirds, with its dominant forms: methyl-Hg (MeHg) and inorganic Hg (iHg). Adapted from Monteiro and Furness (1995), Carravieri (2014) and Chételat et al. (2020). Demethylation occurs in the different tissues, but its degree/intensity varies among tissues and seabird species.

After the assimilation in the digestive tract, dietary MeHg is distributed *via* the blood circulation to the body tissues where it can be stored (Figure 2.1; Boudou and Ribeyre, 1985; Monteiro and Furness, 2001; Oliveira Ribeiro et al., 1999). While some tissues act as a storing endpoint (*i.e.*, kidney and brain), others can store and remobilize MeHg (*i.e.*, liver and blood) in different physiological conditions (Chételat et al., 2020; Li et al., 2022; Renedo et al., 2021). In internal tissues, MeHg can be demethylated and converted into inorganic Hg, a less toxic form that does not experience remobilization (Burger and Gochfeld, 2001b; Renedo et al., 2021; Spalding et al., 2000). The remaining MeHg constitutes a body pool until excretion during egg production (in females) and feather synthesis (in both sexes; Braune and Gaskin, 1987; Monteiro and Furness, 2001), which are the two major excretion pathways for MeHg (Bond and Diamond, 2009; Furness et al., 1986).

2.2. A powerful tool for Hg biomonitoring across space and time

In seabirds, MeHg accumulates between moulting episodes (Furness et al., 1986), up to 90% of which is sequestered into growing feathers during moult (K. Honda et al., 1986). Precisely, MeHg binds to sulhydryl groups of keratin molecules (Crewther et al., 1965), the building blocks of feathers, to form strong and stable bonds that withstand any rigorous physical treatment over time (Appelquist et al., 1984). Besides, MeHg accounts for >90% of the total

Hg burden in feathers (Bond and Diamond, 2009; Renedo et al., 2017; Thompson and Furness, 1989), and is highly correlated with Hg (hence MeHg) levels in seabirds' diet (Monteiro et al., 1998). Feathers thus represent a reliable tissue to investigate Hg contamination in seabirds (Thompson et al., 1998), and hence MeHg availability in marine ecosystems, in a wide range of ocean basins and across different temporal scales.

2.2.1. Different tissues, different scales

On the individual time scale, information on Hg contamination at different temporal scales can be obtained by sampling different seabird tissues. Blood informs about recent Hg intakes (*i.e.*, few weeks/months; Bearhop et al., 2000; Monteiro and Furness, 2001). In comparison, internal tissues (*i.e.*, liver, brain, kidney and muscle) inform about longer term Hg contamination (months/years; Mallory et al., 2018; Mallory and Braune, 2018). Eggs inform about intermediate Hg contamination, between blood and internal tissues, depending on the breeding strategy of birds. In income breeders (*i.e.*, species that use locally derived exogenous nutrients for egg production), eggs reflect Hg contamination during a restricted period before egg laying (Bond and Diamond, 2010). In comparison, eggs reflect a more extended period of time in capital breeders (*i.e.*, species that use endogenous nutrients for egg production; Meijer and Drent, 1999). Feathers are long-term Hg archives, informing about contamination from several months (*e.g.*, auks) to up to one year (*e.g.*, penguins) depending on the moulting strategy of birds (Figure 2.5).

Moult is an energetically expensive process, during which feathers are totally or partially replaced. It generally occurs during the non-breeding period, so as to not compromise foraging abilities during periods of high energetic demands, such as breeding or migration (Harrison et al., 2021). Among seabirds, moulting strategies vary, from a unique and drastic moulting episode in penguins (Cherel et al., 1994), to a biannual molting episode in auks (total and partial moult; Gaston and Jones, 1998) or a continuous moult encompassing several seasons/years in albatrosses (Prince et al., 1997; Weimerskirch, 1991). Therefore, knowledge of moulting patterns is fundamental to accurately infer the ecological meaning of Hg contamination from feathers, both temporally and spatially.

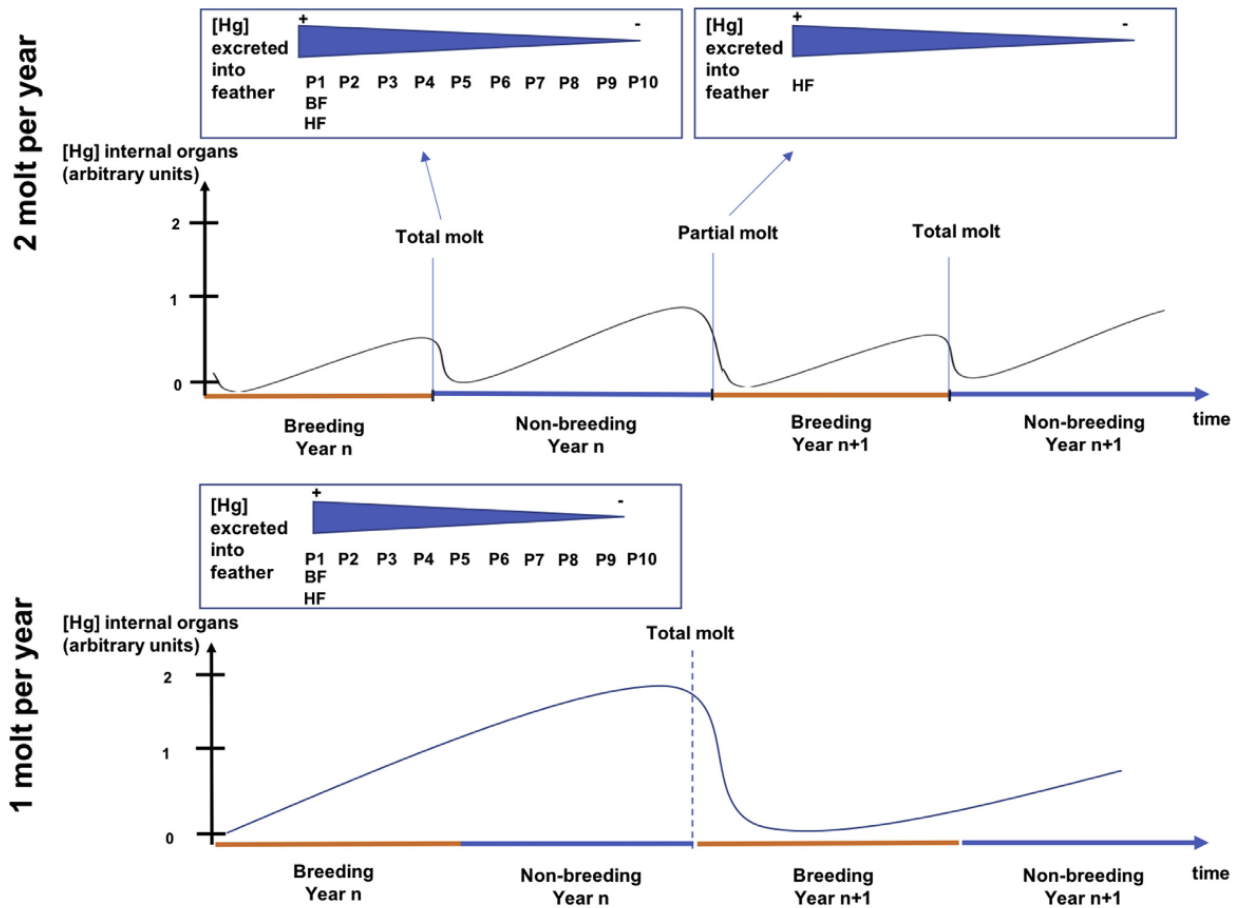


Figure 2.5. Schematic representation of Hg excretion in seabirds, from internal tissues to feathers (*i.e.*, body, head and primary feathers, indicated as BF, HF and PF, respectively), depending on their molting strategy (*i.e.*, one or two molts per year). Extracted from Albert et al. (2019).

Molt in bioindicator species and implications for Hg biomonitoring

Brünnich's guillemots: Like all Alcids, Brünnich's guillemots molt twice a year (Figure 2.5). After breeding, they complete a total molt and replace their entire plumage (*i.e.*, body, head and flight feathers), leading to winter plumage. In spring, they complete a partial molt and only replace their cheek, head and neck feathers, leading to nuptial plumage. Hence, the biannual molt allows to investigate seasonal exposure, with head and **body feathers** providing information about Hg contamination during the non-breeding and the **breeding periods** (Fort et al., 2014). Considering their southward migration towards subarctic and temperate latitudes (Frederiksen et al., 2016), this also allows to investigate Hg contamination in different marine food webs: outside and **inside the Arctic** during the non-breeding and breeding periods, respectively.

Sooty terns: Sooty terns start their post-nuptial molt (*i.e.*, basic molt) and replace all of their feathers (*i.e.*, flight and body feathers) during the following weeks/months (Ashmole, 1963). Therefore, body feathers collected during the breeding season provide information on bird Hg exposure since the previous moult (*i.e.*, **year-round exposure**; Albert et al., 2019; Reynolds et al., 2014).

Adélie penguins: As for all penguins, Adélie penguins present a unique moulting pattern, which results in homogeneous chemical composition in feathers (Brasso et al., 2013; Carravieri et al., 2014a). Following a pre-moulting foraging period of hyperphagia at sea, they renew their entire plumage annually while fasting ashore or on sea ice (a few weeks; Cherel et al., 1994; Emmerson et al., 2019), less frequently at the breeding colonies (Ainley, 2002). All feathers are thus moulted simultaneously every year with the regrowth of the replacement feathers also occurring simultaneously (Figure 2.5). Within each individual penguin, all feathers have thus the same chemical signature, including Hg concentrations and stable isotope ratios (Brasso et al., 2013; Carravieri et al., 2014a), representing a clear advantage when monitoring Hg. Body feathers thus represent **year-round Hg exposure** (Figure 2.6).

Since most seabirds are migratory, the timeframes reflected by feathers encompass different periods of their lifecycle, but are also associated with different spatial distribution in the ocean. Let us take the example of Adélie penguins breeding in Dumont d’Urville (Adélie Land, Antarctica). Given their annual and drastic moult (i.e., all feathers are replaced simultaneously), feathers of Adélie penguins represent year-round Hg exposure. Since feathers are usually moulted after breeding (around March), this includes migration, the non-breeding period and the return migration (~1,200 km away from the colony—mean maximum range; Thiébot et al., 2019), as well as the breeding season (<100 km away; Michelot et al., 2021), from the previous year (Figure 2.6). Feathers thus informs about large spatial and temporal scales in Adélie penguins, and in seabirds in general.

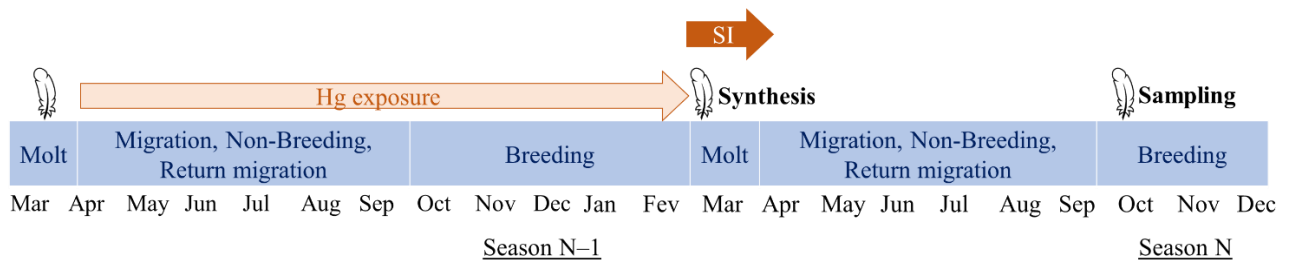


Figure 2.6. Schematic representation of Hg and dietary (as indicated by stable isotopes, SI) exposures and the spatio-temporal scale reflected in body feathers of Adélie penguins. Example from the Dumont d’Urville colony. The reader is referred to Section 4 for further discussion.

2.2.2. Different ages, different scales

An additional means to investigate different temporal and spatial scales of Hg contamination in marine food webs is to study different age classes from the same seabird species. During egg formation, Hg is transferred from the female to the developing egg (Figure 2.4; Ackerman et al., 2016, 2020), and hence to the developing embryo and chick to hatch (Ackerman and Eagles-Smith, 2009; Heinz et al., 2010). Down feathers of newly hatched chicks, which are grown during the embryonic development, thus reflect Hg contamination of the egg and hence maternal transfer during the period of egg formation (Santos et al., 2017). Later during the chick-rearing period, down feathers are moulted and replaced by body feathers (pre-fledging moult), which reflect their dietary intakes (obtained from their parents) and hence Hg exposure since hatching (Blévin et al., 2013). Since the parents are restricted in their foraging trips for breeding constraints, this contamination reflects a short-term Hg exposure (i.e., several weeks to a few months depending on the species) in the local environment (i.e., in the vicinity of the

breeding colony). Thus, comparing feather Hg concentrations in adult (*i.e.*, year-round exposure) and chick seabirds allow to investigate different oceanic environments and marine food webs.

2.2.3. Feathers as a time-machine

Seabird feathers have been commonly used for Hg biomonitoring over both the short- and the long-term (Albert et al., 2019; Burger and Gochfeld, 2004; Cherel et al., 2018), even over multidecadal and century timescales thanks to museum specimens (*e.g.*, Bond et al., 2015; Thompson et al., 1992; Vo et al., 2011). Seabirds have been collected for exhibitions and museum collections worldwide, as part of scientific expeditions that intensified during the last centuries (*i.e.*, mainly since the 19th century). Feather sampling on these invaluable archives thus allow to investigate temporal trends of Hg contamination in marine ecosystems retrospectively (Bond et al., 2015; Thompson et al., 1992; Vo et al., 2011), which is of particular interest in the current context of global change. Resulting from the expansion of human activities since the 19th century, human-caused changes have led to profound changes in marine ecosystems, including climate change, ocean acidification and desoxygenation, overfishing, biodiversity loss and increasing anthropogenic contamination (IPCC, 2019; UN Environment, 2018). All these environmental and anthropogenic changes have influenced the global Hg cycling and hence Hg contamination in marine ecosystems over time.

In this doctoral work, seabird **feathers** were used as biomonitoring tool to assess **Hg contamination of marine food webs** from three remote oceanic regions (the **Arctic**, the **intertropical region** and the **Antarctic**) **at the global scale**.

Specifically, we used **body feathers** (which provide the most representative sample for estimating whole-bird Hg; Furness et al., 1986) from:

- both **adults** and **chicks** (*i.e.*, **contemporary** period) to compare **year-round** and **short-term contamination during the breeding season**, reflected by adult and chick feathers, respectively.
- adults only, but from **museum specimens** and **free-living seabirds**, for the **retrospective assessment**.

2.3. Feather sampling

In this PhD, 7156 feather samples were collected from adults and chicks of three seabird species (Table 2.1), thanks to a large and international network of collaborations, including 58 partners from 35 institutions (Table A2). In total, this represented 2199 individuals, across five ocean basins, spanning over 189 years (1833–2022).

Opportunistically, feather samples from other species were also analysed during this PhD, including Chinstrap (*Pygoscelis antarcticus*; n=22), Gentoo (*P. papua*; n=30) and Emperor (*Aptenodytes forsteri*; n=28) penguins, as part of the Master 1 internship of Pierre Vivion. Main findings for these species are presented in the Annexes (Table A3, Figures A1 and A2).

Table 2.1. Summary of seabird feather samples included in this doctoral work. The sooty tern (*Onychoprion fuscatus*) was used as a bioindicator of tropical marine ecosystems, whereas the Brünnich guillemot (*Uria lomvia*) and the Adélie penguin (*Pygoscelis adeliae*) were used as bioindicators of the Arctic and Southern Oceans, respectively (polar oceans).

Study region	Bioindicator species	Individuals	Sites	Year
Tropical oceans		n=1114	n=28	
Pacific Ocean	Sooty tern	n=358 (204 adults, 154 chicks)	n=9	1887–2022
Atlantic Ocean		n=402 (308 adults, 94 chicks)	n=9	1876–2021
Indian Ocean		n=354 (195 adults, 159 chicks)	n=10	2003–2021
Polar oceans		n=1085	n=64	
Arctic Ocean	Brünnich guillemot	n=547 (481 adults, 66 youngs*)	n=40	1833–2022
Southern Ocean	Adélie penguin	538 (490 adults, 48 chicks)	n=24	2005–2021
Total	All species	n=2199 (1678 adults, 455 chicks, 66 youngs*)		

*Youngs include different age classes: first winter, juvenile, immature and subadult.

3. Laboratory analyses

For simplicity, this section presents the general methodology for laboratory analyses, which was similar for all samples unless stated otherwise, but the reader is referred to the corresponding scientific papers for further analytical details.

3.1. Sample preparation

First, to eliminate any external contamination, feathers were cleaned in the laboratory with a chloroform:methanol mixture (2:1), sonicated for 3 min and rinsed twice in methanol. They were then oven-dried for 48 h at 45°C. For each bird, several feathers (2-4) were pooled to derive the individual mean value (see [Box 3](#) for further details; Carravieri et al., 2014a; Jaeger et al., 2009), then cut with stainless scissors into a homogenous powder to be analysed for both Hg and stable isotopes.

3.2. Mercury analyses

3.2.1. Total mercury analyses

The analysis of THg provides the sum of both inorganic and organic Hg (this latter being mainly MeHg). Since MeHg accounts for >90% of THg in seabird feathers (see Section 2.2 but also Renedo et al. (2017)), THg was used as a proxy of MeHg.

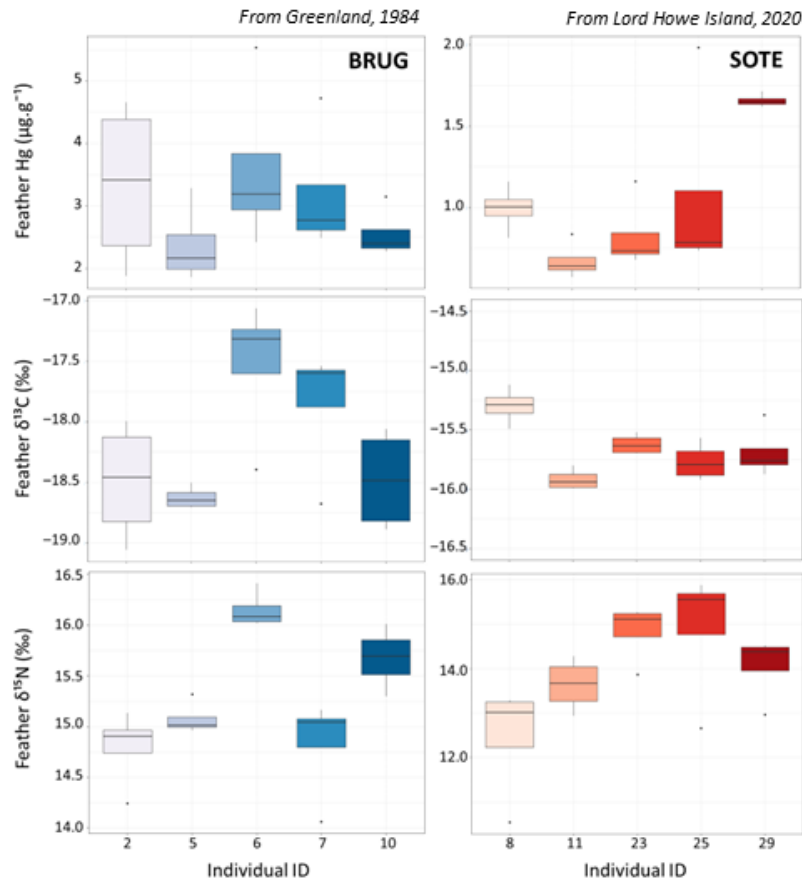
THg analyses were performed on homogenized feathers (0.2-1.5 mg) in duplicate, using two Advanced Mercury Analyzer spectrophotometers (Altec AMA 254). When the relative standard deviation (RSD) between duplicates was < 10%, Hg concentrations were averaged for each sample. When the RSD was > 10%, an additional analysis of homogenate was performed, and the duplicates guaranteeing the lowest RSD were kept for average calculations. Accuracy was verified by running certified reference material (DOLT-5, Dogfish liver; TORT-3, Lobster hepatopancreas; both from the National Research Council, Canada). Certified and measured values, as well as recoveries, are provided in Annexes ([Papers 3](#) and [4](#)). Blanks were run at the beginning of each set of samples. Detection limit of the AMA was 0.05–0.1 ng (depending on the machine used). Mercury concentrations are expressed in $\mu\text{g}\cdot\text{g}^{-1}$ dry weight (dw).

3.2.2. Mercury speciation analyses

Historically, inorganic Hg salts were used by museum curators as preservatives in the preparation of bird specimen, resulting in methodological bias when analysing THg in museum versus free-living specimens (Thompson et al., 1992). This bias was overcome by analysing MeHg specifically (Hogstad et al., 2003).

Box 3**To pool or not to pool ?**

In seabirds, the chemical composition of feathers, including Hg and stable isotopes, varies with moulting patterns. In penguins, which experience a drastic, simultaneous moult, all feathers have similar chemical composition (see Section 2.2.1). In contrast, chemical composition in guillemot and sooty tern feathers, which experience a biannual and continuous moult, respectively (see Section 4), may vary. Therefore, at the early stage of the doctoral work, we investigated intra-individual variation in both feather Hg concentrations and stable isotope values in two species: Brünnich's guillemots (BRUG) and sooty terns (SOTE). For each species, four feathers were analysed individually for five bird individuals.



Considering the intra-individual variability in either feather Hg concentrations or stable isotopes or both, four feathers were pooled for each individual of these two species (all samples of this doctoral work), to derive the mean individual value (Carravieri et al., 2014a; Jaeger et al., 2009).

Mercury speciation analyses were performed at the laboratory IPREM (Pau, France) on the oldest specimens (prior 1950s) to quantify both MeHg and iHg (Renedo et al., 2017, 2018) from feather homogenates (1–12 mg), using an GC-ICP-MS Trace Ultra GC equipped with a Triplus RSH autosampler coupled to an ICP-MS XSeries II (Thermo Scientific, USA; [Table 2.2](#)).

Table 2.2. Summary of Hg speciation analyses performed on feathers of the three bioindicator species: the sooty tern (*Onychoprion fuscatus*), the Brünnich’s guillemot (*Uria lomvia*) and the Adélie penguin (*Pygoscelis adeliae*)

Study region and sites	Bioindicator species	n	Temporal window
Tropical oceans			
Atlantic Ocean			
Ascension Island	Sooty tern	131	1876–1970, 2000
Fernando de Noronha	Sooty tern	5	1884, 1902
Pacific Ocean			
Lord Howe Island	Sooty tern	7	1887, 1913/1914
Polar oceans			
Arctic Ocean			
Greenland	Brünnich’s guillemot	13	1833–1955, 2022
Southern Ocean			
Dumont d’Urville	Adélie penguin	4	1951
Cape Royds	Adélie penguin	10	1912
Signy Island	Adélie penguin	8	1950/1951
Total		178	

Mercury speciation analyses were also performed on a few free-living individuals (n=3 of sooty terns from Ascension Island – 2000; n=5 of Brünnich’s guillemots from Greenland) to determine the precise proportion of MeHg in feathers of both species and hence validate the use of THg as a proxy of MeHg after the 1950s. Certified reference material (NIES-13, human hair) was analysed for validation of feather analyses (keratin-based matrices). Method recovery was checked by comparison of THg values measured with the AMA and the equivalent Σ MeHg + iHg obtained from speciation analyses (see [Papers 3](#) and [4](#) for detailed values). Thus, Hg

concentrations in temporal samples refer to MeHg concentrations before the 1950s and THg concentrations, thereafter.

3.3. Stable isotope analyses

3.3.1. Bulk analyses

Description. Bird trophic ecology is key to understand the mechanisms of Hg contamination and disentangle whether temporal or spatial variations in Hg contamination are linked to changes in environmental Hg contamination and/or dietary shifts (Bond et al., 2015; Carravieri et al., 2016; Choy et al., 2022; Fort et al., 2016; Vo et al., 2011). Historically, seabirds' diet has been determined through the analysis of the stomach contents or from regurgitates (boluses), but these latter only provide a snapshot of recently ingested prey, instead of a time-integrated representation of the assimilated food (Hobson, 1999). Time-integrated trophic ecology can be inferred from stable isotope analyses based on a simple principle: « You are what you eat » (DeNiro and Epstein, 1976). In other words, the chemical composition of an animal's tissues reflects that of its diet in a predictable way (Kelly, 2000). In ecology, two stable isotopes are commonly used to study trophic interactions within marine food webs and hence animal trophic ecology. On the one hand, carbon stable isotopes ($\delta^{13}\text{C}$, $^{13}\text{C}/^{12}\text{C}$) represent a proxy of the feeding habitat (Kelly, 2000). The $\delta^{13}\text{C}$ signatures barely vary within marine food webs, the animal being on average enriched in $\delta^{13}\text{C}$ by around 1 ‰ relative to its diet (DeNiro and Epstein, 1978). Therefore, the animal's $\delta^{13}\text{C}$ signatures provide useful insights into carbon sources at the base of a given food web, which differ depending on marine environments. Classically, $\delta^{13}\text{C}$ signatures allow to distinguish between a benthic/neritic versus a pelagic/oceanic environment (France, 1995). In the Arctic, the distinct $\delta^{13}\text{C}$ signatures of ice algae (i.e., more enriched in ^{13}C ; Fry and Sherr, 1989) and pelagic phytoplankton (Figure 2.7) allow for reconstructing foraging on sympagic (ice-associated) prey and can hence be considered as an ice proxy (Hobson et al., 1995; Søreide et al., 2006). In the Southern Ocean, oceanic waters are characterized by a marked latitudinal gradient in $\delta^{13}\text{C}$ signatures of particulate organic matter (Trull and Armand, 2001), which is reflected in the feathers of seabirds from the Southern Indian Ocean: from Antarctic waters (from -25 to -21.2 ‰) to subantarctic waters (from -21.2 to -18.3 ‰) and subtropical waters (above -18.3 ‰; Carravieri et al., 2014b; Cherel et al., 2013; Cherel and Hobson, 2007; Jaeger et al., 2010b; Quillfeldt et al., 2010).

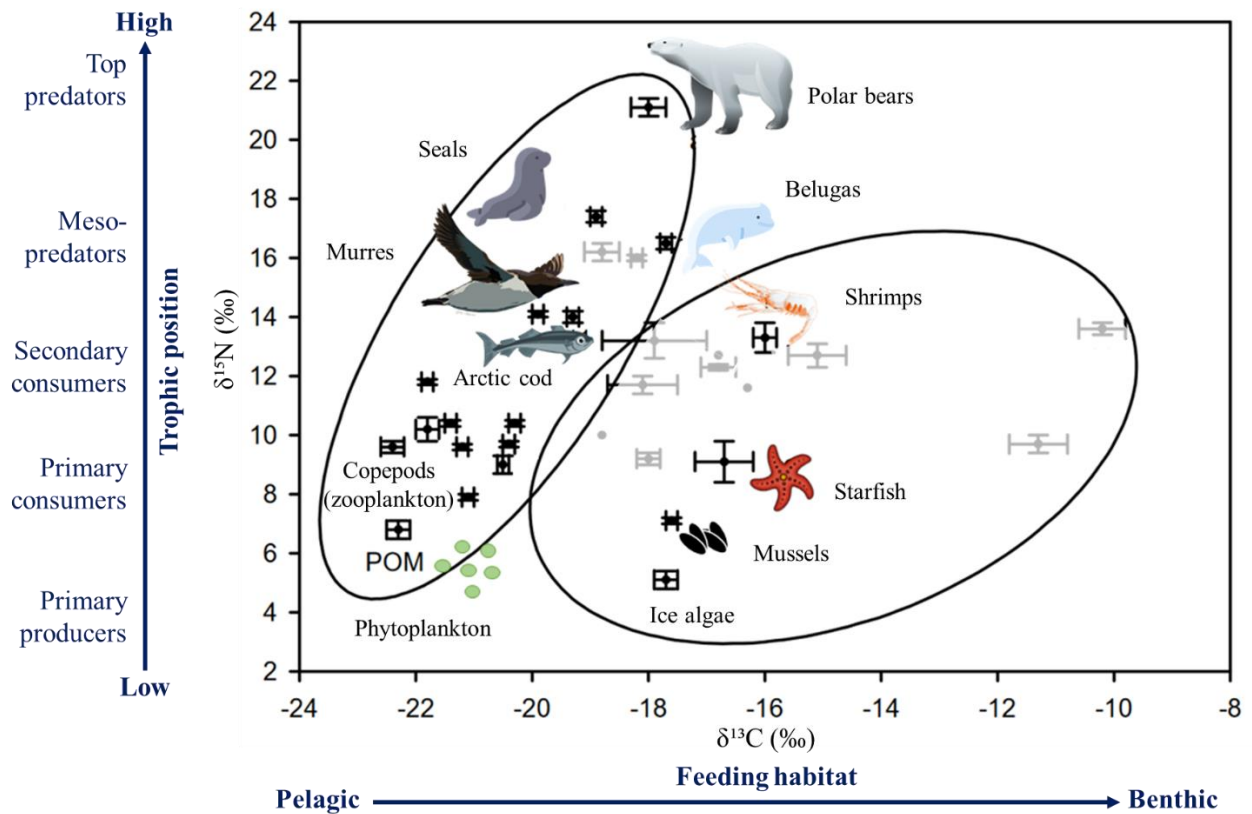


Figure 2.7. Conceptual, simplified representation of the stable isotope method in marine ecology, based on the example of an Arctic marine food web (North Water Polynya, Baffin Bay). Carbon ($\delta^{13}\text{C}$) and nitrogen ($\delta^{15}\text{N}$) stable isotopes (bulk) are proxies of the feeding habitat and trophic position, respectively. This figure was modified from Hobson et al. (2002) and for the complete description of all pelagic and benthic species present, the reader is referred to the original paper.

On the other hand, nitrogen stable isotopes ($\delta^{15}\text{N}$, $^{15}\text{N}/^{14}\text{N}$) represent a proxy of the diet, and hence of the trophic position in marine food webs (Deniro and Epstein, 1981; Hobson et al., 1994). Animals are enriched in ^{15}N relative to their food, because ^{14}N (the light isotope) and ^{15}N (the heavy isotope), respectively, are preferentially excreted, and assimilated by organisms through their diet and incorporated in their tissues. This results in a $\delta^{15}\text{N}$ difference of 3–4 ‰ between each trophic level (Kelly, 2000), with for example $\delta^{15}\text{N}$ values increasing from primary producers (5.1 ‰ and 6.8 ‰ in ice algae and phytoplankton, respectively), to zooplankton (8.3 ‰), fish (14.1 ‰ in Arctic cods), seals (17.0 ‰) up to polar bears (21.1 ‰), at the top of Arctic marine food webs (Figure 2.7; Hobson et al., 2002).

Laboratory analyses. In this doctoral work, carbon and nitrogen stable isotopes (bulk) were analysed in homogenized subsamples of body feathers. Results are expressed in the δ notation

as deviations from standards (Vienna Pee Dee Belemnite for $\delta^{13}\text{C}$ and atmospheric N_2 for $\delta^{15}\text{N}$) following the formula:

$$\delta^{13}\text{C} \text{ or } \delta^{15}\text{N} = (R_{\text{sample}}/R_{\text{standard}} - 1) \times 10^3 \quad (\text{Equation 1})$$

where R is $^{13}\text{C}/^{12}\text{C}$ or $^{15}\text{N}/^{14}\text{N}$, respectively.

Analyses in this thesis were mainly performed at the LIENSs laboratory, but also at the MARE laboratory (University of Coimbra, Portugal) for sooty tern samples (Chapter 4; Paper 4). Feather subsamples (0.2–0.8 mg) were weighed with a microbalance and loaded into tin cups. Values of $\delta^{13}\text{C}$ and $\delta^{15}\text{N}$ were determined with a continuous flow mass spectrometer (Delta V Plus with a ConFlo IV Interface, Thermo Scientific, Bremen, Germany) coupled to an elemental analyzer (Flash 2000 or EA Isolink, Thermo Scientific, Milan, Italy). The analytical precision was $<0.10\text{‰}$ and $<0.15\text{‰}$ for $\delta^{13}\text{C}$ and $\delta^{15}\text{N}$, respectively. Certified materials (USGS-61 and 62) were analysed every 10 samples for QA/QC check.

Since the Industrial Revolution, the combustion of human fossil fuel has increased atmospheric CO_2 , resulting in an accelerating decrease in biosphere $\delta^{13}\text{C}$, mainly influenced by two additive effects: (i) an increase in phytoplankton fractionation (Rau et al., 1992), and (ii) the so-called Suess-Effect (Keeling, 1979), whereby anthropogenic carbon has lower $\delta^{13}\text{C}$ values than natural background carbon. In this thesis work, raw $\delta^{13}\text{C}$ values of historical samples (Chapter 4) were thus corrected accordingly, following calculations from previous work (Eide et al., 2017; Hilton et al., 2006; Jaeger and Cherel, 2011; Körtzinger et al., 2003).

In this doctoral work, **all** feather samples were analysed for **bulk** stable isotopes.

Limitations. Stable isotopes are useful in ecotoxicology, as they provide information on the trophic ecology, which can largely influence exposure to contaminants, including Hg. However, analyses of bulk tissues (*i.e.*, weighed average of all components within a specific tissue; McMahon and Newsome, 2019; described above) involve mixed effects that may complicate the interpretation of the resulting data (McMahon and Newsome, 2019). First, we can mention trophic effects, in relation to changes in diet and trophic position, as well as physiological effects, with respect to variation in metabolic pathway of dietary nutrients to tissue synthesis (Hayes, 2001; Jardine et al., 2006; Ohkouchi et al., 2017). Importantly, we can mention baseline effects, relative to the variation in isotopic composition of primary producers (Jardine et al.,

2006), which are closely tied to variation in isoscapes (*i.e.*, isotopic landscapes). In marine environments, the isotopic composition of elements, including carbon and nitrogen, is influenced by a variety of physical, chemical and biological processes that together produce unique geographic distributions, the so-called «isoscapes» (West et al., 2010). These isoscapes are spatially dynamic, with significant variation within and across ocean systems (both horizontally and vertically; McMahon et al., 2013a, 2013b; Trueman and St John Glew, 2019). For example, baseline $\delta^{13}\text{C}$ values may vary geographically depending on the marine systems (nearshore, benthic and oceanic system; France, 1995), as well as baseline $\delta^{15}\text{N}$ values, which are influenced by the natural nitrogen cycling in the marine environment (including river run-off, atmospheric deposition, N_2 fixation by cyanobacteria, burial in sediments, denitrification; Fry, 1999; McMahon et al., 2013).

On the other hand, marine isoscapes are also temporally dynamic, as they vary along the seasons. For example, changes in baseline $\delta^{13}\text{C}$ can result from seasonal changes in water mass properties and fluctuations in terrestrial run-off, temperature and associated CO_2 concentrations, phytoplankton productivity, as well as changes in the composition of primary producer species and associated growth rate (McMahon et al., 2013). Similarly, changes in baseline $\delta^{15}\text{N}$ may also result from seasonal changes in primary productivity, associated with shifts in nutrient sources and concentrations, microbial nitrogen cycling, as well as phytoplankton species growth rates and composition (Cifuentes et al., 1988; Goering et al., 1990; Ostrom et al., 1997; Vizzini and Mazzola, 2003). In addition, changes in baseline isotope values may be due to anthropogenic influences on nutrients, such as human sewage and agriculture (Anderson and Cabana, 2005; Cabana and Rasmussen, 1996).

Sources of uncertainty are multiple when interpreting isotopic results from bulk tissues, especially in the case of mobile animals such as seabirds, and even more when comparing large spatial scales such as several ocean basins, as is the case in this doctoral work (Chapter 3). A method to reduce the uncertainty and overcome these sources of bias is to perform Compound-Specific Stable Isotope Analyses and particularly on amino-acids (CSIA-AA).

3.3.2. Compound-Specific Stable Isotope Analyses of Amino-Acids

Description. Amino-Acids (AA) constitute the building blocks of proteins and are ubiquitous in living organisms (Sabadel, 2014). In ecology, they have aroused a growing interest, as they

allow to clarify trophic interactions within marine food webs and determine the trophic position of consumers (Chikaraishi et al., 2014), including seabirds (Furtado et al., 2021; Lorrain et al., 2009; Thébault et al., 2021). Whereas stable isotope analyses of bulk tissues average all macromolecules in a sample (including proteins, carbohydrates, lipids and nucleic acids), CSIA-AA takes a molecular approach based on well-established biochemical pathways (focusing on proteins only; McMahon and Newsome, 2019). The power of this approach lies on the differential fractionation of AAs during their transfer in marine food webs (i.e., from diet to consumer), especially in their $\delta^{15}\text{N}$ values (Figure 2.8).

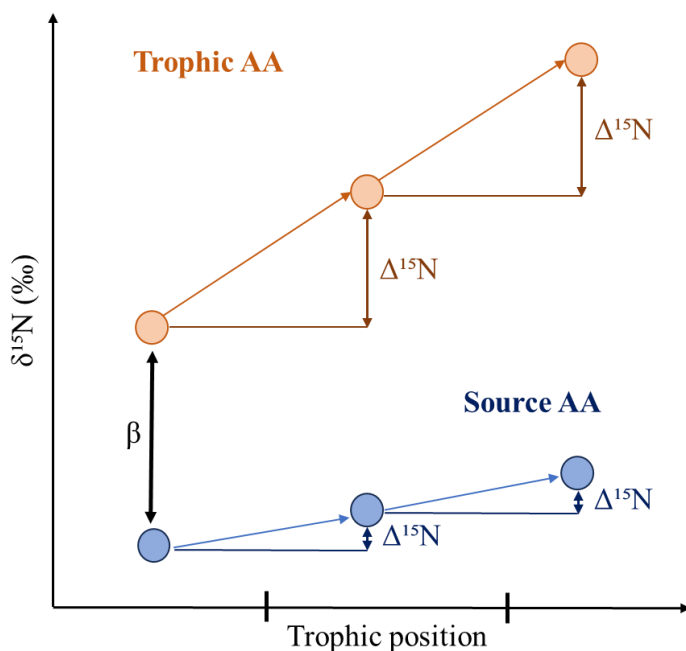


Figure 2.8. Conceptual representation of the differential fractionation of trophic (in orange) and source (in blue) amino acids (AA) with trophic position. β represents the $\delta^{15}\text{N}$ difference between trophic and source AAs in primary producers. Δ represents the ^{15}N enrichment of AAs in a trophic system. Modified from Chikaraishi et al. (2009) and Hoen et al. (2014).

«Source» AAs are AAs that barely enrich for one trophic level to the next (i.e., they do not fractionate), and hence directly reflect the $\delta^{15}\text{N}$ signature of primary producers at the base of the food web (e.g., phenylalanine, Phe; Chikaraishi et al., 2009; Ohkouchi et al., 2017). In contrast, AAs that undergo substantial isotopic enrichment during biochemical processes are called «trophic» AAs (e.g., glutamic acid, Glu; Chikaraishi et al., 2014; Ohkouchi et al., 2017).

Together, $\delta^{15}\text{N}$ values of trophic and source AAs enable to calculate the trophic position of a consumer, accounting for baseline effects (Ohkouchi et al., 2017). Previous studies have used the following equation (Quillfeldt and Masello, 2020; Thébault et al., 2021; adapted from Hoen et al., 2014) :

$$\text{TP (feathers)} = 2 + \frac{\text{Glu} - \text{Phe} - 3.5 \text{ ‰} - 3.4 \text{ ‰}}{6.2 \text{ ‰}} \quad (\text{Equation 2})$$

where:

- Glu and Phe represent $\delta^{15}\text{N}$ values of glutamic acid (trophic AA) and phenylalanine (source AA), respectively;
- 6.2 represents the overall mean Trophic Discrimination Factor (TDF) across wide range of taxa, diet types and modes of nitrogen excretion (McMahon and McCarthy, 2016);
- 3.5 ‰ represents the TDF for seabird feathers (McMahon et al., 2015);
- 3.4 ‰ represents the difference in $\delta^{15}\text{N}$ values between Glu and Phe in primary producers (plankton; Quillfeldt and Masello, 2020).

CSIA-AA have been increasingly used in ecological studies but are still scarce in ecotoxicological ones, with few studies combining this technique with Hg measurements in seabirds. Yet, CSIA-AA are highly relevant to compare trophic positions of seabirds that are distributed across three ocean basins, such as sooty terns. In the intertropical region, environmental conditions and hence isotopic baseline may highly differ from one region to another within a single ocean basin, and between ocean basins. Therefore, baseline effects should be accounted for at such large spatial scale, especially when investigating the role of the trophic ecology on Hg contamination and its spatial variations in marine food webs.

In this doctoral work, CSIA-AA were **only** performed on feathers of **sooty terns** in **Chapter 3**, for a **spatial comparison** of Hg contamination **across ocean basins**.

CSIA measurements are available for **both $\delta^{15}\text{N}$ and $\delta^{13}\text{C}$** , but this work **only** presents **$\delta^{15}\text{N}$** measurements, particularly those of **Glu** and **Phe** that enabled to estimate the **trophic position** of sooty terns.

Laboratory analyses. Complete methodology for laboratory analyses of CSIA-AA is available in the Annexes (i.e., both $\delta^{13}\text{C}$ and $\delta^{15}\text{N}$ values of AAs) and in **Paper 1** (i.e., only $\delta^{15}\text{N}$ of AAs).

Since CSIA-AA is time- and money-consuming, $\delta^{15}\text{N}$ analyses of Phe (*i.e.*, source AA) and Glu (*i.e.*, trophic AA) were performed on a subset of adult individuals ($n=91$), selected across 19 sites in the three ocean basins (see [Table S3](#) in [Paper 1](#)), following previously described protocols (Corr et al., 2007; Styring et al., 2012). Briefly, feather homogenates were hydrolysed to extract AAs, which were purified and derivatized to N-acetyl-iopropyl esters (Styring et al., 2012). Nitrogen analyses were performed using continuous-flow gas chromatography combustion-isotope ratio mass spectrometry (GC-C-IRMS). $\delta^{15}\text{N}$ values were measured using a Thermo Trace Ultra GC coupled to a Delta Plus isotope-ratio mass spectrometer through a GC Isolink combustion interface (Thermo Scientific, Bremen, Germany). Samples were analyzed in duplicate or triplicate. To evaluate drift and accuracy, a standard mixture, thoroughly calibrated by EA-IRMS and derivatized along with the samples, was analysed at the beginning, every three or four samples and at the end of each batch of analyses. Raw data were corrected for instrumental variations and deviations in the isotopic compositions of the products occurring during sample derivatization. AAs values in the standard mixture were used for correction of any instrumental drift during the run (Sabadel et al., 2016) and compound-specific calibration (Yarnes and Herszage, 2017). Precision for AAs values ranged from 0 to 1.5 ‰ (mean 0.3 ‰) for $\delta^{15}\text{N}$ measurements. Finally, AA derivatives were stored at -20°C until analysis (up to one month).

4. Combining feather Hg concentrations and stable isotopes in seabirds

Adults. While Hg and stable isotopes are both incorporated during feather growth, their integration period is temporally decoupled in adult seabirds (Bond, 2010; Thompson et al., 1998). Feathers provide information on bird Hg exposure since the previous moult (integration period: several months to one year depending on species and moulting strategies, but see Cherel et al. (2018) for continuous moulting seabirds such as albatrosses), a temporal period that includes different stages of their life cycle (see Section 2.2). Feathers also retain dietary signatures at the time of their synthesis, as $\delta^{13}\text{C}$ and $\delta^{15}\text{N}$ values are incorporated into feathers as they grow (integration time: few weeks/few months during moult depending on species and moulting strategies; Hobson and Clark, 1992). Nonetheless, stable isotopes provide invaluable information about seabird ecology and are still relevant to understand the ecological drivers of Hg contamination in adult seabirds when no other ecological information is available. A method

to minimize this temporal mismatch in adult feathers is to pool several feathers together (see Section 3.1). This allows to obtain a mean value for Hg concentrations but also for stable isotopes (Carravieri et al., 2014a; Jaeger et al., 2009), that may vary among feathers of the same individual, especially in species that moult their feathers over longer periods of time. Examples of the spatio-temporal scale reflected in body feathers of Brünnich’s guillemots and sooty terns are provided in Figures 2.9 and 2.10, respectively.

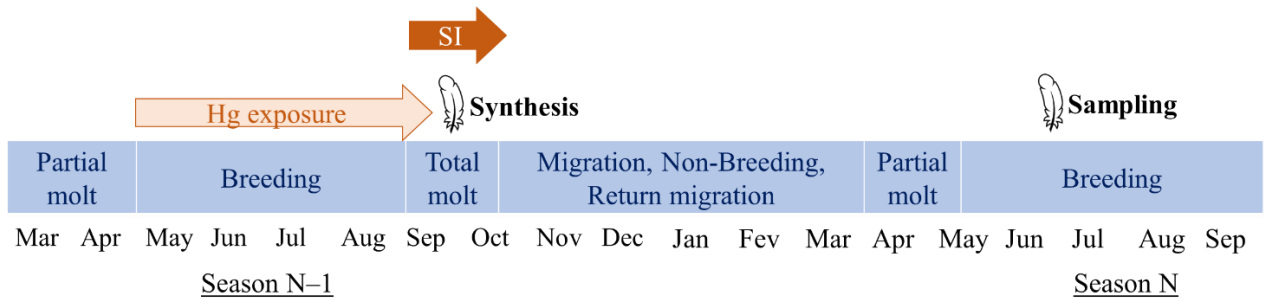


Figure 2.9. Schematic representation of Hg and stable isotope (SI) integration in body feathers of Brünnich’s guillemots, which are replaced during the total moult (post-breeding).

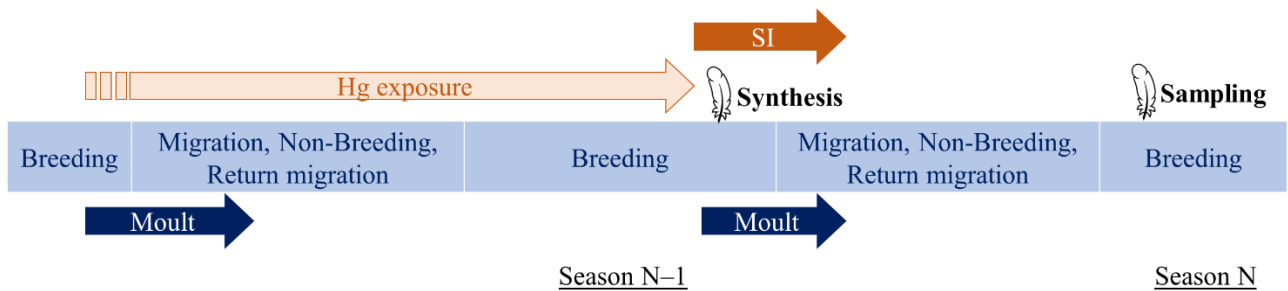


Figure 2.10. Schematic representation of Hg and stable isotope (SI) integration in body feathers of sooty terns. Example for Ascension Island: no date is indicated as sooty terns breed sub-annually at this site.

However, in temporal investigations, combining Hg and stable isotope from feathers is still relevant, considering that we do not associate their respective temporal frames directly (year-round Hg exposure versus trophic ecology during the moulting period). Instead, we associate their respective long-term trends to determine if century-scale changes in Hg exposure have evolved simultaneously to those in trophic ecology.

Chicks. In contrast, the temporal mismatch between Hg concentrations and stable isotopes is minimal in chicks, as the integration time is almost identical between Hg and stable isotopes in

body feathers (Blévin et al., 2013). Large chicks that have not fledged obtain all their food from their parents, which forage in the vicinity of the breeding colony during the chick-rearing period. During the pre-fledging moult (*i.e.*, end of the chick-rearing period), Hg excreted in body feathers corresponds to Hg exposure since initial chick moult (replacement of down by feathers; Stewart et al., 1997). This time-integration period is slightly longer than that of stable isotopes, which correspond to the second part of chick-rearing only (*i.e.*, feather synthesis; Carravieri et al., 2014a). Apart from this fine-scale difference, chick Hg concentrations and stable isotopes reflect, overall, local contamination and diet during the same period (*i.e.*, the chick-rearing period).

All these considerations need to be accounted for when interpreting Hg concentrations and stable isotopes in seabird feathers, on both temporal and spatial scales.

5. Data analyses

Statistical analyses and graphical representations were conducted with R version 4.2.2 (R Core Team, 2022). Briefly, two main types of statistical analyses were conducted in this doctoral work. First, unifactorial analyses were carried out to test for differences in feather Hg concentrations and stable isotopes between sites, oceans or epochs. (*e.g.*, ANOVA, Kruskal-Wallis). Second, multifactorial analyses were performed to investigate the influence of bird's trophic ecology (as indicated by stable isotopes) on either spatial or temporal trends in Hg contamination (*e.g.*, Generalized Linear Models, GLM; Generalized Additive Models, GAM). For each chapter and section, the reader is referred to the corresponding scientific papers for the complete statistical methodology.

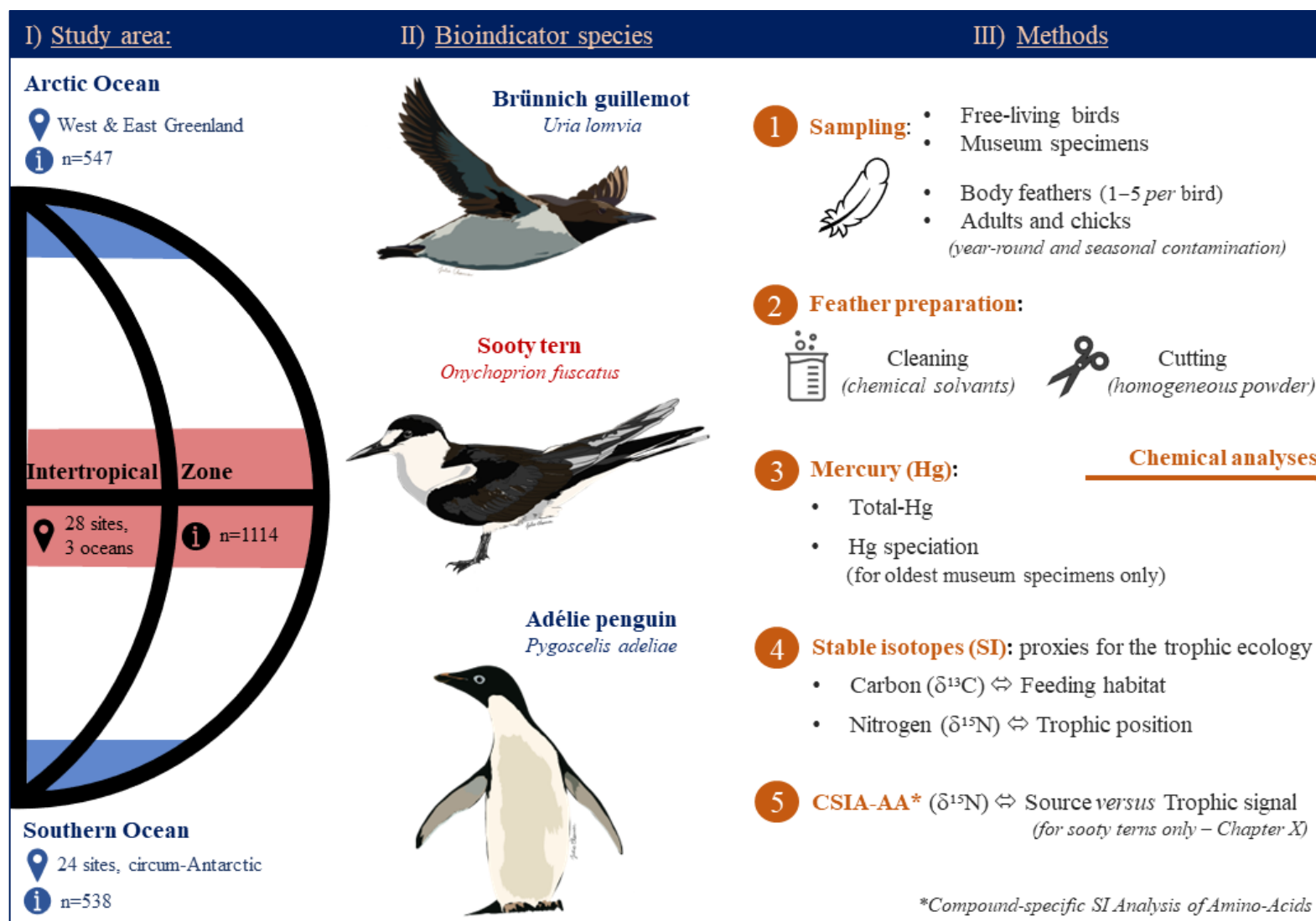


Figure 2.11. Summary of the methodological approach developed in this PhD work, with study areas and their respective bioindicator species, as well as laboratory analyses.

Chapter 3

Spatial monitoring of Hg contamination in tropical and polar marine ecosystems

1. Arctic marine food webs



Prince Leopold Island, Canadian Arctic

1.1. Context

Climate change is a global concern, but its impacts are particularly pronounced in the Arctic, which has experienced profound changes in all ecosystems (*i.e.*, terrestrial, freshwater and marine ; see AMAP, 2021a; McKinney et al., 2022). « Climate change alters how Hg is transported to and within the Arctic, and how it accumulates and cycles through the Arctic environments and living creatures. These changes are complex, inter-related and difficult to predict. » (AMAP, 2021b). Considering the vulnerability of Arctic ecosystems and its inhabitants, this has led to growing scientific efforts over the last decades, to document levels, trends, pathways and effects of Hg contamination in Arctic ecosystems, biota and humans (AMAP, 2021c). This includes national monitoring programs, such as the Canadian Northern Contaminant Program – an integrated initiative for Hg monitoring throughout Canada’s northern territories, which provides Hg measurements in fish, wildlife and traditional foods of Indigenous people (NCP, 2017) – as well as international monitoring programs that provide pan-Arctic assessments of Hg, such as the ARCTOX program.

ARCTOX is a pan-Arctic network that aims to track Hg contamination across Arctic marine food webs, by using seabirds as bioindicators. Initiated in 2014, this network relies on multiple, long-standing collaborations with Canada, Denmark, Estonia, Faroe Islands, France, Iceland, Japan, Norway, Poland, Russia, Scotland and the USA. Since then, 26 seabird species from various families (*i.e.*, Alcidae, Anatidae, Laridae, Procellariidae, Phalacrocoracidae) have been sampled yearly across 72 breeding sites around the Arctic, for feathers and blood. For more information (*e.g.*, species, sites, publications), the reader is referred to the ARCTOX website (www.arctox.cnrs.fr). This scientific network offers a unique playground to explore, in various ways, Hg contamination in marine food webs of rapidly changing Arctic ecosystems. For example, this has led to the thesis of Céline Albert, which was entitled « Exposure of Arctic seabirds to pollutants and the role played by individual migratory movements and non-breeding distribution » (Albert, 2020).

For its long-term monitoring in Arctic ecosystems (Chapter 4), the present doctoral work relied substantially on the ARCTOX database and the PhD thesis of Céline Albert for existing Hg measurements in Brünnich’s guillemots. More specifically, this work complements the existing Hg measurements (2015–2019; n=782) with the analysis of new, more recent samples (2018–2022; n=109), extending the number of sampling years and sites for Brünnich’s guillemots (Table 3.1).

Table 3.1. Body feather Hg concentrations (mean, SD, min, max) measured in adult Brünnich’s guillemots (*Uria lomvia*) sampled as part of the ARCTOX program (2015-2022) across 20 Arctic sites. Mean values for each site (in bold) were used for Figure 3.1. n indicates sample sizes for each site, each year and all years combined.

Ocean, Area, Site	Year	n	Body feather Hg ($\mu\text{g}\cdot\text{g}^{-1}$ dw)			
			Mean	SD	Min	Max
Atlantic Ocean		807	1.37	0.89	0.28	8.52
Bjørnøya	2015–2019	70	0.55	0.13	0.29	1.05
	2015	20	0.56	0.07	0.44	0.68
	2016	20	0.45	0.08	0.29	0.64
	2017	10	0.48	0.10	0.33	0.64
	2019	20	0.67	0.14	0.47	1.05
Franz Josef Land, Cape Flora	2015–2017	61	0.74	0.21	0.35	1.31
	2015	21	0.70	0.20	0.35	1.14
	2016	20	0.77	0.19	0.50	1.31
	2017	20	0.76	0.24	0.40	1.22
Iceland, Grimsey	2016–2017	19	1.50	0.21	1.17	1.91
	2016	8	1.49	0.16	1.21	1.64
	2017	11	1.52	0.24	1.17	1.91
Iceland, Langanes	2015–2017	27	1.35	0.21	0.95	1.77
	2015	14	1.31	0.25	0.95	1.77
	2016	4	1.47	0.20	1.23	1.72
	2017	9	1.36	0.13	1.20	1.56
Jan Mayen	2015–2019	85	1.66	0.31	0.91	2.34
	2015	20	1.54	0.31	1.12	2.34
	2016	25	1.84	0.25	1.46	2.31
	2017	20	1.45	0.25	0.91	2.17
	2019	20	1.74	0.29	1.37	2.31
Newfoundland, Gannet Islands	2015–2017	41	2.39	0.95	1.27	5.90
	2015	17	2.86	1.23	1.65	5.90
	2017	24	2.06	0.47	1.27	3.48
Greenland, Kippaku	2016–2022	86	2.08	0.62	1.10	3.92
	2016	20	1.79	0.44	1.10	3.19
	2018	17	2.36	0.75	1.52	3.92
	2019	19	2.13	0.64	1.33	3.76
	2020	15	2.04	0.54	1.43	3.14
	2022	15	2.12	0.64	1.35	3.54
Greenland, Maniitsoq	2019–2022	37	1.28	0.30	0.74	1.91
	2019	8	1.52	0.19	1.23	1.91
	2020	14	1.25	0.28	0.74	1.69
	2022	15	1.17	0.30	0.78	1.68
Greenland, Qaanaaq/Thule	2015–2022	31	2.99	1.34	1.45	8.52
	2015	17	2.61	0.71	1.45	3.77
	2022	14	3.44	1.76	1.86	8.52

Table 3.1. (following)

Ocean, Area, Site	Year	n	Feather Hg ($\mu\text{g}\cdot\text{g}^{-1}$ dw)				PhD
			Mean	SD	Min	Max	
Norway, Hornøya	2015–2019	66	0.76	0.20	0.37	1.39	-
	2015	20	0.78	0.24	0.37	1.39	CA
	2016	20	0.65	0.15	0.42	0.93	CA
	2017	20	0.80	0.17	0.53	1.17	CA
	2019	6	0.95	0.12	0.86	1.17	CA
Novaya Zemlya, Kara Gate	2015–2019	47	0.69	0.26	0.28	1.71	-
	2015	20	0.71	0.19	0.37	1.22	CA
	2016	20	0.56	0.19	0.28	1.17	CA
	2019	7	1.02	0.32	0.82	1.71	CA
Novaya Zemlya, Oranskie Islands	2016–2017	34	0.70	0.20	0.35	1.32	-
	2016	16	0.64	0.20	0.35	1.21	CA
	2017	18	0.75	0.20	0.51	1.32	CA
Nunavut, Baffin Island	2018	20	3.03	0.46	2.14	4.07	-
Nunavut, Coats Island	2015–2018	50	2.27	0.84	1.20	5.91	-
	2015	20	1.61	0.32	1.20	2.36	CA
	2018	30	2.71	0.79	1.81	5.91	CA
Russia, Cape Gorodetskiy	2015–2019	40	0.82	0.25	0.53	1.39	-
	2015	10	0.75	0.16	0.56	1.09	CA
	2017	19	0.66	0.10	0.53	0.88	CA
	2018	1	1.16	-	1.16	1.16	CA
	2019	10	1.14	0.21	0.80	1.39	CA
Spitsbergen, Alkefjellet	2016–2019	49	0.63	0.19	0.34	1.12	-
	2016	17	0.63	0.22	0.39	1.12	CA
	2017	15	0.62	0.18	0.34	0.89	CA
	2019	17	0.62	0.17	0.44	1.04	CA
Spitsbergen, Isfjorden	2015–2019	44	1.29	0.43	0.60	2.11	-
	2015	13	1.19	0.50	0.60	2.11	CA
	2016	11	1.26	0.29	0.72	1.81	CA
	2017	8	1.02	0.16	0.78	1.26	CA
	2019	12	1.61	0.43	0.77	2.00	CA
Pacific Ocean		84	0.79	0.39	0.32	2.87	
Aleutian Islands, Buldir Island	2018	2	2.36	0.73	1.85	2.87	CA
Pribilofs, Saint George Island	2015–2017	42	0.72	0.24	0.43	1.35	-
	2015	20	0.61	0.19	0.43	1.35	CA
	2016	12	0.77	0.28	0.44	1.24	CA
	2017	10	0.89	0.20	0.64	1.18	CA
Saint Lawrence Island	2016–2017	40	0.77	0.33	0.32	1.92	-
	2016	20	0.59	0.25	0.32	1.45	CA
	2017	20	0.96	0.31	0.42	1.92	CA
Total		891	1.32	0.87	0.28	8.52	

The present work does not include an exhaustive spatial assessment of Hg contamination in Arctic marine food webs, as for other remote oceanic regions (*i.e.*, intertropical region and Southern Ocean), as this was already being covered by the ARCTOX network. Instead, the objective here was to update spatial comparisons of feather Hg concentrations in Brünnich's guillemots and briefly put these new results into the broader context of ARCTOX monitoring. As they will be included in a comprehensive scientific paper on ARCTOX in the near future (combining multiple species, sites and tissues), these results will not be discussed extensively in this section.

1.2. Main findings and discussion

Overall, 891 adult guillemots were sampled across 20 breeding sites, between 2015 and 2022 (Table 3.1). This included 782 and 109 Brünnich's guillemots from the PhD thesis of Céline Albert and the current thesis, respectively.

As a reminder, body feathers in guillemots reflect Hg exposure **during the previous breeding season**, hence **Hg exposure when feeding on Arctic marine food webs** (see Chapter 2, Section 2.2.1).

a) Does Hg contamination during the breeding season vary across the Arctic?

Results obtained from new samples of Brünnich's guillemot (2018–2022) reinforce the spatial gradient described previously, not only on Brünnich's guillemots but on several species combined (Albert et al., 2021). Here, Hg concentrations were the lowest in Europe and increased westwards, with the highest concentrations observed in the Canadian Arctic and West Greenland (Figure 3.2). A similar East-to-West gradient was previously reported in ringed seals and polar bears (Brown et al., 2016; Dietz et al., 2022, 2000; Riget et al., 2005; Routti et al., 2011). Most of these studies revealed that the Canadian Arctic Archipelago and northwestern Greenland are hotspots for Hg exposure in biota. These two regions were also identified as hotspots of seawater MeHg (Wang et al., 2018). In fact, MeHg concentrations were found to be the highest at shallow depths (150–200 m), just below the productive surface layer (Heimbürger et al., 2015). Elevated MeHg concentrations in marine predators, including Brünnich's

guillemots, could result from enhanced MeHg bioavailability in seawater in these regions and enhanced biological uptake at the base of Arctic marine food webs.

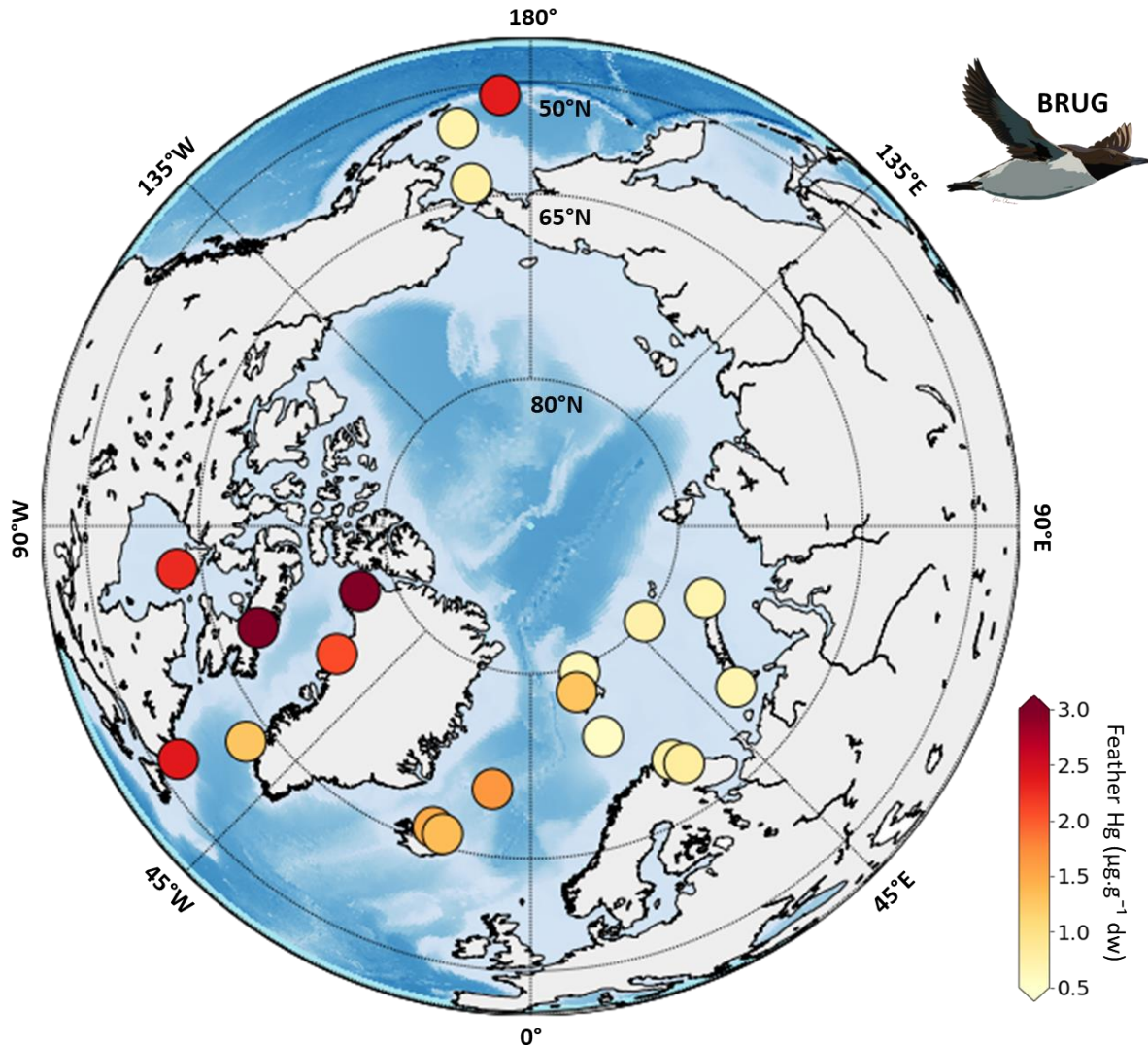


Figure 3.1. Mean Hg concentrations measured in body feathers of adult breeding Brünnich's guillemots (*Uria lomvia*; BRUG) between 2015 and 2022, across 20 breeding sites in the Arctic.

Interestingly, mean Hg concentrations in Brünnich's guillemots decreased from North to South along the western coast of Greenland (Figure 3.2). In Arctic marine ecosystems, the melting of glaciers, particularly in Greenland, represent an important source of Hg (Chételat et al., 2022; Hawkings et al., 2021), potentially enhancing Hg bioaccumulation in fjords and surrounding coastal waters. From an oceanographic point of view, Greenland is mainly surrounded by the Greenland Current (GC), which flows north to south along the eastern coast (*i.e.*, Eastern GC)

and south to north along the western coast (*i.e.*, Western GC), in Davis Strait, and south along the coast of Baffin Island in the Canadian Arctic. Thus, the melting of glaciers may release Hg to ocean waters, which may accumulate Hg with the successive fjord inputs during their transport along the east and west coast of Greenland. This may explain the Hg gradient measured in feathers of Brünnich's guillemots, in West Greenland, but also in the Canadian Arctic where Hg concentrations are also higher. Although the Hg cycle is complex and influenced by both abiotic and biotic interactions (Chételat et al., 2022; McKinney et al., 2022), further research is needed to confirm this hypothesis, for instance by sampling both seawater and biota along the entire coast of Greenland and the Canadian coasts.

Besides, feather Hg concentrations suggest a Hg hotspot in the Pacific Sector, in Buldir Island (Figure 3.2), which is a volcanic island (Coats, 1953). As volcanoes represent a source of natural Hg (Schneider et al., 2023), we could hypothesize that higher Hg concentrations in Brünnich's guillemots could result from local Hg inputs. However, the sample size at this particular site was very low ($n=2$) and prevents us to actually identify this site as potential Hg hotspot. Increasing the sample size at Buldir Island would clearly help to determine if these individual concentrations are anecdotal and if a Hg hotspot truly exists in this region. In both cases, stable isotope analyses would also help to determine if and how these high Hg concentrations are associated with bird feeding ecology.

Most breeding sites were sampled over several years (from 2 to 5 years, but not necessarily consecutively). Inter-annual variation seems to exist in several sites, as St George Island for example, where feather Hg concentrations increased over three consecutive years (Table 3.1). One perspective could thus explore fine-scale temporal variation of Hg contamination in guillemots at the local scale (site or region) and investigate whether these trends differ spatially (for example between the Aleutian Islands, Greenland and Barents Sea). Besides, temporal variation on the longer term (century timescale) of both Hg contamination and trophic ecology of Brünnich's guillemots will be fully addressed in Chapter 4. To date, stable isotope ($\delta^{13}\text{C}$ and $\delta^{15}\text{N}$) analyses are still in progress in the ARCTOX monitoring. Future results should help to investigate the drivers of this temporal and spatial patterns (e.g., trophic ecology, Hg exposure during the non-breeding period, migration, environmental parameters) and determine the role of the feeding habitat and the diet on Hg contamination.

b) Are Brünnich's guillemots at risk in the Arctic?

Recently, an extensive review provided Hg exposure and potential risk assessments for 36 species of Arctic seabirds and shorebirds (Chastel et al., 2022). This review, which included ARCTOX data from 2014 to 2018, showed that Brünnich's guillemots had at least 95% of the sampled individuals at levels associated to no or low risk of toxicity. Our results, which combine existing and new Hg measurements (from 2018 to 2022) are consistent with these previous findings. Across the 20 breeding sites of Brünnich's guillemots, 14 sites (70%) presented mean Hg concentrations associated to « no risk » (Figure 3.1). In contrast, mean Hg concentrations in the six remaining sites (30%) were associated to « low risk » (*i.e.*, in Greenland and the Canadian Arctic; Figure 3.1). However, it is worth noting that, in three North American sites (*i.e.*, in the Canadian Arctic, Greenland and Newfoundland), few individuals (n=5) showed Hg concentrations associated with « moderate risk » (Figure 3.1). Even though feather Hg concentrations indicate no to low potential risks for most of individuals and sites here, adverse Hg effects could arise at different levels, possibly leading to impaired reproductive success and/or long-term demographic consequences (*e.g.*, parental behaviour, endocrine and immune systems, energy expenditure, genotoxicity, neurology; see Chastel et al., 2022 and references therein). Besides, Arctic seabirds, including Brünnich's guillemots, are exposed to multiple stressors, from both natural and anthropogenic origin (*i.e.*, other contaminants, diseases, parasites, environmental changes; Provencher et al., 2016). So, even though risks associated to Hg exposure alone are low to moderate in Brünnich's guillemots, they may be high or severe with the co-occurrence of multiple stressors that may exacerbate adverse effects in Arctic seabirds.

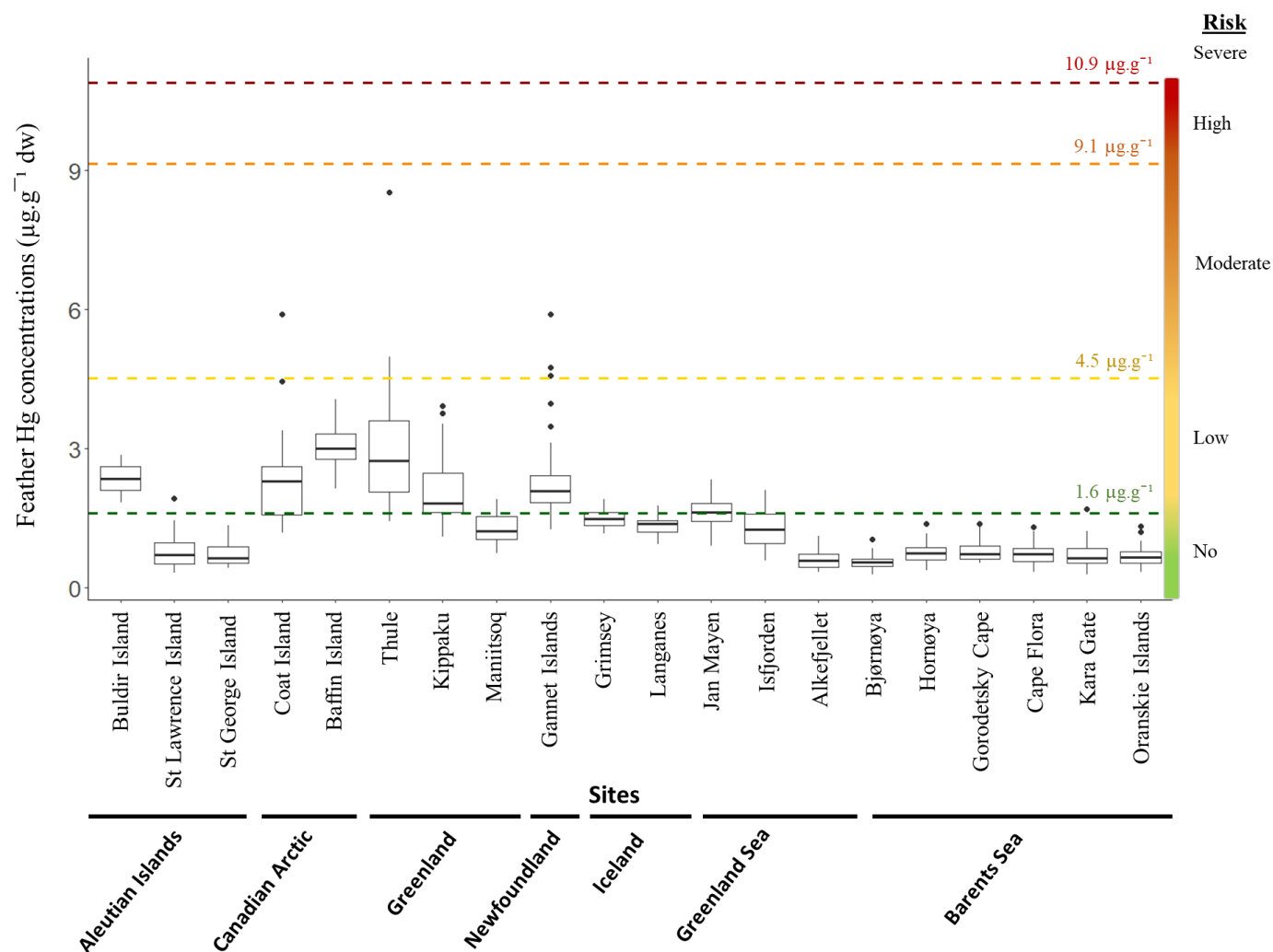


Figure 3.2. Feather Hg concentrations in Brünnich's guillemots (*Uria lomvia*) sampled in 20 sites across the Arctic, as part of the ARCTOX monitoring. The colour gradient indicates the risk gradient associated with threshold Hg concentrations (horizontal dashed lines) established in Chastel et al. (2022) (from low to severe risks in green and red, respectively).

1.3. Conclusion

The present doctoral work builds on the existing database of the ARCTOX monitoring, with the principal aim of investigating long-term Hg contamination in Arctic marine food webs (Chapter 4). Yet, the ARCTOX monitoring provides a pan-Arctic assessment of Hg in Arctic seabirds, including Brünnich's guillemots, the bioindicator species in this chapter. Here, the aim was to take advantage of this tremendous, existing database to briefly investigate spatial patterns of Hg contamination at the pan-Arctic scale. Recent Hg measurements from Greenland corroborated the East-to-West gradient in feather Hg concentrations that was previously documented in Albert et al. (2021) and in the literature. Also, they revealed the existence of a North-to-South gradient along the western coast of Greenland, which would deserve more research in the future, to investigate the role of oceanic currents and melting glaciers in Greenland on the spatial distribution of Hg in marine ecosystems.

The Arctic is particularly vulnerable to climate change and pollution (AMAP, 2021). Since 1991, the Arctic Monitoring Assessment Programme (AMAP) has produced high-quality reports, detailing the status of the Arctic with respect to climate change and pollution issues, including Hg pollution (see www.amap.no for more information). For more than 30 years, these up-to-date reports have built on the growing scientific literature to document the levels and trends, pathways and processes, and effects of Hg on both ecosystems and human populations of the Arctic. The ARCTOX monitoring program represents a valuable contribution to the AMAP, which has been recognized as one of the best examples of regional Hg monitoring system that can help to assess the effectiveness of the Minamata Convention. Pursuing such global initiatives on the long-term is vital to acquire a full understanding of the fate and impacts of Hg in the Arctic, especially in the context of climate change. To this end, interdisciplinary Hg research is now encouraged more than ever, to (i) disentangle the complex interactions between the physical, chemical and biological processes that drives Hg exposure in the Arctic and (ii) determine the cumulative effects of multiple stressors (e.g., contaminants, climate-related environmental changes, diseases) that could represent a major threat for Arctic wildlife and human populations.

1.4. Summary

- The **Brünnich's guillemot** was used as a **pan-Arctic bioindicator** of Arctic marine food webs.
- Feather Hg concentrations confirmed **Hg hotspots in West Greenland, the Canadian Arctic and Newfoundland.**
- **Further research** is needed to identify the **drivers** of these spatial patterns (trophic ecology, Hg biogeochemical cycle, environmental changes).
- These results complement the **ARCTOX monitoring**, which will lead to a comprehensive scientific paper to be published soon.

2. Tropical marine food webs



2.1. Context

Tropical oceans, especially in the Southern Hemisphere, were recently identified as regions where Hg data and scientific understanding are most lacking (Selin et al., 2018; Chen and Evers, 2023 and references therein). Yet, tropical oceans may represent hotspot regions of Hg contamination, as they receive a large fraction of global Hg emissions, mainly from atmospheric deposition, gold-mining, and deforestation of rainforests (see Chapter 1, Section 2.3; Fisher et al., 2023; Schneider et al., 2023). Assessing Hg contamination and its spatial variations in tropical oceans and biota is thus urgently needed to better understand the threat of environmental Hg loads in these key but undocumented oceanic regions.

2.2. Aim and predictions

The present work aims to document spatial variations of Hg contamination in tropical marine ecosystems at the global scale. In the last Global Mercury Assessment (UN Environment, 2018), terns were defined as ecological health bioindicator for tropical marine ecosystems. As the most abundant seabird in the three tropical oceans, we selected the sooty tern (*Onychoprion fuscatus*) as a bioindicator species to:

(1) Quantify current Hg contamination of tropical marine food webs on a pantropical scale.

Specifically, we quantified Hg concentrations in feathers of sooty terns across 28 colonies, distributed in three ocean basins (*i.e.*, the Pacific, Atlantic and Indian Oceans).

(2) Compare long-term (year-round) and short-term (during chick-rearing) Hg contamination, by analysing adult and chick feathers, respectively (see Chapter 2, Section 2.2).

Considering their shorter exposure period, we expected lower Hg concentrations in chicks compared to adults.

- (3) Determine the trophic ecology of sooty terns across ocean basins**, by performing carbon- ($\delta^{13}\text{C}$) and nitrogen ($\delta^{15}\text{N}$) **stable isotope analyses** (*i.e.*, trophic proxies) on both **adult** and **chick feathers** (**bulk** analyses; see Chapter 2, Section 3.3.1).
- (4) Investigate and compare the influence of tern trophic ecology on Hg contamination across ocean basins**, by performing **CSIA-AA** on a subset of **adult** individuals (*i.e.*, only $\delta^{15}\text{N}$ values of phenylalanine (Phe) and glutamic acid (Glx; see Chapter 2, Section 3.3.2).

Considering the large spatial scale, encompassing both latitudinal and longitudinal site distribution, we expected both baseline (from primary producers) and trophic signatures to vary among and across ocean basins, potentially influencing Hg contamination differently.

2.3. Results and discussion

Overall, feathers were collected from 971 sooty terns (564 adults and 407 large fledging chicks) in 28 sites, across the Pacific (n=9), Atlantic (n=9) and Indian (n=10) Oceans ([Figure 3.3](#)).

a) What are the spatial patterns of Hg contamination in tropical marine food webs ?

Overall, feather Hg concentrations measured here in adults ($1.19 \mu\text{g}\cdot\text{g}^{-1}$; all sites combined) were similar to those reported in the literature on sooty terns (see [Table 1](#) in [Paper 1](#)) and on other tropical sternids at similar locations, such as the brown noddy (*Anous stolidus*; $1.11 \mu\text{g}\cdot\text{g}^{-1}$; (Burger et al., 1992, 2001; Burger and Gochfeld, 1995, 2000; Catry et al., 2008; Kojadinovic et al., 2007), bridled tern (*Onychoprion anaethetus*; $1.36 \mu\text{g}\cdot\text{g}^{-1}$; Burger and Gochfeld, 1991; Catry et al., 2008) and roseate tern (*Sterna dougalii*; $1.57 \mu\text{g}\cdot\text{g}^{-1}$; Burger and Gochfeld, 1991; Monticelli et al., 2008). This low Hg contamination agrees with the feeding ecology of sooty terns that largely rely on small epipelagic fish and invertebrates from surface waters (Ashmole, 1963), which have lower Hg concentrations than other mesopelagic and benthic prey species (Chouvelon et al., 2012; Monteiro and Furness, 1997; Ochoa-Acuña et al., 2002).

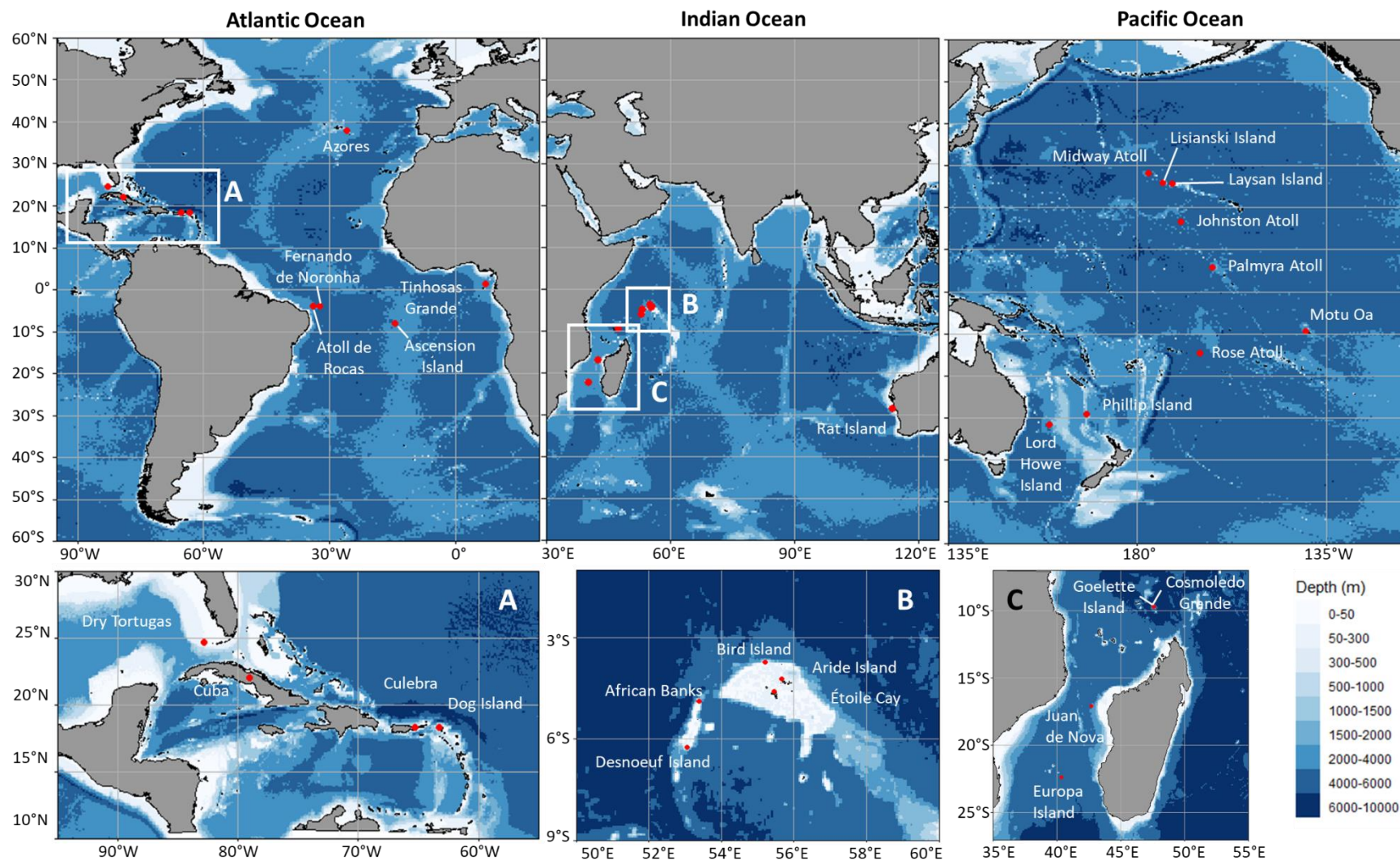


Figure 3.3. Location of feather sampling sites (red dots) of sooty terns (*Onychoprion fuscatus*) in the intertropical region, including the Atlantic Ocean (n=9), Indian Ocean (n=10) and the Pacific Ocean (n=9). Bathymetry is represented by the blue gradient.

In adult sooty terns, Hg archived in feathers includes both local exposure during the breeding season and remote exposure during the non-breeding period, resulting in a year-round exposure to Hg over a large spatial oceanic area. Our pantropical sampling of sooty tern feathers allowed a comprehensive comparison of year-round Hg contamination between colonies, both between and within ocean basins. At the global scale, feather Hg concentrations were higher in the Atlantic Ocean, intermediate in the Indian Ocean and lower in the Pacific Ocean (Figure 3.4).

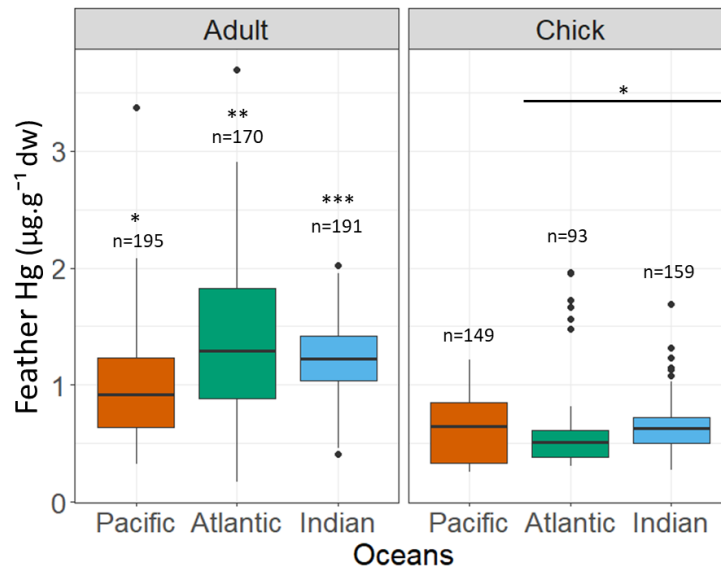


Figure 3.4. Ocean comparison of feather Hg concentrations in adult (left) and chick (right) sooty terns (global subset; only includes sites where $n > 4$). n indicates sample sizes. * indicates when statistical difference was detected (Kruskal-Wallis) and identifies different groups.

However, the Atlantic and Pacific Oceans showed great variability between colonies in terms of feather Hg concentrations (Figure 3.5), particularly when the hemispheres were compared. In both the Pacific and Atlantic Oceans, feathers Hg concentrations were higher in the Northern hemisphere than in the SH (Figure 3.6). This result is consistent with spatial disparities in historical Hg emissions globally. Historically, Hg emissions have been more prevalent in the Northern hemisphere compared to the SH and tropics (Fisher et al., 2023), mainly for two reasons: (1) more historical use of Hg (*i.e.*, 86% of all Hg produced between 1500 and 1900 originated from the Northern hemisphere; Hylander and Meili, 2003), and (2) more historical industrial activities and related consumption of Hg (*i.e.*, 4-fold larger deposition in the Northern Hemisphere than in the Southern Hemisphere; Li et al., 2020).

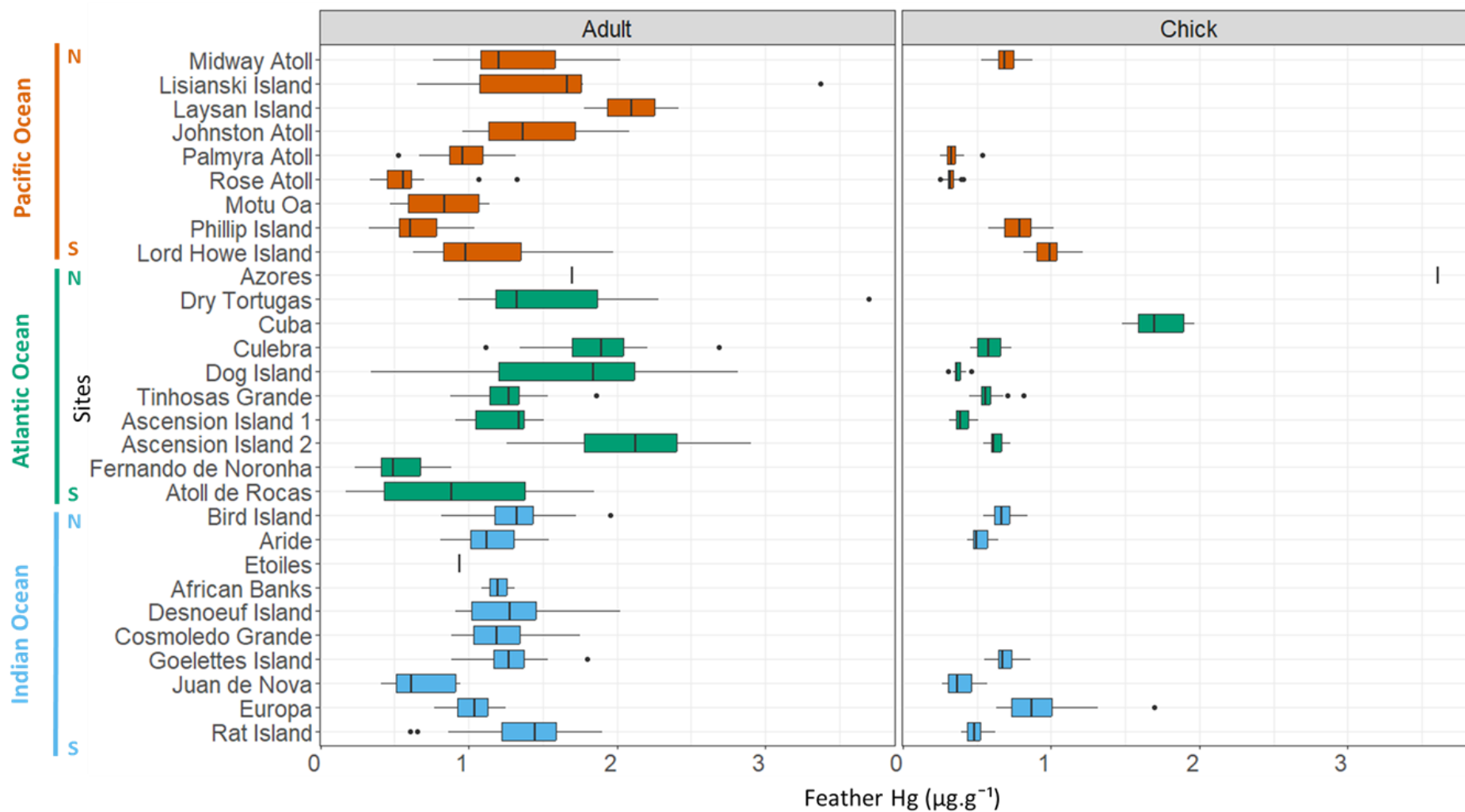


Figure 3.5. Feather Hg concentrations in adults (left) and chicks (right) of sooty terns (*Onychoprion fuscatus*), sampled in 28 sites over three ocean basins. Sample sizes are indicated in [Paper 1 \(Table 1\)](#). Two consecutive years were sampled in Ascension Island: 2020 (Ascension Island 1) and 2021 (Ascension Island 2).

Recent findings in the Pacific Ocean revealed that these hemispheric disparities were also visible in different oceanic compartments, where Hg values were systematically higher in the Northern Hemisphere, including the atmosphere, seawater, sediments and tunas (Médiéu et al., 2022 and references therein), which is consistent with our findings for adult sooty terns. In their study, Médiéu et al. (2022) investigated large-scale Hg contamination in the entire Pacific Ocean thanks to skipjack tuna (*Katsuwonus pelamis*). They revealed an east-to-west gradient in Hg concentrations, with a Hg hotspot near Asia that was attributed to elevated atmospheric and/or river Hg inputs to coastal waters in the region. These large spatial differences were explained by spatial differences in both seawater Hg concentrations at the base of marine food webs and inorganic Hg deposition among distinct oceanic regions. Unfortunately, our results did not allow to confirm this specific spatial gradient, considering the lack of feather sampling in the South-East Asia (e.g., Indonesia, Philippines, Papua New Guinea), where sooty terns are thought to be abundantly distributed (Schreiber et al., 2020). Yet, in the Southern Hemisphere, 15–30% of the total use of Hg in gold-mining occurs in this specific region (Fisher et al., 2023). Therefore, the addition of new colonies in South-East Asia would substantially improve the present spatial Hg assessment and could help to identify anthropogenic Hg hotspots.

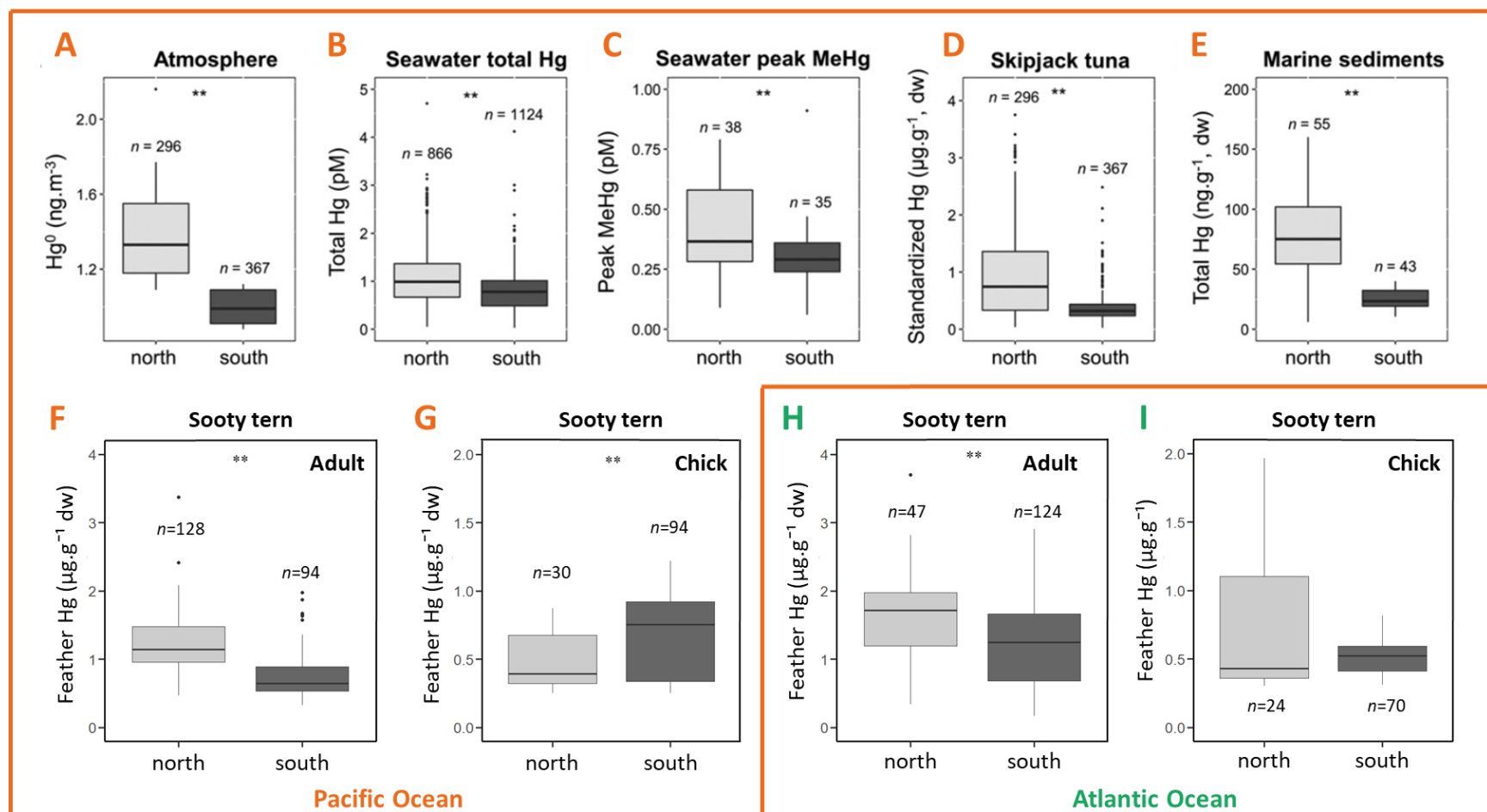


Figure 3.6. Hemispheric Hg gradients in different reservoirs of the Pacific (orange) and Atlantic (green) Oceans, including (A) atmospheric Hg^0 model estimates, (B) observed total Hg concentrations in seawater, (C) observed MeHg concentrations at peak in seawater, (D) standardized total Hg concentrations in skipjack tuna, (E) observed total Hg concentrations in marine sediments and feather concentrations in (F, H) adult and (G, I) chick sooty terns. ** indicates significant differences between the northern and southern hemispheres (Kruskal-Wallis test, $p < 0.001$). Adapted from Médiéu et al. (2022).

In contrast to adults, sooty tern chicks are bioindicators of local Hg contamination during the breeding period (*i.e.*, chick-rearing period). As might be expected from their young age and therefore shorter exposure to Hg, mean Hg concentrations in chick feathers ($0.62 \pm 0.30 \mu\text{g}\cdot\text{g}^{-1}$, $n=402$) were two times lower than in adults ($1.19 \pm 0.51 \mu\text{g}\cdot\text{g}^{-1}$, $n=563$). Overall, chick Hg concentrations were relatively homogenous across ocean basins (Figure 3.7.B). However, two colonies exhibited high Hg concentrations compared to the others: Azores ($3.61 \mu\text{g}\cdot\text{g}^{-1}$) and Cuba ($1.72 \mu\text{g}\cdot\text{g}^{-1}$). The very low sample size in Azores ($n=1$) prevents us to conclude on the contamination level in this region, but clearly, further research is required to investigate a potential, local Hg hotspot or determine if this individual constitutes an outlier. Concerning Cuba, feather Hg concentrations were 2.8 times higher than the chicks' average (*i.e.*, $0.62 \mu\text{g}\cdot\text{g}^{-1}$; all sites combined). Interestingly, feather Hg concentrations seem to be also high in other larids breeding in Cuba, including laughing gulls (*Leucophaeus atricilla*), and bridled, roseate, royal (*Thalasseus maximus*) and sandwich (*T. sandvicensis*) terns (A.G. Quintas, pers.comm.). Clearly, future research in the Caribbean Sea, particularly in Cuba, would help to confirm a Hg hotspot in these tropical waters and to further investigate the influence of anthropogenic releases, from chlor-alkali plants for example, which represent major sources of Hg in this region (Feng et al., 2019).

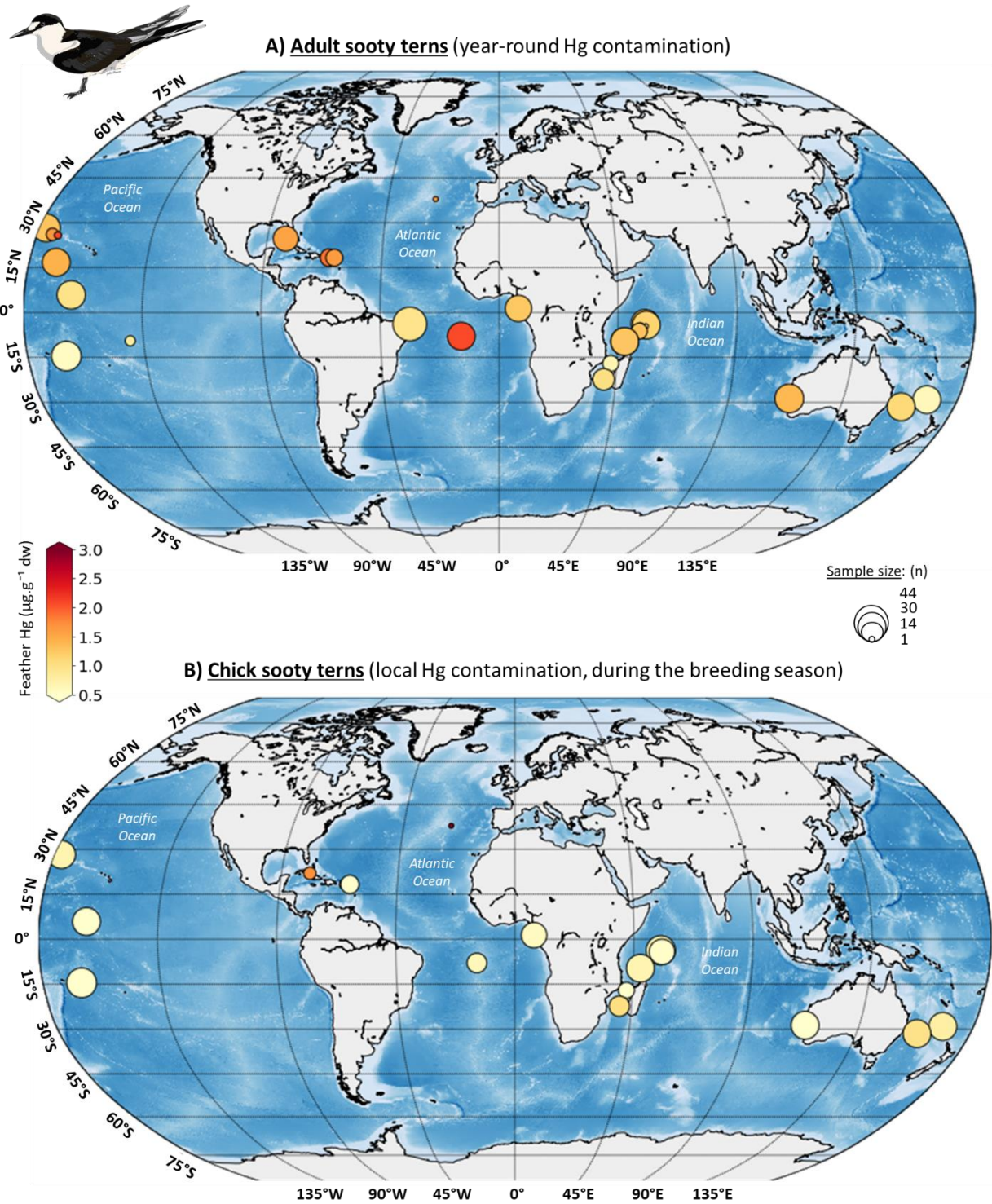


Figure 3.7. Mean feather Hg concentrations of (A) adult and (B) chick sooty terns across tropical oceans (*i.e.*, the Pacific, Atlantic and Indian Oceans), indicated by the colour gradient (from yellow to red for low to high concentrations, respectively). Sample sizes for each site and age class are indicated by the size of the circles (cf. Table 1 in Paper 1 for more details). Adult data for Ascension Island are from 2021.

b) What are the drivers of Hg contamination and its spatial patterns ?

In seabirds, trophic ecology is key to understand the mechanisms of Hg contamination and disentangle whether spatial variation in Hg contamination is related to changes in environmental Hg and/or dietary shifts (Brasso et al., 2015; Carravieri et al., 2016; Gatt et al., 2020). In this study, bulk $\delta^{13}\text{C}$ values (*i.e.*, proxy of feeding habitat) did not show strong variation across the colonies and oceans (Figure 3.8.A), whereas bulk $\delta^{15}\text{N}$ values (*i.e.*, proxy of diet) exhibited high intra- and inter-colony variability, especially in the Pacific Ocean where they ranged from 8.1 to 23.5 ‰ (Figure 3.8.B; see values in Table S3 in Paper 1). Theoretically, this 15.4 ‰ difference in $\delta^{15}\text{N}$ values would mean a variation of four trophic levels (assuming 3.4 ‰ between each trophic level). This large difference clearly indicates strong variation in baseline isotopic values across the Pacific Ocean, and prevents the use of bulk $\delta^{15}\text{N}$ values as a reliable proxy of trophic position (TP) in sooty terns at large spatial scale (Cattry et al., 2008). Therefore, on a subset that only represented 16% of the entire dataset (n=91), we performed CSIA-AA to calculate the TP of adult sooty terns, accounting for both baseline and trophic isotopic variation across sites, as indicated by $\delta^{15}\text{N}$ values of Phe and Glx. Through multifactorial analyses, we then investigated the influence of trophic ecology and colony location on Hg contamination. GLMs were defined with different combinations of three explanatory variables (*i.e.*, bulk $\delta^{13}\text{C}$, TP and colony), as presented in Paper 1 (Table 2), and were then subject to model selection to obtain the best model (*i.e.*, the model that explained the highest proportion of Hg variation). The reader is referred to Paper 1 in the Annexes, for the complete description of statistical methodology.

Results of model selection revealed that feather Hg concentrations were driven by both bulk $\delta^{13}\text{C}$ values and colony location (*i.e.*, 68% of variation explained), and not by TP (Table 2 in Paper 1). The absence of TP in the predictors of feather Hg concentrations is consistent with our single bioindicator approach. It is very likely that sooty terns have a similar trophic ecology across their pantropical distribution range, even though prey species and their corresponding proportions may vary between oceanic regions and oceans. We could expect the opposite result (*i.e.*, presence of TP in the predictors) if several seabird species with distinct trophic ecologies would have been studied. On the other hand, the presence of bulk $\delta^{13}\text{C}$ values in the predictors of feather Hg concentrations suggests that $\delta^{13}\text{C}$ values during the moulting period (*i.e.*, several weeks) influences Hg contamination during the inter-moult period (*i.e.*, several months) of adult sooty terns.

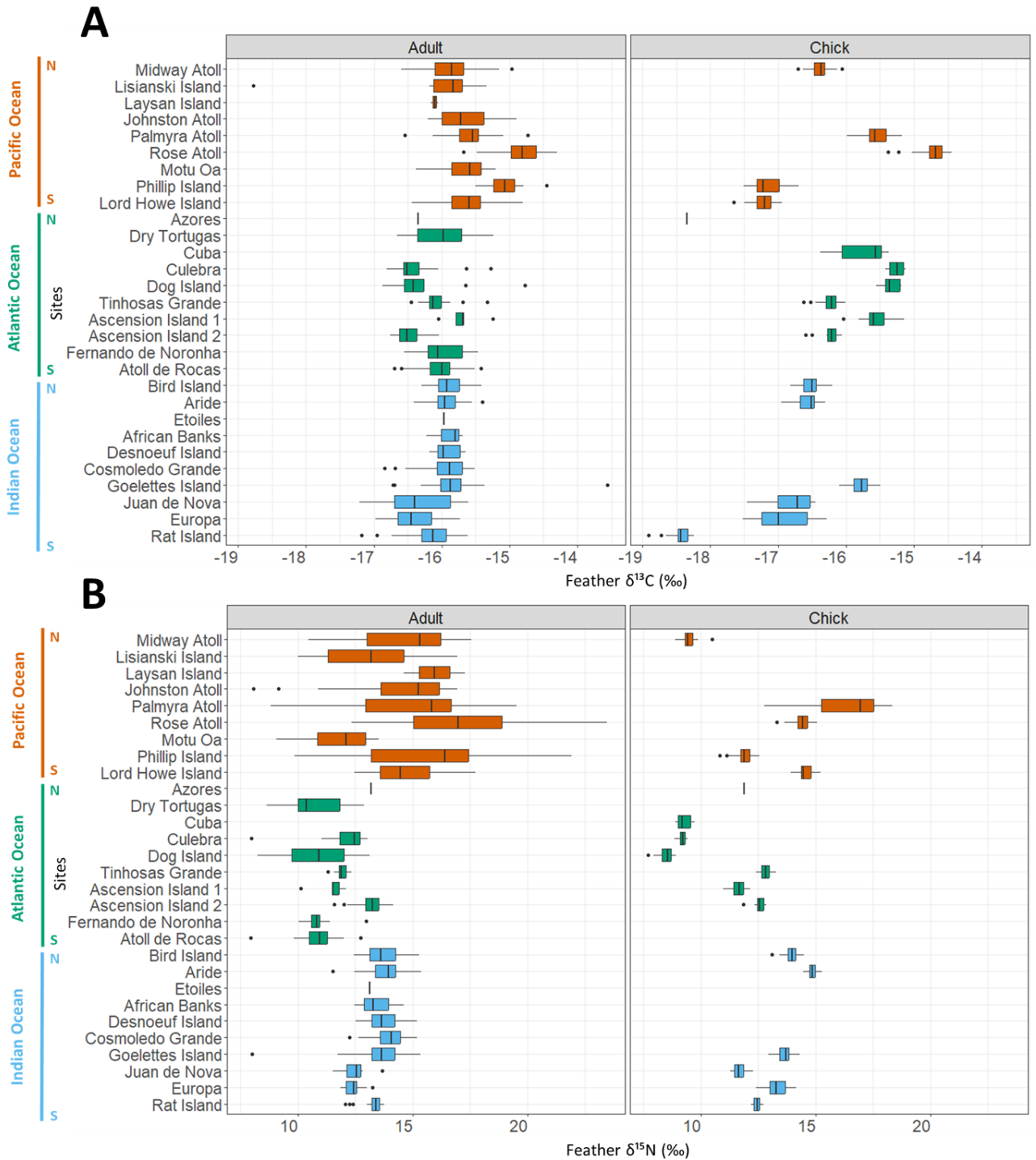


Figure 3.8. Feather (A) $\delta^{13}\text{C}$ and (B) $\delta^{15}\text{N}$ values in adults (left) and chicks (right) of sooty terns (*Onychoprion fuscatus*), sampled in 28 sites over three ocean basins. Sample sizes are indicated in Table 1 (Paper 1). Two consecutive years were sampled in Ascension Island: 2020 (Ascension Island 1) and 2021 (Ascension Island 2).

Unlike the Southern Ocean where the marked latitudinal gradient in $\delta^{13}\text{C}$ values enables to track foraging areas of seabirds during moult (Carravieri et al., 2014b; Cherel and Hobson, 2007;

Quillfeldt et al., 2010), tropical waters usually lack such latitudinal variations, as previously showed in the western Indian Ocean (Catry et al., 2008). Without the ability to track movements of sooty terns within oceanic areas, we cannot associate inshore-offshore patterns of their foraging ecology with potential Hg hotspots and coldspots in tropical oceans.

The other predictor of feather Hg concentrations was colony location, suggesting the role of geographical localization on Hg contamination. Because adult feathers reflect both large spatial and temporal scales, one could argue that colony location may not be the most accurate spatial parameter (*i.e.*, Hg exposure during the inter-moult period mostly occurs away from the colony). However, we assumed that sooty terns would be relatively constrained regionally around their breeding colonies worldwide. Even though they can travel very long distances during the non-breeding period (Jaeger et al., 2017; Reynolds et al., 2021), it is very unlikely for sooty terns breeding on Ascension Island to travel to the Caribbean Sea for example. Besides, defining the ocean basins as spatial parameter instead of the colonies in the models would imply a substantial loss of spatial information and lead to lower statistical power. Biologging approaches, combined to Hg and stable isotope analyses, could thus provide further insights into precise, geographical areas of Hg exposure of sooty terns, and investigate whether they are associated with different types of foraging habitats in tropical oceans.

When accounting for $\delta^{13}\text{C}$ values (that influenced feather Hg concentrations negatively; see [Figure S5 in Paper 1](#)), feather Hg concentrations did not show any specific spatial pattern in the Pacific Ocean, with values slightly varying close to the species average ([Figure 3.9](#)). In the Atlantic Ocean, 71% of the colonies showed higher Hg concentrations than the species average, except for Fernando de Noronha that could represent a Hg coldspot (*i.e.*, low year-round contamination). Yet, Fernando de Noronha is located in the South Atlantic Ocean, approximately 350 km away from Brazil, which represents a major Hg emitter through deforestation of tropical forest and gold-mining (Fisher et al., 2023). A possible explanation for this unexpected result could be the non-breeding distribution of sooty terns, which may forage in remote oceanic regions in the South Atlantic Ocean, instead of the coastal regions of South America.

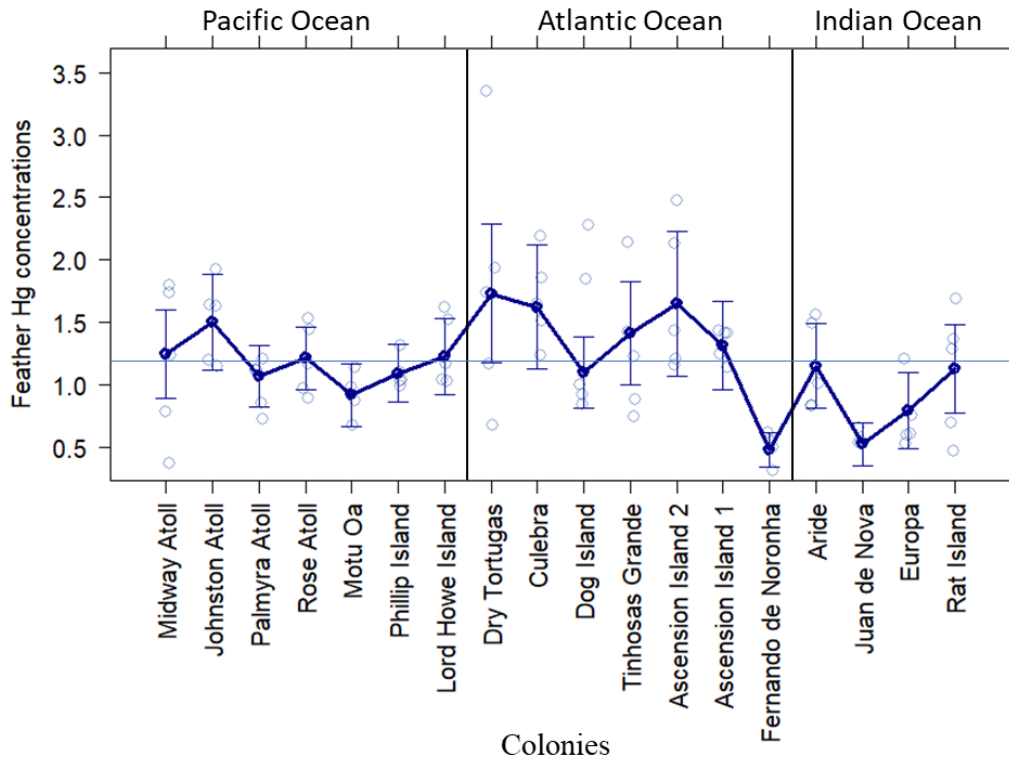


Figure 3.9. Spatial differences in feather Hg concentrations in adult sooty terns (*Onychoprion fuscaus*) from 18 tropical colonies (n=88) when controlled by their feeding ecology (feather bulk $\delta^{13}\text{C}$ values). Relationships result from the extraction of partial residuals of the best Generalized Linear Model (GLM; see Table 2 and Material and Methods in Paper 1 for further details). Individual data are represented in light blue (open circle). Points (filled circle) are means \pm SD. The dark blue line links all mean Hg concentrations. The horizontal line (in blue) represents the species' average (i.e., $1.19 \mu\text{g}\cdot\text{g}^{-1}$). Ascension Island 1 and 2 refer to samples from 2020 and 2021, respectively.

In the Indian Ocean, all colonies showed low Hg contamination, with Juan de Nova and Europa Islands differing from the other colonies. Interestingly, Fernando de Noronha, Juan de Nova and Europa Islands have one feature in common: unlike all other sites that were sampled between 2020 and 2022, these three sites were sampled in 2010 and 2003, respectively, hence more than 10 years ago. It is difficult to determine here whether Hg contamination is lower in these three specific oceanic regions due spatial or temporal variation (i.e., presumed increase in Hg contamination over time) without any additional years of sampling.

c) What about temporal patterns in tropical ecosystems ?

Decadal differences. For sooty terns, Hg temporal data are very limited. Still, we could compare our adult results for the 2020s with previous findings in the 1990s and the 2000s, in five colonies (Figure 3.10; see corresponding references in Paper 1, Table 1).

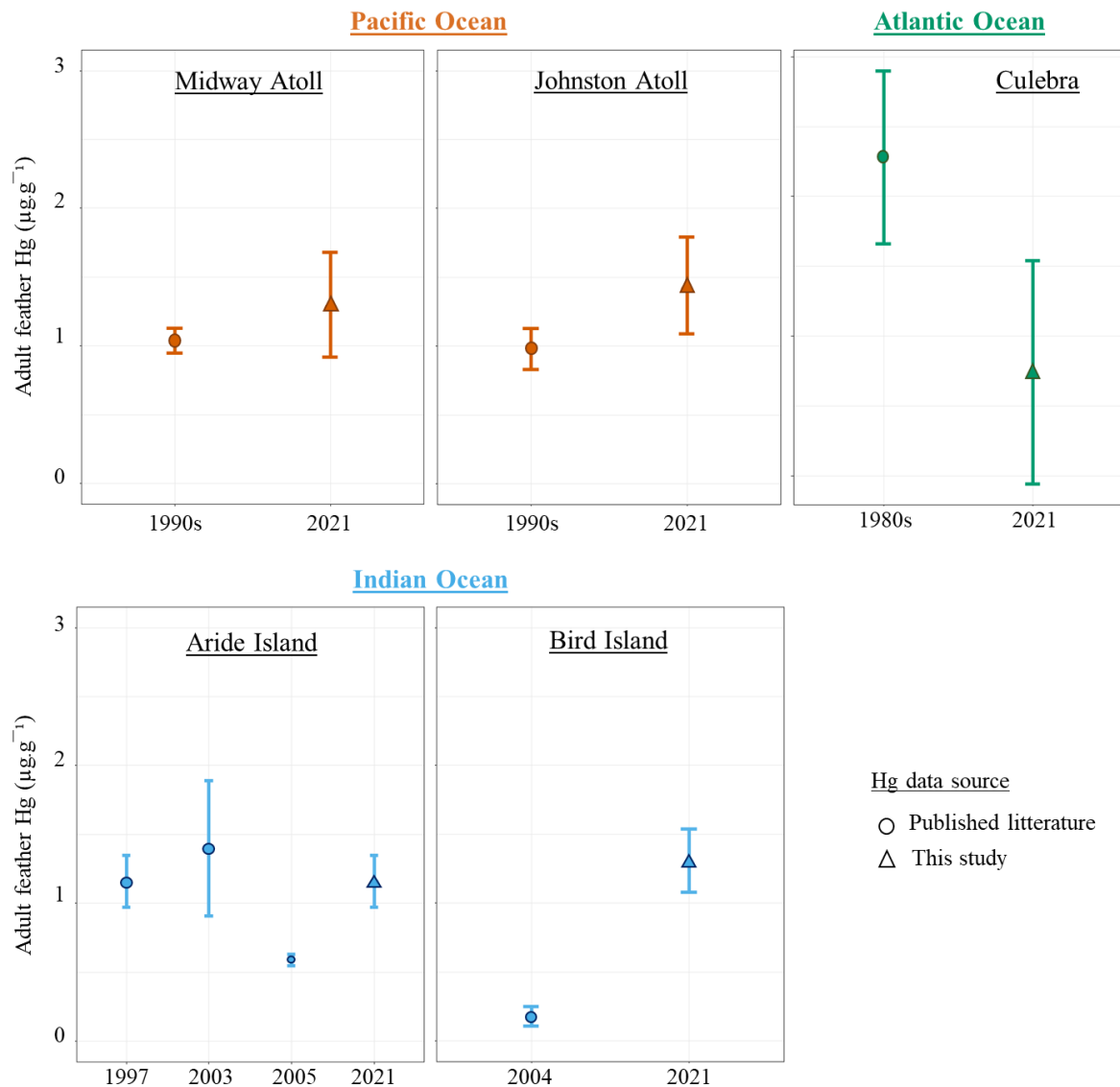


Figure 3.10. Temporal comparisons of feather Hg concentrations in adult sooty terns (*Onychoprion fuscatus*) in five colonies across three ocean basins.

In three colonies (*i.e.*, Midway and Johnston Atolls, and Bird Island), feather Hg concentrations were higher in the 2020s than in the 1990s/2000s (by 25%, 47% and 628%, respectively). This result is consistent with temporal trends of Hg reported worldwide in seabirds (Bond et al.,

2015; Thompson et al., 1992; Vo et al., 2011), including tropical waters where long-term increase in Hg were documented in sooty terns since the 1890s (Cusset et al., 2023). In contrast, in Aride Island, feather Hg concentrations did not show any significant temporal pattern between 1997 and 2021, whereas a 53% decrease appeared in Culebra between 1980s and 2021. Further research could investigate fine-scale temporal patterns of Hg contamination to confirm the observed trends, and determine if these temporal patterns are similar at the global scale.

Interannual differences. In Ascension Island, feathers were collected during two consecutive years for both adults and chicks, allowing to investigate interannual differences in both Hg and stable isotopes (bulk and compound specific). Both feather Hg concentrations and bulk $\delta^{15}\text{N}$ values (from the global subset) were higher in 2021 than in 2020, for both adults and chicks (Figure 3.11.A and C). Consequently, we could hypothesize that the higher Hg concentrations could result from the consumption of higher trophic level prey, and hence from higher TP of sooty terns, both during the inter-moult and chick-rearing periods. However, CSIA-AA (from the CSIA subset) revealed that adult TP remained relatively constant during these two years (Figure 3.11.D). Actually, it is the isotopic baseline that substantially changed between 2020 and 2021, as indicated by the $\delta^{15}\text{N}$ values of phenylalanine (source AA; Figure 3.11.F). Therefore, higher year-round Hg contamination in 2021 did not result from trophic variation of adult sooty terns, but rather from baseline variation, suggesting other environmental drivers of increased Hg bioavailability and transfer and marine food webs of the South Atlantic Ocean. Still, we cannot exclude the possibility that, despite similar TP between years, sooty terns may have consumed different prey in different proportions, resulting in different Hg bioaccumulation between the two years. This could only be verified with Hg and stable isotope analyses of prey species, but obtaining these samples during the non-breeding period of sooty terns without having precise locations precludes any further verification. Clearly, this illustrates the limits of the conventional stable isotope analyses in spatial ecological studies. When considering large spatial scales, we therefore strongly recommend performing CSIA-AA that may help to disentangle the trophic and environmental drivers of Hg contamination in marine food webs.

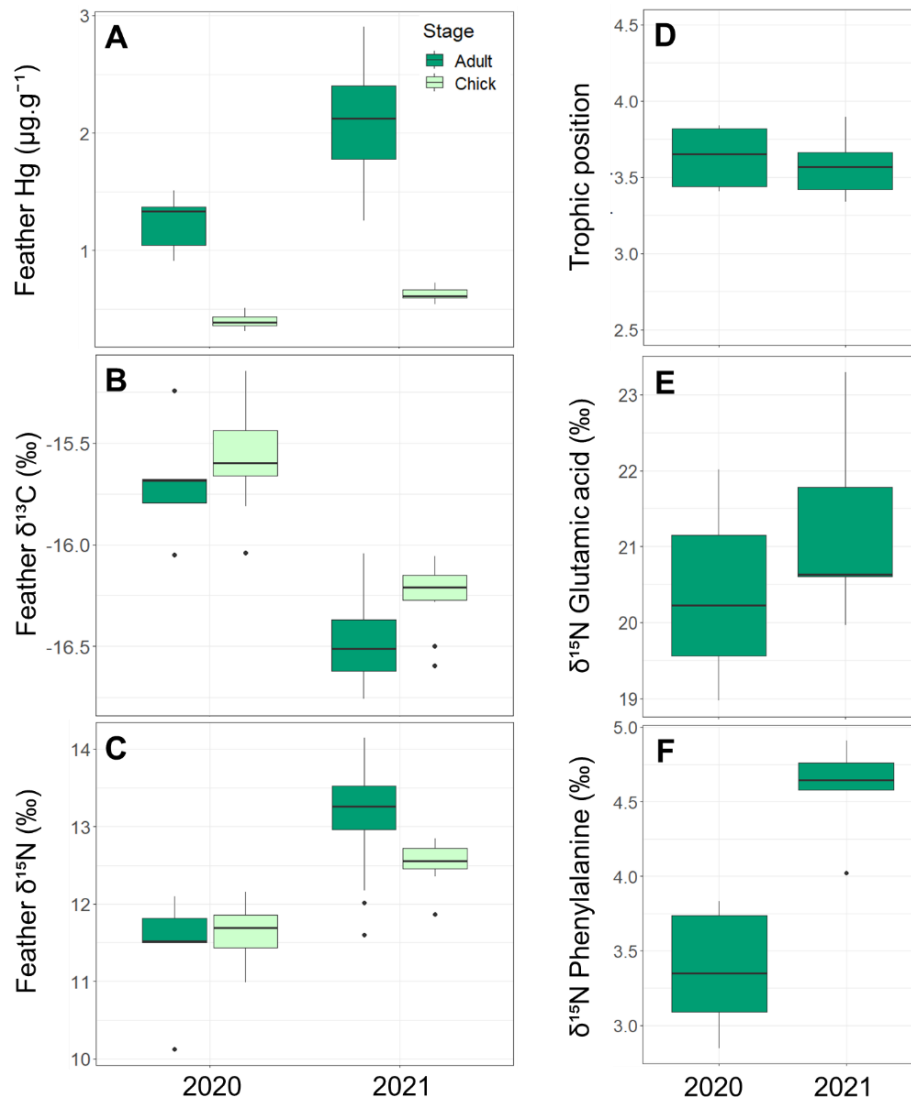


Figure 3.11. Interannual differences in feather (A) Hg concentrations, (B) bulk $\delta^{13}\text{C}$ and (C) $\delta^{15}\text{N}$ values of adults ($n=5$ and $n=30$ in 2020 and 2021, respectively) and chicks ($n=30$ and $n=15$ in 2020 and 2021, respectively) of sooty terns (*Onychoprion fuscatus*), sampled on Ascension Island (South Atlantic Ocean). For a subset of adults ($n=5$ per year), the (D) trophic position (TP) was estimated with the $\delta^{15}\text{N}$ values of (E) glutamic acid (trophic amino acid) and (F) phenylalanine (source amino acid).

2.4. Conclusions and perspectives

Thanks to a large, field-based scientific network, this work provides a unique assessment of Hg contamination in tropical marine food webs, by using the sooty tern as a pantropical bioindicator species. Overall, the low Hg concentrations in adult and chick sooty terns is consistent with their foraging behaviour and diet (*i.e.*, epipelagic prey, including invertebrates and small fish), and are below toxicity threshold recognized for seabird feathers (*i.e.*, $1.62\text{--}10 \mu\text{g.g}^{-1}$; Chastel et al., 2022). This suggests low risks of toxicity for this species, although

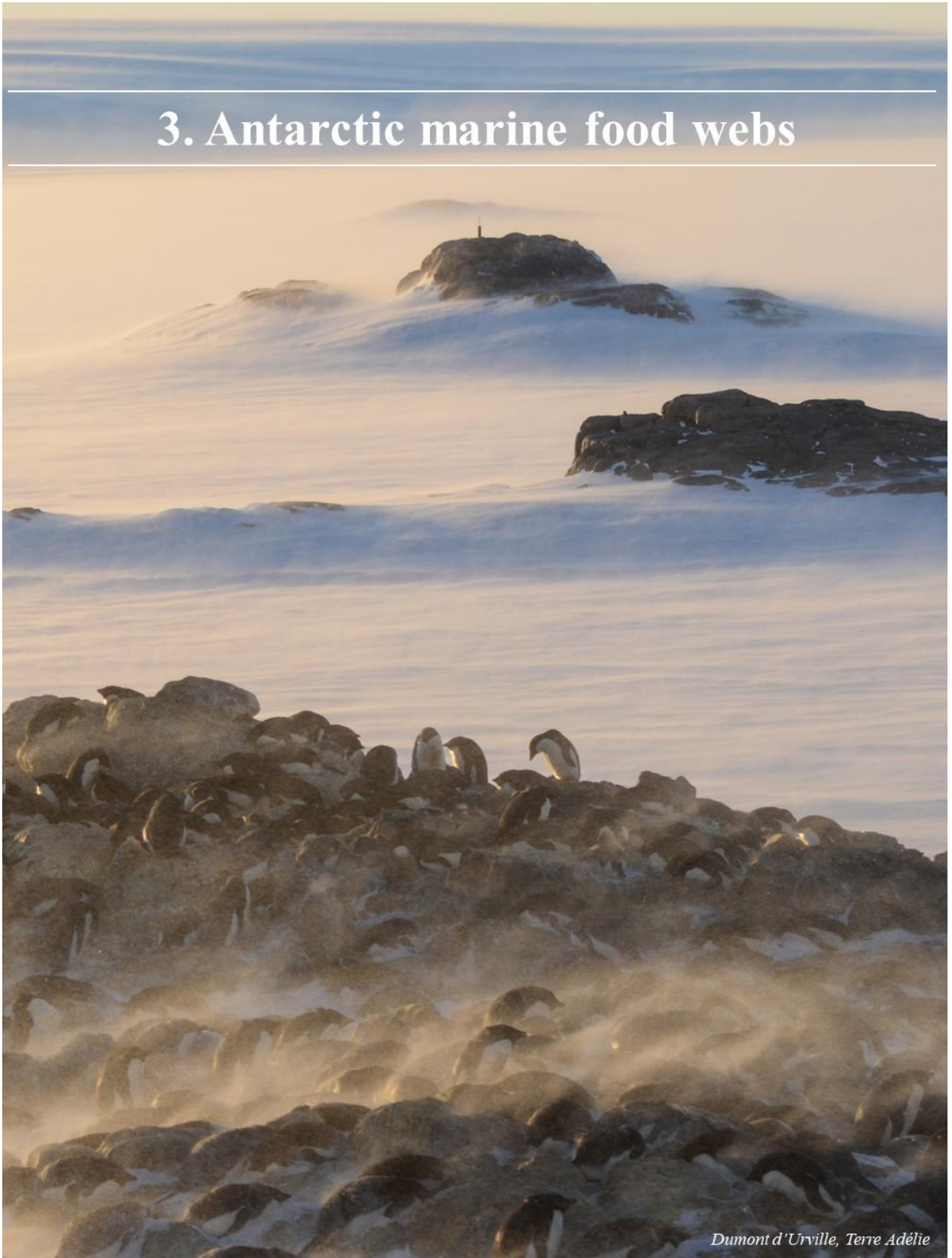
adverse effects may arise at low Hg concentrations. Our results revealed spatial patterns in year-round contamination (as indicated by Hg concentrations in adult feathers) at different spatial scales. At the global scale, the highest Hg concentrations were observed in the Atlantic Ocean, compared to the Pacific and the Indian Ocean. At the hemispheric scale, the highest concentrations were measured in the NH compared to SH. Despite the large number of sampled colonies (n=28), several regions remain undocumented and would clearly deserve further investigations, such as South-East Asia in the Pacific Ocean (*e.g.*, Indonesia, Philippines, Papua New Guinea), as well as the central and eastern Indian Ocean (*e.g.*, Chagos Archipelago). Still, such global assessment represents a valuable asset for international Hg biomonitoring programs (*e.g.*, Global Biotic Mercury Synthesis, Global Mercury Assessment) that aim to protect the environment, wildlife and human populations from the adverse effects of deleterious contaminants, such as Hg.

In seabirds, trophic ecology is key to understand the drivers of Hg contamination (trophic and/or environmental) and investigate its spatial patterns in marine food webs. Despite the temporal mismatch between Hg and stable isotopes in feathers, these latter provide essential knowledge about birds' trophic ecology when no other information is available (during the non-breeding season). Still, caution is necessary when interpreting Hg and stable isotope data together. At the global scale, CSIA-AA represent valuable and essential tools that allow spatial comparison of TP within and between ocean basins and can help to clarify the drivers of Hg contamination. In this study, we used the $\delta^{15}\text{N}$ values of source (Phe) and trophic (Glx) AAs, to determine the trophic position of a subset of adult sooty terns in three ocean basins. TP did not drive feather Hg concentrations, unlike bulk $\delta^{13}\text{C}$ values and colony location, suggesting environmental rather than trophic drivers of Hg contamination in sooty terns. In this work, $\delta^{13}\text{C}$ values of AAs were not explored, mainly because of time constraints, but they are available for future investigations of differences in baseline $\delta^{13}\text{C}$ values and accurate large-scale comparisons.

2.5. Summary

- The **sooty tern** was used as a **pantropical bioindicator species of Hg contamination of tropical marine food webs**.
- Feather Hg concentrations were **higher** in the **Atlantic** than in the Pacific and Indian Oceans.
- Feather Hg concentrations were **higher in the NH than in SH**.
- **Drivers** of feather Hg concentrations were **bulk $\delta^{13}\text{C}$** and **colony location**, and **not TP**, suggesting environmental drivers at the regional scale.

3. Antarctic marine food webs



Dumont d'Urville, Terre Adélie

3.1. Context

Polar oceans are facing significant modifications due to climate change, which alters the biogeochemical cycle of Hg (Chételat et al., 2022; McKinney et al., 2022) and ultimately its transfer in marine food webs (Zhou et al., 2023). In the Arctic Ocean, Hg contamination has been extensively documented over large temporal and spatial scales (e.g., Albert et al., 2021; AMAP, 2021; Bond et al., 2015; Desforges et al., 2022; Dietz et al., 2022). In the Southern Ocean (*sensu lato*, i.e., water masses south of the Subtropical Front; Carter et al., 2008; Orsi et al., 1995), studies are more spatially restricted mainly due to logistical constraints, with a focus on local and/or regional scales (but see Brasso et al., 2015; Carravieri et al., 2017; Cherel et al., 2018), especially in the Antarctic Zone (i.e., water masses south of the Polar Front; Carter et al., 2008; Orsi et al., 1995). This critical gap in sampling areas can be filled by using penguins as bioindicators, since they closely rely on marine food webs from these specific areas (e.g., Burger and Gochfeld, 2004; Carravieri et al., 2013).

Penguins constitute the largest seabird biomass in the Southern Ocean and consume several million tons of marine resources annually (Knox, 2006; Southwell et al., 2017; Williams, 1995). They exploit similar marine resources over both the short-term (breeding season) and the long-term (non-breeding season; Cherel et al., 2007; Polito et al., 2016; Tierney et al., 2009). Therefore, penguins are adequate bioindicator species to monitor Hg contamination in Antarctic marine food webs (Brasso et al., 2015; Carravieri et al., 2013). Besides, they present a unique moulting pattern that leads to homogeneous chemical composition in their plumage (Brasso et al., 2013; Carravieri et al., 2014a), making penguin feathers valuable biomonitoring tools (see Chapter 2). Since the 1980s, 20 studies documented Hg contamination in feathers of eight penguin species from the Southern Ocean, including both breeding in the Subantarctic (i.e., water masses between the Subtropical and Polar Fronts) and Antarctic Zones (see [Table S1](#) in [Paper 2](#) for a complete review). Whereas contamination from subantarctic islands has been well documented, spatial coverage is limited to local and regional investigations in the Antarctic. For example, out of the 14 studies in the Antarctic Zone, nine (64%) were carried out in the South Shetland Islands only. Other documented regions include the coasts of the Queen Maud Land, Adélie Land and Victoria Land (Ross Sea). To date, most Antarctic regions where penguins breed remain unexplored. Large-scale sampling of penguin feathers is thus crucial to identify potential hotspots of Hg contamination and toxicological risk to Antarctic marine biodiversity, simultaneously threatened by other anthropogenic stressors including climate change (Barbraud et al., 2012; Clucas et al., 2014; Lee et al., 2017; Morley et al., 2019).

3.2. Aims and predictions

Here, we take advantage of a large, international field-based scientific network, to evaluate the extent of year-round, circumpolar Hg contamination in Antarctic marine ecosystems, using feathers of Adélie penguins breeding across Antarctic regions. The aims of this study were three-fold:

(1) Quantify current Hg contamination of Antarctic marine food webs by focussing on this key higher-order indicator species **on a circumpolar scale**.

Given the unique oceanographic features of the Southern Ocean (*i.e.*, circumpolar circulation), relatively homogenous Hg concentrations were expected across all Adélie penguin colonies.

(2) Assess Hg contamination over different spatial and temporal scales by using **feathers** of **fledging-chick**, which reflect short-term, local contamination (~two months during the breeding season only), and **adults**, which integrate a geographically larger scale over one year, incorporating both the breeding and non-breeding seasons (see Chapter 2, Section 2.2).

Because of longer exposure to Hg, adults were expected to show higher Hg concentrations than chicks (Stewart et al., 1997; Thompson et al., 1991).

(3) Investigate the influence of penguin trophic ecology on spatial patterns of Hg contamination, by using feather carbon- ($\delta^{13}\text{C}$) and nitrogen ($\delta^{15}\text{N}$) stable isotopes, which are well-known proxies of feeding habitat and trophic position, respectively (see Chapter 2, Section 3.3).

As for other species and regions, trophic ecology was expected to be a major driver of spatial differences of Hg contamination in Antarctic marine ecosystems (*e.g.*, Becker et al., 2002; Bustamante et al., 2016; Carravieri et al., 2014c; Mills et al., 2020).

3.3. Results and discussion

The Southern Ocean hosts some of the most extreme and least accessible environments on Earth. As such, it has commonly been considered to be a pristine ocean, free from substantial anthropogenic contamination. Nevertheless, latitudinal gradients in contaminants, such as Hg, were previously described in the Southern Ocean (Carravieri et al., 2014b; Renedo et al., 2020b), with lower Hg concentrations in Antarctic compared to subantarctic and subtropical seabirds. Whether this Hg gradient is locally restricted or widespread in the Southern Ocean is still unknown. Here, we studied the Adélie penguin as a circumpolar bioindicator species to investigate ocean-wide patterns in Hg contamination across Antarctic marine ecosystems.

a) Circumpolar assessment of Hg contamination in Adélie penguins

The present comprehensive assessment brought together published and new Hg concentrations for Adélie penguin feathers. Overall, 538 individuals of Adélie penguins (490 adults and 48 pre-fledging chicks) were sampled between 2005 and 2021, in 24 breeding colonies around Antarctica (Figure 3.12). Geographical coordinates of sampling sites are provided in Paper 2 (Table S2). Feather Hg concentrations and stable isotope values (mean \pm SD, min–max) for both adult and chick Adélie penguins are provided in Paper 2 (Tables 1 and 2).

Overall, feather Hg concentrations found in this work were similar to those reported by previous studies on Adélie penguins (Paper 2, Table 1). In the Antarctic Zone, Adélie penguins exhibited lower Hg concentrations ($0.45 \mu\text{g}\cdot\text{g}^{-1}$) compared to chinstrap (*Pygoscelis antarcticus*; $0.71 \mu\text{g}\cdot\text{g}^{-1}$), gentoo (*P. papua*; $1.34 \mu\text{g}\cdot\text{g}^{-1}$) and emperor (*Aptenodytes forsteri*) penguins ($1.37 \mu\text{g}\cdot\text{g}^{-1}$) on average (Figure 3.13; Paper 2, Table S1).

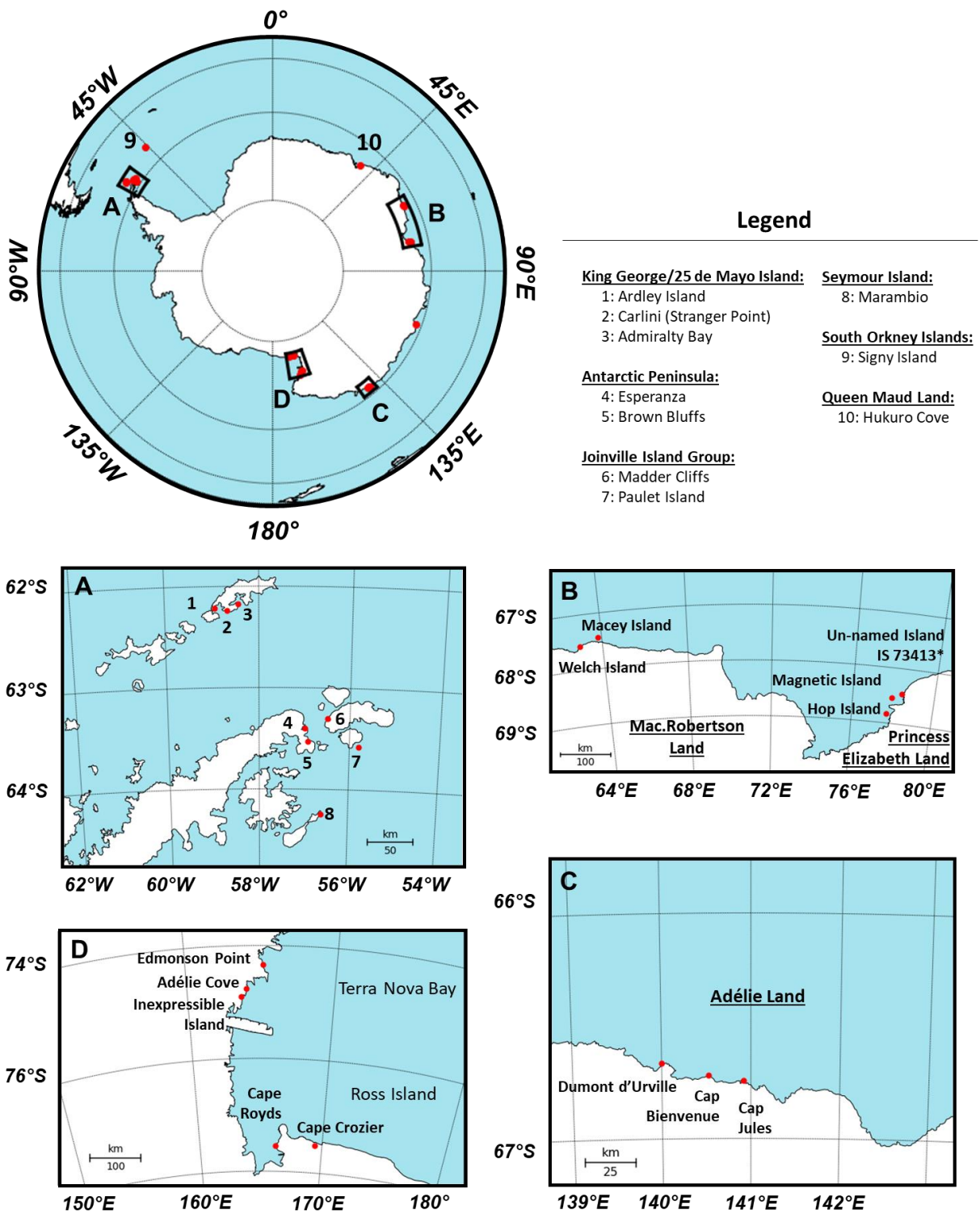


Figure 3.12. Sampling colonies of the present study (n=24), where feathers of Adélie penguins (*Pygoscelis adeliae*; both adult and chick) were collected during the breeding season, between 2005 and 2021 (see [Tables 1 and 2](#) in [Paper 2](#) for further details).

This was also the case when comparing with other penguin species elsewhere in the Southern Ocean (Figure 3.13; Paper 2, Table S1), such as southern rockhopper (*Eudyptes chrysocome*; $2.03 \mu\text{g}\cdot\text{g}^{-1}$), king (*A. patagonicus*; $2.19 \mu\text{g}\cdot\text{g}^{-1}$) and macaroni (*E. chrysolophus*; $2.73 \mu\text{g}\cdot\text{g}^{-1}$) penguins; and with other flying seabirds from the Southern Ocean, including storm petrels ($5.47 \mu\text{g}\cdot\text{g}^{-1}$; Pacyna et al., 2019) or albatrosses ($22.14 \mu\text{g}\cdot\text{g}^{-1}$; Bustamante et al., 2016). Our results highlight an overall low contamination in Adélie penguins, in agreement with the latitudinal gradient in Hg contamination described previously in the Southern Ocean (Carravieri et al., 2014b; Renedo et al., 2020b).

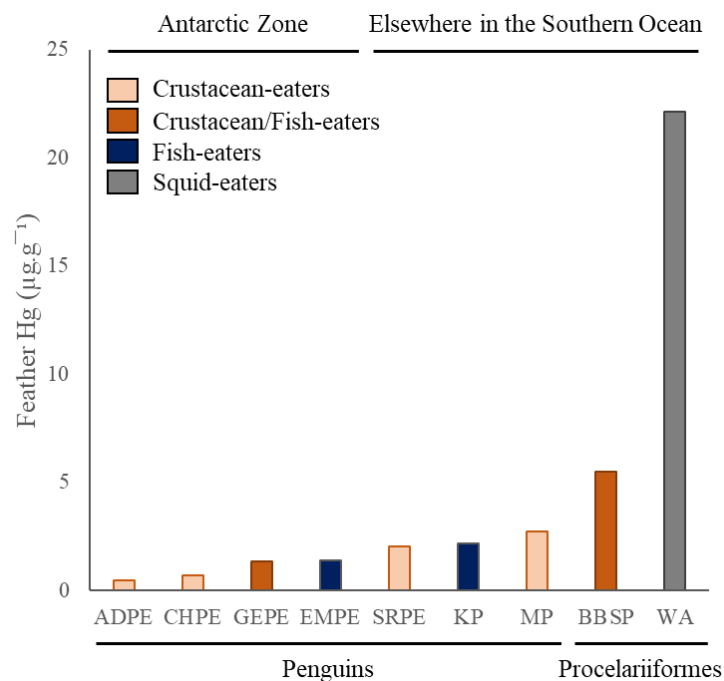


Figure 3.13. Comparison of mean feather Hg concentrations in Adélie penguins (ADPE; this work), with other seabird species (i.e., penguins and Procelariiformes) in the Antarctic Zone and elsewhere in the Southern Ocean, including the chintrap (CHPE), gentoo (GEPE), emperor (EMPE), southern rockhopper (SRPE), king (KP) and macaroni (MP) penguins, black-bellied storm-petrels (BBSP) and wandering albatross (WA). Colours refer to their diet, distinguishing between crustaceans-, crustaceans/fish-, fish- and squid-eaters.

At the circumpolar scale, our results revealed spatial variation in feather Hg concentrations of both age classes (Figure 3.14). In adults, Hg concentrations were the lowest in West Antarctica (i.e., King George/25 de Mayo, Seymour and Joinville Islands, and the Antarctic Peninsula), intermediate in East Antarctica, and the highest in the Ross Sea (Figure 3.14.A).

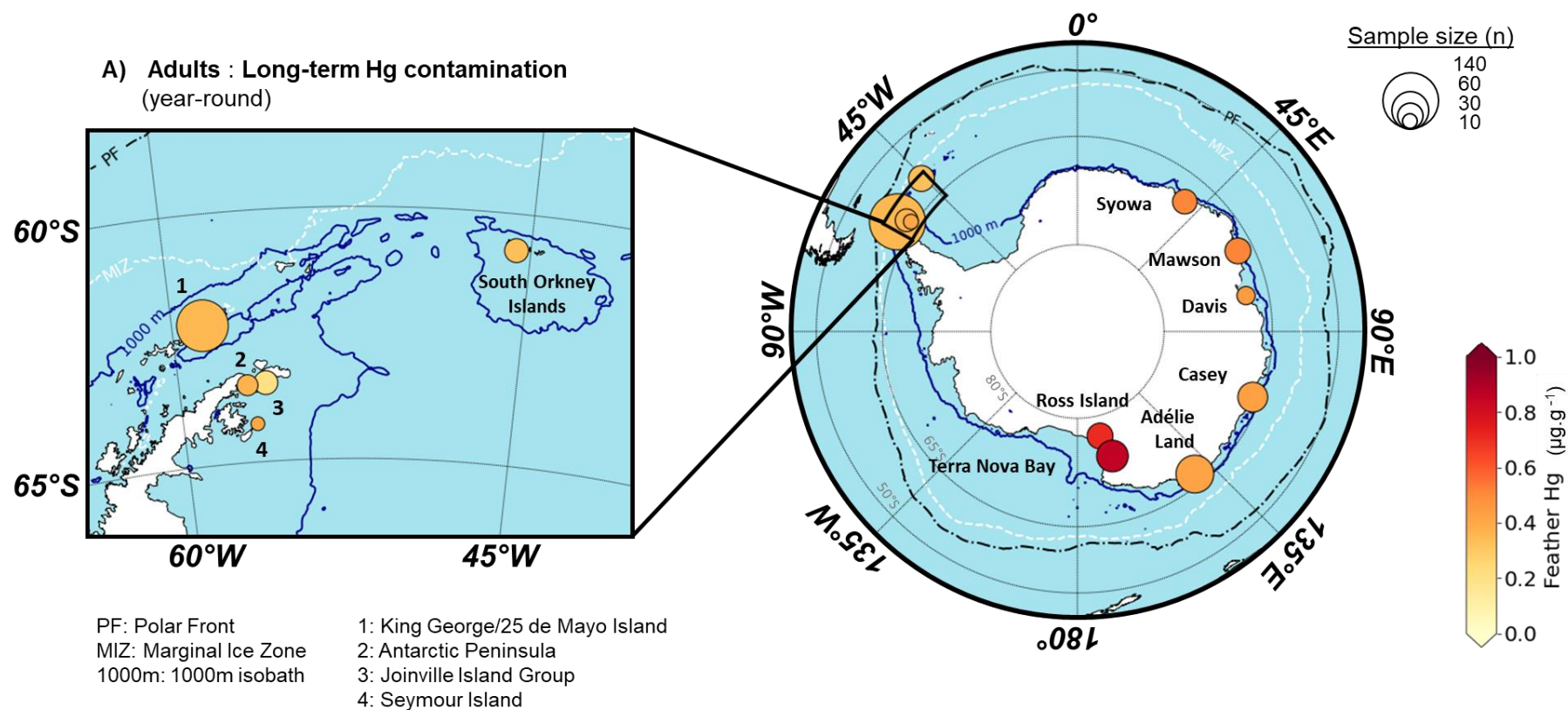


Figure 3.14. Circumpolar assessment of feather Hg concentrations measured in (A) adults and (B) large-fledging chicks of Adélie penguins (*Pygoscelis adeliae*). The colour gradient reflects increasing Hg concentrations (from low to high concentrations in yellow and red, respectively). The size of circles and triangles indicate sample sizes at each site for adult and chicks, respectively. Relevant ecological parameters include the Polar Front (PF; dashed black line), the Marginal Ice Zone (MIZ, dashed white line) and the 1000 m isobath (dark blue line). For more methodological details, the reader is referred to the Materials and Methods in Paper 2.

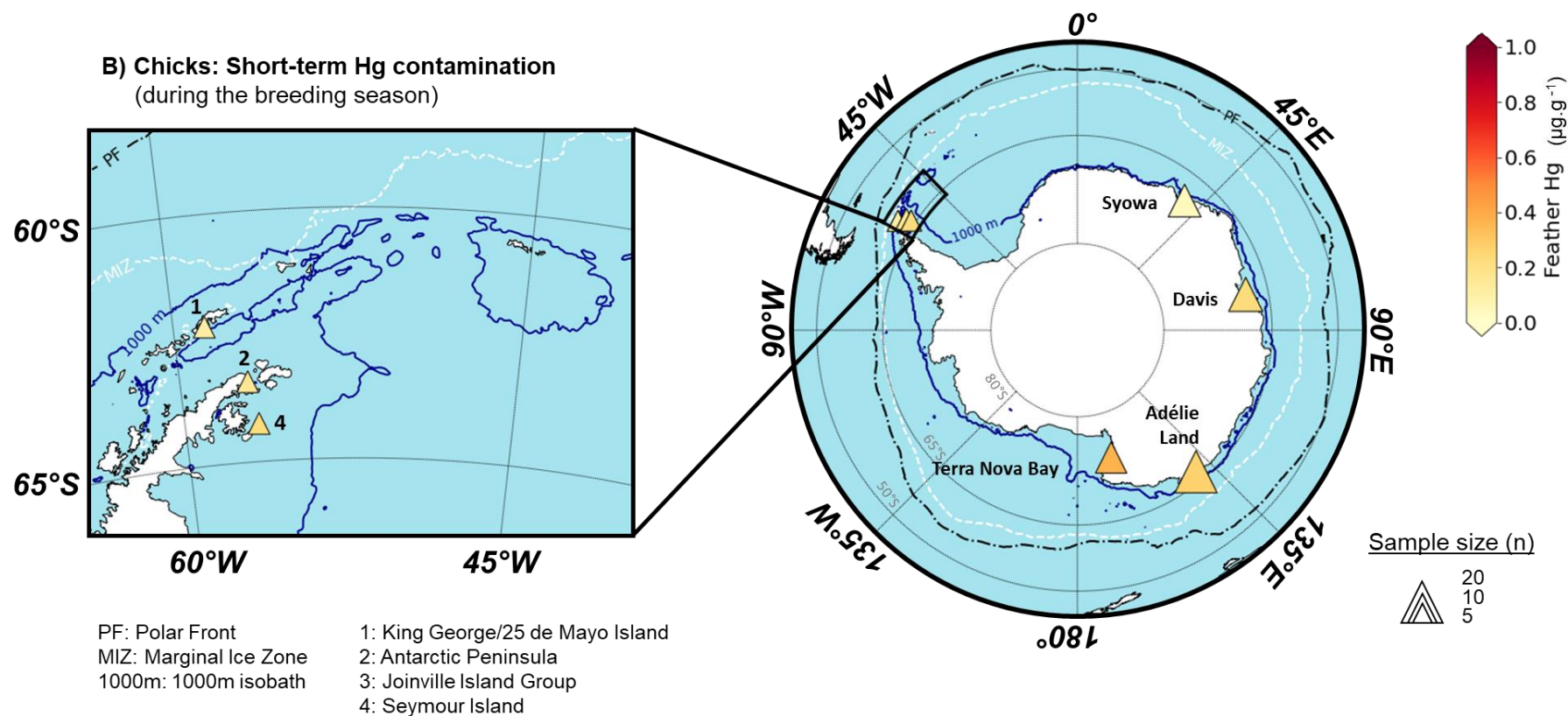


Figure 3.14. (following)

In chicks, the Ross Sea (*i.e.*, Terra Nova Bay) also exhibited the highest feather Hg concentrations (Figure 3.14.B). Clearly, Adélie penguins are more exposed to Hg in this region compared to others, both locally during the breeding season (as indicated by chick concentrations) and on the larger spatial scale, year-round (as indicated by adult concentrations). The Ross Sea could thus be considered as Hg hotspot in Antarctica, but why?

b) Does the trophic ecology of Adélie penguins drive spatial variation in Hg contamination?

Multifactorial analyses enabled to investigate the drivers of spatial variation in Hg contamination of Adélie penguins. These drivers included $\delta^{13}\text{C}$ and $\delta^{15}\text{N}$ values, and colonies. GLMs were defined with different combinations of these three explanatory variables, as presented in Paper 2 (Table 3), and were then subject to model selection to obtain the best model (*i.e.*, the model that explained the highest proportion of Hg variation). The reader is referred to Paper 2 for the complete description of statistical methodology.

As expected, trophic position was a significant predictor of feather Hg concentrations, as showed by the higher $\delta^{15}\text{N}$ values in the Ross Sea (Figure 3.15). This suggests that penguins, during the moulting period, foraged at higher trophic position at these locations. Adélie penguins are strongly associated with sea-ice environments, both during the breeding (Emmerson and Southwell, 2008; Guen et al., 2018; Kokubun et al., 2021) and non-breeding seasons (Emmerson and Southwell, 2011). Their diet may vary significantly according to the geographical localization of the colony, but also the year (Tierney et al., 2009; see Chapter 2, Section 1 for a complete description of the species' diet). For example, Adélie penguins feed almost exclusively on Antarctic krill along the Antarctic Peninsula and in the Scotia Sea (Coria et al., 1995; Juárez et al., 2018; Lynnes et al., 2004). In contrast, Adélie penguins from the Ross Sea consume higher proportions of Antarctic silverfish (Ainley et al., 1998; Olmastroni et al., 2020), which are abundant in continental shelf waters (Gon and Heemstra, 1990).

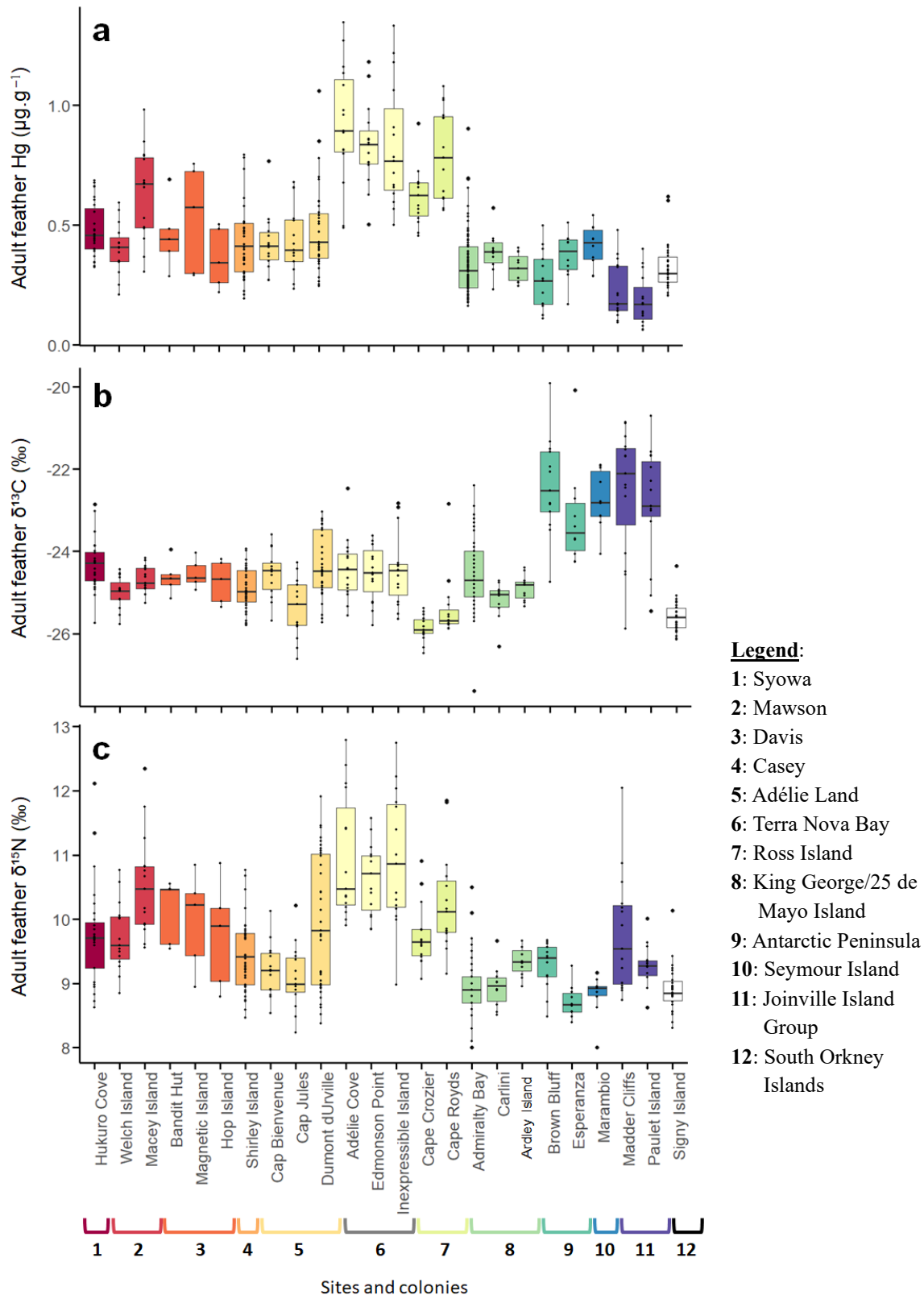


Figure 3.15. Spatial comparison of feather (a) Hg concentrations, (b) $\delta^{13}\text{C}$ and (c) $\delta^{15}\text{N}$ values in adult Adélie penguins (*Pygoscelis adeliae*) collected in 24 Antarctic colonies, represented by a clockwise colour gradient (from East-Antarctica in dark red to South Orkney Islands in grey). Feather $\delta^{13}\text{C}$ and $\delta^{15}\text{N}$ values are proxies for penguin feeding habitat and trophic position, respectively. Numbers (bottom) refers to sampling sites (cf. Legend). Individual values (smaller dots) are presented with boxplots, representing median values (midlines), errors bars (whiskers) and outliers (black dots outside whiskers).

Yet, the silverfish is also a zooplankton predator itself and thus exhibits a higher trophic position than krill (Everson, 2000; Hodum and Hobson, 2000; Polito et al., 2011). Previous studies showed that Hg concentrations in several species of Antarctic fish were 4 to 20 times higher than in other krill species (Polito et al., 2016; Seco et al., 2021, 2019; Sontag et al., 2019). Consequently, Adélie penguins consuming silverfish in higher proportions than krill could thus accumulate more Hg, probably explaining the higher feather Hg concentrations in the Ross Sea.

c) Are environmental drivers involved in the circumpolar variation of Hg contamination?

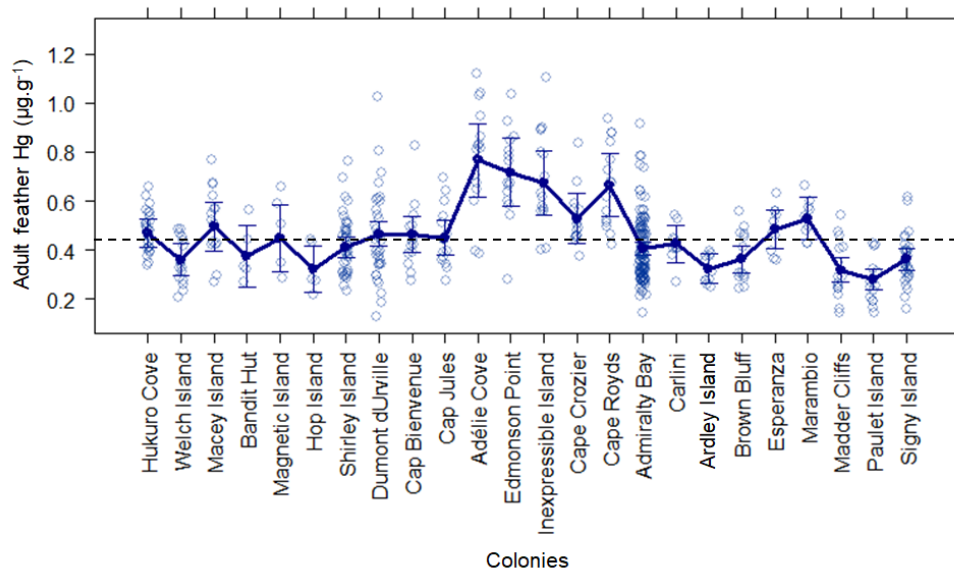


Figure 3.16. Spatial differences in feather Hg concentrations in adult Adélie penguins (*Pygoscelis adeliae*) from 24 Antarctic colonies (n=485) when controlled by their feeding ecology (feather $\delta^{13}\text{C}$ and $\delta^{15}\text{N}$ values). Relationships result from the extraction of partial residuals of the best Generalized Linear Model (GLM; see Table 3 and Material and Methods in Paper 2 for further details). Individual data are represented in light blue (open circle). Points (filled circle) are means \pm SD. The dark blue line links all mean Hg concentrations. The dotted black line indicates the global average Hg concentrations (*i.e.*, $0.45 \mu\text{g.g}^{-1}$, all pooled data from all colonies).

In addition to trophic drivers, feather Hg concentrations were also associated with regional colony location, as revealed by the results of model selection (Paper 2, Table 3). This suggests that environmental factors are involved in explaining spatial patterns in Hg contamination. When accounting for feeding ecology (*i.e.*, $\delta^{13}\text{C}$ and $\delta^{15}\text{N}$ values), colonies from the Ross Sea still appeared to have higher Hg concentrations than all other colonies (Figure 3.16). Hence,

penguins in the Ross Sea have disproportionately higher Hg concentrations than would be expected on the basis of their diet alone.

Two non-exclusive factors may explain this result: (1) **volcanism** and (2) katabatic winds. The West-Antarctic Rift System runs from the base of the Antarctic Peninsula through the Weddell Sea to the Ross Sea (Rocchi et al., 2003), resulting in numerous volcanoes present in Western versus Eastern Antarctica. Despite low activity levels, two main active volcanoes border the coast of the Ross Sea: Mount Erebus and Mount Melbourne, which are located on Ross Island and in Terra Nova Bay, respectively (Behrendt, 1990; Edwards and Smellie, 2016; Ferraccioli et al., 2000; Global Volcanism Program, 2022). Since volcanoes represent a primary source of Hg to the atmosphere (Grasby et al., 2019), they are likely to constitute a local source of Hg for the ocean and associated marine food webs as well. On the other hand, **katabatic winds** may also influence Hg deposition in the Ross Sea. Katabatic winds are strong winds that blow from the large and elevated Antarctic ice sheets toward the coast and represent a major environmental feature in Antarctica (Parish, 1988; Parish and Cassano, 2003) that can transport dust and debris. The Ross Sea is strongly exposed to katabatic winds (Turner, 2015) and in Terra Nova Bay, regions exposed to strong katabatic winds showed enhanced Hg deposition on the coast (Bargagli, 2008, 2016). Consequently, by carrying air masses originating from the Antarctic continent towards coastal regions, katabatic winds could represent a local natural source of Hg in marine ecosystems of the Ross Sea. Still, the biogeochemical cycle of Hg is complex and includes several chemical processes and biological transformations with both abiotic and biotic interactions (Chételat et al., 2022; McKinney et al., 2022): methylation/demethylation, redox reactions, MeHg production, bioavailability and transfer through marine food webs; especially in polar environments with the influence of sea ice (Cossa et al., 2011). The presence of **sea ice**, which harbour microbial source of MeHg in the Southern Ocean (Gionfriddo et al., 2016; Yue et al., 2023), may thus influence Hg contamination in Antarctic marine food webs. Further research is needed to disentangle the biogeochemical processes at the circumpolar scale, but also those that could result in higher year-round Hg exposure in Adélie penguins from the Ross Sea.

d) Could spatial patterns result from temporal patterns of Hg contamination?

In Antarctic environments, sample collection is challenging and implied a relatively large temporal scale period (between 2005 and 2021) here. Even if interannual variations were very

low in one colony where adult Hg concentrations were available for six consecutive years (i.e., Admiralty Bay, King George/25 de Mayo Island), observed spatial variations could result from the combination of both spatial and temporal variations. It is worth noting that Hg concentrations in two colonies were different from those reported previously. In Queen Maud Land, feather Hg concentrations in the 2010s were five times higher than in the 1980s and the 1990s (Honda et al., 1986; Yamamoto et al., 1996; Paper 2, Table 1). In Adélie Land, feather Hg concentrations dropped by 30% between 2006 and the following years (2011 and 2017; Carravieri et al., 2016; this study; Paper 2, Table 1). However, this temporal difference ($0.2 \mu\text{g}\cdot\text{g}^{-1}$) is still low compared to the spatial difference measured among adult Hg concentrations ($1.2 \mu\text{g}\cdot\text{g}^{-1}$). Further studies should thus investigate mid- and long-term Hg trends in Antarctic food webs, for instance by increasing the temporal resolution in Hg monitoring.

e) Was Hg contamination different between the sexes in adult Adélie penguins?

In seabirds, sexual foraging segregation has been suggested as a strategy to reduce intra-specific competition (Bearhop et al., 2006; Forero et al., 2002; González-Solís et al., 2000; Phillips et al., 2011). In Adélie penguins, foraging segregation between sexes was observed during the breeding season: females foraged for more krill than fish in more offshore, pelagic waters, in contrast to males which fed equally on both prey types in more inshore, benthic waters (Clarke et al., 1998; Colominas-Ciuró et al., 2018). In theory, such sexual foraging segregation should therefore be reflected in stable isotopes and then in Hg concentrations.

Information about the sex was available for a dataset that only represented half of the total sample size (see Paper 2, Table S5). We therefore investigated sex differences in both Hg contamination and trophic ecology across different Antarctic sites. Here, **no clear sexual segregation** could be deduced from the observed $\delta^{13}\text{C}$ and $\delta^{15}\text{N}$ values (Figure 3.17.b,c). However, differences between sexes in feather Hg concentrations could be noticed when differences in either $\delta^{13}\text{C}$ or $\delta^{15}\text{N}$ values or both were present (Figure 3.17.a). Feather Hg concentrations were similar between sexes at Adélie Cove (Terra Nova Bay) and Admiralty Bay (King George/25 de Mayo Island), as previously reported (Polito et al., 2016). In contrast, females had lower Hg concentrations in five colonies, in Queen Maud Land and the Ross Sea, probably resulting from egg production that represents an additional route of Hg elimination in females compared to males (Bond and Diamond, 2009; Braune and Gaskin, 1987b).

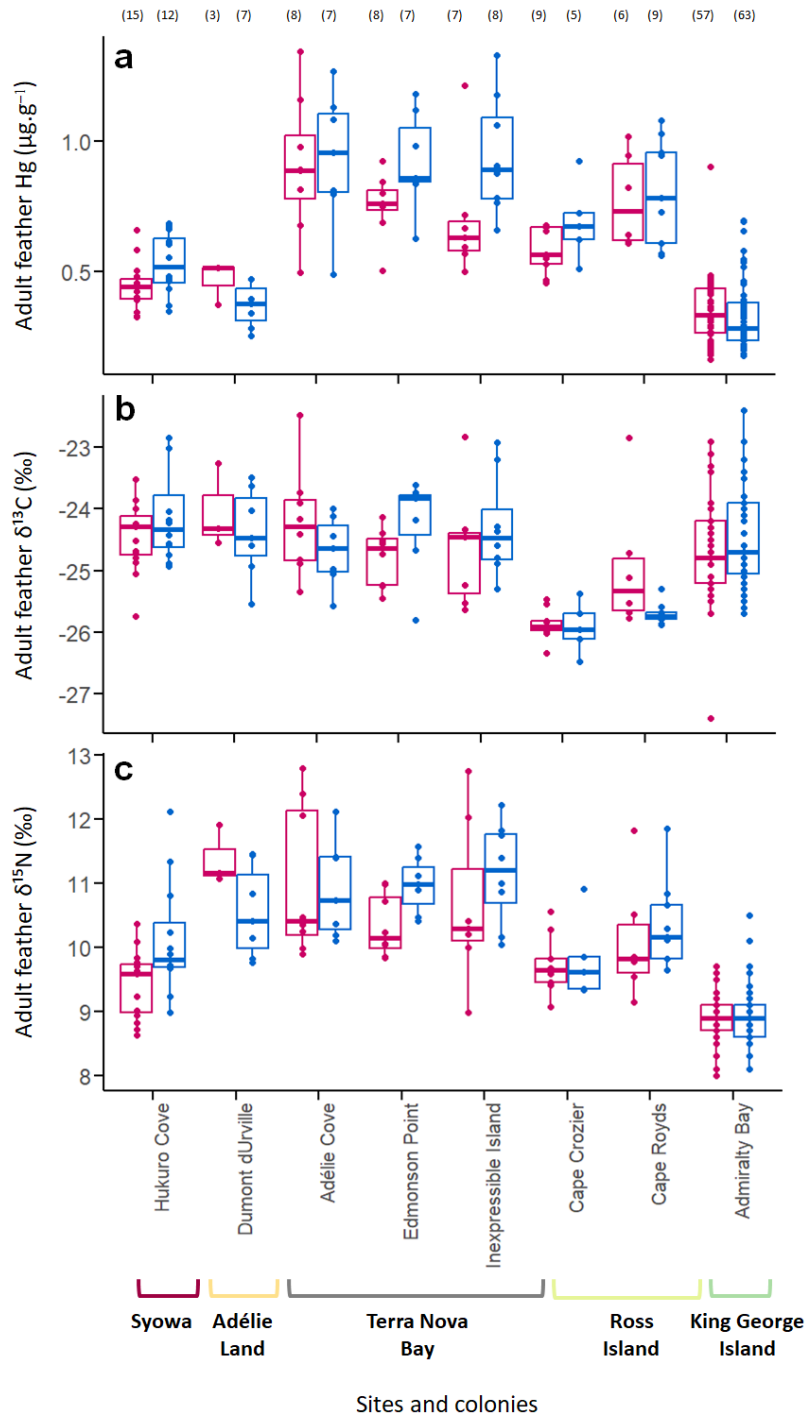


Figure 3.17. Sex differences in feather (a) Hg concentrations, and (b) $\delta^{13}\text{C}$ and (c) $\delta^{15}\text{N}$ values measured in adult Adélie penguins (*Pygoscelis adeliae*) from eight Antarctic colonies. Females and males are represented in pink and blue, respectively. Feather $\delta^{13}\text{C}$ and $\delta^{15}\text{N}$ values are proxies for penguin feeding habitat and trophic position, respectively. Numbers in brackets represent sample sizes for each sex and colony. Individual values (smaller dots) are presented with boxplots, representing median values (midlines), errors bars (whiskers) and outliers (black dots outside whiskers)

Despite these potential differences between sexes, **sex did not significantly drive spatial variation** in adult Hg contamination (Paper 2, Table 3). Complete sexing analyses, either determined through morphological or molecular approaches, should help to further investigate differences in Hg contamination between sexes and its drivers (either extrinsic or intrinsic), on a circumpolar scale.

3.4. Conclusions and perspectives

This study provides a unique assessment of Hg contamination in Antarctic marine food webs, by using the Adélie penguin as a circum-Antarctic bioindicator. To the best of our knowledge, this work is the first to document Hg contamination over such a large spatial scale, encompassing a total of 24 continental and coastal island colonies around Antarctica. Feathers represent a valuable, non-destructive and non-invasive monitoring tool, in complete agreement with Antarctic Treaty protocols, to examine the variation in Hg contamination across temporal and spatial scales. Feather Hg concentrations detected in Adélie penguins ($< 2 \mu\text{g}\cdot\text{g}^{-1}$) were below toxicity thresholds recognized for seabird feathers ($1.62\text{--}10 \mu\text{g}\cdot\text{g}^{-1}$ dw; Ackerman et al., 2016; Chastel et al., 2022). Currently, this suggests low risks of toxicity for this species, although toxic effects may arise at low Hg concentrations, particularly in co-occurrence with other natural and/or anthropogenic stressors. At the circumpolar scale, Hg contamination was relatively homogeneous across regions. This is consistent with the circumpolar structure of the Southern Ocean, which is characterized by a unique stratification of annular fronts and water masses encircling the Antarctic Continent (Carter et al., 2008).

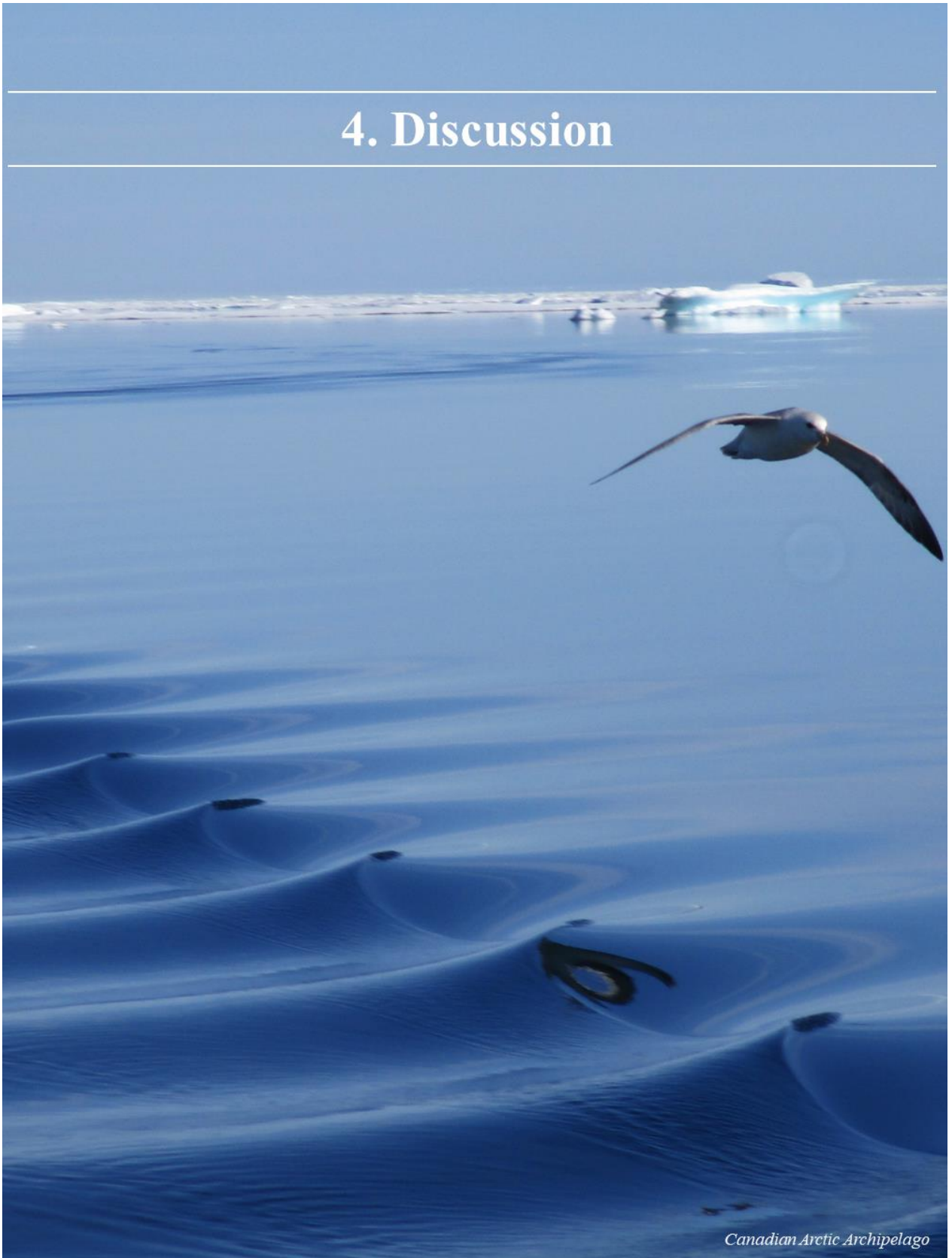
Trophic ecology (feeding habitat and trophic position, as indicated by stable isotopes) was crucial to explain spatial variations of Hg contamination. The Hg hotspot observed in the Ross Sea was associated with higher trophic position of Adélie penguins, probably due to a higher proportion of fish in their diet. This reinforces the need to account systematically for the diet when monitoring Hg contamination in seabirds, especially at such large spatial scales. However, results also suggested that unknown environmental drivers may influence Hg contamination of marine food webs in the Ross Sea. Based on their ability to detect spatial variation in Hg contamination in circum-Antarctic ecosystems, this reinforces the suitability of Adélie penguins as bioindicator species for Antarctic marine ecosystems. Further research is now required to explore and identify these environmental drivers and the biogeochemical mechanisms involved

in the enhanced transfer of Hg in marine food webs in the Ross Sea, and in Antarctic regions in general.

3.5. Summary

- The **Adélie penguin** was used as a **circumpolar bioindicator species of Hg contamination of Antarctic marine food webs**.
- The **Ross Sea** appeared as **Hg hotspot**.
- Drivers included both **trophic ecology** (as indicated by stable isotopes) and **colony location**, suggesting the role of environmental drivers.
- Further research is required to explore and identify these environmental drivers and the biogeochemical mechanisms involved in the enhanced transfer of Hg in marine food webs in the Ross Sea, and in other Antarctic regions.

4. Discussion



Canadian Arctic Archipelago

This doctoral work provides a large-scale biomonitoring of Hg contamination in marine food webs of remote oceanic regions, including the Arctic Ocean (to a lesser extent), the intertropical region and the Southern Ocean (exhaustively), by using seabirds as bioindicators. In total, this included 2400 seabird individuals (1945 adults, 455 chicks) from the three bioindicator species (Brünnich's guillemots, sooty terns and Adélie penguins), distributed over 72 sites across all ocean basins (Figure 3.18). This work represents a valuable subset for the Global Biotic Mercury Synthesis database, by further documenting large oceanic regions that were scarcely documented previously.

4.1. Highlights

- In the **Arctic**, results confirmed the **East-to-West gradient**, with Hg hotspots in Greenland, Canadian Arctic and Newfoundland, and also revealed a South-to-North gradient in West-Greenland.
- In the **intertropical region**, adult feather concentrations revealed that Hg contamination was **higher**:
 - in the **Atlantic Ocean** compared to the Pacific and Indian Oceans,
 - in the **Northern Hemisphere** compared to the Southern Hemisphere.
- In the **Antarctic Zone** (i.e., south of Polar Front), Hg contamination was relatively homogenous around Antarctica, except for a **Hg hotspot in the Ross Sea**.
- **Trophic ecology** was a significant driver of Hg spatial patterns, in combination with colony location, suggesting both trophic and environmental drivers in Hg contamination in Antarctic ecosystems. This was not the case in tropical ecosystems, as only $\delta^{13}\text{C}$ values and colony location were the main drivers.

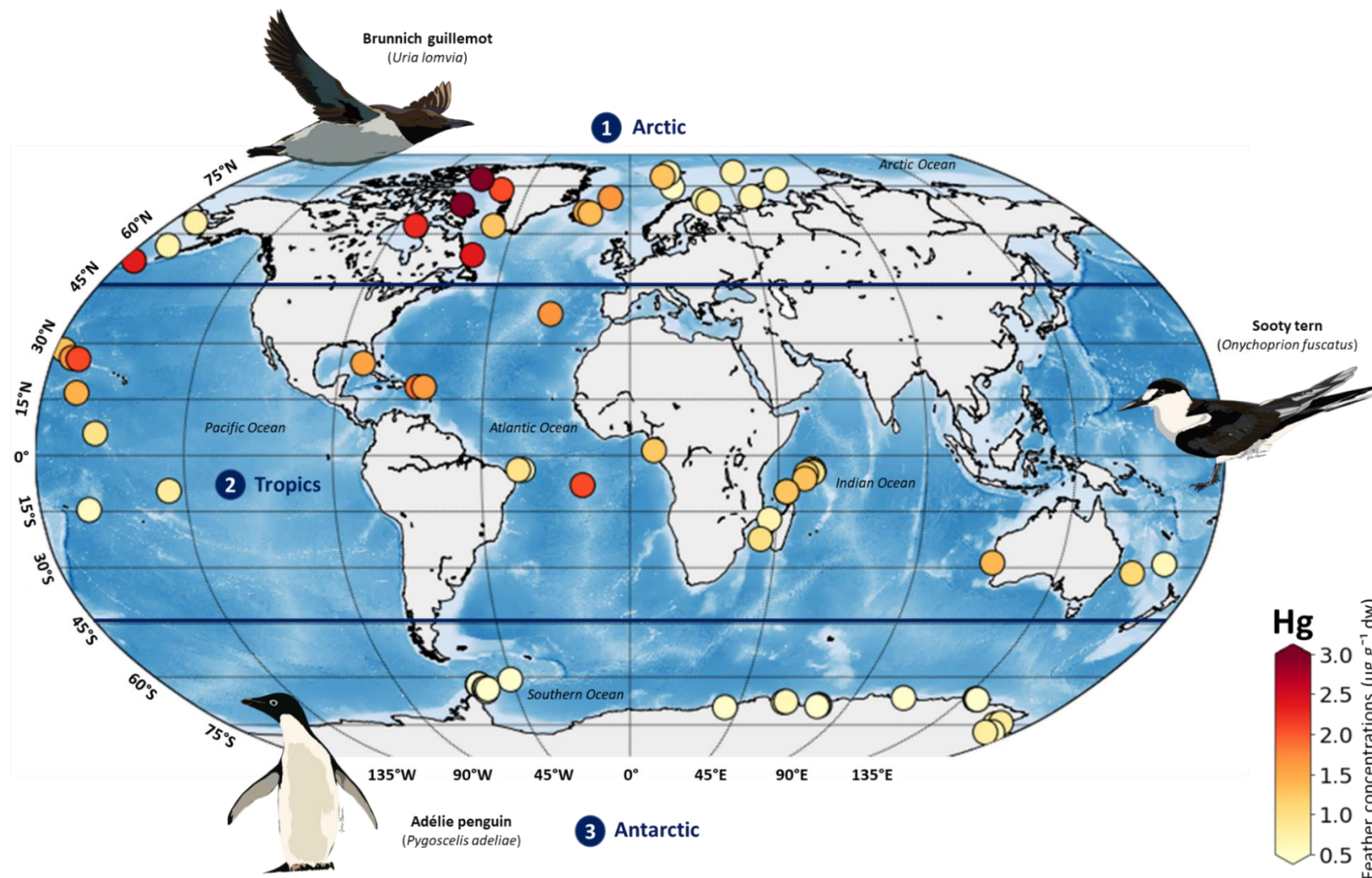


Figure 3.18. Spatial biomonitoring of feather Hg concentrations in three remote oceanic regions using three bioindicator species (adults): the Brunnich's guillemot (the Arctic; 20 sites), the sooty tern (Tropics: Pacific, Atlantic and Indian Oceans; 28 sites) and the Adélie penguin (the Antarctic; 24 sites). Values are mean feather Hg concentrations for each site (from low to high Hg concentrations in yellow and red, respectively).

4.2. Can we associate feather Hg concentrations of seabirds with geographical areas?

This large-scale Hg assessment aimed to identify potential Hg hotspots and coldspots in marine food webs in remote oceanic regions. To this end, seabird feathers were used as biomonitoring tools, as they provide integrated information about Hg contamination of marine food webs, on both large temporal and spatial scales (*cf.* Chapter 2, Section 2). Identifying Hg hotspots or coldspots means associating feather Hg information to geographical areas where seabirds are exposed to Hg. Thus, knowledge of the movement ecology of the seabird species across the different oceanic regions is essential. Unfortunately, tracking devices were not deployed on the sampled individuals here, neither during the breeding or the non-breeding periods, preventing the identification of exposure areas *in situ*. In the absence of precise tracking positions, published tracking studies could help to obtain hypothetical geographical areas to be associated with feather Hg concentrations. In the Southern Ocean for example, we used the existing studies (n=6) that tracked Adélie penguins during the non-breeding period (*i.e.*, the integrated period of Hg exposure) and determined the maximum geographical zone that included all individual tracks (Figure 3.19).

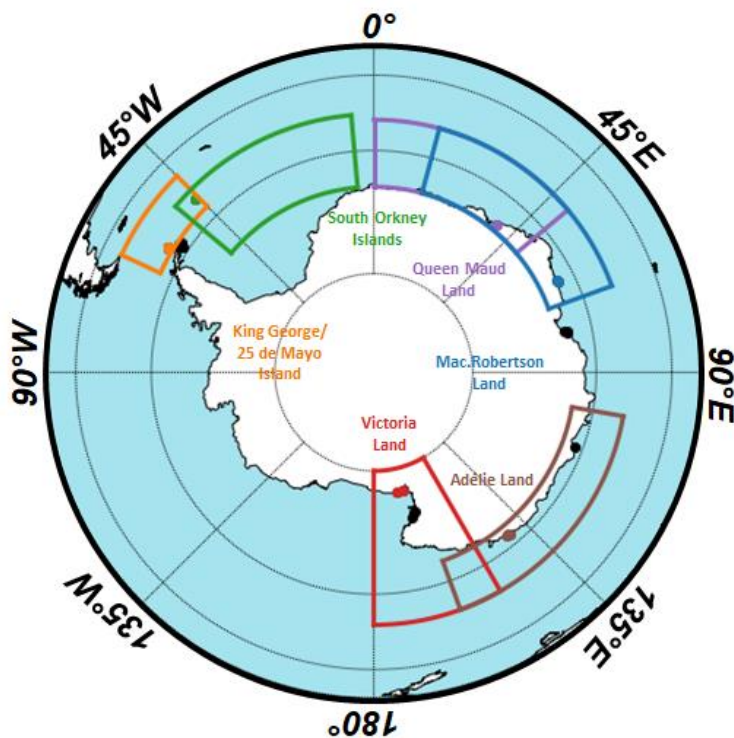


Figure 3.19. Literature review of non-breeding distributions of Adélie penguins (*Pygoscelis adeliae*) tracked in six Antarctic sites: South Orkney Islands (Signy Island, in green), Queen Maud Land (Hukuro Cove, in purple), Mac.Robertson Land (Mawson Station, Béchervaise Island, in blue), Adélie Land (Dumont d’Urville, in brown), Victoria Land (Ross Sea, Cap Bird, in red) and King George/25 de Mayo Island (Admiralty Bay, in orange). Associated references are provided in Paper 2. Black dots represent other sites sampled in the present study (see Paper 2 for further details).

These geographical areas represented the zone that was reflected by their feathers, both spatially (*i.e.*, integrating intermoult movements) and temporally (*i.e.*, year-round contamination; see Chapter 2, Section 2.2). In the end, this represented a large spatial region, encompassing most

of Adélie penguins' habitat in the Antarctic Zone, from the Antarctic Peninsula to the Ross Sea. Clearly, a large part of the Antarctic Zone could not be documented in either tracking studies (Figure 3.19) or this circumpolar Hg monitoring (Figure 3.19): in East-Antarctica, between the Ross Sea and the Antarctic Peninsula (i.e., Edward VII Land, Marie Byrd Land and Ellsworth Land). In fact, these Antarctic regions constitute a « no man's land » that unfortunately prevents any scientific research in these regions, including feather sampling of penguins.

Regarding tropical oceans, only two studies determined the non-breeding distribution of sooty terns: in Ascension Island (South Atlantic Ocean; Reynolds et al., 2021) and Bird Island in the Seychelles (Indian Ocean; Jaeger et al., 2017; Figure 3.20).

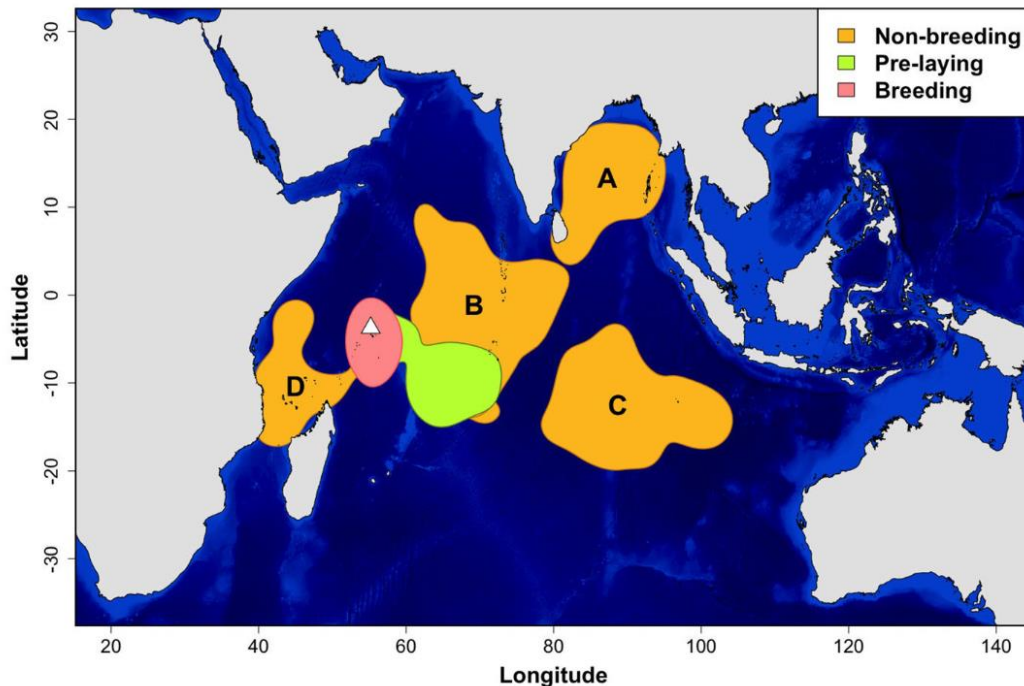


Figure 3.20. Distributions of sooty terns (i.e., 36 birds, 53 annual tracks) breeding in Bird Island (Seychelles; white triangle) during the non-breeding (orange), the pre-laying (green) and the breeding (red) periods. During the non-breeding period, locations were concentrated in (A) the Bay of Bengal, (B) on each side of the Chagos-Laccadive plateau, (C) on each side of 90 East Ridge and (D) around the Comoros. Units are in degree. From Jaeger et al. (2017). For more information, the reader is referred to the original study.

Unlike Adélie penguins that are restricted to the Antarctic Zone, sooty terns disperse widely during the non-breeding period, travelling several thousands of kilometres from their breeding

colonies (up to 2,900 and 4,500 km, respectively). Besides, individuals from the same colony can spend the non-breeding period in distinct oceanic regions, as indicated by their distribution in the Indian Ocean (Figure 3.20). Sooty terns from Bird Island concentrate in four main regions during the non-breeding period: the Bay of Bengal, on each side of the Chagos-Laccadive plateau, on each side of 90 East Ridge and around the Comoros. Clearly, these four regions may largely differ in Hg availability and transfer, in the composition and structure of marine food webs, and also in environmental conditions. The lack of tracking positions and studies prevents us from associating feather Hg information to geographical areas where sooty terns are exposed to Hg, even if approximated with the published literature.

Detailed spatial information of seabird movements during their annual cycle is essential to quantify precisely the spatial variation in their Hg exposure and then identify Hg hotspots in the ocean. Obviously, the present work constitutes a qualitative approach that paves the way for future quantitative approaches in spatial ecotoxicology that would combine Hg biomonitoring and biologging. Several successful examples already exist in the literature, in the North Pacific (Fleishman et al., 2019; Shoji et al., 2021), North Atlantic Ocean (Albert et al., 2021; Fort et al., 2014; Renedo et al., 2020a) and the Southern Ocean (Carravieri et al., 2018), but the number of these studies globally is still limited to date. In the North Atlantic Ocean, more studies should come thanks to ARCTOX (see Section 1.1) and SEATRACK, a collaborative project that aims to map the non-breeding distributions of 11 seabird species from 56 breeding sites (Figure 3.21; more information on www.seapop.no/seatrack). In a similar way, the large-scale Hg assessment in tropical and polar oceans (specifically the Southern Ocean), which was carried out in this doctoral work, would be substantially improved by the deployment of tracking devices, allowing connection to be made between spatial and seasonal distributions of both sooty terns and Adélie penguins, at the individual level, with contaminants at the ocean scale.

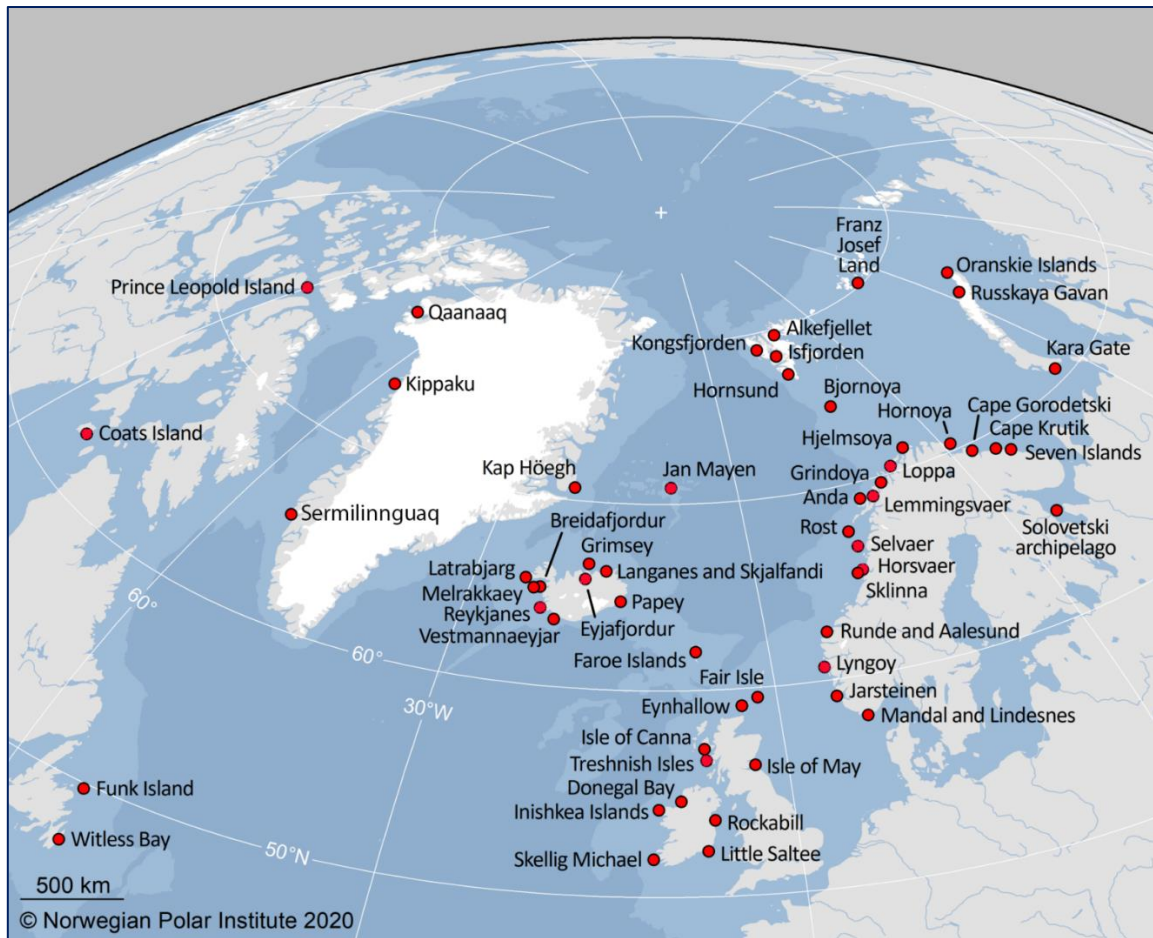


Figure 3.21. Sampling sites within the SEATRACK project.

Chapter 4

Long-term monitoring of Hg contamination in tropical and polar marine ecosystems

Human activities have released Hg globally, to the atmosphere, land and water bodies (rivers and oceans), since the expansion of silver and gold mining in the sixteenth century (Sonke et al., 2023). Later, the Industrial Revolution in the nineteenth and twentieth centuries has led to increasing releases of Hg through Hg mining and production, technological applications of Hg, chemical manufacturing, and more recently (*i.e.*, since the 1960s) from coal burning and metallurgy (Sonke et al., 2023; Streets et al., 2017). For instance, this represents a three- to five-fold global increase of Hg on land, in the atmosphere and the ocean (Lamborg et al., 2014; Selin, 2009). Concurrently, human activities have also led to a multitude of alterations on the climate and the environment, including air and ocean warming, and ocean acidification that have resulted mainly from the increasing release of greenhouse gases (*e.g.*, carbon dioxide, CO₂) and alteration of the carbon cycle, as well as ocean desoxygenation or deforestation for example (see Chapter 1; IPCC, 2023). More recently, in addition to direct anthropogenic Hg (described above), these anthropogenic alterations have also shaped the global increase of Hg releases over time, by modifying Hg cycle and transfer in all ecosystems and allowing re-emissions of legacy Hg (Fisher et al., 2023). Today, it is estimated that atmospheric re-emissions of legacy Hg are two times larger than current atmospheric emissions from anthropogenic origin (Amos et al., 2013; UN Environment, 2018). Anthropogenic emissions of both current and legacy Hg shape long-term trends of environmental Hg, with different contributions. In the context of ongoing global change, this raises considerable concern for the fate of environmental Hg pollution and the subsequent impact on both wildlife and humans worldwide. Therefore, exploring the past may help to better understand the fate of environmental Hg and the role of anthropogenic Hg over time, and ultimately to assess the effectiveness of international regulations that were implemented recently (*e.g.*, Minamata Convention on Mercury).

Exploring the past is a challenge, as this requires to access archives that have recorded environmental Hg over years, decades and centuries. Natural archives such as sediment (lake and marine sediment), peat and ice cores, as well as tree rings have been used to reconstruct past Hg atmospheric concentrations and deposition over large temporal scales (*i.e.*, decadal to millennial timescales; Cooke et al., 2020 and references therein). However, they do not inform about post-depositional processes, such as Hg availability and transfer in food webs. Biotic archives represent a relevant alternative to reconstruct past Hg contamination of food webs, particularly of hardly accessible marine food webs (see Chapter 1, Section 2.2). In biota, temporal trends of Hg are generally limited. Despite a general lack of regional initiatives worldwide, some key biomonitoring efforts exist in some regions, such as the Arctic (with the

AMAP; see Chapter 3), North-East USA (with Great Lakes Monitoring Programs; <https://www.epa.gov/great-lakes-monitoring>) and Canada (with the Northern Contaminants Program; <https://science.gc.ca/site/science/en/northern-contaminants-program>), but only since the 1990s. Similarly, the majority of temporal studies has monitored marine biotic Hg over the last 30–50 years (*e.g.*, Aubail et al., 2012; Braune et al., 2016; Evans et al., 2013). In contrast, investigations over multi-decadal and century timescales are scarce, mainly because tissue samples that reflect such temporal scales are limited and hard to obtain retrospectively. Unlike soft tissues (*e.g.*, organs, blood), hard tissues such as bones, teeth, hair and feathers are easier to preserve, as they hardly deteriorate over years, decades or centuries, especially when kept in controlled conditions, as is the case in museum collections. Therefore, museum specimens, which were collected for exhibitions and museum collections worldwide over the last centuries, are invaluable to reconstruct past Hg availability and transfer in marine food webs, in particular in remote oceanic regions that are the focus of this doctoral work.

To date, only a very limited number of studies have investigated Hg in museum-held specimens over the last century, including marine mammals ($n=9$; see [Table A5](#) for a review) and seabirds ($n=14$; see [Table A4](#) for a review). In this chapter, feathers of seabird specimens were used to study temporal trends of Hg contamination in marine food webs. Out of the 14 seabird studies, only four of these have considered trophic ecology as a factor that could influence Hg contamination ([Table A4](#)). Yet, bird trophic ecology is key in understanding the mechanisms of Hg contamination and to disentangle whether temporal variations in Hg contamination are linked to dietary shifts and/or changes in environmental Hg contamination (Bond et al., 2015; Carravieri et al., 2016; Choy et al., 2022; Fort et al., 2016; Vo et al., 2011). Over multi-decadal timescales, decreases and stable trends in Hg contamination have been documented in only one temperate Atlantic species (Thompson et al., 1992) and one temperate Pacific species (Choy et al., 2022), respectively. In contrast, increases in Hg contamination have been observed in 12 temperate Atlantic species (Monteiro and Furness, 1997; Thompson et al., 1992, 1993a), one temperate/subtropical Pacific species (Vo et al., 2011) and one Arctic species (Bond et al., 2015). Considering remote oceanic regions, which are the focus of this doctoral work, **long-term monitoring** of Hg contamination (at multidecadal/century time scales) in seabirds is still **very scarce in the Arctic Ocean and clearly lacking in tropical oceans** to date. The present chapter thus aims to fill this research gap by assessing Hg contamination in polar and tropical marine food webs retrospectively, by using seabirds as bioindicators. These temporal trends were investigated at the multi-decadal time scales for both the Arctic (Greenland) and the

intertropical region (Ascension Island, South Atlantic Ocean), but were only investigated through epoch comparisons in the intertropical region (other sites) and the Southern Ocean, because of lower sampling efforts over time in these specific regions.



Ukaleqarteq (Kap Höegh), Greenland

1.1. Context

Despite its remoteness, the Arctic is no longer considered as a pristine environment. Anthropogenic contaminants, such as Hg, are transported from their emission sources outside the region (mostly at mid-latitudes) to the Arctic via long-range ocean and air transport (Dastoor et al., 2022). Over millennia, Arctic soils have accumulated atmospheric Hg (both from natural and anthropogenic origin), which may be re-emitted to the atmosphere or released to surface waters via melting of ice and permafrost, river run-offs and coastal erosion (Dastoor et al., 2022; Lim et al., 2020, p. 20; Schuster et al., 2018). This has led to elevated Hg concentrations in Arctic fish, marine mammals and seabirds compared to lower latitudes (AMAP, 2011; UN Environment, 2018). Because they heavily rely on Arctic animals in their traditional diets, Indigenous People that live in the Arctic year-round are among the highest Hg exposed populations in the world (Basu et al., 2018). Therefore, Hg biomonitoring in the Arctic has been conducted since the 1970s in coordination with the AMAP (see Chapter 3, Section 1.3), in various ecosystems (*i.e.*, marine, freshwater and terrestrial) and species (*i.e.*, bivalves, fish, birds and mammals; see AMAP, 2021 for a review). Such modern monitoring is key to assess the risks for Arctic wildlife and human populations, but also the effectiveness of national and international regulations implemented over the last years and decades. Yet, long-term monitoring that documents Hg bioavailability in Arctic ecosystems over multidecadal and century timescales provides a unique opportunity to determine the influence of human activities since the Industrial Revolution, which represents a critical point in the global history. To date, only a few studies have investigated such large temporal scales in the Arctic. Out of the six Arctic studies that were conducted on marine mammals (see [Table A5](#) for a review), only four of them dated back to the 19th century and all reported considerable increase in Hg concentrations in the Canadian Arctic, Greenland and Svalbard, including in belugas (Desforges et al., 2022), narwhals (Dietz et al., 2021), ringed seals (Aubail et al., 2010) and polar bears (Dietz et al., 2011, 2006). Over the last century, a substantial increase in Hg contamination was also reported in ivory gulls in the Canadian Arctic and West Greenland (Bond et al., 2015). Yet, this is the only published long-term study conducted on Arctic seabirds.

1.2. Aims and predictions

In this context, the present study aims to further investigate long-term trends of Hg contamination in Arctic seabirds, which can be used as bioindicator species of Arctic marine

food webs. In particular, this work focused on Greenland, as this represents an emblematic Arctic region that is underrepresented in Hg monitoring in general. To document Greenland marine ecosystems, we analysed body feathers of Brünnich's guillemots, which informs about Hg exposure during the breeding season and thus solely reflects Hg exposure in the Arctic. More specifically, the aim was two-fold:

(1) Document the temporal trend of feather Hg concentrations in guillemots breeding in Greenland from the 1830s to the 2020s.

(2) Investigate the influence of their trophic ecology (reflected by $\delta^{13}\text{C}$ and $\delta^{15}\text{N}$ values) on this temporal trend.

As most retrospective studies conducted on seabirds previously reported increasing Hg trends over the last century, we expected similar results in feather Hg concentrations of guillemots in the Arctic.

1.3. Results and discussion

Overall, 547 Brünnich's guillemots were sampled in Greenland, including 481 adults and 66 youngs (*i.e.*, juveniles, immatures, subadults). Details on sample sizes and time frames for all age classes are presented in [Table A6](#). In this chapter, we only focused on the adult individuals, which included museum-held ($n=153$) and free-living ($n=328$) Brünnich's guillemots. Museums specimens originated from three natural history museums, including the Bird Group Tring (Natural History Museum, UK; $n=6$), Natural History Museum of Denmark (Copenhagen; $n=143$) and the French National History Museum (Paris; $n=4$). Overall, this represented a time frame of 189 years, from 1833 to 2022. However, the adult sampling included different regions from Greenland, mainly West Greenland ($n=448$, from 1841 to 2022) and East Greenland ($n=21$, from 1833 to 1936), and for some individuals ($n=12$, from 1834–1977), the precise region was unknown. For each region, feather Hg concentrations and stable isotope values are presented in the Annexes ([Tables A7, A8 and A9](#)). Because these two main regions face distinct environmental conditions, we decided to not pool them. In this section, we focused on West Greenland, as they represented most (93%) of our adult sampling.

a) Long-term trends of Hg contamination and trophic ecology in Brünnich's guillemots

Mercury contamination. Overall, our results are consistent with the range of average concentrations observed for Brünnich's guillemots in Arctic colonies, such as Hornøya (Norway; $0.78 \pm 0.18 \mu\text{g}\cdot\text{g}^{-1}$; Wenzel and Gabrielsen, 1995), the Canadian Arctic ($1.63 \pm 0.33 \mu\text{g}\cdot\text{g}^{-1}$; Albert et al., 2021) and Iceland ($2.1 \pm 0.7 \mu\text{g}\cdot\text{g}^{-1}$; Thompson et al., 1992). However, Brünnich's guillemots from West Greenland ($1.72 \pm 1.09 \mu\text{g}\cdot\text{g}^{-1}$) exhibit Hg concentrations in the upper part of this range, similar to other colonies from the West Atlantic that display higher Hg values than those from the East Atlantic or the Pacific Arctic (Albert et al., 2021). Among Arctic seabirds, feather Hg concentrations were intermediate compared to other alcids, such as common guillemots (*Uria aalge*; $0.59 \pm 0.17 \mu\text{g}\cdot\text{g}^{-1}$; Albert et al., 2021), crested auklets (*Aethia cristella*; $1.0 \pm 0.51 \mu\text{g}\cdot\text{g}^{-1}$; Albert et al., 2021), little auks (*Alle alle*; $1.53 \pm 0.84 \mu\text{g}\cdot\text{g}^{-1}$; Fort et al., 2014), razorbills (*Alca torda*; $2.89 \pm 1.84 \mu\text{g}\cdot\text{g}^{-1}$) and rhinoceros auklets (*Cerorhinca monocerata*; $3.47 \pm 1.63 \mu\text{g}\cdot\text{g}^{-1}$; Albert et al., 2021). Intermediate Hg contamination in Brünnich's guillemots is consistent with their foraging ecology that largely relies on macrozooplankton and fish, such as the ice-associated Arctic cod (*Boreogadus saida*; Gaston and Nettleship, 1981; Provencher et al., 2012).

Over the last two centuries, our results revealed a non-linear increase in feather Hg concentrations (Figure 4.1.A). This represents a 251.7% increase in feather Hg concentrations over the entire period, corresponding to a 1.39% increase per year in Brünnich's guillemots. In the Arctic, only one study has documented century-time trends of Hg in seabirds, reporting a 1.6% increase per year in feather Hg concentrations of ivory gulls (*Pagophila eburnea*) in the Canadian Arctic and West Greenland, between 1877 and 2007 (*i.e.*, 45-fold increase overall; Bond et al., 2015). Although our result is consistent with this previous temporal trend, the 3.5-fold increase observed here in Brünnich's guillemots is much lower than in ivory gulls. Still, this also agrees with similar findings in Arctic marine mammals: (i) a 3- to 5-fold increase between historical and modern Hg concentrations in beluga teeth from the Canadian Arctic and West Greenland (1854–2000; Desforges et al., 2022), and (ii) a 1.6 to 1.7% increase per year documented in polar bears from Northwest Greenland (1892-2008; Dietz et al., 2011). Overall, this study provides additional evidence that Hg contamination in Arctic marine food webs has increased since the Industrial Revolution.

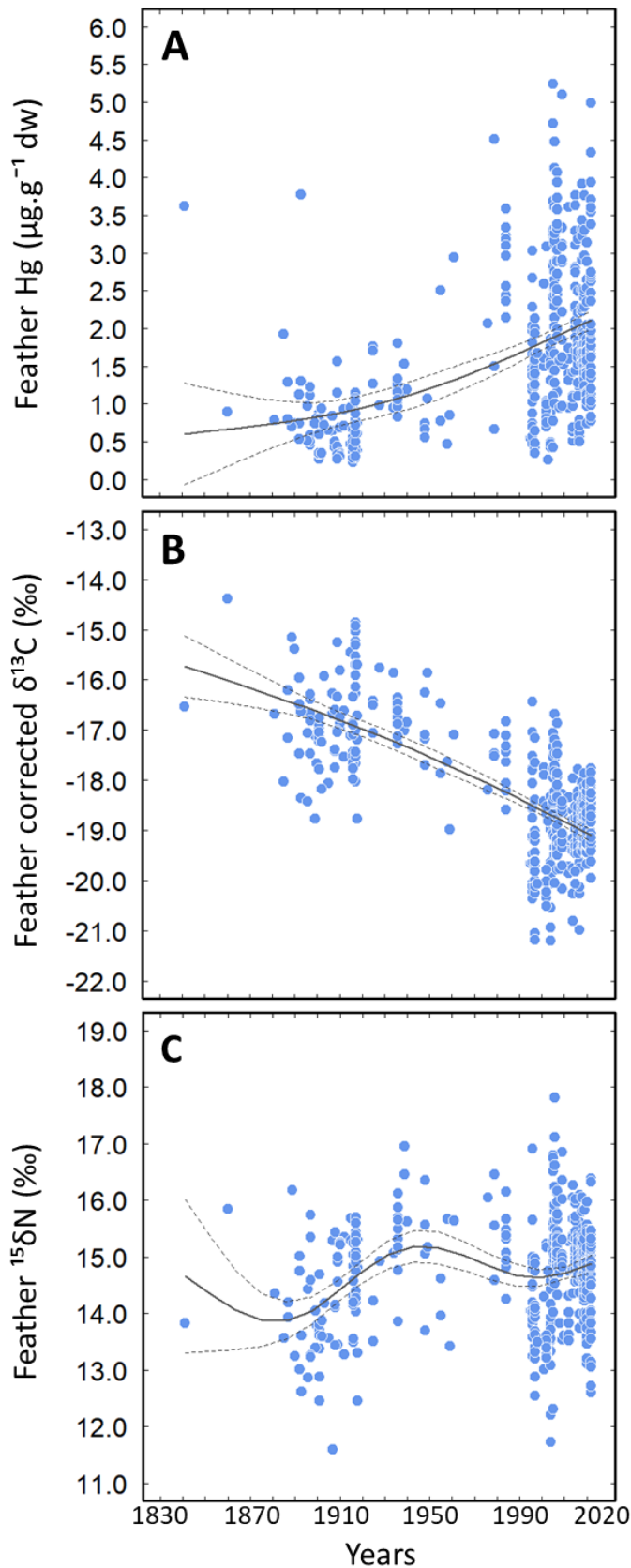


Figure 4.1. Long-term trends of feather (A) Hg concentrations, (B) carbon ($\delta^{13}\text{C}$) and (C) nitrogen ($\delta^{15}\text{N}$) isotopic values in Brünnich's guillemots breeding in Greenland between 1841 and 2022 (*i.e.*, 181 years). The $\delta^{13}\text{C}$ values are corrected for the Suess Effect and phytoplankton fractionation (see Chapter 2, Section 3.3 for further details). Solid and dotted curves represent the best-fitting model detected from construction of GAMs and the confidence interval, respectively.

To better understand Hg cycling at the Arctic scale and its evolution over time, temporal trends of biotic Hg, such as ours, can then be compared to those of other environmental archives that informs about different processes in Arctic Hg cycling. Whereas feathers of Brünnich's guillemots informs about Hg contamination in marine ecosystems, marine sediment cores inform about Hg deposition and subsequent burial in deep ocean sediments. In Greenland, marine sediments cores highlighted a two-fold increase in Hg flux over the last 100 years (Asmund and Nielsen, 2000), which coincides with our rate of increase in seabirds. On the other hand, tree rings provide temporal insights into atmospheric deposition of Hg in Arctic terrestrial ecosystems (Clackett et al., 2018; Eccles et al., 2020; Ghotra et al., 2020).

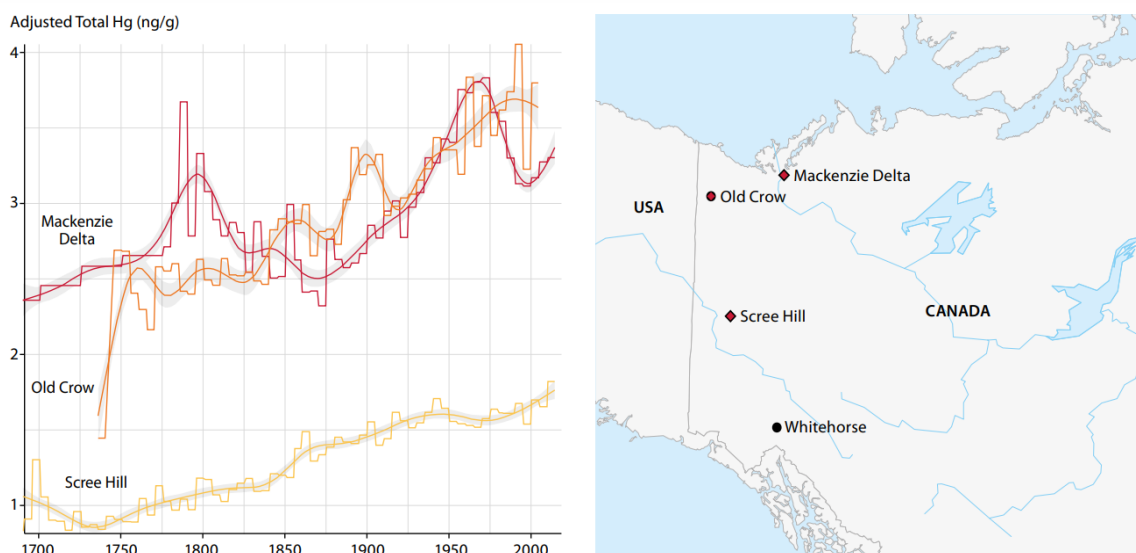


Figure 4.2. Temporal trends of gaseous Hg (Hg^0) concentrations in tree rings of white spruce (*Picea gluca*) at three locations in Canada, including the Mackenzie Delta (Northwest Territories; in red), Old Crow (Yukon, in orange) and Scree Hill (Yukon; in yellow). Extracted from AMAP, 2021. For further details, the reader is referred to the original studies (Clackett et al., 2018; Eccles et al., 2020; Ghotra et al., 2020).

In the Canadian Arctic, tree ring records revealed that atmospheric Hg concentrations increased since the 16th century, and that Hg started to accumulate in the Arctic simultaneously with the European Industrial Revolution (Figure 4.2; AMAP, 2021). The concordance between our biotic archives and other environmental archives, such as sediment cores and tree ring records, further confirms the global influence of anthropogenic emissions and re-emissions of Hg, even in the remote polar ecosystems such as the Arctic.

Trophic ecology. Over the last 181 years, feather $\delta^{13}\text{C}$ values decreased drastically and non-linearly in Brünnich's guillemots, with a 3.4 ‰ difference between the 1840s and the 2020s (Figure 4.1.B). This drastic temporal trend is consistent with similar findings reported in other marine species elsewhere. In the South Atlantic Ocean, a 1.4 ‰ and 3 ‰ declines in $\delta^{13}\text{C}$ values were observed in the muscle of tunas between 2000 and 2015 (Lorrain et al., 2020) and in feathers of sooty terns between the 1890s and the 2010s (Reynolds et al., 2019), respectively. In the Bering Sea, this was also the case in ringed seals, where bone $\delta^{13}\text{C}$ values declined by 2.3 ‰ from the 19th century until the present day (Szpak et al., 2018). Previously, declines in $\delta^{13}\text{C}$ values observed in marine consumers have been associated with those of primary productivity and carrying capacity of marine ecosystems (Hirons et al., 2001; O'Reilly et al., 2003; Schell, 2000), and even led to population declines in sub-Antarctic penguins (Hilton et al., 2006; Jaeger and Cherel, 2011). Our results thus suggest a global shift in phytoplankton productivity and ecosystem-wide changes in the structure of Arctic marine ecosystems over the last centuries.

In contrast, feather $\delta^{15}\text{N}$ values measured in Brünnich's guillemots showed a slight, non-linear increase over the study period (Figure 4.1.C). After a first increase from the 1870s to the 1950s, feather $\delta^{15}\text{N}$ values decreased slightly until the 2000s and appeared to increase again until the present days. Overall, this represented a slow increase of 0.21 ‰ over 181 years. This result agrees with similar findings reported in Arctic (Bond et al., 2015) and Pacific seabirds (Vo et al., 2011), and Arctic mammals (Desforges et al., 2022), where the absence of significant temporal trend in $\delta^{15}\text{N}$ values suggested the absence of dietary change over time. The observed Hg increase in the absence of dietary changes (as indicated by $\delta^{15}\text{N}$ values) surely reflects the impact of anthropogenic Hg on Arctic marine ecosystems in West Greenland. However, this long-term trend in $\delta^{15}\text{N}$ values could incorporate temporal variation in both the diet of Brünnich's guillemots and isotopic baselines. Isotopic baseline values (i.e., at the base of the food web) may vary over the seasons and years, due to changes in the cycling of nutrient sources, as well as changes in species composition and growth rates of phytoplankton communities, which result all together in changes in primary productivity (Cifuentes et al., 1988; Goering et al., 1990; Ostrom et al., 1997; Vizzini and Mazzola, 2003). One way to dissociate dietary changes from baseline changes over time would be to perform Compound-Specific Stable Isotope Analyses of Amino-Acids (CSIA-AA), to estimate the trophic position of Brünnich's guillemots (McMahon and Newsome, 2019; Ohkouchi et al., 2017), using source

and trophic AAs (see Chapter 2, Section 3.3.2 for further details), and investigate its temporal trend over the last centuries.

b) What is the influence of trophic ecology on the temporal trend of Hg contamination?

Multifactorial analyses were conducted to investigate the influence of the temporal trends of trophic proxies (*i.e.*, feeding habitat and diet) on the long-term trend of Hg contamination. The complete description of the statistical methodology is described in Paper 3. Briefly, Generalized Additives Models (GAM) were defined for each variable with year as smoother. Then, the residuals of each GAM were extracted to obtain time-detrended variables (*i.e.*, for Hg, $\delta^{13}\text{C}$ and $\delta^{15}\text{N}$). These latter were then tested in different combinations (see Paper 3, Table 2) and subject to model selections (with linear models).

Results from model selection revealed that the best model explaining temporal variation in time detrended Hg concentrations included both time-detrended $\delta^{13}\text{C}$ and $\delta^{15}\text{N}$ values (Table 2 in Paper 3). Over the entire period, Hg concentrations increased marginally with increasing $\delta^{13}\text{C}$ values (Figure 4.3.A) and significantly with increasing $\delta^{15}\text{N}$ values (Figure 4.3.B). However, the best model including both isotopic values explained only 17% of the total variation in Hg contamination, which suggests that other unknown factors mainly influenced long-term Hg contamination in Brünnich's guillemots from Greenland. As stated previously, isotopic variations at century timescales are not simply or solely driven by changes in feeding habitat and diet, but likely by changes at the base of food webs, driven by environmental and ecological processes (Fort et al., 2016). Thus, our results suggest that the temporal trend in Hg contamination in Arctic marine ecosystems is driven by both trophic factors linked to ecosystem-wide changes and other unknown factors.

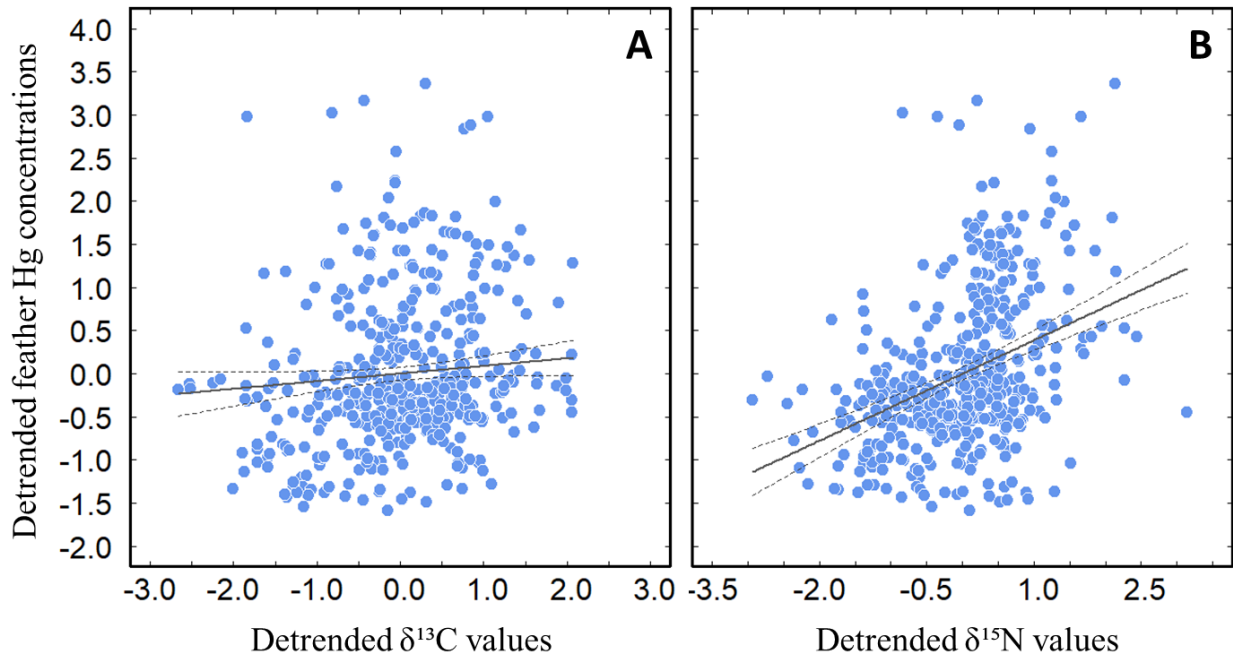


Figure 4.3. Relationship between time-detrended Hg concentrations and time-detrended stable isotope values: **(A)** $\delta^{13}\text{C}$ and **(B)** $\delta^{15}\text{N}$ values, in feathers of Brünnich’s guillemots breeding in West Greenland, between 1841 and 2022 (i.e., 181 years). All data (blue dots) were scaled. Solid and dashed lines represent the best-fitting linear model and the 95% confidence interval, respectively.

c) Which unknown factors?

The Arctic is particularly vulnerable to climate change and pollution and has experienced profound changes in all ecosystems (*i.e.*, terrestrial, freshwater and marine; AMAP, 2021a). Climate change affects Hg transport, chemistry and bioaccumulation in the Arctic, through a multitude of physical, biogeochemical, biological and ecological processes, both at local and regional scales (Figure 4.4; Chételat et al., 2022; McKinney et al., 2022).

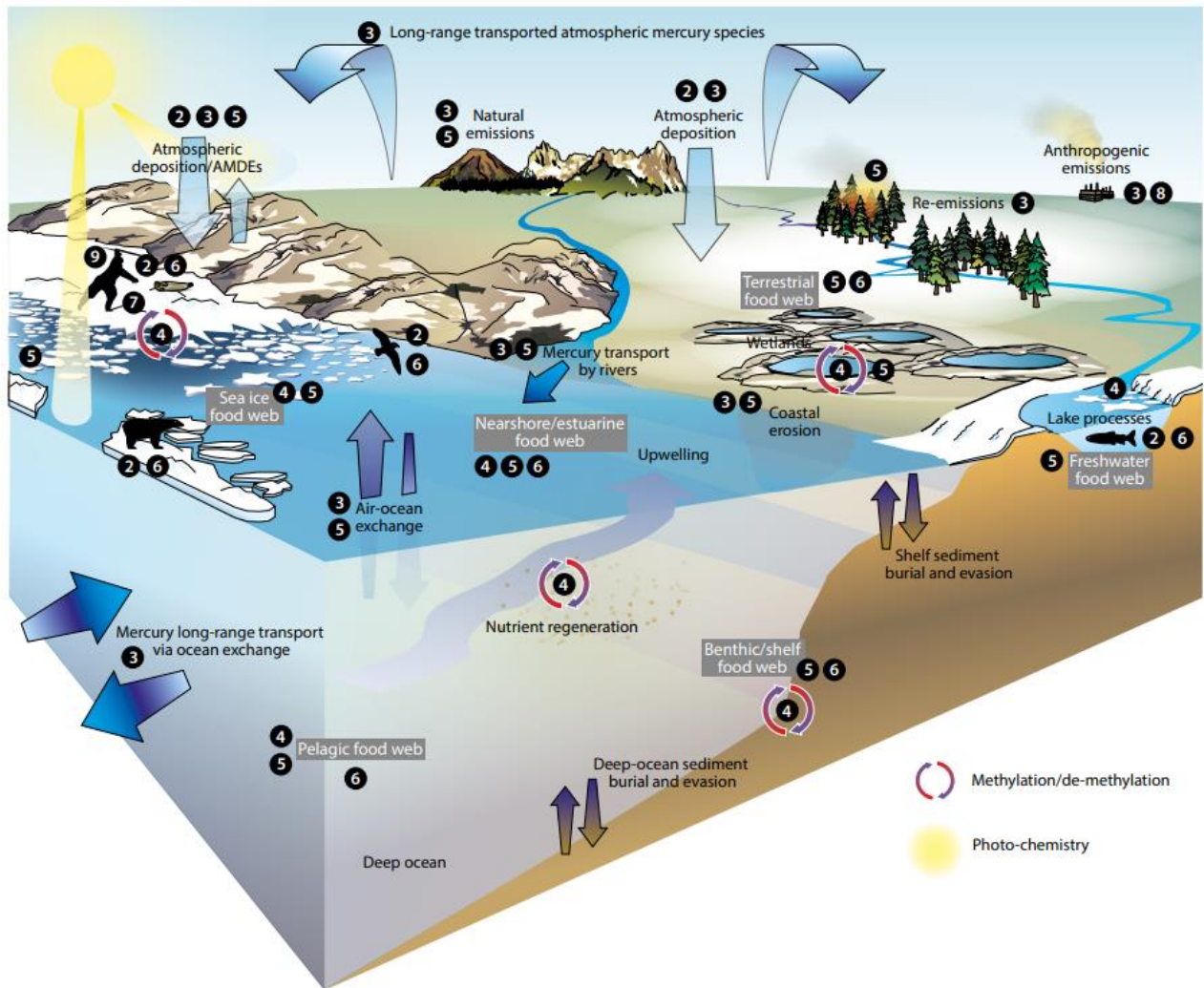


Figure 4.4. Conceptual representation of key components of Hg cycle in the Arctic. Extracted from AMAP (2021). Numbers indicate the chapters where information can be found in the assessment report.

One of the most striking impacts of climate change in the Arctic is sea-ice loss. **Sea ice** plays a central role in the biogeochemical cycle of Hg, in its bioavailability to marine wildlife and hence in the contamination of Arctic marine ecosystems, in several ways. First, sea ice may store Hg deposited from the atmosphere for long periods of time (Beattie et al., 2014). The melting of sea ice may thus represent a significant route of Hg deposition to the ocean (Schartup et al., 2020), where it can be assimilated by primary producers and transferred along Arctic food webs (Campbell et al., 2005). Second, sea ice influences Hg biogeochemistry by regulating air-sea exchanges of Hg species (DiMento et al., 2019) and controlling the photochemical transformation of Hg (Zheng et al., 2021). These processes further modify Hg bioavailability and the contamination of Arctic marine consumers. Finally, sea ice also drives indirectly Hg exposure in marine predators through ecological changes, such as changes in their

trophic ecology. In marine mammals, different contaminant patterns were observed in different sea-ice conditions and were related to prey shifts (Gaden and Stern, 2010; McKinney et al., 2009). In seabirds, changing ice conditions in northern Hudson Bay has resulted in prey shifts (Gaston et al., 2003) toward a higher consumption of less contaminated prey (i.e., capelin instead of Arctic cod; Braune et al., 2014; Gaston et al., 2012). On the other hand, in the Canadian High Arctic, higher Hg concentrations were measured in eggs of Brünnich's guillemots during years of heavier ice conditions (Mallory and Braune, 2018), and were related with a higher consumption of ice-associated prey (Cusset et al., submitted). Through all these processes (i.e., physical, chemical and ecological), sea ice influences Hg bioavailability and transfer in Arctic marine food webs and hence Hg exposure in Brünnich's guillemots, which occupy ice-covered waters while breeding in West Greenland. Thus, the drastic loss of sea-ice that has resulted from climate change over the last century is very likely to have influenced Hg exposure in Brünnich's guillemots and its temporal variation. Therefore, determining the simultaneous temporal trend of sea-ice concentrations in the region would clearly help to investigate the influence of sea ice loss on Hg transfer to Arctic predators over century-time scales. However, obtaining long-term sea-ice data could be challenging, as the satellites that have monitored the Arctic sea-ice cover only date back to the 1970s. Alternatively, sediments cores may provide a proxy of sea-ice extent over centuries and millennia in the Arctic (Belt et al., 2015; Brennan and Hakim, 2022), thanks to lipid biomarkers (i.e., Highly Branched Isoprenoids) that are specifically synthesized by Arctic primary producers and preserved in marine sediments (see Belt and Müller, 2013 for a review). Previous studies have reconstructed past sea-ice and oceanic conditions over the last thousand years, from marine sediment cores in West Greenland (Georgiadis et al., 2020; Limoges et al., 2020; Ribeiro et al., 2021). Although the spatial coverage from these sediments cores and our bird sampling may not be exactly the same, such temporal information could still be relevant to overlap sea-ice and Hg long term trends. Clearly, this would deserve further investigations.

In addition to sea ice, other environmental factors would deserve further research, as they may also contribute to the temporal variation of Hg contamination observed here. This includes **sea surface temperature**, **primary productivity** (i.e., chlorophyll *a*) and **climate indices**, such as the Northern Arctic Oscillation (NAO; Foster et al., 2019; Tartu et al., 2022). However, Hg exposure in Arctic seabirds is influenced by weather patterns over multiple years, with time-lags between the variation in environmental parameters and the subsequent biotic Hg concentrations (Foster et al., 2019). For example, egg Hg concentrations in Brünnich's

guillemots were influenced by summer NAO and summer temperature 4 years before, local snowfall 5 years before and sea-ice concentrations 7 years before, presumably due both to deposition but also release or access to Hg already stored in Arctic archives (*e.g.*, glaciers and permafrost; Dastoor et al., 2022).

The clearer evidence of the effects of current climate change on Hg cycling in the Arctic is Hg transport from terrestrial reservoirs, including the **melting of glaciers and icecaps** and **permafrost thaw** (Chételat et al., 2022; Dastoor et al., 2022; Hawkings et al., 2021; St. Pierre et al., 2018). Recently, a study conducted on polar bears from the Barents Sea showed that the increase in Hg contamination over the last two decades was attributed to re-emissions of previously stored Hg from thawing sea ice, glaciers and permafrost (Lippold et al., 2020). Glacier melt represents a large source of both water and Hg to downstream ecosystems (St Pierre et al., 2019; Zdanowicz et al., 2018). Glacier meltwaters include two principal sources of Hg: (i) legacy and current Hg archived in glacial ice and snow, and (ii) geogenic Hg transported by meltwaters as they flow downstream (Zdanowicz et al., 2013). On the other hand, climate change (*i.e.*, warming) is predicted to continue enhancing Hg mobilization through permafrost thaw, which has also stored both geogenic and anthropogenic (both legacy and current) Hg since the last centuries or millennia (Schaefer et al., 2020; St. Pierre et al., 2018). In this context, we could hypothesize that Hg exposure of Brünnich's guillemots in West Greenland could be largely impacted by glacier melt and permafrost thaw. Greenland is covered by 80% ice and represents one of the largest icecaps in the world (Rastner et al., 2012). The melting of Greenland glaciers could likely release Hg in fjords and surrounding coastal waters, and enhance Hg accumulation in surrounding marine ecosystems (if conditions are favourable to Hg methylation and uptake). Similarly, the melting of permafrost soils in Greenland may also influence the temporal trend of Hg contamination observed here. Through the analysis of Hg isotopes, future research could determine the origin of Hg (*e.g.*, marine or terrestrial) measured in feathers of Brünnich's guillemots and investigate associated long-term trends and potential shifts in Hg sources over the last centuries.

1.4. Conclusions and perspectives

This work provides a unique assessment of Hg contamination in Arctic marine ecosystems from West Greenland by using Brünnich's guillemots as bioindicators. Thanks to the feather collection of museum-held and free-living birds, this represents the longest timeseries for biotic

Hg to date (*i.e.*, 181 years). Over the two last centuries, our results revealed a 3.5-fold increase in feather Hg concentrations, which was consistent with the temporal trends observed in other Arctic predators (seabirds and marine mammals), as well as other paleoarchives (*i.e.*, tree rings and sediments cores). Clearly, this is further evidence of the impact of anthropogenic Hg on Arctic marine ecosystems. Although trophic ecology was key to understanding the temporal variation in Hg, our results suggest that trophic factors have little direct influence on the long-term Hg trend of Brünnich's guillemots, and that other unknown factors, including ecosystem-wide changes, drive Hg contamination of Arctic marine food webs over the last centuries. Further research is now needed to better understand the drivers of the temporal trend in Hg contamination at the century scale, including environmental factors such as sea ice concentrations, warming temperatures and primary productivity. Still, our work provides further evidence that long-term monitoring is fundamental to evaluate the global impacts of Hg pollution and to guide future directions of international regulatory policies.

As this work is still in progress, further temporal investigations could also focus, at a finer scale, on the last decades, which have been extensively monitored thanks to international sampling networks (*e.g.*, ARCTOX program) and for which environmental parameters are available from satellite measurements. Despite a general increase observed over the last 189 years, our temporal trends in feather Hg concentrations and $\delta^{15}\text{N}$ values since the 1970s show more complex patterns at the finer scale, with fluctuating values over time (Figure 4.5). The next step would be to explore the drivers of these successive oscillations in Hg contamination and whether they are associated with climate change in the Arctic.

Moreover, in this section, we presented long-term trends of Hg contamination in West Greenland, a region that included most of our adult sampling (93%). However, several individuals were also collected in East Greenland ($n=21$) and the associated temporal trends (from 1833 to 1936) seem to show different patterns than those observed in West Greenland, particularly for $\delta^{15}\text{N}$ values (see Figure A3). Further data analyses are now needed to allow comparison between these two regions in Greenland and investigate spatial differences in long-term Hg trends in the Arctic.

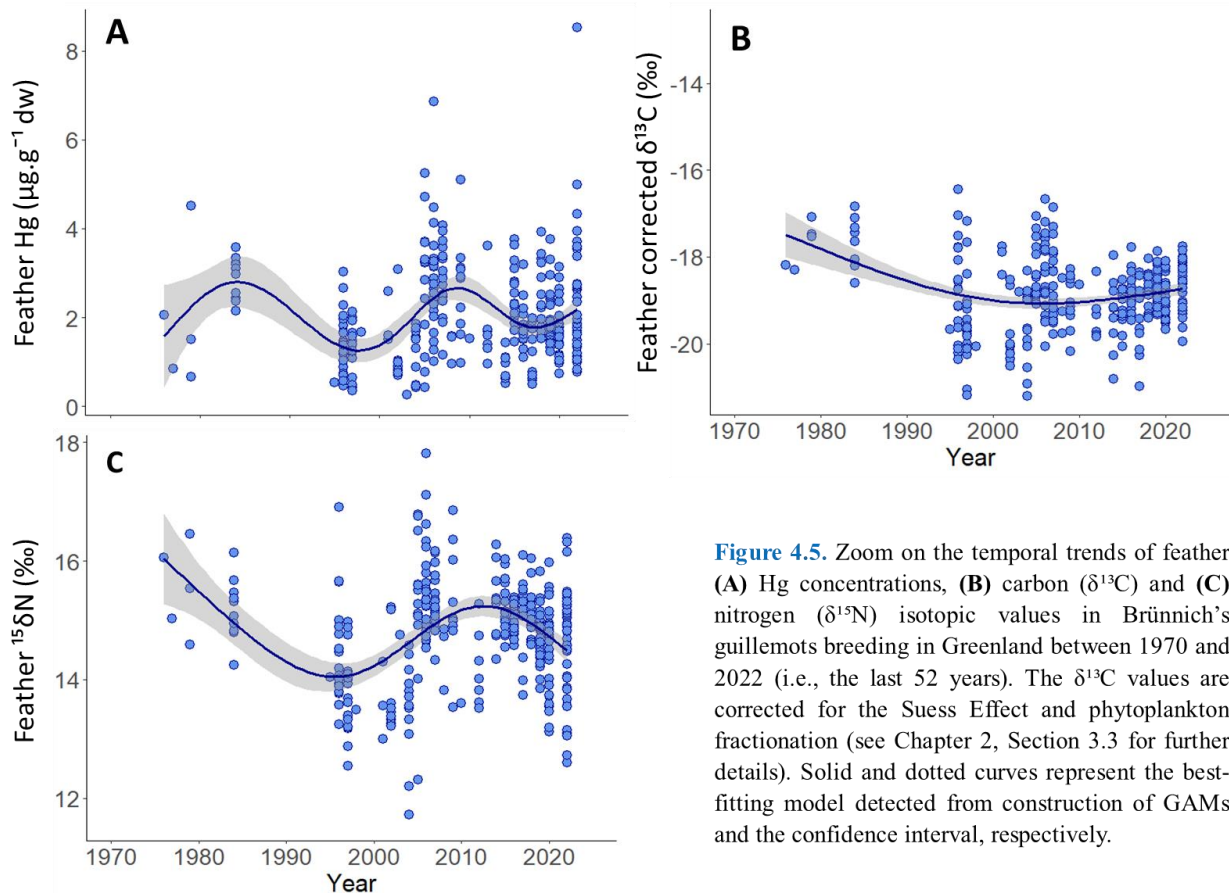


Figure 4.5. Zoom on the temporal trends of feather (A) Hg concentrations, (B) carbon ($\delta^{13}\text{C}$) and (C) nitrogen ($\delta^{15}\text{N}$) isotopic values in Brünnich's guillemots breeding in Greenland between 1970 and 2022 (i.e., the last 52 years). The $\delta^{13}\text{C}$ values are corrected for the Suess Effect and phytoplankton fractionation (see Chapter 2, Section 3.3 for further details). Solid and dotted curves represent the best-fitting model detected from construction of GAMs and the confidence interval, respectively.

1.5. Summary

- Brünnich's guillemots act as bioindicators of Hg temporal trends in Arctic marine ecosystems from West Greenland.
- Feather Hg concentrations **increased non-linearly** over 181 years ($\times 3.5$).
- The observed **Hg increase** in the **absence of dietary changes** (as indicated by $\delta^{15}\text{N}$ values) surely reflects the **impacts of anthropogenic Hg** on Arctic marine ecosystems.
- **Trophic position** ($\delta^{15}\text{N}$) and **feeding habitat** ($\delta^{13}\text{C}$) influenced Hg long-term trend, but **only** explained **17%** of temporal variation in Hg, suggesting trophic factors linked to ecosystem-wide changes, and unknown factors.
- **Climate change** may influence Hg long-term trends in various ways.

2. Tropical marine food webs



Ascension Island, South Atlantic Ocean

Part 1: Retrospective investigation of Hg contamination: century time series

2.1. Context and objectives

Ascension Island (07°57' S, 14°24' W) is an isolated 97 km² volcanic island in the tropical South Atlantic Ocean (see Chapter 3, Figure 3.3 for a map). It accommodates the largest breeding population of sooty terns in the entire Atlantic Ocean, containing on average >200,000 pairs (Hughes et al., 2012). Currently, they nest on bare ground across the Wideawake Fairs – an Important Bird Area (IBA SH009) – at two Nature Reserves (NRs) called Mars Bay and Waterside Fairs. As epipelagic seabirds, sooty terns feed on small pelagic fish and squid caught at or near the ocean surface (Ashmole, 1963a; Reynolds et al., 2019). Globally, sooty terns are listed as of «Least Concern» in the IUCN Red List of Threatened Species. Yet, the population from Ascension Island has drastically declined by approximately 84% between the 1960s and 1990s from a peak of approximately two million birds (Hughes et al., 2017). Many factors may have contributed to this precipitous decline, including the depletion of food resources and predation by introduced species such as domestic cats (*Felis silvestris catus*), black rats (*Rattus rattus*) and common mynas (*Acridotheres tristis*) (Reynolds et al., 2019 and references therein). To better understand the drivers of this population decline, Reynolds and colleagues (2019) investigated long-term trends in feeding ecology of sooty terns from Ascension Island from the 1890s to the 2010s, by using feathers of both museum and free-living birds. Over this period, they highlighted long-term changes in both feeding habitat and diet, as indicated by the declines in feather $\delta^{13}\text{C}$ and $\delta^{15}\text{N}$ values since the 1890s, respectively. Their results revealed that the dramatic decline in the size of the breeding population on Ascension Island coincided with a dietary shift from predominantly teleost fish (from the 1890s to the 1940s) to squid (from the 1970s to the 2010s).

The present work builds on previous long-term investigations of Reynolds et al. (2019), by extending the recent time series by an additional decade (*i.e.*, the 2020s), and providing feather-derived Hg concentrations. More specifically, the aim here was three-fold:

(2) Document the temporal trend of feather Hg concentrations in Ascension Island sooty terns between the 1890s and the 2020s.

(3) Investigate the influence of their trophic ecology (reflected by $\delta^{13}\text{C}$ and $\delta^{15}\text{N}$ values) on this temporal trend.

(4) Compare Hg contamination before and after the population collapse.

As for other remote oceanic regions, we predict that there will be a general increase in feather Hg concentrations to the present day, linked to the previously documented changes in their diet and foraging behaviours.

2.2. Result and discussion

Body feathers were sampled from 220 sooty terns from seven different decades, spanning 145 years (*i.e.*, 1876-2021), including feathers from skins (n=134) held in 10 natural history museum collections (see details in [Paper 4](#), [Table S2](#)) and free-living birds (n=86) sampled in the 2000s, 2010s and 2020s. Details on sample sizes, decades, feather Hg concentrations and stable isotope values (mean \pm SD, min–max) are provided in [Table 1](#) in [Paper 4](#). Temporal trends of feather Hg concentrations, $\delta^{13}\text{C}$ and $\delta^{15}\text{N}$ values are provided in [Figure 4.6](#). The reader is referred to [Paper 4](#) in Annexes for the complete methodological description, including statistical analyses.

Few individuals were available prior to the 1920s, leading to high variability and large uncertainty in temporal trends of Hg concentrations before the 1920s ([Figure 4.6.A](#)). Thus, interpretation of GAM temporal trends could only be carried out from the 1920s onward. Therefore, results presented in this section mainly focus on the period between the 1920s and the 2020s. Detailed output from GAMs describing temporal variations in Hg, $\delta^{13}\text{C}$ and $\delta^{15}\text{N}$ values are provided in [Paper 4](#) ([Table S7](#)).

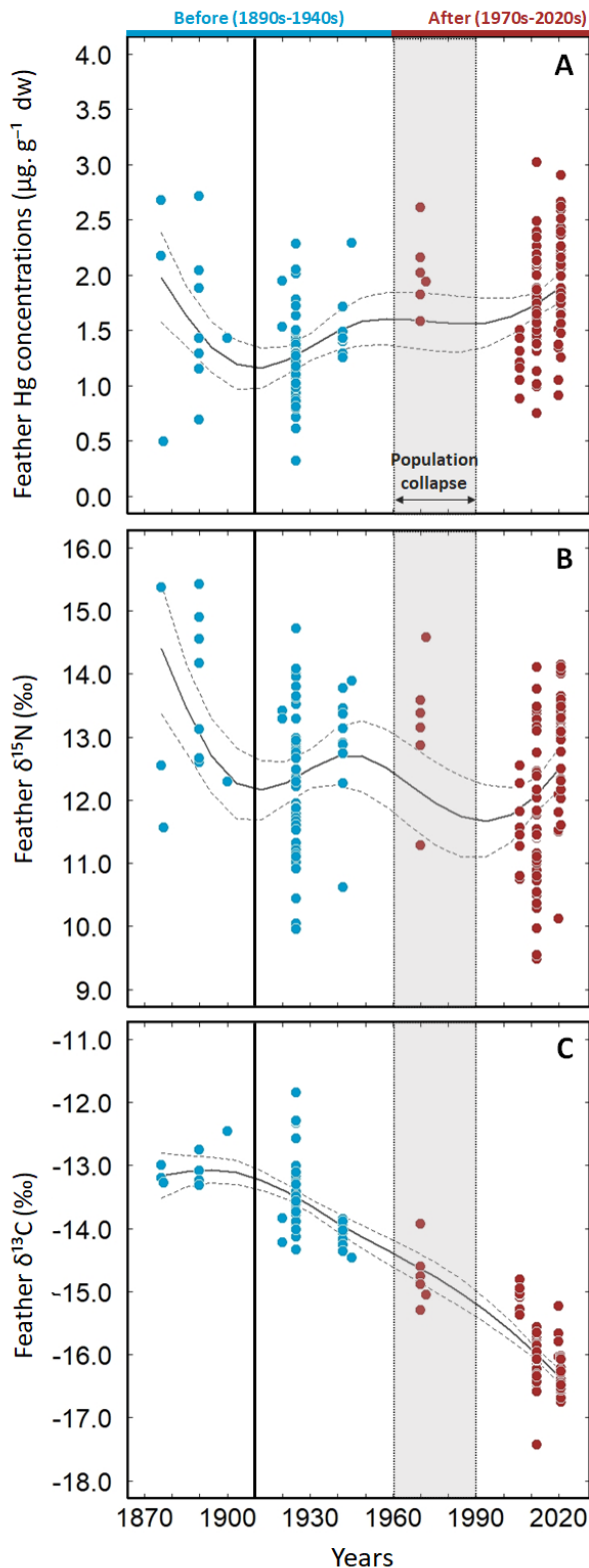


Figure 4.6. Long-term trends in (A) feather Hg concentrations, (B) nitrogen ($\delta^{15}\text{N}$) and (C) carbon ($\delta^{13}\text{C}$) isotopic values of sooty terns breeding on Ascension Island (South Atlantic Ocean) between 1876 and 2021 (*i.e.*, over 145 years). The $\delta^{13}\text{C}$ values are corrected for the Suess Effect and phytoplankton fractionation. The grey area represents the transition between the period before (blue) and after (red) population collapse that occurred between the 1960s and the 1990s (see Reynolds et al., 2019 for further details). Solid and dotted lines represent the best-fitting model detected from construction of GAMs and the confidence interval, respectively. To the right of the vertical solid line at 1910 is the period of realistic interpretation. For further details, the reader is referred to the Material and Methods and Discussion in [Paper 4](#).

a) Long-term trend in foraging ecology: an update

Reynolds et al. (2019) found a linear decreasing trend in both feather $\delta^{13}\text{C}$ and $\delta^{15}\text{N}$ values from the 1890s to the 2010s. In contrast, we did not detect any further significant linear trend in $\delta^{15}\text{N}$ values,

by extending the time series with the inclusion of feathers obtained in 2020 and 2021. Instead, we detected a non-linear trend (Figure 4.6.B; GAM, $p < 0.0001$, deviance explained was 0.13), which followed three distinct phases: (i) a 5.8% increase between the 1900s and the 1940s (i.e., +0.75 ‰), (ii) a 10.4% decrease between the 1940s and the 2000s (−1.34 ‰), and (iii) a 10.4% increase from the 2000s to the present day (i.e., +1.33 ‰; Paper 4, Tables 1 and S6). The addition of the most recent decade in the time series clearly highlights the importance of such long-term monitoring, by revealing recent and unpredictable patterns in the foraging ecology of sooty terns. These long-term variations in feather $\delta^{15}\text{N}$ values could reflect variations in seabird diet over time (Reynolds et al., 2019), but also changes in the isotopic baseline (McMahon et al., 2013a). Isoscapes of $\delta^{15}\text{N}$ can vary seasonally due to changes in primary productivity, which stem from variation and cycling of nutrient sources, as well as changes in species composition and growth rates of phytoplankton (Cifuentes et al., 1988; Goering et al., 1990; Ostrom et al., 1997; Vizzini and Mazzola, 2003). The changing $\delta^{15}\text{N}$ isoscape could then have cascading effects on feather isotopic values of seabird consumers at upper trophic levels and hence, drive the temporal variations in their trophic position. One way to disentangle these hypotheses would be to perform compound-specific stable isotope analysis of amino acids (CSIA-AA) (McMahon and Newsome, 2019), which would help distinguish the specific signatures of the baseline («source» $\delta^{15}\text{N}$ -AAs) and the diet-consumer transfer («trophic» $\delta^{15}\text{N}$ -AAs), and hence elucidate the «true» trophic position of sooty terns over time.

Extending the results of Reynolds et al. (2019), corrected $\delta^{13}\text{C}$ values (see Chapter 2, Section 3.3 for further details) exhibited a similar and even stronger decreasing trend to the present day (Figure 4.6.C; GAM, $p < 0.001$, deviance explained was 0.91), with a 2.85 ‰ decline between the 1920s and the 2020s. This represents a 3.24 ‰ decline when considering the trend between the 1890s and the 2020s. A comparable decrease in $\delta^{13}\text{C}$ values over time was previously described in thin-billed prions (*Pachyptila belcheri*) in the Southern Ocean (Cherel et al., 2014; Quillfeldt et al., 2010), and was interpreted as a result of latitudinal change in their moulting area, switching from sub-Antarctic to Antarctic waters over more than 90 years (1913-2005). Similarly, moulting areas of Ascension sooty terns could have changed spatially over time but, to date, their post-breeding migrations have only been studied using geolocators between 2011 and 2015 (Reynolds et al., 2021) and far more research is required. Continuing such tracking work over the next few decades would allow trophic ecology of sooty terns to be directly related to long-term changes in their spatial distribution in the South Atlantic Ocean.

Carbon isotope values reflect phytoplankton productivity in aquatic environments (DeNiro and Epstein, 1978; France, 1995; Hobson, 1999). Declines in $\delta^{13}\text{C}$ values have been associated with those

in primary productivity, and hence with the carrying capacity of ecosystems (Hirons et al., 2001; O'Reilly et al., 2003; Schell, 2000), and ultimately with declines of penguin (Spheniscidae) populations, for example, in the sub-Antarctic region (Hilton et al., 2006; Jaeger and Cherel, 2011). In the South Atlantic Ocean, a 1.38 ‰ decline in $\delta^{13}\text{C}$ values was observed in the muscle of tuna species in the between 2000 and 2015, suggesting a global shift in phytoplankton community structure (Lorrain et al., 2020). This coincides with the 1.24 ‰ decline we observed in feather $\delta^{13}\text{C}$ values of Ascension sooty terns between the 2000s and the 2020s in the same region. So, the global 2.85 ‰ decline in feather $\delta^{13}\text{C}$ values in this study (between the 1920s and the 2020s) could likely result from a change in phytoplankton productivity in the surrounding tropical marine ecosystems.

b) Long-term trend in Hg contamination

Comparison with other sites and species

Overall, our results are consistent with the range of average Hg concentrations observed for sooty terns elsewhere, such as in the Mozambique Channel ($0.2 \mu\text{g}\cdot\text{g}^{-1}$; Jaquemet et al., 2008; Kojadinovic et al., 2007), in the Pacific Islands ($0.8 \mu\text{g}\cdot\text{g}^{-1}$; Burger et al., 1992), in the Seychelles ($1.2 \mu\text{g}\cdot\text{g}^{-1}$; Ramos and Tavares, 2010) and in Puerto Rico ($2.6 \mu\text{g}\cdot\text{g}^{-1}$; Burger and Gochfeld, 1991). However, sooty terns from Ascension Island exhibit Hg concentrations in the upper part of this range ($1.5 \mu\text{g}\cdot\text{g}^{-1}$). Among tropical birds, feather Hg values were intermediate compared with other sternids at other locations, such as brown noddies (*Anous stolidus*) in Hawaii ($0.6 \mu\text{g}\cdot\text{g}^{-1}$; Burger et al., 2001) and bridled terns (*Onychoprion anaethetus*; $1.4 \mu\text{g}\cdot\text{g}^{-1}$) and roseate terns (*Sterna dougallii*) in Puerto Rico ($2.3 \mu\text{g}\cdot\text{g}^{-1}$; Burger and Gochfeld, 1991). Low Hg contamination in sooty terns is consistent with their foraging ecology that largely depends on small epipelagic fish and invertebrates from surface waters (Ashmole, 1963a). Epipelagic prey exhibit lower Hg concentrations than mesopelagic and benthic prey (Chouvelon et al., 2012; Monteiro and Furness, 1997; Ochoa-Acuña et al., 2002), mainly because Hg methylation occurs in mesopelagic waters (Blum et al., 2013; Bowman et al., 2020; Cossa et al., 2009; Wang et al., 2018).

Long-term Hg trend in Ascension Island

Since the 1920s, Hg concentrations increased non-linearly with time (GAM, $p < 0.0001$, deviance explained was 0.25), following three distinct phases (Figure 4.6.A). First, Hg concentrations increased by 62.9% between the 1920s and the 1970s. This increase was likely facilitated by growing

Hg emissions during the Industrial Era with developing human activities, such as the Gold Rush, the burning of coal and intensifying manufacturing efforts to meet the military demands of World War II (Thompson et al., 1993a). Then, Hg concentrations exhibited an unclear pattern of change between the 1970s and the 2000s. Although Hg concentrations appeared to stabilize during this phase, this latter included a very low number of available samples *per* year with a high variability, implying a large uncertainty in the generated models. Thus, whether Hg concentrations really remained stable between the 1970s and the 2000s is difficult to confirm. Finally, Hg concentrations increased by 62.8% from the 2000s onwards, despite strong regulations restricting Hg emissions since the 1990s in the Northern Hemisphere and 2017 globally (Minamata Convention on Mercury). Overall, Hg concentrations were 58.9% higher in the 2020s than in the 1920s. This, together with other recently detected increases (*e.g.*, Bond et al., 2015; Carravieri et al., 2016; Tartu et al., 2022) raises concerns for potential consequences on wildlife health.

Comparison with temporal trends of Hg elsewhere

Few studies (n=14) have investigated long-term Hg trends in seabirds by using feathers as archives (Table S1 in Paper 4). Most have focussed on temperate (*e.g.*, Appelquist et al., 1985; Thompson et al., 1993, 1992) and polar regions (*e.g.*, Bond et al., 2015; Carravieri et al., 2016; Scheifler et al., 2005). Only two have focussed on subtropical regions, in the Azores (Monteiro and Furness, 1997) and Pacific islands (Vo et al., 2011). Monteiro and Furness (1997) measured a 1.1% increase in Hg contamination *per* year between the 1880s and the 1990s in epipelagic Cory's shearwaters (*Calonectris borealis*) that share similar habitat with sooty terns, albeit in the North Atlantic Ocean. This was a stronger annual increase than that of 0.37% that we found if considering simply a linear trend. Despite different temporal coverage between studies, it appears that Hg transfer to predators has increased more slowly in the South than in the North Atlantic Ocean. Similar spatial disparities in Hg contamination between hemispheres were observed in tunas (Médieu et al., 2022), probably as a result of inorganic Hg deposition among distinct oceanic regions and spatial differences in seawater Hg concentrations at the base of the food web. Mercury deposition could be higher in the subtropical than in the tropical Atlantic Ocean for two reasons. First, anthropogenic Hg was historically mainly emitted by industrialized countries from the Northern Hemisphere (Pacyna et al., 2006). Secondly, Hg is globally distributed by atmospheric circulation (Selin, 2009), which includes successive atmospheric circulation cells from the pole to the tropics, namely the Polar, the Ferrel and the Hadley Cells. As such, Hg emitted in Europe, for example, could be more easily deposited in the subtropical

North Atlantic Ocean (*i.e.*, one circulation cell away) than in the tropical South Atlantic Ocean (*i.e.*, two circulation cells away).

c) Drivers of Hg contamination over time

Despite the temporal mismatch between feather Hg and stable isotopes (Bond, 2010), we assumed that both trophic ecology and Hg contamination are comparable over time, allowing to investigate the influence of the temporal variation of trophic ecology on the temporal variation of Hg contamination. Knowing this, our results revealed that the trophic ecology of sooty terns influenced significantly their Hg contamination over time. The best model explaining feather Hg contamination included both $\delta^{13}\text{C}$ and $\delta^{15}\text{N}$ values (Table 2 in Paper 4). Feather Hg concentrations decreased with increasing $\delta^{13}\text{C}$ values and increased with $\delta^{15}\text{N}$ values (Figure 4.7).

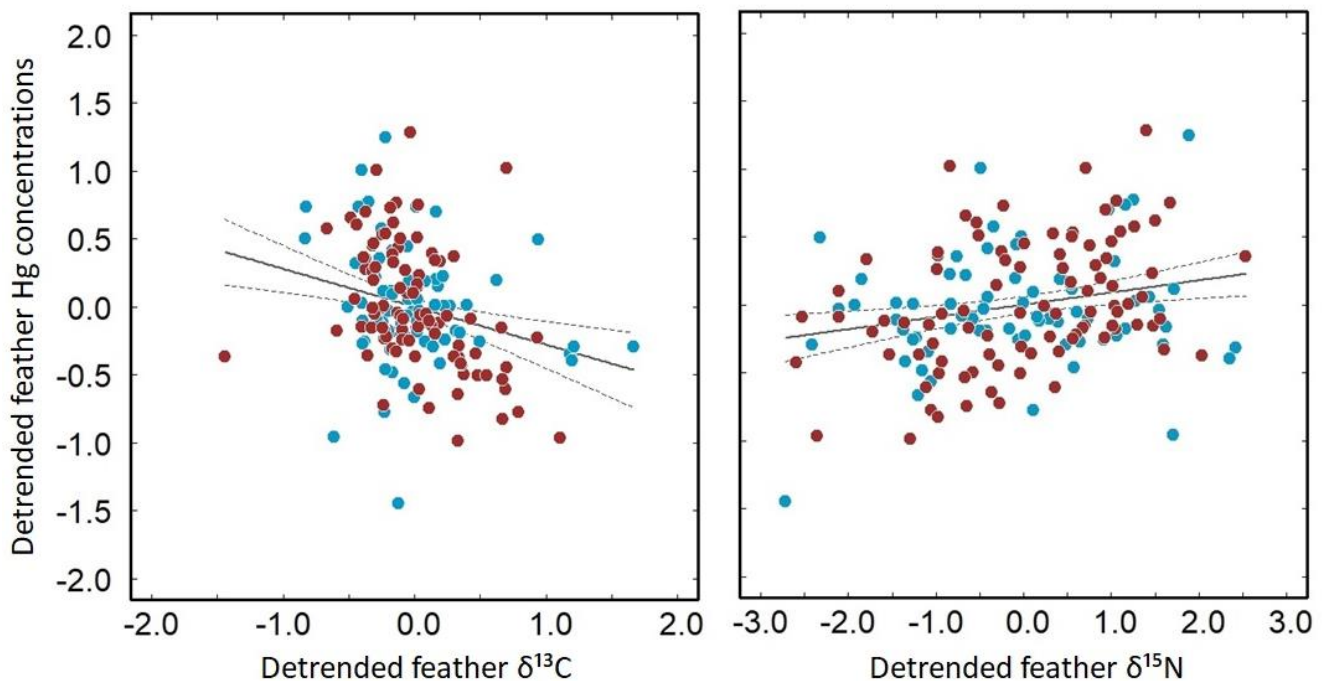


Figure 4.7. Relationship between time-detrended Hg concentrations and time-detrended stable isotope values in feathers of adult sooty terns breeding on Ascension Island in the South Atlantic Ocean between 1876 and 2021 (*i.e.*, over 145 years). The tern population collapsed between the 1960s and the 1990s (see Reynolds et al., 2019 for further details), with data before- (in blue) and after (in red) the collapse. All data were scaled. Solid and dashed lines represent the best-fitting linear model and the 95% confidence interval, respectively. For further details, the reader is referred to Paper 4.

This indicates that the temporal increase in feather Hg concentrations was associated with the strong decrease in $\delta^{13}\text{C}$ values and fluctuating $\delta^{15}\text{N}$ values observed over the past century. However, the best model including both isotopic values explained only 14% of the total variation in Hg contamination, which suggests that other unknown factors (discussed below in the next section) also influenced long-term Hg contamination in sooty terns from Ascension Island. Although the temporal mismatch may be involved to a certain extent, this is consistent with previous studies on other species (Bond et al., 2015; Carravieri et al., 2016; Vo et al., 2011). In addition, isotopic variations at the century scale are not simply or solely driven by changes in feeding habitat and trophic position, but likely by changes at the base of the food web, which are driven by several environmental and ecological processes (see previous section above). Therefore, our results suggest that the temporal trend in Hg transfer to predators in the South Atlantic Ocean was driven by trophic factors linked to ecosystem-wide changes, and other unknown factors.

d) Influence of climate change and fisheries on tropical Hg contamination

Reynolds et al. (2019) highlighted the importance of increasing sea surface temperatures (SST) and tuna extraction by fisheries in explaining long-term changes in the trophic ecology of sooty terns breeding on Ascension Island. Sooty terns are heavily reliant on large schools of surface-swimming tunas, such as yellowfin (*Thunnus albacares*) and skipjack (*Katsuwonus pelamis*) tuna, to drive their common prey to the ocean surface, where many tropical seabirds forage in so-called « facilitated foraging » (Ashmole, 1963a; Au and Pitman, 1986; Ballance and Pitman, 1999; Maxwell and Morgan, 2013). Sooty terns are therefore susceptible to any over-exploitation and major declines in these associated species (Cullis-Suzuki and Pauly, 2010; Juan-Jordá et al., 2011). Nonetheless, under climate change, and specifically with changes in temperatures and salinity, global abundances of tunas are predicted to increase in tropical waters (Erauskin-Extramiana et al., 2019). Specifically, Ascension Island is predicted to become more suitable for several tuna species, including sooty tern associates (Townhill et al., 2021). Climate change and fishing pressure are therefore likely to impact Hg contamination in sooty terns, and hence in tropical marine ecosystems, even though the direction and the extent of these impacts are difficult to predict precisely.

Since seabird Hg contamination is heavily associated with their foraging ecology, climate change and fishing pressure also have indirect effects on Hg contamination through dietary changes (prey switching), species' interactions and transfer through marine food webs (biotic factors). For example, MeHg concentrations increased in marine fish as a result of dietary shifts initiated by overfishing and

with increasing SST (Schartup et al., 2019). Other environmental factors can also influence seabird Hg contamination, such as Hg transport, deposition, uptake and methylation rates in the ocean (Krabbenhoft and Sunderland, 2013). Mercury is mainly deposited in oceans by atmospheric fallouts (Eagles-Smith et al., 2018). Although Ascension Island is isolated, with its nearest neighbour, St Helena, located more than 1,300 km away, it is highly unlikely that Hg contamination results from local anthropogenic sources. As a volcanic island, Hg contamination might alternatively result from local geological activities, but there is no record of volcanic activity of Ascension Island over the last 500 to 1000 years (Preece et al., 2018). Instead, Hg contamination in sooty terns likely results from global Hg transport. In the ocean, sources of MeHg are multiple: methylation can occur in the sediments of continental shelves (Hammerschmidt and Fitzgerald, 2006) and estuaries (Heyes et al., 2006), within the water column (Cossa, 2013; Hammerschmidt and Bowman, 2012) and at deep-ocean hydrothermal vents (Bowman et al., 2016, 2015). Mercury methylated through these processes can then be widely distributed by ocean currents, both spatially (global ocean circulation) and vertically (vertical mixing and upwellings) (Mason et al., 2012b). Climate change will likely influence all of these processes and could ultimately influence sooty tern contamination on different temporal and spatial scales. Methylation rate and bioavailability of Hg are also affected by other processes such as acidification, eutrophication and/or deoxygenation (Clayden et al., 2013; Gong et al., 2021; Jardine et al., 2013; Zhang et al., 2021). For instance, oxygen-depleted zones (*i.e.*, «dead zones») are increasing with increasing ocean temperatures (Breitburg et al., 2018; Watson, 2016). Mercury methylation is substantially enhanced in low-oxygen zones in the ocean, that at low latitudes (*i.e.*, tropics) are the most vulnerable to further deoxygenation (Gruber, 2011). Tropical oceans should thus be a priority for further studies of Hg contamination, especially in the context of climate change. Further research should focus on Hg stable isotopes to disentangle the different environmental and ecological factors involved, by identifying Hg sources and exploring the associated biogeochemical and trophic processes in the different compartments of tropical marine ecosystems (Renedo et al., 2020a).

e) Was Hg contamination involved in the population decline of sooty terns in Ascension Island?

On Ascension Island, sooty terns suffered a 80% population collapse between the 1960s and the 1990s (Hughes et al., 2017). Reynolds et al. (2019) attributed this in part to a dietary shift from predominantly fish in the 1890s to the 1940s prior to the decline, to predominantly squid in the 1970s to the 2010s after it. With additional feather samples from the 2020s, our results revealed that isotopic

niches, during the moulting period, were different between the two periods (Figure 4.8.B). There was a significant difference in foraging habitat, with ~ 2.5 ‰ lower $\delta^{13}\text{C}$ values after than before the population collapse (agreeing with $\delta^{13}\text{C}$ values documented in Reynolds et al., 2019), but with an equivalent trophic position ($\delta^{15}\text{N}$ values).

Mercury concentrations were 38.8% higher after ($1.79 \pm 0.48 \mu\text{g}\cdot\text{g}^{-1}$) than before ($1.29 \pm 0.46 \mu\text{g}\cdot\text{g}^{-1}$) the population collapse (Figure 4.8.A). These results are consistent with previous temporal comparisons, in which Hg concentrations have increased between historical and contemporary time periods in marine environments worldwide (Carravieri et al., 2016; Furness et al., 1995; Vo et al., 2011). During the period of population collapse, all Hg concentrations were relatively high with low variability, likely reflecting a generally high contamination in sooty terns. In comparison, there was more variability before and after the period of population collapse, probably because of slight differences in either diet or the proportions of different prey species constituting the diet. Given measured levels of Hg in sooty tern feathers – although elevated after the population collapse – it seems unlikely that Hg contamination drove the population decline of sooty terns on Ascension Island. Indeed, the extent of Hg contamination detected was below severe toxicity thresholds for seabird feathers ($4\text{-}10 \mu\text{g}\cdot\text{g}^{-1}$; Ackerman et al., 2016; Chastel et al., 2022). However, information on selenium (Se) levels in sooty terns might be relevant to determine the risk related to low concentrations of Hg, as Se plays a protective role against Hg toxicity (Goutte et al., 2014). Further insights into the causes of the population decline of Ascension Island may be provided by additional analyses of other trace elements, such as cadmium (Cd). Cadmium is present in high concentrations in cephalopods and cephalopod predators (Bustamante et al., 1998).

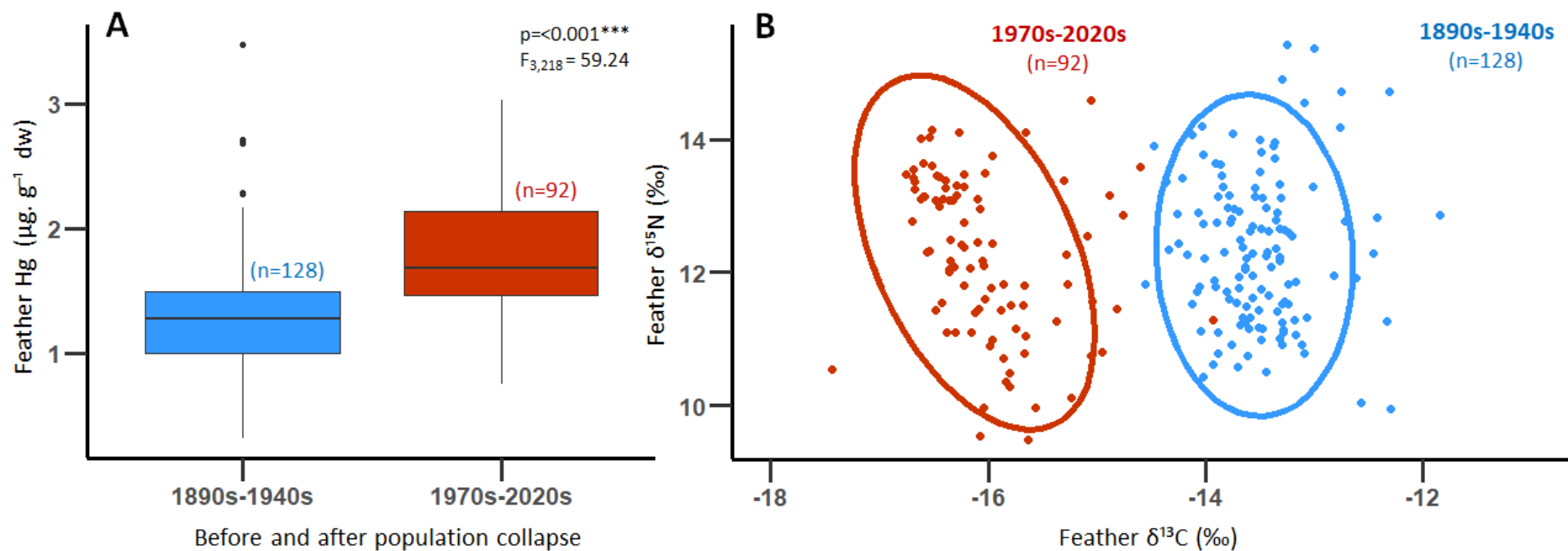


Figure 4.8. Difference in (A) Hg concentrations and (B) isotopic niches ($\delta^{13}\text{C}$ and $\delta^{15}\text{N}$ values) from feathers of adult sooty terns relative to the population collapse on Ascension Island between the 1960s and the 1990s. Points, ellipses (including 90% of the data) and bars in blue and red are before (n=128) and after (n=92) the population collapse, respectively. n indicates the sample sizes. Boxplots indicate median values (midlines), errors bars (whiskers) and outliers (black dots).

Because it has deleterious impacts on calcium metabolism, Cd may impact the reproduction of cephalopod-eating seabirds, such as sooty terns (Sarkar et al., 2013; Elinder, 1992). The switch from a fish- to a cephalopod-diet, simultaneously to the population decline, may have resulted in increasing Cd exposure, potentially leading to impaired reproduction in sooty terns from Ascension Island. This hypothesis could be verified by analysing blood and internal tissues (particularly kidneys) of sooty terns that might have been preserved over time, but individuals sampled prior the collapse might be difficult to obtain. Still, investigating contamination by other pollutants (such as pesticides or plastics) would undoubtedly allow further insights into the risks and demographic stressors for this population, but our results reinforce the conclusions of Reynolds et al. (2019), that overharvesting of large predatory fish and climate change likely negatively impacted sooty tern trophic ecology, thereby resulting in elevated Hg contamination.

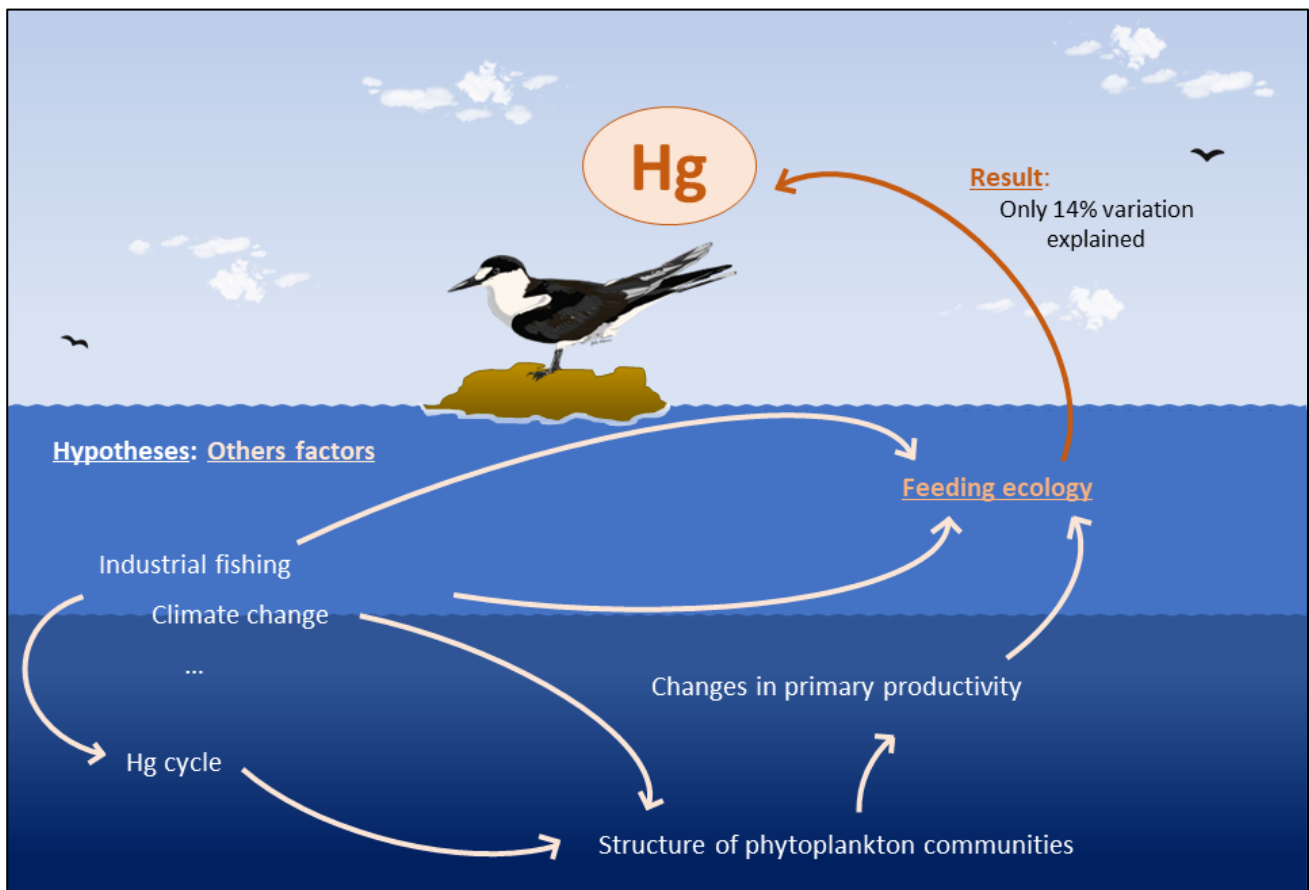


Figure 4.9. Graphical representation of potential drivers influencing long-term Hg trends (from the 1890s to the 2020s) in marine food webs of the tropical South Atlantic Ocean, as indicated by sooty terns breeding on Ascension Island.

2.3. Conclusions

In this work, sooty terns act as bioindicators of temporal trends in Hg contamination of food webs in the tropical South Atlantic Ocean. We have built on previous long-term investigations of the feeding ecology of breeding sooty terns on Ascension Island (1890s–2010s; Reynolds et al., 2019), by extending the recent time series by an additional decade and providing feather-derived Hg concentrations. To the best of our knowledge, this is the first study to determine Hg contamination over such an extensive multidecadal timescale in the tropical oceans. Our results revealed a global non-linear increase in Hg contamination of sooty terns over the last 145 years, because of both trophic and environmental changes over time (Figure 4.9). Overall, this work provides invaluable information on how ecosystem-wide changes can increase Hg contamination of tropical marine predators and reinforces the need for long-term regulations of harmful contaminants at the global scale.

Part 2: Retrospective investigation of Hg contamination: epoch comparison

2.4. Context

In July 2022, I took advantage of my visit at the Bird Group Tring to collect feathers on museum-held sooty terns whose sampling locations were matching those of free-living individuals collected recently (i.e., in the 2010s and 2020s) for Chapter 3. Overall, this represented 12 adult individuals from two colonies (Table 4.1): Lord Howe Island in the South Pacific Ocean, and Fernando de Noronha in the South Atlantic Ocean (Figure 4.10). For each site, the aim was to perform temporal comparisons in feather Hg concentrations and stable isotope values between two epochs, one century apart.

Table 4.1. Feather sampling of sooty terns, including museum-held specimens (kept at Bird Group Tring, Natural History Museum, UK; BNHM) and free-living birds, from two tropical colonies. This included Lord Howe Island and Fernando de Noronha in the South Pacific and South Atlantic Oceans, respectively. n indicates sample sizes.

Colonies	n	Year	Epochs	Source
Lord Howe Island	3	1887	1880s-1910s	Museum (BNHM)
	4	1913		Museum (BNHM)
	30	2020	2020s	Free-living
Fernando de Noronha	1	1884	1880s-1900s	Museum (BNHM)
	4	1902		Museum (BNHM)
	18	2011	2010s	Free-living

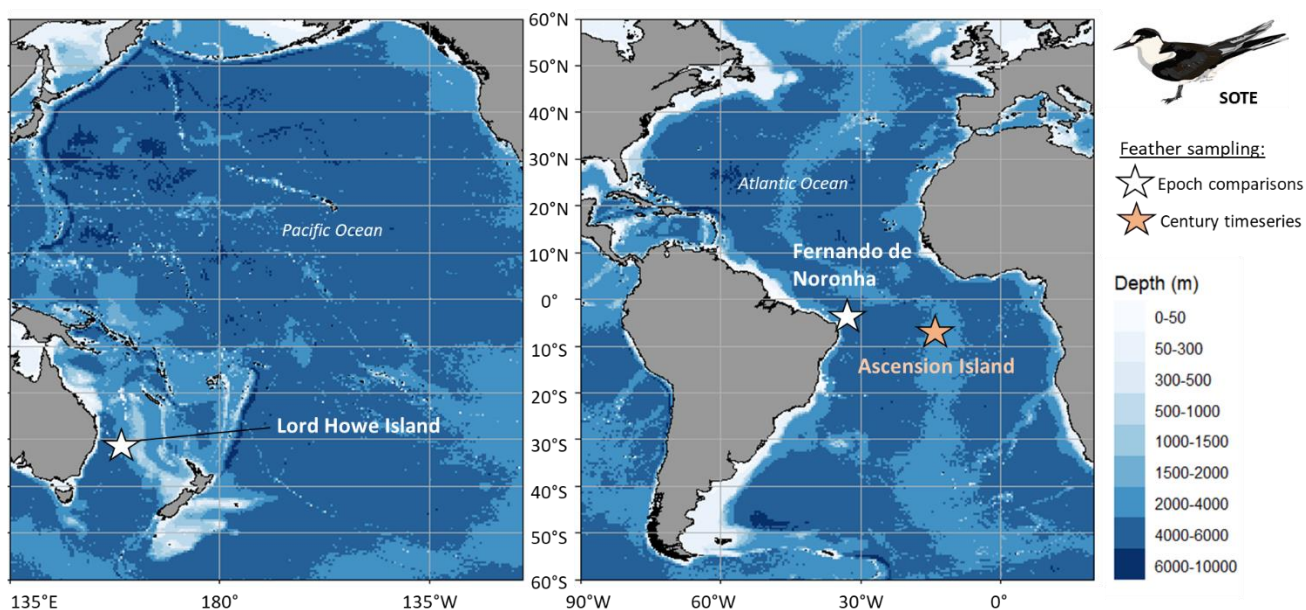


Figure 4.10. Location of sampling sites (stars) of sooty terns (SOTE) used for temporal Hg monitoring, including epoch comparisons (in white) and century time-series (in orange). The ocean bathymetry is represented by the blue gradient.

2.5. Results and Discussion

Statistical results are presented in the Annexes, as well as feather Hg concentrations, bulk $\delta^{13}\text{C}$ and $\delta^{15}\text{N}$ values (mean \pm SD, min–max) that are provided in [Table A11](#).

In Fernando de Noronha, our results revealed simultaneous and marked differences for all variables between the 1880s/1900s and the 2010s ([Figure 4.11.A](#)). Over this period, average feather Hg concentrations decreased by 64.5%, $\delta^{13}\text{C}$ values by 15.5% and $\delta^{15}\text{N}$ values by 9.6% ([Table A10](#)). As for our results on Ascension Island (see Section 2.2), three hypotheses arise for these temporal trends. First, sooty terns may have changed their moulting area between the two epochs, resulting in changes in feeding habitat and diet (reflected in feather stable isotope values) and in subsequent changes in year-round Hg exposure. Second, considering that sooty terns occupy similar moulting areas between the two epochs, changes in year-round Hg exposure over time may result from temporal changes in feeding habitat and diet during the moulting period, with lower trophic position (as indicated by lower $\delta^{15}\text{N}$ values) leading to lower Hg bioaccumulation and lower feather Hg concentrations. However, as discussed previously, these temporal trends of bulk stable isotopes could integrate both trophic changes (feeding habitat and diet) and baseline changes over time. CSIA-AA could help to determine if the trophic position of sooty terns changed over time, and thereby if the decrease in feather Hg concentrations could be attributed to trophic changes or baseline changes in marine food webs.

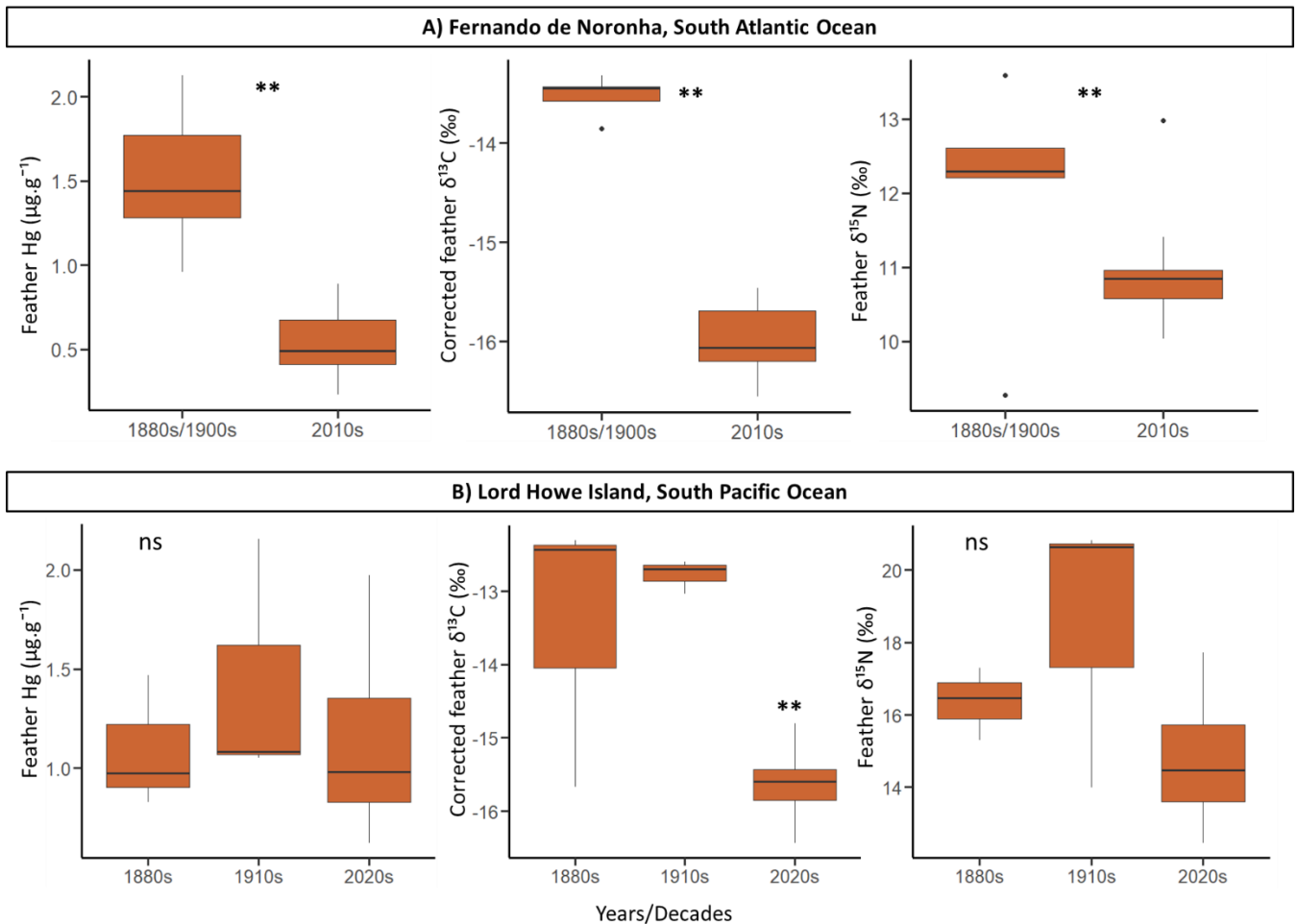


Figure 4.11. Temporal comparisons of feather Hg concentrations, bulk $\delta^{13}\text{C}$ and $\delta^{15}\text{N}$ values in sooty terns (adults) from two tropical colonies: **(A)** Fernando de Noronha (South Atlantic Ocean) and **(B)** Lord Howe Island (South Pacific Ocean). Sample sizes are provided in Table 4.1. ns and ** indicate when statistical differences were non-significant and detected, respectively (ANOVA or Kruskal-Wallis; cf. Table A11 for further details). Values of $\delta^{13}\text{C}$ were corrected for the Suess Effect (cf. Chapter 2, Section 3.3.1).

In contrast, temporal trends in Lord Howe Island were not synchronous and differed depending on the variables. After removing one outlier from 1913 ($\text{Hg}=6.98 \mu\text{g}\cdot\text{g}^{-1}$; $\delta^{13}\text{C}=-13.03 \text{‰}$, $\delta^{15}\text{N}=15.92 \text{‰}$), non-significant differences were observed in feather Hg concentrations and $\delta^{15}\text{N}$ values over time (Figure 4.11.B). However, there were marked differences in $\delta^{13}\text{C}$ values between museum-held and free-living sooty terns (*i.e.*, 18.4% decrease between the 1880s and the 2020s; Table A11). This result is consistent with previous findings in tropical seabirds (*i.e.*, results from Ascension Island in the previous section) and fish (tunas; Lorrain et al., 2020), but also in seabirds from other oceanic regions (Hirons et al., 2001; O'Reilly et al., 2003; Schell, 2000), where a drastic decrease in $\delta^{13}\text{C}$ values over time was associated with a global shift in phytoplankton community structure, and hence in primary

productivity in marine ecosystems (see discussion in Section 2.2.a). Thus, our results further confirm this global trend in the South Atlantic and Pacific Oceans.

Based on our century timeseries in sooty terns from Ascension Island and the literature, we expected feather Hg concentrations from the two colonies to increase between the different epochs. Surprisingly, our results revealed the opposite trend in Fernando de Noronha and no temporal trend in Lord Howe Island. Although these results do not coincide with the expansion of human activities and associated releases in Hg globally, they are consistent with previous findings in seabirds from the Southeast Indian Ocean (Bond and Lavers, 2020) and the Southern Ocean (Gilmour et al., 2019). Yet, it is worth noting that both our tropical colonies and those from these two studies were all located in the Southern Hemisphere. The lack of temporal trends or the decreasing trends observed between the early 20th and the 21st centuries there could thus coincide with the hemispheric Hg gradients (*i.e.*, high Hg concentrations in the Northern Hemisphere compared to the SH; Médiéu et al., 2022 and references therein; see Chapter 3), and the spatial disparities in historical Hg emissions globally (Fisher et al., 2023; Hylander and Meili, 2003; Li et al., 2020). Clearly, this illustrates the heterogeneity in Hg bioavailability and transfer in marine food webs over time, and the importance of long-term monitoring with high temporal frequency, to better understand the fate of anthropogenic Hg in marine environments and anticipate the potential risks associated. Despite the stable and decreasing trends described here, future research should further investigate past Hg contamination with the addition of feather samples between the different epochs, to confirm the observed differences or highlight potential fluctuations until the present day. More importantly, further monitoring is required in the next years and decades, to track Hg contamination in tropical ecosystems, which may face enhanced Hg emissions from ever-growing human activities and enhanced remobilization from legacy Hg, particularly under the influence of global change (Sonke et al., 2023).

2.6. Summary: Retrospective assessment of Hg contamination in tropical marine food webs

Sooty terns act as bioindicators of Hg temporal trends in the South Atlantic and Pacific Oceans.

Century time series in Ascension Island:

- Feather Hg concentrations were **59% higher** in the **1920s** than in the **2020s**.
- **Trophic position** ($\delta^{15}\text{N}$) and **feeding habitat** ($\delta^{13}\text{C}$) influenced Hg long-term trend.
- **Climate change** and **overfishing** may influence Hg long-term trends.

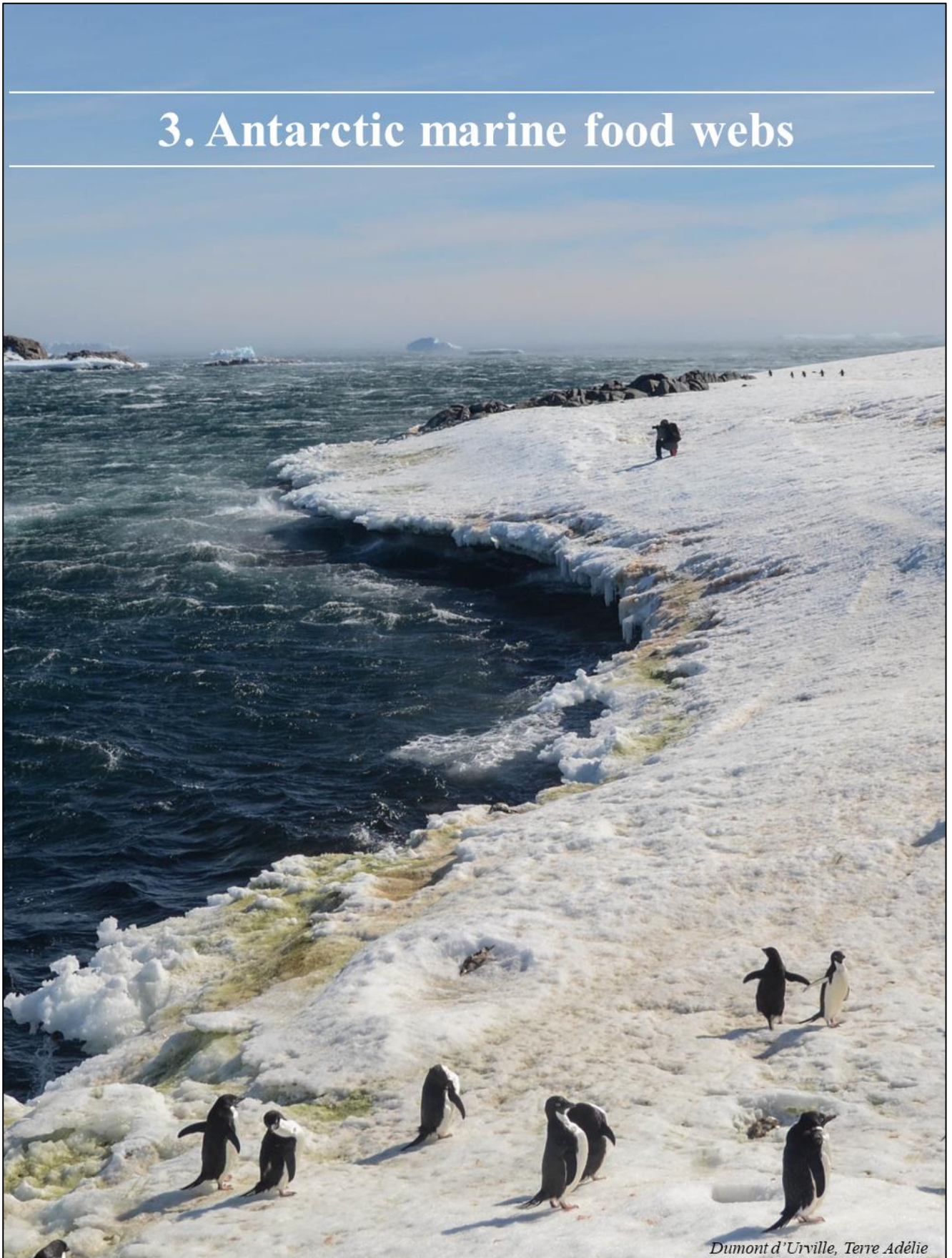
Epoch comparison in two other colonies:

Feather Hg concentrations were:

- **65% lower** in **Fernando de Noronha** between the **1880s/1900s** and **2010s**.
- **similar** in **Lord Howe Island** between the **1880s** and the **2020s**.

To the best of our knowledge, this work represents the first temporal assessment of Hg contamination in tropical marine food webs, both through century timescales and epoch comparisons.

3. Antarctic marine food webs



Dumont d'Urville, Terre Adélie

3.1. Context

Out of the 14 studies that investigated long-term trends of Hg in seabirds (see [Table A4](#) for a review), only four (*i.e.*, 29%) were conducted in the Southern Ocean. All of them were conducted in sub-Antarctic islands (Carravieri et al., 2016; Gilmour et al., 2019; Scheifler et al., 2005; Thompson et al., 1993b), and only one in Antarctica (Carravieri et al., 2016). The present work further investigates temporal trends of Hg contamination in Antarctic marine food webs, by analysing feathers of museum-held and free-living (from Chapter 3) Adélie penguins in three Antarctic colonies: Signy Island (South Orkney Islands), Dumont d'Urville (Adélie Land) and Cape Royds (Ross Island; [Figure 4.12](#)). Overall, this represented 22 museum specimens, kept at the Bird Group Tring (Natural History Museum, UK; n=18) and the French National Museum of Natural History (n=4; [Table 4.2](#)). Similar to sooty terns in the previous section, the aim was to perform epoch comparisons of feather Hg concentrations and stable isotope values for each site, one century apart.

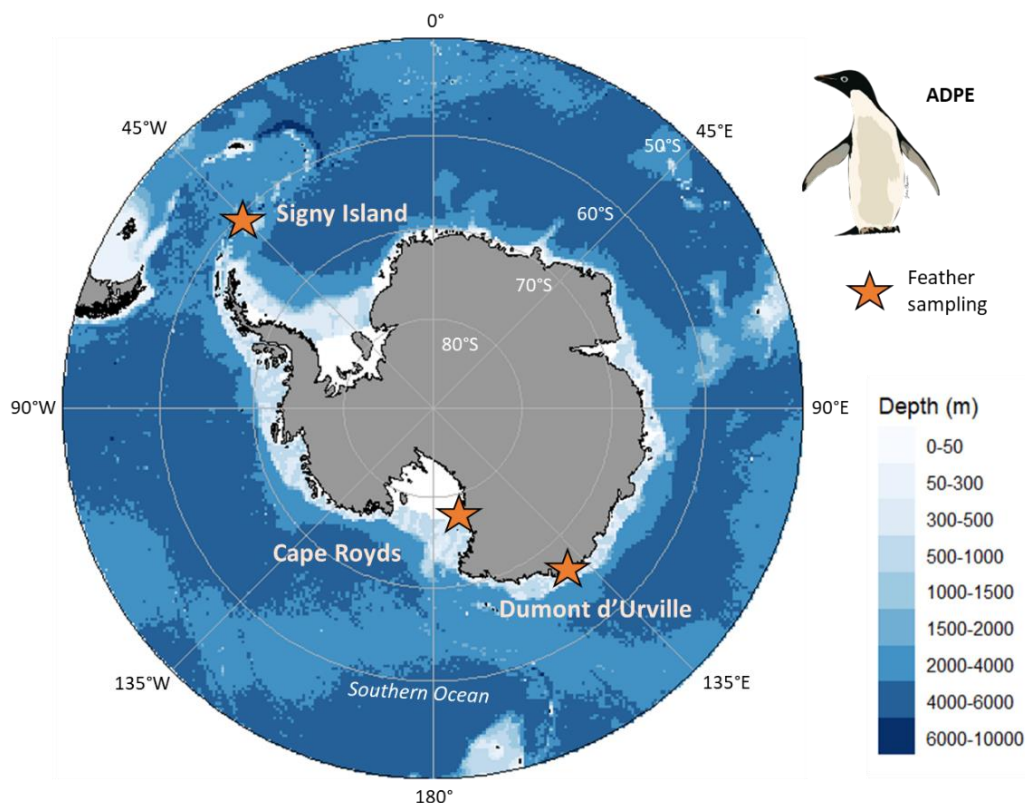


Figure 4.12. Location of sampling sites (orange stars) of Adélie penguins (ADPE) used for epoch comparisons in three Antarctic colonies: Signy Island (South Orkney Islands), Dumont d'Urville (Adélie Land) and Cape Royds (Ross Island). The ocean bathymetry is represented by the blue gradient.

Table 4.2. Feather sampling of Adélie penguins from museum-held specimens and free-living birds, in three Antarctic colonies, including Signy Island (South Orkney Islands), Dumont d’Urville (Adélie Land) and Cape Royds (Ross Island). n indicates sample sizes. Museum-held specimens were kept at Bird Group Tring (Natural History Museum, UK; BNHM) and the French National Museum of Natural History (Paris; MNHN).

Colony	n	Year	Epoch	Source	References
Signy Island	8	1950–1951	1950s	Museum (BNHM)	This thesis
	30	2022	2020s	Free-living	This thesis
Dumont d’Urville	4	1951	1950s	Museum (MNHN)	This thesis; Carravieri et al. (2016)
	10	2007	2007	Free-living	This thesis
	10	2012	2012	Free-living	This thesis
	15	2017	2017	Free-living	This thesis
Cape Royds	10	1912	1910s	Museum (BNHM)	This thesis
	15	2019	2010s	Free-living	This thesis

3.2. Results and Discussion

Statistical results are presented in the Annexes, as well as feather Hg concentrations, bulk $\delta^{13}\text{C}$ and $\delta^{15}\text{N}$ values (mean \pm SD, min–max) that are provided in [Table A10](#).

Overall, our results are consistent with the range of feather Hg concentrations reported in the literature for Adélie penguins (see [Table 1](#) in [Paper 2](#) for a complete review) and in our circum-Antarctic Hg assessment (Chapter 3, Section 3). Regarding temporal comparisons of Hg contamination, we found contrasting patterns according to the different colonies ([Figure 4.13](#)). In Signy Island, feather Hg concentrations were not statistically different between the 1950s and the 2020s ([Figure 4.13.A](#)), although average values were 27% lower in the 2020s than in the 1950s ([Table A10](#)). In contrast, we detected significant differences between the four periods in Dumont d’Urville, with average Hg concentrations 53% higher after the 2000s (*i.e.*, 2007, 2012, 2017) compared to the 1950s ([Figure 4.13.B](#)). Finally, we did not observe significant temporal differences in feather Hg concentrations in Cape Royds, although average concentrations were 5% higher in the 2020s than in the 1910s ([Figure 4.13.C](#)).

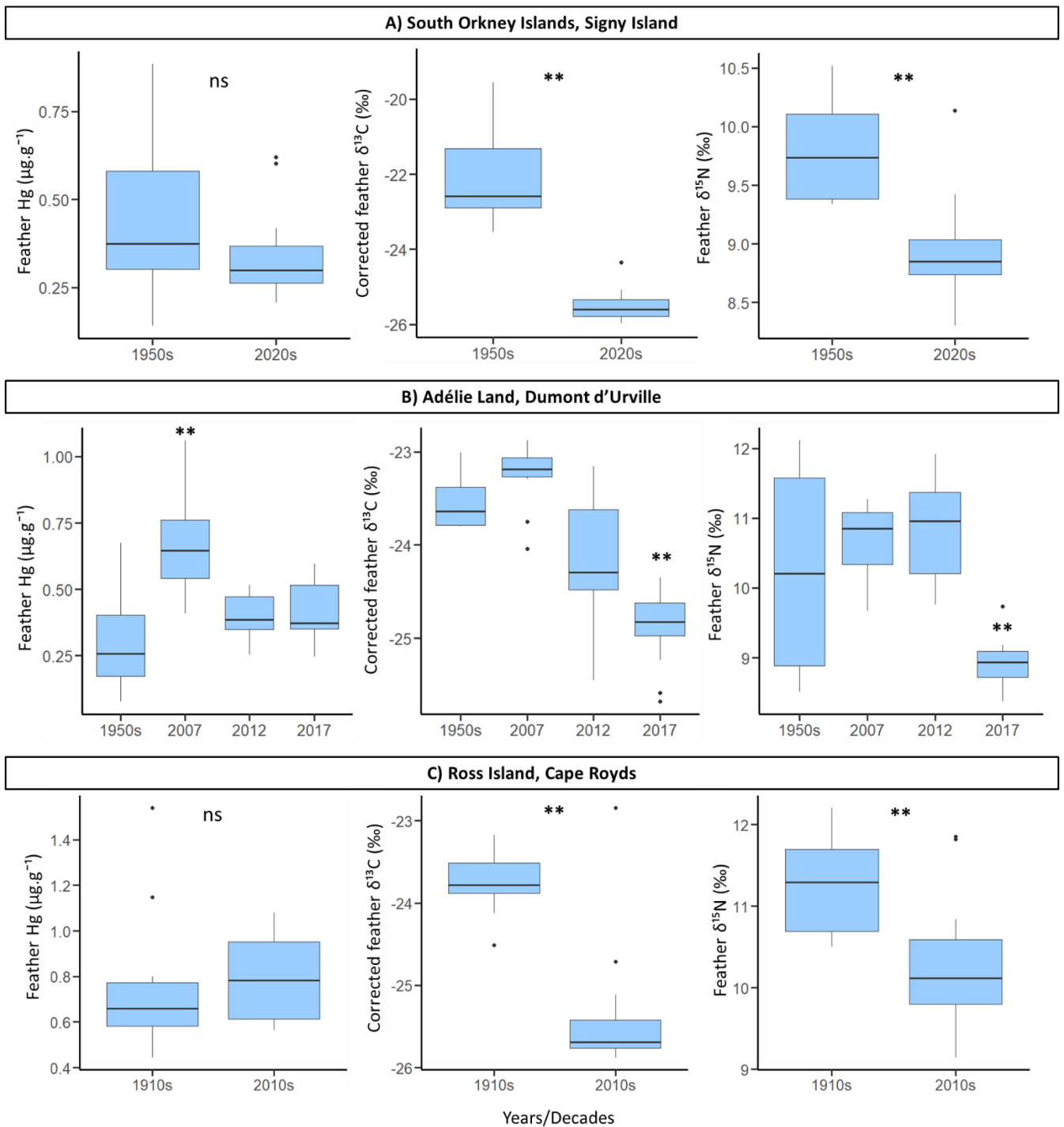


Figure 4.13. Temporal comparisons of feather Hg concentrations, bulk $\delta^{13}\text{C}$ and $\delta^{15}\text{N}$ values in Adélie penguins (adults) from three Antarctic colonies: **(A)** Signy Island (South Orkney Islands), **(B)** Dumont d'Urville (Adélie Land) and **(C)** Cape Royds (Ross Island). Sample sizes are provided in Table 4.2. ns and ** indicate when statistical differences were non-significant and detected, respectively (ANOVA or Kruskal-Wallis; cf. Table A11 for further details). Values of $\delta^{13}\text{C}$ were corrected for the Suess Effect (cf. Chapter 2, Section 3.3.1).

Regarding stable isotopes values, temporal differences were similar in all colonies, with marked decreases in both $\delta^{13}\text{C}$ and $\delta^{15}\text{N}$ values between epochs (Figure 4.13). In Dumont d'Urville, however, average $\delta^{15}\text{N}$ values in feathers remained stable from the 1950s to 2012 and then decreased in 2017 (Figure 4.13.B). Despite lower $\delta^{15}\text{N}$ values in the most recent years at all sites (*i.e.*, 2020s, 2017 and 2010s for Signy Island, Dumont d'Urville and Cape Royds, respectively), feather Hg concentrations were not systematically lower recently compared to the 1910s or the 1950s, suggesting that changes in trophic ecology alone do not explain temporal changes in Hg contamination. As for sooty terns in the previous section, we observed contrasting temporal differences within one single species but in different Antarctic regions. However, the low sample sizes for museum specimens likely led to the low detection of statistical differences between the different epochs. This could be overcome with the addition of new individuals collected in these sites but kept in other natural history museums, particularly in countries that have established research stations in Antarctica in the past (*e.g.*, USA, UK). Besides, this could help to fill the temporal gaps in the timeseries and further investigate these temporal scales at a finer scale. This could be the case in Dumont d'Urville, where feathers of several seabird species are collected yearly, for more than 60 years, as part of long-term monitoring programs such as the ORNITHOECO program, which uses seabirds and marine mammals as sentinels of global changes in the Southern Ocean (More information is available here: https://institut-polaire.fr/en/programmes_soutenus/seabirds-and-marine-mammals-as-sentinels-of-global-changes-in-the-southern-ocean-2/).

In Chapter 3, we provided a circum-Antarctic assessment of Hg contamination in marine food webs for the contemporary period (*i.e.*, 2000s-2020s). To further investigate long-term trends of Hg contamination in Antarctic marine food webs but at a larger spatial scale, future research could extend the present work (*i.e.*, museum archives from three Antarctic colonies) with the addition of new colonies around Antarctica focusing on the early 20th century. Unfortunately, due to the more recent discovery of Antarctica compared to other regions of the world, chances to obtain museum specimens of Adélie penguins earlier than the 1900s are low. To explore longer temporal scales, the alternative would be to use sediment cores in breeding colonies of Adélie penguins, in search of feathers to reconstruct past Hg contamination until the present day (Lorenzini et al., 2014). Still, obtaining a snapshot of such large-scale Hg contamination at different epochs over time, both in the past and the future, will help to determine the impacts of human activities and their extent on the contamination status of marine ecosystems, even in the remote polar oceans.

3.3. Conclusion

Temporal monitoring is key to assess the effectiveness of international regulations on anthropogenic Hg emissions (*i.e.*, the Minamata Convention), particularly in remote oceans such as the Southern Ocean. This work provides new insights into the temporal trends of Hg contamination in Antarctic marine food webs, by using the Adélie penguin as bioindicator species. Our results revealed contrasting temporal patterns in Hg contamination between different Antarctic colonies (*i.e.*, increase, no trend, decrease). Still, temporal changes in Hg contamination were relatively low compared to other temperate or Arctic regions (Bond et al., 2015; Thompson et al., 1993a), probably due to the higher historical Hg emissions of anthropogenic origin in the Northern Hemisphere compared to the Southern Hemisphere (Fisher et al., 2023; Médieu et al., 2022). Further research is now required to fill the temporal gaps, extend the number of Antarctic colonies and to continue long-term monitoring in the future. In the context of global change, which is particularly visible in polar oceans, further research is also needed to investigate the drivers of these temporal trends, including environmental parameters (*e.g.*, sea-ice concentrations, primary productivity, sea-surface temperatures) and ecological drivers (*e.g.*, changes in trophic ecology) that may influence the fate of contaminants in marine environments.

4. Discussion

...som samlere, der opgjorde
og fiskere tog ud for
fugle, ofte for en lille,
handler, der solgte fugl
hænder eller muse

I museets samlinger
stoppede gejrfugle. De
som er i sommerdragt,
1832. Det andet - som il
et af ganske få i verden,
vinterdragt. Museet ejer d
glas med indhold og d
fra det sidste gejrfugle
blev fanget på den islandske



Natural History Museum, Copenhagen

Over the last century, seabirds have been collected for exhibitions and museum collections worldwide and represent invaluable archives to reconstruct past Hg availability and transfer in marine food webs, particularly in remote oceanic regions that are the focus of this doctoral work. Feathers of museum specimens enable both ecological and ecotoxicological investigations on multidecadal and century timescales. However, any retrospective investigation at a single location is challenging, because it is highly dependent on sampling effort each year over a large time scale. Gaps in retrospective time-series are thus very common and can make statistical analyses and the interpretation of temporal data more complicated. Still, such long-term monitoring is crucial to determine the influence of expanding human activities and climate change on marine ecosystems and biota.

By using feathers of three seabird species, we have documented long-term Hg contamination in marine food webs of three remote oceanic regions, including the Arctic, the South Atlantic and the Southern Oceans. This doctoral work represents a valuable contribution to Hg research by providing century-scale Hg assessments in both the South Atlantic Ocean and the Arctic, two oceanic regions where such temporal data were either lacking or scarce. Our results revealed that Hg contamination increased in both regions over the last century and that the temporal Hg trends were little explained by those of trophic proxies (*i.e.*, birds' feeding habitat and diet, as indicated by stable isotopes). This suggested ecosystem-wide changes (*e.g.*, shift in primary productivity) that may influence Hg cycling in marine ecosystems and hence Hg exposure in seabirds over time, particularly in the context of global changes. In contrast, epoch comparisons in two tropical and three Antarctic colonies revealed contrasting temporal patterns in Hg contamination depending on the colonies (*i.e.*, increase, no trend and decrease), both in the intertropical region (South Atlantic and Pacific Oceans) and the Southern Ocean. Clearly, this illustrates the heterogeneity of Hg cycling in the oceans, including both its natural and anthropogenic drivers under the influence of global changes, that together influence the temporal responses of marine biota globally. Because of the noise induced by biological processes that interfere with Hg geochemical signal, a high temporal frequency and number of measurements (*i.e.*, sample size) is crucial to obtain a clear and complete overview of the drivers of Hg contamination in marine ecosystems.

Since the eighteenth century, human activities have released Hg globally, mainly to the atmosphere (Eagles-Smith et al., 2018; Streets et al., 2017). Natural archives, such as ice and sediment cores and peat bogs, have recorded the subsequent increase in air Hg concentrations and atmospheric deposition even in remote regions (*e.g.*, mountainous and polar regions; Beal et al., 2015; Kang et al., 2016; Zheng, 2015). Following an increasing input of Hg into all ecosystems, including marine ecosystems, we could expect a subsequent increase in biotic Hg concentrations, so that trends in biota would track

those of atmospheric deposition over time. Yet, a mismatch exists between biotic and environmental trends of Hg over time (Wang et al., 2019), as illustrated in [Figure 4.14](#).

Starting in the 19th century, with sharp anthropogenic uses and releases of Hg globally (Outridge et al., 2018), both air and biotic Hg concentrations increased steadily until reaching a maximum in the 1970s–1980s (Dietz et al., 2009; Rig  t et al., 2011). Then, although anthropogenic releases to air stabilized after the 1980s (*i.e.*, in the Northern Hemisphere), trends in biotic Hg have diverged in some regions and co-occurring species and have continued synchronously in other regions and species (AMAP, 2021; Un Environment, 2018). These divergent patterns result from the combination of several co-occurring processes. First, they reflect a switch from emission-driven to processes-driven Hg bioaccumulation in biota, that is not only influenced by Hg inputs alone (both natural and anthropogenic), but also by ecosystem processes that control the recycling, speciation, methylation, bioavailability and biological uptake of Hg (Ch  telat et al., 2022; McKinney et al., 2022; Wang et al., 2010, 2019). Then, these divergent patterns may also be attributed to the growing contribution over time of legacy Hg inventories (in soil and ocean reservoirs), relative to those of newly emitted Hg. Finally, they result from the considerable sensitivity of Hg biogeochemical cycling to any type of changes, including changes in physical (*e.g.*, temperature, light, hydrology), geochemical (*e.g.*, pH, redox status), biological (*e.g.*, feeding behavior, migration) and ecological conditions (*e.g.*, primary productivity, microbial processes, food web structure and dynamics; see Hsu-Kim et al., 2018). Many of these changes have been recently exacerbated by climate change, reinforcing the decoupling between biotic and environmental Hg. Together, all these processes create a large variability in the response of Hg temporal trends in biota and lead to a temporal mismatch between atmospheric Hg emissions and biotic responses ([Figure 4.14](#)).

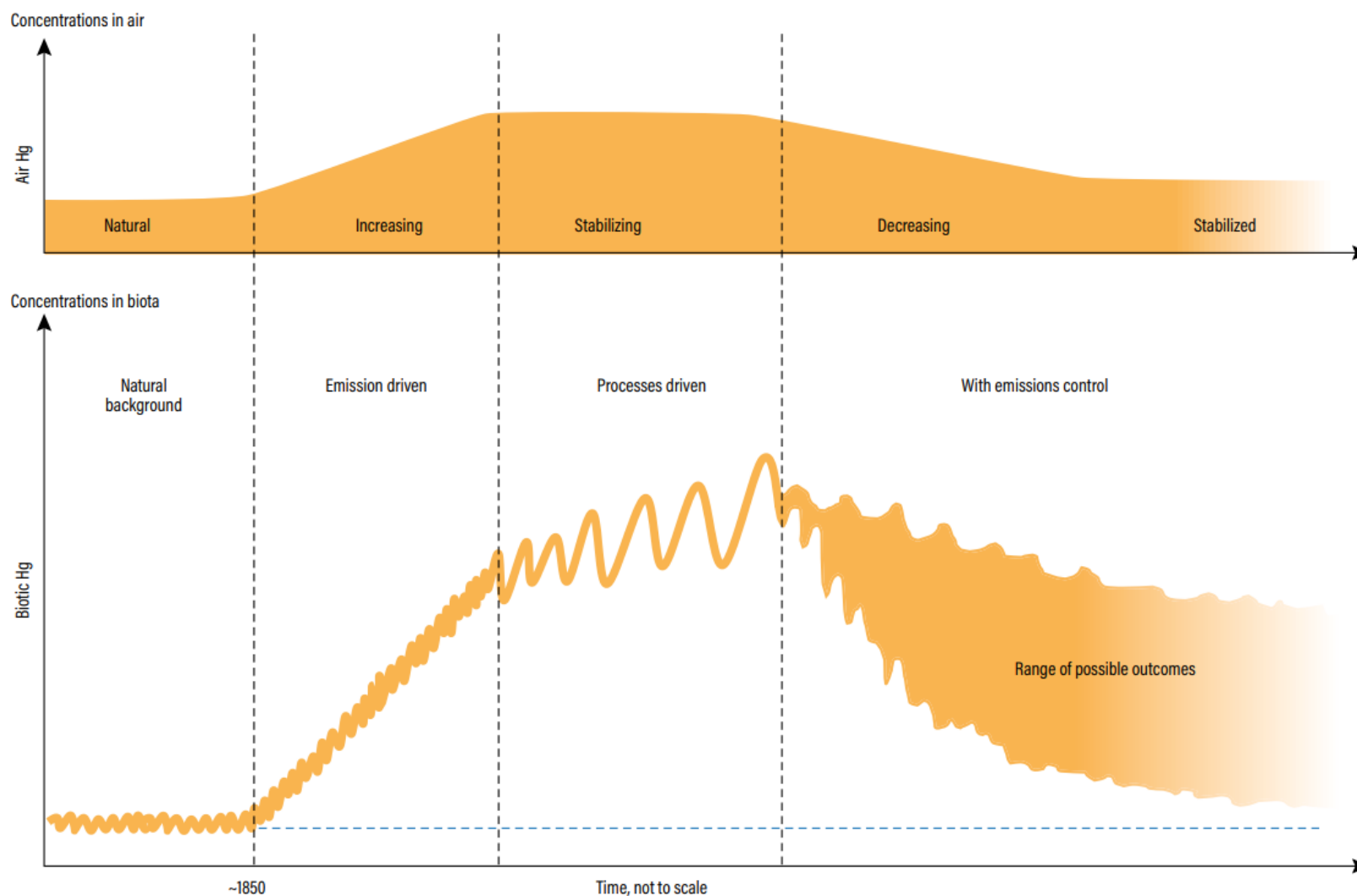


Figure 4.14. Conceptual representation of the response of biotic Hg concentrations to changes in atmospheric Hg concentrations, as the limiting factors in bioaccumulation change. Extracted from the Global Mercury Assessment (UN Environment, 2018), which was adapted from Wang et al. (2019).

Mercury contamination of marine environments results from long-term processes, influenced by Hg transport, methylation and bioavailability, as well as from ecological interactions, both locally and globally. Undoubtedly, there is a time lag of years, decades or even centuries between Hg emissions and deposition in the ocean and the resulting Hg contamination of marine food webs (Driscoll et al., 2013; Foster et al., 2019; Sunderland and Mason, 2007; UN Environment, 2018). In a similar way, there is a time lag between the implementation of international regulations such as the Minamata Convention on Mercury, which aim to control and reduce anthropogenic releases of Hg in the environment, and the subsequent decrease in marine biota. Therefore, long-term monitoring of biotic Hg, as is the case in this doctoral work, is fundamental to assess the effectiveness of the Minamata Convention in the next years and decades, and help guiding future directions of international policies. The Montreal Protocol, designed to protect the ozone layer in the atmosphere, is a good example of the effectiveness of international treaties, as a recent study estimated that its implementation in 1989 has postponed the occurrence of the first ice-free Arctic by as much as 15 years (England and Polvani, 2023). This represents a hopeful example for the Minamata Convention to follow.

Chapter 5

Conclusion, critical evaluation and perspectives

5.1. Highlights of the doctoral work

This doctoral work provides a unique, large-scale assessment of Hg contamination in marine ecosystems of remote oceanic regions, which were poorly documented in global monitoring programs until then. Seabirds were used as bioindicators to document past and current trends in Hg contamination, in three main oceanic regions: the Arctic Ocean, the intertropical region that included tropical waters of the Pacific, Atlantic and Indian Oceans, and the Southern Ocean. Feathers of three seabird species (one for each oceanic region) revealed past and current Hg trends in these three regions, both across space and time. Overall, this represented around 2200 individuals, across five ocean basins, spanning over 189 years (1833-2022).

1) Spatial monitoring of Hg contamination in tropical and marine ecosystems

Thanks to large, field-based scientific networks in both the intertropical region and Antarctica, this thesis provides contemporary assessments of Hg in tropical and polar marine ecosystems. Our results revealed spatial patterns in year-round contamination, as indicated by feather Hg concentrations of adults. Highlights for this chapter are the following:

- In the **Arctic**, results confirmed the **East-to-West gradient**, with Hg hotspots in West Greenland, Canadian Arctic and Newfoundland, and also revealed a **South-to-North gradient** in West-Greenland.
- In the **intertropical region**, adult feather concentrations revealed that Hg contamination was **higher**:
 - in the **Atlantic Ocean** compared to the Pacific and Indian Oceans,
 - in the **Northern Hemisphere** compared to the Southern Hemisphere.
- In the **Antarctic Zone** (i.e., south of Polar Front), Hg contamination was relatively homogenous around Antarctica, except for a **Hg hotspot in the Ross Sea**.

- **In Antarctic ecosystems, trophic ecology** was a **significant driver** of Hg spatial patterns, in combination with **colony location**, suggesting **both trophic and environmental drivers** in Hg contamination.
- **In tropical ecosystems**, trophic ecology was **not a major driver**, as only $\delta^{13}\text{C}$ values and **colony location** were the main drivers.
- **Further research** is needed to **identify the drivers** of these spatial patterns (e.g., Hg biogeochemical cycle, environmental changes).

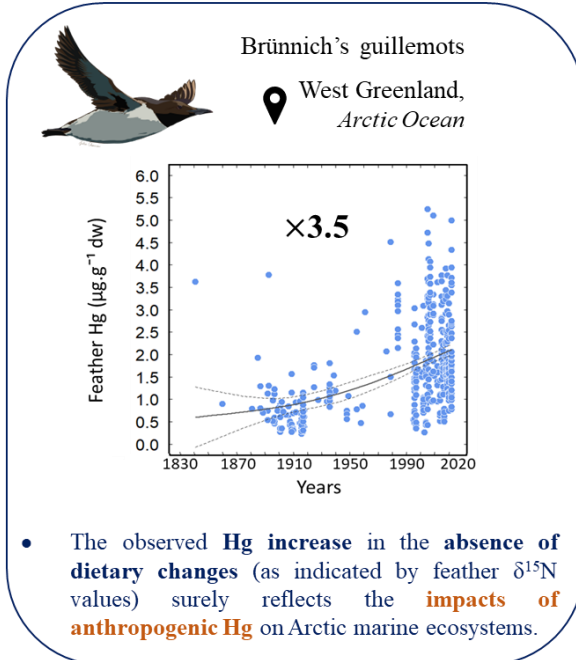
2) Long-term monitoring of Hg contamination in tropical and marine ecosystems

Our combined sampling of museum-held and free-living seabirds allowed two types of retrospective assessments of Hg contamination since the 19th century: (i) long-term assessments with high temporal frequency (*i.e.*, century time series), and (ii) temporal comparisons between different epochs (*i.e.*, epoch comparison). Highlights for each assessment are provided on the following page.

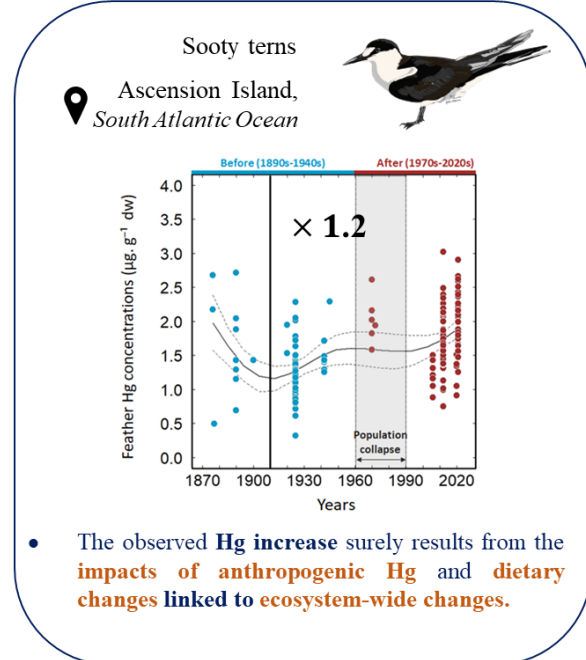
Considering the increasing Hg trends recorded both in the Arctic and tropical bioindicator species until the present (*i.e.*, century time series), the impacts of global regulatory policies that were implemented over the last years and decades, including the Minamata Convention on Mercury, are not yet visible in the response of these specific marine ecosystems. However, other environmental compartments and regions of the world have responded positively to the implementation of national and international regulations (Figure 5.1; Sonke et al., 2023). At the global scale, long-term biomonitoring and reconstructions of past Hg concentrations in natural archives (*e.g.*, peat cores, Greenland firn air; *i.e.*, air trapped in land ice) revealed several simultaneous decreasing trends since the 1970s, in atmospheric (panel b) and biotic (panel c) concentrations, as well as in accumulation rates (*i.e.*, deposition; from peat cores; panel d). This coincides with the clear decline in global Hg emissions to air (panel a) that followed international controls on Hg emissions in the mid-1970s (Sonke et al., 2023 and references therein). However, the different components of the Hg cycle (*i.e.*, emissions, air, deposition and biota) show diverse temporal trends, both in direction and extent.

(1) The **century time series** revealed that Hg contamination **has increased non-linearly** over the last century both **in Arctic and tropical marine ecosystems**.

Arctic marine ecosystems



Tropical marine ecosystems



- Trophic position** ($\delta^{15}\text{N}$) and **feeding habitat** ($\delta^{13}\text{C}$) influenced Hg long-term trends in both species, but **only explained 17% and 14%** of the temporal variation in Hg in Arctic and tropical ecosystems, respectively, suggesting the **role of ecosystem-wide changes and other unknown factors**.
- Climate change** and **anthropogenic activities** may influence Hg long-term trends in various ways (i.e., ocean warming, sea ice loss, industrial fishing, anthropogenic Hg emissions).

(2) In contrast, **epoch comparisons** in tropical and Antarctic marine ecosystems revealed **contrasting temporal patterns** depending on the colonies.

Antarctic marine ecosystems

Feather Hg concentrations were:

- 53% higher** in the 2000s/2010s than in the 1950s in **Adélie Land**.
- similar** in the 2020s than in the 1950s in **South Orkney Islands** (non-significant difference)
- similar** in the 2020s than in the 1910s in **the Ross Sea** (non-significant difference).

Tropical marine ecosystems

Feather Hg concentrations were:

- 65% lower** in the 2010s than in the 1880s/1900s in **Fernando de Noronha**.
- similar** in **Lord Howe Island** between the 1880s and the 2020s (non-significant difference).

For example, out of the five documented temporal trends in biota, four show a continuous decline since the 1970s and one shows a drastic increase until 2000, before decreasing thereafter (Figure 5.1.c). Similarly, accumulation rates differ over time between peat and sediment cores (panel d), which reveal opposite trends from the 1970s onwards (*i.e.*, Hg continues to increase in sediment cores). These contrasting patterns reflect the heterogeneity of Hg cycling in the various ecosystems (*i.e.*, terrestrial, freshwater and marine), which are subject to different environmental forcings (*i.e.*, physical, chemical, biological) that are exacerbated by global change and modulate their response to Hg emissions control (see Figure 4.14 and Chapter 4 for discussion; Chételat et al., 2022; McKinney et al., 2022; Sonke et al., 2023; Wang et al., 2019). Clearly, this reinforces the need to maintain the regulations of anthropogenic Hg emissions globally, and continuing long-term monitoring in the coming years will inform about the need to strengthen them in the future.

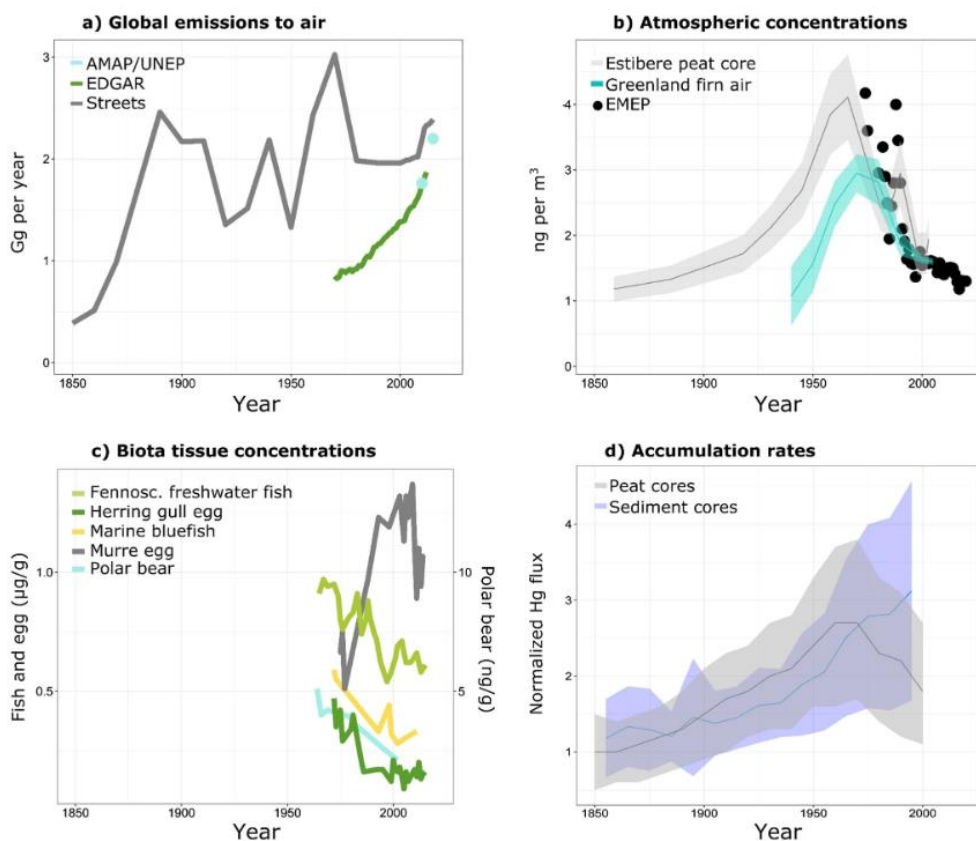


Figure 5.1. Temporal Hg trends since 1850, in different environmental compartments and different components of the Hg cycle, including (a) global Hg emissions to air, (b) atmospheric concentrations, (c) biotic Hg (*i.e.*, fish, seabirds and marine mammals) and (d) Hg deposition, as indicated by accumulation rates in peat and sediment cores. Extracted from Sonke et al. (2023). For further details, the reader is referred to the original study.

5.2. Critical evaluation

5.2.1. Are seabirds *really* good bioindicators of Hg contamination in marine food webs?

Due to their high sensitivity to changes in oceanographic conditions, food supply and pollution (Cairns, 1988; Provencher et al., 2012; Vihtakari et al., 2018), seabirds have been extensively used as bioindicators of marine ecosystems (Burger and Gochfeld, 2004; Furness, 1993). Despite the numerous advantages of this approach, in particular to document remote oceanic regions (see Chapter 1, Section 3), using seabirds as bioindicators can also have several limitations (Burger and Gochfeld, 2004). Because they forage over large oceanic areas and exploit marine resources in various ecosystems, adult seabirds and their feathers do not inform about point sources of Hg pollution. As they are migratory, it is difficult to determine with precision where Hg exposure occurs, except when combining ecotoxicology with biologging approaches (see Discussion in Chapter 3). However, this requires a good understanding of seabird molt cycles, as feathers reflect integrated Hg exposure since the previous molt (Albert et al., 2019; Furness et al., 1986). For example, the combined use of ecotoxicology and biologging appears more suitable for seabirds that have either a biannual (*e.g.*, alcids) or continuous molt (*e.g.*, albatross). In addition, understanding life cycles, migratory routes, diet, foraging range and habitat of seabirds is fundamental to understand their Hg exposure and draw conclusion about the state of contamination of marine ecosystems. Yet, such information is not always fully known depending on the species, particularly during the non-breeding season where seabirds are hardly accessible. Seabirds constitute the most threatened bird group and pelagic seabirds are particularly threatened globally (Croxall et al., 2012). Although monitoring Hg, and contaminants in general, in threatened species can provide further insights into the causes of their decline, obtaining samples, even non-destructive samples such as feathers, from these specific species can be challenging or potentially impossible in some cases. Fortunately, this was not the case in this work, as our three species are classified as «Least Concern» in the ICUN Red List. Yet, the conservation status of a seabird species represents an additional criterion when selecting a bioindicator species. In contrast to adults, seabird chicks present clear advantage when interpreting Hg exposure, since they provide local information (*i.e.*, in the vicinity of their colony; see Chapter 2, Section 4).

In this work, we selected one bioindicator species for each oceanic region of interest, the Brünnich's guillemot for the Arctic Ocean, the sooty tern for the intertropical region and the Adélie penguin for the Southern Ocean (Chapter 2, Section 1). However, the question arises as

to whether the use of one single bioindicator species is really sufficient to obtain robust information on the state of Hg contamination of marine ecosystems. In fact, this depends on the scientific question. If the region of interest is a specific region or ocean, then monitoring different species locally is relevant to document different compartments of the marine ecosystems (both vertically and horizontally), and obtain a comprehensive overview of their contamination status (see Ochoa-Acuña et al., 2002). A good example for regional, integrative Hg assessment is the AMAP (see Chapter 3, Section 1), which combines Hg monitoring in air, precipitation, biota (both terrestrial and marine species, from different trophic levels) and humans (Figure 5.2).

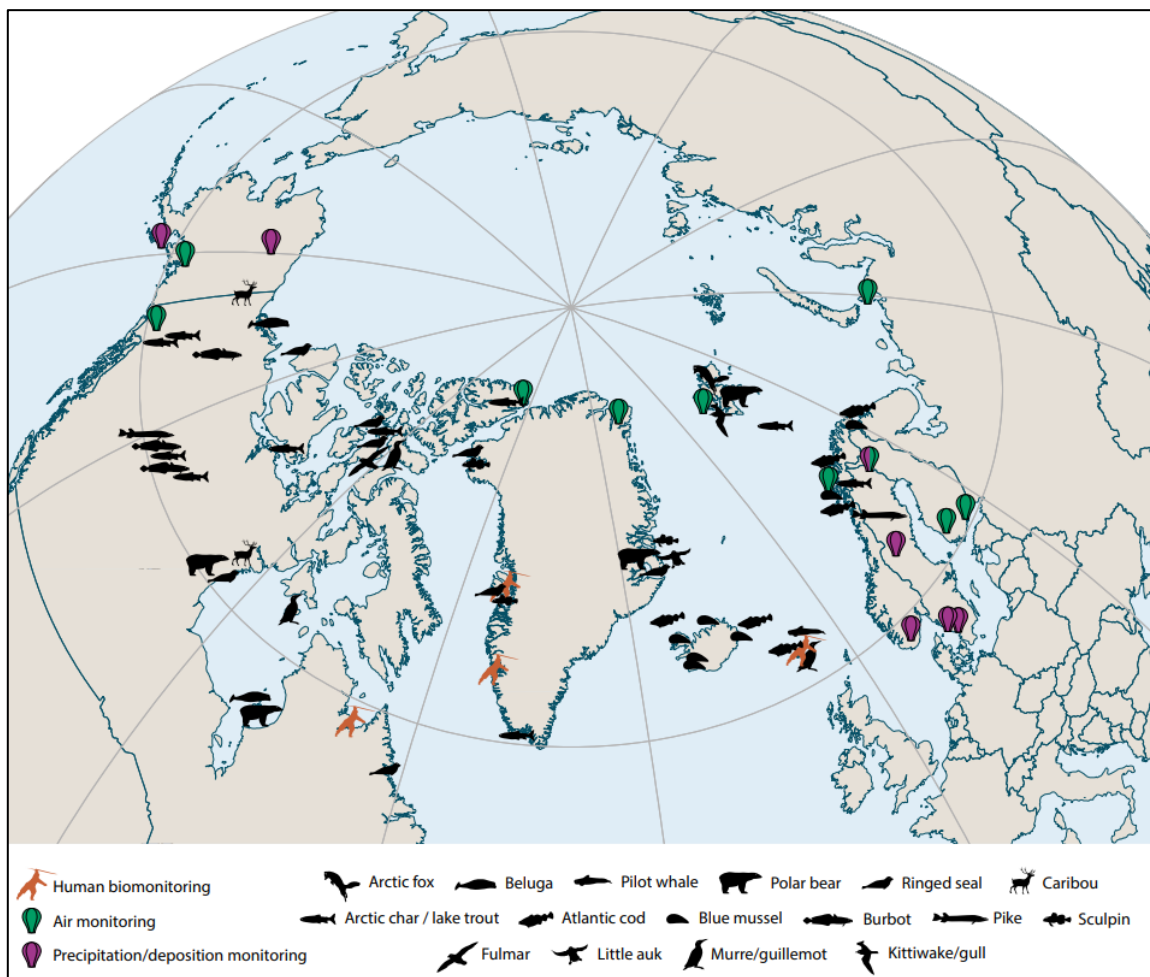


Figure 5.2. Sampling locations of Hg monitoring in the Arctic, including air, precipitation/deposition, biota (*i.e.*, terrestrial mammals, as well as bivalves, fish seabirds and marine mammals) and human monitoring. Extracted from AMAP (2021).

On the other hand, if the focus is on a specific oceanic compartment at the global scale, then one single bioindicator approach can be powerful when considering large spatial scales. Such approach allows to reach a considerable number of sites, as showed in Chapter 3 for both the intertropical region and Antarctica, that would have been necessarily reduced in the case of multi-species monitoring. Besides, in multi-species monitoring, it can be challenging to have exactly the same seabird community (*i.e.*, same species) across the global study area. Although one species might differ in its diet composition and proportions of prey spatially, here we assumed that our bioindicator species had relatively similar foraging habitat and diet across their distribution range. This works specifically for seabirds that have specialized foraging strategies, such as Adélie penguins. Still, we cannot exclude certain variability in foraging habitat and diet between regions and oceans in our three bioindicator species, when comparing Hg exposure over such large spatial scales. Although individuals from the same species may differ in their foraging ecology across their large distribution range, their physiological and metabolic responses to Hg contamination are the same (*e.g.*, identical molt cycle, breeding characteristics, detoxification processes). While single bioindicator approaches are powerful for large-scale Hg assessments, they are also challenging, as they require huge sampling efforts, including the setting-up of new collaborations, coordination, administrative management (permits, authorizations), and the associated analytical efforts.

In conclusion, this doctoral work aimed to provide biotic Hg assessments in remote oceanic regions at the global scale. To cover both large spatial and temporal scales, feathers appeared to be the most appropriate tissue for Hg biomonitoring.

5.2.2. Are feathers *really* relevant for Hg biomonitoring?

In monitoring programs using protected species, particular attention is given to effective, non-destructive and non-invasive sampling that do not jeopardize the health or the survival of the monitored organisms. For seabirds, this is the case with blood, eggs and feathers, which were identified in the GBMS as tissues of interest for Hg biomonitoring and recommended for international monitoring programs (Evers et al., 2019). The utility of a particular tissue varies with the contaminant and the research question. For large-scale monitoring, it is more appropriate to promote non-lethal sampling of feathers, which incorporate Hg accumulated in the body since the last molt and reflect bird's contamination over time (Furness et al., 1986; Furness, 1993).

Feathers are particularly suitable for long-term monitoring of Hg, as they represent valuable archives to investigate Hg contamination in marine ecosystems retrospectively, thanks to museum-held seabirds (Chapter 3; Thompson et al., 1992; Vo et al., 2011). As they reflect large spatial scales, they are also useful for spatial monitoring (see Chapter 2, Section 2.2; Albert et al., 2019), but still present some limitations when interpreting Hg exposure, as previously discussed in Chapter 3. In the absence of biologging, no information is available about the precise geographical distribution of seabirds during the non-breeding season, whose integrated signal is incorporated in feathers. The Southern Ocean represents one of the rare exceptions, where the marked latitudinal gradient in $\delta^{13}\text{C}$ of organic matter and hence in marine consumers enables to estimate the spatial distribution of seabirds and acquire information that would not be available otherwise (Carravieri et al., 2014b; Cherel and Hobson, 2007). Still, this $\delta^{13}\text{C}$ gradient provides information about latitudinal movements, but not on longitudinal distribution of seabirds. Due to the oceanographic characteristics of the Southern Ocean (i.e., annular circulation), variation in longitudinal movements within the relatively homogeneous ocean waters may not be detected through stable isotope analyses.

Blood represents another non-destructive alternative to feather sampling. However, the associated temporal window of Hg exposure reflected in blood is shorter (i.e., few weeks/months; Bearhop et al., 2000; Monteiro and Furness, 2001). Since blood samples are usually collected at the colony during the breeding period, they usually inform about Hg exposure during the early breeding season and not during the non-breeding season. However, to extend seasonal and spatial comparisons of Hg exposure, we could consider blood sampling at two different stages: (i) the period of colony attendance (i.e., when birds return for the breeding season), which would reflect the last weeks/months from the non-breeding period, and (ii) at the end of the breeding season (i.e., after chick-rearing and before colony departure), which would reflect Hg exposure during the breeding season. This way, we could determine if Hg contamination is higher in remote marine ecosystems (i.e., during the non-breeding period) or in local ecosystems during the breeding season, or vice versa.

In conclusion, the utility of feathers in Hg monitoring is dependent on the research question, and interpretation of Hg concentrations requires caution and key biological knowledge about the studied species. Here, feathers have succeeded in their mission: inform about Hg contamination at large spatial and temporal scales.

5.2.3. Are stable isotopes *really* informative when monitoring Hg contamination at large-spatial scale?

Since the main exposure route of Hg in seabirds is through the diet (see Chapter 2, [Figure 2.4](#); (Burger and Gochfeld, 2001a; Monteiro and Furness, 1995), knowledge about their trophic ecology is key to understand drivers of Hg contamination and disentangle between dietary and environmental changes (Bond et al., 2015; Carravieri et al., 2016; Fort et al., 2016). However, feathers present one major issue when combining Hg and stable isotopes, which are proxies of the trophic ecology (see Chapter 2, Section 3.3). While they are both incorporated during feather growth, their integration period is temporally decoupled in adult seabirds (Bond, 2010; Thompson et al., 1998). Feathers retain information on year-round Hg exposure, but dietary signatures for the time of feather growth (i.e., moulting period). Clearly, this temporal mismatch makes interpretation more complex and need to be considered systematically. Yet, despite this temporal mismatch, feathers provide insights into time-integrated, assimilated food, when no other biological information is available.

Oceans are dynamic environments that are subject to a multitude of physical, chemical, geological and biological factors, both temporally (with seasons, years) and spatially (both vertically, horizontally). This results in large variation in baseline isotopic signatures of carbon and nitrogen in the oceans, which are then reflected in marine consumers (see Chapter 2, Section 3.3; McMahon et al., 2013a, 2013b). Thus, not accounting for these baseline variations when investigating large spatial scales can bias the interpretation of trophic proxies, and have cascading effects on the interpretation of Hg exposure in seabirds. In that sense, CSIA-AA represent a powerful tool in marine ecology and spatial ecotoxicology that compensates for this bias. Unfortunately, because they are expensive and time-consuming, CSIA-AA in this doctoral work were only performed on a subset of feather samples, from the region where more environmental variability was expected: the intertropical region (Chapter 3, Section 2). In the literature, few studies (n=5) have combined CSIA-AA with Hg exposure in seabirds, and even fewer on large temporal scales (n=1; [Table A12](#)). In large-scale studies, as is the case in Chapter 3, we strongly recommend this technique to allow large-scale comparison of trophic position, through the use of $\delta^{15}\text{N}$ values of source and trophic AAs (see Chapter 2, Section 3.3.2; Chikaraishi et al., 2014; Ohkouchi et al., 2017). In this work, AA- $\delta^{13}\text{C}$ values could not be explored, mainly due to time constraints, but similar investigations could potentially provide further insights into the foraging habitat of sooty terns across their distribution range and help to further explore its relationship with Hg contamination.

5.3. Perspectives: what's next?

Spatial ecotoxicology. Detailed spatial information of seabird movements during their annual cycle is essential to quantify precisely the spatial variation in their Hg exposure and then identify Hg hotspots in the ocean. Obviously, the present work constitutes a qualitative approach that paves the way for future quantitative approaches in spatial ecotoxicology that would combine Hg biomonitoring and biologging. As such research efforts are currently engaged in the Arctic (e.g., collaboration between the SEATRACK and ARCTOX projects; see Chapter 3, Section 4.2), the intertropical region and the Southern Ocean could be ideal scientific playground in that sense.

Investigating the role of environmental drivers. As discussed in Chapters 3 and 4, environmental parameters may influence Hg cycle in the oceans and bioavailability in marine ecosystems. This could include sea surface temperature, primary productivity (chlorophyll a) in all ecosystems and sea-ice concentrations in polar oceans for example (Foster et al., 2019; Tartu et al., 2022). Such investigations could be relevant for both spatial and temporal monitoring. However, it would be challenging to associate environmental parameters to a specific, precise geographical area, since feathers reflect Hg exposure on both large temporal and spatial scales (i.e., several months, including breeding and non-breeding periods). Actually, for spatial monitoring, this would not be relevant to calculate an average value of a physical parameter (e.g., sea ice) for this long period, considering the seasonality and strong variability in environmental conditions (e.g., in the Southern Ocean). In contrast, this could be relevant for temporal monitoring by considering climatology of the physical parameters of interest (i.e., averaged indices over time for a specific region). In the Arctic for example, we could consider sea ice climatology (i.e., average concentrations of sea-ice over the last decades). Still, in this case we would be limited by the availability of satellite measurements, which only date back to the 1970s. To go back to the 19th century or more, the alternative would be environmental proxies in paleoarchives (e.g., marine sediments), which can inform about past ocean conditions (e.g., sea ice conditions, ocean circulation and temperature, Hg oceanic deposition; see Chapter 4; Asmund and Nielsen, 2000; Georgiadis et al., 2020; Shemesh et al., 1992).

Monitoring multiple species and/or marine compartments. Thanks to our single bioindicator approach for each remote oceanic region, we could highlight Hg hotspots in the Ross Sea, in the Southern Ocean, and potentially in the Caribbean Sea. To further investigate

point-source Hg pollution or the drivers that result in enhanced bioavailability of Hg in these specific marine ecosystems, several species, trophic levels and marine compartments could be simultaneously monitored, as was the case in Antarctica in the 1990s (*i.e.*, in Terra Nova Bay; Bargagli et al., 1998) or today with the AMAP (Figure 5.2). Yet, it is logistically challenging, as this would require a research vessel with different sampling techniques (*e.g.*, for benthos, water column and on land for top predators). Alternatively, the present Hg assessments could be complemented with seabird species that occupy the same oceanic regions as our three bioindicator species. For example, through Adélie penguins, this work documented circumpolar Hg contamination in the epipelagic compartment of the Southern Ocean. A complementary approach could investigate the mesopelagic compartment, where high concentrations of dissolved MeHg were recorded (Cossa et al., 2011). This could be done by studying the circumpolar breeding emperor penguin (*Aptenodytes forsteri*), which mainly feeds on prey of higher trophic position in both epipelagic and mesopelagic waters (Cherel, 2008; Wienecke and Robertson, 1997). In a similar way, our tropical assessment using sooty terns could be complemented with the Bulwer's petrel that feeds on mesopelagic prey, also in tropical waters (Monteiro and Furness, 1997).

Considering multi-stressor approaches. Hg is a toxic pollutant that causes deleterious effects in both wildlife and humans (Basu et al., 2023; Dietz et al., 2013; Evers et al., 2008). Overall, in this doctoral work we found relatively low Hg concentrations in sooty terns and Adélie penguins, and intermediate Hg concentrations in Brünnich's guillemots. However, adverse effects may arise even at low Hg concentrations, particularly in co-occurrence with other stressors, including other trace elements and contaminants (Goutte et al., 2014).

Selenium (Se) is a trace element that plays a protective role against Hg toxicity (Cuvin-Aralar and Furness, 1991), but knowledge about its spatial distribution is still very scarce. A recent study conducted in the Arctic has investigated the spatial distribution of both Hg and Se (Cruz-Flores et al., 2023). This represented a large sampling of two seabird species, distributed in 17 colonies in Arctic and sub-arctic regions, from West to East Atlantic Ocean. Overall, they found that Brünnich's guillemots and black-legged kittiwakes (*Rissa tridactyla*) were better protected from Hg toxicity in the European Arctic. Similarly, investigate the co-exposure of Hg and Se spatially in our bioindicator species could provide additional information on the presence of Hg hotspots in specific regions, such as the Ross Sea in Antarctica. On the other hand, temporal

trends of this co-exposure could also be investigated at the century timescale, as this has never been reported in the literature to date.

Seabirds are exposed to a multitude of stressors, and the impact of Hg probably act synergetically with both natural and anthropogenic stressors, including contaminants (*e.g.*, persistent organic pollutants, emerging pollutants), diseases, parasites and environmental changes (Amélineau et al., 2019; Carravieri et al., 2020; Esparza et al., 2022; Provencher et al., 2016). Both our spatial and long-term monitoring assessments of Hg could be complemented by the analyses of the aforementioned stressors (*e.g.*, contaminants, trace elements) to investigate synergic or contrasting patterns both across space and time.

Tracing the origin of Hg. Seabirds represent unique biological samplers to study Hg contamination in marine ecosystems, as highlighted in this PhD thesis, but more importantly they allow to study the biogeochemical cycle of Hg, through analyses of its stable isotopes. Hg has seven stable isotopes that experience mass-dependent and mass-independent isotopic fractionation. The combined use of Hg isotopic mass-dependent (MDF; *e.g.*, $\delta^{202}\text{Hg}$) and mass-independent (MIF; *e.g.*, $\Delta^{199}\text{Hg}$) fractionation enables to quantify the processes (*e.g.*, photodemethylation, photoreduction, biotic methylation) and identify the sources and pathways of Hg in the environment (Blum et al., 2014), including marine ecosystems (Cransveld et al., 2017; Day et al., 2012; Jackson et al., 2008; Li et al., 2014; Point et al., 2011; Senn et al., 2010). Together, Hg MDF and MIF were used in seabirds, as tracers of Hg sources and transformation pathways in marine ecosystems of the Arctic Ocean (Renedo et al., 2020a) and the Southern Indian Ocean (Renedo et al., 2020b), and revealed large-scale variation in Hg cycling. Our spatial Hg assessment could thus be enhanced by the additional analyses of Hg stable isotopes, to investigate large-scale variation in sources and pathways of Hg in both tropical and Antarctic waters. Specifically, this may help to precisely identify the drivers of the Hg hotspots observed in the Ross Sea, as indicated by feather Hg concentrations of adult and chick Adélie penguins (Chapter 3, Section 3). On the other hand, temporal investigations have also been conducted with Hg stable isotopes in sediment profiles in Antarctic over the last 1500 years and showed that Hg stable isotopes could record historical changes of sea ice conditions by studying Hg pathways, and particularly changes in photodemethylation linked to sea ice changes (Liu et al., 2023). In a similar way, yet on shorter temporal windows (*i.e.*, the last centuries), temporal trends in biogeochemical Hg cycling could be investigated with our long-term monitoring in

both Arctic and tropical marine ecosystems, to explore potential shifts in Hg sources and pathways concurrently to the increase of anthropogenic Hg emissions and climate change.

5.4. Conclusion

«Currently, the Minamata Convention Secretariat is developing guidance for monitoring programs in member countries to evaluate the effectiveness of the Minamata Convention. Scientific input is critical for guiding the policies related to effectiveness evaluation» (Chen and Evers, 2023), including large-scale Hg assessments of biotic Hg. In general, identifying biota species for Hg biomonitoring is complex, because their suitability differs according to geographic area, timescale of interest, conservation concern, and whether the overall goal is for ecological or human health (UN Environment, 2018). Through single bioindicator approaches, this doctoral work represents a valuable contribution to international monitoring programs, such as the AMAP from the Arctic Council and the Global Mercury Assessment from the United Nations, which are closely tied to the implementation and effectiveness evaluation of the Minamata Convention. For this purpose, maintaining large-scale monitoring on the long-term is crucial. Renewing global assessments, such as those presented in this doctoral work, on a regular basis (*e.g.*, every few years or decade for example) is fundamental to monitor the contamination status of marine ecosystems over time and to further investigate global trends, especially in the context of climate change.

Bibliography

A

- Ackerman, J.T., Eagles-Smith, C.A., 2009. Integrating toxicity risk in bird eggs and chicks: Using chick down feathers to estimate mercury concentrations in eggs. *Environ. Sci. Technol.* 43, 2166–2172. <https://doi.org/10.1021/es803159c>
- Ackerman, J.T., Eagles-Smith, C.A., Herzog, M.P., Hartman, C.A., 2016a. Maternal transfer of contaminants in birds: Mercury and selenium concentrations in parents and their eggs. *Environ. Pollut.* 210, 145–154. <https://doi.org/10.1016/j.envpol.2015.12.016>
- Ackerman, J.T., Eagles-Smith, C.A., Herzog, M.P., Hartman, C.A., Peterson, S.H., Evers, D.C., Jackson, A.K., Elliott, J.E., Vander Pol, S.S., Bryan, C.E., 2016b. Avian mercury exposure and toxicological risk across western North America: A synthesis. *Sci. Total Environ.* 568, 749–769. <https://doi.org/10.1016/j.scitotenv.2016.03.071>
- Ackerman, J.T., Herzog, M.P., Evers, D.C., Cristol, D.A., Kenow, K.P., Heinz, G.H., Lavoie, R.A., Brasso, R.L., Mallory, M.L., Provencher, J.F., Braune, B.M., Matz, A., Schmutz, J.A., Eagles-Smith, C.A., Savoy, L.J., Meyer, M.W., Hartman, C.A., 2020. Synthesis of maternal transfer of mercury in birds: Implications for altered toxicity risk. *Environ. Sci. Technol.* 54, 2878–2891. <https://doi.org/10.1021/acs.est.9b06119>
- Adams, N. J., Brown, C.R., 1990. Energetic of molt in penguins, in: *Penguin Biology*. Academic Press, London.
- Ainley, D.G., Wilson, P.R., Barton, K.J., Ballard, G., Nur, N., Karl, B., 1998. Diet and foraging effort of Adélie penguins in relation to pack-ice conditions in the southern Ross Sea. *Polar Biol.* 20, 311–319. <https://doi.org/10.1007/s003000050308>
- Albert, C., 2020. Exposure of Arctic seabirds to pollutants and the role played by individual migratory movements and non-breeding distribution. La Rochelle Université, La Rochelle.
- Albert, C., Bråthen, V.S., Descamps, S., Anker-Nilssen, T., Cherenkov, A., Christensen-Dalsgaard, S., Danielsen, J., Erikstad, K.E., Gavrilov, M., Hanssen, S.A., Helgason, H.H., Jónsson, J.E., Kolbeinsson, Y., Krasnov, Y., Langset, M., Lorentzen, E., Olsen, B., Reiertsen, T.K., Strøm, H., Systad, G.H., Tertitski, G., Thompson, P.M., Thórarinnsson, T.L., Bustamante, P., Moe, B., Fort, J., 2021. Inter-annual variation in winter distribution affects individual seabird contamination with mercury. *Mar. Ecol. Prog. Ser.* 676, 243–254. <https://doi.org/10.3354/meps13793>
- Albert, Céline, Helgason, H.H., Brault-Favrou, M., Robertson, G.J., Descamps, S., Amélineau, F., Danielsen, J., Dietz, R., Elliott, K., Erikstad, K.E., Eulaers, I., Ezhov, A., Fitzsimmons, M.G., Gavrilov, M., Golubova, E., Grémillet, D., Hatch, S., Huffeldt, N.P., Jakubas, D., Kitaysky, A., Kolbeinsson, Y., Krasnov, Y., Lorentzen, S.-H., Lorentzen, E., Mallory, M.L., Merkel, B., Merkel, F.R., Montevecchi, W., Mosbech, A., Olsen, B., Orben, R.A., Patterson, A., Provencher, J., Plumejeaud, C., Pratte, I., Reiertsen, T.K., Renner, H., Rojek, N., Romano, M., Strøm, H., Systad, G.H., Takahashi, A., Thiebot, J.-B., Thórarinnsson, T.L., Will, A.P., Wojczulanis-Jakubas, K., Bustamante, P., Fort, J., 2021. Seasonal variation of mercury contamination in Arctic seabirds: A pan-Arctic assessment. *Sci. Total Environ.* 750, 142201. <https://doi.org/10.1016/j.scitotenv.2020.142201>
- Albert, C., Renedo, M., Bustamante, P., Fort, J., 2019. Using blood and feathers to investigate large-scale Hg contamination in Arctic seabirds: A review. *Environ. Res.* 177, 108588. <https://doi.org/10.1016/j.envres.2019.108588>
- AMAP, 2021a. Arctic climate change update 2021: Key trends and impacts. Summary for policy-makers. Arctic Monitoring and Assessment Programme.
- AMAP, 2021b. 2021 Mercury Assessment. Summary for policy-makers. Arctic Monitoring and Assessment Programme.
- AMAP, 2021c. AMAP Assessment 2021: Mercury in the Arctic. Arctic Monitoring and Assessment Programme (AMAP), Tromsø, Norway. viii + 324pp
- Amélineau, F., Grémillet, D., Harding, A.M.A., Walkusz, W., Choquet, R., Fort, J., 2019. Arctic climate change and pollution impact little auk foraging and fitness across a decade. *Sci. Rep.* 9, 1014. <https://doi.org/10.1038/s41598-018-38042-z>
- Amirbahman, A., Ruck, P.L., Fernandez, I.J., Haines, T.A., Kahl, J.S., 2004. The Effect of Fire on Mercury Cycling in the Soils of Forested Watersheds: Acadia National Park, Maine, U.S.A. *Water. Air. Soil Pollut.* 152, 315–331. <https://doi.org/10.1023/B:WATE.0000015369.02804.15>
- Amos, H.M., Jacob, D.J., Streets, D.G., Sunderland, E.M., 2013. Legacy impacts of all-time anthropogenic emissions on the global mercury cycle. *Glob. Biogeochem. Cycles* 27, 410–421. <https://doi.org/10.1002/gbc.20040>
- Anderson, C., Cabana, G., 2005. $\delta^{15}\text{N}$ in riverine food webs: effects of N inputs from agricultural watersheds. *Can. J. Fish. Aquat. Sci.* 62, 333–340. <https://doi.org/10.1139/f04-191>
- Appelquist, H., Asbirk, S., Drabæk, I., 1984. Mercury monitoring: Mercury stability in bird feathers. *Mar. Pollut. Bull.* 15, 22–24. [https://doi.org/10.1016/0025-326X\(84\)90419-3](https://doi.org/10.1016/0025-326X(84)90419-3)

- Ashmole, N.P., 1963. The biology of the wideawake or sooty tern *Sterna Fuscata* on Ascension Island. *Ibis* 103b, 297–351. <https://doi.org/10.1111/j.1474-919X.1963.tb06757.x>
- Asmund, G., Nielsen, S.P., 2000. Mercury in dated Greenland marine sediments. *Sci. Total Environ.* 245, 61–72. [https://doi.org/10.1016/S0048-9697\(99\)00433-7](https://doi.org/10.1016/S0048-9697(99)00433-7)
- Au, D.W.K., Pitman, R.L., 1986. Seabird interactions with dolphins and tuna in the Eastern tropical Pacific. *The Condor* 88, 304–317. <https://doi.org/10.2307/1368877>
- Aubail, A., Dietz, R., Rigét, F., Simon-Bouhet, B., Caurant, F., 2010. An evaluation of teeth of ringed seals (*Phoca hispida*) from Greenland as a matrix to monitor spatial and temporal trends of mercury and stable isotopes. *Sci. Total Environ.* 408, 5137–5146. <https://doi.org/10.1016/j.scitotenv.2010.07.038>
- Aubail, A., Dietz, R., Rigét, F., Sonne, C., Wiig, Ø., Caurant, F., 2012. Temporal trend of mercury in polar bears (*Ursus maritimus*) from Svalbard using teeth as a biomonitoring tissue. *J. Environ. Monit.* 14, 56–63. <https://doi.org/10.1039/C1EM10681C>

B

- Balance, L.T., and Pitman, R.L. 1999. Foraging ecology of tropical seabirds. In: Adams, N.J. & Slotow, R.H. (eds) *Proc. 22 Int. Ornithol. Congr., Durban:2057-2071*. Johannesburg: BirdLife South Africa
- Barbraud, C., Rolland, V., Jenouvrier, S., Nevoux, M., Delord, K., Weimerskirch, H., 2012. Effects of climate change and fisheries bycatch on Southern Ocean seabirds: A review. *Mar. Ecol. Prog. Ser.* 454, 285–307.
- Bargagli, R., 2016. Atmospheric chemistry of mercury in Antarctica and the role of cryptogams to assess deposition patterns in coastal ice-free areas. *Chemosphere* 163, 202–208. <https://doi.org/10.1016/j.chemosphere.2016.08.007>
- Bargagli, R., 2008. Environmental contamination in Antarctic ecosystems. *Sci. Total Environ.* 400, 212–226. <https://doi.org/10.1016/j.scitotenv.2008.06.062>
- Bargagli, R., Monaci, F., Sanchez-Hernandez, J.C., Cateni, D., 1998. Biomagnification of mercury in an Antarctic marine coastal food web. *Mar. Ecol. Prog. Ser.* 169, 65–76. <https://doi.org/10.3354/meps169065>
- Basu, N., Bastiansz, A., Dórea, J.G., Fujimura, M., Horvat, M., Shroff, E., Weihe, P., Zastenskaya, I., 2023. Our evolved understanding of the human health risks of mercury. *Ambio*. <https://doi.org/10.1007/s13280-023-01831-6>
- Basu, N., Horvat, M., Evers, D.C., Zastenskaya, I., Weihe, P., Tempowski, J., 2018. A state-of-the-science review of mercury biomarkers in human populations worldwide between 2000 and 2018. *Environ. Health Perspect.* 126, 106001. <https://doi.org/10.1289/EHP3904>
- Beal, S.A., Osterberg, E.C., Zdanowicz, C.M., Fisher, D.A., 2015. Ice core perspective on mercury pollution during the past 600 years. *Environ. Sci. Technol.* 49, 7641–7647. <https://doi.org/10.1021/acs.est.5b01033>
- Bearhop, S., Phillips, R.A., McGill, R., Cherel, Y., Dawson, D.A., Croxall, J.P., 2006. Stable isotopes indicate sex-specific and long-term individual foraging specialisation in diving seabirds. *Mar. Ecol. Prog. Ser.* 311, 157–164. <https://doi.org/10.3354/meps311157>
- Bearhop, S., Ruxton, G.D., Furness, R.W., 2000. Dynamics of mercury in blood and feathers of great skuas. *Environ. Toxicol. Chem.* 19, 1638–1643. <https://doi.org/10.1002/etc.5620190622>
- Beattie, S.A., Armstrong, D., Chaulk, A., Comte, J., Gosselin, M., Wang, F., 2014. Total and methylated mercury in Arctic multiyear sea ice. *Environ. Sci. Technol.* 48, 5575–5582. <https://doi.org/10.1021/es5008033>
- Becker, P.H., González-Solís, J., Behrends, B., Croxall, J., 2002. Feather mercury levels in seabirds at South Georgia: Influence of trophic position, sex and age. *Mar. Ecol. Prog. Ser.* 243, 261–269. <https://doi.org/10.3354/meps243261>
- Becker, P.H., Goutner, V., Ryan, P.G., González-Solís, J., 2016. Feather mercury concentrations in Southern Ocean seabirds: Variation by species, site and time. *Environ. Pollut.* 216, 253–263. <https://doi.org/10.1016/j.envpol.2016.05.061>
- Behrendt, J.C., 1990. *Ross Sea. Antarct. Res. Ser.* 48, 89–90.
- Belt, S.T., Cabedo-Sanz, P., Smik, L., Navarro-Rodriguez, A., Berben, S.M.P., Knies, J., Husum, K., 2015. Identification of paleo Arctic winter sea ice limits and the marginal ice zone: Optimised biomarker-based reconstructions of late Quaternary Arctic sea ice. *Earth Planet. Sci. Lett.* 431, 127–139. <https://doi.org/10.1016/j.epsl.2015.09.020>
- Belt, S.T., Müller, J., 2013. The Arctic sea ice biomarker IP₂₅: A review of current understanding, recommendations for future research and applications in palaeo sea ice reconstructions. *Quat. Sci. Rev., Sea ice in the paleoclimate system: The challenge of reconstructing sea ice from proxies* 79, 9–25. <https://doi.org/10.1016/j.quascirev.2012.12.001>
- Blévin, P., Carravieri, A., Jaeger, A., Chastel, O., Bustamante, P., Cherel, Y., 2013. Wide range of mercury contamination in chicks of Southern Ocean seabirds. *PLOS ONE* 8, e54508. <https://doi.org/10.1371/journal.pone.0054508>

- Blum, J.D., Popp, B.N., Drazen, J.C., Anela Choy, C., Johnson, M.W., 2013. Methylmercury production below the mixed layer in the North Pacific Ocean. *Nat. Geosci.* 6, 879–884. <https://doi.org/10.1038/ngeo1918>
- Blum, J.D., Sherman, L.S., Johnson, M.W., 2014. Mercury isotopes in Earth and Environmental sciences. *Annu. Rev. Earth Planet. Sci.* 42, 249–269. <https://doi.org/10.1146/annurev-earth-050212-124107>
- Bond, A.L., 2010. Relationships between stable isotopes and metal contaminants in feathers are spurious and biologically uninformative. *Environ. Pollut.* 158, 1182–1184. <https://doi.org/10.1016/j.envpol.2010.01.004>
- Bond, A.L., Diamond, A.W., 2010. Nutrient allocation for egg production in six Atlantic seabirds. *Can. J. Zool.* 88, 1095–1102. <https://doi.org/10.1139/Z10-082>
- Bond, A.L., Diamond, A.W., 2009. Total and methyl mercury concentrations in seabird feathers and eggs. *Arch. Environ. Contam. Toxicol.* 56, 286–291. <https://doi.org/10.1007/s00244-008-9185-7>
- Bond, A.L., Hobson, K.A., Branfireun, B.A., 2015. Rapidly increasing methyl mercury in endangered ivory gull (*Pagophila eburnea*) feathers over a 130 year record. *Proc. Biol. Sci.* 282, 1–8.
- Bond, A.L., Lavers, J.L., 2020. Biological archives reveal contrasting patterns in trace element concentrations in pelagic seabird feathers over more than a century. *Environ. Pollut.* 263, 114631. <https://doi.org/10.1016/j.envpol.2020.114631>
- Boudou, A., Ribeyre, F., 1985. Experimental study of trophic contamination of *Salmo gairdneri* by two mercury compounds — HgCl₂ and CH₃HgCl — analysis at the organism and organ levels. *Water. Air. Soil Pollut.* 26, 137–148. <https://doi.org/10.1007/BF00292064>
- Bowman, K.L., Hammerschmidt, C.R., Lamborg, C.H., Swarr, G., 2015. Mercury in the North Atlantic Ocean: The U.S. GEOTRACES zonal and meridional sections. *Deep Sea Res. Part II Top. Stud. Oceanogr., GEOTRACES GA-03 - The U.S. GEOTRACES North Atlantic Transect 116*, 251–261. <https://doi.org/10.1016/j.dsr2.2014.07.004>
- Bowman, K.L., Hammerschmidt, C.R., Lamborg, C.H., Swarr, G.J., Agather, A.M., 2016. Distribution of mercury species across a zonal section of the eastern tropical South Pacific Ocean (U.S. GEOTRACES GP16). *Mar. Chem.* 186, 156–166. <https://doi.org/10.1016/j.marchem.2016.09.005>
- Bowman, K.L., Lamborg, C.H., Agather, A.M., 2020. A global perspective on mercury cycling in the ocean. *Sci. Total Environ.* 710, 136166. <https://doi.org/10.1016/j.scitotenv.2019.136166>
- Brasso, R.L., Chiaradia, A., Polito, M.J., Raya Rey, A., Emslie, S.D., 2015. A comprehensive assessment of mercury exposure in penguin populations throughout the Southern Hemisphere: Using trophic calculations to identify sources of population-level variation. *Mar. Pollut. Bull.* 97, 408–418. <https://doi.org/10.1016/j.marpolbul.2015.05.059>
- Brasso, R.L., Drummond, B.E., Borrett, S.R., Chiaradia, A., Polito, M.J., Rey, A.R., 2013. Unique pattern of molt leads to low intraindividual variation in feather mercury concentrations in penguins. *Environ. Toxicol. Chem.* 32, 2331–2334. <https://doi.org/10.1002/etc.2303>
- Braune, B., Chételat, J., Amyot, M., Brown, T., Clayden, M., Evans, M., Fisk, A., Gaden, A., Girard, C., Hare, A., Kirk, J., Lehnerr, I., Letcher, R., Loseto, L., Macdonald, R., Mann, E., McMeans, B., Muir, D., O’Driscoll, N., Poulain, A., Reimer, K., Stern, G., 2015. Mercury in the marine environment of the Canadian Arctic: Review of recent findings. *Sci. Total Environ., Special Issue: Mercury in Canada’s North 509–510*, 67–90. <https://doi.org/10.1016/j.scitotenv.2014.05.133>
- Braune, B.M., Gaskin, D.E., 1987a. A mercury budget for the Bonaparte’s gull during autumn moult. *Ornis Scand. Scand. J. Ornithol.* 18, 244–250. <https://doi.org/10.2307/3676891>
- Braune, B.M., Gaskin, D.E., 1987b. Mercury levels in Bonaparte’s gulls (*Larus Philadelphi*) during autumn molt in the Quoddy region, New Brunswick, Canada. *Arch. Environ. Contam. Toxicol.* 16, 539–549. <https://doi.org/10.1007/BF01055810>
- Braune, B.M., Gaston, A.J., Elliott, K.H., Provencher, J.F., Woo, K.J., Chambellant, M., Ferguson, S.H., Letcher, R.J., 2014a. Organohalogen contaminants and total mercury in forage fish preyed upon by thick-billed murrelets in northern Hudson Bay. *Mar. Pollut. Bull.* 78, 258–266. <https://doi.org/10.1016/j.marpolbul.2013.11.003>
- Braune, B.M., Gaston, A.J., Hobson, K.A., Gilchrist, H.G., Mallory, M.L., 2014b. Changes in food web structure alter trends of mercury uptake at two seabird colonies in the Canadian Arctic. *Environ. Sci. Technol.* 48, 13246–13252. <https://doi.org/10.1021/es5036249>
- Braune, B.M., Gaston, A.J., Mallory, M.L., 2016. Temporal trends of mercury in eggs of five sympatrically breeding seabird species in the Canadian Arctic. *Environ. Pollut.* 214, 124–131. <https://doi.org/10.1016/j.envpol.2016.04.006>
- Breitburg, D., Levin, L.A., Oschlies, A., Grégoire, M., Chavez, F.P., Conley, D.J., Garçon, V., Gilbert, D., Gutiérrez, D., Isensee, K., Jacinto, G.S., Limburg, K.E., Montes, I., Naqvi, S.W.A., Pitcher, G.C., Rabalais, N.N., Roman, M.R., Rose, K.A., Seibel, B.A., Telszewski, M., Yasuhara, M., Zhang, J., 2018. Declining oxygen in the global ocean and coastal waters. *Science* 359, eaam7240. <https://doi.org/10.1126/science.aam7240>

- Brennan, M.K., Hakim, G.J., 2022. Reconstructing arctic sea ice over the Common Era using data assimilation. *J. Clim.* 35, 1231–1247. <https://doi.org/10.1175/JCLI-D-21-0099.1>
- Brooke M., 2004. The food consumption of the world's seabirds. *Proc. R. Soc. Lond. B Biol. Sci.* 271, S246–S248. <https://doi.org/10.1098/rsbl.2003.0153>
- Brown, T.M., Fisk, A.T., Wang, X., Ferguson, S.H., Young, B.G., Reimer, K.J., Muir, D.C.G., 2016. Mercury and cadmium in ringed seals in the Canadian Arctic: Influence of location and diet. *Sci. Total Environ.* 545–546, 503–511. <https://doi.org/10.1016/j.scitotenv.2015.12.030>
- Burger, J., 1993. Metals in avian feathers: bioindicators of environmental pollution. *Reviews of Environmental Toxicology* 5:203–311
- Burger, J., 2002. Food chain differences affect heavy metals in bird eggs in Barnegat Bay, New Jersey. *Environ. Res.* 90, 33–39. <https://doi.org/10.1006/enrs.2002.4381>
- Burger, J., Gochfeld, M., 2004. Marine birds as sentinels of environmental pollution. *EcoHealth* 1, 263–274. <https://doi.org/10.1007/s10393-004-0096-4>
- Burger, J., Gochfeld, M., 2001a. On developing bioindicators for human and ecological health. *Environ. Monit. Assess.* 66, 23–46. <https://doi.org/10.1023/A:1026476030728>
- Burger, J., Gochfeld, M., 2001b. Effects of chemicals and pollution on seabirds, in: *Biology of Marine Birds*. CRC Press, pp. 485–525. <https://doi.org/10.1201/9781420036305>
- Burger, J., Gochfeld, M., 2000. Metal levels in feathers of 12 species of seabirds from Midway Atoll in the northern Pacific Ocean. *Sci. Total Environ.* 257, 37–52. [https://doi.org/10.1016/S0048-9697\(00\)00496-4](https://doi.org/10.1016/S0048-9697(00)00496-4)
- Burger, J., Gochfeld, M., 1995. Biomonitoring of heavy metals in the Pacific basin using avian feathers. *Environ. Toxicol. Chem.* 14, 1233–1239. <https://doi.org/10.1002/etc.5620140716>
- Burger, J., Gochfeld, M., 1991. Lead, mercury, and cadmium in feathers of tropical terns in Puerto Rico and Australia. *Arch. Environ. Contam. Toxicol.* 21, 311–315. <https://doi.org/10.1007/BF01055351>
- Burger, J., Schreiber, E.A.E., Gochfeld, M., 1992. Lead, cadmium, selenium and mercury in seabird feathers from the tropical mid-Pacific. *Environ. Toxicol. Chem.* 11, 815–822. <https://doi.org/10.1002/etc.5620110610>
- Burger, J., Shukla, T., Dixon, C., Shukla, S., McMahon, M.J., Ramos, R., Gochfeld, M., 2001. Metals in feathers of sooty tern, white tern, gray-backed tern, and brown noddy from islands in the North Pacific. *Environ. Monit. Assess.* 71, 71–89. <https://doi.org/10.1023/A:1011695829296>
- Bustamante, P., Carravieri, A., Goutte, A., Barbraud, C., Delord, K., Chastel, O., Weimerskirch, H., Cherel, Y., 2016. High feather mercury concentrations in the wandering albatross are related to sex, breeding status and trophic ecology with no demographic consequences. *Environ. Res.* 144, 1–10. <https://doi.org/10.1016/j.envres.2015.10.024>
- Bustamante, P., Caurant, F., Fowler, S.W., Miramand, P., 1998. Cephalopods as a vector for the transfer of cadmium to top marine predators in the north-east Atlantic Ocean. *Sci. Total Environ.* 220, 71–80. [https://doi.org/10.1016/S0048-9697\(98\)00250-2](https://doi.org/10.1016/S0048-9697(98)00250-2)

C

- Cabana, G., Rasmussen, J.B., 1996. Comparison of aquatic food chains using nitrogen isotopes. *Proc. Natl. Acad. Sci.* 93, 10844–10847. <https://doi.org/10.1073/pnas.93.20.10844>
- Cairns, D.K., 1988. Seabirds as indicators of marine food supplies. *Biol. Oceanogr.* 5, 261–271. <https://doi.org/10.1080/01965581.1987.10749517>
- Campbell, L.M., Norstrom, R.J., Hobson, K.A., Muir, D.C.G., Backus, S., Fisk, A.T., 2005. Mercury and other trace elements in a pelagic Arctic marine food web (Northwater Polynya, Baffin Bay). *Sci. Total Environ., Contaminants in Canadian Arctic Biota and Implications for Human Health* 351–352, 247–263. <https://doi.org/10.1016/j.scitotenv.2005.02.043>
- Carravieri, A., 2014. Seabirds as bioindicators of Southern Ocean ecosystems: Concentrations of inorganic and organic contaminants, ecological explanation and critical evaluation. La Rochelle Université, La Rochelle, France.
- Carravieri, A., Burthe, S.J., de la Vega, C., Yonehara, Y., Daunt, F., Newell, M.A., Jeffreys, R.M., Lawlor, A.J., Hunt, A., Shore, R.F., Pereira, M.G., Green, J.A., 2020. Interactions between environmental contaminants and gastrointestinal parasites: Novel insights from an integrative approach in a marine predator. *Environ. Sci. Technol.* 54, 8938–8948. <https://doi.org/10.1021/acs.est.0c03021>
- Carravieri, A., Bustamante, P., Churlaud, C., Cherel, Y., 2013. Penguins as bioindicators of mercury contamination in the Southern Ocean: Birds from the Kerguelen islands as a case study. *Sci. Total Environ.* 454–455, 141–148. <https://doi.org/10.1016/j.scitotenv.2013.02.060>
- Carravieri, A., Bustamante, P., Churlaud, C., Fromant, A., Cherel, Y., 2014a. Moulting patterns drive within-individual variations of stable isotopes and mercury in seabird body feathers: Implications for monitoring of the marine environment. *Mar. Biol.* 161, 963–968. <https://doi.org/10.1007/s00227-014-2394-x>

- Carravieri, A., Bustamante, P., Tartu, S., Meillère, A., Labadie, P., Budzinski, H., Peluhet, L., Barbraud, C., Weimerskirch, H., Chastel, O., Cherel, Y., 2014b. Wandering Albatrosses document latitudinal variations in the transfer of persistent organic pollutants and mercury to Southern Ocean predators. *Environ. Sci. Technol.* 48, 14746–14755. <https://doi.org/10.1021/es504601m>
- Carravieri, A., Cherel, Y., Blévin, P., Brault-Favrou, M., Chastel, O., Bustamante, P., 2014c. Mercury exposure in a large subantarctic avian community. *Environ. Pollut.* 190, 51–57. <https://doi.org/10.1016/j.envpol.2014.03.017>
- Carravieri, A., Cherel, Y., Brault-Favrou, M., Churlaud, C., Peluhet, L., Labadie, P., Budzinski, H., Chastel, O., Bustamante, P., 2017. From Antarctica to the subtropics: Contrasted geographical concentrations of selenium, mercury, and persistent organic pollutants in skua chicks (*Catharacta spp.*). *Environ. Pollut.* 228, 464–473. <https://doi.org/10.1016/j.envpol.2017.05.053>
- Carravieri, A., Cherel, Y., Jaeger, A., Churlaud, C., Bustamante, P., 2016. Penguins as bioindicators of mercury contamination in the southern Indian Ocean: Geographical and temporal trends. *Environ. Pollut. Barking Essex* 1987 213, 195–205. <https://doi.org/10.1016/j.envpol.2016.02.010>
- Carravieri, A., Fort, J., Tarrow, A., Cherel, Y., Love, O.P., Prieur, S., Brault-Favrou, M., Bustamante, P., Descamps, S., 2018. Mercury exposure and short-term consequences on physiology and reproduction in Antarctic petrels. *Environ. Pollut.* 237, 824–831. <https://doi.org/10.1016/j.envpol.2017.11.004>
- Carter, L., McCave, I.N., Williams, M.J.M., 2008. Chapter 4 Circulation and water masses of the Southern Ocean: A Review, in: Florindo, F., Siegert, M. (Eds.), *Developments in Earth and Environmental Sciences, Antarctic Climate Evolution*. Elsevier, pp. 85–114. [https://doi.org/10.1016/S1571-9197\(08\)00004-9](https://doi.org/10.1016/S1571-9197(08)00004-9)
- Catry, T., Ramos, J.A., Le Corre, M., Kojadinovic, J., Bustamante, P., 2008. The role of stable isotopes and mercury concentrations to describe seabird foraging ecology in tropical environments. *Mar. Biol.* 155, 637–647. <https://doi.org/10.1007/s00227-008-1060-6>
- Chastel, O., Fort, J., Ackerman, J.T., Albert, C., Angelier, F., Basu, N., Blévin, P., Brault-Favrou, M., Bustnes, J.O., Bustamante, P., Danielsen, J., Descamps, S., Dietz, R., Erikstad, K.E., Eulaers, I., Ezhov, A., Fleishman, A.B., Gabrielsen, G.W., Gavrilov, M., Gilchrist, G., Gilg, O., Gíslason, S., Golubova, E., Goutte, A., Grémillet, D., Hallgrímsson, G.T., Hansen, E.S., Hanssen, S.A., Hatch, S., Huffeldt, N.P., Jakubas, D., Jónsson, J.E., Kitaysky, A.S., Kolbeinsson, Y., Krasnov, Y., Letcher, R.J., Linnebjerg, J.F., Mallory, M., Merkel, F.R., Moe, B., Montevecchi, W.J., Mosbech, A., Olsen, B., Orben, R.A., Provencher, J.F., Ragnarsdóttir, S.B., Reiertsen, T.K., Rojek, N., Romano, M., Søndergaard, J., Strøm, H., Takahashi, A., Tartu, S., Thórarinnsson, T.L., Thiebot, J.-B., Will, A.P., Wilson, S., Wojczulanis-Jakubas, K., Yannic, G., 2022. Mercury contamination and potential health risks to Arctic seabirds and shorebirds. *Sci. Total Environ.* 156944. <https://doi.org/10.1016/j.scitotenv.2022.156944>
- Chen, C.Y., Evers, D.C., 2023. Global mercury impact synthesis: Processes in the Southern Hemisphere. *Ambio.* <https://doi.org/10.1007/s13280-023-01842-3>
- Cherel, Y., 2008. Isotopic niches of emperor and Adélie penguins in Adélie Land, Antarctica. *Mar. Biol.* 154, 813–821. <https://doi.org/10.1007/s00227-008-0974-3>
- Cherel, Y., Barbraud, C., Lahournat, M., Jaeger, A., Jaquemet, S., Wanless, R.M., Phillips, R.A., Thompson, D.R., Bustamante, P., 2018. Accumulate or eliminate? Seasonal mercury dynamics in albatrosses, the most contaminated family of birds. *Environ. Pollut.* 241, 124–135. <https://doi.org/10.1016/j.envpol.2018.05.048>
- Cherel, Y., Charrassin, J.B., Challet, E., 1994. Energy and protein requirements for molt in the king penguin *Aptenodytes patagonicus*. *Am. J. Physiol.* 266, R1182–1188. <https://doi.org/10.1152/ajpregu.1994.266.4.R1182>
- Cherel, Y., Connan, M., Jaeger, A., Richard, P., 2014. Seabird year-round and historical feeding ecology: Blood and feather $\delta^{13}\text{C}$ and $\delta^{15}\text{N}$ values document foraging plasticity of small sympatric petrels. *Mar. Ecol. Prog. Ser.* 505, 267–280. <https://doi.org/10.3354/meps10795>
- Cherel, Y., Hobson, K.A., 2007. Geographical variation in carbon stable isotope signatures of marine predators: A tool to investigate their foraging areas in the Southern Ocean. *Mar. Ecol. Prog. Ser.* 329, 281–287. <https://doi.org/10.3354/meps329281>
- Cherel, Y., Hobson, K.A., Guinet, C., Vanpe, C., 2007. Stable isotopes document seasonal changes in trophic niches and winter foraging individual specialization in diving predators from the Southern Ocean. *J. Anim. Ecol.* 76, 826–836. <https://doi.org/10.1111/j.1365-2656.2007.01238.x>
- Cherel, Y., Jaeger, A., Alderman, R., Jaquemet, S., Richard, P., Wanless, R.M., Phillips, R.A., Thompson, D.R., 2013. A comprehensive isotopic investigation of habitat preferences in nonbreeding albatrosses from the Southern Ocean. *Ecography* 36, 277–286. <https://doi.org/10.1111/j.1600-0587.2012.07466.x>
- Chételat, J., Ackerman, J.T., Eagles-Smith, C.A., Hebert, C.E., 2020. Methylmercury exposure in wildlife: A review of the ecological and physiological processes affecting contaminant concentrations and their interpretation. *Sci. Total Environ.* 711, 135117. <https://doi.org/10.1016/j.scitotenv.2019.135117>

- Chételat, J., McKinney, M.A., Amyot, M., Dastoor, A., Douglas, T.A., Heimbürger-Boavida, L.-E., Kirk, J., Kahilainen, K.K., Outridge, P.M., Pelletier, N., Skov, H., St. Pierre, K., Vuorenmaa, J., Wang, F., 2022. Climate change and mercury in the Arctic: Abiotic interactions. *Sci. Total Environ.* 824, 153715. <https://doi.org/10.1016/j.scitotenv.2022.153715>
- Chikaraishi, Y., Ogawa, N.O., Kashiyama, Y., Takano, Y., Suga, H., Tomitani, A., Miyashita, H., Kitazato, H., Ohkouchi, N., 2009. Determination of aquatic food-web structure based on compound-specific nitrogen isotopic composition of amino acids. *Limnol. Oceanogr. Methods* 7, 740–750. <https://doi.org/10.4319/lom.2009.7.740>
- Chikaraishi, Y., Steffan, S.A., Ogawa, N.O., Ishikawa, N.F., Sasaki, Y., Tsuchiya, M., Ohkouchi, N., 2014. High-resolution food webs based on nitrogen isotopic composition of amino acids. *Ecol. Evol.* 4, 2423–2449. <https://doi.org/10.1002/ece3.1103>
- Chouvelon, T., Spitz, J., Caurant, F., Méndez-Fernandez, P., Autier, J., Lassus-Débat, A., Chappuis, A., Bustamante, P., 2012. Enhanced bioaccumulation of mercury in deep-sea fauna from the Bay of Biscay (north-east Atlantic) in relation to trophic positions identified by analysis of carbon and nitrogen stable isotopes. *Deep Sea Res. Part Oceanogr. Res. Pap.* 65, 113–124. <https://doi.org/10.1016/j.dsr.2012.02.010>
- Choy, E.S., Blight, L.K., Elliott, J.E., Hobson, K.A., Zanuttig, M., Elliott, K.H., 2022. Stable mercury trends support a long-term diet shift away from marine foraging in Salish Sea glaucous-winged gulls over the last century. *Environ. Sci. Technol.* 56, 12097–12105. <https://doi.org/10.1021/acs.est.1c03760>
- Cifuentes, L.A., Sharp, J.H., Fogel, M.L., 1988. Stable carbon and nitrogen isotope biogeochemistry in the Delaware estuary. *Limnol. Oceanogr.* 33, 1102–1115. <https://doi.org/10.4319/lo.1988.33.5.1102>
- Clackett, S.P., Porter, T.J., Lehnerr, I., 2018. 400-Year record of atmospheric mercury from tree-rings in Northwestern Canada. *Environ. Sci. Technol.* 52, 9625–9633. <https://doi.org/10.1021/acs.est.8b01824>
- Clarke, J., Manly, B., Kerry, K., Gardner, H., Franchi, E., Corsolini, S., Focardi, S., 1998. Sex differences in Adélie penguin foraging strategies. *Polar Biol.* 20, 248–258. <https://doi.org/10.1007/s003000050301>
- Clayden, M.G., Kidd, K.A., Wyn, B., Kirk, J.L., Muir, D.C.G., O'Driscoll, N.J., 2013. Mercury biomagnification through food webs is affected by physical and chemical characteristics of lakes. *Environ. Sci. Technol.* 47, 12047–12053. <https://doi.org/10.1021/es4022975>
- Clucas, G.V., Dunn, M.J., Dyke, G., Emslie, S.D., Levy, H., Naveen, R., Polito, M.J., Pybus, O.G., Rogers, A.D., Hart, T., 2014. A reversal of fortunes: Climate change ‘winners’ and ‘losers’ in Antarctic Peninsula penguins. *Sci. Rep.* 4, 5024. <https://doi.org/10.1038/srep05024>
- Coats, R.R., 1953. *Geology of Buldir Island, Aleutian Islands, Alaska*. U.S. Government Printing Office.
- Colominas-Ciuró, R., Santos, M., Coria, N., Barbosa, A., 2018. Sex-specific foraging strategies of Adélie penguins (*Pygoscelis adeliae*): Females forage further and on more krill than males in the Antarctic Peninsula. *Polar Biol.* 41, 2635–2641. <https://doi.org/10.1007/s00300-018-2395-1>
- Cooke, C.A., Martínez-Cortizas, A., Bindler, R., Sexauer Gustin, M., 2020. Environmental archives of atmospheric Hg deposition – A review. *Sci. Total Environ.* 709, 134800. <https://doi.org/10.1016/j.scitotenv.2019.134800>
- Coria, N.R., Spairani, H., Vivequin, S., Fontana, R., 1995. Diet of Adélie penguins *Pygoscelis adeliae* during the post-hatching period at Esperanza Bay, Antarctica, 1987/88. *Polar Biol.* 15, 415–418. <https://doi.org/10.1007/BF00239717>
- Corr, L.T., Berstan, R., Evershed, R.P., 2007. Development of N-acetyl methyl ester derivatives for the determination of $\delta^{13}\text{C}$ values of amino acids using gas chromatography-combustion- isotope ratio mass spectrometry. *Anal. Chem.* 79, 9082–9090. <https://doi.org/10.1021/ac071223b>
- Cossa, D., 2013. Methylmercury manufacture. *Nat. Geosci.* 6, 810–811. <https://doi.org/10.1038/ngeo1967>
- Cossa, D., Averty, B., Pirrone, N., 2009. The origin of methylmercury in open Mediterranean waters. *Limnol. Oceanogr.* 54, 837–844. <https://doi.org/10.4319/lo.2009.54.3.0837>
- Cossa, D., Heimbürger, L.-E., Lannuzel, D., Rintoul, S.R., Butler, E.C.V., Bowie, A.R., Averty, B., Watson, R.J., Remenyi, T., 2011. Mercury in the Southern Ocean. *Geochim. Cosmochim. Acta* 75, 4037–4052. <https://doi.org/10.1016/j.gca.2011.05.001>
- Cransveld, A., Amouroux, D., Tessier, E., Koutrakis, E., Ozturk, A.A., Bettoso, N., Mieiro, C.L., Bérail, S., Barre, J.P.G., Sturaro, N., Schnitzler, J., Das, K., 2017. Mercury stable isotopes discriminate different populations of European seabass and trace potential Hg sources around Europe. *Environ. Sci. Technol.* 51, 12219–12228. <https://doi.org/10.1021/acs.est.7b01307>
- Crewther, W.G., Fraser, R.D., Lennox, F.G., Lindley, H., 1965. The chemistry of keratins. *Adv. Protein Chem.* 20, 191–346. [https://doi.org/10.1016/s0065-3233\(08\)60390-3](https://doi.org/10.1016/s0065-3233(08)60390-3)
- Croll, D.A., Gaston, A.J., Burger, A.E., Konnoff, D., 1992. Foraging behavior and physiological adaptation for diving in thick-billed murre. *Ecology* 73, 344–356. <https://doi.org/10.2307/1938746>
- Croxall, J.P., Butchart, S.H.M., Lascelles, B., Stattersfield, A.J., Sullivan, B., Symes, A., Taylor, P., 2012. Seabird conservation status, threats and priority actions: A global assessment. *Bird Conserv. Int.* 22, 1–34. <https://doi.org/10.1017/S0959270912000020>

- Cruz-Flores, M., Lemaire, J., Brault-Favrou, M., Christensen-Dalsgaard, S., Churlaud, C., Descamps, S., Elliott, K., Erikstad, K.E., Ezhov, A., Gavrilov, M., Grémillet, D., Guillou, G., Hatch, S., Huffeldt, N., Kitaysky, A.S., Kolbeinsson, Y., Krasnov, Y., Langset, M., Leclair, S., Linnebjerg, J.F., Lorentzen, E., Mallory, M.L., Merkel, F.R., Montevicchi, W., Mosbech, A., Patterson, A., Perret, S., Provencher, J.F., Reiertsen, T.K., Renner, H., Strøm, H., Takahashi, A., Thiebot, J.B., Thórarinnsson, T.L., Will, A., Bustamante, P., Fort, J., 2024. Spatial distribution of selenium-mercury in Arctic seabirds. *Env. Pol.*, 343:123110. <https://doi.org/10.1016/j.envpol.2023.123110>.
- Cusset, F., Fort, J., Mallory, M., Braune, B., Massicotte, P., Massé, G., 2019. Arctic seabirds and shrinking sea ice: Egg analyses reveal the importance of ice-derived resources. *Sci. Rep.* 9, 1–15. <https://doi.org/10.1038/s41598-019-51788-4>
- Cusset, F., Reynolds, S.J., Carravieri, A., Amouroux, D., Asensio, O., Dickey, R.C., Fort, J., Hughes, B.J., Paiva, V.H., Ramos, J.A., Shearer, L., Tessier, E., Wearn, C.P., Cherel, Y., Bustamante, P., 2023. A century of mercury: Ecosystem-wide changes drive increasing contamination of a tropical seabird species in the South Atlantic Ocean. *Environ. Pollut.* 121187. <https://doi.org/10.1016/j.envpol.2023.121187>
- Cuvin-Aralar, Ma.L.A., Furness, R.W., 1991. Mercury and selenium interaction: A review. *Ecotoxicol. Environ. Saf.* 21, 348–364. [https://doi.org/10.1016/0147-6513\(91\)90074-Y](https://doi.org/10.1016/0147-6513(91)90074-Y)

D

- Dastoor, A., Angot, H., Bieser, J., Christensen, J.H., Douglas, T.A., Heimbürger-Boavida, L.-E., Jiskra, M., Mason, R.P., McLagan, D.S., Obrist, D., Outridge, P.M., Petrova, M.V., Ryjkov, A., St. Pierre, K.A., Schartup, A.T., Soerensen, A.L., Toyota, K., Travnikov, O., Wilson, S.J., Zdanowicz, C., 2022. Arctic mercury cycling. *Nat. Rev. Earth Environ.* 3, 270–286. <https://doi.org/10.1038/s43017-022-00269-w>
- Day, R.D., Roseneau, D.G., Beraill, S., Hobson, K.A., Donard, O.F.X., Vander Pol, S.S., Pugh, R.S., Moors, A.J., Long, S.E., Becker, P.R., 2012. Mercury stable isotopes in seabird eggs reflect a gradient from terrestrial geogenic to oceanic mercury reservoirs. *Environ. Sci. Technol.* 46, 5327–5335. <https://doi.org/10.1021/es2047156>
- DeNiro, M., and Epstein, S. 1976. You are what you eat (plus a few ‰): The carbon isotope cycle in food chains. *Geol. Soc. Am. Abs. Prog.* 8, 834-835.
- DeNiro, M.J., Epstein, S., 1981. Influence of diet on the distribution of nitrogen isotopes in animals. *Geochim. Cosmochim. Acta* 45, 341–351. [https://doi.org/10.1016/0016-7037\(81\)90244-1](https://doi.org/10.1016/0016-7037(81)90244-1)
- DeNiro, M.J., Epstein, S., 1978. Influence of diet on the distribution of carbon isotopes in animals. *Geochim. Cosmochim. Acta* 42, 495–506. [https://doi.org/10.1016/0016-7037\(78\)90199-0](https://doi.org/10.1016/0016-7037(78)90199-0)
- Desforges, J.-P., Outridge, P., Hobson, K.A., Heide-Jørgensen, M.P., Dietz, R., 2022. Anthropogenic and climatic drivers of long-term changes of mercury and feeding ecology in Arctic beluga (*Delphinapterus leucas*) populations. *Environ. Sci. Technol.* 56, 271–281. <https://doi.org/10.1021/acs.est.1c05389>
- Dietz, R., Born, E.W., Rigét, F., Aubail, A., Sonne, C., Drimmie, R., Basu, N., 2011. Temporal trends and future predictions of mercury concentrations in Northwest Greenland polar bear (*Ursus maritimus*) hair. *Environ. Sci. Technol.* 45, 1458–1465. <https://doi.org/10.1021/es1028734>
- Dietz, R., Desforges, J.-P., Rigét, F.F., Aubail, A., Garde, E., Ambus, P., Drimmie, R., Heide-Jørgensen, M.P., Sonne, C., 2021. Analysis of narwhal tusks reveals lifelong feeding ecology and mercury exposure. *Curr. Biol.* 31, 2012-2019.e2. <https://doi.org/10.1016/j.cub.2021.02.018>
- Dietz, R., Letcher, R.J., Aars, J., Andersen, M., Boltunov, A., Born, E.W., Ciesielski, T.M., Das, K., Dastnai, S., Derocher, A.E., Desforges, J.-P., Eulaers, I., Ferguson, S., Hallanger, I.G., Heide-Jørgensen, M.P., Heimbürger-Boavida, L.-E., Hoekstra, P.F., Jenssen, B.M., Kohler, S.G., Larsen, M.M., Lindstrøm, U., Lippold, A., Morris, A., Nabe-Nielsen, J., Nielsen, N.H., Peacock, E., Pinzone, M., Rigét, F.F., Rosing-Asvid, A., Routti, H., Siebert, U., Stenson, G., Stern, G., Strand, J., Søndergaard, J., Treu, G., Víkingsson, G.A., Wang, F., Welker, J.M., Wiig, Ø., Wilson, S.J., Sonne, C., 2022. A risk assessment review of mercury exposure in Arctic marine and terrestrial mammals. *Sci. Total Environ.* 829, 154445. <https://doi.org/10.1016/j.scitotenv.2022.154445>
- Dietz, R., Letcher, R.J., Desforges, J.-P., Eulaers, I., Sonne, C., Wilson, S., Andersen-Ranberg, E., Basu, N., Barst, B.D., Bustnes, J.O., Bytingsvik, J., Ciesielski, T.M., Drevnick, P.E., Gabrielsen, G.W., Haarr, A., Hylland, K., Jenssen, B.M., Levin, M., McKinney, M.A., Nørregaard, R.D., Pedersen, K.E., Provencher, J., Styriehave, B., Tartu, S., Aars, J., Ackerman, J.T., Rosing-Asvid, A., Barrett, R., Bignert, A., Born, E.W., Branigan, M., Braune, B., Bryan, C.E., Dam, M., Eagles-Smith, C.A., Evans, M., Evans, T.J., Fisk, A.T., Gamberg, M., Gustavson, K., Hartman, C.A., Helander, B., Herzog, M.P., Hoekstra, P.F., Houde, M., Hoydal, K., Jackson, A.K., Kucklick, J., Lie, E., Loseto, L., Mallory, M.L., Miljeteig, C., Mosbech, A., Muir, D.C.G., Nielsen, S.T., Peacock, E., Pedro, S., Peterson, S.H., Polder, A., Rigét, F.F., Roach, P., Saunes, H., Sinding, M.-H.S., Skaare, J.U., Søndergaard, J., Stenson, G., Stern, G., Treu, G., Schuur, S.S.,

- Víkingsson, G., 2019. Current state of knowledge on biological effects from contaminants on Arctic wildlife and fish. *Sci. Total Environ.* 696, 133792. <https://doi.org/10.1016/j.scitotenv.2019.133792>
- Dietz, R., Outridge, P.M., Hobson, K.A., 2009. Anthropogenic contributions to mercury levels in present-day Arctic animals—A review. *Sci. Total Environ.* 407, 6120–6131. <https://doi.org/10.1016/j.scitotenv.2009.08.036>
- Dietz, R., Riget, F., Born, E.W., 2000. Geographical differences of zinc, cadmium, mercury and selenium in polar bears (*Ursus maritimus*) from Greenland. *Sci. Total Environ.* 245, 25–47. [https://doi.org/10.1016/S0048-9697\(99\)00431-3](https://doi.org/10.1016/S0048-9697(99)00431-3)
- Dietz, R., Riget, F., Born, E.W., Sonne, C., Grandjean, P., Kirkegaard, M., Olsen, M.T., Asmund, G., Renzoni, A., Baagøe, H., Andreasen, C., 2006. Trends in mercury in hair of Greenlandic polar bears (*Ursus maritimus*) during 1892–2001. *Environ. Sci. Technol.* 40, 1120–1125. <https://doi.org/10.1021/es051636z>
- Dietz, R., Sonne, C., Basu, N., Braune, B., O'Hara, T., Letcher, R.J., Scheuhammer, T., Andersen, M., Andreasen, C., Andriashek, D., Asmund, G., Aubail, A., Baagøe, H., Born, E.W., Chan, H.M., Derocher, A.E., Grandjean, P., Knott, K., Kirkegaard, M., Krey, A., Lunn, N., Messier, F., Obbard, M., Olsen, M.T., Ostertag, S., Peacock, E., Renzoni, A., Rigét, F.F., Skaare, J.U., Stern, G., Stirling, I., Taylor, M., Wiig, Ø., Wilson, S., Aars, J., 2013. What are the toxicological effects of mercury in Arctic biota? *Sci. Total Environ.* 443, 775–790. <https://doi.org/10.1016/j.scitotenv.2012.11.046>
- DiMento, B.P., Mason, R.P., Brooks, S., Moore, C., 2019. The impact of sea ice on the air-sea exchange of mercury in the Arctic Ocean. *Deep Sea Res. Part Oceanogr. Res. Pap.* 144, 28–38. <https://doi.org/10.1016/j.dsr.2018.12.001>
- Dittman, J.A., Shanley, J.B., Driscoll, C.T., Aiken, G.R., Chalmers, A.T., Towse, J.E., Selvendiran, P., 2010. Mercury dynamics in relation to dissolved organic carbon concentration and quality during high flow events in three northeastern U.S. streams. *Water Resour. Res.* 46. <https://doi.org/10.1029/2009WR008351>
- Driscoll, C.T., Mason, R.P., Chan, H.M., Jacob, D.J., Pirrone, N., 2013. Mercury as a global pollutant: Sources, pathways, and effects. *Environ. Sci. Technol.* 47, 4967–4983. <https://doi.org/10.1021/es305071v>

E

- Eagles-Smith, C.A., Silbergeld, E.K., Basu, N., Bustamante, P., Diaz-Barriga, F., Hopkins, W.A., Kidd, K.A., Nyland, J.F., 2018. Modulators of mercury risk to wildlife and humans in the context of rapid global change. *Ambio* 47, 170–197. <https://doi.org/10.1007/s13280-017-1011-x>
- Eccles, K.M., Majeed, H., Porter, T.J., Lehnerr, I., 2020. A continental and marine-influenced tree-ring mercury record in the Old Crow Flats, Yukon, Canada. *ACS Earth Space Chem.* 4, 1281–1290. <https://doi.org/10.1021/acsearthspacechem.0c00081>
- Editorial (2021, April 29) Many Minamata disease victims still waiting for overdue relief. *The Asahi Shimbun*. <https://www.asahi.com/ajw/articles/14340051> (consulted in 2023, April 18th)
- Edwards, B.R., Smellie, J.L. (Eds.), 2016. Distribution of glaciovolcanism on Earth, in: *Glaciovolcanism on Earth and Mars: Products, Processes and Palaeoenvironmental Significance*. Cambridge University Press, Cambridge, pp. 15–56. <https://doi.org/10.1017/CBO9781139764384.003>
- Eide, M., Olsen, A., Ninnemann, U.S., Eldevik, T., 2017. A global estimate of the full oceanic ¹³C Suess effect since the preindustrial. *Glob. Biogeochem. Cycles* 31, 492–514. <https://doi.org/10.1002/2016GB005472>
- Elinder, C.G., 1992. Cadmium as an environmental hazard. *IARC Sci. Publ.* 123–132.
- Emmerson, L., Southwell, C., 2011. Adélie penguin survival: Age structure, temporal variability and environmental influences. *Oecologia* 167, 951–965. <https://doi.org/10.1007/s00442-011-2044-7>
- Emmerson, L., Southwell, C., 2008. Sea ice cover and its influence on Adélie penguin reproductive performance. *Ecology* 89, 2096–2102. <https://doi.org/10.1890/08-0011.1>
- England, M.R., Polvani, L.M., 2023. The Montreal Protocol is delaying the occurrence of the first ice-free Arctic summer. *Proc. Natl. Acad. Sci.* 120, e2211432120. <https://doi.org/10.1073/pnas.2211432120>
- EPA, U.S. 1997. Mercury study report to congress. Washington, DC: EPA.
- Esparza, I., Elliott, K.H., Choy, E.S., Braune, B.M., Letcher, R.J., Patterson, A., Fernie, K.J., 2022. Mercury, legacy and emerging POPs, and endocrine-behavioural linkages: Implications of Arctic change in a diving seabird. *Environ. Res.* 212, 113190. <https://doi.org/10.1016/j.envres.2022.113190>
- Evans, M., Muir, D., Brua, R.B., Keating, J., Wang, X., 2013. Mercury trends in predatory fish in Great Slave Lake: The influence of temperature and other climate drivers. *Environ. Sci. Technol.* 47, 12793–12801. <https://doi.org/10.1021/es402645x>
- Evers, D.C., Savoy, L.J., DeSorbo, C.R., Yates, D.E., Hanson, W., Taylor, K.M., Siegel, L.S., Cooley, J.H., Bank, M.S., Major, A., Munney, K., Mower, B.F., Vogel, H.S., Schoch, N., Pokras, M., Goodale, M.W., Fair, J., 2008. Adverse effects from environmental mercury loads on breeding common loons. *Ecotoxicology* 17, 69–81. <https://doi.org/10.1007/s10646-007-0168-7>
- Evers, D.C. and E. Sunderland. 2019. Technical information report on mercury monitoring in biota: Proposed

- components towards a strategic long-term plan for monitoring mercury in fish and wildlife globally. UN Environment Programme, Chemicals and Health Branch, Geneva, Switzerland. 40 pp.
- Everson, I., 2000. Roles of krill in marine food webs: the Southern Ocean, in: Everson, I. (Ed.). Blackwell Science, Oxford, pp. 194–201.

F

- Feng, C., Pedrero, Z., Lima, L., Olivares, S., de la Rosa, D., Berail, S., Tessier, E., Pannier, F., Amouroux, D., 2019. Assessment of Hg contamination by a Chlor-Alkali Plant in riverine and coastal sites combining Hg speciation and isotopic signature (Sagua la Grande River, Cuba). *J. Hazard. Mater.* 371, 558–565. <https://doi.org/10.1016/j.jhazmat.2019.02.092>
- Ferraccioli, F., Armadillo, E., Bozzo, E., Privitera, E., 2000. Magnetism and gravity image tectonic framework of the Mount Melbourne volcano area (Antarctica). *Phys. Chem. Earth Part Solid Earth Geod.* 25, 387–393. [https://doi.org/10.1016/S1464-1895\(00\)00061-2](https://doi.org/10.1016/S1464-1895(00)00061-2)
- Fisher, J.A., Schneider, L., Fostier, A.-H., Guerrero, S., Guimarães, J.R.D., Labuschagne, C., Leaner, J.J., Martin, L.G., Mason, R.P., Somerset, V., Walters, C., 2023. A synthesis of mercury research in the Southern Hemisphere, part 2: Anthropogenic perturbations. *Ambio*. <https://doi.org/10.1007/s13280-023-01840-5>
- Fleishman, A.B., Orben, R.A., Kokubun, N., Will, A., Paredes, R., Ackerman, J.T., Takahashi, A., Kitaysky, A.S., Shaffer, S.A., 2019. Wintering in the Western Subarctic Pacific increases mercury contamination of red-legged kittiwakes. *Environ. Sci. Technol.* 53, 13398–13407. <https://doi.org/10.1021/acs.est.9b03421>
- Forero, M.G., Hobson, K.A., Bortolotti, G.R., Donázar, J.A., Bertellotti, M., Blanco, G., 2002. Food resource utilisation by the Magellanic penguin evaluated through stable-isotope analysis: Segregation by sex and age and influence on offspring quality. *Mar. Ecol. Prog. Ser.* 234, 289–299. <https://doi.org/10.3354/meps234289>
- Fort, J., Grémillet, D., Traisnel, G., Amélineau, F., Bustamante, P., 2016. Does temporal variation of mercury levels in Arctic seabirds reflect changes in global environmental contamination, or a modification of Arctic marine food web functioning? *Environ. Pollut.* 211, 382–388. <https://doi.org/10.1016/j.envpol.2015.12.061>
- Fort, J., Robertson, G.J., Grémillet, D., Traisnel, G., Bustamante, P., 2014. Spatial ecotoxicology: Migratory Arctic seabirds are exposed to mercury contamination while overwintering in the Northwest Atlantic. *Environ. Sci. Technol.* 48, 11560–11567. <https://doi.org/10.1021/es504045g>
- Foster, K.L., Braune, B.M., Gaston, A.J., Mallory, M.L., 2019. Climate influence on mercury in Arctic seabirds. *Sci. Total Environ.* 693, 133569. <https://doi.org/10.1016/j.scitotenv.2019.07.375>
- France, R., 1995. Carbon-13 enrichment in benthic compared to planktonic algae: Foodweb implications. *Mar. Ecol. Prog. Ser.* 124, 307–312. <https://doi.org/10.3354/meps124307>
- Fry, B., 1999. Using stable isotopes to monitor watershed influences on aquatic trophodynamics. *Can. J. Fish. Aquat. Sci.* 56, 2167–2171. <https://doi.org/10.1139/f99-152>
- Fry, B., Sherr, E.B., 1989. $\delta^{13}\text{C}$ measurements as indicators of carbon flow in marine and freshwater ecosystems, in: Rundel, P.W., Ehleringer, J.R., Nagy, K.A. (Eds.), *Stable Isotopes in Ecological Research*, Ecological Studies. Springer New York, pp. 196–229.
- Furness, R.W., 1993. Birds as monitors of pollutants, in: Furness, R.W., Greenwood, J.J.D. (Eds.), *Birds as Monitors of Environmental Change*. Springer Netherlands, Dordrecht, pp. 86–143. https://doi.org/10.1007/978-94-015-1322-7_3
- Furness, R.W., Camphuysen, K. (C J.), 1997. Seabirds as monitors of the marine environment. *ICES J. Mar. Sci.* 54, 726–737. <https://doi.org/10.1006/jmsc.1997.0243>
- Furness, R.W., Muirhead, S.J., Woodburn, M., 1986. Using bird feathers to measure mercury in the environment: Relationships between mercury content and moult. *Mar. Pollut. Bull.* 17, 27–30. [https://doi.org/10.1016/0025-326X\(86\)90801-5](https://doi.org/10.1016/0025-326X(86)90801-5)
- Furness, R.W., Thompson, D.R., Becker, P.H., 1995. Spatial and temporal variation in mercury contamination of seabirds in the North Sea. *Helgoländer Meeresunters.* 49, 605–615. <https://doi.org/10.1007/BF02368386>
- Furtado, R., Granadeiro, J.P., Gatt, M.C., Rounds, R., Horikoshi, K., Paiva, V.H., Menezes, D., Pereira, E., Catry, P., 2021. Monitoring of mercury in the mesopelagic domain of the Pacific and Atlantic oceans using body feathers of Bulwer's petrel as a bioindicator. *Sci. Total Environ.* 775, 145796. <https://doi.org/10.1016/j.scitotenv.2021.145796>

G

- Gaden, A., Stern, G.A., 2010. Temporal Trends in Beluga, Narwhal and Walrus Mercury Levels: Links to Climate Change, in: Ferguson, S.H., Loseto, L.L., Mallory, M.L. (Eds.), *A little less Arctic: Top predators in the world's largest Northern inland sea, Hudson Bay*. Springer Netherlands, Dordrecht, pp. 197–216. https://doi.org/10.1007/978-90-481-9121-5_10

- Gaston, A.J., Gilchrist, H.G., Hipfner, J.M., 2005. Climate change, ice conditions and reproduction in an Arctic nesting marine bird: Brunnich's guillemot (*Uria lomvia* L.). *J. Anim. Ecol.* 74, 832–841. <https://doi.org/10.1111/j.1365-2656.2005.00982.x>
- Gaston, A. J. and J. M. Hipfner (2020). Thick-billed Murre (*Uria lomvia*), version 1.0. In *Birds of the World* (S. M. Billerman, Editor). Cornell Lab of Ornithology, Ithaca, NY, USA. <https://doi.org/10.2173/bow.thbmur.01>
- Gaston, A.J., Jones, I.L., 1998. *The Auks: Alcidae, Bird Families of the World*. Oxford University Press.
- Gaston, A.J., Nettleship, D.N., 1981. *The thick-billed murre of Prince Leopold Island*, Monograph Series. Environment Canada - Canadian Wildlife Service, Ottawa.
- Gaston, A.J., Smith, P.A., Provencher, J.F., 2012. Discontinuous change in ice cover in Hudson Bay in the 1990s and some consequences for marine birds and their prey. *ICES J. Mar. Sci.* 69, 1218–1225. <https://doi.org/10.1093/icesjms/fss040>
- Gaston, A.J., Woo, K., Hipfner, M., 2003. Trends in forage fish populations in Northern Hudson Bay since 1981, as determined from the diet of nestling thick-billed murre *Uria Lomvia*. *Arctic* 56, 227.
- Gatt, M.C., Reis, B., Granadeiro, J.P., Pereira, E., Catry, P., 2020. Generalist seabirds as biomonitors of ocean mercury: The importance of accurate trophic position assignment. *Sci. Total Environ.* 740, 140159. <https://doi.org/10.1016/j.scitotenv.2020.140159>
- Georgiadis, E., Giraudeau, J., Jennings, A., Limoges, A., Jackson, R., Ribeiro, S., Massé, G., 2020. Local and regional controls on Holocene sea ice dynamics and oceanography in Nares Strait, Northwest Greenland. *Mar. Geol.* 422, 106115. <https://doi.org/10.1016/j.margeo.2020.106115>
- Ghotra, A., Lehnerr, I., Porter, T.J., Pisaric, M.F.J., 2020. Tree-ring inferred atmospheric mercury concentrations in the Mackenzie Delta (NWT, Canada) peaked in the 1970s but are increasing once more. *ACS Earth Space Chem.* 4, 457–466. <https://doi.org/10.1021/acsearthspacechem.0c00003>
- Gilmour, C.C., Podar, M., Bullock, A.L., Graham, A.M., Brown, S.D., Somenahally, A.C., Johs, A., Hurt, R.A., Bailey, K.L., Elias, D.A., 2013. Mercury methylation by novel microorganisms from new environments. *Environ. Sci. Technol.* 47, 11810–11820. <https://doi.org/10.1021/es403075t>
- Gilmour, M.E., Holmes, N.D., Fleishman, A.B., Kriwoken, L.K., 2019. Temporal and interspecific variation in feather mercury in four penguin species from Macquarie Island, Australia. *Mar. Pollut. Bull.* 142, 282–289. <https://doi.org/10.1016/j.marpolbul.2019.03.051>
- Gionfriddo, C.M., Tate, M.T., Wick, R.R., Schultz, M.B., Zemla, A., Thelen, M.P., Schofield, R., Krabbenhoft, D.P., Holt, K.E., Moreau, J.W., 2016. Microbial mercury methylation in Antarctic sea ice. *Nat. Microbiol.* 1, 1–12. <https://doi.org/10.1038/nmicrobiol.2016.127>
- Gochfeld, J.B., Michael, 2000. Effects of lead on birds (Laridae): A Review of laboratory and field Studies. *J. Toxicol. Environ. Health Part B* 3, 59–78. <https://doi.org/10.1080/109374000281096>
- Goering, J., Alexander, V., Haubenstock, N., 1990. Seasonal variability of stable carbon and nitrogen isotope ratios of organisms in a North Pacific Bay. *Estuar. Coast. Shelf Sci.* 30, 239–260. [https://doi.org/10.1016/0272-7714\(90\)90050-2](https://doi.org/10.1016/0272-7714(90)90050-2)
- Gon, O., Heemstra, P.C., 1990. *Fishes of the Southern Ocean*, First edition. ed. J.L.B. Smith Institute of Ichthyology, Grahamstown, South Africa.
- Gong, H., Li, C., Zhou, Y., 2021. Emerging global ocean deoxygenation across the 21st century. *Geophys. Res. Lett.* 48, e2021GL095370. <https://doi.org/10.1029/2021GL095370>
- González-Bergonzoni Ivan, Johansen Kasper L., Mosbech Anders, Landkildehus Frank, Jeppesen Erik, Davidson Thomas A., 2017. Small birds, big effects: the little auk (*Alle alle*) transforms high Arctic ecosystems. *Proc. R. Soc. B Biol. Sci.* 284, 20162572. <https://doi.org/10.1098/rspb.2016.2572>
- González-Solís, J., Croxall, J.P., Wood, A.G., 2000. Sexual dimorphism and sexual segregation in foraging strategies of northern giant petrels, *Macronectes halli*, during incubation. *Oikos* 90, 390–398. <https://doi.org/10.1034/j.1600-0706.2000.900220.x>
- Goutte, A., Bustamante, P., Barbraud, C., Delord, K., Weimerskirch, H., Chastel, O., 2014. Demographic responses to mercury in two closely related Antarctic top predators 95, 1075–1086. <https://doi.org/10.1890/13-1229.1>
- Grasby, S.E., Them, T.R., Chen, Z., Yin, R., Ardakani, O.H., 2019. Mercury as a proxy for volcanic emissions in the geologic record. *Earth-Sci. Rev.* 196, 102880. <https://doi.org/10.1016/j.earscirev.2019.102880>
- Gruber, N., 2011. Warming up, turning sour, losing breath: Ocean biogeochemistry under global change. *Philos. Trans. R. Soc. Math. Phys. Eng. Sci.* 369, 1980–1996. <https://doi.org/10.1098/rsta.2011.0003>
- Guen, C.L., Kato, A., Raymond, B., Barbraud, C., Beaulieu, M., Bost, C.-A., Delord, K., MacIntosh, A.J.J., Meyer, X., Raclot, T., Sumner, M., Takahashi, A., Thiebot, J.-B., Ropert-Coudert, Y., 2018. Reproductive performance and diving behaviour share a common sea-ice concentration optimum in Adélie penguins (*Pygoscelis adeliae*). *Glob. Change Biol.* 24, 5304–5317. <https://doi.org/10.1111/gcb.14377>

H

- Hammerschmidt, C.R., Bowman, K.L., 2012. Vertical methylmercury distribution in the subtropical North Pacific Ocean. *Mar. Chem.* 132–133, 77–82. <https://doi.org/10.1016/j.marchem.2012.02.005>
- Hammerschmidt, C.R., Fitzgerald, W.F., 2006. Methylmercury cycling in sediments on the continental shelf of southern New England. *Geochim. Cosmochim. Acta* 70, 918–930. <https://doi.org/10.1016/j.gca.2005.10.020>
- Harrison, P., Perrow, M.R. and Larsson, H. 2021. *Seabirds. The New Identification Guide*, Lynx Edicions, Barcelona.
- Hawkings, J.R., Linhoff, B.S., Wadham, J.L., Stibal, M., Lamborg, C.H., Carling, G.T., Lamarche-Gagnon, G., Kohler, T.J., Ward, R., Hendry, K.R., Falteisek, L., Kellerman, A.M., Cameron, K.A., Hatton, J.E., Tingey, S., Holt, A.D., Vinšová, P., Hofer, S., Bulínová, M., Větrovský, T., Meire, L., Spencer, R.G.M., 2021. Large subglacial source of mercury from the southwestern margin of the Greenland Ice Sheet. *Nat. Geosci.* 14, 496–502. <https://doi.org/10.1038/s41561-021-00753-w>
- Hayes, J.M., 2001. Fractionation of carbon and hydrogen isotopes in biosynthetic processes. *Rev. Mineral. Geochem.* 43, 225–277. <https://doi.org/10.2138/gsrmg.43.1.225>
- Heimbürger, L.-E., Sonke, J.E., Cossa, D., Point, D., Lagane, C., Laffont, L., Galfond, B.T., Nicolaus, M., Rabe, B., van der Loeff, M.R., 2015. Shallow methylmercury production in the marginal sea ice zone of the central Arctic Ocean. *Sci. Rep.* 5, 10318. <https://doi.org/10.1038/srep10318>
- Heinz, G.H., Hoffman, D.J., Klimstra, J.D., Stebbins, K.R., 2010. Predicting mercury concentrations in mallard eggs from mercury in the diet or blood of adult females and from duckling down feathers. *Environ. Toxicol. Chem.* 29, 389–392. <https://doi.org/10.1002/etc.50>
- Heyes, A., Mason, R.P., Kim, E.-H., Sunderland, E., 2006. Mercury methylation in estuaries: Insights from using measuring rates using stable mercury isotopes. *Mar. Chem.*, 8th International Estuarine Biogeochemistry Symposium - Introduction 102, 134–147. <https://doi.org/10.1016/j.marchem.2005.09.018>
- Hilton, G.M., Thompson, D.R., Sagar, P.M., Cuthbert, R.J., Cherel, Y., Bury, S.J., 2006. A stable isotopic investigation into the causes of decline in a sub-Antarctic predator, the rockhopper penguin *Eudyptes chrysocome*. *Glob. Change Biol.* 12, 611–625. <https://doi.org/10.1111/j.1365-2486.2006.01130.x>
- Hirons, A.C., Schell, D.M., Finney, B.P., 2001. Temporal records of $\delta^{13}\text{C}$ and $\delta^{15}\text{N}$ in North Pacific pinnipeds: Inferences regarding environmental change and diet. *Oecologia* 129, 591–601. <https://doi.org/10.1007/s004420100756>
- Hobson, K.A., 1999. Tracing origins and migration of wildlife using stable isotopes: A review. *Oecologia* 120, 314–326. <https://doi.org/10.1007/s004420050865>
- Hobson, K.A., Ambrose Jr, W.G., Renaud, P.E., 1995. Sources of primary production, benthic-pelagic coupling and trophic relationships within the Northeast Water Polynya: insights from $\delta^{13}\text{C}$ and $\delta^{15}\text{N}$ analysis. *Mar. Ecol. Prog. Ser.* 128, 1–10.
- Hobson, K.A., Clark, R.G., 1992. Assessing avian diets using stable isotopes I: Turnover of ^{13}C in tissues. *The Condor* 94, 181–188. <https://doi.org/10.2307/1368807>
- Hobson, K.A., Fisk, A., Karnovsky, N., Holst, M., Gagnon, J.-M., Fortier, M., 2002. A stable isotope ($\delta^{13}\text{C}$, $\delta^{15}\text{N}$) model for the North Water food web: Implications for evaluating trophodynamics and the flow of energy and contaminants. *Deep Sea Res. Part II Top. Stud. Oceanogr.*, The International North Water Polynya Study 49, 5131–5150. [https://doi.org/10.1016/S0967-0645\(02\)00182-0](https://doi.org/10.1016/S0967-0645(02)00182-0)
- Hobson, K.A., Piatt, J.F., Pitocchelli, J., 1994. Using stable isotopes to determine seabird trophic relationships. *J. Anim. Ecol.* 63, 786–798. <https://doi.org/10.2307/5256>
- Hodum, P.J., Hobson, K.A., 2000. Trophic relationships among Antarctic fulmarine petrels: insights into dietary overlap and chick provisioning strategies inferred from stable-isotope ($\delta^{15}\text{N}$ and $\delta^{13}\text{C}$) analyses. *Mar. Ecol. Prog. Ser.* 198, 273–281. <https://doi.org/10.3354/meps198273>
- Hoen, D.K., Kim, S.L., Hussey, N.E., Wallsgrove, N.J., Drazen, J.C., Popp, B.N., 2014. Amino acid ^{15}N trophic enrichment factors of four large carnivorous fishes. *J. Exp. Mar. Biol. Ecol.* 453, 76–83. <https://doi.org/10.1016/j.jembe.2014.01.006>
- Hogstad, O., Nygård, T., Gätzschmann, P., Lierhagen, S., Thingstad, P.G., 2003. Bird skins in museum collections: are they suitable as indicators of environmental metal load after conservation procedures? *Environ. Monit. Assess.* 87, 47–56. <https://doi.org/10.1023/A:1024485829174>
- Honda, K., Nasu, T., Tatsukawa, R., 1986. Seasonal changes in mercury accumulation in the black-eared kite, *Milvus migrans lineatus*. *Environ. Pollut. Ser. Ecol. Biol.* 42, 325–334. [https://doi.org/10.1016/0143-1471\(86\)90016-4](https://doi.org/10.1016/0143-1471(86)90016-4)
- Honda K., Yamamoto Y., Hidaka H., Tatsukawa R., 1986. Heavy metal accumulations in Adelie penguin, *Pygoscelis adeliae*, and their variations with the reproductive processes 40, 443–453.

- Horowitz, H.M., Jacob, D.J., Zhang, Y., Dibble, T.S., Slemr, F., Amos, H.M., Schmidt, J.A., Corbitt, E.S., Marais, E.A., Sunderland, E.M., 2017. A new mechanism for atmospheric mercury redox chemistry: Implications for the global mercury budget. *Atmospheric Chem. Phys.* 17, 6353–6371. <https://doi.org/10.5194/acp-17-6353-2017>
- Hsu-Kim, H., Eckley, C.S., Achá, D., Feng, X., Gilmour, C.C., Jonsson, S., Mitchell, C.P.J., 2018. Challenges and opportunities for managing aquatic mercury pollution in altered landscapes. *Ambio* 47, 141–169. <https://doi.org/10.1007/s13280-017-1006-7>
- Hughes, B.J., Martin, G.R., Giles, A.D., Reynolds, S.J., 2017. Long-term population trends of sooty terns *Onychoprion fuscatus*: Implications for conservation status. *Popul. Ecol.* 59, 213–224. <https://doi.org/10.1007/s10144-017-0588-z>
- Hughes, B.J., Martin, G.R., Reynolds, S.J., 2012. Estimate of sooty tern *Onychoprion fuscatus* population size following cat eradication on Ascension Island, central Atlantic. *Bull ABC* 19, 166–171.
- Hylander, L.D., Meili, M., 2003. 500 years of mercury production: Global annual inventory by region until 2000 and associated emissions. *Sci. Total Environ.*, Pathways and processes of mercury in the environment. Selected papers presented at the sixth International Conference on Mercury as Global Pollutant, Minamata, Japan, Oct. 15-19, 2001 304, 13–27. [https://doi.org/10.1016/S0048-9697\(02\)00553-3](https://doi.org/10.1016/S0048-9697(02)00553-3)

I

- IPCC, 2019: Technical Summary [H.-O. Pörtner, D.C. Roberts, V. Masson-Delmotte, P. Zhai, E. Poloczanska, K. Mintenbeck, M. Tignor, A. Alegría, M. Nicolai, A. Okem, J. Petzold, B. Rama, N.M. Weyer (eds.)]. In: IPCC Special Report on the Ocean and Cryosphere in a Changing Climate [H.- O. Pörtner, D.C. Roberts, V. Masson-Delmotte, P. Zhai, M. Tignor, E. Poloczanska, K. Mintenbeck, A. Alegría, M. Nicolai, A. Okem, J. Petzold, B. Rama, N.M. Weyer (eds.)]. Cambridge University Press, Cambridge, UK and New York, NY, USA, pp. 39–69. <https://doi.org/10.1017/9781009157964.002>
- IPCC, 2023: Climate Change 2023: Synthesis Report. A Report of the Intergovernmental Panel on Climate Change. Contribution of Working Groups I, II and III to the Sixth Assessment Report of the Intergovernmental Panel on Climate Change [Core Writing Team, H. Lee and J. Romero (eds.)]. IPCC, Geneva, Switzerland, (in press)

J

- Jackson, T.A., Whittle, D.M., Evans, M.S., Muir, D.C.G., 2008. Evidence for mass-independent and mass-dependent fractionation of the stable isotopes of mercury by natural processes in aquatic ecosystems. *Appl. Geochem.*, Transport and Fate of Mercury in the Environment 23, 547–571. <https://doi.org/10.1016/j.apgeochem.2007.12.013>
- Jaeger, A., Blanchard, P., Richard, P., Cherel, Y., 2009. Using carbon and nitrogen isotopic values of body feathers to infer inter- and intra-individual variations of seabird feeding ecology during moult. *Mar. Biol.* 156, 1233–1240. <https://doi.org/10.1007/s00227-009-1165-6>
- Jaeger, A., Cherel, Y., 2011. Isotopic investigation of contemporary and historic changes in penguin trophic niches and carrying capacity of the Southern Indian Ocean. *PLOS ONE* 6, e16484. <https://doi.org/10.1371/journal.pone.0016484>
- Jaeger, A., Feare, C.J., Summers, R.W., Lebarbenchon, C., Larose, C.S., Le Corre, M., 2017. Geolocation reveals year-round at-sea distribution and activity of a superabundant tropical seabird, the sooty tern *Onychoprion fuscatus*. *Front. Mar. Sci.* 4. <https://doi.org/10.3389/fmars.2017.00394>
- Jaeger, A., Lecomte, V.J., Weimerskirch, H., Richard, P., Cherel, Y., 2010. Seabird satellite tracking validates the use of latitudinal isoscapes to depict predators' foraging areas in the Southern Ocean. *Rapid Commun. Mass Spectrom.* 24, 3456–3460. <https://doi.org/10.1002/rcm.4792>
- Jaquemet, S., Potier, M., Cherel, Y., Kojadinovic, J., Bustamante, P., Richard, P., Catry, T., Ramos, J.A., Le Corre, M., 2008. Comparative foraging ecology and ecological niche of a superabundant tropical seabird: The sooty tern *Sterna fuscata* in the southwest Indian Ocean. *Mar. Biol.* 155, 505–520. <https://doi.org/10.1007/s00227-008-1049-1>
- Jardine, T.D., Kidd, K.A., Fisk, A.T., 2006. Applications, considerations and sources of uncertainty when using stable isotope analysis in ecotoxicology. *Environ. Sci. Technol.* 40, 7501–7511. <https://doi.org/10.1021/es061263h>
- Jardine, T.D., Kidd, K.A., O' Driscoll, N., 2013. Food web analysis reveals effects of pH on mercury bioaccumulation at multiple trophic levels in streams. *Aquat. Toxicol.* 132–133, 46–52. <https://doi.org/10.1016/j.aquatox.2013.01.013>
- Juan-Jordá, M.J., Mosqueira, I., Cooper, A.B., Freire, J., Dulvy, N.K., 2011. Global population trajectories of tunas and their relatives. *Proc. Natl. Acad. Sci.* 108, 20650–20655. <https://doi.org/10.1073/pnas.1107743108>

Juárez, M.A., Casaux, R., Corbalán, A., Blanco, G., Pereira, G.A., Perchivale, P.J., Coria, N.R., Santos, M.M., 2018. Diet of Adélie penguins (*Pygoscelis adeliae*) at Stranger Point (25 de Mayo/King George Island, Antarctica) over a 13-year period (2003–2015). *Polar Biol.* 41, 303–311. <https://doi.org/10.1007/s00300-017-2191-3>

K

- Kang, S., Huang, J., Wang, F., Zhang, Q., Zhang, Y., Li, C., Wang, L., Chen, P., Sharma, C.M., Li, Q., Sillanpää, M., Hou, J., Xu, B., Guo, J., 2016. Atmospheric mercury depositional chronology reconstructed from lake sediments and ice core in the Himalayas and Tibetan Plateau. *Environ. Sci. Technol.* 50, 2859–2869. <https://doi.org/10.1021/acs.est.5b04172>
- Keane, S., Bernaudat, L., Davis, K.J., Stylo, M., Mutemeri, N., Singo, P., Twala, P., Mutemeri, I., Nakafecero, A., Etui, I.D., 2023. Mercury and artisanal and small-scale gold mining: Review of global use estimates and considerations for promoting mercury-free alternatives. *Ambio.* <https://doi.org/10.1007/s13280-023-01843-2>
- Keeling, C.D., 1979. The Suess effect: ¹³Carbon-¹⁴Carbon interrelations. *Environ. Int.* 2, 229–300. [https://doi.org/10.1016/0160-4120\(79\)90005-9](https://doi.org/10.1016/0160-4120(79)90005-9)
- Kelly, J.F., 2000. Stable isotopes of carbon and nitrogen in the study of avian and mammalian trophic ecology. *Can. J. Zool.* 78, 1–27. <https://doi.org/10.1139/z99-165>
- Knox, G.A., 2006. *Biology of the Southern Ocean*. CRC Press.
- Kojadinovic, J., Bustamante, P., Churlaud, C., Cosson, R.P., Le Corre, M., 2007. Mercury in seabird feathers: Insight on dietary habits and evidence for exposure levels in the western Indian Ocean. *Sci. Total Environ.* 384, 194–204. <https://doi.org/10.1016/j.scitotenv.2007.05.018>
- Kokubun, N., Emmerson, L., McInnes, J., Wienecke, B., Southwell, C., 2021. Sea-ice and density-dependent factors affecting foraging habitat and behaviour of Adélie penguins throughout the breeding season. *Mar. Biol.* 168, 97. <https://doi.org/10.1007/s00227-021-03899-8>
- Körtzinger, A., Quay, P.D., Sonnerup, R.E., 2003. Relationship between anthropogenic CO₂ and the ¹³C Suess effect in the North Atlantic Ocean. *Glob. Biogeochem. Cycles* 17, 5-1-5–20. <https://doi.org/10.1029/2001GB001427>
- Kozak, N., Ahonen, S.A., Keva, O., Østbye, K., Taipale, S.J., Hayden, B., Kahilainen, K.K., 2021. Environmental and biological factors are joint drivers of mercury biomagnification in subarctic lake food webs along a climate and productivity gradient. *Sci. Total Environ.* 779, 146261. <https://doi.org/10.1016/j.scitotenv.2021.146261>
- Krabbenhoft, D.P., Sunderland, E.M., 2013. Global change and mercury. *Science* 341, 1457–1458. <https://doi.org/10.1126/science.1242838>

L

- Lamborg, C.H., Hammerschmidt, C.R., Bowman, K.L., Swarr, G.J., Munson, K.M., Ohnemus, D.C., Lam, P.J., Heimbürger, L.-E., Rijkenberg, M.J.A., Saito, M.A., 2014. A global ocean inventory of anthropogenic mercury based on water column measurements. *Nature* 512, 65–68. <https://doi.org/10.1038/nature13563>
- Lee, J.R., Raymond, B., Bracegirdle, T.J., Chadès, I., Fuller, R.A., Shaw, J.D., Terauds, A., 2017. Climate change drives expansion of Antarctic ice-free habitat. *Nature* 547, 49–54. <https://doi.org/10.1038/nature22996>
- Li, C., Sonke, J.E., Le Roux, G., Piotrowska, N., Van der Putten, N., Roberts, S.J., Daley, T., Rice, E., Gehrels, R., Enrico, M., Mauquoy, D., Roland, T.P., De Vleeschouwer, F., 2020. Unequal anthropogenic enrichment of mercury in Earth's Northern and Southern Hemispheres. *ACS Earth Space Chem.* <https://doi.org/10.1021/acsearthspacechem.0c00220>
- Li, F., Ma, C., Zhang, P., 2020. Mercury deposition, climate change and anthropogenic activities: A review. *Front. Earth Sci.* 8.
- Li, M., Sherman, L.S., Blum, J.D., Grandjean, P., Mikkelsen, B., Weihe, P., Sunderland, E.M., Shine, J.P., 2014. Assessing sources of human methylmercury exposure using stable mercury isotopes. *Environ. Sci. Technol.* 48, 8800–8806. <https://doi.org/10.1021/es500340r>
- Li, M.-L., Kwon, S.Y., Poulin, B.A., Tsui, M.T.-K., Motta, L.C., Cho, M., 2022. Internal dynamics and metabolism of mercury in biota: A review of insights from mercury stable isotopes. *Environ. Sci. Technol.* 56, 9182–9195. <https://doi.org/10.1021/acs.est.1c08631>
- Lim, A.G., Jiskra, M., Sonke, J.E., Loiko, S.V., Kosykh, N., Pokrovsky, O.S., 2020. A revised pan-Arctic permafrost soil Hg pool based on Western Siberian peat Hg and carbon observations. *Biogeosciences* 17, 3083–3097. <https://doi.org/10.5194/bg-17-3083-2020>
- Limoges, A., Weckström, K., Ribeiro, S., Georgiadis, E., Hansen, K.E., Martinez, P., Seidenkrantz, M.-S., Giraudeau, J., Crosta, X., Massé, G., 2020. Learning from the past: Impact of the Arctic Oscillation on

- sea ice and marine productivity off northwest Greenland over the last 9,000 years. *Glob. Change Biol.* 26, 6767–6786. <https://doi.org/10.1111/gcb.15334>
- Lippold, A., Aars, J., Andersen, M., Aubail, A., Derocher, A.E., Dietz, R., Eulaers, I., Sonne, C., Welker, J.M., Wiig, Ø., Routti, H., 2020. Two decades of mercury concentrations in Barents Sea polar bears (*Ursus maritimus*) in relation to dietary carbon, sulfur and nitrogen. *Environ. Sci. Technol.* 54, 7388–7397. <https://doi.org/10.1021/acs.est.0c01848>
- Liu, H., Zheng, W., Bergquist, B.A., Gao, Y., Yue, F., Yang, L., Sun, L., Xie, Z., 2023. A 1500-year record of mercury isotopes in seal feces documents sea ice changes in the Antarctic. *Commun. Earth Environ.* 4, 1–10. <https://doi.org/10.1038/s43247-023-00921-3>
- Liu, M., Zhang, Q., Maavara, T., Liu, S., Wang, X., Raymond, P.A., 2021. Rivers as the largest source of mercury to coastal oceans worldwide. *Nat. Geosci.* 14, 672–677. <https://doi.org/10.1038/s41561-021-00793-2>
- Lorenzini, S., Baroni, C., Baneschi, I., Salvatore, M.C., Fallick, A.E., Hall, B.L., 2014. Adélie penguin dietary remains reveal Holocene environmental changes in the western Ross Sea (Antarctica). *Palaeogeogr. Palaeoclimatol. Palaeoecol.* 395, 21–28. <https://doi.org/10.1016/j.palaeo.2013.12.014>
- Lorrain, A., Graham, B., Ménard, F., Popp, B., Bouillon, S., Breugel, P. van, Cherel, Y., 2009. Nitrogen and carbon isotope values of individual amino acids: A tool to study foraging ecology of penguins in the Southern Ocean. *Mar. Ecol. Prog. Ser.* 391, 293–306. <https://doi.org/10.3354/meps08215>
- Lorrain, A., Pethybridge, H., Cassar, N., Receveur, A., Allain, V., Bodin, N., Bopp, L., Choy, C.A., Duffy, L., Fry, B., Goñi, N., Graham, B.S., Hobday, A.J., Logan, J.M., Ménard, F., Menkes, C.E., Olson, R.J., Pagendam, D.E., Point, D., Revill, A.T., Somes, C.J., Young, J.W., 2020. Trends in tuna carbon isotopes suggest global changes in pelagic phytoplankton communities. *Glob. Change Biol.* 26, 458–470. <https://doi.org/10.1111/gcb.14858>
- Lynch, H.J., LaRue, M.A., 2014. First global census of the Adélie Penguin. *The Auk* 131, 457–466. <https://doi.org/10.1642/AUK-14-31.1>
- Lynnes, A.S., Reid, K., Croxall, J.P., 2004. Diet and reproductive success of Adélie and chinstrap penguins: linking response of predators to prey population dynamics. *Polar Biol.* 27, 544–554. <https://doi.org/10.1007/s00300-004-0617-1>

M

- Mallory, M.L., Braune, B.M., 2018. Do concentrations in eggs and liver tissue tell the same story of temporal trends of mercury in high Arctic seabirds? *J. Environ. Sci., Mercury Fate and Biogeochemistry* 68, 65–72. <https://doi.org/10.1016/j.jes.2017.10.017>
- Mallory, M.L., Braune, B.M., 2012. Tracking contaminants in seabirds of Arctic Canada: Temporal and spatial insights. *Mar. Pollut. Bull.* 64, 1475–1484. <https://doi.org/10.1016/j.marpolbul.2012.05.012>
- Mallory, M.L., Provencher, J.F., Robertson, G.J., Braune, B.M., Holland, E.R., Klapstein, S., Stevens, K., O’Driscoll, N.J., 2018. Mercury concentrations in blood, brain and muscle tissues of coastal and pelagic birds from northeastern Canada. *Ecotoxicol. Environ. Saf.* 157, 424–430. <https://doi.org/10.1016/j.ecoenv.2018.04.004>
- Martínez, I., D. A. Christie, F. Jutglar, E.F.J. Garcia, and C.J. Sharpe (2020). Adélie Penguin (*Pygoscelis adeliae*), version 1.0. In *Birds of the World* (J. del Hoyo, A. Elliott, J. Sargatal, D. A. Christie, and E. de Juana, Editors). Cornell Lab of Ornithology, Ithaca, NY, USA. <https://doi.org/10.2173/bow.adepen1.01>
- Mason, R.P., 2012. The methylation of metals and metalloids in aquatic systems, in: *Methylation - From DNA, RNA and Histones to Diseases and Treatment*. IntechOpen. <https://doi.org/10.5772/51774>
- Mason, R.P., 2009. Mercury emissions from natural processes and their importance in the global mercury cycle, in: Mason, R., Pirrone, N. (Eds.), *Mercury Fate and Transport in the Global Atmosphere: Emissions, Measurements and Models*. Springer US, Boston, MA, pp. 173–191. https://doi.org/10.1007/978-0-387-93958-2_7
- Mason, R.P., Choi, A.L., Fitzgerald, W.F., Hammerschmidt, C.R., Lamborg, C.H., Soerensen, A.L., Sunderland, E.M., 2012a. Mercury biogeochemical cycling in the ocean and policy implications. *Environ. Res., Mercury in Marine Ecosystems: Sources to Seafood Consumers* 119, 101–117. <https://doi.org/10.1016/j.envres.2012.03.013>
- Mason, R.P., Choi, A.L., Fitzgerald, W.F., Hammerschmidt, C.R., Lamborg, C.H., Soerensen, A.L., Sunderland, E.M., 2012b. Mercury biogeochemical cycling in the Ocean and policy implications. *Environ. Res.* 119, 101–117. <https://doi.org/10.1016/j.envres.2012.03.013>
- Maxwell, S.M., Morgan, L.E., 2013. Foraging of seabirds on pelagic fishes: Implications for management of pelagic marine protected areas. *Mar. Ecol. Prog. Ser.* 481, 289–303. <https://doi.org/10.3354/meps10255>
- McKinney, M.A., Atwood, T.C., Pedro, S., Peacock, E., 2017. Ecological change drives a decline in mercury concentrations in Southern Beaufort Sea Polar Bears. *Environ. Sci. Technol.* 51, 7814–7822. <https://doi.org/10.1021/acs.est.7b00812>

- McKinney, M.A., Chételat, J., Burke, S.M., Elliott, K.H., Fernie, K.J., Houde, M., Kahilainen, K.K., Letcher, R.J., Morris, A.D., Muir, D.C.G., Routti, H., Yurkowski, D.J., 2022. Climate change and mercury in the Arctic: Biotic interactions. *Sci. Total Environ.* 834, 155221. <https://doi.org/10.1016/j.scitotenv.2022.155221>
- McKinney, M.A., Peacock, E., Letcher, R.J., 2009. Sea ice-associated diet change increases the levels of chlorinated and brominated contaminants in polar bears. *Environ. Sci. Technol.* 43, 4334–4339. <https://doi.org/10.1021/es900471g>
- McMahon, K.W., Hamady, L.L., Thorrold, S.R., 2013a. Ocean ecogeochemistry: A review. *Oceanogr. Mar. Biol. Annu. Rev.* 51, 327–374.
- McMahon, K.W., Hamady, L.L., Thorrold, S.R., 2013b. A review of ecogeochemistry approaches to estimating movements of marine animals. *Limnol. Oceanogr.* 58, 697–714. <https://doi.org/10.4319/lo.2013.58.2.0697>
- McMahon, K.W., McCarthy, M.D., 2016. Embracing variability in amino acid $\delta^{15}\text{N}$ fractionation: Mechanisms, implications, and applications for trophic ecology. *Ecosphere* 7, e01511. <https://doi.org/10.1002/ecs2.1511>
- McMahon, K.W., Newsome, S.D., 2019. Chapter 7 - Amino acid isotope analysis: A new frontier in studies of animal migration and foraging ecology, in: Hobson, K.A., Wassenaar, L.I. (Eds.), *Tracking Animal Migration with Stable Isotopes (Second Edition)*. Academic Press, pp. 173–190. <https://doi.org/10.1016/B978-0-12-814723-8.00007-6>
- McMahon, K.W., Polito, M.J., Abel, S., McCarthy, M.D., Thorrold, S.R., 2015. Carbon and nitrogen isotope fractionation of amino acids in an avian marine predator, the gentoo penguin (*Pygoscelis papua*). *Ecol. Evol.* 5, 1278–1290. <https://doi.org/10.1002/ece3.1437>
- Médiéu, A., Point, D., Itai, T., Angot, H., Buchanan, P.J., Allain, V., Fuller, L., Griffiths, S., Gillikin, D.P., Sonke, J.E., Heimbürger-Boavida, L.-E., Desgranges, M.-M., Menkes, C.E., Madigan, D.J., Brosset, P., Gauthier, O., Tagliabue, A., Bopp, L., Verheyden, A., Lorrain, A., 2022. Evidence that Pacific tuna mercury levels are driven by marine methylmercury production and anthropogenic inputs. *Proc. Natl. Acad. Sci.* 119, e2113032119. <https://doi.org/10.1073/pnas.2113032119>
- Meijer, T., Drent, R., 1999. Re-examination of the capital and income dichotomy in breeding birds. *Ibis* 141, 399–414. <https://doi.org/10.1111/j.1474-919X.1999.tb04409.x>
- Michelot, C., Kato, A., Raclot, T., Ropert-Coudert, Y., 2021. Adélie penguins foraging consistency and site fidelity are conditioned by breeding status and environmental conditions. *PLOS ONE* 16, e0244298. <https://doi.org/10.1371/journal.pone.0244298>
- Mills, W.F., Bustamante, P., McGill, R.A.R., Anderson, O.R.J., Bearhop, S., Cherel, Y., Votier, S.C., Phillips, R.A., 2020. Mercury exposure in an endangered seabird: Long-term changes and relationships with trophic ecology and breeding success. *Proc. R. Soc. B Biol. Sci.* 287, 20202683. <https://doi.org/10.1098/rspb.2020.2683>
- Monteiro, L.R., Furness, R.W., 2001. Kinetics, dose–response and excretion of methylmercury in free-living adult Cory’s Shearwaters. *Environ. Sci. Technol.* 35, 739–746. <https://doi.org/10.1021/es000114a>
- Monteiro, L.R., Furness, R.W., 1997. Accelerated increase in mercury contamination in North Atlantic mesopelagic food chains as indicated by time series of seabird feathers. *Environ. Toxicol. Chem.* 16, 2489–2493. <https://doi.org/10.1002/etc.5620161208>
- Monteiro, L.R., Furness, R.W., 1995. Seabirds as monitors of mercury in the marine environment. *Water, Air, Soil Pollut.* 80, 851–870. <https://doi.org/10.1007/BF01189736>
- Monteiro, L.R., Granadeiro, J.P., Furness, R.W., 1998. Relationship between mercury levels and diet in Azores seabirds. *Mar. Ecol. Prog. Ser.* 166, 259–265. <https://doi.org/10.3354/meps166259>
- Monticelli, D., Ramos, J.A., Tavares, P.C., Bataille, B., Lepoint, G., Devillers, P., 2008. Diet and foraging ecology of roseate terns and lesser noddies breeding sympatrically on Aride Island, Seychelles. *Waterbirds* 31, 231–240. [https://doi.org/10.1675/1524-4695\(2008\)31\[231:DAFEOR\]2.0.CO;2](https://doi.org/10.1675/1524-4695(2008)31[231:DAFEOR]2.0.CO;2)
- Morley, S.A., Barnes, D.K.A., Dunn, M.J., 2019. Predicting which species succeed in climate-forced polar seas. *Front. Mar. Sci.* 5.

N

- NCP, 2017. Northern Contaminants Program (NCP). Indigenous and Northern Affairs, Government of Canada. www.science.gc.ca/eic/site/063.nsf/eng/h_7A463.thml

O

- Obrist, D., Kirk, J.L., Zhang, L., Sunderland, E.M., Jiskra, M., Selin, N.E., 2018. A review of global environmental mercury processes in response to human and natural perturbations: Changes of emissions, climate, and land use. *Ambio* 47, 116–140. <https://doi.org/10.1007/s13280-017-1004-9>

- Ochoa-Acuña, H., Sepúlveda, M.S., Gross, T.S., 2002. Mercury in feathers from Chilean birds: Influence of location, feeding strategy, and taxonomic affiliation. *Mar. Pollut. Bull.* 44, 340–345. [https://doi.org/10.1016/S0025-326X\(01\)00280-6](https://doi.org/10.1016/S0025-326X(01)00280-6)
- Ohkouchi, N., Chikaraishi, Y., Close, H.G., Fry, B., Larsen, T., Madigan, D.J., McCarthy, M.D., McMahon, K.W., Nagata, T., Naito, Y.I., Ogawa, N.O., Popp, B.N., Steffan, S., Takano, Y., Tayasu, I., Wyatt, A.S.J., Yamaguchi, Y.T., Yokoyama, Y., 2017. Advances in the application of amino acid nitrogen isotopic analysis in ecological and biogeochemical studies. *Org. Geochem.* 113, 150–174. <https://doi.org/10.1016/j.orggeochem.2017.07.009>
- Oliveira Ribeiro, C.A., Rouleau, C., Pelletier, É., Audet, C., Tjälve, H., 1999. Distribution kinetics of dietary methylmercury in the Arctic char (*Salvelinus alpinus*). *Environ. Sci. Technol.* 33, 902–907. <https://doi.org/10.1021/es980242n>
- Olmastroni, S., Fattorini, N., Pezzo, F., Focardi, S., 2020. Gone fishing: Adélie penguin site-specific foraging tactics and breeding performance. *Antarct. Sci.* 32, 199–209. <https://doi.org/10.1017/S0954102020000085>
- O'Reilly, C.M., Alin, S.R., Plisnier, P.-D., Cohen, A.S., McKee, B.A., 2003. Climate change decreases aquatic ecosystem productivity of Lake Tanganyika, Africa. *Nature* 424, 766–768. <https://doi.org/10.1038/nature01833>
- Orsi, A.H., Whitworth, T., Nowlin, W.D., 1995. On the meridional extent and fronts of the Antarctic Circumpolar Current. *Deep Sea Res. Part Oceanogr. Res. Pap.* 42, 641–673. [https://doi.org/10.1016/0967-0637\(95\)00021-W](https://doi.org/10.1016/0967-0637(95)00021-W)
- Ostrom, N.E., Macko, S.A., Deibel, D., Thompson, R.J., 1997. Seasonal variation in the stable carbon and nitrogen isotope biogeochemistry of a coastal cold ocean environment. *Geochim. Cosmochim. Acta* 61, 2929–2942. [https://doi.org/10.1016/S0016-7037\(97\)00131-2](https://doi.org/10.1016/S0016-7037(97)00131-2)
- Outridge, P.M., Mason, R.P., Wang, F., Guerrero, S., Heimbürger-Boavida, L.E., 2018. Updated global and oceanic mercury budgets for the United Nations Global Mercury Assessment 2018. *Environ. Sci. Technol.* 52, 11466–11477. <https://doi.org/10.1021/acs.est.8b01246>

P

- Pacyna, A.D., Jakubas, D., Ausems, A.N.M.A., Frankowski, M., Polkowska, Ż., Wojczulanis-Jakubas, K., 2019. Storm petrels as indicators of pelagic seabird exposure to chemical elements in the Antarctic marine ecosystem. *Sci. Total Environ.* 692, 382–392. <https://doi.org/10.1016/j.scitotenv.2019.07.137>
- Pacyna, E.G., Pacyna, J.M., Steenhuisen, F., Wilson, S., 2006. Global anthropogenic mercury emission inventory for 2000. *Atmos. Environ.* 40, 4048–4063. <https://doi.org/10.1016/j.atmosenv.2006.03.041>
- Parish, T.R., 1988. Surface winds over the Antarctic continent: A review. *Rev. Geophys.* 26, 169–180. <https://doi.org/10.1029/RG026i001p00169>
- Parish, T.R., Cassano, J.J., 2003. The role of katabatic winds on the Antarctic surface wind regime. *Mon. Weather Rev.* 131, 317–333. [https://doi.org/10.1175/1520-0493\(2003\)131<0317:TROKWO>2.0.CO;2](https://doi.org/10.1175/1520-0493(2003)131<0317:TROKWO>2.0.CO;2)
- Pedro, S., Xavier, J.C., Tavares, S., Trathan, P.N., Ratcliffe, N., Paiva, V.H., Medeiros, R., Vieira, R.P., Ceia, F.R., Pereira, E., Pardal, M.A., 2015. Mercury accumulation in gentoo penguins *Pygoscelis papua*: Spatial, temporal and sexual intraspecific variations. *Polar Biol.* 38, 1335–1343. <https://doi.org/10.1007/s00300-015-1697-9>
- Phillips, R.A., McGill, R.A.R., Dawson, D.A., Bearhop, S., 2011. Sexual segregation in distribution, diet and trophic level of seabirds: Insights from stable isotope analysis. *Mar. Biol.* 158, 2199–2208. <https://doi.org/10.1007/s00227-011-1725-4>
- Piatt, J.F., Harding, A.M.A., Shultz, M., Speckman, S.G., Pelt, T.I. van, Drew, G.S., Kettle, A.B., 2007. Seabirds as indicators of marine food supplies: Cairns revisited. *Mar. Ecol. Prog. Ser.* 352, 221–234. <https://doi.org/10.3354/meps07078>
- Point, D., Sonke, J.E., Day, R.D., Roseneau, D.G., Hobson, K.A., Vander Pol, S.S., Moors, A.J., Pugh, R.S., Donard, O.F.X., Becker, P.R., 2011. Methylmercury photodegradation influenced by sea-ice cover in Arctic marine ecosystems. *Nat. Geosci.* 4, 188–194. <https://doi.org/10.1038/ngeo1049>
- Polito, M.J., Brasso, R.L., Trivelpiece, W.Z., Karnovsky, N., Patterson, W.P., Emslie, S.D., 2016. Differing foraging strategies influence mercury (Hg) exposure in an Antarctic penguin community. *Environ. Pollut.* 218, 196–206. <https://doi.org/10.1016/j.envpol.2016.04.097>
- Polito, M.J., Lynch, H.J., Naveen, R., Emslie, S.D., 2011. Stable isotopes reveal regional heterogeneity in the pre-breeding distribution and diets of sympatrically breeding *Pygoscelis spp.* penguins. *Mar. Ecol. Prog. Ser.* 421, 265–277. <https://doi.org/10.3354/meps08863>
- Preece, K., Mark, D.F., Barclay, J., Cohen, B.E., Chamberlain, K.J., Jowitt, C., Vye-Brown, C., Brown, R.J., Hamilton, S., 2018. Bridging the gap: $^{40}\text{Ar}/^{39}\text{Ar}$ dating of volcanic eruptions from the ‘Age of Discovery.’ *Geology* 46, 1035–1038. <https://doi.org/10.1130/G45415.1>

- Prince, P.A., Weimerskirch, H., Huin, N., Rodwell, S., 1997. Molt, maturation of plumage and ageing in the Wandering Albatross. *The Condor* 99, 58–72. <https://doi.org/10.2307/1370224>
- Provencher, J.F., Gaston, A.J., O'Hara, P.D., Gilchrist, H.G., 2012. Seabird diet indicates changing Arctic marine communities in eastern Canada. *Mar. Ecol. Prog. Ser.* 454, 171–182. <https://doi.org/10.3354/meps09299>
- Provencher, J.F., Gilchrist, H.G., Mallory, M.L., Mitchell, G.W., Forbes, M.R., 2016. Direct and indirect causes of sex differences in mercury concentrations and parasitic infections in a marine bird. *Sci. Total Environ.* 551–552, 506–512. <https://doi.org/10.1016/j.scitotenv.2016.02.055>

Q

- Quillfeldt, P., Masello, J.F., 2020. Compound-specific stable isotope analyses in Falkland Islands seabirds reveal seasonal changes in trophic positions. *BMC Ecol.* 20, 21. <https://doi.org/10.1186/s12898-020-00288-5>
- Quillfeldt, P., Masello, J.F., McGill, R.A., Adams, M., Furness, R.W., 2010. Moving polewards in winter: A recent change in the migratory strategy of a pelagic seabird? *Front. Zool.* 7, 15. <https://doi.org/10.1186/1742-9994-7-15>

R

- R Core Team (2022). R: A language and environment for statistical computing. R Foundation for Statistical Computing, Vienna, Austria. URL <https://www.R-project.org/>.
- Ramos, J.A., Tavares, P.C., 2010. Mercury levels in the feathers of breeding seabirds in the Seychelles, western Indian Ocean, from 1996 to 2005. *Emu - Austral Ornithol.* 110, 87–91. <https://doi.org/10.1071/MU09055>
- Rastner, P., Bolch, T., Mölg, N., Machguth, H., Le Bris, R., Paul, F., 2012. The first complete inventory of the local glaciers and ice caps on Greenland. *The Cryosphere* 6, 1483–1495. <https://doi.org/10.5194/tc-6-1483-2012>
- Rau, G.H., Takahashi, T., Des Marais, D.J., Repeta, D.J., Martin, J.H., 1992. The relationship between $\delta^{13}\text{C}$ of organic matter and $[\text{CO}_2(\text{aq})]$ in ocean surface water: Data from a JGOFS site in the northeast Atlantic Ocean and a model. *Geochim. Cosmochim. Acta* 56, 1413–1419. [https://doi.org/10.1016/0016-7037\(92\)90073-R](https://doi.org/10.1016/0016-7037(92)90073-R)
- Renedo, M., Amouroux, D., Albert, C., Bérail, S., Br'athen, V.S., Gavriilo, M., Grémillet, D., Helgason, H.H., Jakubas, D., Mosbech, A., Strøm, H., Tessier, E., Wojczulanis-Jakubas, K., Bustamante, P., Fort, J., 2020a. Contrasting spatial and seasonal trends of methylmercury exposure pathways of Arctic seabirds: Combination of large-scale tracking and stable isotopic approaches. *Environ. Sci. Technol.* 54, 13619–13629. <https://doi.org/10.1021/acs.est.0c03285>
- Renedo, M., Amouroux, D., Duval, B., Carravieri, A., Tessier, E., Barre, J., Bérail, S., Pedrero, Z., Cherel, Y., Bustamante, P., 2018. Seabird tissues as efficient biomonitoring tools for Hg isotopic investigations: Implications of using blood and feathers from chicks and adults. *Environ. Sci. Technol.* 52, 4227–4234. <https://doi.org/10.1021/acs.est.8b00422>
- Renedo, M., Bustamante, P., Cherel, Y., Pedrero, Z., Tessier, E., Amouroux, D., 2020b. A “seabird-eye” on mercury stable isotopes and cycling in the Southern Ocean. *Sci. Total Environ.* 742, 140499. <https://doi.org/10.1016/j.scitotenv.2020.140499>
- Renedo, M., Bustamante, P., Tessier, E., Pedrero, Z., Cherel, Y., Amouroux, D., 2017. Assessment of mercury speciation in feathers using species-specific isotope dilution analysis. *Talanta* 174, 100–110. <https://doi.org/10.1016/j.talanta.2017.05.081>
- Renedo, M., Pedrero, Z., Amouroux, D., Cherel, Y., Bustamante, P., 2021. Mercury isotopes of key tissues document mercury metabolic processes in seabirds. *Chemosphere* 263, 127777. <https://doi.org/10.1016/j.chemosphere.2020.127777>
- Reynolds, S.J., Hughes, B.J., Wearn, C.P., Dickey, R.C., Brown, J., Weber, N.L., Weber, S.B., Paiva, V.H., Ramos, J.A., 2019. Long-term dietary shift and population decline of a pelagic seabird—A health check on the tropical Atlantic? *Glob. Change Biol.* 25, 1383–1394. <https://doi.org/10.1111/gcb.14560>
- Reynolds, S.J., Wearn, C.P., Hughes, B.J., Dickey, R.C., Garrett, L.J.H., Walls, S., Hughes, F.T., Weber, N., Weber, S.B., Leat, E.H.K., Andrews, K., Ramos, J.A., Paiva, V.H., 2021. Year-round movements of sooty terns (*Onychoprion fuscatus*) nesting within one of the Atlantic's largest Marine Protected Areas. *Front. Mar. Sci.* 8.
- Ribeiro, S., Limoges, A., Massé, G., Johansen, K.L., Colgan, W., Weckström, K., Jackson, R., Georgiadis, E., Mikkelsen, N., Kuijpers, A., Olsen, J., Olsen, S.M., Nissen, M., Andersen, T.J., Strunk, A., Wetterich, S., Syväranta, J., Henderson, A.C.G., Mackay, H., Taipale, S., Jeppesen, E., Larsen, N.K., Crosta, X., Giraudeau, J., Wengrat, S., Nuttall, M., Grønnow, B., Mosbech, A., Davidson, T.A., 2021. Vulnerability of the North Water ecosystem to climate change. *Nat. Commun.* 12, 4475. <https://doi.org/10.1038/s41467-021-24742-0>

- Rigét, F., Braune, B., Bignert, A., Wilson, S., Aars, J., Born, E., Dam, M., Dietz, R., Evans, M., Evans, T., Gamberg, M., Gantner, N., Green, N., Gunnlaugsdóttir, H., Kannan, K., Letcher, R., Muir, D., Roach, P., Sonne, C., Stern, G., Wiig, Ø., 2011. Temporal trends of Hg in Arctic biota, an update. *Sci. Total Environ.* 409, 3520–3526. <https://doi.org/10.1016/j.scitotenv.2011.05.002>
- Riget, F., Muir, D., Kwan, M., Savinova, T., Nyman, M., Woshner, V., O'Hara, T., 2005. Circumpolar pattern of mercury and cadmium in ringed seals. *Sci. Total Environ., Contaminants in Canadian Arctic Biota and Implications for Human Health* 351–352, 312–322. <https://doi.org/10.1016/j.scitotenv.2004.05.032>
- Rocchi, S., Storti, F., Di Vincenzo, G., Rossetti, F., 2003. Intraplate strike-slip tectonics as an alternative to mantle plume activity for the Cenozoic rift magmatism in the Ross Sea region, Antarctica. *Geol. Soc. Lond. Spec. Publ.* 210, 145–158. <https://doi.org/10.1144/GSL.SP.2003.210.01.09>
- Routti, H., Letcher, R.J., Born, E.W., Branigan, M., Dietz, R., Evans, T.J., Fisk, A.T., Peacock, E., Sonne, C., 2011. Spatial and temporal trends of selected trace elements in liver tissue from polar bears (*Ursus maritimus*) from Alaska, Canada and Greenland. *J. Environ. Monit.* 13, 2260–2267. <https://doi.org/10.1039/C1EM10088B>

S

- Sabadel, A., 2014. Stable isotope analyses of amino-acids: A tool to understand trophic relationships in terrestrial and marine food webs. University of Otago, Dunedin, New Zealand.
- Sabadel, A.J.M., Woodward, E.M.S., Van Hale, R., Frew, R.D., 2016. Compound-specific isotope analysis of amino acids: A tool to unravel complex symbiotic trophic relationships. *Food Webs* 6, 9–18. <https://doi.org/10.1016/j.fooweb.2015.12.003>
- Santos, C.S.A., Blondel, L., Sotillo, A., Müller, W., Stienen, E.W.M., Boeckx, P., Soares, A.M.V.M., Monteiro, M.S., Loureiro, S., de Neve, L., Lens, L., 2017. Offspring Hg exposure relates to parental feeding strategies in a generalist bird with strong individual foraging specialization. *Sci. Total Environ.* 601–602, 1315–1323. <https://doi.org/10.1016/j.scitotenv.2017.05.286>
- Sarkar, A., Ravindran, G., & Krishnamurthy, V. (2013). A brief review on the effect of cadmium toxicity: From cellular to organ level. *Int J Biotechnol Res*, 3(1), 17-36.
- Schaefer, K., Elshorbany, Y., Jafarov, E., Schuster, P.F., Striegl, R.G., Wickland, K.P., Sunderland, E.M., 2020. Potential impacts of mercury released from thawing permafrost. *Nat. Commun.* 11, 4650. <https://doi.org/10.1038/s41467-020-18398-5>
- Schartup, A.T., Soerensen, A.L., Heimbürger-Boavida, L.-E., 2020. Influence of the Arctic sea-ice regime shift on sea-ice methylated mercury trends. *Environ. Sci. Technol. Lett.* 7, 708–713. <https://doi.org/10.1021/acs.estlett.0c00465>
- Schartup, A.T., Thackray, C.P., Qureshi, A., Dassuncao, C., Gillespie, K., Hanke, A., Sunderland, E.M., 2019. Climate change and overfishing increase neurotoxicant in marine predators. *Nature* 572, 648–650. <https://doi.org/10.1038/s41586-019-1468-9>
- Scheifler, R., Gauthier-Clerc, M., Bohec, C.L., Crini, N., Cœurdassier, M., Badot, P.-M., Giraudoux, P., Maho, Y.L., 2005. Mercury concentrations in king penguin (*Aptenodytes patagonicus*) feathers at Crozet Islands (sub-Antarctic): Temporal trend between 1966–1974 and 2000–2001. *Environ. Toxicol. Chem.* 24, 125–128. <https://doi.org/10.1897/03-446.1>
- Schell, D.M., 2000. Declining carrying capacity in the Bering Sea: Isotopic evidence from whale baleen. *Limnol. Oceanogr.* 45, 459–462. <https://doi.org/10.4319/lo.2000.45.2.0459>
- Scheuhammer, A.M., Basu, N., Evers, D.C., Heinz, G.H., Sandheinrich, M.B., Bank, M.S., 2012. Ecotoxicology of mercury in fish and wildlife: Recent advances, in: Bank, M. (Ed.), *Mercury in the Environment: Pattern and Process*. University of California Press, p. 0. <https://doi.org/10.1525/california/9780520271630.003.0011>
- Schneider, L., Fisher, J.A., Diéguez, M.C., Fostier, A.-H., Guimaraes, J.R.D., Leaner, J.J., Mason, R., 2023. A synthesis of mercury research in the Southern Hemisphere, part 1: Natural processes. *Ambio*. <https://doi.org/10.1007/s13280-023-01832-5>
- Schreiber, E. A., C. J. Feare, B. A. Harrington, B. G. Murray Jr., W. B. Robertson Jr., M. J. Robertson, and G. E. Woolfenden (2020). Sooty Tern (*Onychoprion fuscatus*), version 1.0. In *Birds of the World* (S. M. Billerman, Editor). Cornell Lab of Ornithology, Ithaca, NY, USA. <https://doi.org/10.2173/bow.sooter1.01>
- Schuster, P.F., Schaefer, K.M., Aiken, G.R., Antweiler, R.C., Dewild, J.F., Gryziec, J.D., Gusmeroli, A., Hugelius, G., Jafarov, E., Krabbenhoft, D.P., Liu, L., Herman-Mercer, N., Mu, C., Roth, D.A., Schaefer, T., Striegl, R.G., Wickland, K.P., Zhang, T., 2018. Permafrost stores a globally significant amount of mercury. *Geophys. Res. Lett.* 45, 1463–1471. <https://doi.org/10.1002/2017GL075571>
- Seco, J., Aparício, S., Brierley, A.S., Bustamante, P., Ceia, F.R., Coelho, J.P., Phillips, R.A., Saunders, R.A., Fielding, S., Gregory, S., Matias, R., Pardal, M.A., Pereira, E., Stowasser, G., Tarling, G.A., Xavier, J.C.,

2021. Mercury biomagnification in a Southern Ocean food web. *Environ. Pollut.* 275, 116620. <https://doi.org/10.1016/j.envpol.2021.116620>
- Seco, J., Xavier, J.C., Coelho, J.P., Pereira, B., Tarling, G., Pardal, M.A., Bustamante, P., Stowasser, G., Brierley, A.S., Pereira, M.E., 2019. Spatial variability in total and organic mercury levels in Antarctic krill *Euphausia superba* across the Scotia Sea. *Environ. Pollut.* 247, 332–339. <https://doi.org/10.1016/j.envpol.2019.01.031>
- Selin, H., Keane, S.E., Wang, S., Selin, N.E., Davis, K., Bally, D., 2018. Linking science and policy to support the implementation of the Minamata Convention on Mercury. *Ambio* 47, 198–215. <https://doi.org/10.1007/s13280-017-1003-x>
- Selin, N.E., 2009. Global biogeochemical cycling of mercury: A review. *Annu. Rev. Environ. Resour.* 34, 43–63. <https://doi.org/10.1146/annurev.enviro.051308.084314>
- Senn, D.B., Chesney, E.J., Blum, J.D., Bank, M.S., Maage, A., Shine, J.P., 2010. Stable isotope (N, C, Hg) study of methylmercury sources and trophic transfer in the Northern Gulf of Mexico. *Environ. Sci. Technol.* 44, 1630–1637. <https://doi.org/10.1021/es902361j>
- Shemesh, A., Charles, C.D., Fairbanks, R.G., 1992. Oxygen isotopes in biogenic silica: Global changes in Ocean temperature and isotopic composition. *Science* 256, 1434–1436. <https://doi.org/10.1126/science.256.5062.1434>
- Shoji, A., Elliott, K.H., Watanuki, Y., Basu, N., Whelan, S., Cunningham, J., Hatch, S., Mizukawa, H., Nakayama, S.M.M., Ikenaka, Y., Ishizuka, M., Aris-Brosou, S., 2021. Geolocators link marine mercury with levels in wild seabirds throughout their annual cycle: Consequences for trans-ecosystem biotransport. *Environ. Pollut.* 284, 117035. <https://doi.org/10.1016/j.envpol.2021.117035>
- Sonke, J.E., Angot, H., Zhang, Y., Poulain, A., Björn, E., Schartup, A., 2023. Global change effects on biogeochemical mercury cycling. *Ambio*. <https://doi.org/10.1007/s13280-023-01855-y>
- Sontag, P.T., Steinberg, D.K., Reinfelder, J.R., 2019. Patterns of total mercury and methylmercury bioaccumulation in Antarctic krill (*Euphausia superba*) along the West Antarctic Peninsula. *Sci. Total Environ.* 688, 174–183. <https://doi.org/10.1016/j.scitotenv.2019.06.176>
- Søreide, J.E., Hop, H., Carroll, M.L., Falk-Petersen, S., Hegseth, E.N., 2006. Seasonal food web structures and sympagic–pelagic coupling in the European Arctic revealed by stable isotopes and a two-source food web model. *Prog. Oceanogr.* 71, 59–87. <https://doi.org/10.1016/j.pocean.2006.06.001>
- Southwell, C., Emmerson, L., Takahashi, A., Barbraud, C., Delord, K., Weimerskirch, H., 2017. Large-scale population assessment informs conservation management for seabirds in Antarctica and the Southern Ocean: A case study of Adélie penguins. *Glob. Ecol. Conserv.* 9, 104–115. <https://doi.org/10.1016/j.gecco.2016.12.004>
- Spalding, M.G., Frederick, P.C., McGill, H.C., Bouton, S.N., McDowell, L.R., 2000. Methylmercury accumulation in tissues and its effects on growth and appetite in captive great egrets. *J. Wildl. Dis.* 36, 411–422. <https://doi.org/10.7589/0090-3558-36.3.411>
- St. Pierre, K.A., St. Louis, V.L., Lehnher, I., Gardner, A.S., Serbu, J.A., Mortimer, C.A., Muir, D.C.G., Wiklund, J.A., Lemire, D., Szostek, L., Talbot, C., 2019. Drivers of mercury cycling in the rapidly changing glacierized watershed of the High Arctic’s largest lake by volume (Lake Hazen, Nunavut, Canada). *Environ. Sci. Technol.* 53, 1175–1185. <https://doi.org/10.1021/acs.est.8b05926>
- St. Pierre, K.A., Zolkos, S., Shakil, S., Tank, S.E., St. Louis, V.L., Kokelj, S.V., 2018. Unprecedented increases in total and methyl mercury concentrations downstream of retrogressive thaw slumps in the Western Canadian Arctic. *Environ. Sci. Technol.* 52, 14099–14109. <https://doi.org/10.1021/acs.est.8b05348>
- Stewart, F., Phillips, R., Catry, P., Furness, R., 1997. Influence of species, age and diet on mercury concentrations in Shetland seabirds. *Mar. Ecol. Prog. Ser.* 151, 237–244. <https://doi.org/10.3354/meps151237>
- Streets, D.G., Horowitz, H.M., Jacob, D.J., Lu, Z., Levin, L., ter Schure, A.F.H., Sunderland, E.M., 2017. Total Mercury released to the environment by human activities. *Environ. Sci. Technol.* 51, 5969–5977. <https://doi.org/10.1021/acs.est.7b00451>
- Streets, D.G., Horowitz, H.M., Lu, Z., Levin, L., Thackray, C.P., Sunderland, E.M., 2019. Five hundred years of anthropogenic mercury: Spatial and temporal release profiles. *Environ. Res. Lett.* 14. <https://doi.org/10.1088/1748-9326/ab281f>
- Styring, A.K., Kuhl, A., Knowles, T.D.J., Fraser, R.A., Bogaard, A., Evershed, R.P., 2012. Practical considerations in the determination of compound-specific amino acid $\delta^{15}\text{N}$ values in animal and plant tissues by gas chromatography-combustion-isotope ratio mass spectrometry, following derivatisation to their N-acetylisopropyl esters. *Rapid Commun. Mass Spectrom.* RCM 26, 2328–2334. <https://doi.org/10.1002/rcm.6322>
- Sunderland, E.M., Krabbenhoft, D.P., Moreau, J.W., Strobe, S.A., Landing, W.M., 2009. Mercury sources, distribution, and bioavailability in the North Pacific Ocean: Insights from data and models. *Glob. Biogeochem. Cycles* 23. <https://doi.org/10.1029/2008GB003425>

- Sunderland, E.M., Mason, R.P., 2007. Human impacts on open ocean mercury concentrations. *Glob. Biogeochem. Cycles* 21. <https://doi.org/10.1029/2006GB002876>
- Szpak, P., Buckley, M., Darwent, C.M., Richards, M.P., 2018. Long-term ecological changes in marine mammals driven by recent warming in northwestern Alaska. *Glob. Change Biol.* 24, 490–503. <https://doi.org/10.1111/gcb.13880>

T

- Takeuchi, T., Morikawa, N., Matsumoto, H., Shiraishi, Y., 1962. A pathological study of Minamata disease in Japan. *Acta Neuropathol. (Berl.)* 2, 40–57. <https://doi.org/10.1007/BF00685743>
- Tan, S.W., Meiller, J.C., Mahaffey, K.R., 2009. The endocrine effects of mercury in humans and wildlife. *Crit. Rev. Toxicol.* 39, 228–269. <https://doi.org/10.1080/10408440802233259>
- Tartu, S., Blévin, P., Bustamante, P., Angelier, F., Bech, C., Bustnes, J.O., Chierici, M., Fransson, A., Gabrielsen, G.W., Goutte, A., Moe, B., Sauser, C., Sire, J., Barbraud, C., Chastel, O., 2022. A U-turn for mercury concentrations over 20 Years: How do environmental conditions affect exposure in Arctic seabirds? *Environ. Sci. Technol.* 56, 2443–2454. <https://doi.org/10.1021/acs.est.1c07633>
- Teitelbaum, C.S., Ackerman, J.T., Hill, M.A., Satter, J.M., Casazza, M.L., De La Cruz, S.E.W., Boyce, W.M., Buck, E.J., Eadie, J.M., Herzog, M.P., Matchett, E.L., Overton, C.T., Peterson, S.H., Plancarte, M., Ramey, A.M., Sullivan, J.D., Prosser, D.J., 2022. Avian influenza antibody prevalence increases with mercury contamination in wild waterfowl. *Proc. R. Soc. B Biol. Sci.* 289, 20221312. <https://doi.org/10.1098/rspb.2022.1312>
- Thébault, J., Bustamante, P., Massaro, M., Taylor, G., Quillfeldt, P., 2021. Influence of species-specific feeding ecology on mercury concentrations in seabirds breeding on the Chatham Islands, New Zealand. *Environ. Toxicol. Chem.* 40, 454–472. <https://doi.org/10.1002/etc.4933>
- Thiébot, J.-B., Ropert-Coudert, Y., Raclot, T., Poupart, T., Kato, A., Takahashi, A., 2019. Adélie penguins' extensive seasonal migration supports dynamic Marine Protected Area planning in Antarctica. *Mar. Policy* 109, 103692. <https://doi.org/10.1016/j.marpol.2019.103692>
- Thompson, D.R., Bearhop, S., Speakman, J.R., Furness, R.W., 1998. Feathers as a means of monitoring mercury in seabirds: Insights from stable isotope analysis. *Environ. Pollut.* 101, 193–200. [https://doi.org/10.1016/S0269-7491\(98\)00078-5](https://doi.org/10.1016/S0269-7491(98)00078-5)
- Thompson, D.R., Becker, P.H., Furness, R.W., 1993a. Long-term changes in mercury concentrations in herring gulls *Larus argentatus* and common terns *Sterna hirundo* from the German North Sea Coast. *J. Appl. Ecol.* 30, 316–320. <https://doi.org/10.2307/2404633>
- Thompson, D.R., Furness, R.W., 1989. The chemical form of mercury stored in South Atlantic seabirds. *Environ. Pollut.* 60, 305–317. [https://doi.org/10.1016/0269-7491\(89\)90111-5](https://doi.org/10.1016/0269-7491(89)90111-5)
- Thompson, D.R., Furness, R.W., Lewis, S.A., 1993b. Temporal and spatial variation in mercury concentrations in some albatrosses and petrels from the sub-Antarctic. *Polar Biol.* 13, 239–244. <https://doi.org/10.1007/BF00238759>
- Thompson, D.R., Furness, R.W., Walsh, P.M., 1992. Historical changes in mercury concentrations in the marine ecosystem of the North and North-East Atlantic Ocean as indicated by seabird feathers. *J. Appl. Ecol.* 29, 79–84. <https://doi.org/10.2307/2404350>
- Thompson, D.R., Hamer, K.C., Furness, R.W., 1991. Mercury accumulation in great skuas *Catharacta skua* of known age and sex, and its effects upon breeding and survival. *J. Appl. Ecol.* 28, 672–684. <https://doi.org/10.2307/2404575>
- Tierney, M., Emmerson, L., Hindell, M., 2009. Temporal variation in Adélie penguin diet at Béchervaise Island, east Antarctica and its relationship to reproductive performance. *Mar. Biol.* 156, 1633–1645. <https://doi.org/10.1007/s00227-009-1199-9>
- Townhill, B.L., Couce, E., Bell, J., Reeves, S., Yates, O., 2021. Climate change impacts on Atlantic oceanic island Tuna Fisheries. *Front. Mar. Sci.* 8.
- Trasande, L., Landrigan, P.J., Schechter, C., 2005. Public health and economic consequences of methyl mercury toxicity to the developing brain. *Environ. Health Perspect.* 113, 590–596. <https://doi.org/10.1289/ehp.7743>
- Trueman, C.N., St John Glew, K., 2019. Chapter 6 - Isotopic tracking of marine animal movement, in: Hobson, K.A., Wassenaar, L.I. (Eds.), *Tracking Animal Migration with Stable Isotopes* (Second Edition). Academic Press, pp. 137–172. <https://doi.org/10.1016/B978-0-12-814723-8.00006-4>
- Trull, T.W., Armand, L., 2001. Insights into Southern Ocean carbon export from the $\delta^{13}\text{C}$ of particles and dissolved inorganic carbon during the SOIREE iron release experiment. *Deep Sea Res. Part II Top. Stud. Oceanogr., The Southern Ocean Iron Release Experiment (SOIREE)* 48, 2655–2680. [https://doi.org/10.1016/S0967-0645\(01\)00013-3](https://doi.org/10.1016/S0967-0645(01)00013-3)

Turner, J., 2015. Arctic and Antarctic,| Antarctic Climate, in: North, G.R., Pyle, J., Zhang, F. (Eds.), *Encyclopedia of Atmospheric Sciences (Second Edition)*. Academic Press, Oxford, pp. 98–106. <https://doi.org/10.1016/B978-0-12-382225-3.00044-X>

V

- Vihtakari, M., Welcker, J., Moe, B., Chastel, O., Tartu, S., Hop, H., Bech, C., Descamps, S., Gabrielsen, G.W., 2018. Black-legged kittiwakes as messengers of Atlantification in the Arctic. *Sci. Rep.* 8, 1178. <https://doi.org/10.1038/s41598-017-19118-8>
- Villar, E., Cabrol, L., Heimbürger-Boavida, L.-E., 2020. Widespread microbial mercury methylation genes in the global ocean. *Environ. Microbiol. Rep.* 12, 277–287. <https://doi.org/10.1111/1758-2229.12829>
- Vizzini, S., Mazzola, A., 2003. Seasonal variations in the stable carbon and nitrogen isotope ratios ($^{13}\text{C}/^{12}\text{C}$ and $^{15}\text{N}/^{14}\text{N}$) of primary producers and consumers in a western Mediterranean coastal lagoon. *Mar. Biol.* 142, 1009–1018. <https://doi.org/10.1007/s00227-003-1027-6>
- Vo, A.-T.E., Bank, M.S., Shine, J.P., Edwards, S.V., 2011. Temporal increase in organic mercury in an endangered pelagic seabird assessed by century-old museum specimens. *Proc. Natl. Acad. Sci.* 108, 7466–7471. <https://doi.org/10.1073/pnas.1013865108>

W

- Wang, F., Macdonald, R.W., Stern, G.A., Outridge, P.M., 2010. When noise becomes the signal: Chemical contamination of aquatic ecosystems under a changing climate. *Mar. Pollut. Bull.* 60, 1633–1635. <https://doi.org/10.1016/j.marpolbul.2010.05.018>
- Wang, F., Outridge, P.M., Feng, X., Meng, B., Heimbürger-Boavida, L.-E., Mason, R.P., 2019. How closely do mercury trends in fish and other aquatic wildlife track those in the atmosphere? – Implications for evaluating the effectiveness of the Minamata Convention. *Sci. Total Environ.* 674, 58–70. <https://doi.org/10.1016/j.scitotenv.2019.04.101>
- Wang, K., Munson, K.M., Beaupré-Laperrière, A., Mucci, A., Macdonald, R.W., Wang, F., 2018. Subsurface seawater methylmercury maximum explains biotic mercury concentrations in the Canadian Arctic. *Sci. Rep.* 8, 1–5. <https://doi.org/10.1038/s41598-018-32760-0>
- Watson, A.J., 2016. Oceans on the edge of anoxia. *Science* 354, 1529–1530. <https://doi.org/10.1126/science.aaj2321>
- Weimerskirch, H., 1991. Sex-specific differences in molt strategy in relation to breeding in the Wandering Albatross. *The Condor* 93, 731–737. <https://doi.org/10.2307/1368205>
- Welch, H.E., Bergmann, M.A., Siferd, T.D., Martin, K.A., Curtis, M.F., Crawford, R.E., Conover, R.J., Hop, H., 1992. Energy flow through the marine ecosystem of the Lancaster Sound region, Arctic Canada. *Arctic* 45, 343–357.
- Wenzel, C., Gabrielsen, G.W., 1995. Trace element accumulation in three seabird species from Hornøya, Norway. *Arch. Environ. Contam. Toxicol.* 29, 198–206. <https://doi.org/10.1007/BF00212971>
- West, J.B., Bowen, G.J., Dawson, T.E., Tu, K.P., 2010. *Isoscapes: Understanding movement, pattern, process on Earth through isotope mapping*, Springer. ed.
- Whitney, M.C., Cristol, D.A., 2018. Impacts of sublethal mercury exposure on birds: A detailed review, in: de Voogt, P. (Ed.), *Reviews of Environmental Contamination and Toxicology Volume 244, Reviews of Environmental Contamination and Toxicology*. Springer International Publishing, Cham, pp. 113–163. https://doi.org/10.1007/398_2017_4
- Wienecke, B.C., Robertson, G., 1997. Foraging space of emperor penguins *Aptenodytes forsteri* in Antarctic shelf waters in winter. *Mar. Ecol. Prog. Ser.* 159, 249–263. <https://doi.org/10.3354/meps159249>
- Williams, T.D., 1995. *The penguins: Spheniscidae, Bird families of the world*. Oxford University Press, Oxford.
- Wolfe, M.F., Schwarzbach, S., Sulaiman, R.A., 1998. Effects of mercury on wildlife: A comprehensive review. *Environ. Toxicol. Chem.* 17, 146–160. <https://doi.org/10.1002/etc.5620170203>
- World Health Organization, WHO. (2020) 10 chemicals of public health concern. Available on <https://www.who.int/news-room/photo-story/photo-story-detail/10-chemicals-of-public-health-concern> (consulted on April, 18th 2023)

Y

- Yamamoto, Y., Kanesaki, S., Kuramochi, T., Miyazaki, N., Watanuki, Y., Naito, Y., 1996. Comparison of trace element concentrations in tissues of the chick and adult Adelie penguins. *Proc. NIPR Symp. Polar Biol. Natl. Inst. Polar Res.* 253–262.

- Yarnes, C.T., Herszage, J., 2017. The relative influence of derivatization and normalization procedures on the compound-specific stable isotope analysis of nitrogen in amino acids. *Rapid Commun. Mass Spectrom.* 31, 693–704. <https://doi.org/10.1002/rcm.7832>
- Yue, F., Li, Y., Zhang, Y., Wang, L., Li, Dan, Wu, P., Liu, H., Lin, L., Li, Dong, Hu, J., Xie, Z., 2023. Elevated methylmercury in Antarctic surface seawater: The role of phytoplankton mass and sea ice. *Sci. Total Environ.* 882, 163646. <https://doi.org/10.1016/j.scitotenv.2023.163646>

Z

- Zdanowicz, C., Karlsson, P., Beckholmen, I., Roach, P., Poulain, A., Yumvihoze, E., Martma, T., Ryjkov, A., Dastoor, A., 2018. Snowmelt, glacial and atmospheric sources of mercury to a subarctic mountain lake catchment, Yukon, Canada. *Geochim. Cosmochim. Acta* 238, 374–393. <https://doi.org/10.1016/j.gca.2018.06.003>
- Zdanowicz, C., Krümmel, E.M., Lean, D., Poulain, A.J., Yumvihoze, E., Chen, J., Hintelmann, H., 2013. Accumulation, storage and release of atmospheric mercury in a glaciated Arctic catchment, Baffin Island, Canada. *Geochim. Cosmochim. Acta* 107, 316–335. <https://doi.org/10.1016/j.gca.2012.11.028>
- Zhang, P., Zhang, Y., 2022. Earth system modeling of mercury using CESM2 – Part 1: Atmospheric model CAM6-Chem/Hg v1.0. *Geosci. Model Dev.* 15, 3587–3601. <https://doi.org/10.5194/gmd-15-3587-2022>
- Zhang, Y., Dutkiewicz, S., Sunderland, E.M., 2021. Impacts of climate change on methylmercury formation and bioaccumulation in the 21st century ocean. *One Earth* 4, 279–288. <https://doi.org/10.1016/j.oneear.2021.01.005>
- Zhang, Y., Jaeglé, L., Thompson, L., Streets, D.G., 2014. Six centuries of changing oceanic mercury. *Glob. Biogeochem. Cycles* 28, 1251–1261. <https://doi.org/10.1002/2014GB004939>
- Zhang, Y., Zhang, P., Song, Z., Huang, S., Yuan, T., Wu, P., Shah, V., Liu, M., Chen, L., Wang, X., Zhou, J., Agnan, Y., 2023. An updated global mercury budget from a coupled atmosphere-land-ocean model: 40% more re-emissions buffer the effect of primary emission reductions. *One Earth* 6, 316–325. <https://doi.org/10.1016/j.oneear.2023.02.004>
- Zheng, J., 2015. Archives of total mercury reconstructed with ice and snow from Greenland and the Canadian High Arctic. *Sci. Total Environ.*, Special Issue: Mercury in Canada's North 509–510, 133–144. <https://doi.org/10.1016/j.scitotenv.2014.05.078>
- Zheng, W., Chandan, P., Steffen, A., Stupple, G., De Vera, J., Mitchell, C.P.J., Wania, F., Bergquist, B.A., 2021. Mercury stable isotopes reveal the sources and transformations of atmospheric Hg in the high Arctic. *Appl. Geochem.* 131, 105002. <https://doi.org/10.1016/j.apgeochem.2021.105002>
- Zhou, Z., Wang, H., Li, Y., 2023. Mercury stable isotopes in the ocean: Analytical methods, cycling, and application as tracers. *Sci. Total Environ.* 874, 162485. <https://doi.org/10.1016/j.scitotenv.2023.162485>

Annexes

Chapter 1: Introduction

Table A1. Summary of Hg samples by major taxa across major oceanic and continental regions from the Global Biotic Hg Synthesis Database (Evers, 2019).

	Fish	Sea turtles	Birds	Marine Mammals	Subtotal
Ocean Basins					
Antarctic	593	-	3,299	196	4,088
Arctic	1,776	-	2,613	2,693	7,082
Gulf of Mexico-Caribbean	6,515	259	45	169	6,988
Indian	3,264	60	1,447	180	4,951
Mediterranean	4,521	156	638	358	5,673
North Atlantic	12,770	955	13,624	2,381	29,730
North Pacific	14,590	211	17,116	1,024	32,941
South Atlantic	9,659	125	1,429	658	11,871
South Pacific	2,140	-	1,331	82	3,553
Subtotal	55,828	1,766	41,542	7,741	106,877
Continents					
Africa	5,877	391	865	253	7,386
Antarctica	564	49	2,881	196	3,690
Asia	11,978	-	1,535	1,029	14,542
Australia	1,887	-	906	64	2,857
Europe	16,177	254	11,138	1,476	29,045
North America	197,851	950	60,596	4,512	263,909
South America	28,940	363	685	546	30,534
Subtotal	263,274	2,007	78,606	8,076	351,963
Total	319,102	3,773	120,148	15,817	458,840

Description of the three bioindicator seabird species:



The Brunnich guillemot

Uria lomvia

Other common name: Thick-billed murre

Conservation Status: Least Concern 

Scientific classification:
 Animalia > Chordata > Aves > Charadriiformes > Alcidae > Uria

Description: Diving seabird (20–50 m deep on average, up to 100m deep)

 45 cm

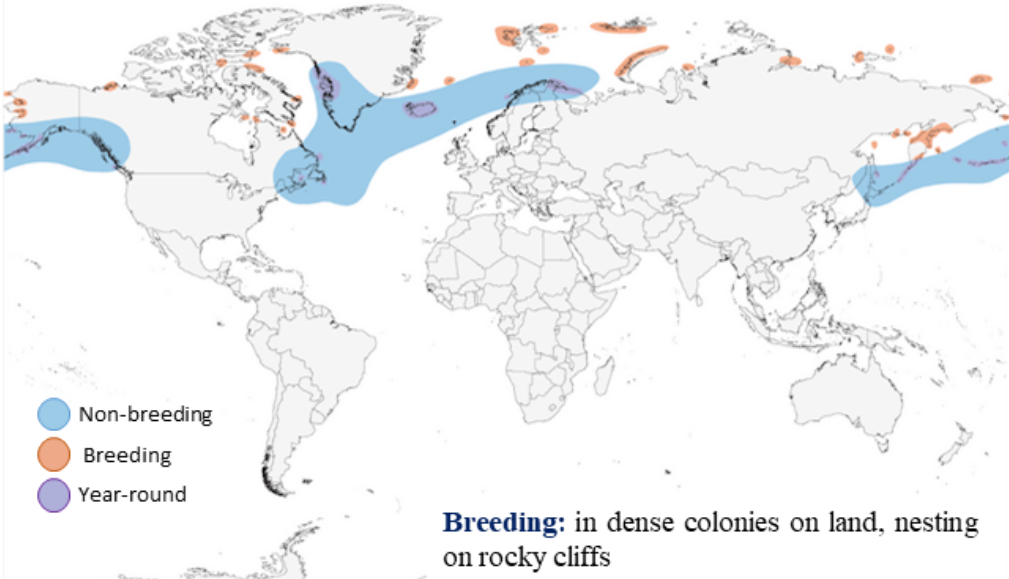
 0.75–1.5 kg

Lifespan: 20-30 years

Habitat
 Oceans, typical in marginal ice zones and ice-covered waters

Diet
 Fish, Zooplankton
 Pelagic and sympagic* prey

Distribution: Circumpolar (Northern Hemisphere), subarctic and Arctic regions



Breeding: in dense colonies on land, nesting on rocky cliffs

Moult: Biannual

- pre-breeding in Spring (nuptial plumage; partial moult)
- post-breeding in Autumn (wintering plumage; complete moult)

Source: Gaston, A. J. and J. M. Hipfner (2020). Thick-billed Murre (*Uria lomvia*), version 1.0. In Birds of the World (S. M. Billerman, Editor). Cornell Lab of Ornithology, Ithaca, NY, USA. <https://doi.org/10.2173/bow.thbmur.01>

*Sympagic = sea ice-associated



The sooty tern

Onychoprion fuscatus

Other name: «Ewa ewa»

Conservation Status: Least Concern



Scientific classification:

Animalia > Chordata > Aves > Charadriiformes > Alcidae > Uria

Description: Surface-feeding seabird (fews cm, above the sea surface; no dive)



36–45 cm



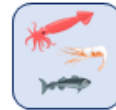
200 g

Lifespan: ~32 year



Habitat

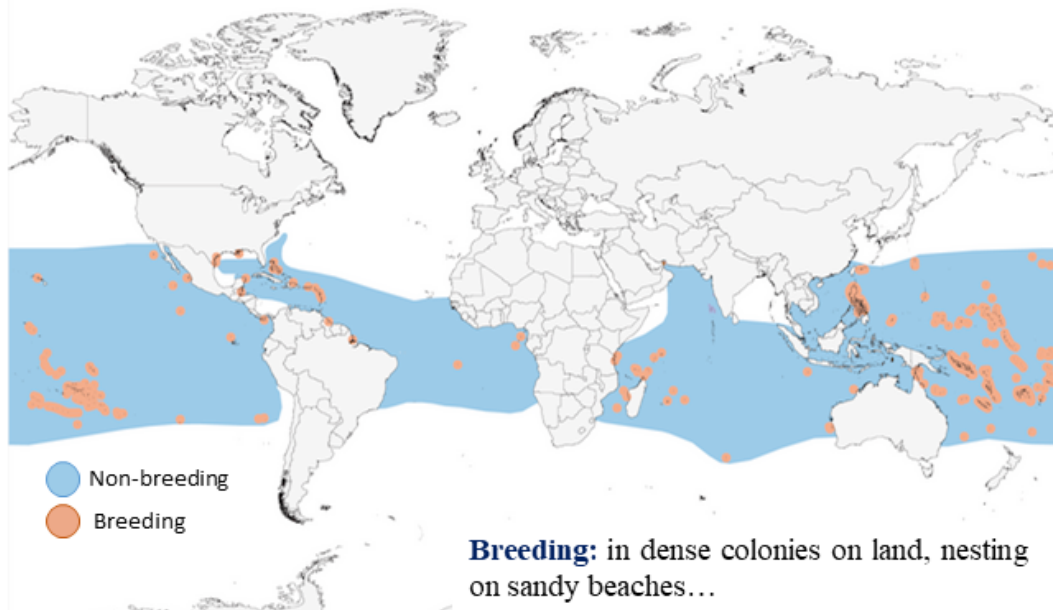
Tropical and subtropical oceans, nesting on remote islands



Diet

Fish, Zooplankton, Squids

Distribution: Pantropical



Moult: Start moulting primary feathers while still breeding, and all their feathers the following weeks/months

Sources: Schreiber, E. A., C. J. Feare, B. A. Harrington, B. G. Murray Jr., W. B. Robertson Jr., M. J. Robertson, and G. E. Woolfenden (2020). Sooty Tern (*Onychoprion fuscatus*), version 1.0. In *Birds of the World* (S. M. Billerman, Editor). Cornell Lab of Ornithology, Ithaca, NY, USA. <https://doi.org/10.2173/bow.sooter1.01>



The Adélie penguin

Pygoscelis adeliae

Conservation Status: Least Concern



Scientific classification:

Animalia > Chordata > Aves > Sphenisciformes > Spheniscidae

Description: Ice-obligated diving seabird
(2-35 m deep, up to 175 meters; pursuit-diving)



70 cm



3.2–8.2 kg

Lifespan: 15-20 years



Habitat

ice-covered waters



Diet

Krill, Fish

Distribution: Circumpolar (Southern Ocean, solely south of the Polar Front)



Moult: Unique, simultaneous, annual (post-breeding, usually on ice-floes)

Breeding: in dense colonies on land, nesting on snow and ice-free rocky coasts

Sources: Martinez, I., D. A. Christie, F. Jutglar, E. F. J. Garcia, and C. J. Sharpe (2020). Adélie Penguin (*Pygoscelis adeliae*), version 1.0. In *Birds of the World* (J. del Hoyo, A. Elliott, J. Sargatal, D. A. Christie, and E. de Juana, Editors). Cornell Lab of Ornithology, Ithaca, NY, USA. <https://doi.org/10.2173/bow.adepen1.01>

Chapter 2: Methodological approach

Table A2. List of collaborators and associated institutions involved in feather sampling during this PhD.

Collaborators	Institutions
Spatial Hg assessment in tropical ecosystems	
Charlie Bost	Centre d'Études Biologiques de Chizé, CNRS, France
Leandro Bugoni	Universidade Federal do Rio Grande, Brazil
Nicholas Carlisle	Department of Planning, Industry and Environment, Australia
Annabelle Cupidon	Island Conservation Society, Seychelles
Nina Darocha	Fundação Príncipe, Sao Tomé-et-Príncipe
Nic Dunlop	Conservation Council of Western Australia, Australia
Chris Feare	WildWings Bird Management, Seychelles
Antonia Garcia Quintas	Marine Biodiversity, Exploitation and Conservation, France-Cuba
Thomas Ghestemme	Société d'Ornithologie de Polynésie (SOP Manu), France
Daniel Link	US Fish and Wildlife Service, Papahānaumokuākea Marine National Monument, USA
Estrela Matilde	Fundação Príncipe, Sao Tomé-et-Príncipe
Matthew Morgan	Island Conservation Society, Seychelles
Terry O'Dwyer	Department of Planning, Industry and Environment, Australia
Brian Peck	US Fish and Wildlife Service, Rose Atoll National Wildlife Refuge, USA
Stuart Pimm	Nicholas School of the Environment, Duke University, USA
Veronica Rodrigues Costa Neves	Oceanos Center, Azores University, Portugal
Ana Roman	US Fish and Wildlife Service, Culebra National Wildlife Refuge Puerto Rico, USA
Gerard Rocamora	Island Biodiversity and Conservation Centre, University of Seychelles, Seychelles
Laura Shearer	Ascension Island Government Conservation and Fisheries Directorate, Ascension Island, UK
Louise Soanes	University of Roehampton, UK
Kate Toniolo	US Fish and Wildlife Service, Pacific Remote Islands Marine National Monument, USA
Eduardo Ventosa	Effective Environmental Restoration, Puerto Rico, USA
Tehani Withers	Société d'Ornithologie de Polynésie (SOP Manu), France
Spatial Hg assessment in Antarctic ecosystems	
Rebecka Brasso	Department of Zoology, Weber State University, USA
Ilaria Costi	Department of Physical, Earth and Environmental Sciences, University of Siena, Italy
Michael Dunn	British Antarctic Survey, UK
Louise Emmerson	Australian Antarctic Division, Australia
Tom Hart	Department of Biology, University of Oxford
Mariana Juárez	Instituto Antártico Argentino, Argentina

Akiko Kato	Centre d'Études Biologiques de Chizé, CNRS, France
Ana Laura Machado	Centro Universitario Regional del Este, Universidad de la República, Uruguay
Candice Michelot	Centre d'Études Biologiques de Chizé, La Rochelle Université, France
Silvia Olmastroni	Museo Nazionale dell' Antartide, Italy
Michael Polito	Louisiana State University, USA
Thierry Raclot	Institut Pluridisciplinaire Hubert Curien, Université de Strasbourg, France
Mercedes Santos	Instituto Antártico Argentino, Argentina
Annie Schmidt	Point Blue Conservation, USA
Colin Southwell	Australian Antarctic Division, Australia
Alvaro Soutullo	Centro Universitario Regional del Este, Universidad de la República, Uruguay
Akinori Takahashi	National Institute of Polar Research, Japan
Jean-Baptiste Thiébot	Graduate School of Fisheries Sciences, Hokkaido University, Japan
Phil Trathan	British Antarctic Survey, UK
Claire Waluda	British Antarctic Survey, UK

Temporal Hg assessment in Arctic ecosystems

Mark Adams, Hein van Grouw,	Bird Group Tring, Natural History Museum, UK
Alexander Bond	
Peter Hosner	Bird Collections, Natural History Museum, Copenhagen, Denmark
Flemming Merkel	Aarhus University, Denmark
Jannie Linnebjerg	Aarhus University, Denmark
Jérôme Fort	Littoral, Environnement et Sociétés, CNRS, France

Temporal Hg assessment in tropical ecosystems

Roger Dickey	Army Ornithological Society, UK
John Hughes	Centre for Ornithology, University of Birmingham, UK
Vitor Paiva	Marine and Environmental Sciences Centre, University of Coimbra, Portugal
Jaime Ramos	Marine and Environmental Sciences Centre, University of Coimbra, Portugal
James Reynolds	Centre for Ornithology, University of Birmingham, UK
Laura Shearer	Ascension Island Government Conservation and Fisheries Directorate, Ascension Island, UK
Colin Wearn	Royal Air Force Ornithological Society, UK

Opportunistic monitoring of penguin species

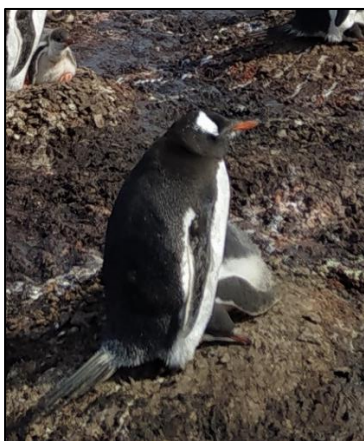
Context. Thanks to the collaboration with the Australian Antarctic Division (Louise Emmerson and Colin Southwell) and the Spanish National Research Council (Andr s Barbosa), additional feather samples from three other penguin species were collected and shipped to the LIENSs for chemical analyses. This included chinstrap (*Pygoscelis antarcticus*; n=22), gentoo (*Pygoscelis papua*; n=30) and Emperor penguins (*Aptenodytes forsteri*; n=27). Samples of chinstrap and gentoo penguins were analysed as part of the Master 1 internship of Pierre Vivion. Samples of Emperor penguins were analysed by myself.

Methods. Laboratory analyses included both total-Hg and stable isotope analyses ($\delta^{13}\text{C}$, $\delta^{15}\text{N}$). Complete methodology is detailed in Chapter 2.

Main findings. Feather Hg concentrations and stable isotope values are provided in Table A3 (mean \pm SD, min–max) for all species, in Figure A1 for gentoo penguins and Figure A2 for Emperor penguins. For a comparison with existing measurements of both Hg and stable isotopes, the reader is referred to Paper 2 (Supplementary Material, Table S1).



Chinstrap penguin



Gentoo penguin



Emperor penguin

Table A3. Feather Hg concentrations and stable isotope values measured in body feathers of Emperor (*Aptenodytes forsteri*), Chinstrap (*Pygoscelis antarcticus*) and Gentoo (*P. papua*) penguins, sampled in Antarctica.

Species, site, colony	Year	Age class	n	Feather Hg ($\mu\text{g}\cdot\text{g}^{-1}$)	Feather $\delta^{13}\text{C}$ (‰)	Feather $\delta^{15}\text{N}$ (‰)
Emperor penguins						
Mawson						
Auster Rockery	2019/2020	Adult	4	2.19 ± 0.21 (1.93–2.43)	-24.12 ± 0.26 (-24.36, -23.78)	12.84 ± 0.57 (12.18–13.53)
Davis						
Amanda Bay	2019/2020	Adult	23	0.72 ± 0.74 (0.19–2.91)	-24.56 ± 1.31 (-26.07, -21.86)	10.43 ± 1.95 (8.53–14.11)
		Chick	1	0.41	-23.34	13.84
Chinstrap penguins						
South Shetland Islands						
Deception Island	2017/2018	Adult	22	1.36 ± 0.31 (0.85–2.11)	-25.20 ± 0.39 (-25.82, -24.34)	9.31 ± 0.25 (8.71–9.81)
Gentoo penguins						
Antarctic Peninsula						
Hope Bay/Esperanza	2013/2014	Adult	15	1.81 ± 0.66 (0.74–3.11)	-22.19 ± 1.45 (-25.76, -20.54)	11.79 ± 1.12 (9.90–13.11)
Cierva Point	2018/2019	Adult	15	0.25 ± 0.06 (0.17–0.9)	-25.29 ± 0.30 (-25.96, -24.93)	9.68 ± 0.27 (9.25–10.13)

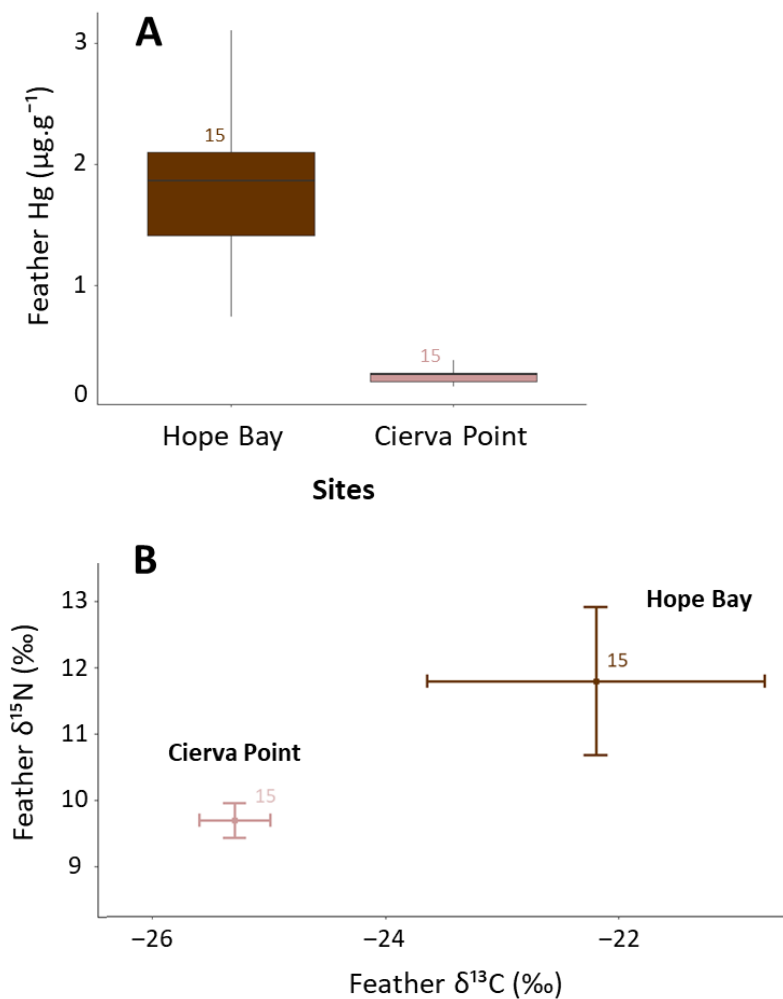
Gentoo penguin

Figure A1. Feather (A) Hg concentrations and (B) stable isotope analyses of adult gentoo penguins (*Pygoscelis papua*) sampled in two sites: Hope Bay/Esperanza and Cierva Point, both located in the Antarctic Peninsula. Numbers indicate sample sizes. Values of $\delta^{13}\text{C}$ and $\delta^{15}\text{N}$ (mean \pm SD) indicate the feeding habitat (carbon source) and the trophic position (diet), respectively. Boxplots indicate the median values (horizontal bar), ranges (min–max; vertical bar), with the box encompassing 50% of all data.

Emperor penguins

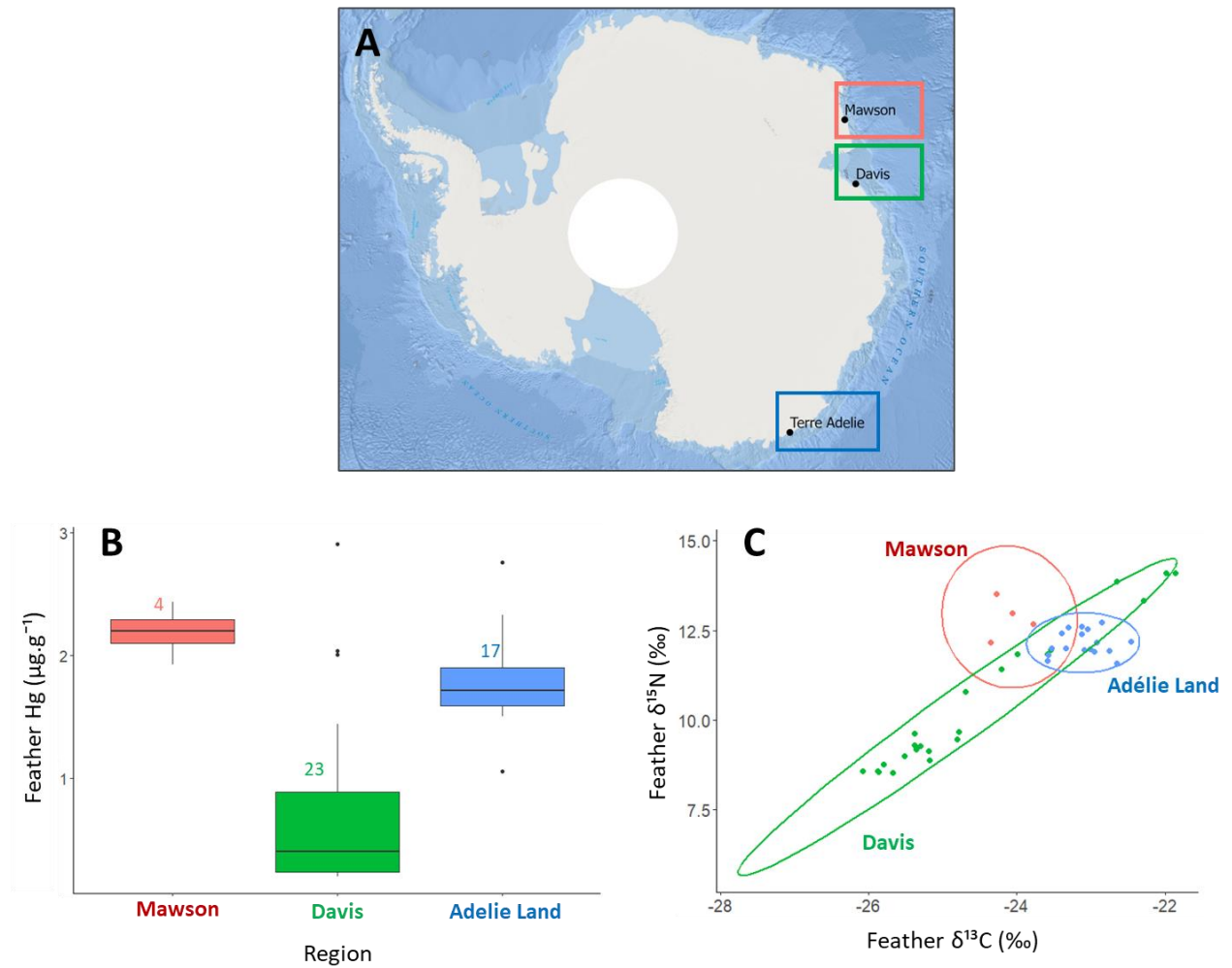


Figure A2. (A) Locations of feather sampling of Emperor penguin (*Aptenodytes forsteri*) in Antarctica, on which (B) Hg concentrations and (C) stable isotope were measured. Feathers were collected in two Australian Antarctic Stations: Mawson (in 2019) and Davis (in 2019), and results were compared to Adélie Land (in 2007; from Carravieri et al., 2016).

Methodology: Compound-Specific Stable Isotope Analyses of Amino-Acids (CSIA-AA)

Context: In this doctoral work, CSIA-AA were only performed on feathers of sooty terns in Chapter 3, for a spatial comparison of Hg contamination across ocean basins. Considering the high dispersal of adult sooty terns and the lack of knowledge about precise geographical localisation during the non-breeding period, spatial comparison of bulk stable isotopes seems inappropriate, as terns may rely on marine food webs that are isotopically highly contrasted. Since CSIA-AA is time- and money-consuming, analyses were performed on a subset of adult individuals (n=91), selected across 19 sites in the three ocean basins (see Paper 1, Table S3).

Laboratory analyses: Amino acids (AA) must be derivative to be amenable to gas chromatographic separation. The methodology used here leads to the production of N-acetyl isopropyl esters. These derivatives have two main interests: a low number of C atoms added, that improves the measurement precision, and a relatively long stability during storage. The protocols described below are derived from Corr et al. (2007) and Styring et al. (2012).

Standards, reagents and solvents

All reagents were of high purity grade ($\geq 99\%$) from Sigma-Aldrich, including NH_4OH 30-33% solution (puriss), HCl (37% ACS), acetyl chloride (puriss), acetic anhydride, triethylamine and NaCl. MilliQ® water was used for water dilutions of reagents. Solvents were of GC or GC-MS Suprasolv grade from Merck (acetone, dichloromethane, ethyl acetate) or Sigma-Aldrich (2-Propanol puriss ACS). A standard mixture (10 mM in 0.1 M HCl) of 16 high purity AAs, precisely determined for their $\delta^{13}\text{C}$ and $\delta^{15}\text{N}$ values, was prepared. This included alanine (Ala), valine (Val), leucine (Leu), isoleucine (Ile), threonine (Thr), serine (Ser), proline (Pro), methionine (Met), glutamic acid (Glu), hydroxyproline (Hyp), tyrosine (Tyr), histidine (His), lysine (Lys) from Sigma- Aldrich, and glycine (Gly), aspartic acid (Asp), phenylalanine (Phe) from Alfa Aesar. Norleucine (Nle, Alfa Aesar) and alpha-aminoadipic acid (AAA, Sigma-Aldrich) were added as internal standards. A third internal standard was prepared from a caffeine reference material (USGS-61, 10 mM in ethyl acetate).

Sample hydrolysis and AA purification

Feather homogenates (1–1.5 mg) were hydrolysed (110°C, 22 h) in 200 μL 6 M HCl under nitrogen in pre-combusted screw cap tubes. They were then dried under a stream of N_2 at 70°C and finally re-dissolved in 2 ml HCl 0.5 M. During hydrolysis, asparagine (Asn) and glutamine (Gln) are converted to Asp and Glu, respectively. Data for Asp and Glu thus represent the total Asp + Asn and Glu + Gln, respectively, noted Asx and Glx thereafter.

AA purification was done by ion-exchange chromatography on a Dowex 50W-X8 200-400 mesh resin (Sigma-Aldrich), packed in glass columns (5 cm height, 6 mm i.d.; resin volume $V = 1.4$ mL). The resin was washed successively with 3V of HCl (1M), H₂O, NaOH (1M) and H₂O. It was activated with 3V HCl 1M followed by 3V H₂O just before introducing the sample in the column, through a pre-combusted GF/C (Whatman) glass fiber filter. After rinsing the tube and the filter with 1 mL HCl 0.5 M, and complete elution, salts were washed with 3V H₂O, then AAs eluted with 3V NH₄OH 10% in clean screw cap tubes. Finally, after addition of two internal standards (Norleucine and α -amino adipic acid, 10 mM, 20 μ L), the purified AAs were dried at 80°C under a stream of N₂.

Amino acid derivatisation

A standard mixture (20 μ L, 10 mM) was derivatized with each batch of 6 to 9 samples. Esterification was performed by addition of 0.9 mL of acidified isopropanol (isopropanol: acetyl chloride, 4:1 v/v) at 100°C for 1h under nitrogen. After cooling, samples were placed at 60°C under a gentle stream of N₂, to evaporate isopropanol until complete dryness. Acetylation was carried out by adding 0.75 mL of a mixture of acetone, triethylamine and acetic anhydride (5:2:1 v/v/v), sealing tubes under nitrogen, and heating at 60°C for 10 min. After cooling, the reagents were evaporated under a N₂ stream at 60°C during 5 min, then at room temperature. Dryness was achieved by addition of 0.5 mL of dichloromethane flowed by evaporation. AA derivatives were cleaned by liquid-liquid extraction by addition of 1 mL of ethyl acetate, and 1 mL of a saturated NaCl water solution. Tubes were capped under nitrogen then shaken and vortexed. After phase separation, the organic phase was transferred in a pre-combusted tube, and extraction of the residual derivatives was repeated with 1 mL of ethyl acetate. Finally, caffeine (20 μ L, 10 mM) was added in sample and standard mixture derivatives, and 50 μ L transferred to a glass autosampler vial insert for AA $\delta^{13}\text{C}$ analysis. The rest of the derivatives was dried under a gentle stream of N₂, and re-dissolved in 100 μ L ethylacetate further transferred to an autosampler vial insert for AA $\delta^{15}\text{N}$ analysis. AA derivatives were stored at -20°C until analysis, during a few days for $\delta^{13}\text{C}$ measurements, and up to one month for $\delta^{15}\text{N}$ ones.

GC-C-IRMS analysis

GC-C-IRMS analysis of the derivatized AAs was performed on a Thermo Trace Ultra GC, fitted with a TriPlus autosampler and coupled to a Delta Plus isotope-ratio mass spectrometer through a GC Isolink combustion interface (Thermo Scientific, Bremen, Germany). The combustion furnace was held at 1000°C, and a 1 min seed oxidation was applied before each sample injection to maintain reactor efficiency. The GC was equipped with a TG-624 SilMS (60 m x 0.25 mm i.d., 1.4 μ m film thickness, Thermo Scientific). Injections were performed in splitless mode (1 min) at 255°C, the helium carrier gas flow was constant (1.2 mL/min). GC temperature program was set as follows: 70°C (hold 1 min),

165°C at 16°C/min, 274°C at 4.5°C/min (hold 22 min), 285°C at 10°C/min (hold 4 min). For $\delta^{15}\text{N}$ analysis, CO_2 generated during combustion was removed from the carrier gas using a cryogenic trap, and released after the end of each analysis. Good chromatographic separation was effective for the three internal standards (Nle, AAA and caffeine), and 14 AAs among the 16 AAs of the standard mixture. Values obtained for some AAs were not usable as they co-eluted (Tyr and His) or were in too small quantities in samples (peaks <200 mV, Met, Lys).

Data correction and calibration

Similar to bulk analyses, data are expressed in delta notation relative to V-PDB for carbon and atmospheric N_2 for nitrogen. Obtained raw data were corrected for instrumental variations and deviations in the isotopic compositions of the products occurring during sample derivatization, in particular kinetic fractionation and addition of C atoms from reagents to the derivatives, in the case of $\delta^{13}\text{C}$ measurements. The standard mixture was analysed at the beginning, every three or four samples and at the end of each batch of analyses. Data were normalized by using internal standard values (Sabadel et al., 2016): caffeine was used for $\delta^{15}\text{N}$ measurements, but due to its low peak and a co-elution with a small contaminant in samples, was less useful for $\delta^{13}\text{C}$ measurements, for which AAA was used. AAs values in the standard mixture were used for correction of any instrumental drift during the run (Sabadel et al., 2016) and compound-specific calibration (Yarnes and Herszage, 2017). Precision ($1\ \sigma$) for AAs values (excluding unusable AAs), ranged from 0 to 1.2 ‰ (mean 0.3 ‰) for $\delta^{13}\text{C}$ measurements and from 0 to 1.5 ‰ (mean 0.3 ‰) for $\delta^{15}\text{N}$ measurements.

Chapter 4: Temporal monitoring - Introduction

Table A4. Studies investigating long-term trends in Hg contamination in feathers of museum specimens. n indicates sample sizes for each species and study.

Reference, Species	n	Feather	Time range	Site, Region (Ocean)	Main findings	Isotopes
<u>Choy et al. (2022)</u>						
Glaucous-winged gull (<i>Larus glaucescens</i>)	65	Body	1887–1996	Salish Sea (Northeast Pacific Ocean)	No trend (stable)	Yes
<u>Bond and Lavers (2020)</u>						
Flesh-footed shearwater (<i>Puffinus carneipes</i>)	137	Body	1946–2011	Australia (Southeast Indian Ocean)	No significant trend (-0.3 % per year)	No
<u>Sun et al. (2019)</u>						
White-tailed eagle (<i>Haliaeetus albicilla</i>)	124	Body	1884–2013	West Greenland (Arctic Ocean)	No significant trend	Yes
	102		1866–2015	Norway (Baltic Sea)	Non-linear increase (+60% from 1866 to 1957; -40% until 2015)	
	87		1967–2011	Sweden (Baltic Sea)	Drastic decline (-70%) from 1967 to 2011	
<u>Gilmour et al. (2019)</u>						
Gentoo penguin (<i>Pygoscelis papua</i>)	37	Body	1950s–2003	Macquarie Island, (Southern Ocean; sub-Antarctic)	No trend	No
King penguin (<i>Aptenodytes patagonicus</i>)	30		1940s–2003		Decrease	
Rockhopper penguin (<i>Eudyptes sp.</i>)	34		1940s–2003		Non-significant increase	
Royal penguin (<i>Eudyptes schlegeli</i>)	42		1930s–2003		Decrease	
<u>Gagné et al. (2019)</u>						

Laysan albatross (<i>Phoebastria immutabilis</i>)	-		1897–1992	Hawaiian Islands (North Pacific Ocean), American Samoa (South Pacific Ocean), Florida Keys (Atlantic Ocean)	Decreasing from the 1980s to 2015 for Hawaiian Islands only	No
Bulwer's petrel (<i>Bulweria bulweri</i>)	-		1891–2014			
Wedge-tailed shearwater (<i>Puffinus pacificus</i>)	-		1897–2014			
White-tailed tropicbird (<i>Phaethon lepturus</i>)	-	Body/	1892–2015			
Brown booby (<i>Sula leucogaster</i>)	-	Primary	1891–2015			
Brown noddy (<i>Anous stolidus</i>)	-		1939–1996			
White tern (<i>Gygis alba</i>)	-		1891–2013			
Sooty tern (<i>Onychoprion fuscatus</i>)	-		1896–2015			
<u>Carravieri et al. (2016)</u>						
Emperor penguin (<i>Aptenodytes forsteri</i>)	28	Body	1950s–2007	Adélie Land, Antarctica (Southern Ocean)	No change	Yes
Adelie penguin (<i>Pygoscelis adeliae</i>)	15		1950s–2007		Decrease (-77%)	
King penguin (<i>Aptenodytes patagonicus</i>)	38		1970s–2007	Crozet Islands (Southern Ocean; sub-Antarctic waters)	No significant change (+14%)	
Macaroni penguin (<i>Eudyptes chrysolophus</i>)	30		1970s–2007		Increase (+32%)	
Gentoo penguin (<i>Pygoscelis papua</i>)	24		1970s–2007		Increase (+53%)	
<u>Bond et al. (2015)</u>						
Ivory gull (<i>Pagophila eburnea</i>)	80	Body	1877–2007	Canadian Arctic, Greenland and Eastern Canadian waters (Arctic Ocean)	45-fold increase (+1.6% per year)	Yes
<u>Vo et al. (2011)</u>						
Black-footed albatross (<i>Phoebastria nigripes</i>)	25	Body	1880–2002	Multiple sites (North Pacific Ocean)	Increase	Yes
<u>Scheifler et al. (2005)</u>						
King penguin (<i>Aptenodytes patagonicus</i>)	41	Body	1966–2001	Crozet Islands (Southern Ocean; sub-Antarctic waters)	Significant decrease (-34%)	No
<u>Monteiro and Furness (1997)</u>						
Cory's shearwater (<i>Calonectris borealis</i>)	267	Body	1886–1994	Azores, Madeira, Salvages (Northeast Atlantic Ocean)	Increase by 1.1 – 1.9% per year	No
Little shearwater (<i>Puffinus assimilis</i>)	49				-	
Common tern (<i>Sterna hirundo</i>)	37				-	

Bulwer's petrel (<i>Bulweria bulweri</i>)	85				Increase by 3.5 – 4.8% per year	
Madeiran storm petrel (<i>Oceanodroma castro</i>)	63				-	
<u>Furness et al. (1995)</u>						
Herring gull (<i>Larus argentatus</i>)	-	Body	1880–1990	German Bight, East Scotland, Shetland (North Sea, North Atlantic Ocean)	Increase	No
Common tern (<i>Sterna hirundo</i>)	-					
Kittiwakes (<i>Rissa sp.</i>)	-					
Guillemots (<i>Uria sp.</i>)	-					
<u>Thompson et al. (1993a)</u>						
Common tern (<i>Sterna hirundo</i>)	42	Body	1866–1990s	German North Sea coast, (Northeast Atlantic Ocean)	4-fold increase in adults (+377%), 2-fold in juveniles (+139%)	No
Herring gull (<i>Larus argentatus</i>)	140		1884–1990s		2-fold increase (adults: +75%, juveniles: +110%)	
<u>Thompson et al. (1993b)</u>						
Wandering albatross (<i>Diomedea exulans</i>)	35	Body	<1950–1980s	New Zealand, South Georgia, Gough Island, Marion Island (Southern Ocean; sub-Antarctic waters)	Significant increase in 3 species, but lack of widespread increase	No
Black-browed albatross (<i>Thalassarche melanorhynchus</i>)	20					
Grey-headed albatross (<i>Thalassarche chrysotoma</i>)	16					
Shy albatross (<i>Thalassarche cauta</i>)	9					
Northern giant petrel (<i>Macronectes halli</i>)	7					
Southern giant petrel (<i>Macronectes giganteus</i>)	42					
<u>Thompson et al. (1992)</u>						
Northern fulmar (<i>Fulmarus glacialis</i>)	57	Body	1850s–1980s	St Kilda, Foula, southern Ireland (Northeast Atlantic Ocean)	Decrease (-65% in Shetland, -35% in St Kilda)	No
Manx shearwater (<i>Puffinus puffinus</i>)	96			Skomer, Wales (Northeast Atlantic Ocean)	Increase (+125%)	
North Atlantic gannet (<i>Morus bassanus</i>)	57			Bass Rock (North Atlantic Ocean)	Increase (+20%)	
Great skua (<i>Stercorarius skua</i>)	225			Foula, southern Ireland (Northeast Atlantic Ocean)	Increase (+53%)	

Atlantic puffin (<i>Fratercula arctica</i>)	110			St Kilda, Foula, Great Saltee, southern Ireland (Northeast Atlantic Ocean)	Increase (+120%)	
---	-----	--	--	--	------------------	--

Appelquist et al. (1985)

Black guillemot (<i>Cepphus grille</i>)	137	Primary	1830s–1979	Baltic Sea, Faroe Islands, Greenland (North Atlantic Ocean)	Substantial increase	No
Common, Brunnich guillemots (<i>Uria sp.</i>)	140					

∴ Information not available in the original study

Table A5. Review of Hg long-term trends using museum archives - Arctic mammals. Polar bear (*Ursus maritimus*), narwhal (*Monodon monoceros*), ringed seal (*Phoca hispida*).

Region, Species	n	Tissue	Time range	Main findings	Isotopes	References
Canadian High Arctic						
Beluga	135	Teeth	1854–2000	Increase (x3-5)	Yes	Desforges et al. (2022)
Greenland						
Northwest Greenland						
Narwhal	10	Tusk	1962–2010	Log-linear increase (+0.3% per year) but +1.9% per year after 2000	Yes	Dietz et al. (2021)
Polar bear	117	Hair	1892–2008	Increase (+1.6–1.7% per year)	Yes (partially)	Dietz et al. (2011)
Polar bear	69	Hair	1892–2001	Increase (+2.1% per year) until 1991	No ?	Dietz et al. (2006)
Central West Greenland						
Ringed seal	115	Teeth	1982–2006	Decrease until the 1990s, increase until 2006	Yes (no Suess?)	Aubail et al. (2010)
East Greenland						
Polar bear	322	Hair	?	Increase (+0.8% per year) after 1973	No ?	Dietz et al. (2006)
Polar bear	27	Hair	1892–1973	Increase (+3.1% per year)	No ?	Dietz et al. (2006)
Central East Greenland						
Ringed seal	170	Teeth	1986–2006	Decrease until the 1990s, increase until 2004, decrease in 2006	Yes (no Suess ?)	Aubail et al. (2010)
Svalbard						
Polar bear	87	Teeth	1964–2003	Decrease (–2.1% per year) over four decades	Yes (no Suess?)	Aubail et al. (2011)

Chapter 4 – Section 1: Temporal monitoring Arctic marine food webs

Table A6. Description of different age classes of Brünnich’s guillemots sampled in Greenland for the temporal Hg monitoring.

	n	Time frame (n years)
Adults	481	1833–2022 (76 years)
Youngs	66	–
First winter	27	1995–2013 (5 years)
Juvenile	9	2014 (1 year)
Immature	27	1995–2017 (6 years)
Subadult	2	2014 (1 year)
Unknown	1	2011 (1 year)

Table A7. Feather Hg concentrations and stable isotopes in Brünnich’s guillemots from Greenland (unknown site; n=12), collected from the 1830s and the 1970s.

Decades	n	Feather Hg ($\mu\text{g}\cdot\text{g}^{-1}$)	Feather corrected $\delta^{13}\text{C}$ (‰)	Feather $\delta^{15}\text{N}$ (‰)
1830	1	0.84	–15.01	17.07
1870	1	0.62	–17.38	13.19
1880	2	0.89 \pm 0.68 (0.41–1.37)	–15.34 \pm 0.57 (–15.75, –14.94)	13.34 \pm 2.21 (11.78–14.90)
1890	1	0.70	–15.23	14.37
1920	1	1.19	–15.79	15.13
1930	3	1.10 \pm 0.72 (0.58–1.92)	–16.36 \pm 0.07 (–16.30, –15.51)	15.51 \pm 0.26 (15.21–15.70)
1950	2	1.12 0.38 (0.85 1.38)	–14.70 \pm 2.81 (–16.69, –12.72)	15.15 \pm 0.47 (14.81–15.48)
1970	1	0.84	–18.29	15.03

Table A8. Feather Hg concentrations and stable isotopes in Brünnich's guillemots (adults) from East Greenland (n=21), collected between the 1830s and 19730s.

Decades	n	Feather Hg ($\mu\text{g}\cdot\text{g}^{-1}$)	Feather corrected $\delta^{13}\text{C}$ (‰)	Feather $\delta^{15}\text{N}$ (‰)
1830	1	1.11	-15.78	13.13
1890	1	0.61	-15.66	15.47
1900	2	1.23 ± 0.22 (1.08–1.39)	-15.87 ± 0.03 (-15.89, -15.85)	15.49 ± 0.38 (15.52–15.76)
1910	1	0.93	-16.09	15.44
1920	11	1.01 ± 0.36 (0.59–1.59)	-16.52 ± 0.34 (-16.95, -15.91)	13.49 ± 0.49 (12.63–14.57)
1930	5	1.20 ± 0.52 (0.79–2.10)	-17.27 ± 0.69 (-18.06, -16.27)	13.89 ± 0.83 (12.56–14.80)

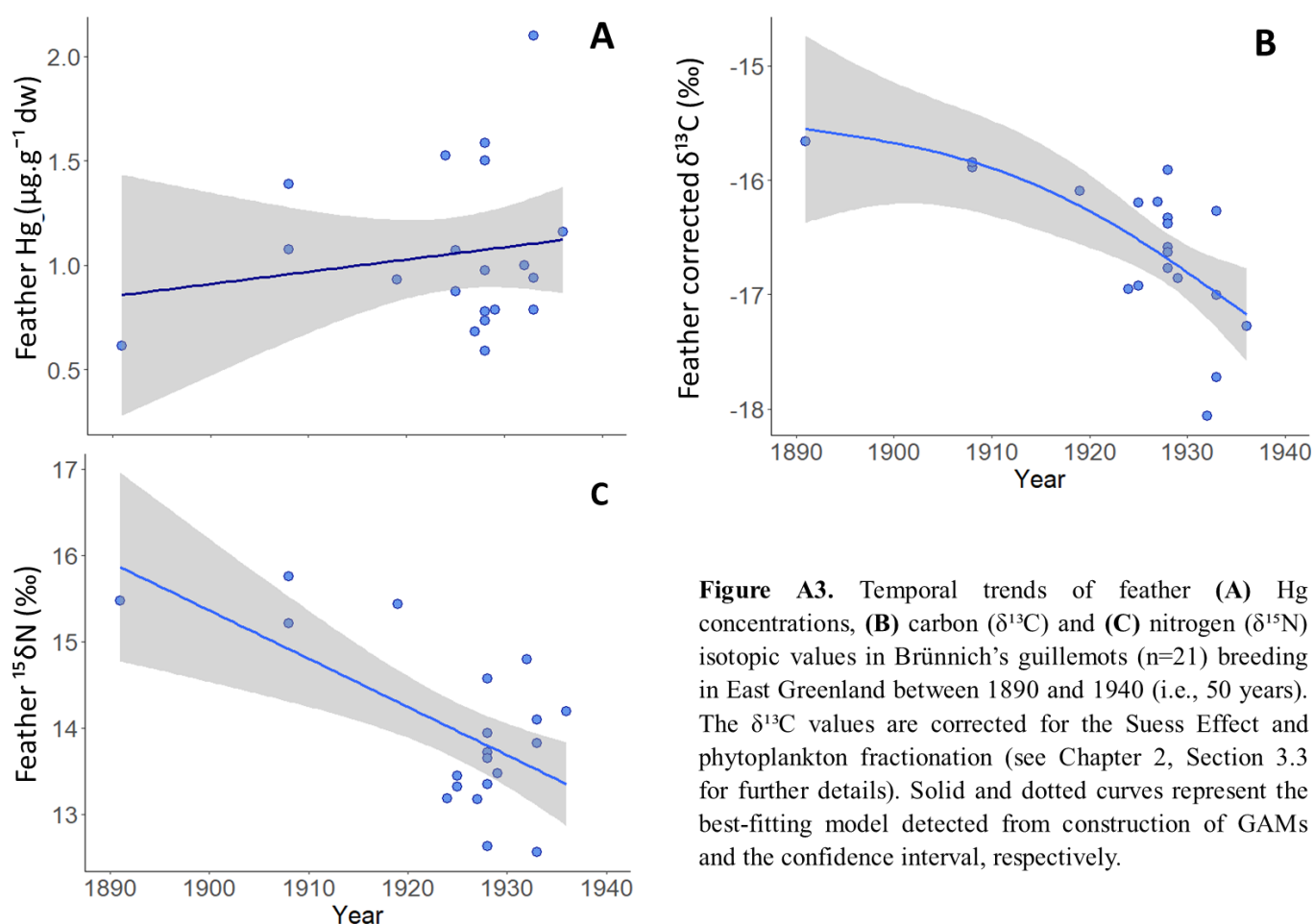


Figure A3. Temporal trends of feather (A) Hg concentrations, (B) carbon ($\delta^{13}\text{C}$) and (C) nitrogen ($\delta^{15}\text{N}$) isotopic values in Brünnich's guillemots (n=21) breeding in East Greenland between 1890 and 1940 (i.e., 50 years). The $\delta^{13}\text{C}$ values are corrected for the Suess Effect and phytoplankton fractionation (see Chapter 2, Section 3.3 for further details). Solid and dotted curves represent the best-fitting model detected from construction of GAMs and the confidence interval, respectively.

Table A9. Feather Hg concentrations and stable isotope values in Brünnich's guillemots (adults) from West Greenland (n=448), collected between the 1840s and the 2020s.

Decades	n	Feather Hg ($\mu\text{g}\cdot\text{g}^{-1}$)	Feather corrected $\delta^{13}\text{C}$ (‰)	Feather $\delta^{15}\text{N}$ (‰)
1840	1	3.62	-16.54	13.83
1860	1	0.90	-14.38	15.84
1880	5	1.10 \pm 0.52 (0.69–1.92)	-16.65 \pm 1.07 (-18.03, -15.16)	14.44 \pm 1.01 (13.57–16.17)
1890	15	1.00 \pm 0.81 (0.46–3.77)	-17.02 \pm 0.95 (-18.77, -15.38)	13.94 \pm 0.98 (12.62–15.75)
1900	23	0.61 \pm 0.32 (0.27–1.57)	-17.03 \pm 0.68 (-18.18, -15.26)	13.93 \pm 0.91 (11.60–15.44)
1910	39	0.60 \pm 0.26 (0.22–1.15)	-16.59 \pm 1.05 (-18.77, -14.85)	14.71 \pm 0.78 (12.45–15.69)
1920	4	1.43 \pm 0.37 (0.98–1.76)	-16.44 \pm 0.53 (-17.06, -15.76)	14.04 \pm 0.68 (13.50–14.92)
1930	15	1.14 \pm 0.26 (0.82–1.81)	-16.71 \pm 0.36 (-17.27, -15.86)	15.53 \pm 0.73 (13.86–16.96)
1940	6	0.81 \pm 0.25 (0.56–1.19)	-16.83 \pm 0.67 (-17.71, -15.87)	15.24 \pm 0.88 (13.70–16.35)
1950	4	1.15 \pm 0.92 (0.47–2.51)	-17.74 \pm 1.03 (-18.99, -16.47)	14.42 \pm 0.96 (13.43–15.66)
1960	1	2.94	-17.09	15.64
1970	4	2.18 \pm 1.66 (0.66–4.51)	-17.57 \pm 0.46 (-18.19, -17.08)	15.66 \pm 0.81 (14.58–16.46)
1980	10	2.89 \pm 0.48 (2.14–3.58)	-17.75 \pm 0.57 (-18.59, -16.83)	15.19 \pm 0.53 (14.25–16.15)
1990	41	1.33 \pm 0.64 (0.35–3.03)	-19.14 \pm 1.11 (-21.19, -16.44)	14.07 \pm 0.82 (12.54–16.91)
2000	96	2.34 \pm 1.23 (0.26–6.85)	-18.88 \pm 0.94 (-21.21, -16.68)	14.86 \pm 1.12 (11.72–17.81)
2010	110	1.91 \pm 0.79 (0.50–3.92)	-19.00 \pm 0.57 (-20.99, -17.78)	14.96 \pm 0.55 (13.51–16.27)
2020	73	1.99 \pm 1.18 (0.74–8.52)	-18.74 \pm 0.51 (-19.95, -17.76)	14.59 \pm 0.84 (12.60–16.38)

Chapter 4: Temporal monitoring – Epoch comparisons

Table A10. Feather Hg concentrations, bulk $\delta^{13}\text{C}$ and $\delta^{15}\text{N}$ values measured in Adélie penguins and sooty terns in Chapter 4 (Epoch comparisons).

Species, Colonies	Epochs	n	Feather Hg ($\mu\text{g.g}^{-1}$ dw)	Feather corrected $\delta^{13}\text{C}$ (‰)	Feather $\delta^{15}\text{N}$ (‰)
Adélie penguins					
Signy Island	1950s	8	0.45 ± 0.27 (0.14–0.88)	-21.62 ± 1.79 (-23.54, -18.87)	9.80 ± 0.45 (9.34–10.52)
	2020s	30	0.33 ± 0.10 (0.21–0.62)	-25.60 ± 0.38 (-26.14, -24.35)	8.91 ± 0.34 (8.30–10.13)
Dumont d’Urville	1950s	4	0.32 ± 0.26 (0.08–0.67)	-23.52 ± 0.37 (-23.80, -23.01)	10.26 ± 1.77 (8.51–12.11)
	2007	10	0.66 ± 0.20 (0.41–1.06)	-23.27 ± 0.35 (-24.04, -22.88)	10.67 ± 0.56 (9.67–11.27)
	2012	10	0.40 ± 0.09 (0.25–0.52)	-24.18 ± 0.70 (-25.45, -23.16)	10.80 ± 0.74 (9.76–11.91)
	2017	15	0.41 ± 0.11 (0.25–0.60)	-24.86 ± 0.39 (-25.68, -24.35)	8.93 ± 0.33 (8.38–9.73)
Cape Royds	1910s	10	0.76 ± 0.33 (0.44–1.54)	-23.77 ± 0.38 (-24.51, -23.17)	11.26 ± 0.61 (10.51–12.20)
	2010s	15	0.80 ± 0.19 (0.56–1.08)	-25.40 ± 0.77 (-25.88, -22.84)	10.26 ± 0.78 (9.15–11.85)
Sooty terns					
Fernando de Noronha	1880s/1900s	5	1.52 ± 0.45 (0.96–2.13)	-13.53 ± 0.20 (-13.85, -13.32)	12.00 ± 1.61 (9.28–13.59)
	2010s	18	0.54 ± 0.18 (0.23–0.89)	-16.00 ± 0.31 (-16.55, -15.46)	10.84 ± 0.64 (10.03–12.98)
Lord Howe Island	1880s	3	1.09 ± 0.34 (0.83–1.47)	-13.47 ± 1.91 (-15.67, -12.30)	16.35 ± 1.00 (15.31–17.29)
	1910s	3	1.43 ± 0.63 (1.05–2.15)	-12.77 ± 0.23 (-13.03, -12.59)	18.48 ± 3.89 (13.99–20.81)
	2020s	30	1.11 ± 0.39 (0.62–1.97)	-15.64 ± 0.35 (-16.44, -14.81)	14.77 ± 1.57 (12.46–17.72)

Table A11. Statistical results for epoch comparisons of feather Hg concentrations, bulk $\delta^{13}\text{C}$ and $\delta^{15}\text{N}$ values measured in Adélie penguins and sooty terns. Adélie penguins were sampled in three Antarctic colonies, including Signy Island (South Orkney Islands), Dumont d'Urville (Adélie Land) and Cape Royds (Ross Island). Sooty terns were sampled in two tropical colonies, including Fernando de Noronha (South Atlantic Ocean) and Lord Howe Island (South Pacific Ocean). For further information, the reader is referred to Chapter 4, Sections 2 and 3.

Variables	Tests	Sites	Parameters	Difference
Adélie penguins				
Hg ~ Epoch	Kruskal-Wallis	Signy Island	$\chi^2(1)=1.6, p=0.2$	No
	Kruskal-Wallis	Dumont d'Urville	$\chi^2(3)=14.8, p=0.002$	Yes: 2007 different from 2012 and 2017
	ANOVA	Cape Royds	$F_{1,23}=0.08, p=0.8$	No
$\delta^{13}\text{C}$ ~ Epoch	Kruskal-Wallis	Signy Island	$\chi^2(1)=18.5, p<0.0001$	Yes: 1950s different from 2020s
	ANOVA	Dumont d'Urville	$F_{3,35}=24.3, p<0.0001$	Yes: 2017 different from all other years (1950s, 2007, 2012) + 2007 different from 2012
$\delta^{15}\text{N}$ ~ Epoch	ANOVA	Cape Royds	$F_{1,23}=37.9, p<0.0001$	Yes: 1910s different from 2010s
	ANOVA	Signy Island	$F_{1,36}=37.4, p<0.0001$	Yes: 1950s different from 2020s
	Kruskal-Wallis	Dumont d'Urville	$\chi^2(3)=22.3, p<0.0001$	Yes: 2017 different from 2007 and 2012
	ANOVA	Cape Royds	$F_{1,23}=11.7, p=0.002$	Yes: 1910s different from 2010s
Sooty terns				
Hg ~ Epoch	Kruskal-Wallis	Fernando de Noronha	$\chi^2(1)=11.3, p<0.001$	Yes: 1880s/1900s different from 2010s
	Kruskal-Wallis	Lord Howe Island	$\chi^2(2)=1.97, p=0.4$	No
$\delta^{13}\text{C}$ ~ Epoch	ANOVA	Fernando de Noronha	$F_{1,21}=280.6, p<0.0001$	Yes: 1880s/1900s different from 2010s
	Kruskal-Wallis	Lord Howe Island	$\chi^2(2)=9.9, p=0.007$	Yes: 1910s different from 2020s
$\delta^{15}\text{N}$ ~ Epoch	ANOVA	Fernando de Noronha	$F_{1,21}=6.3, p=0.021$	Yes: 1880s/1900s different from 2010s
	Kruskal-Wallis	Lord Howe Island	$\chi^2(2)=5.1, p=0.08$	No (close to $\alpha=0.05$)

Chapter 5: Conclusions and perspectives – Compound-Specific Stable Isotope Analyses of Amino Acids (CSIA-AA)

Table A12. Review of ecological studies where Compound-Specific Stable Isotope Analysis of Amino-Acids (CSIA-AA) were performed in seabirds, and associated with Hg data (indicated by «Yes»).

Region	Year	Species	Tissue	References	Hg
Atlantic Ocean					
Dry Tortugas	2013-2015	Brown noddy Sooty tern	Feathers (flight)	Gagné et al. (2019, 2018)	Yes
Madeiran Archipelago	2016	Cory's shearwater	Feathers (flight) (adult)	Gatt et al. (2020)	Yes
Madeiran Archipelago, Cape Verde	2018	Bulwer's petrel	Feathers (body) (adult + chick)	Furtado et al. (2021)	Yes
Pacific Ocean					
Hawaii, Japan	2018	Bulwer's petrel	Feathers (body) (adult + chick)	Furtado et al. (2021)	Yes
Hawaii, Rose Atoll	2013-2015	Brown noddy Sooty tern	Feathers (flight)	Gagné et al. (2019, 2018)	Yes
Hawaii Archipelago	1891-2016	Laysan albatross Bulwer's petrel Wedge-tailed shearwater White-tailed tropicbird Brown booby Brown noddy White tern Sooty tern	Feathers (body for historic) (flight for contemporary)	Gagné et al. (2019, 2018b)	Yes
Chatham Islands, Zealand	New Zealand 2015	Magenta petrel Broad-billed prion Chatham petrel	Blood + Feathers (body) + muscle	Thébault et al. (2021)	Yes

		Common diving petrel	Sooty shearwater	White-faced storm petrel	+ muscle		
Southern Ocean							
Falkland Islands	2006-2011	Thin-billed prion	Blood/Feathers	Quillfeldt and Masello (2020)	No		
		Rockhopper penguin	Blood/Feathers				
		Gentoo penguin	Blood/Feathers				
		Magellanic penguin	Blood/Feathers				
South Shetland Islands, King George Island	2013/2014	Black-bellied storm-petrels	Feathers (rectrix)	Quillfeldt et al. (2017)	No		
		Wilson's petrel	Feathers (rectrix)				
South Shetland Islands, King George Island, Livingston Island	2011-2013	Adélie penguin	Feathers (tail)	Polito et al. (2017)	No		
		Chinstrap penguin					
Amsterdam Island	2001/2002	Northern rockhopper penguin	Blood (chick)	Lorrain et al. (2009)	No		
Crozet Islands		Southern rockhopper penguin					
Adélie Land		King penguin					
		Adélie Land					
Omaha's Henry Doorly Zoo and Aquarium		Gentoo penguin (captive)	Feathers (breast)	McMahon et al. (2015)	No		
South Shetland Islands, King George Island		(wild)					

Papers

Paper 1

Sooty terns as bioindicators of mercury contamination in marine ecosystems: a pantropical approach

In preparation

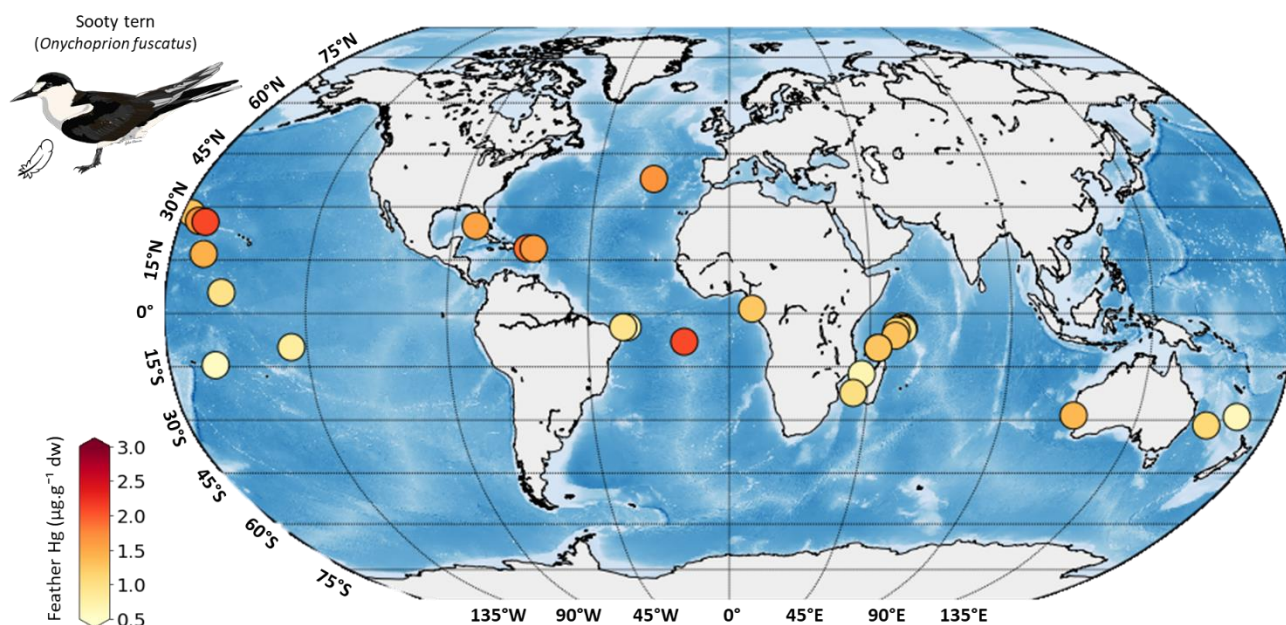
Fanny Cusset, Pierre Richard, Jérôme Fort, Charlie Bost, Leandro Bugoni, Nicholas Carlisle, Michael Charriot, Annabelle Cupidon, Nina Darocha, Nic Dunlop, Chris Feare, Antonio Garcia Quintas, Thomas Gestemme, Gaël Guillou, Estrela Matilde, Matthew Morgan, Terry O'Dwyer, Stuart Pimm, Veronica Rodrigues Costa Neves, Gerard Rocamora, Laura Shearer, Louise Soanes, Eduardo Ventosa, Tehani Withers, Yves Cherel, Paco Bustamante.



KEYWORDS

Hg – Spatial biomonitoring – Seabirds – Feathers – Stable isotopes – CSIA

GRAPHICAL ABSTRACT



INTRODUCTION

Mercury (Hg) is a natural and anthropogenic contaminant of major public health concern (WHO, 2020), which adversely affects human health and the environment. To address this threat, the United Nations Environment Program (UNEP) has produced successive reports of the Global Mercury Assessment, providing the updated state of scientific knowledge of Hg research at the global scale. In its latest report in 2018, oceans were identified as «locations of greatest concern». Oceans are primary reservoirs in Hg cycling, allowing the storage of Hg over long periods and its subsequent remissions over time (Amos et al., 2013; Driscoll et al., 2013). After its release and large-scale transport in the atmosphere, Hg deposits in all oceans (Streets et al., 2019). There, Hg is efficiently transformed to its most toxic and bioavailable form, methyl-Hg (MeHg), by naturally-occurring microorganisms (Driscoll et al., 2007). Once assimilated by phytoplankton, MeHg is transferred along marine food webs (Obrist et al., 2018). MeHg biomagnifies in marine food webs (*i.e.*, concentrations increase along the food web), and also bioaccumulates in marine biota (*i.e.*, concentrations increase in tissues over time), thus causing numerous negative health effects (Basu et al., 2023; Scheuhammer et al., 2012). Due to the methylation

that occurs specifically in their waters, and considering their huge surface and volume, oceans promote the bioavailability and the toxicity of MeHg, posing serious threats to both wildlife and humans that heavily rely on marine resources worldwide.

Overall, oceans receive 80% of total atmospheric Hg deposition, 49% of which is restricted to the tropics (Horowitz et al., 2017). Despite this, Hg monitoring is very scarce in tropical waters. Yet, the intertropical region contains most countries where artisanal and small-scale gold mining occurs (GMA, 2018). This growing activity represents the largest user and emitter of Hg globally, producing more than 35% of total atmospheric Hg emissions of anthropogenic origin (Keane et al., 2023). In addition, tropical waters have experienced increased oxygen-depletion (Breitburg et al., 2018), conditions that promote the formation of MeHg (Cossa, 2013; Mason et al., 2012; Sunderland et al., 2009). They may therefore represent hotspot regions of Hg contamination. Yet, tropical waters, especially in the Southern Hemisphere (SH), were recently identified as regions where Hg data and scientific understanding are most lacking (Selin et al., 2018; Chen and Evers, 2023 and references therein). There is therefore an urgent need to assess Hg contamination and its spatial variations in tropical waters and biota, and better understand the threat posed by environmental Hg loads in these key but undocumented oceanic regions.

When monitoring Hg at the global scale, the use of bioindicator species is critical (Evers et al., 2016). Bioindicators reflect the bioavailability of MeHg, which is generated and made available to marine food webs (Mason et al., 2005). The Article 19 of the Minamata Convention on Mercury has defined ecological health bioindicators, which includes fish, sea turtles, marine mammals and seabirds. Seabirds are meso- and top predators, which occupy high trophic position within marine ecosystems. Thus, they integrate and reflect Hg contamination of marine food webs (Burger and Gochfeld, 2004; Furness, 1993; Furness and Camphuysen, 1997). They represent a very large biomass in all oceans (Brooke, 2004; Paleczny et al., 2016) and hence, they permit Hg monitoring across large geographical (both latitudinal and longitudinal) scales. Considering their colonial nesting and high-site fidelity, numerous individuals can be sampled simultaneously and repeatedly over time (Albert et al., 2019). Feathers represent a reliable, non-destructive tissue to investigate Hg contamination in seabirds (Thompson et al., 1998). Dietary MeHg accumulates in the body between two moulting episodes (Furness et al., 1986), 70–90% of which is transferred into growing feathers during each moult (K. Honda et al., 1986). Because of the strong affinity of MeHg for keratin, the dominant component of feathers, and its stable bond that withstand any treatment (Appelquist et al., 1984; Crewther et al., 1965), feathers represent a valuable tool for Hg biomonitoring across ocean basins.

In this context, the present study aims to document spatial variation of Hg contamination in tropical oceanic ecosystems at the global scale. In the Global Mercury Assessment (UN Environment, 2018), terns were defined as ecological health bioindicator for tropical marine ecosystems. As the most abundant pantropical seabird, we selected the sooty tern (*Onychoprion fuscatus*) as a bioindicator

species for monitoring Hg contamination in the tropics. Specifically, we quantified Hg concentrations in feathers of sooty terns across 28 colonies, distributed in three ocean basins (*i.e.*, the Pacific, the Atlantic and the Indian Oceans). Then, we compared long-term (*i.e.*, year-round) and short-term (*i.e.*, during chick-rearing) Hg contamination by analysing adult and chick feathers, respectively. Considering their shorter exposure period, we expected lower Hg concentrations in chicks compared to adults (Carravieri et al., 2014c). Since the diet is the major exposure route of Hg (Burger and Gochfeld, 2001; Gochfeld, 2000), we investigated the influence of tern feeding ecology, by analysing carbon- ($\delta^{13}\text{C}$) and nitrogen ($\delta^{15}\text{N}$) stable isotopes (bulk), which are well-known proxies of the feeding habitat (*i.e.*, carbon source) and diet (*i.e.*, trophic position), respectively (Kelly, 2000). However, classical isotopic approaches have limitations when considering such a global scale. Baseline isotopic values can differ substantially within and between ocean basins, due to differences in (i) environmental conditions that shape them (both spatially and temporally) and (ii) the composition and structure of phytoplankton communities at the base of marine food webs (Jardine et al., 2006; McMahon et al., 2013). Sources of uncertainty are thus multiple when interpreting isotopic values from bulk tissues, especially at such large spatial scales (Ohkouchi et al., 2017). Compound-Specific Stable Isotope Analyses of Amino-Acids (CSIA-AA) allow to reduce uncertainty and cope with these limitations, as they enable to distinguish between baseline and trophic effects (McMahon and Newsome, 2019). This method is based on the principle that AAs can be distinguished based on their differential fractionation with trophic position (Popp et al., 2007). Source AAs do not fractionate with trophic position and thus directly represents the isotopic signature of primary producers at the base of the food web (*e.g.*, phenylalanine). In contrast, trophic AAs change substantially between the food and the consumer (*e.g.*, glutamic acid). Together, they enable to calculate the trophic position of consumers, accounting for baseline and trophic effects (Chikaraishi et al., 2014). Here, CSIA-AA were performed on a subset of adult individuals, to allow large-scale comparisons of trophic proxies in sooty terns and investigate their interactions with Hg contamination.

MATERIAL AND METHODS

Feather sampling and preparation

Overall, feathers were collected from 971 sooty terns in 28 colonies, across the Pacific (n=9), Atlantic (n=9) and Indian (n=10) Oceans (Figure 1). The complete list of sampling sites and their geographical coordinates is provided in Table S1. Body feathers were collected on both adults (n=564) and large fledging chicks (n=407), preferentially from the breast. Sampled individuals included predominantly free-living birds, but carcasses were also opportunistically sampled in Palmyra Atoll (n=1), Motu Oa

(n=2), Puerto Rico (n=16), Tinhosas Grande (n=1), Desnoeuf Island (n=5), African Banks (n=3), Etoile Cay (n=1) and Rat Island (n=2).

To eliminate any external contamination, feathers were cleaned with a mixture of chloroform:methanol (2:1), sonicated for 3 min, rinsed twice in methanol and finally oven-dried for 48 h at 45°C. For each tern, four feathers were pooled to derive individual mean value (Carravieri et al., 2014a; Jaeger et al., 2009) and cut with stainless scissors to obtain a homogenous powder to be analysed for both Hg and stable isotopes.

Mercury analyses

In seabird feathers, MeHg accounts for >90% of the total Hg (THg; Cusset et al., 2023; Renedo et al., 2017). Thus, we used THg as a relevant proxy of MeHg burden in sooty tern feathers. Therefore, THg analyses were performed on feather homogenates (0.3–1.8 mg) in duplicate, using an Advanced Mercury Analyzer (Altec AMA 254). When the relative standard deviation (RSD) was <10%, Hg concentrations were averaged for each sample. When the RSD was >10%, an additional sample of the homogenate was analysed and the duplicates guaranteeing the lowest RSD were kept for average calculations. Certified reference materials were run to verify accuracy (DOLT-5, Fish liver and TORT-3, Lobster hepatopancreas; National Research Council, Canada). Certified and measured values are provided in Table S2. Recovery values were $96.6 \pm 1.4\%$ and $101.3 \pm 2.4\%$, respectively. Blanks were run at the beginning of each laboratory session (*i.e.*, each day). Detection limit was 0.1 ng. Mercury concentrations are expressed in $\mu\text{g}\cdot\text{g}^{-1}$ dry weight (dw).s

Bulk stable isotope analyses

Feather homogenates (0.2–0.8 mg) were loaded into tin cups (8 mm x 5 mm; Elemental Microanalysis Ltd, Okehampton, UK) using a microbalance (XPRUD5, Mettler Toledo, Greifensee, Switzerland), to perform carbon and nitrogen stable isotope analyses. Values of $\delta^{13}\text{C}$ and $\delta^{15}\text{N}$ were determined with a continuous flow isotope ratio mass spectrometer (Delta V Plus with a ConFlo IV Interface, Thermo Scientific, Bremen, Germany) coupled to an elemental analyzer (Flash 2000 or Flash IRMS EA Isolink CN, Thermo Scientific, Milan, Italy). Results are expressed in the usual δ unit notation relative to Vienna PeeDee Belemnite (V-PDB) for $\delta^{13}\text{C}$ and atmospheric N_2 for $\delta^{15}\text{N}$, following the formula:

$$\delta^{13}\text{C} \text{ or } \delta^{15}\text{N} = [(R_{\text{sample}}/R_{\text{standard}}) - 1] \times 10^3 \quad (\text{Equation 1})$$

where R is $^{13}\text{C}/^{12}\text{C}$ or $^{15}\text{N}/^{14}\text{N}$, respectively. Replicate measurements of reference materials (USGS61 and USGS63, US Geological Survey) indicated measurement uncertainties $<0.10\text{‰}$ for both $\delta^{13}\text{C}$ and $\delta^{15}\text{N}$ values.

Compound-Specific Stable Isotope Analyses of Amino Acids (CSIA-AA)

Since CSIA-AA is time- and money-consuming, $\delta^{15}\text{N}$ analyses of phenylalanine (Phe) and glutamic acid (Glu) were performed on a subset of adult individuals ($n=91$), selected across 19 sites in the three ocean basins (see Table S3), following previously described protocols (Corr et al., 2007; Styring et al., 2012).

Feather homogenates (1–1.5 mg) were hydrolysed under nitrogen (200 μL 6 M HCl, 110°C, 22 h). They were then dried under a stream of N_2 at 70°C and finally re-dissolved in 2 ml HCl 0.5 M. Because glutamine (Gln) is converted to Glu during hydrolysis, data for Glu thus represent the total Glu + Gln, noted Glx thereafter. The resultant AA were purified and derivatized to N-acetyl-isopropyl esters (Styring et al., 2012). Norleucine (Alfa Aesar) and alpha-aminoadipic acid (AAA, Sigma-Aldrich) were added as internal standards after AA purification. Caffeine (USGS-61) was added as an internal standard to the derivatized AA before dilution in ethyl acetate for nitrogen analyses by continuous-flow gas chromatography combustion-isotope ratio mass spectrometry (GC-C-IRMS). $\delta^{15}\text{N}$ values were measured using a Thermo Trace Ultra GC coupled to a Delta Plus isotope-ratio mass spectrometer through a GC Isolink combustion interface (Thermo Scientific, Bremen, Germany). The combustion furnace was maintained at 1000°C, and CO_2 generated during combustion was removed from the carrier gas using a cryogenic trap and released after the end of each analysis. AA were separated on a TG-624 SilMS column (60 m x 0.25 mm i.d., 1.4 μm film thickness, Thermo Scientific). Injections were performed in splitless mode (1 min) at 255°C, the helium carrier gas flow was constant (1.2 mL/min). GC temperature program was set as follows: 70°C (hold 1 min), 165°C at 16°C/min, 274°C at 4.5°C/min (hold 22 min), 285°C at 10°C/min (hold 4 min). Samples were analyzed in duplicate or triplicate. To evaluate drift and accuracy, a standard mixture, thoroughly calibrated by EA-IRMS and derivatized along with the samples, was analysed at the beginning, every three or four samples and at the end of each batch of analyses. Similar to bulk analyses, data are expressed in delta notation relative to atmospheric N_2 for nitrogen. Raw data were corrected for instrumental variations and deviations in the isotopic compositions of the products occurring during sample derivatization. AAs values in the standard mixture were used for correction of any instrumental drift during the run (Sabadel et al., 2016) and compound-specific calibration (Yarnes and Herszage, 2017). Precision for AAs values ranged from 0 to 1.5 ‰ (mean 0.3 ‰) for $\delta^{15}\text{N}$ measurements. Finally, AA derivatives were stored at -20°C until analysis (up to one month).

Combining feather Hg and stable isotopes

Adult sooty terns start to moult (i.e., basic, post-nuptial moult) while still breeding and replace all of their feathers (flight and body feathers) during the following weeks/months (Ashmole, 1963). Body feathers thus reflect tern Hg exposure since the previous moult, including the breeding and non-breeding periods (i.e., for the past 9–12 months depending on the breeding cycle: sub-annual or annual; Reynolds et al., 2014). This temporal window also includes a large spatial scale, as adult sooty terns forage primarily in the vicinity of their colony during the breeding period (50–100 km; Neumann et al., 2018; Soanes et al., 2015, 2016) and travel thousands of kilometres away from their nesting site during the non-breeding period. In Ascension Island (South Atlantic Ocean), the non-breeding range of sooty terns is 2,900 km on average (Reynolds et al., 2021), compared to 4,500 km in Bird Island (the Seychelles; Jaeger et al., 2017). On the other hand, feathers retain dietary values at the time of their synthesis, as stable isotopes ($\delta^{13}\text{C}$ and $\delta^{15}\text{N}$) are incorporated into feathers as they grow (Hobson and Clark, 1992). While Hg and stable isotopes are both incorporated during feather growth, their integration is temporally decoupled (Bond, 2010; Thompson et al., 1998). Nonetheless, stable isotopes provide invaluable information about tern ecology and are still relevant to understand the ecological drivers of Hg contamination in adult sooty terns when no other ecological information is available.

In contrast, the temporal mismatch between feather Hg concentrations and stable isotopes is minimal in chicks, as the integration time is almost identical between Hg and stable isotopes in body feathers (Blévin et al., 2013). Chick feathers thus reflect local Hg exposure (resulting from parents' foraging trips in the vicinity of the colony) during the chick-rearing period (Carravieri et al., 2014a; Stewart et al., 1997).

Data analyses

Determining the trophic position of sooty terns

The CSIA-AA method, and more particularly the analysis of $\delta^{15}\text{N}$ values in Glx and Phe, was used to estimate the trophic position of adult sooty terns during the non-breeding period (see Ohkouchi et al. (2017) for a review). Together, source and trophic AAs enable to calculate bird trophic position from the difference in their $\delta^{15}\text{N}$ values (Lorrain et al., 2009; McClelland and Montoya, 2002), with the following formula:

$$\text{TP (feathers)} = 2 + \frac{\text{Glx} - \text{Phe} - 3.5 - 3.4}{6.2} \quad (\text{Equation 2})$$

where 6.2 is the overall mean trophic discrimination factor (TDF) from McMahon and McCarthy (2016), 3.5 is the TDF for seabird feathers (McMahon et al., 2015) and 3.4 the difference in $\delta^{15}\text{N}$ values between Glx and Phe in primary producers (Quillfeldt and Masello, 2020).

Statistical analyses

Statistical analyses and graphical representations were carried out in R 4.2.2 (R Core Team, 2022), by distinguishing two separate datasets: (i) the entire dataset (*i.e.*, with all variables, all sites, both age classes: 564 adults and 407 large chicks; hereafter the «global subset»), and (ii) a partial dataset that only included individuals selected for CSIA-AA (adults, $n=91$) and all variables (*i.e.*, Hg, bulk and compound specific stable isotopes (hereafter the «CSIA subset»). For all statistical analyses, colonies with sample size <4 were removed (*i.e.*, African Bank, Azores, Etoiles Cay, Laysan Island).

Unifactorial analyses were performed to test for differences in feather Hg concentrations at different spatial scales (between colonies, hemispheres and oceans) in adults and chicks, and between age classes. Because the entire basin is located in the SH, hemispheric differences were not tested in the Indian Ocean. Residual normality and homoscedasticity were examined with Shapiro-Wilk and Breusch-Pagan tests («lmtest» package; Zeileis and Hothorn, 2002), respectively. When test assumptions were met, a one-way ANOVA and posthoc Tukey HSD tests were performed to locate the detected differences. Otherwise, a non-parametric (Kruskal-Wallis) test was used, followed by a multiple comparisons (Pairwise-Wilcoxon) test. Considering the high probability of variation in baseline isotopic values across the three ocean basins (both latitudinal and longitudinal), differences in bulk isotopic values (both $\delta^{13}\text{C}$ and $\delta^{15}\text{N}$ values) were not tested, either at different spatial scales or between age classes. Instead, differences in trophic position (TP; cf. Equation 2), and $\delta^{15}\text{N}$ values of glutamic acid (Glx) and phenylalanine (Phe) were tested on the CSIA subset. Since sooty terns were sampled during two consecutive years in Ascension Island, interannual differences in all variables were also tested in both adults and chicks.

Multifactorial analyses were performed to investigate the influence of trophic ecology and colony location on Hg contamination. Prior to model definition, relationships between continuous variables (*i.e.*, Hg, $\delta^{13}\text{C}$, TP) were tested using a correlation matrix to validate the simultaneous inclusion of non-collinear explanatory variables. Models were Generalized Linear Models (GLMs) with a Gaussian distribution and identity link-function, built using the «nlme» package (Pinheiro and Bates, 2022). We used the CSIA dataset, which included adults only ($n=88$; colonies with $n>4$). The initial model was: $\text{Hg} \sim \delta^{13}\text{C} + \text{TP} + \text{Colony}$. Despite the variation in baseline $\delta^{13}\text{C}$ values that may substantially influence bulk $\delta^{13}\text{C}$ values of sooty tern feathers, bulk $\delta^{13}\text{C}$ values were kept for model selection, as they showed relatively little variation here (-15.86 ± 0.54 ‰, $n=563$). Model selection was based on Akaike's

Information Criterion adjusted for small sample sizes (AIC_c). All potential combinations of variables for each dataset are presented in Table 2. Models were ranked using the «dredge» function («MuMIn» package; Bartoń, 2022). Following Burnham and Anderson (2002), the model with the lowest AIC_c value and a difference of AIC_c (ΔAIC_c) > 2 when compared with the next best model was considered to be the best. Following Johnson and Omland (2004), model performance was assessed using Akaike weights (w_i). Model assumptions (residual normality, homogeneity, independence) were checked with diagnostic functions («plot» and «qqnorm»). The degree of model fit was reported by using the McFadden's R-Squared metric. Differences between colonies were then identified with Estimated Marginal Means (EMMs; «emmeans» package; Length, 2023) following Bond and Diamond (2009a). Finally, partial residuals were extracted from each best model to obtain predictor effect plots («effects» package; Fox and Weisberg, 2018, 2019). This allowed us to control variation in Hg concentrations due to both $\delta^{13}C$ values and TP to quantify and visualise Hg spatial variation.

RESULTS

Feather Hg concentrations (Figure 2) and bulk stable isotope values (Figure 3) for the two age classes and all colonies are detailed in Tables 1 and S3, respectively. The AA- $\delta^{15}N$ values (i.e., Glx and Phe), as well as TP of sooty terns (CSIA subset), are provided in Table S4.

Age and spatial differences in Hg contamination

When comparing adults and chicks, chicks had lower Hg concentrations than adults (Kruskal-Wallis, $\chi^2(1) = 343.3$, $p < 0.0001$, $n = 965$).

In adults (global subset), feather Hg concentrations differed between colonies (Kruskal-Wallis, $\chi^2(23) = 302.1$, $p < 0.0001$, $n = 556$; Figure 2). When comparing hemispheres within each ocean basin, feather Hg concentrations were higher in the Northern compared to the Southern Hemispheres, both in the Pacific (Kruskal-Wallis, $\chi^2(1) = 69.2$, $p < 0.0001$, $n = 222$) and the Atlantic (Kruskal-Wallis, $\chi^2(1) = 12.3$, $p < 0.001$, $n = 171$) Oceans (Figure S1). In addition, differences between ocean basins were also found (Kruskal-Wallis, $\chi^2(2) = 47.3$, $p < 0.0001$, $n = 556$), with the highest Hg concentrations in the Atlantic Ocean ($1.36 \pm 0.66 \mu\text{g.g}^{-1}$, $n = 171$), followed by the Indian ($1.22 \pm 0.29 \mu\text{g.g}^{-1}$, $n = 195$) and the Pacific ($1.02 \pm 0.48 \mu\text{g.g}^{-1}$, $n = 197$) Oceans (Figure S2). On the other hand, using the CSIA subset, TP of adult sooty terns was similar between the 18 colonies (ANOVA, $F_{17,70} = 1.6$, $p = 0.09$; Figure S3.F), but differed when comparing ocean basins (ANOVA, $F_{2,85} = 6.7$, $p = 0.002$; Figure S4), with significantly lower TP in the Atlantic Ocean ($3.54 \pm 0.21 \mu\text{g.g}^{-1}$, $n = 35$) compared to the Indian ($3.76 \pm 0.25 \mu\text{g.g}^{-1}$, $n = 20$) and Pacific ($3.74 \pm 0.30 \mu\text{g.g}^{-1}$, $n = 36$) Oceans (Figure S3.B).

In chicks (global subset), feather Hg concentrations also differed between colonies (Kruskal-Wallis, $\chi^2(16)=338.7$, $p<0.0001$, $n=402$; Figure 2), and ocean basins (Kruskal-Wallis, $\chi^2(2)=16.6$, $p=0.0003$, $n=401$), with the Atlantic Ocean ($0.57 \pm 0.33 \mu\text{g}\cdot\text{g}^{-1}$, $n=93$; lowest concentrations) differing from the Indian Ocean ($0.64 \pm 0.20 \mu\text{g}\cdot\text{g}^{-1}$, $n=159$; highest concentrations), and the Pacific Ocean ($0.61 \pm 0.28 \mu\text{g}\cdot\text{g}^{-1}$, $n=149$; Figure S2). When comparing hemispheres, chick feather Hg concentrations were significantly higher in the North- than in the South- Pacific Ocean (Kruskal-Wallis, $\chi^2(1)=14.9$, $p=0.0001$, $n=124$) and the West- compared to the East-Indian Ocean (Kruskal-Wallis, $\chi^2(1)=38.1$, $p<0.0001$, $n=134$; Figure S1). In contrast, no difference was detected in the Atlantic Ocean (Kruskal-Wallis, $\chi^2(1)=0.01$, $p<0.92$, $n=94$; Figure S1).

Interannual differences in Ascension Island

When comparing 2020 and 2021 in adults (i.e., global subset), statistical differences were found for feather Hg concentrations (ANOVA, $F_{1,33}=20.7$, $p=0.001$; Figure 4.A), bulk $\delta^{13}\text{C}$ (ANOVA, $F_{1,33}=59.7$, $p<0.001$; Figure 4.B) and $\delta^{15}\text{N}$ values (ANOVA, $F_{1,33}=30.7$, $p<0.001$; Figure 4.C). For the CSIA subset, there was no significant difference in TP (ANOVA, $F_{1,8}=0.2$, $p=0.7$; Figure 4.D) nor in $\delta^{15}\text{N}$ values of Glx (ANOVA, $F_{1,8}=1.2$, $p=0.3$; Figure 4.E). In contrast, $\delta^{15}\text{N}$ values of Phe differed significantly between 2020 and 2021 (ANOVA, $F_{1,8}=25.4$, $p=0.001$; Figure 4.F).

In chicks (i.e., global subset), statistical differences were detected between both years for feather Hg concentrations (ANOVA, $F_{1,43}=1.87.1$, $p<0.001$; Figure 4.A), bulk $\delta^{13}\text{C}$ (ANOVA, $F_{1,43}=155.9$, $p<0.001$; Figure 4.B) and $\delta^{15}\text{N}$ values (ANOVA, $F_{1,43}=107.2$, $p<0.001$; Figure 4.C).

Influence of trophic ecology on Hg contamination

Results from model selections performed on the CSIA subset are presented in Table 2. The best model included bulk $\delta^{13}\text{C}$ values and the colony as significant predictors, and explained 68% of the observed variation in feather Hg concentrations (Table 3). Feather Hg concentrations decreased with $\delta^{13}\text{C}$ values (Table 3; Figure S5). When accounting for $\delta^{13}\text{C}$, the colony effect plot showed that: (i) most colonies (61%) exhibited feather Hg concentrations close to the species' average (i.e., $1.19 \mu\text{g}\cdot\text{g}^{-1}$; all colonies combined), (ii) most colonies (75%) in the Atlantic Ocean had Hg concentrations above the average, in contrast to Fernando de Noronha that had three times lower Hg concentrations, (iii) all colonies in the Indian Ocean were below the average, with Juan de Nova and Europa that had two times lower Hg concentrations than the other colonies (Figure 5). These results are reinforced by the EMMs (Figure S6).

DISCUSSION

Tropical waters, especially in the SH, were recently identified as regions where Hg data and scientific understanding are most lacking (Selin et al., 2018; Chen and Evers, 2023 and references therein). Yet, tropical waters may represent hotspot regions of Hg contamination, as they receive a large fraction of global Hg emissions (e.g., atmospheric deposition, gold-mining and deforestation of rainforests; both releases to air and waters; Fisher et al., 2023; Schneider et al., 2023; Selin et al., 2018). This study provides a unique pantropical assessment of biotic Hg in 28 colonies distributed in three ocean basins, and thereby new information on the bioavailability of MeHg in tropical marine food webs, by using sooty terns as bioindicators.

Spatial patterns of Hg contamination in tropical marine food webs

Overall, feather Hg concentrations measured here in adults ($1.19 \mu\text{g}\cdot\text{g}^{-1}$; all sites combined) were similar to those reported in the literature on sooty terns (Table 1) and on other tropical sternids at similar locations, such as the brown noddy (*Anous stolidus*; $1.11 \mu\text{g}\cdot\text{g}^{-1}$; (Burger et al., 1992, 2001; Burger and Gochfeld, 1995, 2000; Catry et al., 2008; Kojadinovic et al., 2007), bridled tern (*Onychoprion anaethetus*; $1.36 \mu\text{g}\cdot\text{g}^{-1}$; Burger and Gochfeld, 1991; Catry et al., 2008) and roseate tern (*Sterna dougalii*; $1.57 \mu\text{g}\cdot\text{g}^{-1}$; Burger and Gochfeld, 1991; Monticelli et al., 2008). This low Hg contamination agrees with the feeding ecology of sooty terns that largely rely on small epipelagic fish and invertebrates from surface waters (Ashmole, 1963), which have lower Hg concentrations than other mesopelagic and benthic prey species (Chouvelon et al., 2012; Monteiro and Furness, 1997; Ochoa-Acuña et al., 2002).

In adult sooty terns, Hg archived in feathers includes both local exposure during the breeding season and remote exposure during the non-breeding period, resulting in a year-round exposure to Hg over a large spatial oceanic area. Our pantropical sampling of sooty tern feathers allowed a comprehensive comparison of year-round Hg contamination between colonies, both between and within ocean basins (Figure 2). At the global scale, feather Hg concentrations were higher in the Atlantic Ocean, intermediate in the Indian Ocean and lower in the Pacific Ocean (Figure S2). However, the Atlantic and Pacific Oceans showed great variability between colonies in terms of feather Hg concentrations (Figure 2), particularly when the hemispheres were compared. In both the Pacific and Atlantic Oceans, feathers Hg concentrations were higher in the northern hemisphere (NH) than in the SH (Figure S1). This result is consistent with spatial disparities in historical Hg emissions globally. Historically, Hg emissions have been more prevalent in the NH compared to the SH and tropics (Fisher et al., 2023), mainly for two reasons: (1) more historical use of Hg (*i.e.*, 86% of all Hg produced between 1500 and 1900 originated from the NH; Hylander and Meili, 2003), and (2) more historical industrial activities and related consumption of Hg (*i.e.*, 4-fold larger deposition in the NH than in the SH; Li et al., 2020). Recent

findings in the Pacific Ocean revealed that these hemispheric disparities were also visible in different oceanic compartments, where Hg values were systematically higher in the NH, including the atmosphere, seawater, sediments and tunas (Médieu et al., 2022 and references therein), which is consistent with our findings for adult sooty terns. In their study, Médieu et al. (2022) investigated large-scale Hg contamination in the entire Pacific Ocean thanks to skipjack tuna (*Katsuwonus pelamis*). They revealed an east-to-west gradient in Hg concentrations, with a Hg hotspot near Asia that was attributed to elevated atmospheric and/or river Hg inputs to coastal waters in the region. These large spatial differences were explained by spatial differences in both seawater Hg concentrations at the base of marine food webs and inorganic Hg deposition among distinct oceanic regions. Unfortunately, our results did not allow to confirm this specific spatial gradient, considering the lack of feather sampling in the South-East Asia (e.g., Indonesia, Philippines, Papua New Guinea), where sooty terns are thought to be abundantly distributed (Schreiber et al., 2020). Yet, in the SH, 15–30% of the total use of Hg in gold-mining occurs in this specific region (Fisher et al., 2023). Therefore, the addition of new colonies in South-East Asia would substantially improve the present spatial Hg assessment and could help to identify anthropogenic Hg hotspots.

In contrast to adults, sooty tern chicks are bioindicators of local Hg contamination during the breeding period (i.e., chick-rearing period). As might be expected from their young age and therefore shorter exposure to Hg, mean Hg concentrations in chick feathers ($0.62 \pm 0.30 \mu\text{g}\cdot\text{g}^{-1}$, $n=402$) were two times lower than in adults ($1.19 \pm 0.51 \mu\text{g}\cdot\text{g}^{-1}$, $n=563$). Overall, chick Hg concentrations were relatively homogenous across ocean basins. However, two colonies exhibited high Hg concentrations compared to the others: Azores ($3.61 \mu\text{g}\cdot\text{g}^{-1}$) and Cuba ($1.72 \mu\text{g}\cdot\text{g}^{-1}$). The very low sample size in Azores ($n=1$) prevents us to conclude on the contamination level in this region, but clearly, further research is required to investigate a potential, local Hg hotspot or determine if this individual constitutes an outlier. Concerning Cuba, feather Hg concentrations were 2.8 times higher than the chicks' average (i.e., $0.62 \mu\text{g}\cdot\text{g}^{-1}$; all sites combined). Interestingly, feather Hg concentrations seem to be also high in other larids breeding in Cuba, including laughing gulls (*Leucophaeus atricilla*), and bridled, roseate, royal (*Thalasseus maximus*) and sandwich (*T. sandvicensis*) terns (Garcia, pers.comm.). Clearly, future research in the Caribbean Sea, particularly in Cuba, would help to confirm a Hg hotspot in these tropical waters and to further investigate the influence of anthropogenic releases, from chlor-alkali plants for example, which represent major sources of Hg in this region (Feng et al., 2019).

Drivers of Hg contamination and its spatial patterns

In seabirds, trophic ecology is key to understand the mechanisms of Hg contamination and disentangle whether spatial variation in Hg contamination is related to changes in environmental Hg and/or dietary

shifts (Brasso et al., 2015; Carravieri et al., 2016; Gatt et al., 2020). In this study, bulk $\delta^{13}\text{C}$ values (*i.e.*, proxy of feeding habitat) did not show strong variation across the colonies and oceans (Figure 3), whereas bulk $\delta^{15}\text{N}$ values (*i.e.*, proxy of diet) exhibited high intra- and inter-colony variability, especially in the Pacific Ocean where they ranged from 8.1 to 23.5 ‰ (Table S3). Theoretically, this 15.4 ‰ difference in $\delta^{15}\text{N}$ values would mean a variation of four trophic levels (assuming 3.4 ‰ between each trophic level). This large difference clearly indicates strong variation in baseline isotopic values across the Pacific Ocean, and prevents the use of bulk $\delta^{15}\text{N}$ values as a reliable proxy of TP in sooty terns at large spatial scale (Catry et al., 2008). Therefore, on a subset that only represented 16% of the entire dataset ($n=91$), CSIA-AA enabled to calculate the trophic position of adult sooty terns, accounting for both baseline and trophic isotopic variation across sites, as indicated by $\delta^{15}\text{N}$ values of Phe and Glx. Results of model selection revealed that feather Hg concentrations were driven by both bulk $\delta^{13}\text{C}$ values and colony location (*i.e.*, 68% of variation explained), and not by TP (Table 2). The absence of TP in the predictors of feather Hg concentrations is consistent with our single bioindicator approach. It is very likely that sooty terns have a similar trophic ecology across their pantropical distribution range, even though prey species and their corresponding proportions may vary between oceanic regions and oceans. We could expect the opposite result (*i.e.*, presence of TP in the predictors) if several seabird species with distinct trophic ecologies would have been studied. On the other hand, the presence of bulk $\delta^{13}\text{C}$ values in the predictors of feather Hg concentrations suggests that $\delta^{13}\text{C}$ values during the moulting period (*i.e.*, several weeks) influences Hg contamination during the inter-moult period (*i.e.*, several months) of adult sooty terns. Unlike the Southern Ocean where the marked latitudinal gradient in $\delta^{13}\text{C}$ values enables to track foraging areas of seabirds during moult (Carravieri et al., 2014b; Cherel and Hobson, 2007; Quillfeldt et al., 2010), tropical waters usually lack such latitudinal variations, as previously showed in the western Indian Ocean (Catry et al., 2008). Without the ability to track movements of sooty terns within oceanic areas, we cannot associate inshore-offshore patterns of their foraging ecology with potential Hg hotspots and coldspots in tropical oceans. The other predictor of feather Hg concentrations was colony location, suggesting the role of geographical localization on Hg contamination. Because adult feathers reflect both large spatial and temporal scales, one could argue that colony location may not be the most accurate spatial parameter (*i.e.*, Hg exposure during the inter-moult period mostly occurs away from the colony). However, we assumed that sooty terns would be relatively constrained regionally around their breeding colonies worldwide. Even though they can travel very long distances during the non-breeding period (Jaeger et al., 2017; Reynolds et al., 2021), it is very unlikely for sooty terns breeding on Ascension Island to travel to the Caribbean Sea for example. Besides, defining the ocean basins as spatial parameter instead of the colonies in the models would imply a substantial loss of spatial information and lead to lower statistical power. Biologging approaches, combined to Hg and stable isotope analyses, could thus provide further insights into precise, geographical areas of Hg exposure of

sooty terns, and investigate whether they are associated with different types of foraging habitats in tropical oceans.

When accounting for $\delta^{13}\text{C}$ values (that influenced feather Hg concentrations negatively; Figure S5), feather Hg concentrations did not show any specific spatial pattern in the Pacific Ocean, with values slightly varying close to the species average (Figure 5). In the Atlantic Ocean, 71% of the colonies showed higher Hg concentrations than the species average, except for Fernando de Noronha that could represent a Hg coldspot (i.e., low year-round contamination). Yet, Fernando de Noronha is located in the South Atlantic Ocean, approximately 350 km away from Brazil, which represents a major Hg emitter through deforestation of tropical forest and gold-mining (Fisher et al., 2023). A possible explanation for this unexpected result could be the non-breeding distribution of sooty terns, which may forage in remote oceanic regions in the South Atlantic Ocean, instead of the coastal regions of South America. Again, biologging approaches would be very useful to confirm this hypothesis in the future. In the Indian Ocean, all colonies showed low Hg contamination, with Juan de Nova and Europa Islands differing from the other colonies. Interestingly, Fernando de Noronha, Juan de Nova and Europa Islands have one feature in common: unlike all other sites that were sampled between 2020 and 2022, these three sites were sampled in 2010 and 2003, respectively, hence more than 10 years ago. It is difficult to determine here whether Hg contamination is lower in these three specific oceanic regions due spatial or temporal variation (i.e., increase in Hg contamination over time) without any additional years of sampling.

For sooty terns, Hg temporal data are very limited. Still, we could compare our adult results for the 2020s with previous findings in the 1990s and the 2000s, in five colonies (Figure 6; see corresponding references in Table 1). In three colonies (i.e., Midway and Johnston Atolls, and Bird Island), feather Hg concentrations were higher in the 2020s than in the 1990s/2000s (by 25%, 47% and 628%, respectively). This result is consistent with temporal trends of Hg reported worldwide in seabirds (Bond et al., 2015; Thompson et al., 1992; Vo et al., 2011), including tropical waters where long-term increase in Hg were documented in sooty terns since the 1890s (Cusset et al., 2023). In contrast, in Aride Island, feather Hg concentrations did not show any significant temporal pattern between 1997 and 2021, whereas a 53% decrease appeared in Culebra between 1980s and 2021. Further research could investigate fine-scale temporal patterns of Hg contamination to confirm the observed trends, and determine if these temporal patterns are similar at the global scale.

Interannual difference in Ascension Island

In Ascension Island, feathers were collected during two consecutive years for both adults and chicks, allowing to investigate interannual differences in both Hg and stable isotopes (bulk and compound specific). Both feather Hg concentrations and bulk $\delta^{15}\text{N}$ values (from the global subset) were higher in

2021 than in 2020, for both adults and chicks (Figure 4.A and C). Consequently, we could hypothesize that the higher Hg concentrations could result from the consumption of higher trophic level prey, and hence from higher TP of sooty terns, both during the inter-moult and chick-rearing periods. However, CSIA-AA (from the CSIA subset) revealed that adult TP remained relatively constant during these two years (Figure 4.D). Actually, it is the isotopic baseline that substantially changed between 2020 and 2021, as indicated by the $\delta^{15}\text{N}$ values of phenylalanine (source AA; Figure 4.F). Therefore, higher year-round Hg contamination in 2021 did not result from trophic variation of adult sooty terns, but rather from baseline variation, suggesting other environmental drivers of increased Hg bioavailability and transfer and marine food webs of the South Atlantic Ocean. Still, we cannot exclude the possibility that, despite similar TP between years, sooty terns may have consumed different prey in different proportions, resulting in different Hg bioaccumulation between the two years. This could only be verified with Hg and stable isotope analyses of prey species, but obtaining these samples during the non-breeding period of sooty terns without having precise locations precludes any further verification. Clearly, this illustrates the limits of the conventional stable isotope analyses in spatial ecological studies. When considering large spatial scales, we therefore strongly recommend performing CSIA-AA that may help to disentangle the trophic and environmental drivers of Hg contamination in marine food webs.

Conclusions and perspectives

Thanks to a large, field-based scientific network, this study provides a unique assessment of Hg contamination in tropical marine food webs, by using the sooty tern as a pantropical bioindicator species. Overall, the low Hg concentrations in adult and chick sooty terns is consistent with their foraging behaviour and diet (i.e., epipelagic prey, including invertebrates and small fish), and are below toxicity threshold recognized for seabird feathers (i.e., 1.62–10 $\mu\text{g}\cdot\text{g}^{-1}$; Chastel et al., 2022). This suggests low risks of toxicity for this species, although adverse effects may arise at low Hg concentrations. Our results revealed spatial patterns in year-round contamination (as indicated by Hg concentrations in adult feathers) at different spatial scales. At the global scale, the highest Hg concentrations were observed in the Atlantic Ocean, compared to the Pacific and the Indian Ocean. At the hemispheric scale, the highest concentrations were measured in the NH compared to SH. Despite the large number of sampled colonies ($n=28$), several regions remain undocumented and would clearly deserve further investigations, such as South-East Asia in the Pacific Ocean (e.g., Indonesia, Philippines, Papua New Guinea), as well as the central and eastern Indian Ocean (e.g., Chagos Archipelago). Still, such global assessment represents a valuable asset for international Hg biomonitoring programs (e.g., Global Biotic Mercury Synthesis, Global Mercury Assessment) that aim to protect the environment, wildlife and human populations from the adverse effects of deleterious contaminants, such as Hg.

In seabirds, trophic ecology is key to understand the drivers of Hg contamination (trophic and/or environmental) and investigate its spatial patterns in marine food webs. Despite the temporal mismatch between Hg and stable isotopes in feathers, these latter provide essential knowledge about birds' trophic ecology when no other information is available (during the non-breeding season). Still, caution is necessary when interpreting Hg and stable isotope data together. At the global scale, CSIA-AA represent valuable and essential tools that allow spatial comparison of TP within and between ocean basins and can help to clarify the drivers of Hg contamination. In this study, we used the $\delta^{15}\text{N}$ values of source (Phe) and trophic (Glx) AAs, to determine the trophic position of a subset of adult sooty terns in three ocean basins. TP did not drive feather Hg concentrations, unlike bulk $\delta^{13}\text{C}$ values and colony location, suggesting environmental rather than trophic drivers of Hg contamination in sooty terns. In this work, $\delta^{13}\text{C}$ values of AAs were not explored, mainly because of time constraints, but they are available for future investigations of differences in baseline $\delta^{13}\text{C}$ values and accurate large-scale comparisons.

Beyond spatial variation, Hg contamination in marine food webs results from long-term processes of years, decades or even centuries (Driscoll et al., 2013; Foster et al., 2019; Sunderland and Mason, 2007; UN Environment, 2018), that influence the cycling of both natural and anthropogenic Hg in the marine environment, particularly in the context of ongoing climate change (Sonke et al., 2023). Therefore, renewing such large-scale assessment on a regular basis (e.g., decades) is essential to monitor Hg availability in tropical marine food webs and evaluate the effectiveness of international regulations of Hg, such as the Minamata Convention.

ACKNOWLEDGMENTS

The authors are thankful to all people who contributed to sample collection, preparation and shipment across the 28 colonies of sooty terns. First, we acknowledge the U.S. Fish and Wildlife Service and the activities conducted under National Wildlife Refuge System Special Use Permits in four American Refuges: (i) the Pacific Remote Islands Marine National Monument (Johnston and Palmyra Atolls; Permit 12543-21002), (ii) the Papahānaumokuākea Marine National Monument (Laysan and Lisianki Islands, Midway Atoll; permit number: PMNM-2021-014), (iii) Rose Atoll National Wildlife Refuge, and (iv) Culebra National Wildlife Refuge (Puerto Rico). Superintendents of these four refuges are acknowledged for their support during permit preparation and sampling organization, namely Kate Toniolo, Daniel Link, Brian Peck and Ana Roman. These activities were conducted in the USA under Migratory Bird Permit Import/Export (N° MBPER0018031).

For the Seychelles, we acknowledge the following persons and institutions for their support in sample collection: (i) the Island Conservation Society (ICS) with Pierre-André Adam, Mickaél Napoleon, Nicky Jean, Liam Padayachy, Annie Gendron and Dillys Pouponeau, as well as the staff of the Ministry of

Agriculture, Climate Change and Environment (MACCE) (Indira Gamatis), and Magali Rocamora (IBC-UniSey) for their assistance in the field; (ii) the Government of Seychelles, MACCE and Seychelles Bureau of Standards (SBS) for granting approval for this research; (iii) the Islands Development Company (IDC), Farquhar, Cosmoledo & Astove, Marie-Louise & Desnoeufts, Rémire & African Banks Foundations for logistical and financial support; and (iv) ICS Head Office Management Team for their support in coordinating and facilitating the administration procedures associated with this project.

Feather samples were then shipped from all collaborating countries under appropriate French import permits (N°: FR17201182LR (2020), FR17 211006LR (2021), FR17211289LR (2022)).

Regarding laboratory analyses, we are grateful to: (i) Louis Troussé and Margaux Mollier for their help in the laboratory during their internships, and (ii) Carine Churlaud and Maud Brault-Favrou from the Plateforme Analyses Élémentaires (LIENSs) for their support during Hg analyses. Thanks are due to the CPER (Contrat de Projet État-Région) and the FEDER (Fonds Européen de Développement Régional) for funding the AMA and the IRMS of LIENSs laboratory. The IUF (Institut Universitaire de France) is acknowledged for its support to Paco Bustamante as a Senior Member. This work benefitted from the French GDR Aquatic Ecotoxicology framework, that aims to foster stimulating scientific discussions for more integrative approaches.

FIGURES

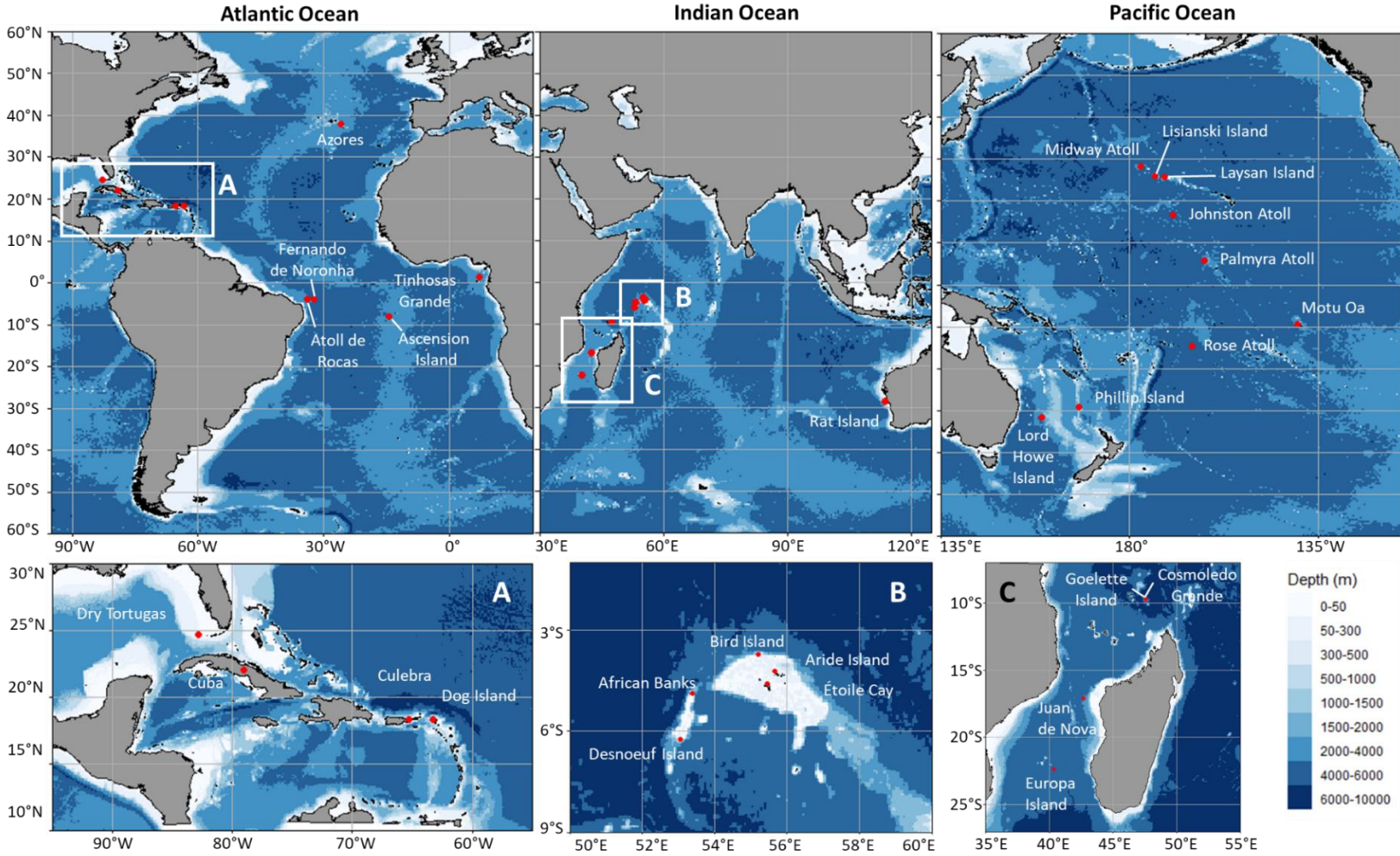


Figure 1. Feather sampling sites (red dots) of sooty terns across tropical waters, including the Atlantic (n=9), Indian (n=10) and Pacific Oceans (n=9). The blue gradient indicates bathymetry.

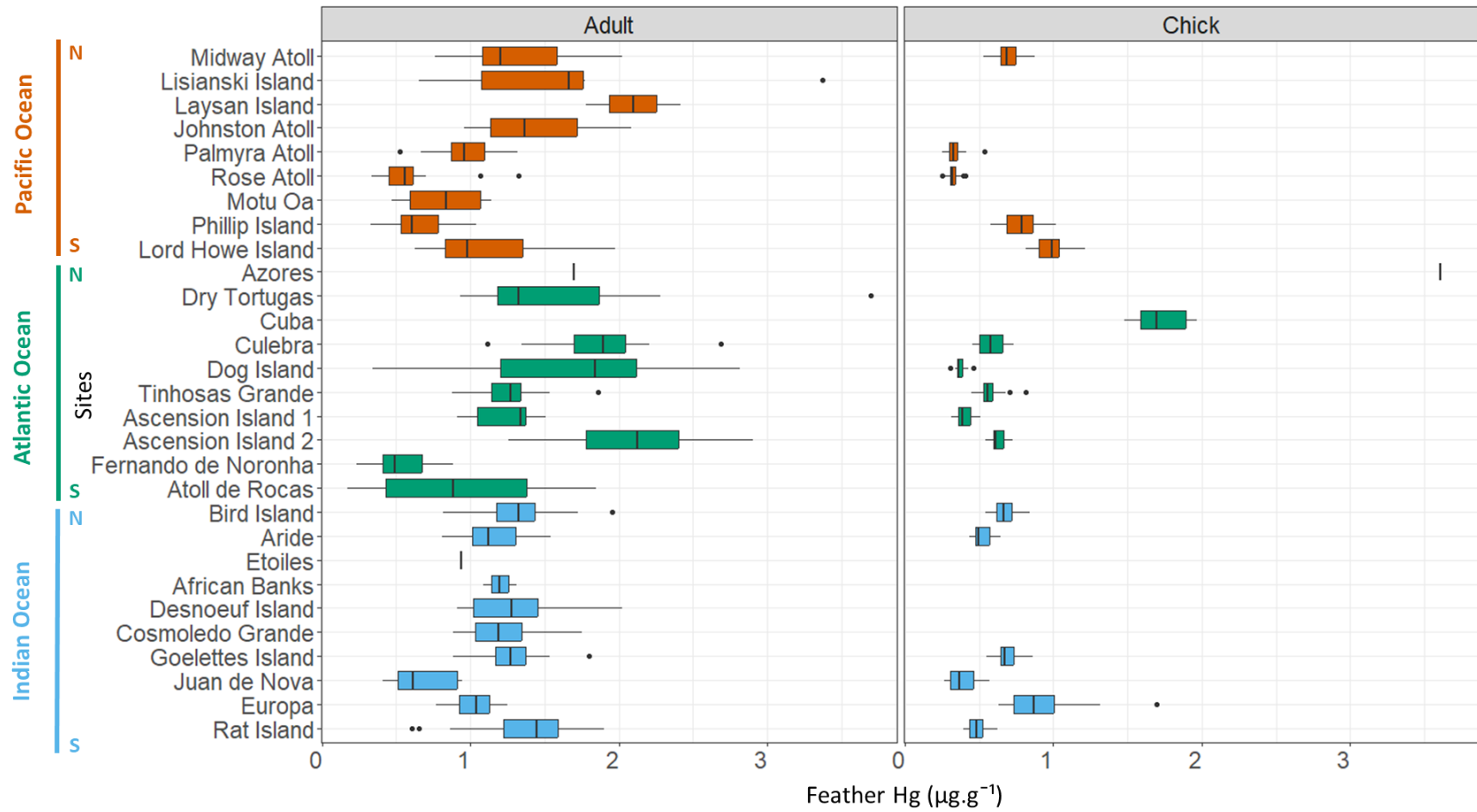


Figure 2. Feather Hg concentrations in adults (left) and chicks (right) of sooty terns (*Onychoprion fuscatus*), sampled in 28 sites over three ocean basins. Sample sizes are indicated in Table 1. Two consecutive years were sampled in Ascension Island: 2020 (Ascension Island 1) and 2021 (Ascension Island 2).

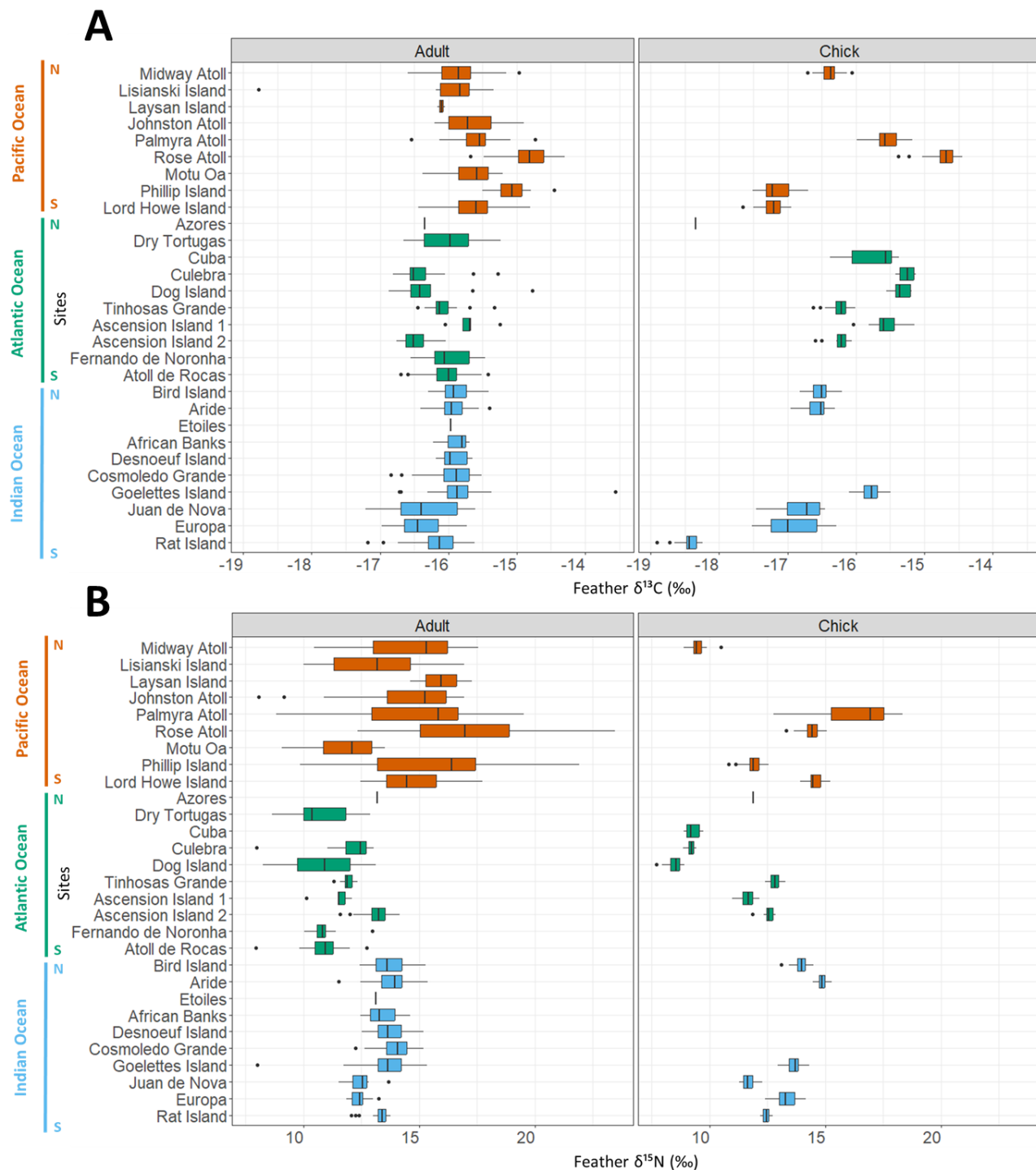


Figure 3. Feather (A) $\delta^{13}\text{C}$ and (B) $\delta^{15}\text{N}$ values in adults (left) and chicks (right) of sooty terns (*Onychoprion fuscatus*), sampled in 28 sites over three ocean basins. Sample sizes are indicated in Table 1. Two consecutive years were sampled in Ascension Island: 2020 (Ascension Island 1) and 2021 (Ascension Island 2).

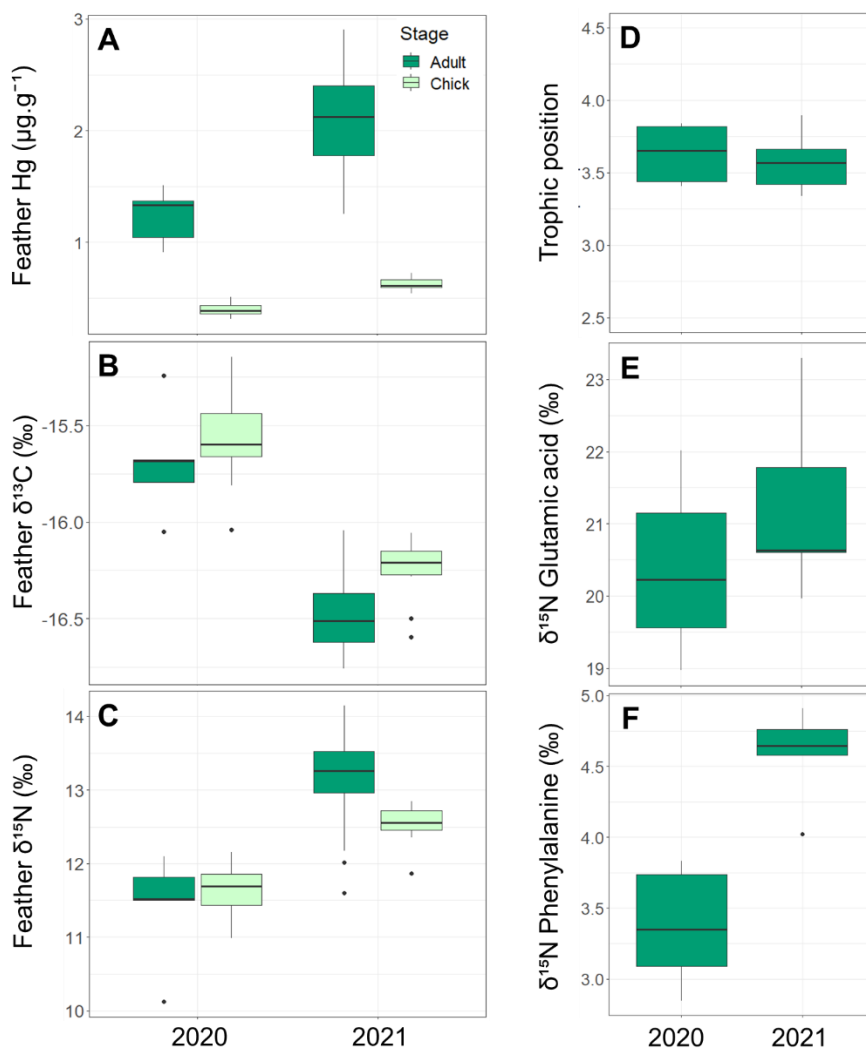


Figure 4. Interannual differences in feather (A) Hg concentrations, (B) bulk $\delta^{13}\text{C}$ and (C) $\delta^{15}\text{N}$ values of adults ($n=5$ and $n=30$ in 2020 and 2021, respectively) and chicks ($n=30$ and $n=15$ in 2020 and 2021, respectively) of sooty terns (*Onychoprion fuscatus*), sampled on Ascension Island (South Atlantic Ocean). For a subset of adults ($n=5$ per year), the (D) trophic position (TP) was estimated with the $\delta^{15}\text{N}$ values of (E) glutamic acid (trophic amino acid) and (F) phenylalanine (source amino acid).

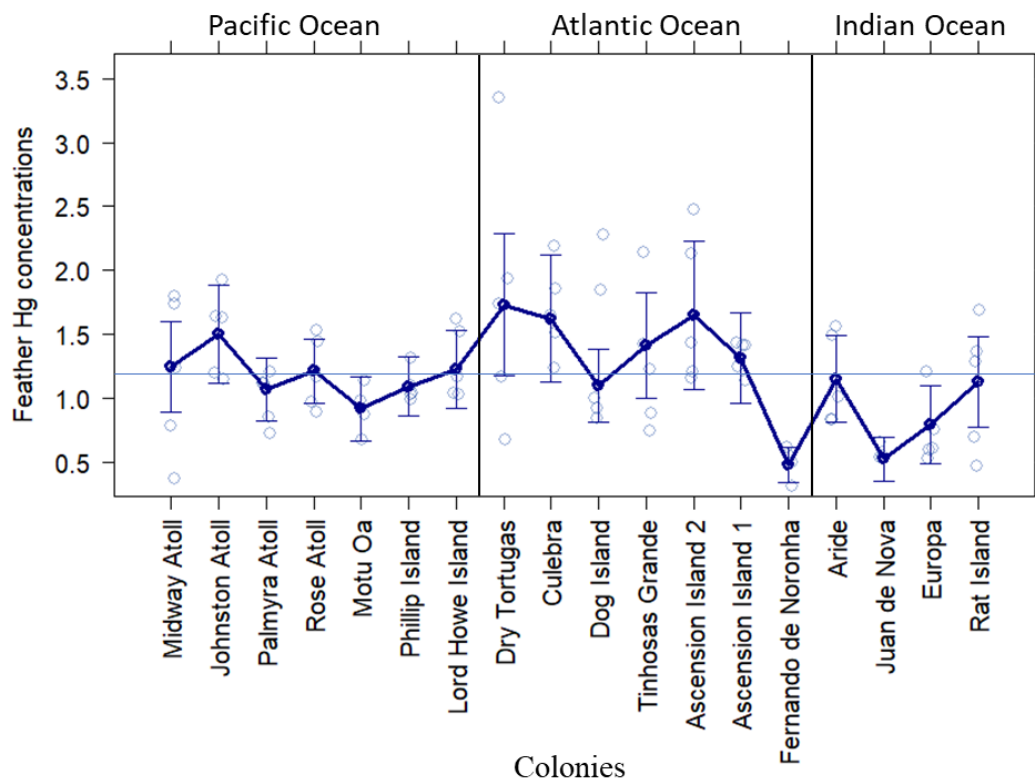


Figure 5. Spatial differences in feather Hg concentrations in adult sooty terns (*Onychoprion fuscaus*) from 18 tropical colonies (n=88) when controlled by their feeding ecology (feather bulk $\delta^{13}\text{C}$ values). Relationships result from the extraction of partial residuals of the best Generalized Linear Model (GLM; see **Table 2** and **Material and Methods** for further details). Individual data are represented in light blue (open circle). Points (filled circle) are means \pm SD. The dark blue line links all mean Hg concentrations. The horizontal line (in blue) represents the species' average (i.e., $1.19 \mu\text{g}\cdot\text{g}^{-1}$). Ascension Island 1 and 2 refer to samples from 2020 and 2021, respectively.

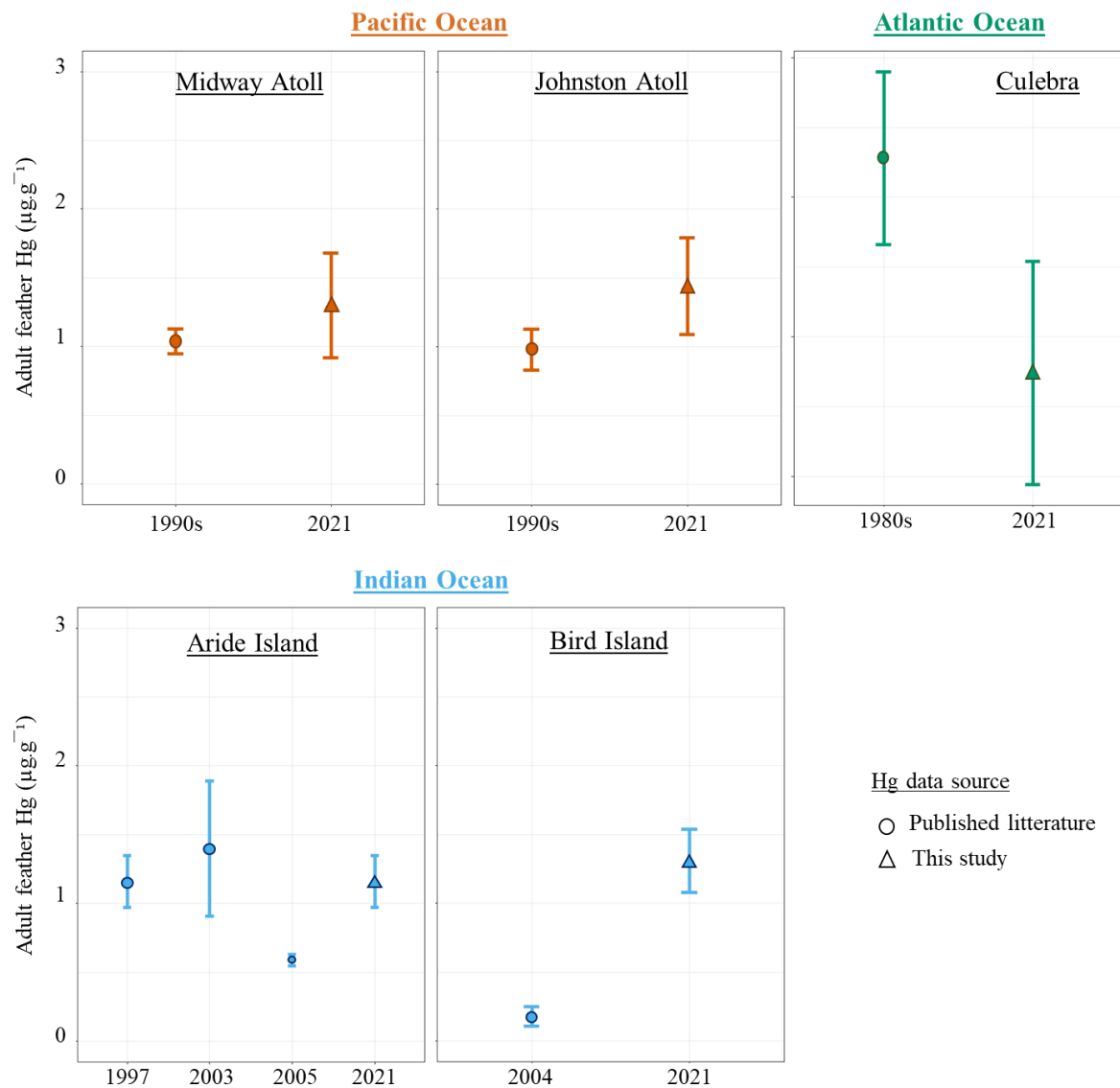


Figure 6. Temporal comparisons of feather Hg concentrations in adult sooty terns (*Onychoprion fuscatus*) in five colonies across three ocean basins.

TABLES

Table 1. Literature review of feather Hg concentrations of sooty terns (*Onychoprion fuscatus*) sampled across three ocean basins.

Sites	Year	Stage	n	Feather Hg ($\mu\text{g}\cdot\text{g}^{-1}$ dw)	References
<u>Pacific Ocean</u>					
Midway Atoll	1990s	Adult	28	1.04 ± 0.09	Burger et al. (2001); Burger and Gochfeld (2000)
	2021	Adult	30	1.30 ± 0.38 (0.76–2.03)	
	2021	Chick	30	0.70 ± 0.08 (0.53–0.87)	
Lisianski Island	2021	Adult	6	1.67 ± 0.95 (0.66–3.37)	This study
Laysan Island	2021	Adult	2	2.10 ± 0.45 (1.78–2.42)	This study
Hawaii	1990s	Adult	26	1.26 ± 0.34	Burger et al. (2001)
	1990	Adult	20	0.77 ± 0.07	Burger et al. (1992)
Johnston Atoll	1990	Adult	12	0.98 ± 0.15	Burger et al. (1992)
	2021	Adult	30	1.44 ± 0.35 (0.96–2.08)	This study
Palmyra Atoll	2021	Adult	31	0.97 ± 0.05 (0.52–1.32)	This study
	2021	Chick	30	0.33 ± 0.05 (0.25–0.54)	This study
Rose Atoll	2021	Adult	34	0.57 ± 0.19 (0.33–1.33)	This study
	2021	Chick	34	0.33 ± 0.03 (0.25–0.41)	This study
Ua Pou, Marquesas	2021/2022	Adult	4	0.82 ± 0.32 (0.47–1.14)	This study
Great Barrier Reef, Michaelmas Cay	1984	Adult	15	0.44 ± 0.18	Burger and Gochfeld (1991)
Phillip Island, Norfolk Islands	2020	Adult	30	0.63 ± 0.19 (0.32–1.04)	This study
	2021	Chick	30	0.78 ± 0.11 (0.58–1.02)	This study
Lord Howe Island	2020	Adult	30	1.11 ± 0.39 (0.62–1.97)	This study
	2020	Chick	30	0.98 ± 0.12 (0.82–1.22)	This study
<u>Atlantic Ocean</u>					
Azores	2021	Adult	1	1.69	This study
	2020	Chick	1	3.61	This study
Dry Tortugas, Florida	2021	Adult	24	1.56 ± 0.61 (0.93–3.70)	This study
Cuba	2021	Chick	6	1.72 ± 0.20 (1.48–1.96)	This study

Culebra, Puerto Rico	1980s	Adult	15	2.64 ± 0.31	Burger and Gochfeld (1991)
	2021	Adult	12	1.87 ± 0.40 (1.12–2.68)	This study
	2021	Chick	4	0.59 ± 0.12 (0.46–0.73)	This study
Dog Island, Anguilla	2021	Adult	11	1.63 ± 0.76 (0.34–2.82)	This study
	2021	Chick	13	0.37 ± 0.04 (0.30–0.46)	This study
Tinhosas Grande	2021	Adult	27	1.27 ± 0.19 (0.87–1.86)	This study
	2021	Chick	25	0.58 ± 0.08 (0.45–0.82)	This study
Fernando de Noronha	2011	Adult	18	0.54 ± 0.18 (0.23–0.89)	This study
Atoll de Rocas	2010	Adult	44	0.95 ± 0.53 (0.17–1.84)	This study
Ascension Island	2020	Adult	5	1.24 ± 0.25 (0.91–1.51)	This study
	2020	Chick	30	0.40 ± 0.05 (0.31–0.51)	This study
	2021	Adult	30	2.09 ± 0.40 (1.25–2.90)	This study
	2021	Chick	15	0.63 ± 0.05 (0.54–0.72)	This study
<u>Indian Ocean</u>					
Bird Island	2004	Adult	37	0.18 ± 0.07 (0.10–0.33)	Kojadinovic et al. (2007)
	2021	Adult	31	1.31 ± 0.23 (0.82–1.96)	This study
	2021	Chick	33	0.67 ± 0.06 (0.54–0.84)	This study
Aride Island	1997	Adult	15	1.16 ± 0.19	Ramos and Tavares (2010)
	2003	Adult	14	1.40 ± 0.49	Ramos and Tavares (2010)
	2005	Adult	10	0.59 ± 0.04	Ramos and Tavares (2010)
	2005	Adult	10	0.59 ± 0.60	Jaquemet et al. (2008)
	2021	Adult	30	1.16 ± 0.19 (0.81–1.54)	This study
	2021	Chick	25	0.52 ± 0.06 (0.43–0.64)	This study
Etoile Cay	2021	Adult	1	0.94	This study
African Banks	2021	Adult	3	1.20 ± 0.11 (1.09–1.31)	This study
Desnoeuf Island	2021	Adult	10	1.31 ± 0.37 (0.91–2.02)	This study
Cosmoledo Grande	2021	Adult	30	1.24 ± 0.26 (0.89–1.75)	This study
Goelette Island	2021	Adult	30	1.28 ± 0.19 (0.88–1.80)	This study
	2021	Chick	30	0.69 ± 0.07 (0.55–0.86)	This study
Lys Island, Glorieuses	2004	Adult	14	0.23 ± 0.10 (0.09–0.39)	Jaquemet et al. (2008); Kojadinovic et al. (2007)

Europa Island	2004	Chick	22	0.05 ± 0.03 (0.02–0.17)	Jaquemet et al. (2008); Kojadinovic et al. (2007)
	2003	Adult	18	1.02 ± 0.15 (0.77–1.25)	This study
	2004	Adult	32	0.21 ± 0.08 (0.05–0.47)	Jaquemet et al. (2008); Kojadinovic et al. (2007)
	2003	Chick	15	0.77 ± 0.14 (0.63–1.01)	This study
Juan de Nova	2021	Chick	16	1.03 ± 0.24 (0.76–1.69)	This study
	2003	Adult	10	0.68 ± 0.22 (0.41–0.94)	This study
	2004	Adult	14	0.39 ± 0.15 (0.16–0.67)	Jaquemet et al. (2008); Kojadinovic et al. (2007)
Rat Island, Houtman Abrolhos	2003	Chick	10	0.39 ± 0.10 (0.27–0.57)	This study
	2020	Adult	32	1.38 ± 0.33 (0.61–1.90)	This study
		Chick	30	0.49 ± 0.06 (0.39–0.62)	This study

Table 2. AICc model ranking from statistical analyses of feather Hg concentrations from sooty terns (n=88). Models are Generalized Linear Models (GLMs) with Gamma distribution, and identity link-function. Abbreviations: k, number of parameters; AICc, Akaike’s Information Criterion adjusted for small sample size; w_i AICc weights. A model with $\Delta\text{AIC}_c = 0$ is interpreted as the best model among all the selected ones (in bold). Weights are cumulative (sum to 1).

Models	k	AIC _c	ΔAIC_c	w _i
Hg ~ C + Colony	21	101.6	0.00	0.85
Hg ~ C + Colony + TP	22	105.1	3.47	0.15
Hg ~ C	3	121.5	19.86	0.00
Hg ~ C + TP	4	123.6	21.90	0.00
Hg ~ Colony	20	138.8	37.11	0.00
Hg ~ Colony + TP	21	140.0	38.36	0.00
NULL	2	158.0	56.39	0.00
Hg ~ TP	3	160.2	58.53	0.00

Table 3. Estimated parameters of variables included in the best model (n=88). Models are Generalized Linear Models (GLMs) with Gamma distribution and identity link-function. McFadden's R^2 indicates the degree of model fit (*i.e.*, from low and high model fit indicated from 0 to 1, respectively). Bulk carbon ($\delta^{13}\text{C}$) values are proxies of the feeding habitat. The «+» symbol indicates that the colony (categorical factor) is included in the best model. Results for site comparisons (estimated marginal means) are provided in **Figure S6**. Abbreviations: CI, confidence interval (95%); SE, standard error.

Variables	Estimates [CI] \pm SE
Intercept	-7.28 [-9.74, -4.76] \pm 1.22
$\delta^{13}\text{C}$	-0.53 [-0.68, -0.37] \pm 0.08
Colony	+
McFadden's R^2	0.68

SUPPLEMENTARY MATERIAL

Supplementary tables

Table S1. Geographical coordinates of sampling sites and collaborators involved in feather sampling of sooty terns across the 28 sites... from Mapcarta.com (following the colour code from the figures).

Sites	Coordinates	Collaborators and/or contact persons
Pacific Ocean		
Midway Atoll	28°13'41" N, 177°23'20" O	Daniel Link
Lisianski Island	26°3'45" N, 173°57'59" O	Daniel Link
Laysan Island	25°46'15" N, 171°44'15" O	Daniel Link
Johnston Atoll	16°43'44" N, 169°32'1" O	Kate Toniolo
Palmyra Atoll	5°52'56" N, 162°4'30" O	Kate Toniolo
Rose Atoll	14°32'45" S, 168°9' O	Brian Peck
Ua Pou, Marqueses	9°28'47" S, 140°2'49" O	Thoma Gestemme, Tehani Withers
Phillip Island, Norfolk Islands	29°7'2" S, 167°56'35" E	Nicholas Carlisle
Lord Howe Island	31°31'24" S, 159°3'49" E	Terry O'Dwyer
Atlantic Ocean		
Azores	37°51'24" N, 25°47'2" O	Veronica Rodrigues Costa Nevess
Dry Tortugas, Florida	24°38'56" N, 82°52'18" O	Stuart Pimm
Cuba	21°59'2" N, 79°3'25" O	Antonio Garcia Quintas
Culebra, Puerto Rico	18°18'11" N, 65°18'0" O	Ana Roman, Eduardo Ventosa
Dog Island, Anguilla	18°16'40" N, 63°14'56" O	Louise Soanes
Tinhas Grande	1°20'32" N, 7°17'31" E	Nina Darocha, Estrela Matilde
Fernando de Noronha	3°51'16" S, 32°25'4" O	Leandro Bugoni
Atoll de Rocas	3°51'21" S, 33°49'3" O	Leandro Bugoni
Ascension Island	7°56'30" S, 14°21'45" O	Laura Shearer
Indian Ocean		
Bird Island	3°43'8" S, 55°12'22" E	Chris Feare
Aride Island	4°12'45" S, 55°40'0" E	Gerard Rocamora
Etoile Cay	4°35'36" S, 55°27'19" E	Matthew Morgan
African Banks	4°52'52" S, 53°23'14" E	Matthew Morgan
Desnoeuf Island	6°14'5" S, 53°2'37" E	Matthew Morgan
Cosmoledo Grande	9°43' S, 47°35' E	Matthew Morgan, Pierre-Andre Adam
Goelette Island	9°42'2" S, 47°38'43" E	Matthew Morgan
Juan de Nova	17° 3' 17" S, 42° 43' 28" E	Jaeger ?
Europa Island	22°21'1" S, 40°21'34" E	Charlie Bost, Jaeger ?
Rat Island, Houtman Abrolhos	28°42'56" S, 113°47'2" E	Nic Dunlop

Table S2. Certified reference materials (NRC Canada) used for total Hg analyses in feathers of sooty terns (*Onychoprion fuscatus*): certified (theoretical) and measured concentrations, and recoveries (calculated as measured/certified value). n indicate sample sizes for each reference material and values are mean ± SD (min–max).

Reference Material	n	Certified value ($\mu\text{g}\cdot\text{g}^{-1}$ dw)	Measured value ($\mu\text{g}\cdot\text{g}^{-1}$ dw)	Recovery (%)
DOLT-5 <i>Fish liver</i>	16	0.44 ± 0.18 (0.26–0.62)	0.42 ± 0.01 (0.41–0.43)	96.6 ± 1.4 (94.3–98.6)
TORT-3 <i>Lobster hepatopancreas</i>	101	0.29 ± 0.02 (0.27–0.31)	0.30 ± 0.01 (0.27–0.31)	101.3 ± 2.4 (94.1–107.7)

Table S3. Literature review of stable isotope values measured in feathers of sooty terns (*Onychoprion fuscatus*) sampled across three ocean basins.

Sites	Year	Stage	n	$\delta^{13}\text{C}$ (‰)	$\delta^{15}\text{N}$ (‰)	References
<u>Pacific Ocean</u>						
Midway Atoll	2021	Adult	30	-15.88 ± 0.38 ($-16.59, -14.97$)	14.72 ± 2.06 ($10.46-17.55$)	This study
		Chick	30	-16.39 ± 0.15 ($-16.71, -16.06$)	9.47 ± 0.33 ($8.88-10.50$)	This study
Lisianski Island	2021	Adult	6	-16.27 ± 1.26 ($-18.78, -15.34$)	13.18 ± 2.60 ($10.0-16.94$)	This study
Laysan Island	2021	Adult	2	-16.10 ± 0.08 ($-16.16, -16.05$)	15.95 ± 1.90 ($14.60-17.29$)	This study
Johnston Atoll	2021	Adult	30	-15.66 ± 0.40 ($-16.20, -14.89$)	14.50 ± 2.24 ($8.06-16.95$)	This study
Palmyra Atoll	2021	Adult	31	-15.59 ± 0.33 ($-16.54, -14.73$)	15.08 ± 2.49 ($8.84-19.52$)	This study
		Chick	30	-15.56 ± 0.21 ($-15.98, -15.17$)	16.36 ± 1.59 ($12.77-18.33$)	This study
Rose Atoll	2021	Adult	34	-14.85 ± 0.33 ($-15.68, -14.30$)	17.15 ± 2.66 ($12.33-23.45$)	This study
		Chick	34	-14.72 ± 0.19 ($-15.38, -14.44$)	14.41 ± 0.40 ($13.30-15.06$)	This study
Ua Pou, Marqueses	2021/2022	Adult	4	-15.69 ± 0.50 ($-16.38, -15.21$)	11.71 ± 1.95 ($9.09-13.53$)	This study
Phillip Island, Norfolk Islands	2020	Adult	30	-15.09 ± 0.24 ($-15.50, -14.45$)	15.26 ± 2.91 ($9.86-21.90$)	This study
	2021	Chick	30	-17.15 ± 0.21 ($-17.52, -16.70$)	11.87 ± 0.89 ($10.81-12.56$)	This study
Lord Howe Island	2020	Adult	30	-15.64 ± 0.35 ($-16.44, -14.81$)	14.77 ± 1.57 ($12.46-17.72$)	This study
		Chick	30	-17.22 ± 0.15 ($-17.65, -16.95$)	14.56 ± 0.34 ($13.92-15.20$)	This study
<u>Atlantic Ocean</u>						
Azores	2021	Adult	1	-16.34	13.20	This study
		Chick	1	-18.35	11.89	This study
Dry Tortugas, Florida	2021	Adult	24	-16.03 ± 0.43 ($-16.65, -15.23$)	10.70 ± 1.21 ($8.64-12.90$)	This study
Cuba		Chick	6	-15.76 ± 0.42 ($-16.38, -15.37$)	9.27 ± 0.35 ($8.89-9.74$)	This study
Culebra, Puerto Rico	2021	Adult	12	-16.35 ± 0.46 ($-16.81, -15.28$)	11.95 ± 1.41 ($7.99-13.05$)	This study
		Chick	4	-15.26 ± 0.14 ($-15.42, 15.12$)	9.18 ± 0.25 ($8.85-9.44$)	This study
Dog Island, Anguilla	2021	Adult	11	-16.26 ± 0.63 ($-16.87, -14.77$)	10.83 ± 1.59 ($8.26-13.14$)	This study
		Chick	13	-15.34 ± 0.13 ($-15.55, -15.18$)	8.44 ± 0.37 ($7.71-8.93$)	This study
Tinhosas Grande	2021	Adult	27	-16.08 ± 0.22 ($-16.45, -15.33$)	11.93 ± 0.24 ($11.32-12.33$)	This study
		Chick	25	-16.24 ± 0.15 ($-16.62, -16.01$)	12.81 ± 0.23 ($12.40-13.28$)	This study
Fernando de Noronha	2011	Adult	18	-16.0 ± 0.31 ($-16.55, -15.46$)	10.84 ± 0.64 ($10.03-12.98$)	This study

Atoll de Rocas	2010	Adult	44	-16.03 ± 0.27 (-16.69, -15.42)	10.88 ± 0.73 (7.95–12.75)	This study
Ascension Island	2020	Adult	5	-15.69 ± 0.29 (-16.05, -15.24)	11.41 ± 0.76 (10.12–12.09)	This study
		Chick	30	-15.47 ± 0.16 (-15.65, 15.29)	11.81 ± 0.05 (11.77–11.89)	This study
	2021	Adult	30	-16.47 ± 0.20 (-16.76, -16.04)	13.18 ± 0.65 (11.60–14.15)	This study
		Chick	15	-16.28 ± 0.15 (-16.50, -16.15)	12.61 ± 0.14 (12.48–12.80)	This study
<u>Indian Ocean</u>						
Bird Island	2021	Adult	31	-15.88 ± 0.22 (-16.29, -15.41)	13.68 ± 0.75 (12.44–15.28)	This study
	2021	Chick	33	-16.52 ± 0.15 (-16.82, -16.21)	13.91 ± 0.31 (13.11–14.50)	This study
Aride Island	2021	Adult	30	-15.91 ± 0.22 (-16.40, -15.40)	13.81 ± 0.86 (11.53–15.37)	This study
	2021	Chick	25	-16.57 ± 0.17 (-16.96, -16.31)	14.85 ± 0.20 (14.47–15.27)	This study
Etoile Cay	2021	Adult	1	-15.97	13.13	This study
African Banks	2021	Adult	3	-15.91 ± 0.28 (-16.22, -15.69)	13.46 ± 1.09 (12.47–14.63)	This study
Desnoeuf Island	2021	Adult	10	-15.92 ± 0.20 (-16.18, -15.65)	13.80 ± 0.84 (12.53–15.18)	This study
Cosmoledo Grande	2021	Adult	30	-15.93 ± 0.32 (-16.84, -15.51)	14.03 ± 0.74 (12.26–15.20)	This study
Goelette Island	2021	Adult	30	-15.81 ± 0.53 (-16.72, -13.56)	13.50 ± 1.33 (8.02–15.34)	This study
	2021	Chick	30	-15.79 ± 0.15 (-16.10, -15.50)	13.65 ± 0.34 (12.95–14.32)	This study
Europa Island	2003	Adult	18	-16.43 ± 0.36 (-16.97, -15.93)	12.42 ± 0.38 (11.86–13.24)	Cherel et al. (2008)
	2003	Chick	15	-16.57 ± 0.18 (-16.89, -16.29)	13.68 ± 0.27 (13.22–14.15)	Cherel et al. (2008)
	2021	Chick	16	-17.25 ± 0.17 (-17.52, -17.00)	12.96 ± 0.36 (12.39–13.55)	This study
Juan de Nova	2003	Adult	10	-16.35 ± 0.53 (-17.21, -15.61)	12.50 ± 0.57 (11.53–13.67)	Jaquemet et al. (2008)
	2003	Chick	10	-16.85 ± 0.34 (-17.46, -16.45)	11.67 ± 0.36 (11.07–12.27)	Jaquemet et al. (2008)
Rat Island, Houtman Abrolhos	2020	Adult	32	-16.17 ± 0.36 (-17.18, -15.62)	13.31 ± 0.41 (12.06–13.76)	This study
	2020	Chick	30	-18.44 ± 0.15 (-18.91, -18.24)	12.44 ± 0.16 (12.17–12.72)	This study

Table S4. Feather $\delta^{15}\text{N}$ values of two amino acids (AA) – glutamic acid (trophic AA) and phenylalanine (source AA) – and resulting trophic position (see **Material and Methods** for further details), in feathers of adult sooty terns in 19 sites across three ocean basins.

Ocean, Site	Year	n	Amino-acid $\delta^{15}\text{N}$ values		
			Glutamic acid	Phenylalanine	Trophic position
Pacific Ocean					
Laysan Island	2021	2	25.56 ± 1.70 (24.36–26.76)	6.09 ± 1.30 (5.17–7.01)	4.03 ± 0.06 (3.98–4.07)
Midway Atoll	2021	5	22.38 ± 2.58 (18.85–24.67)	3.95 ± 1.89 (1.97–6.56)	3.86 ± 0.19 (3.57–4.08)
Johnston Atoll	2021	5	21.91 ± 3.11 (17.36–25.52)	3.98 ± 1.59 (2.51–6.41)	3.78 ± 0.29 (3.28–4.02)
Palmyra Atoll	2021	5	22.45 ± 3.89 (18.01–28.23)	4.74 ± 2.51 (2.06–7.37)	3.74 ± 0.36 (3.43–4.32)
Marquises	2022	4	20.77 ± 1.94 (18.31–22.41)	2.94 ± 1.71 (0.76–4.91)	3.76 ± 0.17 (3.61–4.01)
Rose Atoll	2021	5	19.84 ± 0.73 (19.10–20.69)	3.28 ± 0.84 (2.19–4.47)	3.56 ± 0.11 (3.40–3.66)
Phillip Island	2020	5	21.66 ± 5.21 (17.48–30.34)	6.11 ± 4.50 (0.96–12.36)	3.39 ± 0.46 (2.60–3.79)
Lord Howe Island	2020	5	23.32 ± 2.75 (20.35–25.95)	5.58 ± 1.94 (3.81–8.31)	3.75 ± 0.29 (3.54–4.25)
		36			
Atlantic Ocean					
Azores	2021	1	21.35	3.97	3.69
Dog Island	2021	5	19.02 ± 2.72 (14.56–21.97)	3.44 ± 1.04 (2.36–5.00)	3.40 ± 0.41 (2.81–3.83)
Dry Tortugas	2021	5	18.80 ± 1.10 (17.37–20.27)	3.08 ± 0.79 (2.13–4.16)	3.42 ± 0.10 (3.34–3.56)
Culebra	2021	5	19.38 ± 2.07 (16.16–21.47)	2.85 ± 1.67 (0.60–4.82)	3.55 ± 0.18 (3.38–3.82)
Fernando de Noronha	2011	4	18.76 ± 1.37 (17.29–20.51)	1.93 ± 1.25 (0.59–3.50)	3.60 ± 0.12 (3.45–3.74)
Ascension Island	2020	5	20.38 ± 1.22 (18.98–22.01)	3.37 ± 0.42 (2.85–3.83)	3.63 ± 0.20 (3.41–3.84)
	2021	5	21.26 ± 1.31 (19.97–23.29)	4.58 ± 0.34 (4.02–4.91)	3.58 ± 0.22 (3.34–3.90)
Tinhas Grande	2021	5	19.84 ± 0.73 (19.10–20.69)	3.28 ± 0.84 (2.19–4.47)	3.56 ± 0.11 (3.40–3.66)
		36			
Indian Ocean					
Aride	2021	5	22.17 ± 1.27 (20.62–23.90)	4.34 ± 1.08 (3.51–6.17)	3.76 ± 0.09 (3.65–3.88)
Europa	2003	5	21.36 ± 0.61 (20.81–22.09)	3.40 ± 0.62 (2.74–4.04)	3.78 ± 0.07 (3.66–3.84)
Juan de Nova	2003	5	21.24 ± 0.79 (19.94–22.0)	3.08 ± 0.62 (2.35–3.73)	3.82 ± 0.13 (3.68–4.01)
Rat Island	2020	5	21.53 ± 3.38 (17.48–26.86)	4.12 ± 0.66 (3.17–5.0)	3.70 ± 0.51 (3.02–4.41)
		20			
Total		91			3.67 ± 0.28 (2.60–4.41)

Supplementary figures

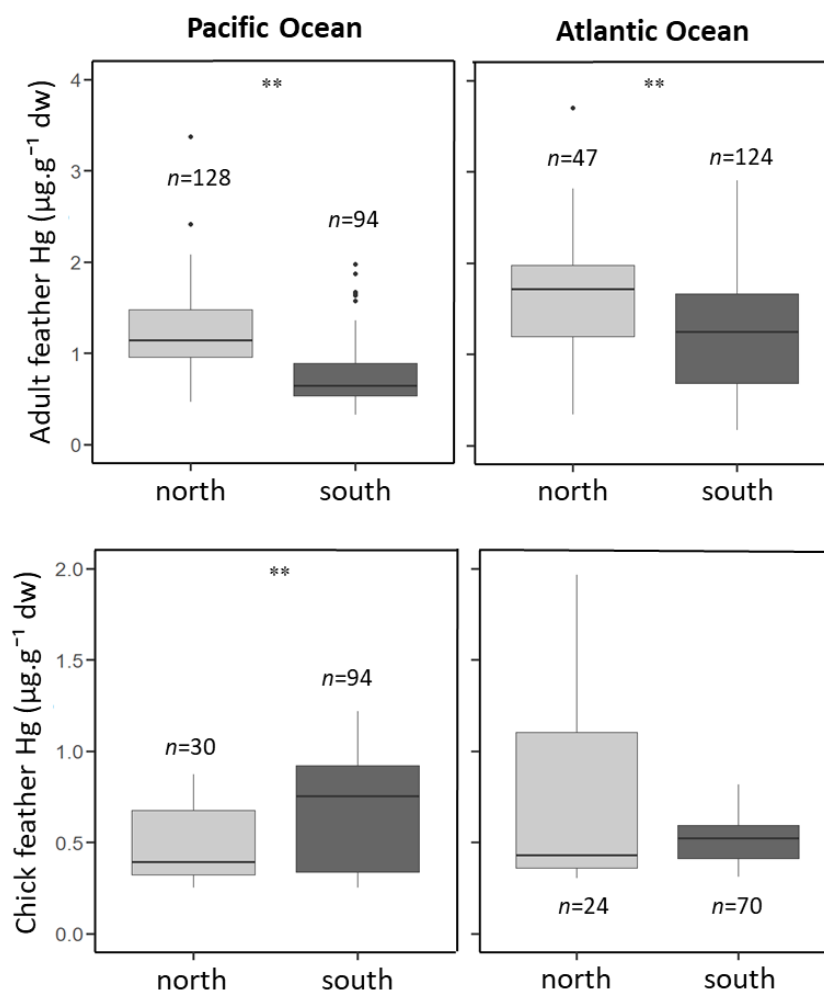


Figure S1. Hemispheric Hg gradients in adult and chick sooty terns (global subset; cf. **Material and Methods**) from two different tropical oceans, including the Pacific and Atlantic Oceans. Comparisons were made between the Northern and the South Hemispheres. n indicates sample sizes. ** indicates statistical difference when detected (Kruskal-Wallis).

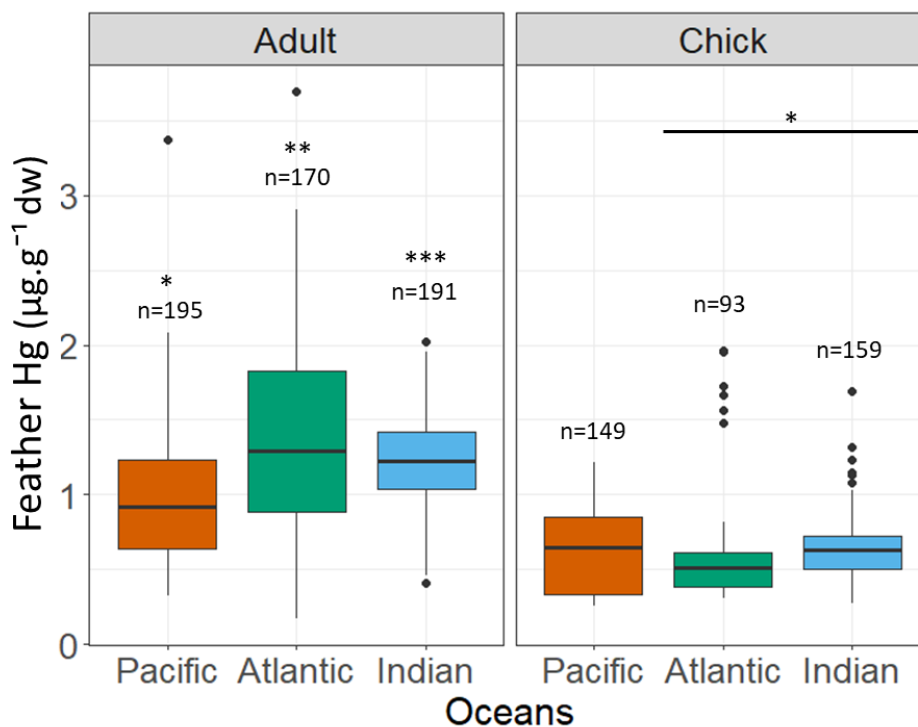


Figure S2. Ocean comparison of feather Hg concentrations in adult (left) and chick (right) sooty terns (global subset; only includes sites where $n > 4$). n indicates sample sizes. * indicates when statistical difference was detected (Kruskal-Wallis) and identifies different groups.

Statistical results

For the CSIA subset ($n=88$), feather Hg concentrations were different between colonies (Kruskal-Wallis, $\chi^2(17) = 43.1$, $p=0.0005$; Figure S3.A) and ocean basins (Kruskal-Wallis, $\chi^2(2) = 12.6$, $p=0.002$; Figure S4), with higher concentrations in the Atlantic Ocean (1.51 ± 0.78 , $n=34$) compared to the Pacific (1.04 ± 0.52 , $n=36$) and Indian (1.01 ± 0.38 , $n=20$) Oceans (Figure S3.A).

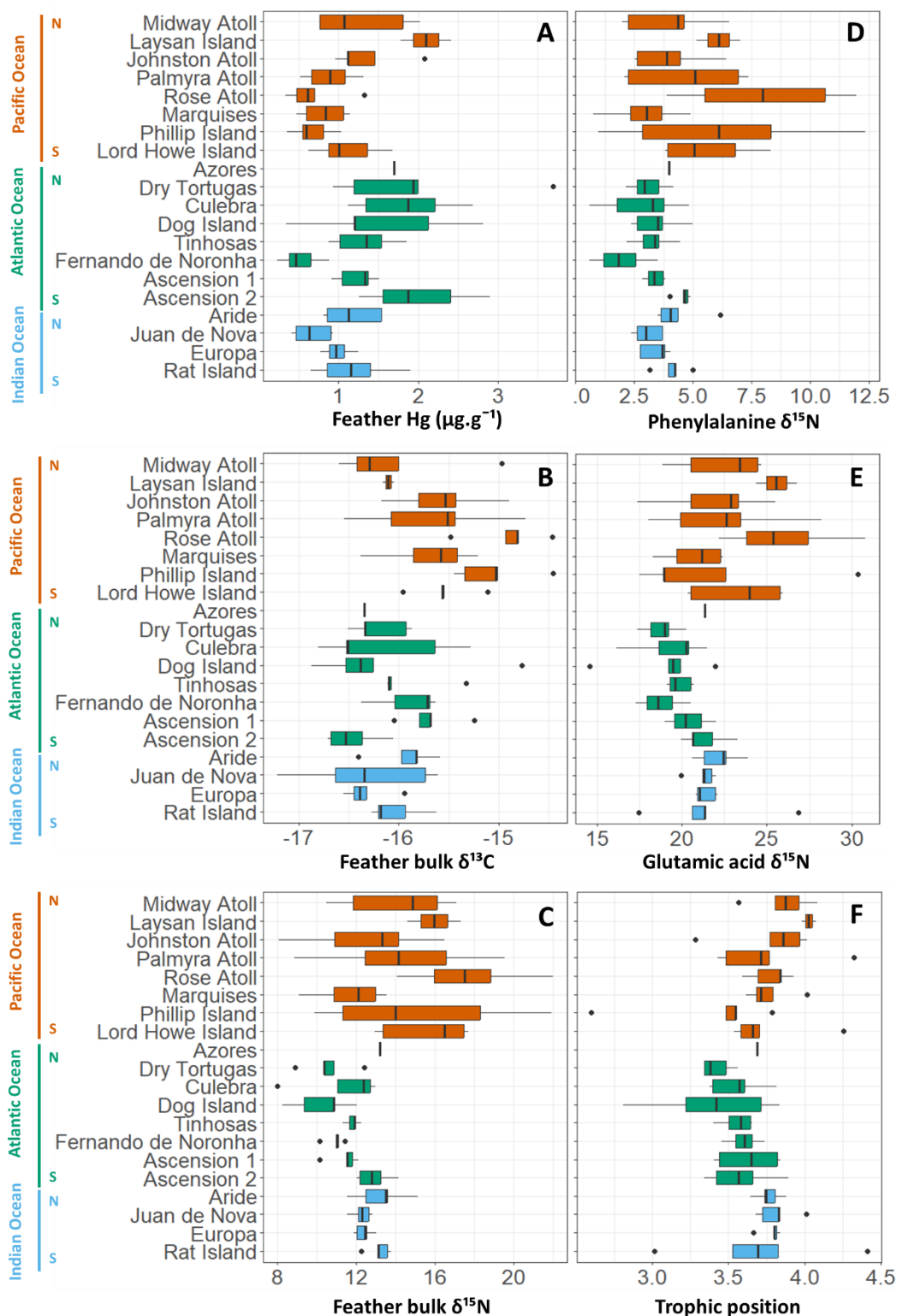


Figure S3. Feather (A) Hg concentrations and stable isotope values of adult sooty terns ($n=91$) in tropical oceans (i.e., 19 sites), including bulk (B) $\delta^{13}\text{C}$ and (C) $\delta^{15}\text{N}$ values, and (D) Phenylalanine and (E) Glutamic acid $\delta^{15}\text{N}$ values, as well as (F) trophic position.

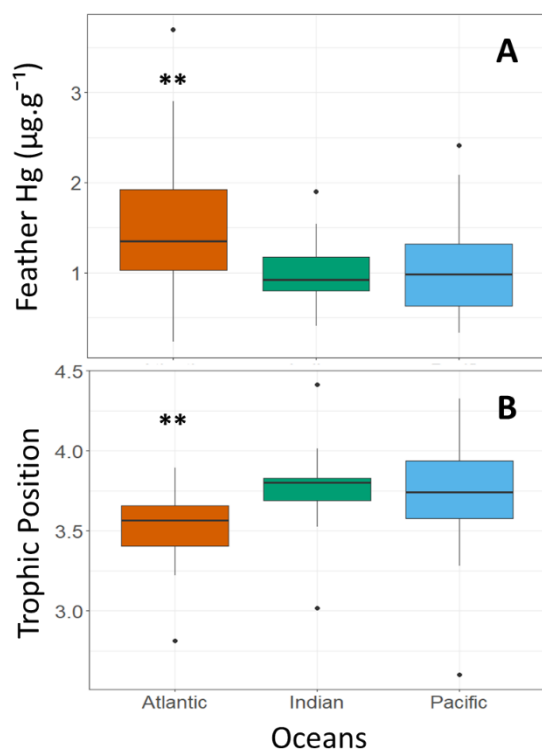


Figure S4. Difference between ocean basins in feather (A) Hg concentrations, (B) trophic position (calculated from $\delta^{15}\text{N}$ values of glutamic acid and phenylalanine; cf. **Material and Methods**) from adult sooty terns ($n=91$; CSIA subset). The symbol ** indicates when a site was statistically different with others.

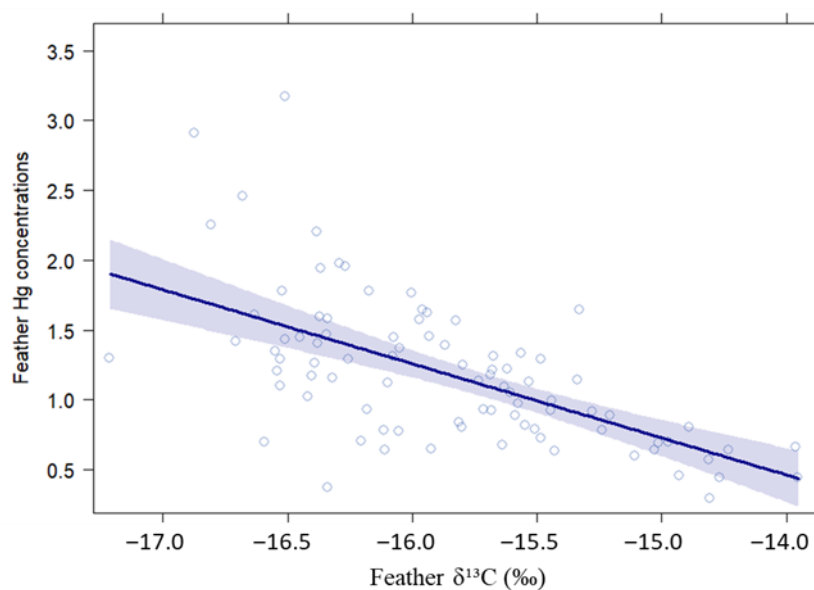


Figure S5. Relationship (regression and confidence interval) between feather Hg concentrations and bulk $\delta^{13}\text{C}$ values in adult sooty terns (CSIA subset; $n=88$), resulting from the extraction of partial residuals of the best Generalized Linear Model (GLM; see Table 2 and Material and Methods for further details). Individual data are represented in light blue (open circle).

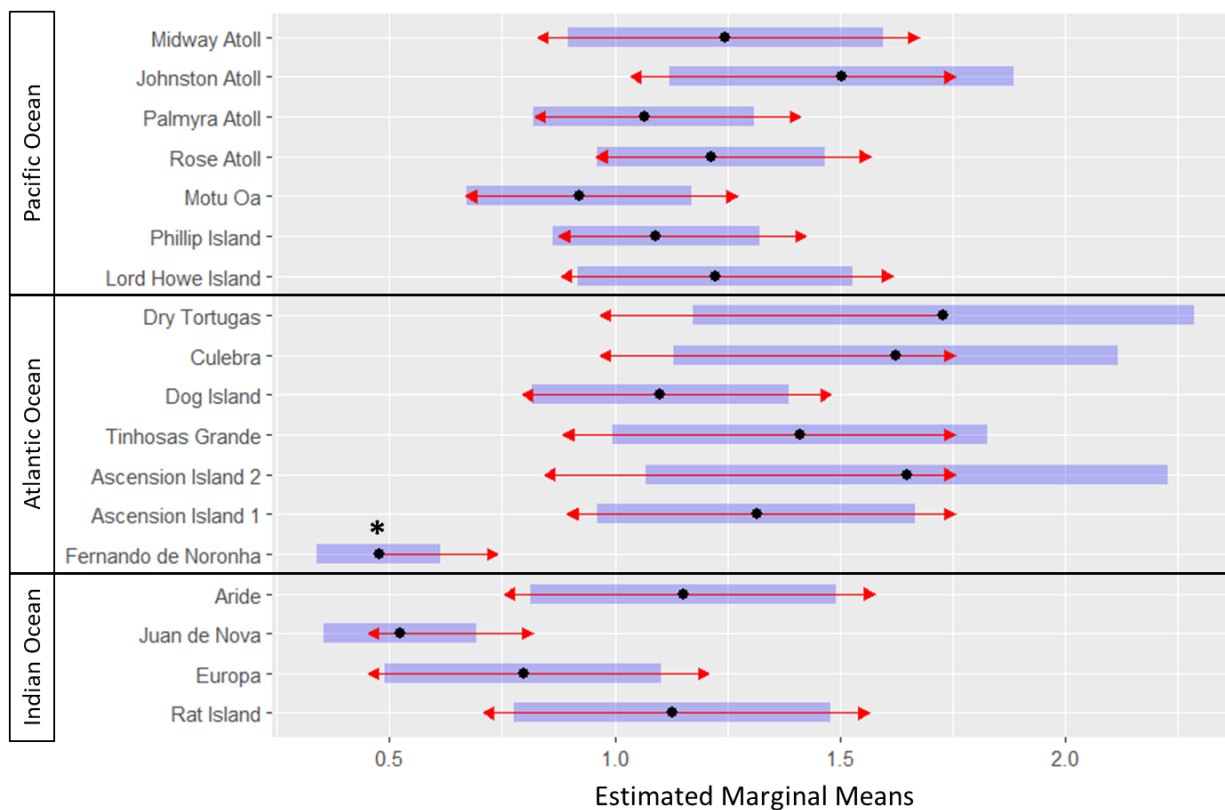


Figure S6. Estimated Marginal Means (EMM) feather Hg concentrations for adult sooty terns ($n=88$) sampled across 17 colonies in three ocean basins (Pacific, Atlantic and Indian Oceans). Estimates were derived from the best-ranked generalized linear model (GLM with Gamma distribution and identity link-function) defined as follows: $Hg \sim \delta^{13}C + Colony$ (see **Table 2** for further details). Differences were considered significant (*) when confidence intervals (red arrows) do not overlap. Ascension Island 1 and 2 refer to samples from 2020 and 2021, respectively.

Paper 2

Circumpolar assessment of mercury contamination: the Adélie penguin as a bioindicator of Antarctic marine ecosystems

Published in *Ecotoxicology*

Special Issue: *Assessing Environmental Mercury Loads in Biota and Impacts on Biodiversity to Meet the Needs of the Minamata Convention*

Fanny Cusset, Paco Bustamante, Alice Carravieri, Clément Bertin, Rebecka Brasso, Ilaria Corsi, Michael Dunn, Louise Emmerson, Gaël Guillou, Tom Hart, Mariana Juárez, Akiko Kato, Ana Laura Machado, Candice Michelot, Silvia Olmastroni, Michael Polito, Thierry Raclot, Mercedes Santos, Annie Schmidt, Colin Southwell, Alvaro Soutullo, Akinori Takahashi, Jean-Baptiste Thiébot, Phil Trathan, Pierre Vivion, Claire Waluda, Jérôme Fort and Yves Cherel.





Circumpolar assessment of mercury contamination: the Adélie penguin as a bioindicator of Antarctic marine ecosystems

Fanny Cusset^{1,2} · Paco Bustamante^{1,3} · Alice Carravieri^{1,2} · Clément Bertin¹ · Rebecka Brasso⁴ · Ilaria Corsi⁵ · Michael Dunn⁶ · Louise Emmerson⁷ · Gaël Guillou¹ · Tom Hart⁸ · Mariana Juárez^{9,10} · Akiko Kato² · Ana Laura Machado-Gaye¹¹ · Candice Michelot^{2,12} · Silvia Olmastroni^{5,13} · Michael Polito¹⁴ · Thierry Raclot¹⁵ · Mercedes Santos⁹ · Annie Schmidt¹⁶ · Colin Southwell⁷ · Alvaro Soutullo¹¹ · Akinori Takahashi¹⁷ · Jean-Baptiste Thiebot^{17,18} · Phil Trathan⁶ · Pierre Vivion¹ · Claire Waluda⁶ · Jérôme Fort¹ · Yves Cherel^{1,2}

Accepted: 11 October 2023 / Published online: 25 October 2023

© The Author(s), under exclusive licence to Springer Science+Business Media, LLC, part of Springer Nature 2023

Abstract

Due to its persistence and potential ecological and health impacts, mercury (Hg) is a global pollutant of major concern that may reach high concentrations even in remote polar oceans. In contrast to the Arctic Ocean, studies documenting Hg contamination in the Southern Ocean are spatially restricted and large-scale monitoring is needed. Here, we present the first circumpolar assessment of Hg contamination in Antarctic marine ecosystems. Specifically, the Adélie penguin (*Pygoscelis adeliae*) was used as a bioindicator species, to examine regional variation across 24 colonies distributed across the entire Antarctic continent. Mercury was measured on body feathers collected from both adults ($n = 485$) and chicks ($n = 48$) between 2005 and 2021. Because penguins' diet represents the dominant source of Hg, feather $\delta^{13}\text{C}$ and $\delta^{15}\text{N}$ values were measured as proxies of feeding habitat and trophic position. As expected, chicks had lower Hg concentrations (mean \pm SD: $0.22 \pm 0.08 \mu\text{g}\cdot\text{g}^{-1}$) than adults ($0.49 \pm 0.23 \mu\text{g}\cdot\text{g}^{-1}$), likely because of their shorter bioaccumulation period. In adults, spatial variation in feather Hg concentrations was driven by both trophic ecology and colony location. The highest Hg concentrations were observed in the Ross Sea, possibly because of a higher consumption of fish in the diet compared to other sites (krill-dominated diet). Such large-scale assessments are critical to assess the effectiveness of the Minamata Convention on Mercury. Owing to their circumpolar distribution and their ecological role in Antarctic marine ecosystems, Adélie penguins could be valuable bioindicators for tracking spatial and temporal trends of Hg across Antarctic waters in the future.

✉ Fanny Cusset
 cussetfanny@gmail.com

¹ Littoral, Environnement et Sociétés (LIENSs), UMR 7266 CNRS - La Rochelle Université, 2 Rue Olympe de Gouges, 17000 La Rochelle, France

² Centre d'Études Biologiques de Chizé (CEBC), UMR 7372 du CNRS - La Rochelle Université, 79360 Villiers-en-Bois, France

³ Institut Universitaire de France (IUF), 1 rue Descartes, 75005 Paris, France

⁴ Department of Zoology, Weber State University, Ogden, UT, USA

⁵ Department of Physical, Earth and Environmental Sciences, University of Siena, 53100 Siena, Italy

⁶ British Antarctic Survey, Cambridge, UK

⁷ Department of Climate Change, Energy, the Environment and Water, Australian Antarctic Division, Canberra, ACT, Australia

⁸ Department of Biological and Medicinal Sciences, Oxford Broke University, Oxford, UK

⁹ Departamento Biología de Predadores Tope, Instituto Antártico Argentino, Buenos Aires, Argentina

¹⁰ Consejo Nacional de Investigaciones Científicas y Técnicas (CONICET), Ciudad Autónoma de Buenos Aires, Buenos Aires, Argentina

¹¹ Centro Universitario Regional del Este, Universidad de la República, Maldonado, Uruguay

¹² Institut Maurice-Lamontagne, Pêches et Océans Canada, Mont-Joli, QC, Canada

¹³ Museo Nazionale dell'Antartide, Siena, Italy

¹⁴ Louisiana State University, Baton Rouge, LA, USA

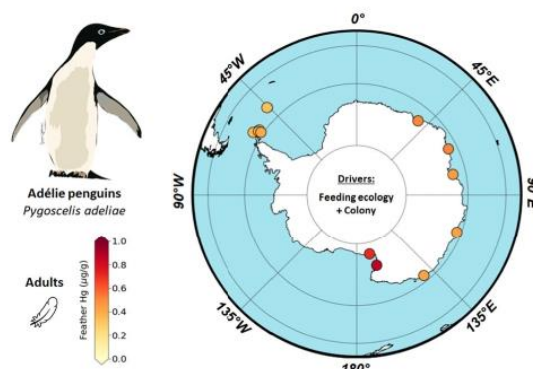
¹⁵ Institut Pluridisciplinaire Hubert Curien, UMR 7178 du CNRS, Université de Strasbourg, 67087 Strasbourg, France

¹⁶ Point Blue Conservation, Petaluma, CA, USA

¹⁷ National Institute of Polar Research, 10-3 Midori-cho, Tachikawa, Tokyo 190-8518, Japan

¹⁸ Graduate School of Fisheries Sciences, Hokkaido University, Minato-cho 3-1-1, Hakodate 041-8611, Japan

Graphical Abstract



Keywords Feathers · Hg · Marine food web · Seabirds · Stable Isotopes · Southern Ocean

Highlights

- Adélie penguins are relevant bioindicators of Hg contamination in Antarctic marine ecosystems.
- Feather Hg concentrations were measured in 24 breeding colonies (adults and chicks).
- The highest Hg concentrations were found in the Ross Sea.
- Both trophic ecology and colony location drove feather Hg concentrations.

Introduction

Mercury (Hg) is a global pollutant of both natural and anthropogenic origin (Sonke et al. 2023). Since the Industrial Revolution, anthropogenic activities, such as chemical manufacturing, gold-mining and coal combustion (Streets et al. 2017), have released considerable amounts of Hg into the environment, resulting in a three- to five-fold increase of Hg globally (Lamborg et al. 2014; Selin 2009). Yet, this non-essential and toxic metal is of global concern due to its adverse effects on wildlife and human health (NRC/NAS 2000; Ackerman et al. 2016; Dietz et al. 2019; Roman et al. 2011; Scheuhammer et al. 2012; Tan et al. 2009). As a reaction, the Minamata Convention on Mercury was adopted in 2013 (implemented in 2017) by more than 140 countries, to protect human health and the environment worldwide. Today, large-scale monitoring of environmental Hg contamination is required to assess the effectiveness of this international treaty and guide its future directions.

Mercury disperses worldwide mainly through atmospheric currents and deposits even in the most remote oceanic regions, such as polar oceans (UN-Environment 2019). These oceans are facing significant modifications due to climate change, which alters the biogeochemical cycle of Hg (Chételat et al. 2022; McKinney et al. 2022) and ultimately its transfer in marine food webs (Zhou

et al. 2023). In the Arctic Ocean, Hg contamination has been extensively documented over large temporal and spatial scales (e.g., Albert et al. 2021; Bond et al. 2015; Desforges et al. 2022; Dietz et al. 2022). In the Southern Ocean (*sensu lato*, i.e., water masses south of the Sub-tropical Front; Carter et al. 2008; Orsi et al. 1995), studies are more spatially restricted mainly due to logistical constraints, with a focus on local and/or regional scales (but see Brasso et al. 2015; Carravieri et al. 2017; Cherel et al. 2018). This is particularly the case in the Antarctic Zone (i.e., water masses south of the Polar Front; Carter et al. 2008; Orsi et al. 1995). This critical gap in sampling areas can be filled by using bioindicator species that closely rely on marine food webs from these specific areas, such as seabirds (e.g., Burger and Gochfeld 2004; Furness and Camphuysen 1997). As meso- to top predators, seabirds are abundant consumers of the world's marine resources. Due to biomagnification processes, they reflect Hg contamination of their marine food webs (Braune et al. 2015; Fort et al. 2016; Piatt et al. 2007). Food intake is the major source of Hg in seabirds, and thus assessing their feeding ecology and spatial distribution is needed to disentangle ecological drivers of Hg contamination (Carravieri et al. 2014b; Cherel et al. 2018). Specifically, accounting for feeding ecology is key to identify whether spatial variation in Hg contamination is linked to dietary differences (Brasso et al. 2015;

Carravieri et al. 2014c; Gatt et al. 2020) and/or to other environmental factors (Foster et al. 2019; Furtado et al. 2021; Tartu et al. 2022).

Once assimilated by seabirds, Hg is distributed *via* blood to internal tissues where it bioaccumulates (i.e., Hg concentrations increase over time) between moulting periods. During moult, stored Hg is remobilised and up to 90% of the total Hg body burden is excreted into growing feathers (Honda et al. 1986), where it binds to keratin proteins (Crewther et al. 1965). Hence, moult represents the main excretion pathway for Hg in seabirds (Thompson et al. 1990; Thompson and Furness 1989). Feathers incorporate the cumulative signal of Hg exposure between two moulting episodes (i.e., over several weeks/months to up to one year in most species; Albert et al. 2019). Sampling seabird feathers thus represent a powerful monitoring opportunity to investigate Hg contamination in marine food webs over large temporal and spatial scales, especially in the remote Southern Ocean.

Penguins constitute the largest seabird biomass in the Southern Ocean and consume several million tons of marine resources annually (Knox 2006; Southwell et al. 2017; Williams 1995). Available evidence suggests that they exploit similar marine resources over both the short-term (breeding season) and the long-term (non-breeding season; Chérel et al. 2007; Polito et al. 2016; Tierney et al. 2009). Therefore, penguins are adequate bioindicator species to monitor Hg contamination in Antarctic marine food webs (Brasso et al. 2015; Carravieri et al. 2013). Among seabirds, penguins present a unique moulting pattern. Following a pre-moult foraging period of hyperphagia at sea, they renew their entire plumage annually while fasting ashore or on sea ice (a few weeks; Chérel et al. 1994; Emmerson et al. 2019), less frequently at the breeding colonies (Ainley 2002). All body feathers are thus moulted simultaneously every year. Within each individual penguin, all body feathers have thus the same chemical signature, including Hg concentrations and stable isotope values (Brasso et al. 2013; Carravieri et al. 2014a). Since the 1980s, 20 studies documented Hg contamination in feathers of eight penguin species from the Southern Ocean, including species breeding both in the Subantarctic (i.e., water masses between the Subtropical and Polar Fronts) and Antarctic Zones (see Table S1 for a complete review). Whereas contamination from sub-antarctic islands has been well documented, spatial coverage is limited to local and regional investigations in the Antarctic. For example, out of the 14 studies on Hg in the Antarctic Zone, nine (64%) were carried out in the South Shetland Islands only (e.g. Álvarez-Varas et al. 2018; Becker et al. 2016; Brasso et al. 2015; Matias et al. 2022; Souza et al. 2020). Other documented regions include the coasts of Queen Maud Land, Adélie Land and Victoria Land (Ross Sea) (Bargagli et al. 1998; Carravieri et al.

2016; Pilcher et al. 2020; Yamamoto et al. 1996). To date, most Antarctic regions where penguins breed remain unexplored. Large-scale sampling of penguin feathers is thus needed to identify potential hotspots of Hg contamination and determine the toxicological risk to Antarctic marine biodiversity, which is simultaneously threatened by other anthropogenic stressors, including climate change (Barbraud et al. 2012; Clucas et al. 2014; Lee et al. 2017; Morley et al. 2019).

The Adélie penguin (*Pygoscelis adeliae*) is an ideal candidate to reflect Hg contamination in Antarctic marine food webs. With its circumpolar distribution, it is the most common and abundant penguin species in both continental and maritime (Antarctic Peninsula and adjacent archipelagos) Antarctica. Adélie penguins forage in Antarctic waters year-round (Ballard et al. 2010; Takahashi et al. 2018; Thiebot et al. 2019) and consistently use similar feeding resources (Ainley 2002; Jafari et al. 2021; Juárez et al. 2016). The Adélie penguin is an indicator species for the Commission for the Conservation of Antarctic Marine Living Resources (CCAMLR) for the Ecosystem Monitoring Program (Agnew 1997). The latter aims (i) to ensure that krill fisheries consider the needs of krill-predators, such as seals and seabirds, and (ii) to distinguish between environmental and fishery-related changes in the Southern Ocean. Here, we take advantage of a large, international field-based scientific network, to provide the first circumpolar assessment of Hg contamination in Antarctic marine ecosystems, using feathers of Adélie penguins that breed across both continental and maritime Antarctica. The aims of this study were four-fold. The first aim was to quantify current Hg contamination of Antarctic marine food webs, by focussing on this key higher-order indicator species at a circumpolar scale. Given the unique oceanographic features of the Southern Ocean (i.e., circumpolar circulation), relatively homogenous Hg concentrations were expected across all Adélie penguin colonies. The second aim was to identify potential Hg hotspots by assessing Hg contamination over different spatial and temporal scales, using pre-fledging chick feathers, which reflect short-term, local contamination (~two months during the breeding season only), and adult feathers, which integrate a geographically larger scale over one year (incorporating both the breeding and non-breeding seasons). Because of longer exposure to Hg, adults were expected to have higher Hg concentrations than chicks (Stewart et al. 1997; Thompson et al. 1991). The third aim was to investigate the influence of penguin trophic ecology on spatial patterns of Hg contamination, by using feather carbon ($\delta^{13}\text{C}$) and nitrogen ($\delta^{15}\text{N}$) stable isotopes, as proxies of feeding habitat and trophic position, respectively (Kelly 2000; Newsome et al. 2007). Mercury and stable isotopes are uncoupled in feathers (Bond 2010), yet provide relevant information on

feeding ecology for the understanding of Hg contamination. As for other species and regions, trophic ecology was expected to be a major driver of spatial differences of Hg contamination in Antarctic marine ecosystems (e.g., Becker et al. 2002; Bustamante et al. 2016; Carravieri et al. 2014c; Mills et al. 2020). Finally, the last aim was to investigate sex differences in both Hg contamination and trophic ecology using a subset of adult Adélie penguins from various colonies.

Material and methods

Feather collection and preparation

This comprehensive assessment brings together published and new Hg concentrations for Adélie penguin feathers (Tables 1 and 2). Overall, 538 individuals of Adélie penguins (490 breeding adults and 48 pre-fledging chicks) were sampled between 2005 and 2021, in 24 colonies around Antarctica ($n = 5\text{--}40$ individuals per colony; Fig. 1). Sample sizes for each colony are provided in Table 1 (adults) and 2 (chicks), and geographical coordinates of sampled colonies are detailed in the Supplementary Material (Table S2). For both adults and chicks, body feathers were sampled for two reasons: (i) they are generally considered to be the best feather type to sample (Furness et al. 1986) and (ii) in penguins, they represent the majority of the plumage (no flight feather). Therefore, 1–5 body feathers from the breast or the back were collected for each individual, because of their complete and drastic moulting strategy (Brasso et al. 2013; Cherel et al. 1994). In a limited number of colonies, where no other pygoscelid penguin breeds, freshly molted feathers were also collected from the ground (i.e., in Shirley Island, Brown Bluffs, Madder Cliffs and Paulet Island; feather sampling locations in each of these colonies were at least several nests away from each other to avoid pseudoreplication; minimum distance = 15 m). Feathers were then stored in either plastic bags or paper envelopes and kept at room temperature until laboratory analyses.

In adults, feather moult starts when the penguins are still at sea, building body reserves during the pre-moulting period (Cherel et al. 1993, 1994; Croxall 1982). The part of the feather that grows at this time (i.e., the tip) thus reflects the pre-moult feeding period at sea. In contrast, the remaining feather that grows during moult reflects the fasting period on sea ice or ashore, and hence the dietary signature from accumulated body reserves. Given the difference in integration of dietary information (stable isotopes) during these two periods, feather's tip (i.e., 5 mm) was cut and discarded. Both Hg and stable isotopes were

analysed in the remaining feather. In order to avoid any external contamination, feathers were cleaned with a chloroform:methanol mixture (2:1), sonicated for 3 min, rinsed twice with methanol and dried at 45 °C for 48 h. Given the homogenous chemical composition of body feathers in penguins (Brasso et al. 2013; Carravieri et al. 2014a), measurements were made on a single randomly-selected feather for each bird, which was cut with precision (stainless steel) scissors to obtain a homogenous powder to be analysed for both Hg and stable isotopes.

Mercury analyses

Total Hg (THg) includes both inorganic and organic Hg (mainly methyl-Hg, MeHg). In feathers, >90% of THg is in the form of MeHg (Renedo et al. 2017), the most toxic and bioavailable form that bioaccumulates and biomagnifies in marine food webs (Cossa 2013). Therefore, we used THg as a proxy of MeHg in Adélie penguin feathers.

Mercury analyses were performed on feather homogenates (0.5–1.5 mg) in duplicate, using an Advanced Mercury Analyser (AMA 254, Altech). When the relative standard deviation (RSD) between duplicates was <10%, Hg concentrations were averaged for each sample. When the RSD was >10%, an additional sample of the homogenate was analysed, and the duplicates guaranteeing the lowest RSD were kept for average calculations. The AMA quantification limit was 0.1 ng. Blanks and two certified reference materials (TORT3 – Lobster hepatopancreas, DOLT5 – Fish liver, NRC Canada) were analysed during each analytical session to guarantee accuracy (Table S3). Recovery values were 100.6 ± 2.3 and $96.7 \pm 2.6\%$, respectively. Concentrations are expressed as $\mu\text{g}\cdot\text{g}^{-1}$ dry weight (dw).

Stable isotope analyses

Carbon and nitrogen stable isotope analyses were performed on feather homogenates (0.2–0.8 mg), loaded into tin cups (8 × 5 mm; Elemental Microanalysis Ltd, Okehampton, UK) using a microbalance (XPRUD5, Mettler Toledo, Greifensee, Switzerland). Values of $\delta^{13}\text{C}$ and $\delta^{15}\text{N}$ were determined with a continuous flow isotope ratio mass spectrometer (Delta V Plus with a Conflo IV Interface, Thermo Scientific, Bremen, Germany) coupled to an elemental analyzer (Flash 2000 or Flash IRMS EA Isolink CN, Thermo Scientific, Milan, Italy). Results are expressed in the usual δ unit notation relative to Vienna PeeDee Belemnite for $\delta^{13}\text{C}$ (‰) and atmospheric N_2 for $\delta^{15}\text{N}$ (‰), following the formula:

$$\delta^{13}\text{C} \text{ or } \delta^{15}\text{N} = \left[\left(\frac{R_{\text{sample}}}{R_{\text{standard}}} \right) - 1 \right] \times 10^3$$

Table 1 Mercury concentrations and stable isotope values from adult Adélie penguins (*Pygoscelis adeliae*) sampled around Antarctica, from both this study (included in the analyses) and literature review (for comparison; not included in the analyses)

Sites, colonies	Season	n	Feather Hg ($\mu\text{g}\cdot\text{g}^{-1}$ dw)	Feather $\delta^{13}\text{C}$ (‰)	Feather $\delta^{15}\text{N}$ (‰)	References	Included
Continental Antarctica							
Queen Maud Land							
Hukuro Cove	2010/2011	27	0.51 ± 0.15 (0.32–0.92)	−23.9 ± 1.5 (−25.7, −22.9)	10.1 ± 1.4 (8.6–12.1)	This study	Yes
	1990/1991	10	0.09 ± 0.05	–	–	Yamamoto et al. (1996)	No
	1981/1982	10	0.17 ± 0.05 (0.11–0.27)	–	–	Honda et al. (1986)	No
Rumapa Island							
Mac. Robertson Land							
Welch Island	2019/2020	15	0.40 ± 0.11 (0.21–0.59)	−25.0 ± 0.4 (−25.8, −24.4)	9.7 ± 0.5 (8.8–10.8)	This study	Yes
Macey Island	2019/2020	15	0.63 ± 0.19 (0.31–0.98)	−25.0 ± 0.3 (−25.3, −24.2)	10.5 ± 0.8 (9.6–12.3)	This study	Yes
Princess Elizabeth Land							
Hop Island	2019/2020	5	0.36 ± 0.13 (0.22–0.50)	−24.7 ± 0.5 (−25.4, −24.2)	9.8 ± 0.9 (8.8–10.9)	This study	Yes
Magnetic Island	2019/2020	5	0.53 ± 0.22 (0.29–0.76)	−24.5 ± 0.4 (−24.9, −24.0)	10.0 ± 0.8 (8.9–10.8)	This study	Yes
Un-named Island IS 73413*	2019/2020	5	0.46 ± 0.15 (0.29–0.69)	−24.6 ± 0.4 (−25.1, −24.0)	10.1 ± 0.5 (9.5–10.6)	This study	Yes
Wilkes Land							
Shirley Island	2020/2021	40	0.43 ± 0.15 (0.19–0.79)	−24.9 ± 0.5 (−25.8, −23.9)	9.5 ± 0.6 (8.5–10.8)	This study	Yes
Adélie Land							
Dumont d'Urville	2006/2007	10	0.66 ± 0.20 (0.41–1.06)	−23.4 ± 0.4 (−24.2, −23.0)	10.7 ± 0.6 (9.7–11.3)	Carravieri et al. (2016)	Yes
	2011/2012	10	0.40 ± 0.09 (0.25–0.52)	−24.3 ± 0.7 (−25.6, −23.3)	10.8 ± 0.7 (9.8–11.9)	Carravieri et al. (2016)	Yes
	2017/2018	15	0.41 ± 0.11 (0.25–0.60)	−24.9 ± 0.4 (−25.7, −24.4)	8.9 ± 0.3 (8.4–9.7)	This study	Yes
Cape Bienvenue	2017/2018	14	0.42 ± 0.13 (0.27–0.77)	−24.5 ± 0.6 (−25.7, −23.6)	9.2 ± 0.4 (8.5–10.1)	This study	Yes
Cape Jules	2017/2018	15	0.44 ± 0.14 (0.23–0.68)	−25.3 ± 0.7 (−26.6, −24.3)	9.1 ± 0.5 (8.2–10.2)	This study	Yes
Victoria Land (Ross Sea)							
Terra Nova Bay							
Adélie Cove	2017/2018	15	0.92 ± 0.25 (0.49–1.35)	−24.4 ± 0.8 (−25.6, −22.5)	11.0 ± 1.0 (9.9–12.8)	This study	Yes
Inexpressible Island	2017/2018	15	0.83 ± 0.26 (0.50–1.33)	−24.5 ± 0.9 (−25.6, −22.8)	10.9 ± 1.0 (9.0–12.8)	This study	Yes
Edmonson Point	2017/2018	15	0.83 ± 0.18 (0.50–1.18)	−24.5 ± 0.7 (−25.8, −23.6)	10.6 ± 0.6 (9.8–11.6)	This study	Yes
Ross Island							
Cape Crozier	2019/2020	15	0.62 ± 0.12 (0.46–0.92)	−25.9 ± 0.3 (−26.5, −25.4)	9.8 ± 0.5 (9.1–10.9)	This study	Yes
Cape Royds	2019/2020	15	0.80 ± 0.19 (0.56–1.08)	−25.4 ± 0.8 (−25.9, −22.8)	10.3 ± 0.8 (9.2–11.9)	This study	Yes
Cape Bird	2004–2016	154	0.59 ± 0.17	–	–	Plicher et al. (2020)	No
Cape Hallett, Cape Adare	2004–2016	20	0.50 ± 0.10	–	–	Plicher et al. (2020)	No
Multiple sites							
Cape Bird, Cape Hallett, Cape Adare	2004–2016	174	0.59 ± 0.02	−25.3 ± 0.6	9.0 ± 0.7	Plicher et al. (2020)	No

Table 1 (continued)

Sites, colonies	Season	n	Feather Hg ($\mu\text{g}\cdot\text{g}^{-1}$ dw)	Feather $\delta^{13}\text{C}$ (‰)	Feather $\delta^{15}\text{N}$ (‰)	References	Included
Maritime Antarctica							
King George/25 de Mayo Island	2021/2022	11	0.32 ± 0.06 (0.24–0.41)	−24.9 ± 0.3 (−25.3, −24.4)	9.3 ± 0.2 (9.0–9.7)	This study	Yes
Ardley Island	2005/2006	20	0.35 ± 0.16 (0.20–0.90)	−24.9 ± 0.7 (−25.7, −23.3)	8.8 ± 0.4 (8.1–9.7)	Brasso et al. (2013, 2014, 2015)	Yes
Admiralty Bay	2006/2007	20	0.25 ± 0.12 (0.16–0.70)	−25.0 ± 0.3 (−25.7, −24.6)	8.7 ± 0.3 (8.1–9.6)	Brasso et al. (2013, 2014, 2015)	Yes
	2007/2008	20	0.38 ± 0.11 (0.21–0.65)	−24.8 ± 0.5 (−25.3, −23.9)	8.9 ± 0.3 (8.5–9.7)	Brasso et al. (2013, 2014, 2015)	Yes
	2008/2009	16	0.35 ± 0.08 (0.18–0.47)	−24.6 ± 0.5 (−25.3, −23.8)	8.9 ± 0.5 (8.3–10.5)	Brasso et al. (2013, 2014, 2015)	Yes
	2009/2010	22	0.35 ± 0.14 (0.18–0.69)	−23.9 ± 0.8 (−25.4, −22.4)	9.1 ± 0.4 (8.0–10.1)	Brasso et al. (2013, 2014, 2015)	Yes
	2010/2011	22	0.35 ± 0.14 (0.18–0.69)	−24.1 ± 1.1 (−27.4, −22.4)	9.1 ± 0.4 (8.0–10.1)	Brasso et al. (2013, 2014, 2015), Polito et al. (2016)	Yes
	2005–2011	120	0.34 ± 0.13 (0.16–0.90)	−24.5 ± 0.8 (−27.4, −22.4)	8.9 ± 0.4 (8.0–10.5)	Brasso et al. (2013, 2014, 2015)	Yes
Carlini (Stranger Point)	2019/2020	10	0.39 ± 0.09 (0.23–0.57)	−25.2 ± 0.5 (−26.3, −24.7)	9.0 ± 0.3 (8.5–9.7)	This study	Yes
Hennequin Point, Hannah Point	2013/2014	31	0.40 ± 0.13 (0.16–0.69)	–	–	Souza et al. (2020)	No
Antarctic Peninsula							
Esperanza/Hope Bay	2019/2020	10	0.37 ± 0.10 (0.17–0.51)	−23.2 ± 1.3 (−24.3, −20.1)	8.7 ± 0.3 (8.4–9.3)	This study	Yes
Brown Bluffs	2019/2020	13	0.37 ± 0.30 (0.11–1.22)	−21.8 ± 1.8 (−24.7, −19.9)	9.7 ± 1.1 (8.5–9.7)	This study	Yes
Seymour Island							
Mirambio	2019/2020	10	0.41 ± 0.09 (0.29–0.54)	−22.7 ± 0.7 (−24.1, −21.9)	8.8 ± 0.3 (8.0–9.2)	This study	Yes
Joinville Island Group							
Madder Cliffs	2019/2020	15	0.23 ± 0.12 (0.09–0.48)	−22.5 ± 1.5 (−25.9, −20.9)	9.8 ± 0.9 (8.7–12.0)	This study	Yes
Paulet Island	2019/2020	15	0.18 ± 0.11 (0.06–0.40)	−22.9 ± 1.4 (−25.5, −20.7)	9.3 ± 0.3 (8.6–10.0)	This study	Yes
Signy Island							
Gourlay	2021/2022	30	0.33 ± 0.10 (0.21–0.62)	−25.6 ± 0.4 (−26.1, −24.4)	8.9 ± 0.3 (8.3–10.1)	This study	Yes

n indicates sample sizes. Feather $\delta^{13}\text{C}$ and $\delta^{15}\text{N}$ values are proxies of penguin feeding habitat and trophic position, respectively. Values are expressed as means ± SD with ranges in parentheses

– No available data (stable isotopes)

*Alpha-numeric identifier in Southwell et al. (2021)

Table 2 Mercury concentrations and stable isotope values from Adélie penguin chicks sampled around Antarctica, from both this study (included in the analyses) and a literature review (for comparison; not included in the analyses)

Sites, colonies	Season	<i>n</i>	Feather Hg ($\mu\text{g}\cdot\text{g}^{-1}\cdot\text{dw}$)	Feather $\delta^{13}\text{C}$ (‰)	Feather $\delta^{15}\text{N}$ (‰)	References	Included
Continental Antarctica							
Queen Maud Land							
Hukuro Cove	1990/1991	12	0.04 ± 0.02	–	–	Yamamoto et al. (1996)	No
Princess Elizabeth Land							
Un-named Island IS 73413*	2019/2020	5	0.25 ± 0.06 (0.19–0.32)	–23.3 ± 1.0 (–24.8, –21.9)	12.0 ± 0.7 (11.3–12.9)	This study	Yes
Magnetic Island	2019/2020	4	0.23 ± 0.03 (0.18–0.25)	–23.4 ± 0.2 (–23.6, –23.2)	11.1 ± 0.2 (10.8–11.3)	This study	Yes
Hop Island	2019/2020	4	0.20 ± 0.08 (0.14–0.32)	–24.3 ± 1.6 (–25.6, –22.2)	10.1 ± 0.8 (9.4–11.1)	This study	Yes
Adélie Land							
Dumont d'Urville	2006/2007	10	0.19 ± 0.06 (0.07–0.27)	–23.5 ± 0.2 (–23.9, –23.2)	10.7 ± 0.4 (10.1–11.3)	Caravieri et al. (2016)	Yes
	2011/2012	10	0.34 ± 0.04 (0.30–0.40)	–22.9 ± 0.5 (–23.2, –21.6)	11.5 ± 0.3 (11.1–12.0)	Caravieri et al. (2016)	Yes
Victoria Land (Ross Sea)							
Edmonson Point	1989–1991	11	0.37 ± 0.15	–	–	Bargagli et al. (1998)	No
Maritime Antarctica							
King George/25 de Mayo Island							
Carlini (Stranger Point)	2019/2020	5	0.12 ± 0.02 (0.09–0.14)	–25.0 ± 0.2 (–25.2, –24.9)	7.6 ± 0.3 (7.2–8.1)	This study	Yes
Hennequin Point + Hannah Point	2013/2014	10	0.10 ± 0.01 (0.07–0.13)	–	–	Souza et al. (2020)	No
Antarctic Peninsula							
Esperanza/Hope Bay	2013/2014	18	0.32 ± 0.14 (0.14–0.63)	–23.7 ± 0.7 (–24.6, –22.0)	8.0 ± 0.5 (7.5–9.7)	McKenzie et al. (2021)	No
	2019/2020	5	0.16 ± 0.01 (0.14–0.18)	–23.5 ± 0.4 (–23.9, –23.0)	7.5 ± 0.3 (7.2–7.8)	This study	Yes
Scymour Island							
Penguin Point	2013/2014	20	0.57 ± 0.20 (0.23–1.05)	–20.0 ± 1.2 (–23.2, –18.9)	11.2 ± 1.1 (7.8–13.4)	McKenzie et al. (2021)	No
Marambio	2019/2020	5	0.23 ± 0.02 (0.19–0.25)	–20.6 ± 0.6 (–21.7, –20.2)	9.1 ± 0.4 (8.6–9.4)	This study	Yes

n indicates sample sizes. Feather $\delta^{13}\text{C}$ and $\delta^{15}\text{N}$ values are proxies of penguin feeding habitat and trophic position, respectively. Values are means ± SD with ranges in parentheses

– No available data (stable isotopes)

*Alpha-numeric identifier in Southwell et al. (2021)

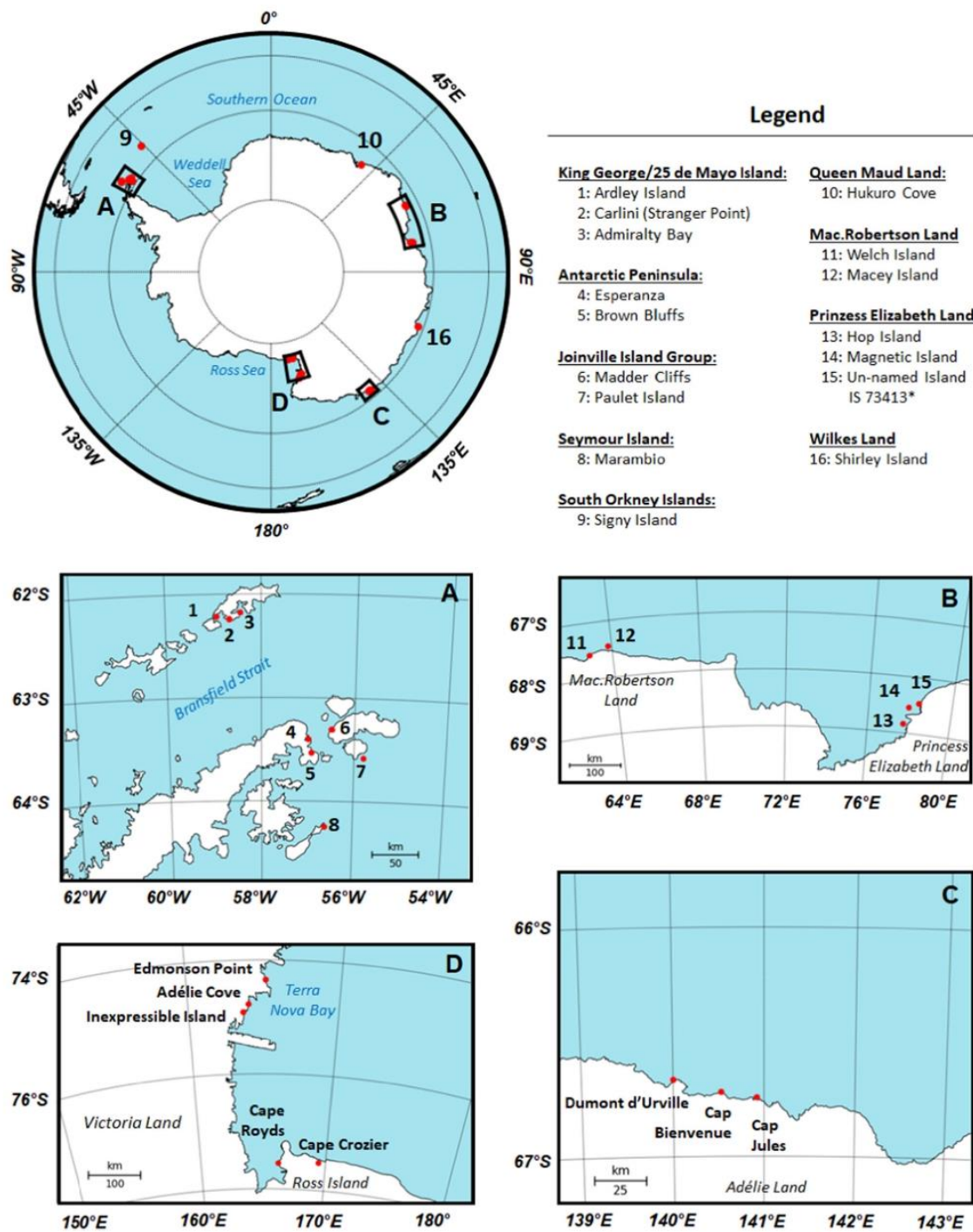


Fig. 1 Sampling colonies of the present study ($n = 24$), where feathers of Adélie penguins (*Pygoscelis adeliae*; both adults and chicks) were collected during the breeding season, between 2005 and 2021 (see Tables 1 and 2 for further details)

where R is $^{13}\text{C}/^{12}\text{C}$ or $^{15}\text{N}/^{14}\text{N}$, respectively. Replicate measurements of reference materials (USGS-61 and USGS-63, US Geological Survey) indicated measurement uncertainties $<0.10\%$ for both $\delta^{13}\text{C}$ and $\delta^{15}\text{N}$ values. Further methodological details are provided in the Supplementary Material.

Combining feather Hg and stable isotopes

While Hg and stable isotopes are both incorporated during feather growth, their integration period is temporally uncoupled in adult seabirds (Bond 2010). Feathers indicate Hg accumulation in the whole body since the previous moult (i.e., integration period: one year in adult penguins), a temporal period that includes different stages of their life cycle (i.e., non-breeding, migration/return to colony, breeding, post-breeding dispersal and moult). In contrast, stable isotopes represent the diet during feather synthesis (i.e., integration period: a few weeks corresponding to the pre-moult foraging period). However, available evidence suggests that Adélie penguins consistently use similar feeding resources during the non-breeding period (Polito et al. 2016; Tierney et al. 2009). Thus, stable isotopes are still relevant to understand the ecological drivers of Hg contamination in adult Adélie penguins. In large fledging chicks, there is no such temporal mismatch between Hg concentrations and stable isotopes, as both are incorporated during the growth of body feathers and reflect local contamination and diet during the same period (chick-rearing period; ~two months in summer).

Statistical analyses

Data analyses and representation («ggplot2» package; Wickham 2016) were carried out with R (Version 4.2.2, R Core Team 2022).

During data exploration, five feather samples showed extremely high $\delta^{13}\text{C}$ values, which are theoretically associated with either a coastal/benthic or a northern environment instead of offshore/pelagic Antarctic $\delta^{13}\text{C}$ values, as expected (Carravieri et al. 2014b; Cherel and Hobson 2007). Feather Hg and stable isotope values for these five individuals are presented in Supplementary Material (Table S4). Following a conservative approach, these values were considered to be outliers and were therefore excluded from statistical analyses and figures.

Spatial variation in Hg contamination and trophic ecology

Unifactorial analyses were performed to investigate independently differences in feather Hg concentrations and $\delta^{13}\text{C}$ and $\delta^{15}\text{N}$ values between colonies. Residual normality and

homoscedasticity were examined with Shapiro-Wilk and Breusch-Pagan tests («lmtest» package; Zeileis and Hothorn 2002), respectively. Since test assumptions were not met, a non-parametric (Kruskal-Wallis) test was used, followed by a multiple comparisons (Pairwise-Wilcoxon) test.

Drivers of Hg contamination and its spatial variation

Multifactorial analyses were performed to investigate simultaneously the influence of trophic ecology, colony location, sex and age class on Hg contamination. Prior to model definition, relationships between continuous variables (i.e., $\delta^{13}\text{C}$, $\delta^{15}\text{N}$) were tested using a correlation matrix to validate the simultaneous inclusion of non-collinear explanatory variables. Models were Generalized Linear Models (GLMs) with a Gaussian distribution and either identity or inverse link-functions, built using the «nlme» R package (Pinheiro et al. 2022).

We used three datasets: adults only ($n = 485$), adults of known sex ($n = 231$), and adults and pre-fledging chicks sampled at the same colony ($n = 113$), to test for different effects with the larger available sample size. Initial models for each dataset were the following: (1) $\text{Hg} \sim \delta^{13}\text{C} + \delta^{15}\text{N} + \text{Colony}$, (2) $\text{Hg} \sim \delta^{13}\text{C} + \delta^{15}\text{N} + \text{Colony} * \text{Sex}$ and (3) $\text{Hg} \sim \delta^{13}\text{C} + \delta^{15}\text{N} + \text{Colony} * \text{Age class}$.

Model selection was based on Akaike's Information Criterion adjusted for small sample sizes (AIC_c) for the three datasets. All potential combinations of variables for each dataset are presented in Table 3. Models were ranked using the «dredge» function («MuMIn» package; Bartoń 2022). Following Burnham and Anderson (2002), the model with the lowest AIC_c value and a difference of AIC_c (ΔAIC_c) > 2 when compared with the next best model was considered to be the best. Following Johnson and Omland (2004), model performance was assessed using Akaike weights (w_i). Model assumptions (residual normality, homogeneity, independence) were checked with diagnostic functions («plot» and «qqnorm»). The degree of model fit was reported by using the McFadden's R-Squared metric. Differences between colonies were then identified with Estimated Marginal Means (EMMs; «emmeans» package; Length 2023) following Bond and Diamond (2009a). Finally, partial residuals were extracted from each best model to obtain predictor effect plots («effects» package; Fox and Weisberg 2018, 2019). This allowed us to quantify and visualise Hg spatial variation by controlling variation due to both $\delta^{13}\text{C}$ and $\delta^{15}\text{N}$ values. Year was not included as an explanatory factor for two reasons: (i) year and colony were confounded for most colonies (92%) and (ii) inter-annual differences in Hg concentrations are expected to be negligible over the short term at remote locations (Brasso et al. 2014; Carravieri et al. 2016). To confirm this, we

Table 3 AIC_c model ranking from statistical analyses of feather Hg concentrations from Adélie penguins

Models	k	AIC _c	ΔAIC _c	w _i
(1) All adults (<i>n</i> = 485)				
δ¹³C + δ¹⁵N + Colony	27	-596.6	0.00	1.00
δ ¹⁵ N + Colony	26	-574.6	21.94	0.00
δ ¹³ C + Colony	26	-538.8	57.94	0.00
Colony	25	-534.1	62.48	0.00
δ ¹⁵ N	3	-393.8	202.73	0.00
δ ¹³ C	3	-204.8	391.79	0.00
NULL	2	-181.0	415.54	0.00
(2) Sexed adults (<i>n</i> = 231)*				
δ¹³C + δ¹⁵N + Colony	11	-258.4	0.00	0.58
δ¹³C + δ¹⁵N + Colony + Sex	12	-257.2	1.20	0.32
δ ¹⁵ N + Colony	10	-253.8	4.54	0.06
δ ¹⁵ N + Colony + Sex	11	-253.2	5.13	0.04
δ ¹³ C + δ ¹⁵ N + Colony * Sex	19	-246.6	11.80	0.00
δ ¹³ N + Colony * Sex	18	-242.5	15.90	0.00
Colony + Sex	10	-236.5	21.89	0.00
Colony	9	-235.4	22.92	0.00
δ ¹³ C + Colony + Sex	11	-234.4	23.95	0.00
δ ¹³ C + Colony	10	-233.4	24.94	0.00
(3) Adults and pre-fledging chicks from the same colony (<i>n</i> = 113)*				
δ¹³C + δ¹⁵N + Colony * Age class	19	-232.7	0.00	0.97
δ ¹⁵ N + Colony * Age class	18	-226.0	6.69	0.03
δ ¹³ C + Colony * Age class	18	-213.5	19.17	0.00
Colony * Age class	17	-213.4	19.28	0.00
δ ¹³ C + δ ¹⁵ N + Age class	5	-200.9	31.80	0.00
δ ¹⁵ N + Age class	4	-200.8	31.86	0.00
δ ¹⁵ N + Colony + Age class	11	-196.7	35.98	0.00
δ ¹³ C + δ ¹⁵ N + Colony + Age class	12	-194.6	38.07	0.00
Colony + Age class	10	-174.5	58.20	0.00
δ ¹³ C + Colony + Age class	11	-173.0	59.71	0.00

Models are Generalized Linear Models (GLMs) with Gamma distribution, and identity (all adults) or inverse (sexed adults and both age classes) link-functions. Models with ΔAIC_c < 2 represent very plausible models (in bold). A model with ΔAIC_c = 0 is interpreted as the best model among all the selected ones. Weights are cumulative (sum to 1)

k number of parameters, AIC_c Akaike's Information Criterion adjusted for small sample size, w_i AIC_c weights

*Only the first 10 models are showed in this table

quantified inter-annual variation in adult feather Hg concentrations of Adélie penguins at Admiralty Bay (King George/25 de Mayo Island), which were sampled across six consecutive years (between 2005 and 2011). Annual mean feather Hg concentrations ranged from 0.25 to 0.35 μg·g⁻¹, a low 0.10 μg·g⁻¹ scope that translated into a marginal statistical significance (one-way ANOVA, F_{5,114} = 2.31, *p* = 0.048).

Visual representation of Hg contamination in the presumed spatial distribution of Adélie penguins

In penguins, body feather Hg concentrations reflect exposure over a large temporal and spatial scale (see previous sections for further details; Brasso et al. 2014; Carravieri et al. 2014a). As a spatial assessment, this study aimed to match visually this year-round Hg accumulation with the presumed, year-round spatial distribution of Adélie penguins. Since the individuals sampled in this study were not tracked precisely with geolocators, their maximum distribution (i.e., including all individual tracks) during the non-breeding season was extracted from published studies (Fig. S1). Tracking data were available for six Antarctic colonies (Ballard et al. 2010; Clarke et al. 2003; Davis et al. 1996; Dunn et al. 2011; Erdmann et al. 2011; Hinke et al. 2015; Takahashi et al. 2018; Thiébot et al. 2019), resulting in a large geographical coverage that can be associated with feather Hg concentrations (Fig. S1). In addition, we used three regionally important habitat characteristics that shape penguins' spatial distribution:

- (i) the Antarctic Polar Front (PF). The PF represents an ecologically meaningful limit for the distribution of Adélie penguins (northernmost limit), as they exploit marine resources within the Antarctic Zone, remaining solely south of the PF. Following Freeman and Lovenduski (2016), the PF was defined here as the average of its weekly positions during the 2002–2014 period, with a resolution of 0.25°.
- (ii) the Marginal Ice Zone (MIZ). Within the Antarctic Zone, Adélie penguins are closely tied to sea ice, which is their main habitat year-round; they migrate to the MIZ (i.e., the transitional zone between consolidated pack ice and open water) to forage during the non-breeding season (Ballard et al. 2010; Dunn et al. 2011; Takahashi et al. 2018). Therefore, the position of the MIZ can be expected to reflect the birds' presumed distribution during their non-breeding period. Following previous work (Bliss et al. 2019; Meier et al., 2014), the MIZ was defined here as areas included within the maximum annual sea ice extent (i.e., in September) covered by at least 15% of ice, averaged on daily sea-ice concentrations over the 2003–2022 period (which encompasses our sampling years; AMSR-E/ASMR2, 3.125 km resolution, downloaded in March 2023 on <https://www.seaice.uni-bremen.de>; Spreen et al. 2008).
- (iii) the 1000 m isobath. To distinguish between neritic (i.e., over the deep Antarctic shelf) and oceanic (i.e., open-ocean) environments that Adélie penguins may exploit, the 1000 m isobath appeared to be a key habitat feature (data downloaded in March 2020 from

<https://www.ncei.noaa.gov/products/etopo-global-relief-model>; Bed Rock ETOPO1; 1 arc-min resolution; Amante and Eakins 2009).

Maps representing these three environmental characteristics with the averaged Hg concentrations for both adults and chicks were computed using Python (Version 3.7.6).

Results

Spatial differences in feather Hg concentrations and isotopic values (unifactorial analyses)

In adult Adélie penguins, individual feather Hg concentrations ranged from 0.06 to 1.35 $\mu\text{g}\cdot\text{g}^{-1}$ dw (Table 1). Unifactorial analyses revealed that mean values were significantly different between colonies (Kruskal-Wallis, $\chi^2(23) = 255.7$, $p < 0.0001$, $n = 485$). Specifically, seven colonies differed from all others (Pairwise Wilcoxon, $p < 0.001$): five colonies from Terra Nova Bay and Ross Island (i.e., highest averaged concentrations; mean: 0.80, range: 0.46–1.35 $\mu\text{g}\cdot\text{g}^{-1}$) and two colonies from Joinville Island Group (i.e., lowest averaged concentrations; mean: 0.21, range: 0.06–0.48 $\mu\text{g}\cdot\text{g}^{-1}$) (Fig. 2a).

Individual feather $\delta^{13}\text{C}$ values ranged from -27.4 to -19.9% (Table 1) and mean values differed among colonies (Kruskal-Wallis, $\chi^2(23) = 226.53$, $p < 0.0001$, $n = 485$), with those from the Antarctic Peninsula, Seymour Island and Joinville Island Group (mean: -22.6 , range: -25.9 , -19.9%) differing from the others (mean: -24.8 , range: -27.4 , -22.4% ; Fig. 2b). Individual feather $\delta^{15}\text{N}$ values ranged from 8.0 to 12.8‰ (Table 1) and mean values differed among colonies (Kruskal-Wallis, $\chi^2(23) = 249.9$, $p < 0.0001$, $n = 485$), with the lowest and highest $\delta^{15}\text{N}$ values recorded in Seymour Island (mean: 8.83, range: 8.0–9.2 ‰) and Terra Nova Bay (mean: 10.9, range: 9.0–12.8 ‰), respectively (Fig. 2c).

Drivers of feather Hg concentrations (multifactorial analyses)

Results from model selections are presented in Table 3. For all adults ($n = 485$), the best model included $\delta^{13}\text{C}$ and $\delta^{15}\text{N}$ values and the colony as significant predictors (Table 3), and explained 61% of the observed variation in feather Hg concentrations (Table 4). Feather Hg concentrations decreased and increased with $\delta^{13}\text{C}$ ($\beta \pm \text{SE}$: -0.03 ± 0.006 ; CI: -0.05 , -0.02) and $\delta^{15}\text{N}$ values ($\beta \pm \text{SE}$: 0.09 ± 0.01 , CI: 0.06 – 0.11), respectively. When accounting for $\delta^{13}\text{C}$ and $\delta^{15}\text{N}$ values, the colony effect plot showed that: (i) most colonies (71%) exhibited feather Hg concentrations close to the circumpolar average (i.e., 0.45 $\mu\text{g}\cdot\text{g}^{-1}$; all colonies

combined), and (ii) colonies from the Ross Sea had higher Hg concentrations than all other sites (Fig. 5). These results are reinforced by the EMMs (Table 5).

For sexed adults ($n = 231$), two models met the selection criteria for the best model (i.e., $\Delta\text{AIC}_c < 2$), weighing together 90% of all models (Table 3). The first best model ($\Delta\text{AIC}_c = 0$) included $\delta^{13}\text{C}$ and $\delta^{15}\text{N}$ values and colony, but did not include sex as a significant predictor (Table 3). The second best model ($\Delta\text{AIC}_c = 1.2$) included $\delta^{13}\text{C}$ and $\delta^{15}\text{N}$ values, colony and sex (Table 3). Because it was 1.8 times more powerful than the second one, the first best model was selected as the final best model. This model explained 67% of the measured variation in feather Hg concentrations (Table 4). Feather Hg concentrations strongly decreased and increased with $\delta^{13}\text{C}$ ($\beta \pm \text{SE}$: 0.14 ± 0.06 ; CI: 0.03 – 0.26 ; Gamma inverse) and $\delta^{15}\text{N}$ values ($\beta \pm \text{SE}$: -0.29 ± 0.06 ; CI: -0.40 , -0.17 ; Gamma inverse), respectively. Spatial differences are provided with the EMMs in Table S6. Despite no statistical difference between sexes (see Table S5 for more details), differences were observed for Hg concentrations, $\delta^{13}\text{C}$ and $\delta^{15}\text{N}$ values (Fig. S2). Regarding Hg concentrations, females had lower concentrations than males at six colonies (Queen Maud Land: Hukuro Cove, and the Ross Sea: Adélie Cove, Edmonson Point, Inexpressible Island, Cape Crozier and Cape Royds). In contrast, females had higher concentrations than males at two other colonies (Adélie Land and King George/25 de Mayo Island), respectively. Regarding $\delta^{13}\text{C}$ values (Fig. S2), there was no clear difference between sexes in five colonies. Compared to males, females had lower values in one colony (Edmonson Point) and higher values in two colonies from the Ross Sea (Adélie Cove and Cape Royds). For $\delta^{15}\text{N}$ values, females and males had similar values in two colonies (Cape Crozier and Admiralty Bay), but females had lower mean values in five colonies (Hukuro Cove, Adélie Cove, Edmonson Point, Inexpressible Island and Cape Royds) and higher mean values in one colony (Dumont d'Urville) compared to males (Fig. S2).

For the dataset including fledging chicks and adults from the same colonies ($n = 113$), the best model included $\delta^{13}\text{C}$ and $\delta^{15}\text{N}$ values, colony, age class and their interaction as significant predictors (Table 3), explaining 79% of the observed variation in feather Hg concentrations (GLM, Table 4). Feather Hg concentrations were strongly and positively driven by $\delta^{15}\text{N}$ values ($\beta \pm \text{SE}$: -0.58 ± 0.13 ; CI: -0.84 , -0.33 ; Gamma inverse). In contrast, $\delta^{13}\text{C}$ values were positively but only marginally related to feather Hg concentrations (small effect size, Table 4). In chicks, individual Hg concentrations ranged from 0.07 to 0.63 $\mu\text{g}\cdot\text{g}^{-1}$ (Table 2), which is 1.8–3.5 times lower than those measured in adults at any colony (Table 1), with the exception of Dumont d'Urville in 2011/2012 (Fig. 3a, Table 6). Chick feather $\delta^{13}\text{C}$ values ranged from -25.6 to -20.2% , with outlying values in Marambio (Seymour Island) compared to other colonies (Fig. 3b). Chick $\delta^{15}\text{N}$ values varied

Fig. 2 Spatial comparison of feather (a) Hg concentrations, (b) $\delta^{13}\text{C}$ and (c) $\delta^{15}\text{N}$ values in adult Adélie penguins (*Pygoscelis adeliae*) collected in 24 Antarctic colonies, represented by a clockwise colour gradient (from East-Antarctica in dark red to South Orkney Islands in grey). Feather $\delta^{13}\text{C}$ and $\delta^{15}\text{N}$ values are proxies for penguin feeding habitat and trophic position, respectively. Numbers in brackets (top) represent sample sizes for each colony. Numbers (bottom) refer to the sites where the sampling colonies are located: (1) Queen Maud Land, (2) Mac.Robertson Land, (3) Princess Elizabeth Land, (4) Wilkes Land, (5) Adélie Land, Victoria Land: (6) Terra Nova Bay, (7) Ross Island; (8) King George/25 de Mayo Island, (9) Antarctic Peninsula, (10) Seymour Island, (11) Joinville Island Group and (12) South Orkney Islands. Individual values (smaller dots) are presented with boxplots, representing median values (midlines), errors bars (whiskers) and outliers (black dots outside whiskers)

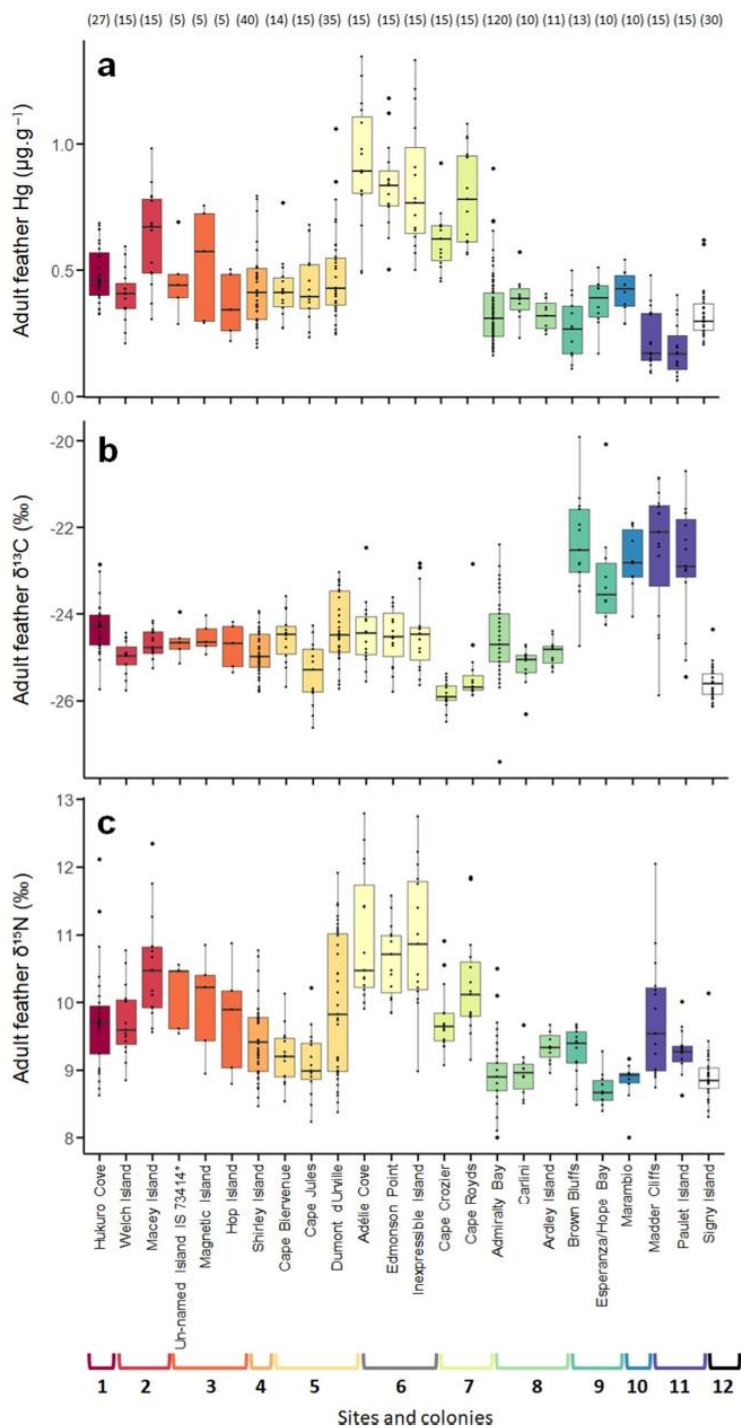


Table 4 Estimated parameters of variables included in the best model for each dataset: (1) adults ($n = 485$), (2) sexed adults ($n = 231$) and (3) both age classes (i.e., adults and pre-fledging chicks from the same colony; $n = 113$)

	Datasets		
	(1) Adults	(2) Sexed adults	(3) Both age classes
Model specification			
Distribution	Gamma	Gamma	Gamma
Link-function	Identity	Inverse	Inverse
Variables			
Intercept	-1.15 [-1.58, -0.72] ± 0.21	8.42 [4.87, 11.97] ± 1.81	16.28 [9.66–23.02] ± 3.41
$\delta^{15}\text{N}$	0.09 [0.06–0.11] ± 0.01	-0.29 [-0.40, -0.17] ± 0.06	-0.58 [-0.84, -0.33] ± 0.13
$\delta^{13}\text{C}$	-0.03 [-0.05, -0.02] ± 0.006	0.14 [0.03, 0.26] ± 0.06	0.33 [0.11–0.56] ± 0.11
Colony	+	+	+
Age class			2.49 [1.45–3.60] ± 0.55
McFadden's R^2	0.61	0.67	0.79

Values are estimates [CI] ± SE. Models are Generalized Linear Models (GLMs) with Gamma distribution and identity or inverse link-function. Results are on the response scale for (1) and the inverse scale for (2) and (3). McFadden's R^2 indicates the degree of model fit (i.e., from low and high model fit indicated from 0 to 1, respectively). Feather $\delta^{13}\text{C}$ and $\delta^{15}\text{N}$ values are proxies of the penguin feeding habitat and trophic position, respectively. When specified, the «+» symbol indicates when the colony (categorical factor) is included in the best model for each dataset. Results for site comparisons (estimated marginal means) are provided in Table 5 (all adults), Table S6 (sexed adults) and Table 6 (both age classes)

CI confidence interval (95%), SE standard error

from 7.2 to 12.9 ‰ (Table 2), with an average 3 ‰ difference between East and West Antarctic colonies (Fig. 3c).

Discussion

The Southern Ocean hosts some of the most extreme and least accessible environments on Earth. As such, it has commonly been considered to be a pristine ocean, free from substantial anthropogenic contamination. Nevertheless, latitudinal gradients in persistent contaminants, such as Hg, were previously described across the Southern Ocean (Carravieri et al. 2014b; Renedo et al. 2020), posing potential threats for its marine ecosystems. Specifically, lower Hg concentrations were observed in Antarctic compared to subantarctic and subtropical seabirds. Whether this Hg gradient is locally restricted or widespread in the Southern Ocean is still unknown. Here, we studied the Adélie penguin as a circumpolar bioindicator species to reveal ocean-wide patterns in Hg contamination across Antarctic marine ecosystems. To the best of our knowledge, this study is the first to use a single bioindicator and document Hg contamination over such a large spatial scale, encompassing a total of 24 colonies around Antarctica (both continental and maritime). This circumpolar assessment revealed notable variation in feather Hg concentrations of Adélie penguins, with a hotspot in the Ross Sea (Victoria Land). Drivers of this spatial variation involved both the trophic ecology and colony location.

Circumpolar Hg contamination in adult Adélie penguins

Overall, feather Hg concentrations found in this study were similar to those reported by previous studies on Adélie penguins (Table 1). In the Antarctic Zone, Adélie penguins exhibited lower Hg concentrations ($0.45 \mu\text{g}\cdot\text{g}^{-1}$) compared to chinstrap (*Pygoscelis antarcticus*; $0.71 \mu\text{g}\cdot\text{g}^{-1}$), gentoo (*P. papua*; $1.34 \mu\text{g}\cdot\text{g}^{-1}$) and emperor (*Aptenodytes forsteri*) penguins ($1.37 \mu\text{g}\cdot\text{g}^{-1}$) on average (Table S1). This was also the case when comparing with other penguin species elsewhere in the Southern Ocean (Table S1), such as the southern rockhopper (*Eudyptes chrysocome*; $2.03 \mu\text{g}\cdot\text{g}^{-1}$), king (*A. patagonicus*; $2.19 \mu\text{g}\cdot\text{g}^{-1}$) and macaroni (*E. chrysolophus*; $2.73 \mu\text{g}\cdot\text{g}^{-1}$) penguins; and with other flying seabirds from the Southern Ocean, including storm petrels ($5.47 \mu\text{g}\cdot\text{g}^{-1}$; Pacyna et al. 2019) or albatrosses ($22.14 \mu\text{g}\cdot\text{g}^{-1}$; Bustamante et al. 2016). Our results thus confirm that the overall Hg concentrations are consistent around the Antarctic continent. We propose that the Adélie penguin, which is also a relevant indicator species for CCAMLR, is a good indicator for Hg contamination in Antarctic marine food webs.

In adult Adélie penguins, body feather Hg concentrations reflect a large temporal and spatial scale of exposure (see Material and Methods for further details; Brasso et al. 2014; Carravieri et al. 2014a). During the breeding season, Adélie penguins are central place foragers (Ainley 2002): they forage in a restricted area immediately adjacent to the colony, within a few hundred kilometres (Ainley et al. 2004; Davis and Miller 1992; Michelot et al. 2021; Riaz et al.

Table 5 Estimated marginal mean (EMM) feather Hg concentrations for adult Adélie penguins ($n = 485$) from 24 Antarctic colonies

Colony	EMM	SE	95% CI		Group
			Lower	Upper	
Hukuro Cove	0.46	0.029	0.41	0.52	A
Welch Island	0.37	0.033	0.30	0.43	A
Macey Island	0.52	0.052	0.42	0.62	AB
Un-named Island*	0.39	0.065	0.26	0.52	A
Magnetic Island	0.46	0.071	0.32	0.60	AB
Hop Island	0.32	0.049	0.23	0.42	A
Shirley Island	0.41	0.021	0.37	0.46	A
Dumont d'Urville	0.45	0.026	0.40	0.50	A
Cape Bienvenue	0.46	0.037	0.38	0.53	A
Cape Jules	0.44	0.036	0.37	0.51	A
Adélie Cove	0.78	0.077	0.63	0.93	B
Edmonson Point	0.73	0.070	0.60	0.87	B
Inexpressible Island	0.69	0.068	0.56	0.82	AB
Cape Crozier	0.55	0.052	0.45	0.66	AB
Cape Royds	0.70	0.066	0.57	0.83	AB
Admiralty Bay	0.39	0.012	0.37	0.41	A
Carlini	0.41	0.039	0.33	0.49	A
Ardley Island	0.32	0.031	0.26	0.38	A
Brown Bluffs	0.35	0.029	0.30	0.41	A
Esperanza/Hope Bay	0.48	0.039	0.40	0.55	AB
Marambio	0.53	0.044	0.44	0.61	A
Madder Cliffs	0.29	0.023	0.25	0.34	AC
Paulet Island	0.27	0.021	0.23	0.31	AC
Signy Island	0.34	0.021	0.30	0.38	A

Estimates were derived from the best-ranked generalized linear model (GLM with Gamma distribution and identity link-function) defined as follows: $Hg \sim \delta^{13}C + \delta^{15}N + Colony$ (see Table 3 for further details)

Differences were considered significant when confidence intervals of each colony did not overlap with those of others. Colonies sharing the same Group letters were not significantly different from each other. Colonies with two letters were not significantly different from either group

CI confidence interval, SE standard error

Un-named Island refers to Un-named Island IS 73413

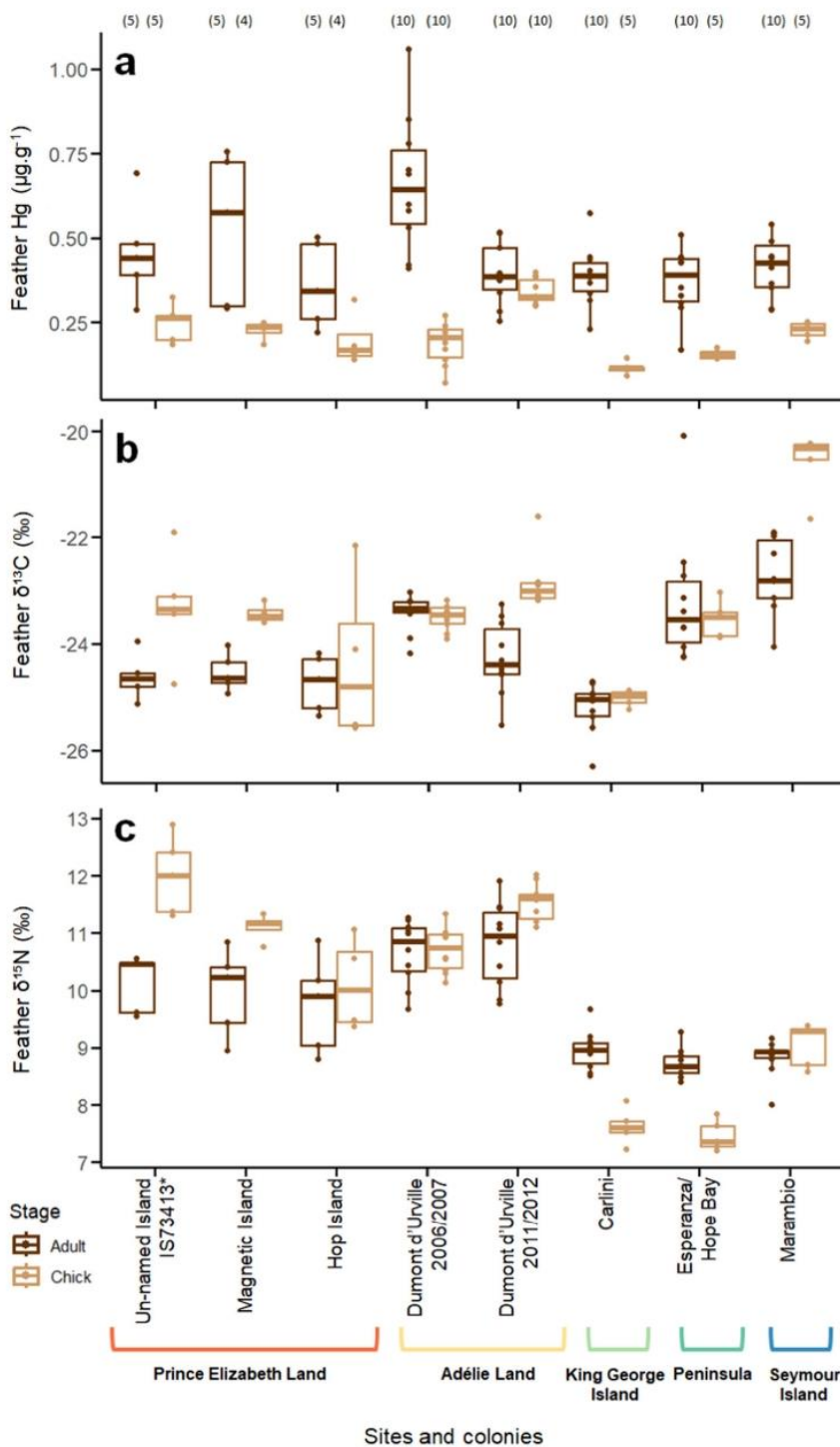
2021). During the non-breeding period, they travel several hundred to thousand of kilometres away from their breeding grounds (e.g., 500–2500 km on average; Ballard et al. 2010; Clarke et al. 2003; Davis et al. 1996; Dunn et al. 2011; Erdmann et al. 2011; Hinke et al. 2015; Takahashi et al. 2018; Thiébot et al. 2019) and are assumed to forage in the MIZ (Dunn et al. 2011; Wilson et al. 2001). In the absence of precise tracking positions, feather Hg concentrations could be qualitatively associated with a large spatial region, encompassing most of the Antarctic Zone from the Antarctic Peninsula to the Ross Sea, thanks to published tracking studies (Fig. S1). At the circumpolar scale, our results revealed spatial variation in feather Hg

concentrations, which were the lowest in West Antarctica (i.e., maritime Antarctica: King George/25 de Mayo, Seymour and Joinville Islands, and the Antarctic Peninsula), intermediate in East Antarctica, and the highest in the Ross Sea (Figs. 2a, 4).

As expected, penguin feeding ecology was a major driver of among colony variation, as indicated by the results of model selection (Table 3). Trophic position was a significant predictor of feather Hg concentrations, as showed by the higher $\delta^{15}N$ values in the Ross Sea (Fig. 2c). This suggests that penguins foraged at higher trophic position at these locations. Adélie penguins are strongly associated with sea-ice environments, both during the breeding (Emmerson and Southwell 2008; Guen et al. 2018; Kokubun et al. 2021) and non-breeding seasons (Emmerson and Southwell 2011). They feed preferentially in waters covered by 10 to 80% sea ice, but also in the open sea (Ballard et al. 2019; Cottin et al. 2012; Guen et al. 2018; Michelot et al. 2020). In these habitats, their diet comprises different euphausiid crustaceans, mainly the Antarctic krill (*Euphausia superba*) and smaller amounts of the ice krill (*Euphausia crystallophias*) (Tierney et al. 2009). Their diet also includes fish species such as the Antarctic silverfish (*Pleuragramma antarcticum*) in different proportions according to colony location and season (Ainley et al. 1998; Ainley 2002). Thus, their diet may vary significantly according to the geographical localization of the colony, but also the year (Tierney et al. 2009). For example, Adélie penguins feed almost exclusively on Antarctic krill along the Antarctic Peninsula and in the Scotia Sea (Coria et al. 1995; Juárez et al. 2018; Lynnes et al. 2004). In East Antarctica, they have a mixed diet depending on feeding habitat: fish and ice krill in neritic waters (continental shelf) versus Antarctic krill in pelagic waters (shelf break; Green and Johnstone 1988; Kent et al. 1998; Puddicombe and Johnstone 1988; Watanuki et al. 1997; Wienecke et al. 2000). In contrast, Adélie penguins from the Ross Sea consume higher proportions of Antarctic silverfish (Ainley et al. 1998; Olmastroni et al. 2020), which are abundant in continental shelf waters (Gon and Heemstra 1990). Yet, the silverfish is also a zooplankton predator itself and thus exhibits a higher trophic position than krill (Everson 2000; Hodum and Hobson 2000; Polito et al. 2011). Hence, a higher consumption of silverfish could explain the higher Hg concentrations observed in Adélie penguins from Victoria Land (Ross Sea). This is supported by previous studies showing that Hg concentrations in several species of Antarctic fish, including the Antarctic silverfish, were 4 to 20 times higher than in different krill species (Polito et al. 2016; Seco et al. 2021, 2019; Sontag et al. 2019).

Nevertheless, the diet of adult Adélie penguins (as detailed above) has been studied mainly determined during the chick-rearing season, when individuals are directly

Fig. 3 Adult and chick comparison in feather (a) Hg concentrations, and (b) $\delta^{13}\text{C}$ and (c) $\delta^{15}\text{N}$ values in Adélie penguins (*Pygoscelis adeliae*) from eight Antarctic colonies. Adult and chicks are represented in dark and light brown, respectively. Feather $\delta^{13}\text{C}$ and $\delta^{15}\text{N}$ values are proxies for penguin feeding habitat and trophic position, respectively. Individual values (smaller dots) are presented with boxplots, representing median values (midlines), errors bars (whiskers) and outliers (black dots outside whiskers). Numbers in brackets indicate sample sizes for each age class and colony



accessible on land, but scarcely during the non-breeding season (also the period of Hg exposure). Given the lack of dietary information available for the non-breeding period,

we assumed here that Adélie penguins use similar marine resources during both periods (Polito et al. 2016; Tierney et al. 2009). However, seasonal variation in feeding ecology

Table 6 Estimated marginal mean (EMM) feather Hg concentrations for adults and pre-fledging chicks of Adélie penguins from the same Antarctic colonies ($n = 113$)

Age class Colonies	Adults				Chicks				Age class Difference
	EMM	SE	95% CI		EMM	SE	95% CI		
			Lower	Upper			Lower	Upper	
Un-named Island*	0.38	0.037	0.32	0.47	0.19	0.019	0.16	0.24	yes
Magnetic Island	0.44	0.044	0.36	0.54	0.20	0.022	0.16	0.25	yes
Hop Island	0.33	0.033	0.27	0.41	0.19	0.021	0.15	0.24	yes
Dumont d'Urville 1	0.52	0.044	0.45	0.63	0.17	0.013	0.15	0.20	yes
Dumont d'Urville 2	0.30	0.024	0.26	0.36	0.27	0.023	0.24	0.33	no
Carlini	0.39	0.041	0.32	0.49	0.13	0.016	0.10	0.17	yes
Esperanza/Hope Bay	0.52	0.070	0.41	0.71	0.20	0.031	0.15	0.29	yes
Marambio	0.65	0.11	0.49	0.96	0.34	0.073	0.24	0.59	yes

Estimates were derived from the best-ranked generalized linear model (GLM with Gamma distribution and inverse link-function) defined as follows: $Hg \sim \delta^{13}C + \delta^{15}N + Colony * Age\ class$ (see Table 3 for further details)

Differences were considered significant when confidence intervals of adults and chicks from the same colony do not overlap. Dumont d'Urville 1 and 2 refers to samples from 2006/2007 and 2011/2012, respectively
CI confidence interval, SE standard error

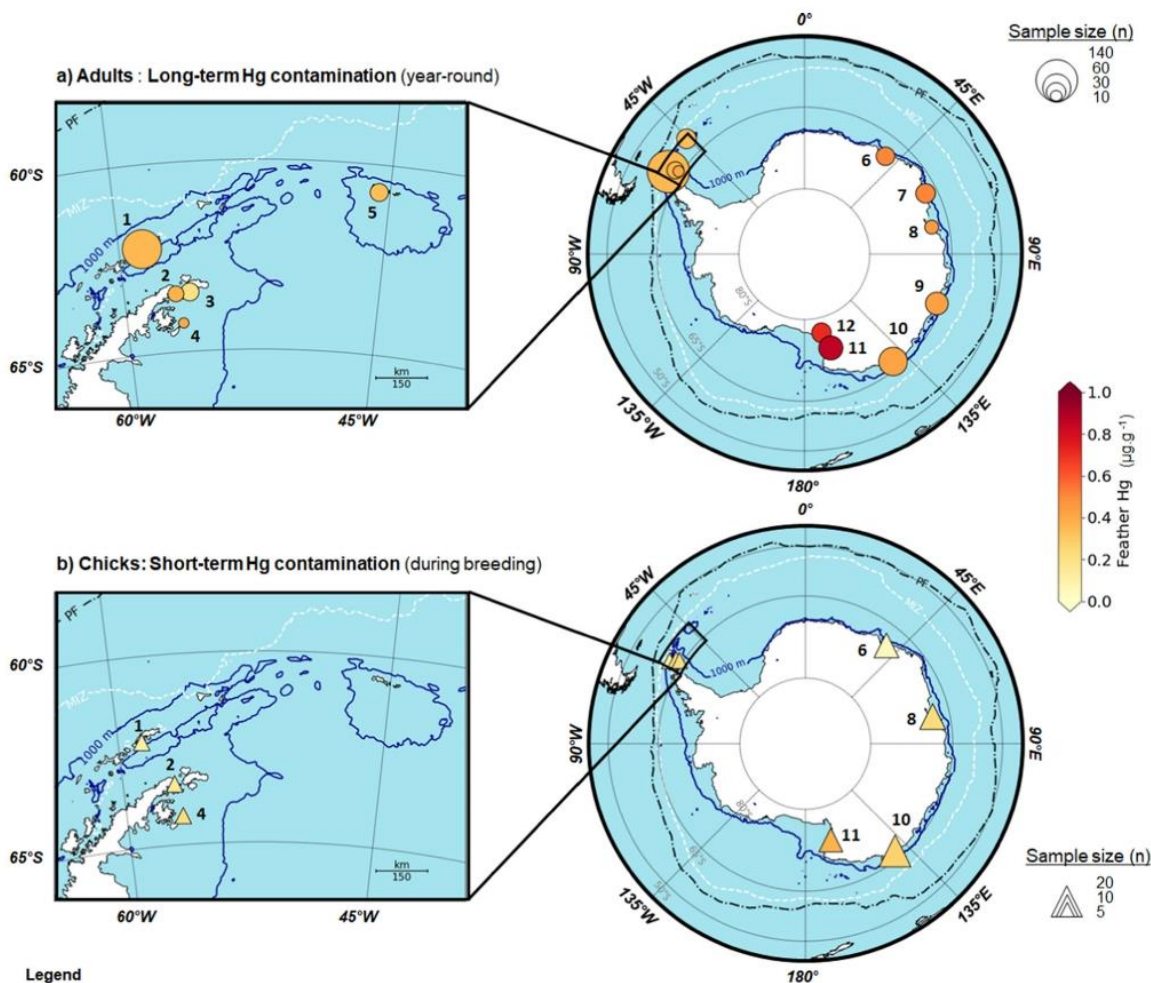
Un-named Island refers to Un-named Island IS 73413

of Adélie penguins cannot be excluded and could thus influence feather Hg concentrations.

Five penguins from Hukuro Cove and Brown Bluffs were excluded from analyses (Table S4) because they had unexpected high positive $\delta^{13}C$ values for Antarctic environments (Carravieri et al. 2014b; Cherel and Hobson 2007) and high $\delta^{15}N$ values for this species. Since it is unlikely that these individuals were associated with northern ecosystems, such values would rather indicate that the birds had foraged in more coastal/benthic habitats (Cherel et al. 2011), possibly resulting in high feather Hg concentrations. One way to better understand why these five individuals had different isotopic signatures would be to perform Compound-Specific Stable Isotope Analysis of Amino-Acids (CSIA-AA). Indeed, CSIA-AA enables to distinguish between source (i.e., baseline) and trophic $\delta^{15}N$ values. In other words, it could clarify whether the $\delta^{15}N$ baseline is different (environmental driver) or whether the diet is the major driver (trophic driver). Similarly, CSIA-AA analyses are likely to help clarify whether the differences in $\delta^{15}N$ values observed in the Ross Sea came from different $\delta^{15}N$ baseline, trophic position or both, and how this could translate into a higher Hg contamination.

Regional colony location was also associated with feather Hg concentrations (Table 3), suggesting that environmental factors are also involved in explaining spatial differences in feather Hg concentrations. When accounting for feeding ecology (i.e., $\delta^{13}C$ and $\delta^{15}N$ values), colonies from Victoria Land (Ross Sea) still appeared to have higher Hg concentrations than all other colonies (Fig. 5). Hence, penguins in the Ross Sea have a disproportionately higher Hg concentrations than would be expected on the basis of

their diet alone. Two non-exclusive factors could explain this result: (1) volcanism and (2) katabatic winds. The West-Antarctic Rift System runs from the base of the Antarctic Peninsula through the Weddell Sea to the Ross Sea (Rocchi et al. 2003), resulting in numerous volcanoes present in Western versus Eastern Antarctica. Despite low activity levels, two main active volcanoes border the coast of the Ross Sea: Mount Erebus and Mount Melbourne, which are located on Ross Island and in Terra Nova Bay, respectively (Behrendt 1990; Edwards and Smellie 2016; Ferraccioli et al. 2000; Global Volcanism Program 2022). Since volcanoes represent a primary source of Hg to the atmosphere (Grasby et al. 2019), they are likely to constitute a local source of Hg for the ocean and associated marine food webs as well. On the other hand, katabatic winds may also influence Hg deposition in the Ross Sea. Katabatic winds are strong winds that blow from the large and elevated Antarctic ice sheets toward the coast and represent a major environmental feature in Antarctica (Parish 1988; Parish and Cassano 2003) that can transport dust and debris. The Ross Sea is strongly exposed to katabatic winds (Turner 2015) and in Terra Nova Bay, regions exposed to strong katabatic winds showed enhanced Hg deposition on the coast (Bargagli 2008, 2016). Consequently, by carrying air masses originating from the Antarctic continent towards coastal regions, katabatic winds could represent a local natural source of Hg in marine ecosystems of the Ross Sea. Still, the biochemical cycle of Hg is complex and includes several chemical processes and biological transformations with both abiotic and biotic interactions (Chételat et al. 2022; McKinney et al. 2022): methylation/demethylation, redox reactions, MeHg



Legend

Habitat characteristics:

PF: Polar Front
 MIZ: Marginal Ice Zone
 1000m: 1000m isobath

Sites:

- | | | |
|----------------------------------|----------------------------|-----------------------------|
| 1: King George/25 de Mayo Island | 5: South Orkney Islands | 9: Wilkes Land |
| 2: Antarctic Peninsula | 6: Queen Maud Land | 10: Adélie Land |
| 3: Joinville Island Group | 7: Mac.Robertson Land | 11: Terra Nova Bay colonies |
| 4: Seymour Island | 8: Princess Elizabeth Land | 12: Ross Island colonies |
- } Victoria Land

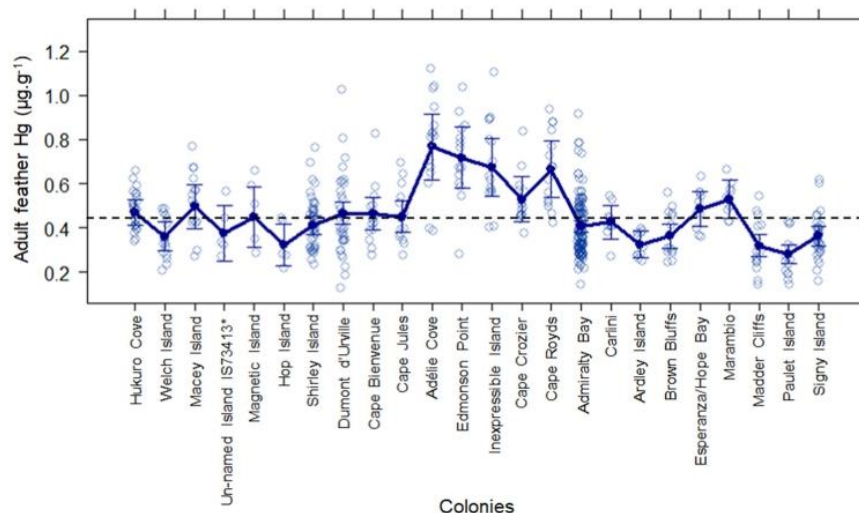
Fig. 4 Spatial variation in feather Hg concentrations of (a) adult and (b) chick Adélie penguins (*Pygoscelis adeliae*) across 24 Antarctic colonies. The colour gradient represents increasing Hg concentrations. Sample sizes (n) are indicated by the size of circles and triangles. The averaged position of the Polar Front (PF, dashed black line) reflects the

northernmost limit of Adélie penguin distribution, whereas the Marginal Ice Zone (MIZ, dashed white line) reflects the presumed northern limit of their non-breeding distribution (i.e., maximum sea ice cover extent in September; see Material and Methods for further details). The darkblue line indicates the 1000 m isobath

production, bioavailability and transfer through marine food webs, especially in polar environments with the influence of sea ice (Cossa et al. 2011). The presence of sea ice, which harbour microbial sources of MeHg in the Southern Ocean (Gionfriddo et al. 2016; Yue et al. 2023), may thus influence Hg contamination in Antarctic marine food webs. Further research is needed to disentangle the biochemical processes at the circumpolar scale, but also those that could result in higher year-round Hg exposure in Adélie penguins from the Ross Sea.

Because sample collection is challenging in Antarctic environments, feathers in this study were collected across a relatively large time period (between 2005 and 2021). Even if interannual variations were very low in one colony where adult Hg concentrations were available for six consecutive years (i.e., Admiralty Bay, King George/25 de Mayo Island), observed spatial variation could result from the combination of both spatial and temporal variations. It is worth noting that Hg concentrations in two colonies were different from those reported previously. In

Fig. 5 Spatial comparison in feather Hg concentrations in adult Adélie penguins (*Pygoscelis adeliae*) from 24 Antarctic colonies ($n = 485$) when controlled by their feeding ecology (feather $\delta^{13}\text{C}$ and $\delta^{15}\text{N}$ values). Relationships result from the extraction of partial residuals of the best Generalized Linear Model (GLM; see Table 3 and Material and Methods for further details). Individual data are represented in light blue (open circle). Points (filled circle) are means \pm SD. The dark blue line links all mean Hg concentrations. The dashed black line indicates the circumpolar average Hg concentrations (i.e., $0.45 \mu\text{g}\cdot\text{g}^{-1}$, all pooled data from all colonies)



Queen Maud Land, feather Hg concentrations in the 2010s were five times higher than in the 1980s and the 1990s (Honda et al. 1986; Yamamoto et al. 1996; Table 1). In Adélie Land, feather Hg concentrations dropped by 30% between 2006 and the following years (2011 and 2017; Carravieri et al. 2016; this study; Table 1). However, this temporal difference ($0.2 \mu\text{g}\cdot\text{g}^{-1}$) is still low compared to the spatial difference measured among adult Hg concentrations ($1.2 \mu\text{g}\cdot\text{g}^{-1}$). Further studies should thus investigate mid- and long-term Hg trends in Antarctic food webs, for instance by increasing the temporal resolution in Hg monitoring.

Potential sex-specific Hg concentrations

In seabirds, sexual segregation in diet has been suggested as a strategy to reduce intra-specific competition (Bearhop et al. 2006; Forero et al. 2002; González-Solís et al. 2000; Phillips et al. 2011). In Adélie penguins, diet segregation between sexes was observed during the breeding season: females foraged for more krill than fish in more offshore, pelagic waters, in contrast to males which fed equally on both prey types in more inshore, benthic waters (Clarke et al. 1998; Colominas-Ciuró et al. 2018). In theory, such sexual segregation in diet should therefore be reflected in stable isotopes and then in Hg concentrations. In our study, no clear sexual segregation could be deduced from the observed feather $\delta^{13}\text{C}$ and $\delta^{15}\text{N}$ values (Fig. S2b, c). However, differences between sexes in feather Hg concentrations could be noticed when differences in either $\delta^{13}\text{C}$ or $\delta^{15}\text{N}$ values or both were present. Feather Hg concentrations were similar between sexes at Adélie Cove (Terra Nova Bay) and Admiralty Bay (King George/25 de Mayo Island), as previously reported (Polito et al. 2016). In contrast, females had lower Hg concentrations in Queen Maud Land

(Hukuro Cove) and the Ross Sea, including Edmonson Point and Inexpressible Island (Terra Nova Bay), and Cape Crozier and Cape Royds (Ross Island). These results were similar to previous studies on Adélie penguins from the Ross Sea (Pilcher et al. 2020), but also in other penguin species (i.e., gentoo and macaroni penguins) from South Georgia/Islands Georgias del Sur (Becker et al. 2002, Pedro et al. 2015). Although moult is the major process responsible for Hg elimination in males, egg production represents an additional route (Bond and Diamond 2009b; Braune and Gaskin 1987), that could lead to lower Hg concentrations in females.

Despite these potential differences between sexes, sex did not significantly drive spatial variation in adult Hg contamination, according to the first best model (Table 3). Indeed, this model included $\delta^{13}\text{C}$ and $\delta^{15}\text{N}$ values and colony location. However, a second model met the selection criteria for the best model (although its weight was lower), which included sex as a predictor in addition to $\delta^{13}\text{C}$ and $\delta^{15}\text{N}$ values and colony location (Table 3). Unfortunately, information on penguin sex was not available for all individuals. Models were thus run on a dataset that only included half of the total sample size. Complete sexing analyses, either determined through morphological or molecular approaches, should help to further investigate differences in Hg contamination between sexes and its drivers (either extrinsic or intrinsic), on a circumpolar scale. Whether sexual segregation in diet and Hg contamination are related during the breeding and the non-breeding season warrants further research.

Comparing Hg contamination on different spatio-temporal scales with adult and chick feathers

Chick and adult feathers reflect different temporal and spatial scales: local accumulation during a few months

during the breeding season *versus* year-round accumulation including their entire distribution (breeding and non-breeding), respectively. In general, chicks exhibit lower feather Hg concentrations relative to adults, as a result of their shorter exposure period (Carravieri et al. 2014c). Our results were coherent with this explanation, with feather concentrations in chicks being 1.8 to 3.6 times lower than in adults on average (Fig. 3).

Feather Hg concentrations were driven by the age class (adult or fledging chick), the trophic ecology (indicated by $\delta^{13}\text{C}$ and $\delta^{15}\text{N}$ values) and colony location (Table 3). In most colonies, chicks exhibited equivalent or higher feather $\delta^{15}\text{N}$ values than adults, suggesting that they were fed with similar prey or with prey of higher trophic position across colonies (for example with higher proportions of fish compared to krill; Cherel 2008). There was one exception to this pattern: in Dumont d'Urville (Adélie Land; in 2011), average feather Hg concentrations were similar between adults and chicks (Table 6), translating into a similar contamination status between age classes. In 2011, sea ice was quite high around the colony (60%) during the chick-rearing period and quite homogenous at a larger scale (Michelot et al. 2021). Whether these sea-ice conditions could be associated with higher Hg exposure for both adults and chicks would deserve further research.

Importantly, Terra Nova Bay (and hence the Ross Sea) exhibited the highest feather Hg concentrations in both chicks and adults (Fig. 4), which reinforces the higher exposure year-round in this region compared to other areas. Since foraging trips are shorter during the chick-rearing period, this also suggests that Hg contamination may be local.

Conclusions and perspectives

This study provides a unique assessment of Hg contamination in Antarctic marine food webs, by using the Adélie penguin as a circum-Antarctic bioindicator. Feathers represent a valuable, non-destructive and non-invasive monitoring tool, in complete agreement with Antarctic Treaty protocols, to examine the variation in Hg contamination across temporal and spatial scales. Feather Hg concentrations detected in Adélie penguins ($<2 \mu\text{g}\cdot\text{g}^{-1}$) were below toxicity thresholds recognized for seabird feathers ($1.6\text{--}10 \mu\text{g}\cdot\text{g}^{-1}$; Ackerman et al. 2016; Chastel et al. 2022). Currently, this suggests low risks of toxicity for this species, although toxic effects may arise at low Hg concentrations, particularly in combination with other stressors (e.g., other contaminants, environmental changes, diseases; Grunst et al., 2023; Provencher et al., 2016). At the circumpolar scale, Hg contamination was relatively homogeneous across regions. This is consistent with the circumpolar structure of the Southern Ocean, which is characterized by a unique stratification of annular fronts and water masses encircling

the Antarctic Continent (Carter et al. 2008). This reinforces the suitability of Adélie penguins as bioindicator species for Antarctic marine ecosystems.

Trophic ecology (indicated by feeding habitat and trophic position) was crucial to explain spatial variation of Hg contamination. The Hg hotspot observed in the Ross Sea was associated with higher trophic position of Adélie penguins, probably due to a higher proportion of fish in their diet. This reinforces the need to account systematically for the diet when monitoring Hg contamination in seabirds, especially at such large spatial scales.

Thanks to published tracking studies, feather Hg concentrations could be qualitatively associated with a large spatial region, encompassing most of the Antarctic Zone, from the Antarctic Peninsula to the Ross Sea. However, detailed spatial information of penguin movements during their annual cycle is essential to quantify precisely the spatial variation in their Hg exposure. The Arctic Monitoring and Assessment Program (AMAP) provides a circumpolar and long-term assessment of Hg contamination in marine ecosystems for the entire Arctic Ocean. In this program, Hg contamination was associated to the spatial and seasonal distributions of seabirds thanks to biologging. In a similar way, such work in the Southern Ocean would be substantially improved by the deployment of individual tracking devices, allowing connection to be made between spatial and seasonal distributions of penguins, at the individual level, with contaminants at the ocean scale.

Through Adélie penguins, this work documented circumpolar Hg contamination in the epipelagic compartment of the Southern Ocean. A complementary approach could investigate the mesopelagic compartment, where high MeHg concentrations were recorded (Cossa et al. 2011), by studying the circumpolar breeding emperor penguin (*Aptenodytes forsteri*), which mainly feeds on prey of higher trophic position in both epipelagic and mesopelagic waters (Cherel 2008; Wienecke and Robertson 1997). Such large-scale monitoring is fundamental for international monitoring programs, such as the Global Mercury Assessment from the United Nations, to assess the effectiveness of the Minamata Convention on Mercury. Renewing a large-scale assessment, such as that presented here, on a regular basis (every few years or decade for example) is highly recommended to monitor the contamination status of Antarctic marine food webs over time and to further investigate global trends, especially in the context of climate change.

Supplementary information The online version contains supplementary material available at <https://doi.org/10.1007/s10646-023-02709-9>.

Acknowledgements The authors are thankful to all people involved in fieldwork, sample preparation and shipment in all Antarctic research stations. In addition, we thank the Mawson seabird field team and Casey station expeditioners for collecting samples, and Marcus Salton

for organising sample transport. Special thanks are due to Yan Ropert-Coudert for his help in the construction of collaborations in the Antarctic research community and to Frédéric Angelier. The authors are grateful to (i) Maud Brault-Favrou and Carine Churlaud from the Plateforme Analyses Élémentaires of the LIENSs for their support during Hg analyses, as well as (ii) Sandy Pascaud for her support in sample preparation in the laboratory, and to (iii) Julie Charrier for the penguin drawings in the figures. The IUF (Institut Universitaire de France) is acknowledged for its support to Paco Bustamante as a Senior Member. This study is also a contribution to the Excellence Chair in Marine Ecology ECOMM funded by the Région Nouvelle Aquitaine (France). This work/review benefitted from the French GDR Aquatic Ecotoxicology framework which aims at fostering stimulating scientific discussions and collaborations for more integrative approaches.

Author contributions Conceptualization: FC, PB, JF, YC. Methodology: FC, PB, AC, YC. Software: FC, AC, CB. Investigation: FC, PV. Formal analysis: FC, AC. Visualization: FC, CB. Writing - original draft preparation: FC, PB, AC, YC. Writing - review and editing: FC, PB, AC, CB, RB, IC, MD, LE, GG, TH, MJ, AK, ALM-G, CM, SO, MP, TR, MS, AS, CS, AS, AT, JBT, PT, CW, JF and YC. Project administration: FC. Funding acquisition: PB, Resources: AC, RB, IC, MD, LE, TH, MJ, ALM-G, CM, SO, MP, TR, MS, AS, CS, AS, AT, JBT, PT, CW. Supervision: PB, JF, YC.

Funding This work relied on several national and international existing monitoring programs in Antarctica, implying several funding sources associated with the logistical support to all research stations. (i) The circumpolar monitoring program led by Jean-Baptiste Thiebot was funded by National Geographic Society grant WW-24R-17. (ii) Samples from MacRobertson Land (Mawson station), Princess Elizabeth Land (Davis station) and Wilkes Land (Casey station) were collected through Australian Antarctic Division support to AAS 4518. (iii) Sampling in Adélie Land was supported financially and logistically by IPEV (Programmes N°109 ORNITHOECO, C. Barbraud, and N°1091 AMMER, A. Kato and T. Raclot) and WWF-UK. (iv) Sampling in Terra Nova Bay was funded by the Ministry and Research (MUR) and National Research Council Italy (CNR) through project #PNRA2016_004 Penguin ERA. (v) Sampling in Ross Island was funded by the National Science Foundation (OPP Award, #1543498). (vi) Fieldwork in Ardley Island was supported by Instituto Antártico Uruguayo (IAU), Ecos Sud Program (project PU20B01/U20B03), Commission for the Conservation of Antarctic Marine Living Resources (CCAMLR) General Capacity Building Fund and Scientific Scholarship Scheme, Agencia Nacional de Investigación e Innovación's (ANII) Clemente Estable Fund (project FCE 1 2021 1 166587), National System of Researchers and National Postgraduate Scholarship Programme, and Basic Science Development Programme (PEDECIBA). (vii) The Instituto Antártico Argentino – Dirección Nacional del Antártico (PINST-05) provided financial and logistical support to carry out the Argentine Antarctic campaign. Finally, funding was provided by CPER (Contrat de Plan Etat-Région) and the FEDER (Fonds Européen de Développement Régional) for the AMA and the IRMS of LIENSs laboratory.

Compliance with ethical standards

Conflict of interest The authors declare no competing interests.

Ethics approval In this work, feather sampling relied on several existing monitoring programs and were carried out at all sites under appropriate permits. More specifically, (i) animal handling and sample collection for Australian stations (Mawson, Davis and Casey stations)

were approved by the Australian Antarctic Division animal ethics committee and ATEP environmental approvals. (ii) Fieldwork in Adélie Land was approved by the Conseil des Programmes Scientifiques et Technologies Polaires of the Institut Polaire Français Paul Emile Victor (IPEV), and procedures were approved by the Animal Ethics Committee of IPEV. (iii) Fieldwork in Terra Nova Bay was approved under permission released from the Programma Nazionale di Ricerca in Antartide (PNRA). All sampling followed SCAR's Code of Conduct for the Use of Animals for Scientific Purposes in Antarctica (<https://www.scar.org/policy/scar-codes-of-conduct>). (iv) The Instituto Antártico Argentino – Dirección Nacional del Antártico (PINST-05) provided financial and logistical support to carry out the Argentine Antarctic campaign. The field work was carried out under the permit granted by the Dirección Nacional del Antártico (Environmental Management Office). (v) Animal handling and sample collection at Signy Island was approved by the British Antarctic Survey Animal Welfare and Ethical Review Board, and permission was granted by the British Foreign and Commonwealth Office on behalf of HM Secretary of State, under Sections 12 and 13 of the Antarctic Act, 1994, 2013.

References

- Ackerman JT, Eagles-Smith CA, Herzog MP, Hartman CA, Peterson SH, Evers DC, Jackson AK, Elliott JE, Vander Pol SS, Bryan CE (2016) Avian mercury exposure and toxicological risk across western North America: a synthesis. *Sci Total Environ* 568:749–769. <https://doi.org/10.1016/j.scitotenv.2016.03.071>
- Agnew DJ (1997) Review—the CCAMLR ecosystem monitoring programme. *Antarct Sci* 9:235–242. <https://doi.org/10.1017/S095410209700031X>
- Ainley DG (2002) The Adélie Penguin: Bellwether of Climate Change. Columbia University Press. <https://doi.org/10.7312/aui12306>
- Ainley DG, Ribic CA, Ballard G, Heath S, Gaffney I, Karl BJ, Barton KJ, Wilson PR, Webb S (2004) Geographic structure of Adélie penguin populations: overlap in colony-specific foraging areas. *Ecol Monogr* 74:159–178. <https://doi.org/10.1890/02-4073>
- Ainley DG, Wilson PR, Barton KJ, Ballard G, Nur N, Karl B (1998) Diet and foraging effort of Adélie penguins in relation to pack-ice conditions in the southern Ross Sea. *Polar Biol* 20:311–319. <https://doi.org/10.1007/s003000050308>
- Albert C, Helgason HH, Brault-Favrou M, Robertson GJ, Descamps S, Amélineau F, Danielsen J, Dietz R, Elliott K, Erikstad KE, Eulaers I, Ezhov A, Fitzsimmons MG, Gavrilov M, Golubova E, Grémillet D, Hatch S, Huffeldt NP, Jakubas D, Kitaysky A, Kolbeinsson Y, Krasnov Y, Lorentsen S-H, Lorentzen E, Mallory ML, Merkel B, Merkel FR, Montevecchi W, Mosbech A, Olsen B, Orben RA, Patterson A, Provencher J, Plumejeaud C, Pratte I, Reierson TK, Renner H, Rojek N, Romano M, Strøm H, Systad GH, Takahashi A, Thiebot J-B, Thórarinnsson TL, Will AP, Wojczulanis-Jakubas K, Bustamante P, Fort J (2021) Seasonal variation of mercury contamination in Arctic seabirds: a pan-Arctic assessment. *Sci Total Environ* 750:142201. <https://doi.org/10.1016/j.scitotenv.2020.142201a>
- Albert C, Renedo M, Bustamante P, Fort J (2019) Using blood and feathers to investigate large-scale Hg contamination in Arctic seabirds: a review. *Environ. Res.* 177:108588. <https://doi.org/10.1016/j.envres.2019.108588>
- Amante, C., Eakins, B.W., (2009), ETOPO1 1 Arc-Minute Global Relief Model: Procedures, data sources and analysis. NOAA Technical Memorandum NESDIS NGDC-24. National Geophysical Data Center, NOAA, Boulder, Colorado, USA.
- Álvarez-Varas R, Morales-Moraga D, González-Acuña D, Klarian SA, Vianna JA (2018) Mercury exposure in Humboldt (*Spheniscus*

- humboldtii*) and chinstrap (*Pygoscelis antarcticus*) penguins throughout the Chilean coast and Antarctica. Arch Environ Contam Toxicol 75:75–86. <https://doi.org/10.1007/s00244-018-0529-7>
- Ballard G, Schmidt AE, Toniolo V, Veloz S, Jongsonjit D, Arrigo KR, Ainley DG (2019) Fine-scale oceanographic features characterizing successful Adélie penguin foraging in the SW Ross Sea. Mar Ecol Prog Ser 608:263–277. <https://doi.org/10.3354/meps12801>
- Ballard G, Toniolo V, Ainley DG, Parkinson CL, Arrigo KR, Trathan PN (2010) Responding to climate change: Adélie penguins confront astronomical and ocean boundaries. Ecology 91:2056–2069. <https://doi.org/10.1890/09-0688.1>
- Barbraud C, Rolland V, Jenouvrier S, Nevoux M, Delord K, Weimerskirch H (2012) Effects of climate change and fisheries bycatch on Southern Ocean seabirds: a review. Mar. Ecol. Prog. Ser. 454:285–307
- Bargagli R (2016) Atmospheric chemistry of mercury in Antarctica and the role of cryptogams to assess deposition patterns in coastal ice-free areas. Chemosphere 163:202–208. <https://doi.org/10.1016/j.chemosphere.2016.08.007>
- Bargagli R (2008) Environmental contamination in Antarctic ecosystems. Sci Total Environ 400:212–226. <https://doi.org/10.1016/j.scitotenv.2008.06.062>
- Bargagli R, Monaci F, Sanchez-Hernandez JC, Cateni D (1998) Biomagnification of mercury in an Antarctic marine coastal food web. Mar Ecol Prog Ser 169:65–76. <https://doi.org/10.3354/meps169065>
- Bartoń K (2022). *MuMIn: Multi-Model Inference*. R package version 1.47.1, <https://CRAN.R-project.org/package=MuMIn>
- Bearhop S, Phillips RA, McGill R, Cherel Y, Dawson DA, Croxall JP (2006) Stable isotopes indicate sex-specific and long-term individual foraging specialisation in diving seabirds. Mar Ecol Prog Ser 311:157–164. <https://doi.org/10.3354/meps311157>
- Becker PH, González-Solís J, Behrens B, Croxall J (2002) Feather mercury levels in seabirds at South Georgia: influence of trophic position, sex and age. Mar Ecol Prog Ser 243:261–269. <https://doi.org/10.3354/meps243261>
- Becker PH, Goutner V, Ryan PG, González-Solís J (2016) Feather mercury concentrations in Southern Ocean seabirds: variation by species, site and time. Environ Pollut 216:253–263. <https://doi.org/10.1016/j.envpol.2016.05.061>
- Behrendt JC (1990) Ross Sea. Antarct. Res. Ser. 48:89–90
- Bless AC, Steele M, Peng G, Meier WN, Dickinson S (2019) Regional variability of Arctic sea ice seasonal change climate indicators from a passive microwave climate data record. Environ Res Lett 14:045003. <https://doi.org/10.1088/1748-9326/aaf84>
- Bond AL (2010) Relationships between stable isotopes and metal contaminants in feathers are spurious and biologically uninformative. Environ Pollut 158:1182–1184. <https://doi.org/10.1016/j.envpol.2010.01.004>
- Bond AL, Diamond AW (2009a) Mercury concentrations in seabird tissues from Machias Seal Island, New Brunswick, Canada. Sci Total Environ 407:4340–4347. <https://doi.org/10.1016/j.scitotenv.2009.04.018>
- Bond AL, Diamond AW (2009b) Total and methyl mercury concentrations in seabird feathers and eggs. Arch Environ Contam Toxicol 56:286–291. <https://doi.org/10.1007/s00244-008-9185-7>
- Bond AL, Hobson KA, Branfireun BA (2015) Rapidly increasing methyl mercury in endangered ivory gull (*Pagophila eburnea*) feathers over a 130 year record. Proc Biol Sci 282:1–8
- Brasso RL, Chiaradia A, Polito MJ, Raya Rey A, Emslie SD (2015) A comprehensive assessment of mercury exposure in penguin populations throughout the Southern Hemisphere: using trophic calculations to identify sources of population-level variation. Mar Pollut Bull 97:408–418. <https://doi.org/10.1016/j.marpolbul.2015.05.059>
- Brasso RL, Drummond BE, Borrett SR, Chiaradia A, Polito MJ, Rey AR (2013) Unique pattern of molt leads to low intraindividual variation in feather mercury concentrations in penguins. Environ Toxicol Chem 32:2331–2334. <https://doi.org/10.1002/etc.2303>
- Brasso RL, Polito MJ, Emslie SD (2014) Multi-tissue analyses reveal limited inter-annual and seasonal variation in mercury exposure in an Antarctic penguin community. Ecotoxicology 23:1494–1504. <https://doi.org/10.1007/s10646-014-1291-x>
- Braune B, Chételat J, Amyot M, Brown T, Clayden M, Evans M, Fisk A, Gaden A, Girard C, Hare A, Kirk J, Lehnher I, Letcher R, Loseto L, Macdonald R, Mann E, McMeans B, Muir D, O'Driscoll N, Poulain A, Reimer K, Stern G (2015) Mercury in the marine environment of the Canadian Arctic: review of recent findings. Sci Total Environ Special Issue: Mercury Canada's North 509–510:67–90. <https://doi.org/10.1016/j.scitotenv.2014.05.133>
- Braune BM, Gaskin DE (1987) Mercury levels in Bonaparte's gulls (*Larus Philadelphica*) during autumn molt in the Quoddy region, New Brunswick, Canada. Arch Environ Contam Toxicol 16:539–549. <https://doi.org/10.1007/BF01055810>
- Burger J, Gochfeld M (2004) Marine birds as sentinels of environmental pollution. EcoHealth 1:263–274. <https://doi.org/10.1007/s10393-004-0096-4>
- Burnham KP, Anderson DR (2002) Model selection and multimodel inference: a practical information - theoretic approach, second ed. Springer, US
- Bustamante P, Carravieri A, Goutte A, Barbraud C, Delord K, Chastel O, Weimerskirch H, Cherel Y (2016) High feather mercury concentrations in the wandering albatross are related to sex, breeding status and trophic ecology with no demographic consequences. Environ Res 144:1–10. <https://doi.org/10.1016/j.envres.2015.10.024>
- Carravieri A, Bustamante P, Churlaud C, Cherel Y (2013) Penguins as bioindicators of mercury contamination in the Southern Ocean: birds from the Kerguelen Islands as a case study. Sci Total Environ 454–455:141–148. <https://doi.org/10.1016/j.scitotenv.2013.02.060>
- Carravieri A, Bustamante P, Churlaud C, Fromant A, Cherel Y (2014a) Moulting patterns drive within-individual variations of stable isotopes and mercury in seabird body feathers: Implications for monitoring of the marine environment. Mar Biol 161:963–968. <https://doi.org/10.1007/s00227-014-2394-x>
- Carravieri A, Bustamante P, Tartu S, Meillère A, Labadie P, Budzinski H, Peluhet L, Barbraud C, Weimerskirch H, Chastel O, Cherel Y (2014b) Wandering Albatrosses document latitudinal variations in the transfer of persistent organic pollutants and mercury to Southern Ocean predators. Environ Sci Technol 48:14746–14755. <https://doi.org/10.1021/es504601m>
- Carravieri A, Cherel Y, Blévin P, Brault-Favrou M, Chastel O, Bustamante P (2014c) Mercury exposure in a large subantarctic avian community. Environ Pollut 190:51–57. <https://doi.org/10.1016/j.envpol.2014.03.017>
- Carravieri A, Cherel Y, Brault-Favrou M, Churlaud C, Peluhet L, Labadie P, Budzinski H, Chastel O, Bustamante P (2017) From Antarctica to the subtropics: contrasted geographical concentrations of selenium, mercury, and persistent organic pollutants in skua chicks (*Catharacta* spp.). Environ Pollut 228:464–473. <https://doi.org/10.1016/j.envpol.2017.05.053>
- Carravieri A, Cherel Y, Jaeger A, Churlaud C, Bustamante P (2016) Penguins as bioindicators of mercury contamination in the southern Indian Ocean: geographical and temporal trends. Environ. Pollut. Barking Essex 1987 213:195–205. <https://doi.org/10.1016/j.envpol.2016.02.010>

- Carter L, McCave IN, Williams MJM (2008) Chapter 4 Circulation and water masses of the Southern Ocean: a review, in: Florindo, F., Siebert, M. (Eds), *Developments in Earth and Environmental Sciences, Antarctic Climate Evolution*. Elsevier, pp. 85–114. [https://doi.org/10.1016/S1571-9197\(08\)00004-9](https://doi.org/10.1016/S1571-9197(08)00004-9)
- Chastel O, Fort J, Ackerman JT, Albert C, Angelier F, Basu N, Blévin P, Brault-Favrou M, Bustnes JO, Bustamante P, Danielsen J, Descamps S, Dietz R, Erikstad KE, Eulaers I, Ezhov A, Fleishman AB, Gabrielsen GW, Gavrilov M, Gilchrist G, Gilg O, Gíslason S, Golubova E, Goutte A, Grémillet D, Hallgrímsson GT, Hansen ES, Hanssen SA, Hatch S, Huffeldt NP, Jakubas D, Jónsson JE, Kitaysky AS, Kolbeinsson Y, Krasnov Y, Letcher RJ, Linnebjerg JF, Mallory M, Merkel FR, Moe B, Montevecchi WJ, Mosbech A, Olsen B, Orben RA, Provencher JF, Ragnarsdóttir SB, Reiersen TK, Rojek N, Romano M, Søndergaard J, Strøm H, Takahashi A, Tartu S, Thórarinnsson TL, Thiebot J-B, Will AP, Wilson S, Wojczulanis-Jakubas K, Yannic G (2022) Mercury contamination and potential health risks to Arctic seabirds and shorebirds. *Sci. Total Environ.* 156944. <https://doi.org/10.1016/j.scitotenv.2022.156944>
- Cherel Y (2008) Isotopic niches of emperor and Adélie penguins in Adélie Land, Antarctica. *Mar Biol* 154:813–821. <https://doi.org/10.1007/s00227-008-0974-3>
- Cherel Y, Barbraud C, Lahoumat M, Jaeger A, Jaquet S, Wanless RM, Phillips RA, Thompson DR, Bustamante P (2018) Accumulate or eliminate? Seasonal mercury dynamics in albatrosses, the most contaminated family of birds. *Environ Pollut* 241:124–135. <https://doi.org/10.1016/j.envpol.2018.05.048>
- Cherel Y, Charrassin JB, Challet E (1994) Energy and protein requirements for molt in the king penguin *Aptenodytes patagonicus*. *Am J Physiol* 266:R1182–1188. <https://doi.org/10.1152/ajpregu.1994.266.4.R1182>
- Cherel Y, Charrassin J-B, Handrich Y (1993) Comparison of body reserve buildup in prefasting chicks and adults of King Penguins (*Aptenodytes patagonicus*). *Physiol Zool* 66:750–770. <https://doi.org/10.1086/physzool.66.5.30163822>
- Cherel Y, Hobson KA (2007) Geographical variation in carbon stable isotope signatures of marine predators: a tool to investigate their foraging areas in the Southern Ocean. *Mar Ecol Prog Ser* 329:281–287. <https://doi.org/10.3354/meps329281>
- Cherel Y, Hobson KA, Guinet C, Vanpe C (2007) Stable isotopes document seasonal changes in trophic niches and winter foraging individual specialization in diving predators from the Southern Ocean. *J Anim Ecol* 76:826–836. <https://doi.org/10.1111/j.1365-2656.2007.01238.x>
- Cherel Y, Koubbi P, Giraldo C, Penot F, Tavernier E, Moteki M, Ozouf-Costaz C, Causse R, Chartier A, Hosie G (2011) Isotopic niches of fishes in coastal, neritic and oceanic waters off Adélie land, Antarctica. *Polar Sci* 5:286–297. <https://doi.org/10.1016/j.polar.2010.12.004>
- Chételat J, McKinney MA, Amyot M, Dastoor A, Douglas TA, Heimbürger-Boavida L-E, Kirk J, Kahilainen KK, Outridge PM, Pelletier N, Skov H, St. Pierre K, Vuorenmaa J, Wang F (2022) Climate change and mercury in the Arctic: Abiotic interactions. *Sci Total Environ* 824:153715. <https://doi.org/10.1016/j.scitotenv.2022.153715>
- Clarke J, Kerry K, Fowler C, Lawless R, Eberhard S, Murphy R (2003) Post-fledging and winter migration of Adélie penguins *Pygoscelis adeliae* in the Mawson region of East Antarctica. *Mar Ecol Prog Ser* 248:267–278. <https://doi.org/10.3354/meps248267>
- Clarke J, Manly B, Kerry K, Gardner H, Franchi E, Corsolini S, Focardi S (1998) Sex differences in Adélie penguin foraging strategies. *Polar Biol* 20:248–258. <https://doi.org/10.1007/s003000050301>
- Clucas GV, Dunn MJ, Dyke G, Emslie SD, Levy H, Naveen R, Polito MJ, Pybus OG, Rogers AD, Hart T (2014) A reversal of fortunes: climate change ‘winners’ and ‘losers’ in Antarctic Peninsula penguins. *Sci Rep* 4:5024. <https://doi.org/10.1038/srep05024>
- Colominas-Ciuró R, Santos M, Coria N, Barbosa A (2018) Sex-specific foraging strategies of Adélie penguins (*Pygoscelis adeliae*): females forage further and on more krill than males in the Antarctic Peninsula. *Polar Biol* 41:2635–2641. <https://doi.org/10.1007/s00300-018-2395-1>
- Coria NR, Spairani H, Vivequin S, Fontana R (1995) Diet of Adélie penguins *Pygoscelis adeliae* during the post-hatching period at Esperanza Bay, Antarctica, 1987/88. *Polar Biol* 15:415–418. <https://doi.org/10.1007/BF00239717>
- Cossa D (2013) Methylmercury manufacture. *Nat Geosci* 6:810–811. <https://doi.org/10.1038/ngeo1967>
- Cossa D, Heimbürger L-E, Lannuzel D, Rintoul SR, Butler ECV, Bowie AR, Averty B, Watson RJ, Remenyi T (2011) Mercury in the Southern Ocean. *Geochim. Cosmochim. Acta* 75:4037–4052. <https://doi.org/10.1016/j.gca.2011.05.001>
- Cottin M, Raymond B, Kato A, Amélineau F, Le Maho Y, Raclot T, Galton-Fenzi B, Meijers A, Ropert-Coudert Y (2012) Foraging strategies of male Adélie penguins during their first incubation trip in relation to environmental conditions. *Mar Biol* 159:1843–1852. <https://doi.org/10.1007/s00227-012-1974-x>
- Crewther WG, Fraser RD, Lennox FG, Lindley H (1965) The chemistry of keratins. *Adv Protein Chem* 20:191–346. [https://doi.org/10.1016/s0065-3233\(08\)60390-3](https://doi.org/10.1016/s0065-3233(08)60390-3)
- Croxall JP (1982) Energy costs of incubation and moult in petrels and penguins. *J Anim Ecol* 51:177–194. <https://doi.org/10.2307/4318>
- Davis LS, Boersma PD, Court GS (1996) Satellite telemetry of the winter migration of Adélie penguins (*Pygoscelis adeliae*). *Polar Biol* 16:221–225. <https://doi.org/10.1007/BF02329210>
- Davis LS, Miller GD (1992) Satellite tracking of Adélie penguins. *Polar Biol* 12:503–506. <https://doi.org/10.1007/BF00238189>
- Desforges J-P, Outridge P, Hobson KA, Heide-Jørgensen MP, Dietz R (2022) Anthropogenic and climatic drivers of long-term changes of mercury and feeding ecology in Arctic Beluga (*Delphinapterus leucas*) populations. *Environ Sci Technol* 56:271–281. <https://doi.org/10.1021/acs.est.1c05389>
- Dietz R, Letcher RJ, Desforges J-P, Eulaers I, Sonne C, Wilson S, Andersen-Ranberg E, Basu N, Barst BD, Bustnes JO, Bytingsvik J, Ciesielski TM, Drevnick PE, Gabrielsen GW, Haarr A, Hylland K, Jenssen BM, Levin M, McKinney MA, Nørregaard RD, Pedersen KE, Provencher J, Styriehave B, Tartu S, Aars J, Ackerman JT, Rosing-Asvid A, Barrett R, Bignert A, Bom EW, Branigan M, Braune B, Bryan CE, Dam M, Eagles-Smith CA, Evans M, Evans TJ, Fisk AT, Gamberg M, Gustavson K, Hartman CA, Helander B, Herzog MP, Hoekstra PF, Houde M, Hoydal K, Jackson AK, Kucklick J, Lie E, Loseto L, Mallory ML, Miljeteig C, Mosbech A, Muir DCG, Nielsen ST, Peacock E, Pedro S, Peterson SH, Polder A, Rigét FF, Roach P, Saunes H, Sinding M-HS, Skaare JU, Søndergaard J, Stenson G, Stern G, Treu G, Schuur SS, Víkingsson G (2019) Current state of knowledge on biological effects from contaminants on arctic wildlife and fish. *Sci Total Environ* 696:133792. <https://doi.org/10.1016/j.scitotenv.2019.133792>
- Dietz R, Wilson S, Loseto LL, Dommergue A, Xie Z, Sonne C, Chételat J (2022) Special issue on the AMAP 2021 assessment of mercury in the Arctic. *Sci Total Environ* 157020. <https://doi.org/10.1016/j.scitotenv.2022.157020>
- Dunn MJ, Silk JRD, Trathan PN (2011) Post-breeding dispersal of Adélie penguins (*Pygoscelis adeliae*) nesting at Signy Island, South Orkney Islands. *Polar Biol* 34:205–214. <https://doi.org/10.1007/s00300-010-0870-4>
- Edwards BR, Smellie JL (Eds) (2016) Distribution of glaciovolcanism on Earth, in: *Glaciovolcanism on Earth and Mars: Products, Processes and Palaeoenvironmental Significance*. Cambridge

- University Press, Cambridge, p 15–56. <https://doi.org/10.1017/CBO9781139764384.003>
- Emmerson L, Southwell C (2011) Adélie penguin survival: age structure, temporal variability and environmental influences. *Oecologia* 167:951–965. <https://doi.org/10.1007/s00442-011-2044-7>
- Emmerson L, Southwell C (2008) Sea ice cover and its influence on Adélie penguin reproductive performance. *Ecology* 89:2096–2102. <https://doi.org/10.1890/08-0011.1>
- Emmerson L, Walsh S, Southwell C (2019) Nonbreeder birds at colonies display qualitatively similar seasonal mass change patterns as breeders. *Ecol Evol* 9:4637–4650. <https://doi.org/10.1002/ece3.5067>
- Erdmann ES, Ribic CA, Patterson-Fraser DL, Fraser WR (2011) Characterization of winter foraging locations of Adélie penguins along the Western Antarctic Peninsula, 2001–2002. *Deep Sea Res. Part II Top. Stud. Oceanogr.*, Understanding the linkages between Antarctic food webs and the environment: a synthesis of Southern Ocean GLOBEC studies 58:1710–1718. <https://doi.org/10.1016/j.dsr2.2010.10.054>
- Everson I (2000) Roles of krill in marine food webs: The Southern Ocean, in: Everson, I. (Ed.), Blackwell Science, Oxford, pp. 194–201.
- Ferraccioli F, Armadillo E, Bozzo E, Privitera E (2000) Magnetics and gravity image tectonic framework of the Mount Melbourne volcano area (Antarctica). *Phys Chem Earth Part Solid Earth Geod* 25:387–393. [https://doi.org/10.1016/S1464-1895\(00\)00061-2](https://doi.org/10.1016/S1464-1895(00)00061-2)
- Forero MG, Hobson KA, Bortolotti GR, Donazar JA, Bertellotti M, Blanco G (2002) Food resource utilisation by the Magellanic penguin evaluated through stable-isotope analysis: Segregation by sex and age and influence on offspring quality. *Mar Ecol Prog Ser* 234:289–299. <https://doi.org/10.3354/meps234289>
- Fort J, Grémillet D, Trainsel G, Amélineau F, Bustamante P (2016) Does temporal variation of mercury levels in Arctic seabirds reflect changes in global environmental contamination, or a modification of Arctic marine food web functioning? *Environ Pollut* 211:382–388. <https://doi.org/10.1016/j.envpol.2015.12.061>
- Foster KL, Braune BM, Gaston AJ, Mallory ML (2019) Climate influence on mercury in Arctic seabirds. *Sci Total Environ* 693:133569. <https://doi.org/10.1016/j.scitotenv.2019.07.375>
- Fox J, Weisberg S (2018) Visualizing fit and lack of fit in complex regression models with predictor effect plots and partial residuals. *J Statist Software* 87(9):1–27. <https://doi.org/10.18637/jss.v087.i09>
- Fox J, Weisberg S (2019) *An R Companion to Applied Regression*, 3rd Edition. Thousand Oaks, CA. <https://socialsciences.mcmaster.ca/jfox/Books/Companion/index.html>
- Freeman NM, Lovenduski NS (2016) Mapping the Antarctic Polar Front: weekly realizations from 2002 to 2014. *Earth Syst Sci Data* 8:191–198. <https://doi.org/10.5194/essd-8-191-2016>
- Furness RW, Camphuysen KJ (1997) Seabirds as monitors of the marine environment *ICES J Mar Sci* 54:726–737. <https://doi.org/10.1006/jmsc.1997.0243>
- Furness RW, Muirhead SJ, Woodburn M (1986) Using bird feathers to measure mercury in the environment: relationships between mercury content and moult. *Mar Pollut Bull* 17:27–30. [https://doi.org/10.1016/0025-326X\(86\)90801-5](https://doi.org/10.1016/0025-326X(86)90801-5)
- Furtado R, Granadeiro JP, Gatt MC, Rounds R, Horikoshi K, Paiva VH, Menezes D, Pereira E, Catty P (2021) Monitoring of mercury in the mesopelagic domain of the Pacific and Atlantic oceans using body feathers of Bulwer's petrel as a bioindicator. *Sci Total Environ* 775:145796. <https://doi.org/10.1016/j.scitotenv.2021.145796>
- Gatt MC, Reis B, Granadeiro JP, Pereira E, Catty P (2020) Generalist seabirds as biomonitors of ocean mercury: the importance of accurate trophic position assignment. *Sci Total Environ* 740:140159. <https://doi.org/10.1016/j.scitotenv.2020.140159>
- Gionfriddo CM, Tate MT, Wick RR, Schultz MB, Zemla A, Thelen MP, Schofield R, Krabbenhoft DP, Holt KE, Moreau JW (2016) Microbial mercury methylation in Antarctic sea ice. *Nat Microbiol* 1:1–12. <https://doi.org/10.1038/nmicrobiol.2016.127>
- Global Volcanism Program (2022) Report on Erebus (Antarctica) (Venzke, E., ed.). Bulletin of the Global Volcanism Network, 47:2. Smithsonian Institution. <https://doi.org/10.5479/si.GVP.BGVN202202-390020>
- Gon O, Heemstra PC (1990) *Fishes of the Southern Ocean*, First edition. ed. J.L.B. Smith Institute of Ichthyology, Grahamstown, South Africa
- González-Solís J, Croxall JP, Wood AG (2000) Sexual dimorphism and sexual segregation in foraging strategies of northern giant petrels, *Macronectes halli*, during incubation. *Oikos* 90:390–398. <https://doi.org/10.1034/j.1600-0706.2000.900220.x>
- Grasby SE, Them TR, Chen Z, Yin R, Ardakani OH (2019) Mercury as a proxy for volcanic emissions in the geologic record. *Earth Sci Rev* 196:102880. <https://doi.org/10.1016/j.earscirev.2019.102880>
- Green K, Johnstone GW (1988) Changes in the diet of Adélie penguins breeding in East-Antarctica. *Wildl Res* 15:103–110. <https://doi.org/10.1071/wr9880103>
- Grunst AS, Grunst ML, Grémillet D, Kato A, Bustamante P, Albert C, Brisson-Curadeau É, Clairbaux M, Cruz-Flores M, Gentès S, Perret S, Ste-Marie E, Wojczulanis-Jakubas K, Fort J (2023) Mercury contamination challenges the behavioral response of a keystone species to Arctic climate change. *Environ Sci Technol* 57(5):2054–2063. <https://doi.org/10.1021/acs.est.2c08893>
- Guen CL, Kato A, Raymond B, Barbraud C, Beaulieu M, Bost C-A, Delord K, MacIntosh AJ, Meyer X, Raclot T, Sumner M, Takahashi A, Thiebot J-B, Ropert-Coudert Y (2018) Reproductive performance and diving behaviour share a common sea-ice concentration optimum in Adélie penguins (*Pygoscelis adeliae*). *Glob Change Biol* 24:5304–5317. <https://doi.org/10.1111/gcb.14377>
- Hinke JT, Polito MJ, Goebel ME, Jarvis S, Reiss CS, Thorrold SR, Trivelpiece WZ, Watters GM (2015) Spatial and isotopic niche partitioning during winter in chinstrap and Adélie penguins from the South Shetland Islands. *Ecosphere* 6:art125. <https://doi.org/10.1890/ES14-00287.1>
- Hodum PJ, Hobson KA (2000) Trophic relationships among Antarctic fulmarine petrels: insights into dietary overlap and chick provisioning strategies inferred from stable-isotope ($\delta^{15}\text{N}$ and $\delta^{13}\text{C}$) analyses. *Mar Ecol Prog Ser* 198:273–281. <https://doi.org/10.3354/meps198273>
- Honda K, Yamamoto Y, Hidaka H, Tatsukawa R (1986) Heavy metal accumulations in Adélie penguin, *Pygoscelis adeliae*, and their variations with the reproductive processes 40, 443–453.
- Jafari V, Maccapan D, Careddu G, Sporta Caputi S, Calizza E, Rossi L, Costantini ML (2021) Spatial and temporal diet variability of Adélie (*Pygoscelis adeliae*) and Emperor (*Aptenodytes forsteri*) penguin: a multi tissue stable isotope analysis. *Polar Biol* 44:1869–1881. <https://doi.org/10.1007/s00300-021-02925-1>
- Johnson JB, Omland KS (2004) Model selection in ecology and evolution. *Trends Ecol Evol* 19:101–108. <https://doi.org/10.1016/j.tree.2003.10.013>
- Juárez MA, Casaux R, Corbalán A, Blanco G, Pereira GA, Perchivalé PJ, Coria NR, Santos MM (2018) Diet of Adélie penguins (*Pygoscelis adeliae*) at Stranger Point (25 de Mayo/King George Island, Antarctica) over a 13-year period (2003–2015). *Polar Biol* 41:303–311. <https://doi.org/10.1007/s00300-017-2191-3>
- Juárez MA, Santos M, Mennucci JA, Coria NR, Mariano-Jelicich R (2016) Diet composition and foraging habitats of Adélie and

- gentoo penguins in three different stages of their annual cycle. *Mar Biol* 163:105. <https://doi.org/10.1007/s00227-016-2886-y>
- Kelly JF (2000) Stable isotopes of carbon and nitrogen in the study of avian and mammalian trophic ecology. *Can J Zool* 78:1–27. <https://doi.org/10.1139/z99-165>
- Kent S, Seddon J, Robertson G, Wienecke BC (1998) Diet of Adélie penguins *Pygoscelis adeliae* at Shirley Island, East Antarctica, January 1992. *Mar Ornithol* 26:7–10
- Knox GA (2006) *Biology of the Southern Ocean* (2nd ed.). CRC Press, Boca Raton, USA. <https://doi.org/10.1201/9781420005134>, <https://www.taylorfrancis.com/books/mono/10.1201/9781420005134/biology-southern-ocean-george-knox>
- Kokubun N, Emmerson L, McInnes J, Wienecke B, Southwell C (2021) Sea-ice and density-dependent factors affecting foraging habitat and behaviour of Adélie penguins throughout the breeding season. *Mar Biol* 168:97. <https://doi.org/10.1007/s00227-021-03899-8>
- Lamborg CH, Hammerschmidt CR, Bowman KL, Swarr GJ, Munson KM, Ohnemus DC, Lam PJ, Heimbürger L-E, Rijkenberg MJA, Saito MA (2014) A global ocean inventory of anthropogenic mercury based on water column measurements. *Nature* 512:65–68. <https://doi.org/10.1038/nature13563>
- Lee JR, Raymond B, Bracegirdle TJ, Chadès I, Fuller RA, Shaw JD, Terauds A (2017) Climate change drives expansion of Antarctic ice-free habitat. *Nature* 547:49–54. <https://doi.org/10.1038/nature22996>
- Length R (2023) `_emmeans`: Estimated Marginal Means, aka Least-Squares Means. R package version 1.8.5, <https://CRAN.R-project.org/package=emmeans>
- Lynnes AS, Reid K, Croxall JP (2004) Diet and reproductive success of Adélie and chinstrap penguins: linking response of predators to prey population dynamics. *Polar Biol* 27:544–554. <https://doi.org/10.1007/s00300-004-0617-1>
- Matias RS, Guimarães HR, Bustamante P, Seco J, Chipev N, Fragão J, Tavares S, Ceia FR, Pereira ME, Barbosa A, Xavier JC (2022) Mercury biomagnification in an Antarctic food web of the Antarctic Peninsula. *Environ Pollut* 304:119199. <https://doi.org/10.1016/j.envpol.2022.119199>
- McKenzie AC, Silvestro AM, Marti LJ, Emslie SD (2021) Intraspecific variation in mercury, $\delta^{15}\text{N}$, and $\delta^{13}\text{C}$ Among three Adélie Penguin (*Pygoscelis adeliae*) populations in the Northern Antarctic Peninsula Region. *Environ Toxicol Chem* 40:2791–2801. <https://doi.org/10.1002/etc.5166>
- McKinney MA, Chételat J, Burke SM, Elliott KH, Fernie KJ, Houde M, Kahilainen KK, Letcher RJ, Morris AD, Muir DCG, Routti H, Yurkowski DJ (2022) Climate change and mercury in the Arctic: biotic interactions. *Sci Total Environ* 834:155221. <https://doi.org/10.1016/j.scitotenv.2022.155221>
- Meier WN et al. (2014) Arctic sea ice in transformation: A review of recent observed changes and impacts on biology and human activity. *Rev. Geophys.* 51:185–217. <https://doi.org/10.1002/2013RG000431>
- Michelot C, Kato A, Raclot T, Ropert-Coudert Y (2021) Adélie penguins foraging consistency and site fidelity are conditioned by breeding status and environmental conditions. *PLOS ONE* 16:e0244298. <https://doi.org/10.1371/journal.pone.0244298>
- Michelot C, Kato A, Raclot T, Shiomi K, Goulet P, Bustamante P, Ropert-Coudert Y (2020) Sea-ice edge is more important than closer open water access for foraging Adélie penguins: evidence from two colonies. *Mar Ecol Prog Ser* 640:215–230. <https://doi.org/10.3354/meps13289>
- Mills WF, Bustamante P, McGill RAR, Anderson ORJ, Bearhop S, Cherel Y, Votier SC, Phillips RA (2020) Mercury exposure in an endangered seabird: long-term changes and relationships with trophic ecology and breeding success. *Proc R Soc B Biol Sci* 287:20202683. <https://doi.org/10.1098/rspb.2020.2683>
- Morley SA, Barnes DKA, Dunn MJ (2019) Predicting which species succeed in climate-forced polar seas. *Front Mar Sci* 5
- NRC/NAS (2000) *Toxicological Effects of Methylmercury*. National Research Council/National Academy of Sciences, Washington, DC
- Newsome SD, del Rio CM, Bearhop S, Phillips DL (2007) A niche for isotopic ecology. *Front Ecol Environ* 5:429–436
- Olmastroni S, Fattorini N, Pezzo F, Focardi S (2020) Gone fishing: Adélie penguin site-specific foraging tactics and breeding performance. *Antarct Sci* 32:199–209. <https://doi.org/10.1017/S0954102020000085>
- Orsi AH, Whitworth T, Nowlin WD (1995) On the meridional extent and fronts of the Antarctic circumpolar current. *Deep Sea Res Part Oceanogr Res Pap* 42:641–673. [https://doi.org/10.1016/0967-0637\(95\)00021-W](https://doi.org/10.1016/0967-0637(95)00021-W)
- Pacyna AD, Jakubas D, Ausems ANMA, Frankowski M, Polkowska Z, Wojczulanis-Jakubas K (2019) Storm petrels as indicators of pelagic seabird exposure to chemical elements in the Antarctic marine ecosystem. *Sci Total Environ* 692:382–392. <https://doi.org/10.1016/j.scitotenv.2019.07.137>
- Parish TR (1988) Surface winds over the Antarctic continent: a review. *Rev Geophys* 26:169–180. <https://doi.org/10.1029/RG026i001p00169>
- Parish TR, Cassano JJ (2003) The role of katabatic winds on the Antarctic surface wind regime. *Mon Weather Rev* 131:317–333. [https://doi.org/10.1175/1520-0493\(2003\)131<0317:TROKWO>2.0.CO;2](https://doi.org/10.1175/1520-0493(2003)131<0317:TROKWO>2.0.CO;2)
- Pedro S, Xavier JC, Tavares S, Trathan PN, Ratcliffe N, Paiva VH, Medeiros R, Vieira RP, Ceia FR, Pereira E, Pardal MA (2015) Mercury accumulation in gentoo penguins *Pygoscelis papua*: spatial, temporal and sexual intraspecific variations. *Polar Biol* 38:1335–1343. <https://doi.org/10.1007/s00300-015-1697-9>
- Phillips RA, McGill RAR, Dawson DA, Bearhop S (2011) Sexual segregation in distribution, diet and trophic level of seabirds: Insights from stable isotope analysis. *Mar Biol* 158:2199–2208. <https://doi.org/10.1007/s00227-011-1725-4>
- Piatt JF, Harding AMA, Shultz M, Speckman SG, Pelt TI, van, Drew GS, Kettle AB (2007) Seabirds as indicators of marine food supplies: Cairns revisited. *Mar Ecol Prog Ser* 352:221–234. <https://doi.org/10.3354/meps07078>
- Pilcher N, Gaw S, Eisert R, Horton TW, Gornley AM, Cole TL, Lyver PO (2020) Latitudinal, sex and inter-specific differences in mercury and other trace metal concentrations in Adélie and Emperor penguins in the Ross Sea, Antarctica. *Mar. Pollut. Bull.* 154:111047. <https://doi.org/10.1016/j.marpolbul.2020.111047>
- Pinheiro J, Bates D, R Core Team (2022) `_nlme`: Linear and Nonlinear Mixed Effects Models. R package version 3.1–160, <https://CRAN.R-project.org/package=nlme>
- Polito MJ, Brasso RL, Trivelpiece WZ, Kamovsky N, Patterson WP, Emslie SD (2016) Differing foraging strategies influence mercury (Hg) exposure in an Antarctic penguin community. *Environ Pollut* 218:196–206. <https://doi.org/10.1016/j.envpol.2016.04.097>
- Polito MJ, Lynch HJ, Naveen R, Emslie SD (2011) Stable isotopes reveal regional heterogeneity in the pre-breeding distribution and diets of sympatrically breeding *Pygoscelis spp.* penguins. *Mar Ecol Prog Ser* 421:265–277. <https://doi.org/10.3354/meps08863>
- Provencher JF, Gilchrist HG, Mallory ML, Mitchell GW, Forbes MR (2016) Direct and indirect causes of sex differences in mercury concentrations and parasitic infections in a marine bird. *Sci Total Environ* 551–552:506–512. <https://doi.org/10.1016/j.scitotenv.2016.02.055>
- Puddicombe RA, Johnstone GW (1988) The breeding season diet of Adélie penguins at the Vestfold Hills, East Antarctica. In: Ferris JM, Burton HR, Johnstone GW, Bayly IAE Eds.) *Biology of the Vestfold Hills, Antarctica, Developments in Hydrobiology*.

- Springer Netherlands, Dordrecht, p 239–253. https://doi.org/10.1007/978-94-009-3089-6_25
- R Core Team (2022) R: A language and environment for statistical computing. R Foundation for Statistical Computing, Vienna, Austria, <https://www.R-project.org/URL>
- Renedo M, Bustamante P, Chérel Y, Pedrero Z, Tessier E, Amouroux D (2020) A “seabird-eye” on mercury stable isotopes and cycling in the Southern Ocean. *Sci Total Environ* 742:140499. <https://doi.org/10.1016/j.scitotenv.2020.140499>
- Renedo M, Bustamante P, Tessier E, Pedrero Z, Chérel Y, Amouroux D (2017) Assessment of mercury speciation in feathers using species-specific isotope dilution analysis. *Talanta* 174:100–110. <https://doi.org/10.1016/j.talanta.2017.05.081>
- Riaz J, Bestley S, Wotherspoon S, Emmerson L (2021) Horizontal-vertical movement relationships: Adélie penguins forage continuously throughout provisioning trips. *Mov Ecol* 9:43. <https://doi.org/10.1186/s40462-021-00280-8>
- Rocchi S, Storti F, Di Vincenzo G, Rossetti F (2003) Intraplate strike-slip tectonics as an alternative to mantle plume activity for the Cenozoic rift magmatism in the Ross Sea region, Antarctica. *Geol Soc Lond Spec Publ* 210:145–158. <https://doi.org/10.1144/GSL.SP.2003.210.01.09>
- Roman HA, Walsh TL, Coull BA, Dewailly É, Guallar E, Hattis D, Mariën K, Schwartz J, Stern AH, Virtanen JK, Rice G (2011) Evaluation of the cardiovascular effects of methylmercury exposures: Current evidence supports development of a dose–response function for regulatory benefits analysis. *Environ Health Perspect* 119:607–614. <https://doi.org/10.1289/ehp.1003012>
- Scheuhammer AM, Basu N, Evers DC, Heinz GH, Sandheinrich MB, Bank MS (2012) Ecotoxicology of mercury in fish and wildlife: Recent advances, in: Bank, M. (Ed.), *Mercury in the environment: Pattern and Process*. University of California Press, p. 0. <https://doi.org/10.1525/california9780520271630.003.0011>
- Seco J, Aparício S, Brierley AS, Bustamante P, Ceia FR, Coelho JP, Philips RA, Saunders RA, Fielding S, Gregory S, Matias R, Pardal MA, Pereira E, Stowasser G, Tarling GA, Xavier JC (2021) Mercury biomagnification in a Southern Ocean food web. *Environ Pollut* 275:116620. <https://doi.org/10.1016/j.envpol.2021.116620>
- Seco J, Xavier JC, Coelho JP, Pereira B, Tarling G, Pardal MA, Bustamante P, Stowasser G, Brierley AS, Pereira ME (2019) Spatial variability in total and organic mercury levels in Antarctic krill *Euphausia superba* across the Scotia Sea. *Environ Pollut* 247:332–339. <https://doi.org/10.1016/j.envpol.2019.01.031>
- Selin NE (2009) Global biogeochemical cycling of mercury: a review. *Annu Rev Environ Resour* 34:43–63. <https://doi.org/10.1146/annurev.environ.051308.084314>
- Sonke JE, Angot H, Zhang Y, Poulain A, Björn E, Schartup A (2023) Global change effects on biogeochemical mercury cycling. *Ambio*. <https://doi.org/10.1007/s13280-023-01855-y>
- Sontag PT, Steinberg DK, Reinfelder JR (2019) Patterns of total mercury and methylmercury bioaccumulation in Antarctic krill (*Euphausia superba*) along the West Antarctic Peninsula. *Sci Total Environ* 688:174–183. <https://doi.org/10.1016/j.scitotenv.2019.06.176>
- Southwell C, Emmerson L, Takahashi A, Barbraud C, Delord K, Weimerskirch H (2017) Large-scale population assessment informs conservation management for seabirds in Antarctica and the Southern Ocean: a case study of Adélie penguins. *Glob Ecol Conserv* 9:104–115. <https://doi.org/10.1016/j.gecco.2016.12.004>
- Southwell C, Smith D, Bender A, Emmerson L (2021) A spatial reference and identification system for coastal ice-free land in East Antarctica. *Polar Rec* 57:e30. <https://doi.org/10.1017/S0032247421000280>
- Souza JS, Kasper D, da Cunha LST, Soares TA, de Lira Pessoa AR, de Carvalho GO, Costa ES, Niedzielski P, Torres JPM (2020) Biological factors affecting total mercury and methylmercury levels in Antarctic penguins. *Chemosphere* 261:127713. <https://doi.org/10.1016/j.chemosphere.2020.127713>
- Spreen G, Kaleschke L, Heygster G (2008) Sea ice remote sensing using AMSR-E 89-GHz channels. *J Geophys Res Oceans* 113. <https://doi.org/10.1029/2005JC003384>
- Stewart F, Phillips R, Catry P, Furness R (1997) Influence of species, age and diet on mercury concentrations in Shetland seabirds. *Mar Ecol Prog Ser* 151:237–244. <https://doi.org/10.3354/meps151237>
- Streets DG, Horowitz HM, Jacob DJ, Lu Z, Levin L, ter Schure AFH, Sunderland EM (2017) Total mercury released to the environment by human activities. *Environ Sci Technol* 51:5969–5977. <https://doi.org/10.1021/acs.est.7b00451>
- Takahashi A, Ito M, Nagai K, Thiebot J-B, Mitamura H, Noda T, Trathan PN, Tamura T, Watanabe YY (2018) Migratory movements and winter diving activity of Adélie penguins in East Antarctica. *Mar Ecol Prog Ser* 589:227–239. <https://doi.org/10.3354/meps12438>
- Tan SW, Meiller JC, Mahaffey KR (2009) The endocrine effects of mercury in humans and wildlife. *Crit Rev Toxicol* 39:228–269. <https://doi.org/10.1080/10408440802233259>
- Tartu S, Blévin P, Bustamante P, Angelier F, Bech C, Bustnes JO, Chierici M, Fransson A, Gabrielsen GW, Goutte A, Moe B, Sauser C, Sire J, Barbraud C, Chastel O (2022) A U-turn for mercury concentrations over 20 Years: How do environmental conditions affect exposure in Arctic seabirds? *Environ Sci Technol* 56:2443–2454. <https://doi.org/10.1021/acs.est.1c07633>
- Thiebot J-B, Ropert-Coudert Y, Raclot T, Poupart T, Kato A, Takahashi A (2019) Adélie penguins’ extensive seasonal migration supports dynamic Marine Protected Area planning in Antarctica. *Mar Policy* 109:103692. <https://doi.org/10.1016/j.marpol.2019.103692>
- Thompson DR, Fumess RW (1989) The chemical form of mercury stored in South Atlantic seabirds. *Environ Pollut* 60:305–317. [https://doi.org/10.1016/0269-7491\(89\)90111-5](https://doi.org/10.1016/0269-7491(89)90111-5)
- Thompson DR, Hamer KC, Furness RW (1991) Mercury accumulation in Great Skuas *Catharacta skua* of known age and sex, and its effects upon breeding and survival. *J Appl Ecol* 28:672–684. <https://doi.org/10.2307/2404575>
- Thompson DR, Stewart FM, Fumess RW (1990) Using seabirds to monitor mercury in marine environments: the validity of conversion ratios for tissue comparisons. *Mar Pollut Bull* 21:339–342. [https://doi.org/10.1016/0025-326X\(90\)90795-A](https://doi.org/10.1016/0025-326X(90)90795-A)
- Tierney M, Emmerson L, Hindell M (2009) Temporal variation in Adélie penguin diet at Béchervaise Island, east Antarctica and its relationship to reproductive performance. *Mar Biol* 156:1633–1645. <https://doi.org/10.1007/s00227-009-1199-9>
- Tumer J (2015) ARCTIC AND ANTARCTIC I Antarctic Climate. In: North GR, Pyle J, Zhang F (Eds.) *Encyclopedia of Atmospheric Sciences* (Second Edition). Academic Press, Oxford, p 98–106. <https://doi.org/10.1016/B978-0-12-382225-3.00044-X>
- UN Environment (2019) *Global Mercury Assessment 2018*. UN-Environment Programme, Chemicals and Health Branch, Geneva, Switzerland, p 59
- Watanuki Y, Kato A, Naito Y, Robertson G, Robinson S (1997) Diving and foraging behaviour of Adélie penguins in areas with and without fast sea-ice. *Polar Biol* 17:296–304. <https://doi.org/10.1007/PL00013371>
- Wickham H (2016) *ggplot2: Elegant Graphics for Data Analysis*. Springer-Verlag, New York
- Wienecke BC, Lawless R, Rodary D, Bost C-A, Thomson R, Pauly T, Robertson G, Kerry KR, LeMaho Y (2000) Adélie penguin foraging behaviour and krill abundance along the Wilkes and

- Adélie land coasts, Antarctica. *Deep Sea Res Part II Top Stud Oceanogr* 47:2573–2587. [https://doi.org/10.1016/S0967-0645\(00\)00036-9](https://doi.org/10.1016/S0967-0645(00)00036-9)
- Wienecke BC, Robertson G (1997) Foraging space of emperor penguins *Aptenodytes forsteri* in Antarctic shelf waters in winter. *Mar Ecol Prog Ser* 159:249–263. <https://doi.org/10.3354/meps159249>
- Williams TD (1995) *The penguins: Spheniscidae, Bird families of the world*. Oxford University Press, Oxford
- Wilson PR, Ainley DG, Nur N, Jacobs SS, Barton KJ, Ballard G, Comiso JC (2001) Adélie penguin population change in the Pacific sector of Antarctica: relation to sea-ice extent and the Antarctic Circumpolar Current. *Mar Ecol Prog Ser* 213:301–309. <https://doi.org/10.3354/meps213301>
- Yamamoto Y, Kanesaki S, Kuramochi T, Miyazaki N, Watanuki Y, Naito Y (1996) Comparison of trace element concentrations in tissues of the chick and adult Adélie penguins. *Proc NIPR Symp Polar Biol Natl Inst Polar Res* 253–262
- Yue F, Li Y, Zhang Y, Wang L, Li Dan, Wu P, Liu H, Lin L, Li Dong, Hu J, Xie Z (2023) Elevated methylmercury in Antarctic surface seawater: the role of phytoplankton mass and sea ice. *Sci Total Environ* 882:163646. <https://doi.org/10.1016/j.scitotenv.2023.163646>
- Zeileis A, Hothorn T (2002) Diagnostic checking in regression relationships. *R News* 2(3):7–10. <https://CRAN.R-project.org/doc/Rnews/>
- Zhou Z, Wang H, Li Y (2023) Mercury stable isotopes in the ocean: analytical methods, cycling, and application as tracers. *Sci Total Environ* 874:162485. <https://doi.org/10.1016/j.scitotenv.2023.162485>

Springer Nature or its licensor (e.g. a society or other partner) holds exclusive rights to this article under a publishing agreement with the author(s) or other rightsholder(s); author self-archiving of the accepted manuscript version of this article is solely governed by the terms of such publishing agreement and applicable law.

SUPPLEMENTARY MATERIAL

1) [Literature review of Hg contamination in penguin feathers from the Southern Ocean](#)

Table S1. Review of feather Hg concentrations in adults of eight penguin species across the Southern Ocean, including both the Subantarctic and the Antarctic Zones. This includes the Adélie (*Pygoscelis adeliae*), chinstrap (*P. antarcticus*) and gentoo penguins (*P. papua*), the emperor (*Aptenodytes forsteri*) and king penguins (*A. patagonicus*), the macaroni (*Eudyptes chrysolophus*), royal (*E. schlegeli*) and southern rockhopper penguins (*E. chrysocome*). Values are means \pm SD with ranges in parentheses.

Zone, Region, Site	Species	Year	n	Feather Hg ($\mu\text{g}\cdot\text{g}^{-1}$)	References
Subantarctic Zone :					
Falkland/Malvinas Islands					
New Island	Gentoo penguin	2016/2017	20	2.97 ± 0.81 (1.77–4.56)	Furtado et al. (2019)
	Southern rockhopper penguin	2016/2017	20	2.24 ± 0.52 (1.43–3.18)	Furtado et al. (2019)
Beauchene Island	Gentoo penguin	2016/2017	20	3.37 ± 0.91 (1.99–4.96)	Furtado et al. (2019)
	Southern rockhopper penguin	2016/2017	20	4.28 ± 0.83 (2.67–5.79)	Furtado et al. (2019)
Kidney Island	Southern rockhopper penguin	2016/2017	25	2.00 ± 0.47 (1.21–3.37)	Furtado et al. (2019)
Crozet Islands					
Possession Island	King penguin	2001	31	1.98 ± 0.73	Scheifler et al. (2005)
	King penguin	2006/2007	12	2.89 ± 0.73 (2.13–4.47)	Carravieri et al. (2016)
	King penguin	2011/2012	11	2.29 ± 0.70 (1.66–4.14)	Renedo et al. (2017)
	Gentoo penguin	2006/2007	11	5.90 ± 1.91 (3.27–8.16)	Carravieri et al. (2016)
	Gentoo penguin	2011/2012	11	4.33 ± 1.85 (1.55–7.59)	Renedo et al. (2017)
	Macaroni penguin	2006/2007	12	2.48 ± 0.35 (1.82–2.92)	Carravieri et al. (2016)
	Macaroni penguin	2011/2012	10	2.27 ± 0.24 (1.85–2.57)	Renedo et al. (2017)
	Southern rockhopper penguin	2006/2007	12	1.79 ± 0.37 (1.20–2.51)	Carravieri et al. (2016)
	Southern rockhopper penguin	2011/2012	10	1.39 ± 0.24 (1.06–1.69)	Renedo et al. (2017)
Kerguelen Islands					
Baie Larose	Southern rockhopper penguin	2006/2007	10	2.54 ± 0.33 (2.00–3.06)	Carravieri et al. (2013)
Cap Cotter	Macaroni penguin	2006/2007	12	2.24 ± 0.29 (1.87–2.75)	Carravieri et al. (2013)
Cap Ratmanoff	King penguin	2006/2007	12	2.22 ± 0.59 (1.45–3.21)	Carravieri et al. (2013)

Estacade	Gentoo penguin	2006/2007	12	5.85 ± 3.00 (1.28–9.43)	Carravieri et al. (2013)
Penn Island	Gentoo penguin	2006/2007	12	1.44 ± 0.44 (0.77–2.06)	Carravieri et al. (2013)
Mayes	Southern rockhopper penguin	2006/2007	12	1.96 ± 0.41 (1.22–2.62)	Carravieri et al. (2013)
Prince Edward Islands					
Marion Island	King penguin	2011	10	3.00 ± 0.71 (2.23–4.65)	Becker et al. (2016)
	Macaroni penguin	2011	10	3.25 ± 0.64 (2.39–4.60)	Becker et al. (2016)
	Southern rockhopper penguin	2011	10	1.80 ± 0.68 (0.93–2.57)	Becker et al. (2016)
Macquarie Island					
	Gentoo penguin	2002/2003	30	0.23 ± 0.29 (0.01–1.50)	Gilmour et al. (2019)
	King penguin	2002/2003	23	0.04 ± 0.02 (0.01–0.09)	Gilmour et al. (2019)
	Royal penguin	2002/2003	23	0.06 ± 0.04 (0.01–0.13)	Gilmour et al. (2019)
	Southern rockhopper penguin	2002/2003	30	0.29 ± 0.23 (0.03–0.91)	Gilmour et al. (2019)
Northern Antarctic Zone :					
South Georgia/Islas Georgias del sur					
Bird Island	Gentoo penguin	1998	14	0.95 ± 0.85 (0.17–3.06)	Becker et al. (2016)
	Gentoo penguin	2009	55	0.97 ± 0.67 (0.15–3.10)	Pedro et al. (2015)
	Gentoo penguin	2011	29	1.13 ± 0.62 (0.23–2.50)	Pedro et al. (2015)
	Macaroni penguin	1998	20	3.42 ± 0.73 (2.08–4.94)	Becker et al. (2016)
Unknown site	King penguin	2008–2012	10	2.92 ± 0.76	Brasso et al. (2013)
Gold Harbour	Gentoo penguin	2008–2012	20	0.85 ± 0.88	Brasso et al. (2015)
	King penguin	2008–2012	20	3.01 ± 0.79	Brasso et al. (2015)
Continental Antarctic Zone :					
Queen Maud Land					
Rumpa Island	Adélie penguin	1981	10	0.17 ± 0.05 (0.11–0.27)	Honda et al. (1986)
Hukuro Cove	Adélie penguin	1991	10	0.09 ± 0.05	Yamamoto et al. (1996)
Adélie Land					
Dumont d'Urville	Adélie penguin	2006/2007	10	0.66 ± 0.20 (0.41–1.06)	Carravieri et al. (2016)
	Adélie penguin	2011/2012	10	0.40 ± 0.09 (0.25–0.52)	Carravieri et al. (2016)
	Emperor penguin	2006/2007	17	1.77 ± 0.37 (1.05–2.76)	Carravieri et al. (2016)

Victoria Land

Cape Bird	Adélie penguin	2004–2006	154	0.59 ± 0.02	Pilcher et al. (2020)
Cape Crozier	Emperor penguin	2016	10	1.35 ± 0.06	Pilcher et al. (2020)
Edmonson Point	Adélie penguin	1989–1991	3	0.82 ± 0.13	Bargagli et al. (1998)
	Emperor penguin	1989–1991	3	0.98 ± 0.21	Bargagli et al. (1998)

Maritime Antarctic Zone:**South Shetland Islands****King George/25 de Mayo Island**

Admiralty Bay	Adélie penguin	2005/2006	20	0.35 ± 0.13 (0.20–0.90)	Brasso et al. (2015, 2014, 2013)	
	Adélie penguin	2006/2007	20	0.25 ± 0.12 (0.16–0.70)	Brasso et al. (2015, 2014, 2013)	
	Adélie penguin	2007/2008	20	0.38 ± 0.11 (0.21–0.65)	Brasso et al. (2015, 2014, 2013)	
	Adélie penguin	2008/2009	16	0.35 ± 0.08 (0.18–0.47)	Brasso et al. (2015, 2014, 2013)	
	Adélie penguin	2009/2010	22	0.35 ± 0.14 (0.18–0.69)	Brasso et al. (2015, 2014, 2013) ; Polito et al. (2016)	
	Adélie penguin	2010/2011	22	0.35 ± 0.14 (0.18–0.69)	Brasso et al. (2015, 2014, 2013)	
	Adélie penguin	2005–2011	120	0.34 ± 0.13 (0.16–0.90)	Brasso et al. (2015, 2014, 2013)	
	Chinstrap penguin	2005/2006	9	0.60 ± 0.14 (0.37–0.76)	Brasso et al. (2015, 2014, 2013)	
	Chinstrap penguin	2006/2007	16	0.53 ± 0.19 (0.24–0.94)	Brasso et al. (2015, 2014, 2013)	
	Chinstrap penguin	2007/2008	9	0.62 ± 0.22 (0.40–1.01)	Brasso et al. (2015, 2014, 2013)	
	Chinstrap penguin	2008/2009	16	0.62 ± 0.30 (0.20–1.32)	Brasso et al. (2015, 2014, 2013)	
	Chinstrap penguin	2009/2010	20	0.74 ± 0.24 (0.40–1.29)	Brasso et al. (2015, 2014, 2013) ; Polito et al. (2016)	
	Chinstrap penguin	2010/2011	20	0.74 ± 0.24 (0.40–1.29)	Brasso et al. (2015, 2014, 2013)	
	Chinstrap penguin	2005–2011	90	0.66 ± 0.24 (0.20–1.32)	Brasso et al. (2015, 2014, 2013) ; Polito et al. (2016)	
	Gentoo penguin	Gentoo penguin	2005/2006	17	0.35 ± 0.21 (0.14–0.80)	Brasso et al. (2015, 2014, 2013)
		Gentoo penguin	2006/2007	17	0.33 ± 0.21 (0.14–0.85)	Brasso et al. (2015, 2014, 2013)
Gentoo penguin		2007/2008	17	0.46 ± 0.47 (0.15–2.08)	Brasso et al. (2015, 2014, 2013)	
Gentoo penguin		2008/2009	20	0.41 ± 0.48 (0.13–2.39)	Brasso et al. (2015, 2014, 2013)	
Gentoo penguin		2009/2010	18	0.54 ± 0.55 (0.18–1.98)	Brasso et al. (2015, 2014, 2013) ; Polito et al. (2016)	
Gentoo penguin		2010/2011	21	0.51 ± 0.51 (0.18–1.98)	Brasso et al. (2015, 2014, 2013)	

	Gentoo penguin	2005–2011	110	$0.44 \pm 0.43(0.13–2.39)$	Brasso et al. (2015, 2014, 2013) ; Polito et al. (2016)
Narębski Point	Chinstrap penguin	2015/2016	30	0.71 ± 0.34	Catán et al. (2017)
Livingston Island					
Cape Shirreff	Chinstrap penguin	2012	16	1.53 ± 0.08	Álvarez-Varas et al. (2018)
Byers Peninsula	Chinstrap penguin	2008/2009	10	$0.40 \pm 0.23 (0.20–0.85)$	Becker et al. (2016)
	Gentoo penguin	2008/2009	10	$0.31 \pm 0.14 (0.11–0.63)$	Becker et al. (2016)
Hannah Point	Chinstrap penguin	2010/2011	30	$0.67 \pm 0.46 (0.24–1.57)$	Matias et al. (2022)
	Gentoo penguin	2010/2011	30	$0.22 \pm 0.09 (0.11–0.38)$	Matias et al. (2022)
King George and Livingston Islands (combined)					
Hennequin + Hannah Points	Adélie penguin	2013/2014	31	$0.40 \pm 0.13 (0.16–0.69)$	Souza et al. (2020)
	Chinstrap penguin	2013/2014	40	$0.63 \pm 0.36 (0.16–1.65)$	Souza et al. (2020)
	Gentoo penguin	2013/2014	45	$0.32 \pm 0.13 (0.17–0.91)$	Souza et al. (2020)

2) Material and methods

a. Feather sampling

Table S2. Geographical coordinates (*i.e.*, degrees minutes seconds and decimals) of sampling colonies (*i.e.*, 12 sites and 24 colonies) of Adélie penguins (body feathers) around Antarctica. Collaborators indicates principal investigators for each site and colony who contributed to the present study with sampling and/or raw data.

<u>Site, colony</u>	<u>Coordinates</u>	<u>Latitude</u>	<u>Longitude</u>	<u>Collaborators</u>
Continental Antarctic Zone				
<u>Queen Maud Land</u> , Hukuro Cove	69° 12' 36" S, 39° 37' 48" E	-69.21	39.63	Akinori Takahashi (Syowa Station)
<u>Mac.Robertson Land</u>	67° 36' 09" S, 62° 52' 25" E	-67.60	62.87	Louise Emmerson, Colin Southwell (Mawson Station)
Welch Island	67° 33' 36" S, 62° 55' 41" E	-67.56	62.93	
Macey Island	67° 26' 21" S, 63° 49' 09" E	-67.44	63.82	
<u>Princess Elizabeth Land</u>	68° 34' 36" S, 77° 58' 03" E	-68.58	77.97	Louise Emmerson, Colin Southwell (Davis Station)
Hop Island	68° 49' 43" S, 77° 42' 08" E	-68.83	77.70	
Magnetic Island	68° 32' 35" S, 77° 54' 32" E	-68.54	77.91	
Un-named Island 73413*	68° 27' 30" S, 78°22' 24" E	-68.46	78.37	
<u>Wilkes Land</u> , Shirley Island	66° 16' 57" S, 110° 31' 36" E	-66.29	110.53	Louise Emmerson, Colin Southwell (Casey Station)
<u>Adélie Land</u>				Thierry Raclot, Candice Michelot, Akiko Kato
Dumont d'Urville	66° 39' 49" S, 140° 0' 4" E	-66.67	140.0	
Cap Bienvenue	66° 43' 14" S, 140° 31' 34" E	-66.72	140.53	
Cap Jules	66° 44' 30" S, 140° 55' E	-66.74	140.92	
<u>Victoria Land</u>				
Edmonson Point	74° 20' S, 165° 08' E	-74.33	165.13	Silvia Olmastroni, Ilaria Corsi (Terra Nova Bay)
Adélie Cove	74° 46' S, 164° 00' E	-74.77	164.0	
Inexpressible Island	74° 54' S, 163° 39' E	-74.90	163.65	
Cap Crozier	77° 31' S, 169° 24' E	-77.52	169.40	Annie Schmidt (Ross Island)
Cap Royds	77° 33' 11" S, 166° 9' 49" E	-77.55	166.16	
Maritime Antarctic Zone				
<u>King George/25 de Mayo Island</u>				
Ardley Island	62° 12' 45" S, 58° 55' 56" W	-62.21	-58.93	Alvaro Soutello, Ana Laura Machado
Admiralty Bay	62° 10' 34" E, 58° 26' 46 W	-62.18	-58.45	Michael Polito, Rebecka Brasso

Carlini (Stranger Point)	62° 14' 17" S, 58° 40' 1" W	-62.24	-58.67	Mercedes Santos, Mariana Juárez
Antarctic Peninsula				
Esperanza/Hope Bay	63° 23' 53" S, 56° 59' 47" W	-63.40	-56.99	Mercedes Santos, Mariana Juárez
Brown Bluff	63° 32' 0" S, 56° 55' 0" W	-63.53	-56.92	Tom Hart
Seymour Island , Marambio	64° 14' 31" S, 56° 37' 33" W	-64.24	-56.63	Mercedes Santos, Mariana Juárez
Joinville Island				
Madder Cliffs	63° 18' 0" S, 56° 29' 0" W	-63.30	-56.48	Tom Hart
Paulet Island	63° 35' 0" S, 55° 47' 0" W	-63.58	-55.78	
Signy Island , Gourlay	60° 43' 30" S, 45° 35' 17" W	-60.73	-45.59	Michael Dunn

*Alpha-numeric identifier in Southwell et al. (2021)

b. Mercury analyses

Table S3. Certified reference materials (NRC Canada) used for Hg analyses in feathers of Adélie penguins (*Pygoscelis adeliae*): certified (theoretical) and measured values, and recoveries (calculated as measured/certified value). n indicates sample size for each reference material and values are means \pm SD with ranges in parentheses.

Reference material	n	Certified value ($\mu\text{g/g dw}$)	Measured value ($\mu\text{g/g dw}$)	Recovery (%)
TORT-3 <i>Lobster hepatopancreas</i>	33	0.29 \pm 0.02 (0.27 – 0.31)	0.29 \pm 0.01 (0.27 – 0.31)	100.6 \pm 2.3 (93.6 – 104.7)
DOLT-5 <i>Fish liver</i>	21	0.44 \pm 0.18 (0.26 – 0.62)	0.43 \pm 0.01 (0.41 – 0.46)	96.7 \pm 2.6 (93.5 – 105.5)

c) Stable isotopes analyses: detailed methodology

Analytical procedure:

Aliquots were placed in tin capsules (8 mm x 5mm, Elemental Microanalysis Ltd, Okehampton, United Kingdom) and analyzed for carbon and nitrogen stable isotope compositions, using a continuous-flow system consisting of an elemental analyzer (Flash 2000, or Flash IRMS EA Isolink CN, Thermo Scientific, Milan, Italy) equipped with the smart EA option and an autosampler (Zero Blank, Costech, Valencia, CA, United States). The elemental analyzer was connected via a Conflo IV peripheral to a Delta V Plus isotope ratio mass spectrometer (Thermo Scientific, Bremen, Germany). In the elemental analyzer, each sample was combusted quantitatively in a first reactor containing copper oxide (Elemental Microanalysis Ltd, Okehampton, United Kingdom) and silvered cobaltous oxide (Elemental Microanalysis Ltd, Okehampton, United Kingdom). Oxygen (grade 99.9999% purity; Air Liquide, France) was pulsed during combustion and helium was used as carrier gas (grade 99.9999% purity, 100 ml.min⁻¹; Air Liquide, France). Gases resulting from the combustion were flushed in a second reactor where NO_x gases were reduced at 650°C using copper wires (Elemental Microanalysis Ltd, Okehampton, United Kingdom) to produce pure N₂. Gases obtained (CO₂, N₂ and H₂O) were carried through a water trap (granular magnesium perchlorate, Elemental Microanalysis Ltd, Okehampton, United Kingdom) and then a GC column. N₂ and CO₂ were then introduced into the isotope ratio mass spectrometer. The instrumentation was controlled and measurement data were obtained using the instrumental software Isodat 3.0 (Thermo Scientific, Bremen, Germany).

Metrological traceability:

Results are reported in per mil (‰) using the delta (δ) notation and were normalized using reference materials: Vienna Pee Dee Belemnite (VPDB) and atmospheric nitrogen (Air-N₂) for carbon and nitrogen, respectively. Normalization was carried out using USGS61 and USG63 (US Geological Survey, Reston, VA, USA) based on their assigned carbon and nitrogen isotope- δ values and standard uncertainties (*i.e.*, $-35.05 \pm 0.04\text{‰}$ and $-1.17 \pm 0.04\text{‰}$ for carbon, respectively, and $-2.87 \pm 0.04\text{‰}$ and $+37.83 \pm 0.06\text{‰}$ for nitrogen, respectively). Each reference material was measured in duplicate at the beginning and the end of each daily group of analysis.

Data processing: Isotope- δ values for the CO₂ and N₂ gas derived from the samples relative to a working gas were obtained using the instrumental software (Isodat 3.0, Thermo Scientific, Bremen, Germany). Working gases were introduced from high-pressure cylinders (CO₂ 99.998 % purity and N₂ 99.9999 % purity; Air Liquide, France) directly into the mass spectrometer. Blank correction was done for both CO₂ and N₂, and “SSH” ¹⁷O correction was applied for CO₂. A drift correction was applied using the results of reference materials analyzed regularly (*i.e.*, after every 20 or 21 sample

measurements) in each analytical batch. Special care was taken to ensure that the amount of yield gas was the same for reference materials and samples, but minor differences were normalized using the signal amplitude of the reference materials ran in each analytical batch. The $\delta^{13}\text{C}$ and $\delta^{15}\text{N}$ values were normalized by two-point normalization. All corrections and normalizations were performed simultaneously using multiple linear least square regression.

Uncertainty evaluation: The uncertainty of the reported isotope- δ values was evaluated as the standard deviation of repeated ($n = 5$ or 8) measurements of each reference material (*i.e.*, USGS61 and USGS63) within a single group of analyses. Uncertainty did not exceed 0.10 ‰ for both $\delta^{13}\text{C}$ and $\delta^{15}\text{N}$ values.

d) Outliers from Hukuro Cove

Table S4. Feather Hg concentrations and stable isotope values in five adult Adélie penguins (*Pygoscelis adeliae*) discarded from analyses because of their outlying high isotopic values ($\delta^{13}\text{C}$ and $\delta^{15}\text{N}$ values are proxies of penguin feeding habitat and trophic position, respectively).

Site, Colony	ID	Feather Hg ($\mu\text{g}\cdot\text{g}^{-1}$ dw)	Feather $\delta^{13}\text{C}$ (‰)	Feather $\delta^{15}\text{N}$ (‰)
Syowa				
Hukuro Cove	10a	0.67	-20.67	13.21
Hukuro Cove	63b	0.92	-18.99	14.49
Hukuro Cove	65b	0.82	-20.14	13.06
Antarctic Peninsula				
Brown Bluff	9	0.83	-18.80	11.06
Brown Bluff	11	1.22	-17.73	13.08

e) Visually representing the non-breeding distribution of Adélie penguins

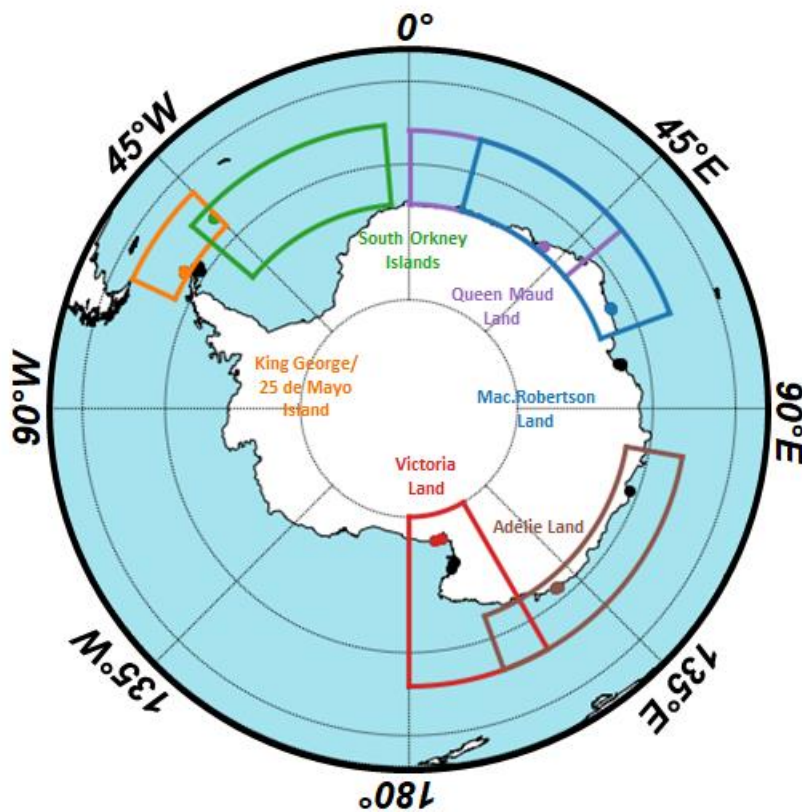


Figure S1. Literature review of non-breeding distributions of Adélie penguins (*Pygoscelis adeliae*) tracked in six Antarctic sites: South Orkney Islands (Signy Island, Dunn et al., 2011; in green), Queen Maud Land (Hukuro Cove, Takahashi et al., 2018; in purple), Mac.Robertson Land (Mawson Station, Béchervaise Island, Clarke et al., 2003; in blue), Adélie Land (Dumont d'Urville, Thiébot et al., 2019; in brown), Victoria Land (Ross Sea, Cap Bird, Davis et al., 1996; in red) and King George/25 de Mayo Island (Admiralty Bay, Hinke et al., 2015; in orange). Distributions were defined as the maximum geographical zone including all individual tracks. Black dots represent other sites sampled in the present study (see **Fig.1** and **Table S2** for further details).

3) Sex differences in Adélie penguins

Table S5. Feather Hg concentrations and stable isotope values from female and male Adélie penguins (*Pygoscelis adeliae*; adults) collected around Antarctica. n indicates sample sizes. Carbon ($\delta^{13}\text{C}$) and nitrogen ($\delta^{15}\text{N}$) stable isotopes are proxies of penguin feeding habitat and trophic position, respectively. Values are means \pm SD with ranges in parentheses.

<u>Site, Colony, Sex (Year)</u>	n	Feather Hg ($\mu\text{g}\cdot\text{g}^{-1}$ dw)	Feather $\delta^{13}\text{C}$ (‰)	Feather $\delta^{15}\text{N}$ (‰)
Continental Antarctic Zone				
<u>Queen Maud Land</u>, Hukuro Cove (2010)				
Female	15	0.44 \pm 0.09 (0.32–0.66)	–24.45 \pm 0.56 (–25.74, –23.52)	9.42 \pm 0.52 (8.63–10.37)
Male	12	0.53 \pm 0.12 (0.35–0.69)	–23.11 \pm 0.77 (–24.93, –22.85)	10.12 \pm 0.89 (8.98–12.11)
<u>Adélie Land</u>, Dumont d’Urville (2012)				
Female	3	0.47 \pm 0.08 (0.37–0.52)	–24.04 \pm 0.69 (–24.55, –23.26)	11.38 \pm 0.46 (11.07–11.91)
Male	7	0.37 \pm 0.09 (0.25–0.47)	–24.38 \pm 0.73 (–25.55, –23.48)	10.55 \pm 0.71 (9.76–11.46)
<u>Victoria Land, Terra Nova Bay</u>: (2017)				
Adélie Cove				
Female	8	0.91 \pm 0.27 (0.50–1.35)	–24.22 \pm 0.89 (–25.34, –22.47)	11.03 \pm 1.18 (9.90–12.79)
Male	7	0.94 \pm 0.26 (0.49–1.27)	–24.68 \pm 0.56 (–25.57, –24.00)	10.90 \pm 0.76 (10.10–12.12)
Edmonson Point				
Female	8	0.75 \pm 0.12 (0.50–0.93)	–24.78 \pm 0.47 (–25.45, –24.13)	10.34 \pm 0.49 (9.84–11.00)
Male	7	0.92 \pm 0.19 (0.63–1.18)	–24.24 \pm 0.78 (–25.80, –23.61)	10.98 \pm 0.44 (10.41–11.58)
Inexpressible Island				
Female	7	0.70 \pm 0.24 (0.50–1.22)	–24.64 \pm 0.97 (–25.64, –22.83)	10.67 \pm 1.28 (8.98–12.75)
Male	8	0.95 \pm 0.23 (0.66–1.33)	–24.29 \pm 0.83 (–25.30, –22.93)	11.16 \pm 0.79 (10.05–12.22)
<u>Victoria Land, Ross Island</u>: (2019)				
Cape Crozier				
Female	9	0.58 \pm 0.09 (0.45–0.68)	–25.87 \pm 0.25 (–26.34, –25.47)	9.72 \pm 0.45 (9.07–10.55)
Male	5	0.69 \pm 0.15 (0.51–0.92)	–25.93 \pm 0.42 (–26.48, –25.38)	9.81 \pm 0.65 (9.34–10.91)
Cape Royds				

Female	6	0.78 ± 0.18 (0.61–1.02)	–24.95 ± 1.10 (–25.77, –22.84)	10.11 ± 0.95 (9.15–11.82)
Male	9	0.81 ± 0.20 (0.56–1.08)	–25.70 ± 0.17 (–25.88, –25.30)	10.36 ± 0.68 (9.65–11.85)

Maritime Antarctic Zone

King George/25 de Mayo Island, Admiralty Bay

(2005)

Female	10	0.37 ± 0.21 (0.20–0.90)	–25.01 ± 0.78 (–25.70, –23.30)	8.87 ± 0.43 (8.30–9.70)
Male	10	0.33 ± 0.08 (0.24–0.52)	–24.83 ± 0.64 (–25.40, –23.50)	8.79 ± 0.34 (8.10–9.20)

(2006)

Female	9	0.21 ± 0.06 (0.16–0.36)	25.00 ± 0.30 (–25.50, –24.60)	8.57 ± 0.25 (8.10–8.90)
Male	11	0.29 ± 0.14 (0.20–0.70)	–25.07 ± 0.39 (–25.70, –24.70)	8.80 ± 0.35 (8.30–9.60)

(2007)

Female	9	0.41 ± 0.06 (0.31–0.47)	–24.87 ± 0.33 (–25.20, –24.30)	8.98 ± 0.15 (8.80–9.20)
Male	11	0.36 ± 0.14 (0.21–0.65)	–24.68 ± 0.54 (–25.30, –23.90)	8.91 ± 0.35 (8.50–9.70)

(2008)

Female	7	0.37 ± 0.07 (0.27–0.47)	–24.60 ± 0.47 (–25.20, –24.00)	8.84 ± 0.19 (8.50–9.00)
Male	9	0.33 ± 0.09 (0.18–0.46)	–24.61 ± 0.56 (–25.30, –23.80)	8.96 ± 0.64 (8.30–10.50)

(2009)

Female	11	0.36 ± 0.09 (0.19–0.49)	–24.06 ± 0.86 (–25.40, –22.90)	9.00 ± 0.43 (8.00–9.60)
Male	11	0.34 ± 0.18 (0.18–0.69)	–23.75 ± 0.83 (–25.00, –22.40)	9.12 ± 0.41 (8.60–10.10)

(2010)

Female	11	0.36 ± 0.09 (0.19–0.49)	–24.43 ± 1.29 (–27.40, –22.90)	9.00 ± 0.43 (8.00–9.60)
Male	11	0.34 ± 0.18 (0.18–0.69)	–23.75 ± 0.83 (–25.00, –22.40)	9.12 ± 0.41 (8.60–10.10)

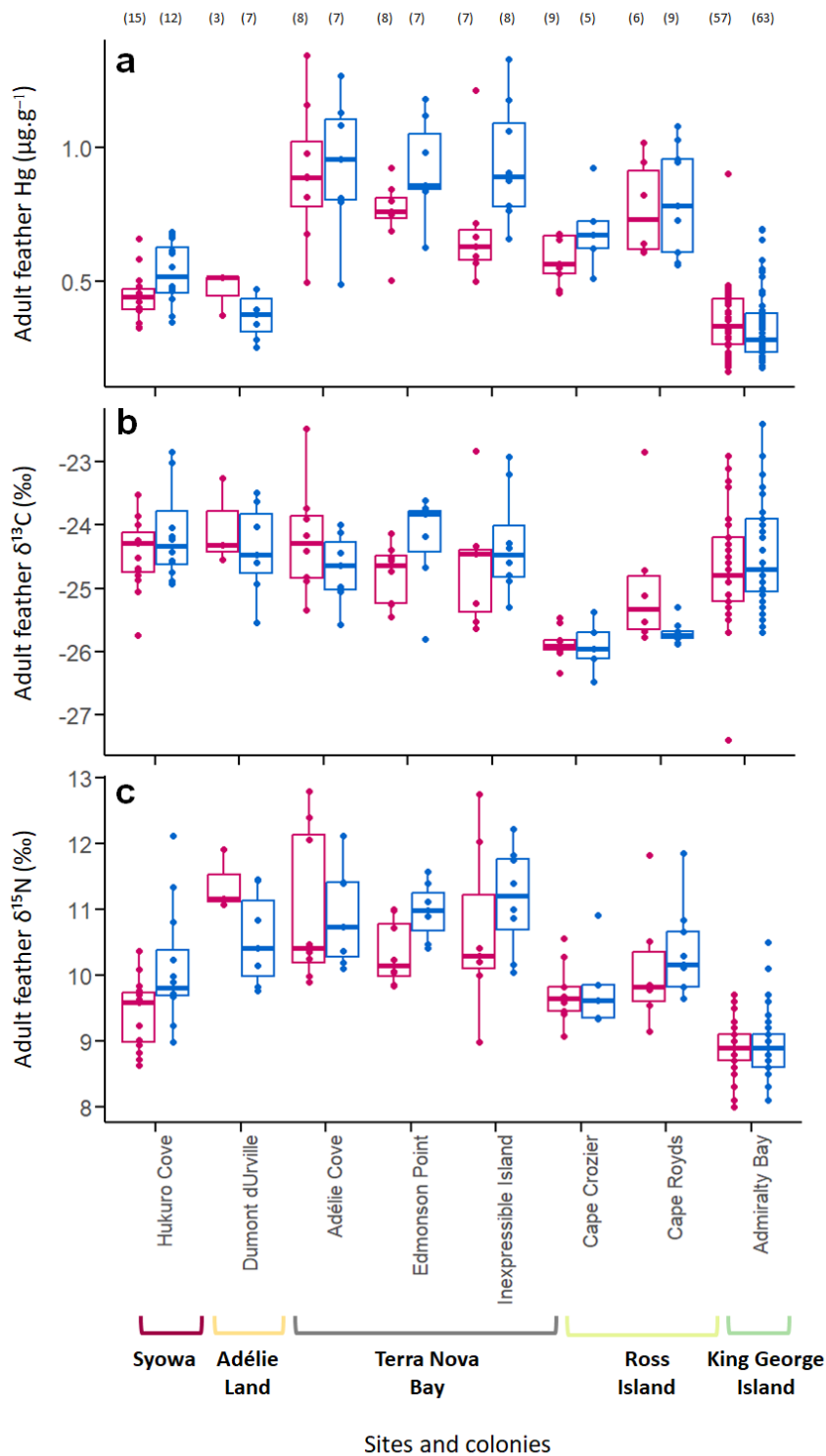


Figure S2. Sex differences in feather (a) Hg concentrations, and (b) $\delta^{13}\text{C}$ and (c) $\delta^{15}\text{N}$ values measured in adult Adélie penguins (*Pygoscelis adeliae*) from eight Antarctic colonies. Females and males are represented in pink and blue, respectively. Feather $\delta^{13}\text{C}$ and $\delta^{15}\text{N}$ values are proxies for penguin feeding habitat and trophic position, respectively. Numbers in brackets represent sample sizes for each sex and colony. Individual values (smaller dots) are presented with boxplots, representing median values (midlines), errors bars (whiskers) and outliers (black dots outside whiskers)

Table S6. Estimated marginal mean (EMM) feather Hg concentrations for sexed adult Adélie penguins (n=231) from eight Antarctic colonies. Estimates were derived from the best-ranked generalized linear model (GLM with Gamma distribution and inverse link-function) defined as follows: $Hg \sim \delta^{13}C + \delta^{15}N + Colony$ (see **Table 3** for further details). Abbreviations: CI, confidence interval; SE, standard error.

Sites	EMM	SE	95% CI		Group
			Lower	Upper	
Hukuro Cove	0.48	0.029	0.43	0.55	A
Dumont d'Urville	0.35	0.032	0.30	0.43	ABD
Adélie Cove	0.67	0.055	0.58	0.80	C
Edmonson Point	0.67	0.051	0.58	0.78	C
Inexpressible Island	0.62	0.051	0.53	0.74	C
Cape Crozier	0.54	0.046	0.46	0.65	AC
Cape Royds	0.63	0.052	0.54	0.75	AC
Admiralty Bay	0.37	0.012	0.34	0.39	D

Differences were considered significant when confidence intervals did not overlap. Sites sharing the same Group letters are not significantly different from each other. Sites with two letters were not significantly different from either group.

Paper 3

Long-term mercury contamination in Arctic marine ecosystems: the Brünnich's guillemot as bioindicator species

In preparation

Fanny Cusset, Paco Bustamante, Céline Albert, David Amouroux, Océane Asensio, Maud Brault-Favrou, Gaël Guillou, Jannie Linnebjerg, Flemming Merkel, Emmanuel Tessier, Yves Cherel and Jérôme Fort.



MATERIAL AND METHODS

Feather sampling and preparation

Body feathers of museum-held specimens were collected from skins of adult Brünnich's guillemots archived in three natural history museum collections, including in Copenhagen (n=143), Tring (n=6) and Paris (n=4). Only specimens sampled in Greenland with known collection year were selected. Feather sampling of free-living birds was conducted in West Greenland between 1984 and 2022. Information about birds' sex was only available for a subset of individuals (i.e., 46 males and 53 females) that included both museum-held and free-living guillemots.

To eliminate any external contamination, all feathers were cleaned in the laboratory with a chloroform:methanol mixture (2:1), sonicated for 3 min, rinsed twice in methanol and oven-dried for 48h at 45°C. For each guillemot, four feathers were pooled to derive the individual mean value in both Hg and stable isotopes (Carravieri et al., 2014a; Jaeger et al., 2009) and cut with stainless scissors into homogenous powder to be analysed for both Hg and stable isotopes.

Mercury analyses

Total-Hg (THg) includes inorganic Hg (iHg) and organic Hg (i.e., MeHg). Since MeHg accounts for 90% of THg in feathers (Bond and Diamond, 2009b; Renedo et al., 2017; D. R Thompson and Furness, 1989), THg was used as proxy of MeHg in feathers of Brünnich's guillemots.

Feather homogenates (0.3–1.0 mg) were analysed using an Advanced Mercury Analyzer spectrophotometer (AMA 254, Altech) to obtain THg concentrations. Each sample was analysed in duplicate to guarantee a relative standard deviation (RSD) < 10%. When the RSD > 10%, an additional analysis was performed and the two best analyses (i.e., with RSD < 10%) were kept to calculate the individual average value. Certified materials (DOLT-5, Fish liver; TORT3, Lobster hepatopancreas; National Research Council, Canada) were analysed during each laboratory session (i.e., every day; at the beginning, middle and end of the session) to guarantee accuracy. Certified Hg concentrations were 0.44 ± 0.18 and 0.292 ± 0.022 $\mu\text{g}\cdot\text{g}^{-1}$ dry weight (dw). Our measured values were 0.427 ± 0.012 (n=16) and 0.289 ± 0.013 (n=72) $\mu\text{g}\cdot\text{g}^{-1}$ dw (Table S1). Detection limit of the AMA was 0.1 ng. Mercury concentrations are expressed in $\mu\text{g}\cdot\text{g}^{-1}$ dw. Recoveries were 97.1 ± 2.7 % and 99.0 ± 4.6 %, respectively (Table S1).

Historically, inorganic Hg salts were used as preservatives in museum collections (approximately until the 1970s), inducing major bias when comparing THg concentrations between old and recent specimens (Thompson et al., 1992). Therefore, Hg speciation analyses were performed on samples that exhibited abnormally high THg concentrations (n=10), to quantify both MeHg and iHg (Renedo et al., 2017) from feather homogenates (2–6 mg), using GC-ICP-MS Trace Ultra GC equipped with a Triplus RSH

autosampler coupled to an ICP-MS XSeries II (Thermo Scientific, USA). Mercury speciation analyses were also performed on a few free-living individuals (n=5 from 2022) to determine precise proportion of MeHg in guillemots and validate the use of THg as a proxy of MeHg (Table S2). Methyl-Hg accounted for 92.2 ± 11.6 (76.4–101.9) % of THg. Further methodological details are provided in Cusset et al. (2023; Supplementary Material). Certified material (NIES-13, human hair; certified concentration = $3.80 \pm 0.40 \mu\text{g}\cdot\text{g}^{-1}$ dw) was analysed with the samples for the validation of feather analyses (keratin-based matrices). Measured values were $3.70 \pm 0.30 \mu\text{g}\cdot\text{g}^{-1}$ dw (n=3; Table S3). Method recovery was checked by comparing AMA (THg concentrations) with speciation values (Σ iHg + MeHg). Recoveries were $102.8 \pm 2.6\%$ (n=5; free-living birds; Table S3). Thereafter, Hg concentrations include MeHg and THg concentrations (depending on the samples and associated Hg analyses).

Stable isotope analyses

Carbon and nitrogen stable isotopes were analysed in homogenized subsamples (0.2–0.8 mg) of body feathers. Results are expressed in the usual delta notation as deviations from standards (Vienna Pee Dee Belemnite for $\delta^{13}\text{C}$ and atmospheric N_2 for $\delta^{15}\text{N}$). $\delta^{13}\text{C}$ and $\delta^{15}\text{N}$, for $^{13}\text{C}/^{12}\text{C}$ and $^{15}\text{N}/^{14}\text{N}$, respectively. Feather subsamples were weighed with a microbalance and loaded into tin cups. Values of $\delta^{13}\text{C}$ and $\delta^{15}\text{N}$ were determined with a continuous flow mass spectrometer (Delta V Plus with a ConFlo IV Interface, Thermo Scientific, Bremen, Germany), coupled to elemental analyzer (Flash 2000 or EA Isolink, Thermo Scientific, Milan, Italy). Analytical precision was $< 0.10 \text{ ‰}$ and 0.15 ‰ for $\delta^{13}\text{C}$ and $\delta^{15}\text{N}$, respectively.

Since the Industrial Revolution, the combustion of human fossil fuel has increased atmospheric CO_2 , resulting in an accelerating decrease in biosphere $\delta^{13}\text{C}$, mainly influenced by two additive effects: (i) an increase in phytoplankton fractionation (Rau et al., 1992), and (ii) the so-called Suess-Effect (Keeling, 1979), whereby anthropogenic carbon has lower $\delta^{13}\text{C}$ values than natural background carbon. Here, raw $\delta^{13}\text{C}$ values were corrected accordingly, following calculations from previous work (Eide et al., 2017; Hilton et al., 2006; Jaeger and Cherel, 2011; Körtzinger et al., 2003).

Statistical analyses

All statistical analyses and graphical representations were conducted in R Version 4.2.2 (R Core Team, 2022). During data exploration three outliers were identified and subsequently removed for all statistical analyses (see Table S4 for further details).

Temporal trends: Data exploration revealed that Hg, $\delta^{13}\text{C}$ and $\delta^{15}\text{N}$ values varied non-linearly with time. Therefore, Generalized Additive Models (GAM) were run to investigate non-linear temporal trends over 181 years, using the «mgcv» package (Wood, 2011). Each variable was modeled independently against year as smoother. For each model, we adapted the smoother term (k) to avoid overfitting and over-simplification, and obtain the best and most realistic fit to the data (k=3 for Hg and $\delta^{13}\text{C}$, k=5 for $\delta^{15}\text{N}$; Table 1). Model assumptions were checked through residual analysis with the «gam.check» function.

Drivers of Hg contamination over time: Multifactorial analyses were used to test for the effect of trophic ecology on feather Hg concentrations over time. To discard the combined effect of time on both feeding habitat and trophic position, we detrended all variables by extracting residuals from GAM temporal trends of Hg, $\delta^{13}\text{C}$ and $\delta^{15}\text{N}$ values. The new response variables were time-detrended Hg concentrations, $\delta^{13}\text{C}$ and $\delta^{15}\text{N}$ values. Relationships between detrended variables were then investigated with linear models using «nlme» package (Pinheiro et al., 2020). Prior to model construction, one-way ANOVA was used to test differences in Hg concentrations between the sexes of Brünnich's guillemots. As no difference was detected ($F_{1,97}=0.002$, $p=0.96$), sex was not included in the procedures of model selection. Models were GLMs with Gaussian distribution and identity link-function. Initial model was: detrended Hg ~ detrended $\delta^{13}\text{C}$ + detrended $\delta^{15}\text{N}$. All potential combinations of variables (Table 2) were subjected to model selection based on Aikake's Information Criterion adjusted for small sample sized (AIC_c), using the «MuMIn» package (Barton, 2022). The model with lowest AIC_c value, with a difference of AIC_c of two or more compared to the next model (ΔAIC_c), was selected as the best model (Burnham and Anderson, 2002). Model performance was assessed using Aikake weights (w_i) (after Johnson and Omland, 2004) and model fit was checked by residual analysis of the initial model.

RESULTS

Body feathers were sampled from 481 adult Brünnich's guillemots, between 1841 and 2022 (i.e., 181 years), from museum skins (n=153) and free-living guillemots (n=328; Table S5).

Temporal trends. Detailed outputs from GAMs describing temporal variation in Hg, $\delta^{13}\text{C}$ and $\delta^{15}\text{N}$ values provided in Table 1.

Since the 1840s, Hg concentrations increased non-linearly with time (GAM, $p<0.0001$, deviance explained was 21.7%; Figure 1A). Over the entire period, this represented a 251.7% increase in feather Hg concentrations, corresponding to a 1.39% increase per year. Feather $\delta^{13}\text{C}$ values decreased drastically and non-linearly (GAM, $p<0.0001$, deviance explained was 52.0%), with a 3.4 % difference between the 1840s and the 2020s (Figure 1B). Feather $\delta^{15}\text{N}$ values showed a slight, non-linear increase over the

study period (GAM, $p < 0.0001$, deviance explained was 7.8%). After a first increase from the 1870s to the 1950s, feather $\delta^{15}\text{N}$ values decreased slightly until the 2000s and appeared to increase again until the present days. Overall, this represented a slow increase of 0.21 ‰ over 181 years (Figure 1C).

Table 1. Outputs from GAM models explaining variation in feather Hg and stable isotope values between the 1830s and the 2020s in adult Brunnich’s guillemots breeding in West Greenland ($n=446$). For the intercept, values are estimates and standard errors. For the smoother (year), values are effective degrees of freedom. K indicates the number of knots in temporal trends of each variable.

Response variable	Intercept	k	s(Year)	p-value	Deviance explained (%)
Hg	1.69 ± 0.0402	3	1.68	$<0.0001^{***}$	21.7
$\delta^{13}\text{C}$	-18.34 ± 0.041	3	1.59	$<0.0001^{***}$	52.0
$\delta^{15}\text{N}$	14.79 ± 0.042	5	3.78	$<0.0001^{***}$	7.8

Drivers. The best model to explain time-detrended Hg concentrations included both detrended $\delta^{13}\text{C}$ and $\delta^{15}\text{N}$ values (linear models, $R^2=0.17$, $p < 0.0001$; Table 2). Whereas Hg concentrations increased marginally with increasing $\delta^{13}\text{C}$ values ($\beta \pm \text{SE} = 0.088 \pm 0.047$; 95% CI: $-0.004, 0.18$), they increased significantly with increasing $\delta^{15}\text{N}$ values ($\beta \pm \text{SE} = 0.38 \pm 0.045$; 95% CI: $0.30, 0.48$; Figure 2).

Table 2. AICc model ranking from statistical analyses of feather concentrations from Brunnich guillemots breeding in Greenland. Models are Generalized Linear Models (Gaussian and identity link-function). Variables are all time-detrended (see Section X for further details). Abbreviations: k, number of parameters; AICc, Akaike’s Information Criterion adjusted for small sample sizes; w_i , AICc weights.

Models	k	AIC _c	ΔAIC_c^a	w_i^b
Detrended $\delta^{13}\text{C}$ + detrended $\delta^{15}\text{N}$	4	1089.5	0.0	0.68
Detrended $\delta^{15}\text{N}$	3	1091.0	1.5	0.32
Detrended $\delta^{13}\text{C}$	3	1155.4	66.0	0.00
NULL	2	1169.6	80.1	0.00

^aA model with $\Delta\text{AIC}_c = 0$ is interpreted as best model among all selected ones (in bold).

^bWeights are cumulative (sum to 1)

FIGURES

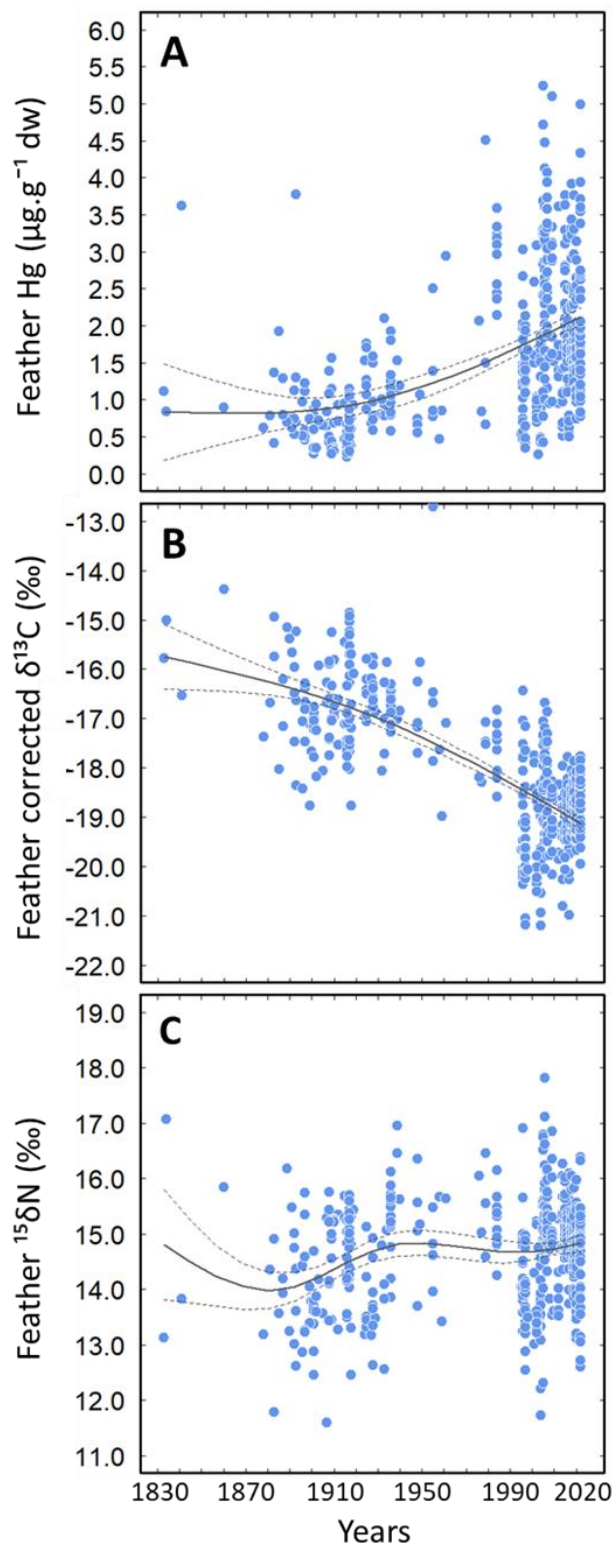


Figure 1. Long-term trends of feather (A) Hg concentrations, (B) carbon ($\delta^{13}\text{C}$) and (C) nitrogen ($\delta^{15}\text{N}$) isotopic values in Brünnich's guillemots breeding in Greenland between 1841 and 2022 (i.e., 181 years). The $\delta^{13}\text{C}$ values are corrected for the Sues Effect and phytoplankton fractionation (see **Material and Methods** for further details). Solid and dotted curves represent the best-fitting model detected from construction of GAMs and the confidence interval, respectively.

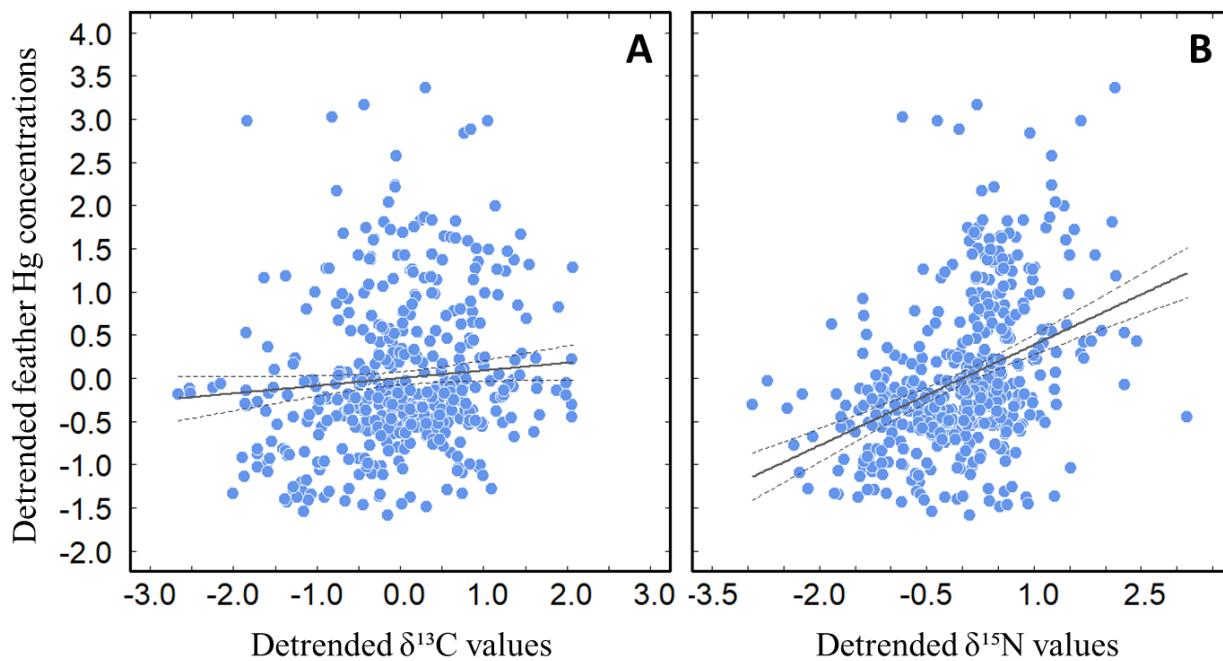


Figure 2. Relationship between time-detrended Hg concentrations and time-detrended stable isotope values: **(A)** $\delta^{13}\text{C}$ and **(B)** $\delta^{15}\text{N}$ values, in feathers of Brünnich's guillemots breeding in West Greenland, between 1841 and 2022 (i.e., 181 years). All data (blue dots) were scaled. Solid and dashed lines represent the best-fitting linear model and the 95% confidence interval, respectively.

SUPPLEMENTARY MATERIAL

Table S1. Certified reference materials (NRC Canada) used for THg analyses in feathers of Brünnich guillemot (*Uria lomvia*): certified (theoretical) and measured values, and recoveries (calculated as measured/certified value). n indicates sample size for each reference material and values are expressed in Mean \pm SD (Min – Max).

Reference Material	n	Certified value ($\mu\text{g}\cdot\text{g}^{-1}$ dw)	Measured value ($\mu\text{g}\cdot\text{g}^{-1}$ dw)	Recovery (%)
TORT-3 <i>Lobster hepatopancreas</i>	72	0.292 \pm 0.022 (0.270–0.314)	0.289 \pm 0.013 (0.270–0.324)	99.0 \pm 4.6 (92.3–110.9)
DOLT-5 <i>Fish liver</i>	16	0.440 \pm 0.180 (0.260–0.620)	0.427 \pm 0.012 (0.409–0.451)	97.1 \pm 2.8 (93.0–102.5)

Table S2. Tests for Hg speciation analyses of feathers from free-living individuals (n=5) of Brünnich's guillemots (*Uria lomvia*), sampled in Western Greenland in 2022. Values are means \pm SD. Concentrations are expressed in $\mu\text{g g}^{-1}$ dw for methyl-Hg (MeHg), inorganic Hg (iHg), total-Hg obtained from Hg speciation analyses (Σ MeHg+iHg) and from AMA analyses (THg). Recovery is calculated as (Σ MeHg + iHg) \times 100 / THg. Samples were analysed in duplicate/triplicates, with certified reference material (NIES-13). Further details are provided in the Materials and Methods.

Site	ID	THg	MeHg	iHg	Σ (iHg + MeHg)	Recovery
Maniitsoq	4284276	0.78	0.79 \pm 0.01	0.03 \pm 0.00	0.82 \pm 0.01	105
Kippaku	4287000	1.35	1.36 \pm 0.00	0.05 \pm 0.00	1.41 \pm 0.00	105
Kippaku	4415028	2.68	2.03 \pm 0.00	0.63 \pm 0.00	2.66 \pm 0.00	99
Kippaku	4286561	3.54	3.61 \pm 0.00	0.06 \pm 0.00	3.68 \pm 0.00	104
Qaanaaq	4415312	8.52	7.13 \pm 0.12	1.44 \pm 0.07	8.57 \pm 0.18	101

Table S3. Summary of Hg speciation analyses performed on feathers of Brünnich's guillemots (*Uria lomvia*) from Greenland (1833–2022): methyl-Hg (MeHg), inorganic Hg (iHg) and the sum of both (equivalent to total-Hg, THg). Values are means \pm SD (range). Concentrations ($\mu\text{g}\cdot\text{g}^{-1}$ dw) were quantified in all samples and in certified reference material (NIES-13). n indicates sample sizes. Individual recovery (%) is calculated as: $(\Sigma \text{MeHg} + \text{iHg}) \times 100 / \text{THg}$. Further details are provided in the Materials and Methods.

	THg	MeHg	iHg	$\Sigma(\text{iHg} + \text{MeHg})$	Recovery
Recent samples (n=5)	3.4 \pm 3.1 (0.8–8.5)	3.0 \pm 2.5 (0.8–8.6)	0.4 \pm 0.6 (0.0–1.4)	3.4 \pm 3.1 (0.8–8.6)	102.8 \pm 2.6 (99.4–105.2)
Museum samples (n=10)	34.9 \pm 41.6 (1.5–126.5)	1.1 \pm 0.5 (0.4–2.1)	32.5 \pm 37.8 (0.2–125.8)	33.6 \pm 37.6 (1.5– 126.8)	–*
NIES-13 (n=3)	4.40 \pm 0.20	3.7 \pm 0.3 (3.5–4.0)	0.8 \pm 0.1 (0.6–0.9)	4.5 \pm 0.2 (4.3–4.6)	101.0 \pm 3.4 (98.3–104.8)

*No recovery is provided for the museum samples, because of the high inorganic contamination in old specimens, which completely biased the recovery percentage.

Table S4. Outliers (n=3) identified during data analyses: feather Hg concentrations and stable isotope values.

ID	Year	Feather Hg ($\mu\text{g}\cdot\text{g}^{-1}$)	Feather $\delta^{13}\text{C}$ (‰)	Feather $\delta^{15}\text{N}$ (‰)
Greenland-6	1955	1.38	–12.72	15.46
BRUG-1	2006	6.85	–18.69	16.36
Qaannaq-4415312	2022	8.52	–18.35	16.15

Table S5. Feather Hg concentrations and stable isotope values in adult Brünnich's guillemots (*Uria lomvia*) from West Greenland (n=448), collected between the 1840s and the 2020s.

Decades	n	Feather Hg ($\mu\text{g}\cdot\text{g}^{-1}$)	Feather corrected $\delta^{13}\text{C}$ (‰)	Feather $\delta^{15}\text{N}$ (‰)
1840	1	3.62	-16.54	13.83
1860	1	0.90	-14.38	15.84
1880	5	1.10 \pm 0.52 (0.69–1.92)	-16.65 \pm 1.07 (-18.03, -15.16)	14.44 \pm 1.01 (13.57–16.17)
1890	15	1.00 \pm 0.81 (0.46–3.77)	-17.02 \pm 0.95 (-18.77, -15.38)	13.94 \pm 0.98 (12.62–15.75)
1900	23	0.61 \pm 0.32 (0.27–1.57)	-17.03 \pm 0.68 (-18.18, -15.26)	13.93 \pm 0.91 (11.60–15.44)
1910	39	0.60 \pm 0.26 (0.22–1.15)	-16.59 \pm 1.05 (-18.77, -14.85)	14.71 \pm 0.78 (12.45–15.69)
1920	4	1.43 \pm 0.37 (0.98–1.76)	-16.44 \pm 0.53 (-17.06, -15.76)	14.04 \pm 0.68 (13.50–14.92)
1930	15	1.14 \pm 0.26 (0.82–1.81)	-16.71 \pm 0.36 (-17.27, -15.86)	15.53 \pm 0.73 (13.86–16.96)
1940	6	0.81 \pm 0.25 (0.56–1.19)	-16.83 \pm 0.67 (-17.71, -15.87)	15.24 \pm 0.88 (13.70–16.35)
1950	4	1.15 \pm 0.92 (0.47–2.51)	-17.74 \pm 1.03 (-18.99, -16.47)	14.42 \pm 0.96 (13.43–15.66)
1960	1	2.94	-17.09	15.64
1970	4	2.18 \pm 1.66 (0.66–4.51)	-17.57 \pm 0.46 (-18.19, -17.08)	15.66 \pm 0.81 (14.58–16.46)
1980	10	2.89 \pm 0.48 (2.14–3.58)	-17.75 \pm 0.57 (-18.59, -16.83)	15.19 \pm 0.53 (14.25–16.15)
1990	41	1.33 \pm 0.64 (0.35–3.03)	-19.14 \pm 1.11 (-21.19, -16.44)	14.07 \pm 0.82 (12.54–16.91)
2000	96	2.34 \pm 1.23 (0.26–6.85)	-18.88 \pm 0.94 (-21.21, -16.68)	14.86 \pm 1.12 (11.72–17.81)
2010	110	1.91 \pm 0.79 (0.50–3.92)	-19.00 \pm 0.57 (-20.99, -17.78)	14.96 \pm 0.55 (13.51–16.27)
2020	73	1.99 \pm 1.18 (0.74–8.52)	-18.74 \pm 0.51 (-19.95, -17.76)	14.59 \pm 0.84 (12.60–16.38)

Paper 4

A century of mercury: Ecosystem-wide changes drive increasing contamination in a tropical seabird species in the South Atlantic Ocean

Published in *Environmental Pollution* (2023)

Fanny Cusset, S. James Reynolds, Alice Carravieri, David Amouroux, Océane Asensio, Roger C. Dickey, Jérôme Fort, John Hughess, Vitor H. Paiva, Jaime A. Ramos, Laura Shearer, Emmanuel Tessier, Colin P. Wearn, Yves Cherel, Paco Bustamante.





Contents lists available at ScienceDirect

Environmental Pollution

journal homepage: www.elsevier.com/locate/envpol

A century of mercury: Ecosystem-wide changes drive increasing contamination of a tropical seabird species in the South Atlantic Ocean[☆]

Fanny Cusset^{a,b,*}, S. James Reynolds^{c,d}, Alice Carravieri^{a,b}, David Amouroux^e, Océane Asensio^e, Roger C. Dickey^d, Jérôme Fort^a, B. John Hughes^{c,d}, Vitor H. Paiva^f, Jaime A. Ramos^f, Laura Shearer^g, Emmanuel Tessier^e, Colin P. Wearn^h, Yves Cherel^b, Paco Bustamante^{a,i}

^a Littoral Environnement et Sociétés (LIENSs), UMR 7266 CNRS - La Rochelle Université, 2 Rue Olympe de Gouges, 17000, La Rochelle, France

^b Centre d'Études Biologiques de Chizé (CEBC), UMR 7372 CNRS - La Rochelle Université, 79360, Villiers-en-Bois, France

^c Centre for Ornithology, School of Biosciences, College of Life & Environmental Sciences, University of Birmingham, Edgbaston, Birmingham, UK

^d Army Ornithological Society (AOS), c/o Prince Consort Library, Knollys Road, Aldershot, Hampshire, UK

^e Institut des Sciences Analytiques et de Physico-Chimie pour l'Environnement et Les Matériaux (IPREM), UMR, 5254, CNRS, Université de Pau et des Pays de l'Adour, Pau, France

^f University of Coimbra, MARE – Marine and Environmental Sciences Centre / ARNET - Aquatic Research Network, Department of Life Sciences, Calçada Martim de Freitas, 3000-456, Coimbra, Portugal

^g Ascension Island Government Conservation and Fisheries Directorate (AIGCFD), Georgetown, Ascension Island, South Atlantic Ocean, UK

^h The Royal Air Force Ornithological Society (RAFOS), High Wycombe, Buckinghamshire, UK The Royal Air Force Ornithological Society (RAFOS) High Wycombe Buckinghamshire UK

ⁱ Institut Universitaire de France (IUF), 1 Rue Descartes, 75005 Paris, France

ARTICLE INFO

Keywords:

Feathers

Hg

Museum

Sooty tern

Stable isotopes

Temporal monitoring

ABSTRACT

Mercury (Hg) is a highly toxic metal that adversely impacts human and wildlife health. The amount of Hg released globally in the environment has increased steadily since the Industrial Revolution, resulting in growing contamination in biota. Seabirds have been extensively studied to monitor Hg contamination in the world's oceans. Multidecadal increases in seabird Hg contamination have been documented in polar, temperate and subtropical regions, whereas in tropical regions they are largely unknown. Since seabirds accumulate Hg mainly from their diet, their trophic ecology is fundamental in understanding their Hg exposure over time. Here, we used the sooty tern (*Onychoprion fuscatus*), the most abundant tropical seabird, as bioindicator of temporal variations in Hg transfer to marine predators in tropical ecosystems, in response to trophic changes and other potential drivers. Body feathers were sampled from 220 sooty terns, from museum specimens ($n = 134$) and free-living birds ($n = 86$) from Ascension Island, in the South Atlantic Ocean, over 145 years (1876–2021). Chemical analyses included (i) total- and methyl-Hg, and (ii) carbon ($\delta^{13}\text{C}$) and nitrogen ($\delta^{15}\text{N}$) stable isotopes, as proxies of foraging habitat and trophic position, respectively, to investigate the relationship between trophic ecology and Hg contamination over time. Despite current regulations on its global emissions, mean Hg concentrations were 58.9% higher in the 2020s ($2.0 \mu\text{g g}^{-1}$, $n = 34$) than in the 1920s ($1.2 \mu\text{g g}^{-1}$, $n = 107$). Feather Hg concentrations were negatively and positively associated with $\delta^{13}\text{C}$ and $\delta^{15}\text{N}$ values, respectively. The sharp decline of 2.9‰ in $\delta^{13}\text{C}$ values over time indicates ecosystem-wide changes (shifting primary productivity) in the tropical South Atlantic Ocean and can help explain the observed increase in terns' feather Hg concentrations. Overall, this study provides invaluable information on how ecosystem-wide changes can increase Hg contamination of tropical marine predators and reinforces the need for long-term regulations of harmful contaminants at the global scale.

[☆] This paper has been recommended for acceptance by Michael Bank.

* Corresponding author. Littoral Environnement et Sociétés (LIENSs), UMR 7266 CNRS - La Rochelle Université, 2 rue Olympe de Gouges, 17000, La Rochelle, France.

E-mail address: fanny.cusset1@univ-lr.fr (F. Cusset).

<https://doi.org/10.1016/j.envpol.2023.121187>

Received 7 November 2022; Received in revised form 10 January 2023; Accepted 30 January 2023

Available online 31 January 2023

0269-7491/© 2023 Elsevier Ltd. All rights reserved.

1. Introduction

Mercury (Hg) is a toxic metal and its impacts on human health are a major concern. Globally, the amount of Hg released into the environment has steadily increased since the Industrial Revolution, resulting in a three- to five-fold increase of Hg on land, in the atmosphere and the ocean (Lamborg et al., 2014; Selin, 2009). Since Hg is primarily emitted in the atmosphere in its volatile form (Hg^0) by both natural and human sources (Eagles-Smith et al., 2018) where it remains for up to one year (Streets et al., 2019), it disperses widely before its deposition in all global ecosystems. Consequently, even remote oceanic regions are affected by this global pollutant. Once in the sea, Hg is methylated by microorganisms into methyl-Hg (MeHg), its most toxic and bioavailable form. Because of its high assimilation efficiency and strong affinity for proteins, MeHg bioaccumulates in marine organisms (i.e., concentrations increase over time in their tissues) and biomagnifies in food webs (i.e., concentrations increase at each trophic level). Marine food resources represent the principal source of Hg for humans and wildlife. Mercury can cause severe physical and neurological harm and even mortality at sufficiently high concentrations, as is the case in Minamata Disease (Takeuchi et al., 1962). This has led to new regulations, such as the Minamata Convention on Mercury, to protect human health and the environment, by controlling and reducing anthropogenic releases of Hg globally.

Oceans receive 80% of total atmospheric Hg deposition, 49% of which is restricted to tropical oceans (Horowitz et al., 2017). Despite this, little is known about the interactions between Hg and ecosystem function in the intertropical zone. Yet, it is here that artisanal and small-scale gold mining occurs, resulting in annual Hg emissions >720 tonnes. Gold mining is the largest contributor to Hg emissions and represents >35% of total global anthropogenic Hg emissions (Eagles-Smith et al., 2018). In addition, tropical oceans have recently experienced increased oxygen-depletion (Breitburg et al., 2018), creating favourable conditions for MeHg formation (Cossa, 2013; Mason et al., 2012; Sunderland et al., 2009). Quantifying Hg contamination and its temporal trends in tropical oceans and wildlife is thus urgently needed.

Monitoring tropical oceans is logistically challenging but can be achieved through investigations of bioindicators that feed extensively across their waters and, thus, provide a lens through which to investigate Hg contamination. Seabirds are effective bioindicators (Burger and Gochfeld, 2004; Furness, 1993) because of their high position in marine trophic webs and longevity, allowing them to integrate and reflect Hg contaminations of their food webs (Fort et al., 2016; Furness and Camphuysen, 1997; Piatt et al., 2007). Furthermore, most seabirds are colonial (i.e., they concentrate in high numbers in breeding colonies) and philopatric (i.e., they have high site fidelity). Thus, several individuals can be sampled simultaneously, and repeatedly through time, in particular through non-lethal collection of feathers (Albert et al., 2019). Feathers are a reliable tissue to investigate Hg contamination in seabirds (Thompson et al., 1998), because dietary MeHg accumulates in body tissues between moulting episodes (Furness et al., 1986). Up to 90% of the accumulated MeHg is sequestered into growing feathers after transportation in the blood and then excreted during moult (Honda et al., 1986). In feathers, MeHg binds to sulfhydryl groups of keratin molecules (Crewther et al., 1965) to form strong, stable bonds that withstand rigorous physical treatments over time (Appelquist et al., 1984). Mercury contained in feathers is mostly in the form of MeHg (>90%, Renedo et al., 2017) and thus seabird feathers are commonly used for Hg biomonitoring over the short- and the long-term (e.g., Albert et al., 2019; Burger and Gochfeld, 2004; Cherel et al., 2018).

Seabirds have been collected for exhibitions and museum collections worldwide over the last centuries and, therefore, their specimens are invaluable to study temporal trends of Hg contamination (Vo et al., 2011). However, inorganic Hg salts were used historically by museum curators as preservatives in specimen preparation, resulting in methodological bias when analysing museum *versus* free-living specimens.

This bias can be overcome by analysing MeHg specifically (Hogstad et al., 2003). Overall, only a limited number of studies ($n = 14$) have quantified Hg in museum-held seabird specimens over the last century, and only four of these have considered trophic ecology as a factor that could influence Hg contamination (see Supplementary Material, Table S1 for species and temporal comparisons). Yet, bird trophic ecology is key to understanding the mechanisms of Hg contamination and to disentangle whether temporal variations in Hg contamination are linked to dietary shifts and/or to changes in environmental Hg contamination (Bond et al., 2015; Carravieri et al., 2016; Choy et al., 2022; Fort et al., 2016; Vo et al., 2011). Over multidecadal timescales, decreases and stable trends in Hg contamination have been documented in only one temperate Atlantic species (Thompson et al., 1992) and one temperate Pacific species (Choy et al., 2022), respectively. In contrast, increases in Hg contamination have been observed in 12 temperate Atlantic species (Monteiro and Furness, 1997; Thompson et al., 1992; Thompson et al., 1993), one temperate/subtropical Pacific species (Vo et al., 2011) and one Arctic species (Bond et al., 2015). Notably, none of these studies involved long-term investigation of tropical regions.

The sooty tern (*Onychoprion fuscatus*) is the most abundant tropical seabird, widely distributed in all three ocean basins. This species is therefore an ideal candidate to monitor Hg contamination in tropical food webs. The present work extends the investigation of Reynolds et al. (2019), who highlighted long-term changes in the feeding ecology of sooty terns breeding on Ascension Island (the largest colony in the South Atlantic Ocean), by using carbon ($\delta^{13}\text{C}$) and nitrogen ($\delta^{15}\text{N}$) stable isotopes, which are proxies of feeding habitat (i.e., carbon source) and diet (i.e., trophic position), respectively (Kelly, 2000). Reynolds et al. (2019) found long-term declines in both feather $\delta^{13}\text{C}$ and $\delta^{15}\text{N}$ values since the 1890s, indicating a fundamental change in their foraging behaviour, including a dietary shift from predominantly teleost fish to squid coinciding with a dramatic decline in the size of the breeding population on Ascension Island. Here, our aim was three-fold to: (i) document the temporal trend of feather Hg concentrations in Ascension sooty terns between the 1890s and the 2020s, (ii) investigate the influence of their trophic ecology (reflected by $\delta^{13}\text{C}$ and $\delta^{15}\text{N}$ values) on this temporal trend and (iii) compare feather Hg contamination before and after population collapse. As for other remote oceanic regions, we predict that there will be a general increase in feather Hg concentrations to the present day, linked to the previously documented changes in their diet and foraging behaviours.

2. Materials and methods

2.1. Study area and museum specimens

Ascension Island (07°57' S, 14°24' W) is an isolated 97 km² volcanic island in the tropical South Atlantic Ocean. It accommodates the largest breeding population of sooty terns in the entire Atlantic Ocean, containing on average > 200,000 pairs (Hughes et al., 2012). Currently, they nest on bare ground across the Wideawake Fairs – an Important Bird Area (IBA SH009) – at two Nature Reserves (NRs) called Mars Bay and Waterside Fairs. As epipelagic seabirds, sooty terns feed on small pelagic fish and squid caught at/ near the ocean surface (Ashmole, 1963a; Reynolds et al., 2019). Globally, sooty terns are listed as 'Least Concern' in the IUCN Red List of Threatened Species. Yet, the population from Ascension Island has drastically declined by approximately 84% between the 1960s and 1990s from a peak of approximately two million birds (Hughes et al., 2017). Many factors may have contributed to this precipitous decline, including the depletion of food resources and predation by introduced species such as domestic cats (*Felis silvestris catus*), black rats (*Rattus rattus*) and common mynas (*Acridotheres tristis*) (Reynolds et al., 2019 and references therein).

2.2. Feather sampling and preparation

Sooty terns from Ascension Island breed sub-annually (~10 months; Reynolds et al., 2014). While still breeding, they start their post-nuptial moult (*i.e.*, basic moult) and replace all of their feathers (*i.e.*, flight and body) during the following weeks/months (Ashmole, 1963b). Therefore, body feathers collected during the breeding season provide information on bird Hg exposure since the previous moult (*i.e.* for the past 10 months; Albert et al., 2019). This includes different stages of their life cycle: (i) the end of the previous breeding season, (ii) the post-breeding migration, (iii) the non-breeding period, (iv) the pre-breeding migration and (v) the beginning of the current breeding season. Consequently, feathers also provide information at different spatial scales, since sooty terns have a maximum non-breeding range of 2900 km in tropical waters around Ascension Island (Reynolds et al., 2021). Feathers also retain dietary signatures at the time of their synthesis, as carbon and nitrogen isotopes are incorporated into feathers as they grow (*i.e.*, over a few weeks). Consequently, Hg concentrations and stable isotope values of feathers are temporally decoupled (Thompson et al., 1998; Bond, 2010). Nonetheless, stable isotope values can provide invaluable information about seabird foraging ecology across century scales by virtue of their constant integration over time, thereby allowing for long-term understanding of Hg temporal trends.

Historical feather samples were collected from skins held in 10 natural history museum collections (see details in Supplementary Table S2). Details of museum skins are provided in Supplementary Table S3. The complete procedure for historical sampling and preparation is detailed in Reynolds et al. (2019). Only specimens with known collection date (*i.e.*, year or decade) were considered for the current study. When the precise year of specimen collection was unknown ($n = 7$), we attributed the first year of the corresponding decade to it. Sex of birds from which skins were prepared was known for some historical samples (*i.e.*, 43 females and 41 males from the 1920s). Feather sampling of free-living birds was carried out at Mars Bay NR and Waterside Fairs NR breeding colonies in 2006 by BJH ($n = 8$), 2012 by CPW and SJR ($n = 40$) and 2020 ($n = 4$) and 2021 ($n = 30$) by LS. These samples were collected by licenced professionals under environmental research permits issued by Ascension Island Government. Incubating sooty terns were caught during ringing activities using a soft mesh hand-held net. While processing the birds (Redfern and Clark, 2001), contour feathers were removed from across the breast on both sides of the keel ridge. Samples were collected from breeding adults and stored at room temperature prior to preparation and analysis.

To eliminate any external contamination, all feathers were cleaned in the laboratory with a chloroform:methanol mixture (2:1), sonicated for 3 min and rinsed twice in methanol. They were then oven-dried for 48 h at 45°C. For each bird specimen, several feathers (2–4) were pooled to derive the individual mean value (Carravieri et al., 2014; Jaeger et al., 2009), then cut with stainless scissors into a homogeneous powder to be analysed for both stable isotopes and Hg.

2.3. Stable isotope analyses

Carbon and nitrogen stable isotopes were analysed in homogenized subsamples of body feathers. Results are expressed in the δ unit notation as deviations from standards (Vienna Pee Dee Belemnite for $\delta^{13}\text{C}$ and atmospheric N_2 for $\delta^{15}\text{N}$) following the formula:

$$\delta^{13}\text{C} \text{ or } \delta^{15}\text{N} = \left(R_{\text{sample}}/R_{\text{standard}} - 1 \right) \times 10^3$$

where R is $^{13}\text{C}/^{12}\text{C}$ or $^{15}\text{N}/^{14}\text{N}$, respectively. Analyses of historical samples (*i.e.*, from the 1890s to the 2010s) were performed at the MARE and results were presented in Reynolds et al. (2019). The present study extends this previous investigation by another decade to the present day. Analyses of these contemporary feathers (*i.e.*, from

the 2020s) were performed at the LIENSs. Feather subsamples (~0.4 mg) were weighed with a microbalance and loaded into tin cups. Values of $\delta^{13}\text{C}$ and $\delta^{15}\text{N}$ were determined with a continuous flow mass spectrometer (Delta V Plus with a ConFlo IV Interface, Thermo Scientific, Bremen, Germany) coupled to an elemental analyzer (Flash 2000 or EA Isolink, Thermo Scientific, Milan, Italy). The analytical precision was <0.10 ‰ and <0.15 ‰ for $\delta^{13}\text{C}$ and $\delta^{15}\text{N}$ values, respectively. Ten samples were analysed in both laboratories to compare analytical performances. No difference in $\delta^{13}\text{C}$ (ANOVA, $F_{1,18} = 0.04$, $p = 0.80$) nor $\delta^{15}\text{N}$ values (ANOVA, $F_{1,18} = 0.008$, $p = 0.90$) was detected between the two laboratories, ensuring data comparability between the older (from Reynolds et al., 2019) and most recent feather samples.

Since the Industrial Revolution, the combustion of human fossil fuel has increased atmospheric CO_2 , resulting in an accelerating decrease in biosphere $\delta^{13}\text{C}$, mainly influenced by two additive effects: (i) an increase in phytoplankton fractionation (Rau et al., 1992), and (ii) the so-called « Suess-Effect » (Keeling, 1979), whereby anthropogenic carbon has lower $\delta^{13}\text{C}$ values than natural background carbon. In our study, raw $\delta^{13}\text{C}$ values were thus corrected accordingly, following calculations from previous work (Eide et al., 2017; Hilton et al., 2006; Jaeger and Chereil, 2011; Körtzinger et al., 2003). For further information, see Supplementary Figure S1 for a comparison of isotopic niches of raw and corrected $\delta^{13}\text{C}$ values.

2.4. Mercury analyses

Generally, total Hg (THg) includes both inorganic (iHg) and organic Hg (*i.e.*, MeHg). In feathers, MeHg accounts for >90% of THg (Bond and Diamond, 2009; Renedo et al., 2017; Thompson and Furness, 1989). So, THg can be used as a proxy of MeHg in feathers. Here, THg analyses were performed on homogenized feathers using an Advanced Mercury Analyzer spectrophotometer (Altec AMA 254). Each sample was analysed in duplicate-triplicate to guarantee a relative standard deviation <10%. Accuracy was verified by running certified reference material (DOLT-5, Fish liver, National Research Council, Canada: certified Hg concentration = $0.44 \pm 0.18 \mu\text{g g}^{-1}$ dry weight [dw]). Our measured values were $0.43 \pm 0.01 \mu\text{g g}^{-1}$ dw ($n = 14$). Blanks were run at the beginning of each set of samples. Detection limit of the AMA was 0.01 ng. Mercury concentrations are expressed in $\mu\text{g g}^{-1}$ dw.

Historically, inorganic Hg salts were used as preservatives in museum collections until approximately the 1970s, creating a major bias in THg comparison between old and recent specimens (Thompson et al., 1992). Therefore, Hg speciation analyses were performed on the oldest specimens ($n = 131$; until the 1970s) to quantify both MeHg and iHg (Renedo et al., 2017, 2018) from feather homogenates (1.1–12.0 mg), using a GC-ICP-MS Trace Ultra GC equipped with a Triplus RSH autosampler coupled to an ICP-MS XSeries II (Thermo Scientific, Bremen, Germany). Mercury speciation analyses were also performed on a few free-living individuals ($n = 3$, from the 2000s) to determine the precise proportion of MeHg in sooty tern feathers and hence validate the use of THg as proxy of MeHg after the 1970s. Further methodological details are provided in Supplementary Material, including a comparison of speciation results between old and recent specimens (Table S4). Certified reference material (NIES-13, human hair; certified MeHg concentration = $3.80 \pm 0.40 \mu\text{g g}^{-1}$ dw) was analysed for validation of feather analyses (keratin-based matrices). Our measured concentrations for MeHg were $3.64 \pm 0.09 \mu\text{g g}^{-1}$ dw ($n = 3$). Method recovery was checked by comparison of THg values measured with AMA and the equivalent Σ MeHg + iHg obtained from speciation analyses. Further details on recovery calculations are shown in Table S5. Average recovery of sooty tern feather Hg was $96.1 \pm 4.9\%$ (92.3–101.3%; $n = 3$; see Supplementary Material). Subsequently, feather Hg concentrations reflect MeHg concentrations before the 1970s and THg concentrations thereafter.

2.5. Data analyses

All statistical analyses and graphical representations were carried out in R 4.0.3 (R Core Team, 2020).

2.5.1. Temporal trends of stable isotopes and Hg over 145 years

Year-specific sample sizes were unbalanced (Table 1), with five times more observations on average in 1925 than in other years. Thus, 50 values were randomly extracted from this specific year and used in all models. One outlier was identified in 1915 (i.e., JR11, Table S3) and removed from all analyses. Data exploration revealed that Hg, $\delta^{13}\text{C}$ and $\delta^{15}\text{N}$ varied non-linearly with time. Therefore, Generalized Additive Models (GAMs) were run to investigate non-linear temporal trends over 145 years, using the « mgcv » package (Wood, 2011). Each variable was modeled independently against year as a smoother. For each model, we adapted the smoothed term (k) to avoid overfitting and over-simplification, and obtain the best and most realistic fit to the data (k = 5 for Hg, $\delta^{13}\text{C}$ and $\delta^{15}\text{N}$ values). Model assumptions were checked via residual analysis through the « gam. check » function.

2.5.2. Drivers of Hg contamination over time

Multifactorial analyses were used to test for the effect of trophic ecology on feather Hg concentrations over time. To discard the combined effect of time on both feeding habitat and trophic position, we detrended all variables by extracting residuals from GAM temporal trends of Hg, $\delta^{13}\text{C}$ and $\delta^{15}\text{N}$ values. The new response variable was time-detrended Hg concentrations and continuous explanatory variables were the time-detrended $\delta^{13}\text{C}$ and $\delta^{15}\text{N}$ values. Relationships between detrended variables were then investigated with linear models using the « nlme » package (Pinheiro et al., 2020). Prior to model construction, one-way ANOVA was used to test for differences in Hg concentrations between the sexes of terns. As no difference was detected ($F_{1,82} = 2.82$, $p = 0.10$; Supplementary Figure S2), sex was not included in model selection procedures. Models were GAMs with a Gaussian distribution and an identity link function. The initial model was: detrended Hg ~ detrended $\delta^{13}\text{C}$ + detrended $\delta^{15}\text{N}$. All potential combinations of variables (Table 2) were subjected to model selection based on the Akaike's Information Criterion adjusted for small sample sizes (AIC_c), using the « MuMIn » package (Bartoń, 2022). The model with the lowest AIC_c value, with a difference of AIC_c of two or more compared to the next model (ΔAIC_c), was selected as the best model (Burnham and Anderson, 2002). Model performance was assessed using Akaike weights (w_i) (after Johnson and Omland, 2004) and model fit was checked by residual analysis of the initial model.

To compare temporal trends with the published literature, we calculated the percentage of change (increase or decrease) for evolution phases identified by GAM temporal trends. Details of empirical calculations are provided in the Supplementary Material (Table S6).

Table 1

Mercury concentrations and stable isotope values (mean \pm SD, range) in feathers of sooty terns (n = 220) breeding on Ascension Island (South Atlantic Ocean) from the 1870s to the 2020s, before (1840s–1940s) and after (1970s–2020s) their population collapse. Total-Hg (THg) was measured in all samples, whereas methyl-Hg (MeHg) was analysed when inorganic contamination by museum preservatives was detected (i.e., prior to the 1970s). Feather $\delta^{13}\text{C}$ (corrected for the Suess Effect) and $\delta^{15}\text{N}$ values are proxies for the foraging habitat and trophic position during moult, respectively. N indicates sample size for each decade or period.

Decade	n	Feather THg ($\mu\text{g g}^{-1}$)	Feather MeHg ($\mu\text{g g}^{-1}$)	Corrected feather $\delta^{13}\text{C}$ (‰)	Feather $\delta^{15}\text{N}$ (‰)
1890	11	70.12 \pm 87.34 (1.65–264.92)	1.63 \pm 0.74 (0.49–2.71)	−13.11 \pm 0.27 (−13.32, −12.46)	13.56 \pm 1.36 (11.57–15.42)
1920	107	5.25 \pm 7.82 (1.65–55.57)	1.24 \pm 0.42 (0.32–3.47)	−13.50 \pm 0.45 (−14.55, −11.85)	12.15 \pm 1.04 (9.96–14.72)
1940	10	9.70 \pm 7.51 (3.36–26.12)	1.51 \pm 0.30 (1.25–2.29)	−14.10 \pm 0.21 (−14.47, −13.85)	12.90 \pm 0.94 (10.61–13.89)
1970	6	5.25 \pm 6.50 (2.20–18.51)	2.02 \pm 0.35 (1.58–2.61)	−14.76 \pm 0.47 (−15.30, −13.93)	13.14 \pm 1.08 (11.28–14.58)
2000	8	1.21 \pm 0.20 (0.88–1.50)	–	−15.11 \pm 0.19 (−15.37, −14.81)	11.56 \pm 0.64 (10.74–12.55)
2010	44	1.72 \pm 0.43 (0.75–3.02)	–	−16.11 \pm 0.33 (−17.44, −15.56)	11.75 \pm 1.19 (9.49–14.11)
2020	34	1.97 \pm 0.49 (0.91–2.90)	–	−16.35 \pm 0.35 (−16.75, −15.23)	12.89 \pm 0.89 (10.12–14.14)
1890–1940	128	–	1.29 \pm 0.46 (0.32–3.47)	−13.51 \pm 0.47 (−14.55, −11.85)	12.33 \pm 1.13 (9.96–15.42)
1970–2020	92	1.79 \pm 0.48 (0.75–3.02)	–	−16.02 \pm 0.58 (−17.44, −13.93)	12.24 \pm 1.19 (9.49–14.58)

Table 2

AIC_c model ranking from statistical analyses of feather Hg concentrations from sooty terns breeding on Ascension Island. Models are Generalized Additive Models (GAMs) with a Gaussian distribution and an identity link function. Variables were all time-detrended (see Section 2.5.2 for further details). Abbreviations: k, number of parameters; AIC_c , Akaike's Information Criterion adjusted for small sample sizes; w_i , AIC_c weights.

Models	k	AIC_c	ΔAIC_c^a	w_i^b
Detrended $\delta^{13}\text{C}$ + Detrended $\delta^{15}\text{N}$	4	184.52	0.00	0.96
Detrended $\delta^{13}\text{C}$	3	191.49	6.97	0.03
Detrended $\delta^{15}\text{N}$	3	193.75	9.23	0.01
NULL	2	206.61	22.09	0.00

^a A model with $\Delta\text{AIC}_c = 0$ is interpreted as the best model among all the selected ones (in bold).

^b Weights are cumulative (sum to 1).

2.5.3. Temporal comparison: before and after population collapse

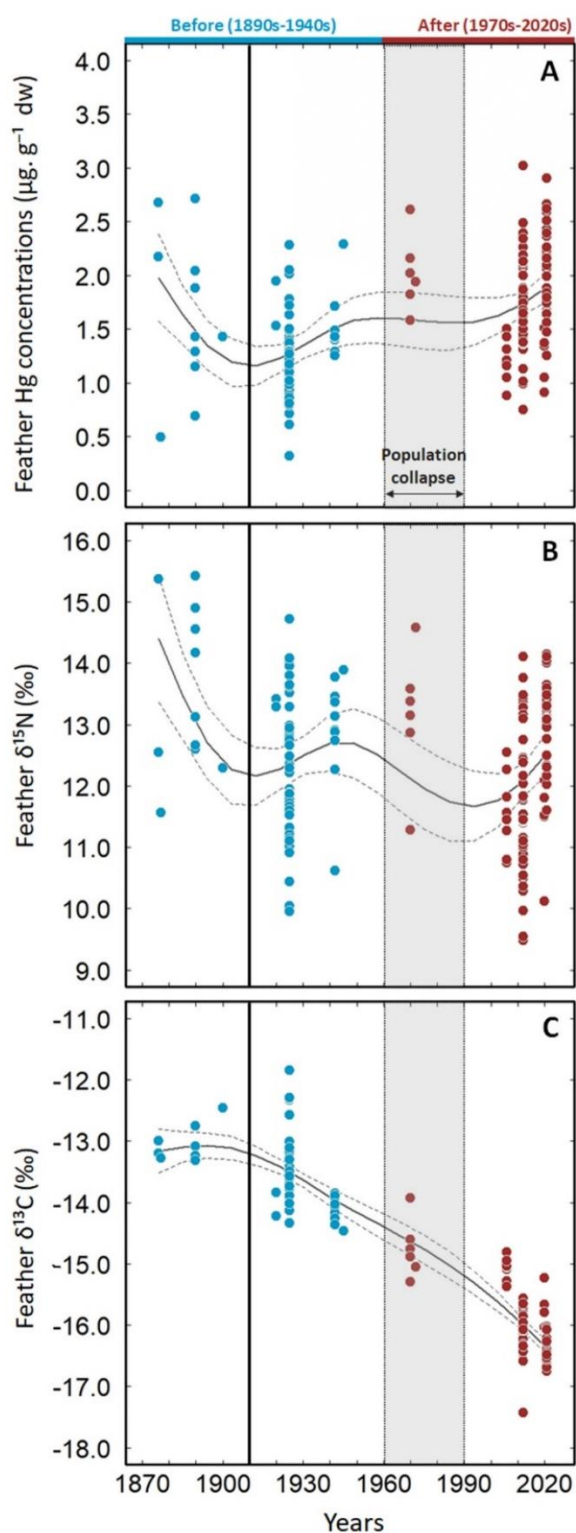
Following Reynolds et al. (2019), we tested for differences in trophic ecology and Hg concentrations of sooty terns relative to their population collapse on Ascension Island (i.e., before: 1890s–1940s; after: 1970s–2020s). First, a Multivariate Analysis of Variance (MANOVA) enabled us to test for differences in isotopic niches (i.e., $\delta^{13}\text{C}$ and $\delta^{15}\text{N}$ values combined) between periods. Differences between periods for individual isotopes were then identified using the « summary. aov » function. Residual normality (« mvnormtest package »; Jarek, 2012), outliers (« rstatix » package; Kassambara, 2022) and multicollinearity (between $\delta^{13}\text{C}$ and $\delta^{15}\text{N}$ values; « cor. test » function) were checked prior to interpretation. Secondly, one-way ANOVA was used to test for differences in Hg concentrations between the two periods. Prior to model construction, normality of residuals and homoscedasticity were tested with Shapiro and Breusch-Pagan tests (« lmtest » package; Zeileis and Hothorn, 2002), respectively. An alpha threshold of 0.05 was used for all statistical analyses.

3. Results

3.1. Temporal trend of Hg contamination and trophic ecology

Body feathers were sampled from 220 sooty terns from seven different decades, spanning 145 years (i.e., 1876–2021; Table 1), from museum skins (n = 134) and free-living birds (n = 86). Few data were available prior to the 1920s, leading to high variability and large uncertainty in temporal trends of Hg concentrations before the 1920s (Fig. 1A). Thus, interpretation of GAM temporal trends could only be carried out from the 1920s onwards. For this reason, results presented here mainly focus on the period between the 1920s and the 2020s. Detailed outputs from GAMs describing temporal variations in Hg, $\delta^{15}\text{N}$ and $\delta^{13}\text{C}$ values are provided in Table S7.

Since the 1920s, Hg concentrations increased non-linearly with time (GAM, $p < 0.0001$, deviance explained was 0.25), following three



(caption on next column)

Fig. 1. Long-term trends in feather (A) Hg concentrations, (B) nitrogen ($\delta^{15}\text{N}$) and (C) carbon ($\delta^{13}\text{C}$) isotopic values of sooty terns breeding on Ascension Island (South Atlantic Ocean) between 1876 and 2021 (i.e., over 145 years). The $\delta^{13}\text{C}$ values are corrected for the Suess Effect and phytoplankton fractionation (cf. see Section 2.3 for further details). The grey area represents the transition between the period before (blue) and after (red) population collapse that occurred between the 1960s and the 1990s (see Reynolds et al., 2019 for further details). Solid and dotted curves represent the best-fitting model detected from construction of GAMs and the confidence interval, respectively. To the right of the vertical solid line at 1910 is the period of realistic interpretation (see Material and methods and Discussion for further details). (For interpretation of the references to colour in this figure legend, the reader is referred to the Web version of this article.)

distinct phases. First, Hg concentrations increased by 62.9% between the 1920s and the 1970s. Then, Hg concentrations exhibited an unclear pattern of change between the 1970s and the 2000s with high variability and large confidence intervals. Finally, Hg concentrations increased again by 62.8% from the 2000s to the present day. Overall, Hg concentrations were 58.9% higher in the 2020s than in the 1920s.

The $\delta^{15}\text{N}$ values ranged from 9.49 ‰ in the 2010s to 15.42 ‰ in the 1890s (Fig. 1B), with values varying non-linearly over time (GAM, $p < 0.0001$, deviance explained was 0.13), following three distinct phases. Values of $\delta^{15}\text{N}$ increased by 5.8% between 1920s and the 1940s (i.e., +0.75 ‰), decreased by 10.4% thereafter until the 2000s (i.e., -1.34 ‰) and increased by 11.5% from 2000s (i.e., +1.33 ‰) to the present day (Table 1 and S6).

Corrected $\delta^{13}\text{C}$ isotopic values ranged between -17.4 ‰ in the 2010s and -11.9 ‰ in the 1920s (Fig. 1C), with values decreasing dramatically over time (GAM, $p < 0.0001$, deviance explained was 0.91). There was a quasi-linear 17.4% change over the century between the 1920s and the 2020s (i.e., +2.85 ‰).

Feather Hg concentrations were 38.8% higher after ($1.79 \pm 0.48 \mu\text{g g}^{-1} \text{ dw}$) than before ($1.29 \pm 0.46 \mu\text{g g}^{-1} \text{ dw}$) (ANOVA; $F_{1,218} = 59.2$, $p < 0.001$) the population collapse that occurred between the 1960s and the 1990s (Fig. 2A). Isotopic niches were statistically different before and after the population collapse (MANOVA; $F_{1,218} = 649.8$, $p < 0.0001$; Fig. 2B), with no significant difference in $\delta^{15}\text{N}$ values (-0.7‰; $p = 0.39$) and -2.5 ‰ lower $\delta^{13}\text{C}$ values after than before the population collapse (-18.6‰; ANOVA; $F_{1,218} = 1271.8$, $p < 0.001$).

3.2. Drivers of Hg contamination over time

Results from model selection are provided in Table 2. The best model to explain time-detrended Hg concentrations included both time-detrended $\delta^{13}\text{C}$ and $\delta^{15}\text{N}$ values (linear models, $R^2 = 0.14$, $p < 0.0001$). Specifically, Hg concentrations decreased with increasing $\delta^{13}\text{C}$ values ($\beta \pm \text{SE}$: -0.279 ± 0.082 , 95% CI: -0.442, -0.117) and increased with increasing $\delta^{15}\text{N}$ values ($\beta \pm \text{SE}$: 0.090 ± 0.030 , 95% CI: 0.031, 0.149) (Fig. 3).

4. Discussion

In this study, sooty terns act as bioindicators of temporal trends in Hg contamination of food webs in the tropical South Atlantic Ocean. We have built on previous long-term investigations of the trophic ecology of breeding sooty terns on Ascension Island (1890s–2010s; Reynolds et al., 2019), by extending the recent time series by an additional decade and providing feather-derived Hg concentrations. To the best of our knowledge, this is the first study to determine Hg contamination over such an extensive multidecadal timescale in the tropical oceans. Our results revealed a global non-linear increase in Hg contamination of sooty terns over the last 145 years, because of both trophic and environmental changes over time.

Museum specimens represent invaluable archives that enable both dietary and ecotoxicological investigations on multidecadal timescales.

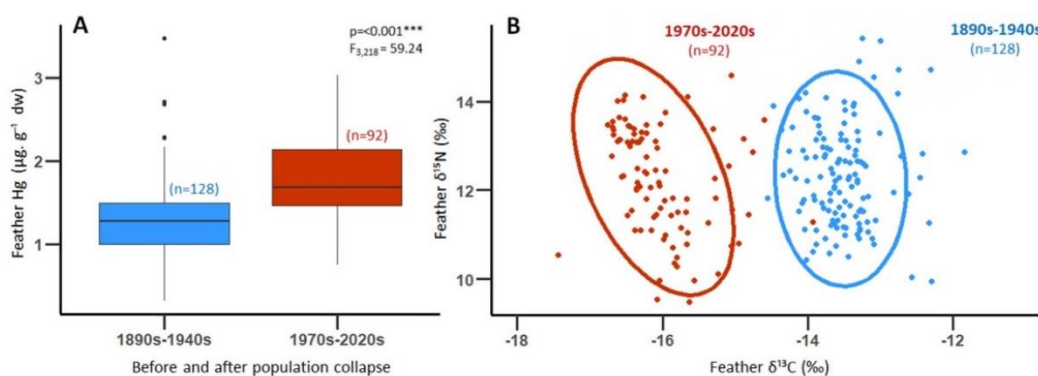


Fig. 2. Difference in (A) Hg concentrations and (B) isotopic niches ($\delta^{13}\text{C}$ and $\delta^{15}\text{N}$ values) from feathers of adult sooty terns relative to the population collapse on Ascension Island between the 1960s and the 1990s. Points, ellipses (including 90% of the data) and bars in blue and red are before ($n = 128$) and after ($n = 92$) the population collapse, respectively. n indicates the sample sizes. Boxplots indicate median values (midlines), errors bars (whiskers) and outliers (black dots). (For interpretation of the references to colour in this figure legend, the reader is referred to the Web version of this article.)

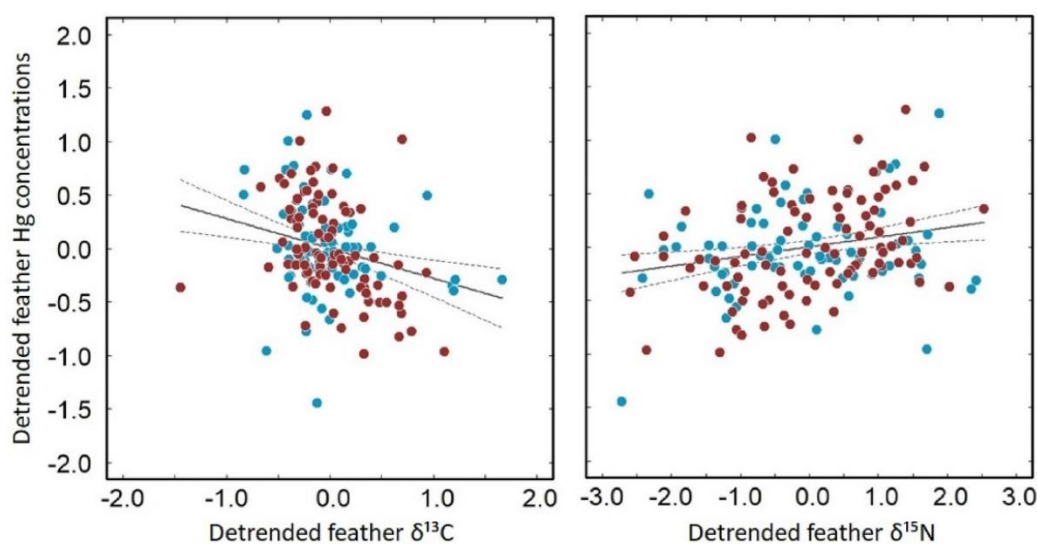


Fig. 3. Relationship between time-detrended Hg concentrations and time-detrended stable isotope values in feathers of adult sooty terns breeding on Ascension Island in the South Atlantic Ocean between 1876 and 2021 (*i.e.*, over 145 years). The tern population collapsed between the 1960s and the 1990s (see Reynolds et al., 2019 for further details), with data before- (in blue) and after (in red) the collapse. All data were scaled. Solid and dashed lines represent the best-fitting linear model and the 95% confidence interval, respectively. (For interpretation of the references to colour in this figure legend, the reader is referred to the Web version of this article.)

However, any retrospective investigation at a single location is challenging because it is highly dependent on sampling effort each year over a large time scale. Gaps in retrospective time-series are thus very common and consequently, analytical statistical approaches that were non-linear in nature were most relevant. Because the oldest specimens in our study were also the least numerous, temporal trends were characterized by high uncertainty between the 1890s and the 1920s (Fig. 1A). For this reason, interpretations of our findings mainly focussed on the 1920s to the 2020s.

4.1. Long-term trend in foraging ecology: an update

Using feathers as a record of sooty tern foraging ecology on the island, Reynolds et al. (2019) found a significant decrease in feather $\delta^{15}\text{N}$ values, suggesting a change in their trophic position over time. By extending the time series in our study with the inclusion of feathers

obtained in 2020 and 2021, we did not detect any further significant linear trend in $\delta^{15}\text{N}$ values. Instead, we detected a non-linear trend (Fig. 1B): initially, there was an increase between the 1900s and the 1940s, followed by a decrease between the 1940s and the 2000s, and a second increase from the 2000s onwards (Table 1 and S6). The addition of the most recent decade in the time series clearly highlights the importance of such long-term monitoring, by revealing recent and unpredictable patterns in the foraging ecology of sooty terns. These long-term variations in feather $\delta^{15}\text{N}$ values could reflect variations in seabird diet over time (Reynolds et al., 2019), but also changes in the isotopic baseline (McMahon et al., 2013). Isoscapes of $\delta^{15}\text{N}$ can vary seasonally due to changes in primary productivity which stem from variation and cycling of nutrient sources, as well as changes in species composition and growth rates of phytoplankton (Cifuentes et al., 1988; Goering et al., 1990; Ostrom et al., 1997; Vizzini and Mazzola, 2003). The changing $\delta^{15}\text{N}$ isoscape could then have cascading effects on feather

isotopic values of seabird consumers at upper trophic levels and hence, drive the temporal variations in their trophic position. One way to disentangle these hypotheses would be to perform compound-specific stable isotope analysis of amino acids (CSIA-AA) (McMahon and Newsome, 2019), which would help distinguish the specific signatures of the baseline («source» $\delta^{15}\text{N}$ -AAs) and the diet-consumer transfer («trophic» $\delta^{15}\text{N}$ -AAs), and hence elucidate the «true» trophic position of sooty terns over time.

Extending the results of Reynolds et al. (2019), corrected $\delta^{13}\text{C}$ values exhibited a similar and even stronger decreasing trend to the present day (Fig. 1C), with a 2.85 ‰ decline between the 1920s and the 2020s. This represents a 3.24 ‰ decline when considering the trend between the 1890s and the 2020s. A comparable decrease in $\delta^{13}\text{C}$ values over time was previously described in thin-billed prions (*Pachyptila belcheri*) in the Southern Ocean (Cherel et al., 2014; Quillfeldt et al., 2010), and was interpreted as a result of latitudinal change in their moulting area, switching from sub-Antarctic to Antarctic waters over more than 90 years (1913–2005). Similarly, moulting areas of Ascension sooty terns could have changed spatially over time but, to date, their post-breeding migrations have only been studied using geolocators between 2011 and 2015 (Reynolds et al., 2021) and far more research is required. Continuing such tracking work over the next few decades would allow trophic ecology of sooty terns to be directly related to long-term changes in their spatial distribution in the South Atlantic Ocean. Alternatively and similar to the hypothesis generated above for changes in feather $\delta^{15}\text{N}$ values, changes in $\delta^{13}\text{C}$ values might reflect baseline changes in the study area. Baseline $\delta^{13}\text{C}$ values vary both spatially (latitudinal gradient influenced by temperature; Sackett et al., 1965) and temporally (seasonal variability) in the marine environment (McMahon et al., 2013). The temporal decline in $\delta^{13}\text{C}$ values of sooty terns could thus reflect fluctuations in baseline $\delta^{13}\text{C}$ values. However, the observed trend appears too marked to be explained solely by a change in $\delta^{13}\text{C}$ baseline values. Carbon isotope values reflect phytoplankton productivity in aquatic environments (DeNiro and Epstein, 1978; France, 1995; Hobson, 1999). Declines in $\delta^{13}\text{C}$ values have been associated with those in primary productivity, and hence with the carrying capacity of ecosystems (Hirons et al., 2001; O'Reilly et al., 2003; Schell, 2000), and ultimately with declines of penguin (Spheniscidae) populations, for example, in the sub-Antarctic region (Hilton et al., 2006; Jaeger and Cherel, 2011). In the South Atlantic Ocean, a 1.38 ‰ decline in $\delta^{13}\text{C}$ values was observed in muscle of tuna species between 2000 and 2015, suggesting a global shift in phytoplankton community structure (Lorrain et al., 2020). This coincides with the 1.24 ‰ decline we observed in feather $\delta^{13}\text{C}$ values of Ascension sooty terns between the 2000s and the 2020s in the same region. So, the global 2.85 ‰ decline in feather $\delta^{13}\text{C}$ values in our study (between the 1920s and the 2020s) could likely result from a change in phytoplankton productivity in the surrounding tropical marine ecosystem.

4.2. Long-term trend in Hg contamination and its drivers

Overall, our results (Table 1) are consistent with the range of average Hg concentrations observed for sooty terns elsewhere, such as in the Mozambique Channel ($0.2 \mu\text{g g}^{-1}$; Jaquet et al., 2008; Kojadinovic et al., 2007), Pacific Islands ($0.8 \mu\text{g g}^{-1}$; Burger et al., 1992), the Seychelles ($1.2 \mu\text{g g}^{-1}$; Ramos and Tavares, 2010) and Puerto Rico ($2.6 \mu\text{g g}^{-1}$; Burger and Gochfeld, 1991). However, Ascension sooty terns exhibit Hg concentrations in the upper part of this range ($1.5 \mu\text{g g}^{-1}$). Among tropical seabirds, feather Hg values were intermediate compared with other sternids at other locations, such as brown noddies (*Anous stolidus*) in Hawaii ($0.6 \mu\text{g g}^{-1}$; Burger et al., 2001) and bridled terns (*Onychoprion anaethetus*) ($1.4 \mu\text{g g}^{-1}$) and roseate terns (*Sterna dougallii*) in Puerto Rico ($2.3 \mu\text{g g}^{-1}$; Burger and Gochfeld, 1991). Low Hg contamination in sooty terns is consistent with their foraging ecology that largely depends on small epipelagic fish and invertebrates from surface waters (Ashmole, 1963a). Epipelagic prey exhibit lower Hg

concentrations than mesopelagic and benthic prey (Chouvelon et al., 2012; Monteiro and Furness, 1997; Ochoa-Acuña et al., 2002), mainly because Hg methylation occurs in mesopelagic waters (Blum et al., 2013; Bowman et al., 2020; Cossa et al., 2009; Wang et al., 2018).

Few studies ($n = 14$) have investigated long-term Hg trends in seabirds by using feathers as archives (Table S1). Most have focused on temperate (e.g., Appelquist et al., 1984; Thompson et al., 1993, 1992) and polar regions (e.g., Bond et al., 2015; Carravieri et al., 2016; Scheifler et al., 2005). Only two have focussed on subtropical regions, in the Azores (Monteiro and Furness, 1997) and islands of the Pacific (Vo et al., 2011). Monteiro and Furness (1997) measured a 1.1% increase in Hg contamination per year between the 1880s and the 1990s in epipelagic Cory's shearwaters (*Calonectris borealis*) that share similar habitat with sooty terns, albeit in the North Atlantic Ocean. This was a stronger annual increase than that of 0.37% that we found if considering simply a linear trend. Despite different temporal coverage between studies, it appears that Hg transfer to predators has increased more slowly in the South than in the North Atlantic Ocean. Similar spatial disparities in Hg contamination were observed in tunas (Médiéu et al., 2022), probably as a result of spatial differences in seawater Hg concentrations at the base of the food web, and inorganic Hg deposition among distinct oceanic regions. Mercury deposition could be higher in the subtropical than in the tropical Atlantic Ocean for two reasons. First, anthropogenic Hg was historically mainly emitted by industrialized countries from the Northern Hemisphere (Pacyna et al., 2006). Secondly, Hg is globally distributed by atmospheric circulation (Selin, 2009), which includes successive atmospheric circulation cells from the pole to the tropics, namely the Polar, the Ferrel and the Hadley Cells. As such, Hg emitted in Europe, for example, could be more easily deposited in the subtropical North Atlantic Ocean (i.e., one circulation cell away) than in the tropical South Atlantic Ocean (i.e., two circulation cells away).

Despite the temporal mismatch between feather Hg and stable isotopes (Bond, 2010), the trophic ecology of sooty terns influenced significantly their feather Hg contamination over time. Indeed, the best model explaining feather Hg contamination included both $\delta^{13}\text{C}$ and $\delta^{15}\text{N}$ values (Table 2), indicating that the temporal increase in feather Hg concentrations was associated with the strong decrease in $\delta^{13}\text{C}$ values and fluctuating $\delta^{15}\text{N}$ values observed over the past century (see Discussion above). However, the best model including both isotopic values explained only 14% of the total variation in Hg contamination, which suggests that other unknown factors (discussed below) also influenced long-term Hg contamination in sooty terns from Ascension Island. This is consistent with previous studies on other species (Bond et al., 2015; Carravieri et al., 2016; Vo et al., 2011). In addition, isotopic variations at the century scale are not simply or solely driven by changes in feeding habitat and trophic position, but likely by changes at the base of the food web, which are driven by several environmental and ecological processes (see Section 4.1). Therefore, our results suggest that the temporal trend in Hg transfer to predators in the South Atlantic Ocean was driven by trophic factors linked to ecosystem-wide changes, and other unknown factors. For instance, the increase in feather Hg concentrations observed from the 1920s to the 1970s was likely facilitated by growing Hg emissions during the Industrial Era with developing human activities, such as the Gold Rush, the burning of coal and intensifying manufacturing efforts to meet the military demands of World War II (Thompson et al., 1993). Between the 1970s and the 2000s, Hg concentrations appeared to stabilize. However, this phase included a very low number of available samples per year with high variability, implying large uncertainty in the generated models. Thus, whether Hg concentrations really remained stable between the 1970s and the 2000s is difficult to confirm. Mercury concentrations increased again from the 2000s to the present day, despite strong regulations restricting Hg emissions since the 1990s in the Northern Hemisphere and 2017 globally (Minamata Convention on Mercury). This, together with other recently detected increases (e.g., Bond et al., 2015; Carravieri et al., 2016; Tartu et al., 2022), raises concerns for potential consequences on

wildlife health.

4.3. Did Hg drive sooty tern population collapse on Ascension Island?

On Ascension Island, sooty terns suffered a 80% population collapse between the 1960s and the 1990s (Hughes et al., 2017). Reynolds et al. (2019) attributed this in part to a dietary shift from predominantly fish in the 1890s to the 1940s prior to the decline, to predominantly squid in the 1970s to the 2010s after it. With additional feather samples from the 2020s, our results revealed that isotopic niches were different between the two periods, with a significant difference in foraging habitat ($\delta^{13}\text{C}$) (agreeing with $\delta^{13}\text{C}$ values documented in Reynolds et al., 2019) but with an equivalent trophic position ($\delta^{15}\text{N}$) (Fig. 2B).

Mercury concentrations were 38.8% higher post-compared to pre-population collapse (Fig. 2A). These results are consistent with previous temporal comparisons, in which Hg concentrations have increased between historical and contemporary time periods in marine environments worldwide (Carravieri et al., 2016; Furness et al., 1995; Vo et al., 2011). During the period of population collapse, all Hg concentrations were relatively high with low variability, likely reflecting a generally high contamination in sooty terns. In comparison, there was more variability before and after the period of population collapse, probably because of slight differences in either diet or the proportions of different prey species constituting the diet. Given measured levels of Hg in sooty tern feathers – although elevated after the population collapse – it seems unlikely that Hg contamination drove the population decline of sooty terns on Ascension Island. Indeed, the extent of Hg contamination detected was below severe toxicity thresholds for seabird feathers (4–10 $\mu\text{g g}^{-1}$; Ackerman et al., 2016; Chastel et al., 2022). Investigating contamination by other pollutants (such as pesticides or plastics) would undoubtedly allow further insights into the risks and demographic stressors for this population, but our results reinforce the conclusions of Reynolds et al. (2019), that overharvesting of large predatory fish and climate change likely negatively impacted sooty tern trophic ecology, thereby resulting in elevated Hg contamination.

4.4. Influence of climate change and fisheries on tropical Hg contamination

Reynolds et al. (2019) highlighted the importance of increasing sea surface temperatures (SST) and tuna extraction by fisheries in explaining long-term changes in the trophic ecology of sooty terns breeding on Ascension Island. Sooty terns are heavily reliant on large schools of surface-swimming tunas, such as yellowfin (*Thunnus albacares*) and skipjack (*Katsuwonus pelamis*), to drive their common prey to the ocean surface, where many tropical seabirds forage in so-called « facilitated foraging » (Ashmole, 1963a; Au and Pitman, 1986; Ballance and Pitman, 1999; Maxwell and Morgan, 2013). Sooty terns are therefore susceptible to any over-exploitation and major declines in these associated species (Cullis-Suzuki and Pauly, 2010; Juan-Jordá et al., 2011). Nonetheless, under climate change, and specifically with changes in temperatures and salinity, global abundances of tunas are predicted to increase in tropical waters (Erauskin-Extramiana et al., 2019). Specifically, Ascension Island is predicted to become more suitable for several tuna species, including sooty tern associates (Townhill et al., 2021). Climate change and fishing pressure are therefore likely to impact Hg contamination in sooty terns, and hence in tropical marine ecosystems, even though the direction and the extent of these impacts are difficult to predict precisely.

Since seabird Hg contamination is heavily associated with their foraging ecology, climate change and fishing pressure also have indirect effects on Hg contamination through dietary changes (prey switching), species' interactions and transfer through marine food webs (biotic factors). For example, MeHg concentrations increased in marine fish as a result of dietary shifts initiated by overfishing and with increasing SST (Schartup et al., 2019). Other environmental factors can also influence

seabird Hg contamination, such as Hg transport, deposition, uptake and methylation rates in the ocean (Krabbenhoft and Sunderland, 2013). Mercury is mainly deposited in oceans by atmospheric fallouts (Eagles-Smith et al., 2018). Although Ascension Island is isolated, with its nearest neighbour, St Helena, located more than 1300 km away, it is highly unlikely that Hg contamination results from local anthropogenic sources. As a volcanic island, Hg contamination might alternatively result from local geological activities, but there is no record of volcanic activity of Ascension Island over the last 500–1000 years (Preece et al., 2018). Instead, Hg contamination in sooty terns likely results from global Hg transport. In the ocean, sources of MeHg are multiple: methylation can occur in the sediments of continental shelves (Hammerschmidt and Fitzgerald, 2006) and estuaries (Heyes et al., 2006), within the water column (Cossa, 2013; Hammerschmidt and Bowman, 2012) and at deep-ocean hydrothermal vents (Bowman et al., 2016, 2015). Mercury methylated through these processes can then be widely distributed by ocean currents, both spatially (global ocean circulation) and vertically (vertical mixing and upwellings) (Mason et al., 2012). Climate change will likely influence all of these processes and could ultimately influence sooty tern contamination on different temporal and spatial scales. Methylation rate and bioavailability of Hg are also affected by other processes such as acidification, eutrophication and/or deoxygenation (Clayden et al., 2013; Gong et al., 2021; Jardine et al., 2013; Zhang et al., 2021). For instance, oxygen-depleted zones (i.e., « dead zones ») are increasing with climate change (Breitburg et al., 2018; Watson, 2016), both in number and size. Mercury methylation is substantially enhanced in low-oxygen zones in the ocean, that at low latitudes (i.e., tropics) are the most vulnerable to further deoxygenation (Gruber, 2011). Tropical oceans should thus be a priority for further studies of Hg contamination, especially in the context of climate change. Further research should focus on Hg stable isotopes to disentangle the different environmental and ecological factors involved, by identifying Hg sources and exploring the associated biogeochemical and trophic processes in the different compartments of tropical marine ecosystems (Renedo et al., 2020).

Mercury contamination of marine environments results from long-term processes, influenced by Hg transport, methylation and bioavailability, as well as from ecological interactions, both globally and locally. Undoubtedly, there is a time lag of years, decades, or even centuries between Hg emissions and deposition in the ocean and its resulting contamination of marine food webs (Driscoll et al., 2013; Foster et al., 2019; Sunderland and Mason, 2007, UN Environment, 2019). Long-term monitoring of Hg is therefore crucial to: (i) assess the ongoing health status of tropical marine ecosystems and its variability over time, and (ii) ultimately minimize the risks of Hg exposure to wildlife and human populations alike, the latter relying heavily on marine food resources worldwide.

Credit author statement

Fanny Cusset: Conceptualization, Methodology, Software, Formal analyses, Investigation, Data curation, Visualization, Writing – Original draft, review and editing, Project administration; **S. James Reynolds:** Conceptualization, Resources, Writing – Reviewing and editing; **Alice Carravieri:** Formal analyses, Investigation, Visualization, Writing – Reviewing and editing; **David Amouroux:** Writing – Reviewing and editing; **Océane Asensio:** Investigation, Writing – Reviewing and editing; **Roger C. Dickey:** Resources, Writing – Reviewing and editing; **Jérôme Fort:** Supervision, Investigation, Validation, Writing – Reviewing and editing; **B. John Hughes:** Resources, Writing – Reviewing and editing; **Vitor H. Paiva:** Conceptualization, Resources, Writing – Reviewing and editing; **Jaime A. Ramos:** Conceptualization, Resources, Writing – Reviewing and editing; **Laura Shearer:** Resources, Writing – Reviewing and editing; **Emmanuel Tessier:** Investigation, Writing – Reviewing and editing; **Colin P. Wearn:** Resources, Writing – Reviewing and editing; **Yves Cherel:** Supervision, Investigation,

Validation, Writing – Reviewing and editing; **Paco Bustamante:** Conceptualization, Supervision, Investigation, Validation, Funding acquisition, Writing – Reviewing and editing.

Declaration of competing interest

The authors declare that they have no known competing financial interests or personal relationships that could have appeared to influence the work reported in this paper.

Data availability

Data will be made available on request.

Acknowledgments

First, we thank all people involved in the original study of Reynolds et al. (2019), for bird sampling, both in museums and in the field. Funding for sample collections was provided by SJR. We are thankful to the Ascension Island Government for granting research permits to sample live birds in the 2000s, the 2010s and the 2020s. The authors are grateful to Carine Churlaud and Maud Brault-Favrou from the Analyses Élémentaires platform (LIENSs) for their support during Hg analysis and to Gaël Guillou from the Analyses Isotopiques platform (LIENSs) for running the stable isotope analyses. Special thanks are due to Sabrina Tartu and Céline Albert for statistical guidance during data exploration. We are grateful to Lucie Machin for the sooty tern drawing on the graphical abstract. Thanks are due to the CPER (Contrat de Projet Etat-Région) and the FEDER (Fonds Européen de Développement Régional) for funding the AMA and IRMS of LIENSs laboratory. The Institut Universitaire de France (IUF) is acknowledged for its support to PB as a Senior Member. This work benefitted from the French GDR “Aquatic Ecotoxicology” framework, that aims to foster stimulating scientific discussions and collaborations for more integrative approaches.

Appendix A. Supplementary data

Supplementary data to accompany this article can be found online at <https://doi.org/10.1016/j.envpol.2023.121187>.

References

Ackerman, J.T., Eagles-Smith, C.A., Herzog, M.P., Hartman, C.A., Peterson, S.H., Evers, D.C., Jackson, A.K., Elliott, J.E., Vander Pol, S.S., Bryan, C.E., 2016. Avian mercury exposure and toxicological risk across western North America: A synthesis. *Sci. Total Environ.* 568, 749–769. <https://doi.org/10.1016/j.scitotenv.2016.03.071>.

Albert, C., Renedo, M., Bustamante, P., Fort, J., 2019. Using blood and feathers to investigate large-scale Hg contamination in Arctic seabirds: A review. *Environ. Res.* 177, 108588. <https://doi.org/10.1016/j.envres.2019.108588>.

Appelquist, H., Asbirk, S., Drabæk, I., 1984. Mercury monitoring: Mercury stability in bird feathers. *Mar. Pollut. Bull.* 15, 22–24. [https://doi.org/10.1016/0025-326X\(84\)90419-3](https://doi.org/10.1016/0025-326X(84)90419-3).

Ashmole, N.P., 1963a. The biology of the Wideawake or sooty tern *Sterna fuscata* on Ascension Island. *Ibis* 103b, 297–351. <https://doi.org/10.1111/j.1474-919X.1963.tb06757.x>.

Ashmole, N.P., 1963b. Molt and breeding in populations of the sooty tern *Sterna fuscata*. *Postilla* 76, 1–18.

Au, D.W.K., Pitman, R.L., 1986. Seabird interactions with dolphins and tuna in the eastern tropical Pacific. *Condor* 88, 304–317. <https://doi.org/10.2307/1368877>.

Ballance, L.T. & Pitman, R.L. 1999. Foraging ecology of tropical seabirds. In: Adams, N.J. & Slotow, R.H. (eds) Proc. 22 Int. Ornithol. Congr., Durban: 2057–2071. Johannesburg: BirdLife South Africa.

Bartoni, 2022. MuMIn: Multi-Model Inference. R Package Version 1.46.0. <https://CRAN.R-project.org/package=MuMIn>.

Blum, J.D., Popp, B.N., Drazen, J.C., Anela Choy, C., Johnson, M.W., 2013. Methylmercury production below the mixed layer in the North Pacific ocean. *Nat. Geosci.* 6, 879–884. <https://doi.org/10.1038/ngeo1918>.

Bond, A.L., 2010. Relationships between stable isotopes and metal contaminants in feathers are spurious and biologically uninformative. *Environ. Pollut.* 158, 1182–1184. <https://doi.org/10.1016/j.envpol.2010.01.004>.

Bond, A.L., Diamond, A.W., 2009. Total and methyl mercury concentrations in seabird feathers and eggs. *Arch. Environ. Contam. Toxicol.* 56, 286–291. <https://doi.org/10.1007/s00244-008-9185-7>.

Bond, A.L., Hobson, K.A., Branfireun, B.A., 2015. Rapidly increasing methyl mercury in endangered ivory gull (*Pagophila eburnea*) feathers over a 130 year record. *Proc. R. Soc. B* 282, 20150032. <https://doi.org/10.1098/rspb.2015.0032>.

Bowman, K.L., Hammerschmidt, C.R., Lamborg, C.H., Swarr, G., 2015. Mercury in the North Atlantic Ocean: The U.S. GEOTRACES zonal and meridional sections, Deep Sea Research Part II: Topical Studies in Oceanography, 116, 251–261. <https://doi.org/10.1016/j.dsr2.2014.07.004>.

Bowman, K.L., Hammerschmidt, C.R., Lamborg, C.H., Swarr, G.J., Agather, A.M., 2016. Distribution of mercury species across a zonal section of the eastern tropical South Pacific Ocean (U.S. GEOTRACES GP16). *Mar. Chem.* 186, 156–166. <https://doi.org/10.1016/j.marchem.2016.09.005>.

Bowman, K.L., Lamborg, C.H., Agather, A.M., 2020. A global perspective on mercury cycling in the ocean. *Sci. Total Environ.* 710, 136166. <https://doi.org/10.1016/j.scitotenv.2019.136166>.

Breitbart, D., Levin, L.A., Oshlies, A., Grégoire, M., Chavez, F.P., Conley, D.J., Garçon, V., Gilbert, D., Gutiérrez, D., Isensee, K., Jacinto, G.S., Limburg, K.E., Montes, I., Naqvi, S.W.A., Pitcher, G.C., Rabalais, N.N., Roman, M.R., Rose, K.A., Seibel, B.A., Telszewski, M., Yasuhara, M., Zhang, J., 2018. Declining oxygen in the global ocean and coastal waters. *Science* 359, eaam7240. <https://doi.org/10.1126/science.aam7240>.

Burger, J., Gochfeld, M., 2004. Marine birds as sentinels of environmental pollution. *Environ. Health* 1, 263–274. <https://doi.org/10.1007/s10393-004-0096-4>.

Burger, J., Gochfeld, M., 1991. Lead, mercury, and cadmium in feathers of tropical terns in Puerto Rico and Australia. *Arch. Environ. Contam. Toxicol.* 21, 311–315. <https://doi.org/10.1007/BF01055351>.

Burger, J., Schreiber, E.A.E., Gochfeld, M., 1992. Lead, cadmium, selenium and mercury in seabird feathers from the tropical mid Pacific. *Environ. Toxicol. Chem.* 11, 815–822. <https://doi.org/10.1002/etc.5620110610>.

Burger, J., Shukla, T., Dixon, C., Shukla, S., McMahon, M.J., Ramos, R., Gochfeld, M., 2001. Metals in feathers of sooty tern, white tern, gray-backed tern, and brown noddy from Islands in the North Pacific. *Environ. Monit. Assess.* 71, 71–89. <https://doi.org/10.1023/A:1011695829296>.

Burnham, K.P., Anderson, D.R., 2002. *Model Selection and Multimodel Inference: A Practical Information Theoretic Approach*, second ed. Springer US.

Carravieri, A., Bustamante, P., Churlaud, C., Fromant, A., Cherel, Y., 2014. Moulting patterns drive within individual variations of stable isotopes and mercury in seabird body feathers: Implications for monitoring of the marine environment. *Mar. Biol.* 161, 963–968. <https://doi.org/10.1007/s00227-014-2394-x>.

Carravieri, A., Cherel, Y., Jaeger, A., Churlaud, C., Bustamante, P., 2016. Penguins as bioindicators of mercury contamination in the southern Indian Ocean: Geographical and temporal trends. *Environ. Pollut.* 213, 195–205. <https://doi.org/10.1016/j.envpol.2016.02.010>.

Chastel, O., Fort, J., Ackerman, J.T., Albert, C., Angelier, F., Basu, N., Blévin, P., Brault-Favrou, M., Bustnes, J.O., Bustamante, P., Danielsen, J., Descamps, S., Dietz, R., Erikstad, K.E., Eulaers, I., Ezhov, A., Fleishman, A.B., Gabrielsen, G.W., Gavrilo, M., Gilchrist, G., Gilg, O., Gíslason, S., Golubova, E., Goutte, A., Grémillet, D., Hallgrímsson, G.T., Hansen, E.S., Hanssen, S.A., Hatch, S., Huffeldt, N.P., Jakubas, D., Jónsson, J.E., Kitaysky, A.S., Kolbeinsson, Y., Krasnov, Y., Letcher, R.J., Linnebjerg, J.F., Mallory, M., Merkel, F.R., Moe, B., Montevecchi, W.J., Mosbech, A., Olsen, B., Orben, R.A., Provencher, J.F., Ragnarsdóttir, S.B., Reiertsen, T.K., Rojck, N., Romano, M., Søndergaard, J., Strøm, H., Takahashi, A., Tartu, S., Thórarinnsson, T.L., Thiebot, J.-B., Will, A.P., Wilson, S., Wojczulanis-Jakubas, K., Yannic, G., 2022. Mercury contamination and potential health risks to Arctic seabirds and shorebirds. *Sci. Total Environ.* 844:156944. <https://doi.org/10.1016/j.scitotenv.2022.156944>.

Cherel, Y., Barbraud, C., Lahournat, M., Jaeger, A., Jaquet, S., Wanless, R.M., Phillips, R.A., Thompson, D.R., Bustamante, P., 2018. Accumulate or eliminate? Seasonal mercury dynamics in albatrosses, the most contaminated family of birds. *Environ. Pollut.* 241, 124–135. <https://doi.org/10.1016/j.envpol.2018.05.048>.

Cherel, Y., Conman, M., Jaeger, A., Richard, P., 2014. Seabird year-round and historical feeding ecology: blood and feather $\delta^{13}\text{C}$ and $\delta^{15}\text{N}$ values document foraging plasticity of small sympatric petrels. *Mar. Ecol. Prog. Ser.* 505, 267–280. <https://doi.org/10.3354/meps10795>.

Chouvelon, T., Spitz, J., Caurant, F., Méndez Fernandez, P., Autier, J., Lassus Débat, A., Chappuis, A., Bustamante, P., 2012. Enhanced bioaccumulation of mercury in deep-sea fauna from the Bay of Biscay (north-east Atlantic) in relation to trophic positions identified by analysis of carbon and nitrogen stable isotopes. *Deep-Sea Res. Part A Oceanogr. Res. Pap.* 65, 113–124. <https://doi.org/10.1016/j.dsr.2012.02.010>.

Choy, E.S., Blight, L.K., Elliott, J.E., Hobson, K.A., Zanuttig, M., Elliott, K.H., 2022. Stable mercury trends support a long-term diet shift away from marine foraging in Salish Sea glaucous-winged gulls over the last century. *Environ. Sci. Technol.* 56, 12097–12105. <https://doi.org/10.1021/acs.est.1c03760>.

Cifuentes, L.A., Sharp, J.H., Fogel, M.L., 1988. Stable carbon and nitrogen isotope biogeochemistry in the Delaware estuary. *Limnol. Oceanogr.* 33, 1102–1115. <https://doi.org/10.4319/lo.1988.33.5.1102>.

Clayden, M.G., Kidd, K.A., Wyn, B., Kirk, J.L., Muir, D.C.G., O’Driscoll, N.J., 2013. Mercury biomagnification through food webs is affected by physical and chemical characteristics of lakes. *Environ. Sci. Technol.* 47, 12047–12053. <https://doi.org/10.1021/es4022975>.

Cossa, D., 2013. Methylmercury manufacture. *Nat. Geosci.* 6, 810–811. <https://doi.org/10.1038/ngeo1967>.

- Cossa, D., Avery, B., Pirrone, N., 2009. The origin of methylmercury in open Mediterranean waters. *Limnol. Oceanogr.* 54, 837–844. <https://doi.org/10.4319/lo.2009.54.3.0837>.
- Crewther, W.G., Fraser, R.D., Lennox, F.G., Lindley, H., 1965. The chemistry of keratins. *Adv. Protein Chem.* 20, 191–346. [https://doi.org/10.1016/s0065-3233\(08\)60390-3](https://doi.org/10.1016/s0065-3233(08)60390-3).
- Cullis Suzuki, S., Pauly, D., 2010. Failing the high seas: A global evaluation of regional fisheries management organizations. *Mar. Policy* 34, 1036–1042. <https://doi.org/10.1016/j.marpol.2010.03.002>.
- DeNiro, M.J., Epstein, S., 1978. Influence of diet on the distribution of carbon isotopes in animals. *Geochem. Cosmochim. Acta* 42, 495–506. [https://doi.org/10.1016/0016-7037\(78\)90199-0](https://doi.org/10.1016/0016-7037(78)90199-0).
- Driscoll, C.T., Mason, R.P., Chan, H.M., Jacob, D.J., Pirrone, N., 2013. Mercury as a global pollutant: Sources, pathways, and effects. *Environ. Sci. Technol.* 47, 4967–4983. <https://doi.org/10.1021/es305071v>.
- Eagles Smith, C.A., Silbergeld, E.K., Basu, N., Bustamante, P., Diaz Barriga, F., Hopkins, W.A., Kidd, K.A., Nyland, J.F., 2018. Modulators of mercury risk to wildlife and humans in the context of rapid global change. *Ambio* 47, 170–197. <https://doi.org/10.1007/s13280-017-1011-x>.
- Eide, M., Olsen, A., Ninnemann, U.S., Eldevik, T., 2017. A global estimate of the full oceanic ^{13}C Suess effect since the preindustrial. *Global Biogeochem. Cycles* 31, 492–514. <https://doi.org/10.1002/2016GB005472>.
- Erauskin Extramiana, M., Arrizabalaga, H., Hobday, A.J., Cabré, A., Ibaibarriaga, L., Arregui, I., Murua, H., Chust, G., 2019. Large-scale distribution of tuna species in a warming ocean. *Glob. Change Biol.* 25, 2043–2060. <https://doi.org/10.1111/gcb.14630>.
- Fort, J., Grémillet, D., Traineau, G., Amélineau, F., Bustamante, P., 2016. Does temporal variation of mercury levels in Arctic seabirds reflect changes in global environmental contamination, or a modification of Arctic marine food web functioning? *Environ. Pollut.* 211, 382–388. <https://doi.org/10.1016/j.envpol.2015.12.061>.
- Foster, K.L., Braune, B.M., Gaston, A.J., Mallory, M.L., 2019. Climate influence on mercury in Arctic seabirds. *Sci. Total Environ.* 693, 133569. <https://doi.org/10.1016/j.scitotenv.2019.07.375>.
- France, R., 1995. Carbon-13 enrichment in benthic compared to planktonic algae: Foodweb implications. *Mar. Ecol. Prog. Ser.* 124, 307–312. <https://doi.org/10.3354/meps124307>.
- Furness, R.W., 1993. Birds as monitors of pollutants. In: Furness, R.W., Greenwood, J.J. D. (Eds.), *Birds as Monitors of Environmental Change*. Springer Netherlands, Dordrecht, pp. 86–143. https://doi.org/10.1007/978-94-015-1322-7_3.
- Furness, R.W., Camphuysen, K. (C. J.), 1997. Seabirds as monitors of the marine environment. *ICES J. Mar. Sci.* 54, 726–737. <https://doi.org/10.1006/jmsc.1997.0243>.
- Furness, R.W., Muirhead, S.J., Woodburn, M., 1986. Using bird feathers to measure mercury in the environment: Relationships between mercury content and moult. *Mar. Pollut. Bull.* 17, 27–30. [https://doi.org/10.1016/0025-326x\(86\)90801-5](https://doi.org/10.1016/0025-326x(86)90801-5).
- Furness, R.W., Thompson, D.R., Becker, P.H., 1995. Spatial and temporal variation in mercury contamination of seabirds in the North Sea. *Helgol. Meeresunters.* 49, 605–615. <https://doi.org/10.1007/BF02368386>.
- Goering, J., Alexander, V., Haubenstock, N., 1990. Seasonal variability of stable carbon and nitrogen isotope ratios of organisms in a North Pacific Bay. *Estuar. Coast Shelf Sci.* 30, 239–260. [https://doi.org/10.1016/0272-7714\(90\)90050-2](https://doi.org/10.1016/0272-7714(90)90050-2).
- Gong, H., Li, C., Zhou, Y., 2021. Emerging global ocean deoxygenation across the 21st Century. *Geophys. Res. Lett.* 48, e2021GL095370. <https://doi.org/10.1029/2021GL095370>.
- Gruber, N., 2011. Warming up, turning sour, losing breath: Ocean biogeochemistry under global change. *Philos. Trans. R. Soc. Math. Phys. Eng. Sci.* 369, 1980–1996. <https://doi.org/10.1098/rsta.2011.0003>.
- Hammerschmidt, C.R., Bowman, K.L., 2012. Vertical methylmercury distribution in the subtropical North Pacific Ocean. *Mar. Chem.* 132–133, 77–82. <https://doi.org/10.1016/j.marchem.2012.02.005>.
- Hammerschmidt, C.R., Fitzgerald, W.F., 2006. Methylmercury cycling in sediments on the continental shelf of southern New England. *Geochem. Cosmochim. Acta* 70, 918–930. <https://doi.org/10.1016/j.gca.2005.10.020>.
- Heyes, A., Mason, R.P., Kim, E.-H., Sunderland, E., 2006. Mercury methylation in estuaries: Insights from using measuring rates using stable mercury isotopes. *Mar. Chem.*, 8th International Estuarine Biogeochemistry Symposium - Introduction 102, 134–147. <https://doi.org/10.1016/j.marchem.2005.09.018>.
- Hilton, G.M., Thompson, D.R., Sagar, P.M., Cuthbert, R.J., Cherel, Y., Bury, S.J., 2006. A stable isotopic investigation into the causes of decline in a sub-Antarctic predator, the rockhopper penguin *Eudyptes chrysocome*. *Global Change Biol.* 12, 611–625. <https://doi.org/10.1111/j.1365-2486.2006.01130.x>.
- Hirons, A.C., Schell, D.M., Finney, B.P., 2001. Temporal records of $\delta^{13}\text{C}$ and $\delta^{15}\text{N}$ in North Pacific pinnipeds: Inferences regarding environmental change and diet. *Oecologia* 129, 591–601. <https://doi.org/10.1007/s004420100756>.
- Hobson, K.A., 1999. Tracing origins and migration of wildlife using stable isotopes: A review. *Oecologia* 120, 314–326. <https://doi.org/10.1007/s004420050865>.
- Hogstad, O., Nygård, T., Gättschmann, P., Lierhagen, S., Thingstad, P.G., 2003. Bird skins in museum collections: Are they suitable as indicators of environmental metal load after conservation procedures? *Environ. Monit. Assess.* 87, 47–56. <https://doi.org/10.1023/A:1024485829174>.
- Honda, K., Nasu, T., Tatsukawa, R., 1986. Seasonal changes in mercury accumulation in the black eared kite, *Milvus migrans lineatus*. *Environ. Pollut. Ser. A Ecol. Biol.* 42, 325–334. [https://doi.org/10.1016/0143-1471\(86\)90016-4](https://doi.org/10.1016/0143-1471(86)90016-4).
- Horowitz, H.M., Jacob, D.J., Zhang, Y., Dibble, T.S., Slenr, F., Amos, H.M., Schmidt, J. A., Corbett, E.S., Marais, E.A., Sunderland, E.M., 2017. A new mechanism for atmospheric mercury redox chemistry: Implications for the global mercury budget. *Atmos. Chem. Phys.* 17, 6353–6371. <https://doi.org/10.5194/acp-17-6353-2017>.
- Hughes, B.J., Martin, G.R., Giles, A.D., Reynolds, S.J., 2017. Long-term population trends of Sooty Terns *Onychoprion fuscatus*: Implications for conservation status. *Popul. Ecol.* 59, 213–224. <https://doi.org/10.1007/s10144-017-0588-z>.
- Hughes, B.J., Martin, G.R., Reynolds, S.J., 2012. Estimate of Sooty Tern *Onychoprion fuscatus* population size following cat eradication on Ascension Island, central Atlantic. *African Bird Club. Bulletin* 19 (2), 166–171.
- Jaeger, A., Blanchard, P., Richard, P., Cherel, Y., 2009. Using carbon and nitrogen isotopic values of body feathers to infer inter- and intra-individual variations of seabird feeding ecology during moult. *Mar. Biol.* 156, 1233–1240. <https://doi.org/10.1007/s00227-009-1165-6>.
- Jaeger, A., Cherel, Y., 2011. Isotopic investigation of contemporary and historic changes in penguin trophic niches and carrying capacity of the Southern Indian Ocean. *PLoS One* 6(2), e16484. <https://doi.org/10.1371/journal.pone.0016484>.
- Jaquemet, S., Potier, M., Cherel, Y., Kojadinovic, J., Bustamante, P., Richard, P., Catry, T., Ramos, J.A., Le Corre, M., 2008. Comparative foraging ecology and ecological niche of a superabundant tropical seabird: The sooty tern *Sterna fuscata* in the southwest Indian Ocean. *Mar. Biol.* 155, 555–520. <https://doi.org/10.1007/s00227-008-1049-1>.
- Jardine, T.D., Kidd, K.A., O' Driscoll, N., 2013. Food web analysis reveals effects of pH on mercury bioaccumulation at multiple trophic levels in streams. *Aquat. Toxicol.* 132–133, 46–52. <https://doi.org/10.1016/j.aquatox.2013.01.013>.
- Jarek, S., 2012. mvnormtest: Normality test for multivariate variables. R package version 0.1-9. <https://CRAN.R-project.org/package=mvnormtest>.
- Johnson, J.B., Omland, K.S., 2004. Model selection in ecology and evolution. *Trends Ecol. Evol.* 19, 101–108. <https://doi.org/10.1016/j.tree.2003.10.013>.
- Juan-Jordá, M.J., Mosqueira, I., Cooper, A.B., Freire, J., Dulvy, N.K., 2011. Global population trajectories of tunas and their relatives. *Proc. Natl. Acad. Sci. USA* 108, 20650–20655. <https://doi.org/10.1073/pnas.1107743108>.
- Kassambara, A., _rstatix: Pipe-Friendly Framework for Basic Statistical Tests. R package version 0.7.1. <https://CRAN.R-project.org/package=rstatix>.
- Keeling, C.D., 1979. The Suess effect: ^{13}C Carbon- ^{14}C Carbon interrelations. *Environ. Int.* 2, 229–300. [https://doi.org/10.1016/0160-4120\(79\)90005-9](https://doi.org/10.1016/0160-4120(79)90005-9).
- Kelly, J.F., 2000. Stable isotopes of carbon and nitrogen in the study of avian and mammalian trophic ecology. *Can. J. Zool.* 78, 1–27. <https://doi.org/10.1139/z99-165>.
- Kojadinovic, J., Bustamante, P., Churlaud, C., Cosson, R.P., Le Corre, M., 2007. Mercury in seabird feathers: Insight on dietary habits and evidence for exposure levels in the western Indian Ocean. *Sci. Total Environ.* 384, 194–204. <https://doi.org/10.1016/j.scitotenv.2007.05.018>.
- Körtzinger, A., Quay, P.D., Sonnerup, R.E., 2003. Relationship between anthropogenic CO_2 and the ^{13}C Suess Effect in the North Atlantic Ocean. *Global Biogeochem. Cycles* 17(1). <https://doi.org/10.1029/2001GB001427>, 1005.
- Krabbenhoft, D.P., Sunderland, E.M., 2013. Global change and mercury. *Science* 341, 1457–1458. <https://doi.org/10.1126/science.1242838>.
- Lamborg, C.H., Hammerschmidt, C.R., Bowman, K.L., Swarr, G.J., Munson, K.M., Ohnenu, D.C., Lam, P.J., Heimbürger, L. E., Rijkenberg, M.J.A., Saito, M.A., 2014. A global ocean inventory of anthropogenic mercury based on water column measurements. *Nature* 512, 65–68. <https://doi.org/10.1038/nature13563>.
- Lorrain, A., Pethybridge, H., Cassar, N., Receveur, A., Allain, V., Bodin, N., Bopp, L., Choy, C.A., Duffy, L., Fry, B., Goni, N., Graham, B.S., Hobday, A.J., Logan, J.M., Ménard, F., Menkes, C.E., Olson, R.J., Pagendam, D.E., Point, D., Revill, A.T., Somes, C.J., Young, J.W., 2020. Trends in tuna carbon isotopes suggest global changes in pelagic phytoplankton communities. *Global Change Biol.* 26, 458–470. <https://doi.org/10.1111/gcb.14858>.
- Mason, R.P., Choi, A.L., Fitzgerald, W.F., Hammerschmidt, C.R., Lamborg, C.H., Soerensen, A.L., Sunderland, E.M., 2012. Mercury biogeochemical cycling in the ocean and policy implications. *Environ. Res.* 119, 101–117. <https://doi.org/10.1016/j.envres.2012.03.013>.
- Maxwell, S.M., Morgan, L.E., 2013. Foraging of seabirds on pelagic fishes: Implications for management of pelagic marine protected areas. *Mar. Ecol. Prog. Ser.* 481, 289–303. <https://doi.org/10.3354/meps10255>.
- McMahon, K.W., Hamady, L.L., Thorrold, S.R., 2013. Ocean ecogeochemistry: A review. *Oceanogr. Mar. Biol. Annu. Rev.* 51, 327–374.
- McMahon, K.W., Newsome, S.D., 2019. Chapter 7 - amino acid isotope analysis: a new frontier in studies of animal migration and foraging ecology. In: Hobson, K.A., Wassenaar, L.I. (Eds.), *Tracking Animal Migration with Stable Isotopes*, second ed. Academic Press, pp. 173–190. <https://doi.org/10.1016/B978-0-12-814723-8.00007-6>.
- Médiéu, A., Point, D., Itai, T., Angot, H., Buchanan, P.J., Allain, V., Fuller, L., Griffiths, S., Gillikin, D.P., Sonke, J.E., Heimbürger-Boavida, L. E., Desgranges, M. M., Menkes, C. E., Madigan, D.J., Brosset, P., Gauthier, O., Tagliabue, A., Bopp, L., Verheyden, A., Lorrain, A., 2022. Evidence that Pacific tuna mercury levels are driven by marine methylmercury production and anthropogenic inputs. *Proc. Natl. Acad. Sci. USA* 119, e2113032119. <https://doi.org/10.1073/pnas.2113032119>.
- Monteiro, L.R., Furness, R.W., 1997. Accelerated increase in mercury contamination in north Atlantic mesopelagic food chains as indicated by time series of seabird feathers. *Environ. Toxicol. Chem.* 16, 2489–2493. <https://doi.org/10.1002/etc.5620161208>.
- Ochoa Acuña, H., Sepúlveda, M.S., Gross, T.S., 2002. Mercury in feathers from Chilean birds: Influence of location, feeding strategy, and taxonomic affiliation. *Mar. Pollut. Bull.* 44, 340–345. [https://doi.org/10.1016/S0025-326X\(01\)00280-6](https://doi.org/10.1016/S0025-326X(01)00280-6).
- O'Reilly, C.M., Alin, S.R., Plismier, P. D., Cohen, A.S., McKee, B.A., 2003. Climate change decreases aquatic ecosystem productivity of Lake Tanganyika, Africa. *Nature* 424, 766–768. <https://doi.org/10.1038/nature01833>.
- Ostrom, N.E., Macko, S.A., Deibel, D., Thompson, R.J., 1997. Seasonal variation in the stable carbon and nitrogen isotope biogeochemistry of a coastal cold ocean

- environment. *Geochem. Cosmochim. Acta* 61(14), 2929–2942. [https://doi.org/10.1016/S0016-7037\(97\)00131-2](https://doi.org/10.1016/S0016-7037(97)00131-2).
- Pacyna, E.G., Pacyna, J.M., Steenhuisen, F., Wilson, S., 2006. Global anthropogenic mercury emission inventory for 2000. *Atmos. Environ.* 40, 4048–4063. <https://doi.org/10.1016/j.atmosenv.2006.03.041>.
- Piatt, J.F., Harding, A.M.A., Shultz, M., Speckman, S.G., Pelt, T.I. van, Drew, G.S., Kettle, A.B., 2007. Seabirds as indicators of marine food supplies: Cairns revisited. *Mar. Ecol. Prog. Ser.* 352, 221–234. <https://doi.org/10.3354/meps07078>.
- Pinheiro, J., Bates, D., DebRoy, S., Sarkar, D., R Core Team, 2020. *Nlme: Linear and Nonlinear Mixed Effects Models*. R Package Version 3, pp. 1–149. <https://CRAN.R-project.org/package=nlme>.
- Preece, K., Mark, D.F., Barclay, J., Cohen, B.E., Chamberlain, K.J., Jowitz, C., Vye-Brown, C., Brown, R.J., Hamilton, S., 2018. Bridging the gap: $^{40}\text{Ar}/^{39}\text{Ar}$ dating of volcanic eruptions from the Age of Discovery. *Geology* 46, 1035–1038. <https://doi.org/10.1130/G45415.1>.
- Quillfeldt, P., Masello, J.F., McGill, R.A., Adams, M., Furness, R.W., 2010. Moving polewards in winter: A recent change in the migratory strategy of a pelagic seabird? *Front. Zool.* 7, 15. <https://doi.org/10.1186/1742-9994-7-15>.
- R Core Team, 2020. *R: A Language and Environment for Statistical Computing*. R Foundation for Statistical Computing, Vienna, Austria. URL: <https://www.R-project.org/>.
- Ramos, J.A., Tavares, P.C., 2010. Mercury levels in the feathers of breeding seabirds in the Seychelles, western Indian Ocean, from 1996 to 2005. *Emu - Austral Ornithol.* 110, 87–91. <https://doi.org/10.1071/MU09055>.
- Rau, G.H., Takahashi, T., Des Marais, D.J., Repeta, D.J., Martin, J.H., 1992. The relationship between $\delta^{13}\text{C}$ of organic matter and $[\text{CO}_2(\text{aq})]$ in ocean surface water: Data from a JGOFS site in the northeast Atlantic Ocean and a model. *Geochem. Cosmochim. Acta* 56, 1413–1419. [https://doi.org/10.1016/0016-7037\(92\)90073-R](https://doi.org/10.1016/0016-7037(92)90073-R).
- Redfern, C.P.F., Clark, J.A., 2001. *British Trust for Ornithology*. In: *Ringers' Manual*. British Trust for Ornithology.
- Renedo, M., Amouroux, D., Albert, C., Bérail, S., Brathen, V.S., Gavrilo, M., Grénillet, D., Helgason, H.H., Jakubas, D., Mosbech, A., Strøm, H., Tessier, E., Wojczulanis Jakubas, K., Bustamante, P., Fort, J., 2020. Contrasting spatial and seasonal trends of methylmercury exposure pathways of Arctic seabirds: Combination of large scale tracking and stable isotopic approaches. *Environ. Sci. Technol.* 54, 13619–13629. <https://doi.org/10.1021/acs.est.1c07633>.
- Renedo, M., Amouroux, D., Pedrero, Z., Bustamante, P., Cherel, Y., 2018. Identification of sources and bioaccumulation pathways of MeHg in subantarctic penguins: A stable isotopic investigation. *Sci. Rep.* 8, 8865. <https://doi.org/10.1038/s41598-018-27079-9>.
- Renedo, M., Bustamante, P., Tessier, E., Pedrero, Z., Cherel, Y., Amouroux, D., 2017. Assessment of mercury speciation in feathers using species specific isotope dilution analysis. *Talanta* 174, 100–110. <https://doi.org/10.1016/j.talanta.2017.05.081>.
- Reynolds, S.J., Hughes, B.J., Wearn, C.P., Dickey, R.C., Brown, J., Weber, N.L., Weber, S. B., Paiva, V.H., Ramos, J.A., 2019. Long term dietary shift and population decline of a pelagic seabird—a health check on the tropical Atlantic? *Global Change Biol.* 25, 1383–1394. <https://doi.org/10.1111/gcb.14560>.
- Reynolds, S.J., Martin, G.R., Dawson, A., Wearn, C.P., Hughes, B.J., 2014. The sub-annual breeding cycle of a tropical seabird. *PLoS One* 9(4), e93582. <https://doi.org/10.1371/journal.pone.0093582>.
- Reynolds, S.J., Wearn, C.P., Hughes, B.J., Dickey, R.C., Garrett, L.J.H., Walls, S., Hughes, F.T., Weber, N., Weber, S.B., Leat, E.H.K., Andrews, K., Ramos, J.A., Paiva, V.H., 2021. Year-round movements of sooty terns (*Onychoprion fuscatus*) nesting within one of the Atlantic's largest Marine Protected Areas. *Front. Mar. Sci.* 8, 744506. <https://doi.org/10.3389/fmars.2021.744506>.
- Sackett, W.M., Eckelmann, W.R., Bender, M.L., Bé, A.W.H., 1965. Temperature dependence of carbon isotope composition in marine plankton and sediments. *Science* 148, 235–237. <https://doi.org/10.1126/science.148.3667.235>.
- Schartup, A.T., Thackray, C.P., Qureshi, A., Dassuncao, C., Gillespie, K., Hanke, A., Sunderland, E.M., 2019. Climate change and overfishing increase neurotoxicant in marine predators. *Nature* 572, 648–650. <https://doi.org/10.1038/s41586-019-1468-9>.
- Scheffler, R., Gauthier-Clerc, M., Bohec, C.L., Crini, N., Cœurassier, M., Badot, P.-M., Giraudoux, P., Maho, Y.L., 2005. Mercury concentrations in king penguin (*Aptenodytes patagonicus*) feathers at Crozet Islands (sub-Antarctic): Temporal trend between 1966–1974 and 2000–2001. *Environ. Toxicol. Chem.* 24, 125–128. <https://doi.org/10.1897/03-446.1>.
- Schell, D.M., 2000. Declining carrying capacity in the Bering Sea: isotopic evidence from whale baleen. *Limnol. Oceanogr.* 45, 459–462. <https://doi.org/10.4319/lo.2000.45.2.0459>.
- Selin, N.E., 2009. Global biogeochemical cycling of mercury: A review. *Annu. Rev. Environ. Resour.* 34, 43–63. <https://doi.org/10.1146/annurev-environ.051308.084314>.
- Streets, D.G., Horowitz, H.M., Lu, Z., Levin, L., Thackray, C.P., Sunderland, E.M., 2019. Five hundred years of anthropogenic mercury: Spatial and temporal release profiles. *Environ. Res. Lett.* 14. <https://doi.org/10.1088/1748-9326/ab281f>.
- Sunderland, E.M., Krabbenhoft, D.P., Moreau, J.W., Strode, S.A., Landing, W.M., 2009. Mercury sources, distribution, and bioavailability in the North Pacific Ocean: Insights from data and models. *Global Biogeochem. Cycles* 23. <https://doi.org/10.1029/2008GB003425>.
- Sunderland, E.M., Mason, R.P., 2007. Human impacts on open ocean mercury concentrations. *Global Biogeochem. Cycles* 21. <https://doi.org/10.1029/2006GB002876>.
- Takeuchi, T., Morikawa, N., Matsumoto, H., Shiraiishi, Y., 1962. A pathological study of Minamata disease in Japan. *Acta Neuropathol.* 2, 40–57. <https://doi.org/10.1007/BF00685743>.
- Tartu, S., Blévin, P., Bustamante, P., Angelier, F., Bech, C., Bustnes, J.O., Chierici, M., Fransson, A., Gabrielsen, G.W., Goutte, A., Moe, B., Sausser, C., Sire, J., Barbraud, C., Chastel, O., 2022. A U-Turn for mercury concentrations over 20 years: How do environmental conditions affect exposure in Arctic seabirds? *Environ. Sci. Technol.* 56, 2443–2454. <https://doi.org/10.1021/acs.est.1c07633>.
- Thompson, D.R., Bearhop, S., Speakman, J.R., Furness, R.W., 1998. Feathers as a means of monitoring mercury in seabirds: Insights from stable isotope analysis. *Environ. Pollut.* 101, 193–200. [https://doi.org/10.1016/S0269-7491\(98\)00078-5](https://doi.org/10.1016/S0269-7491(98)00078-5).
- Thompson, D.R., Becker, P.H., Furness, R.W., 1993. Long term changes in mercury concentrations in herring gulls *Larus argentatus* and common terns *Sterna hirundo* from the German North Sea coast. *J. Appl. Ecol.* 30, 316–320. <https://doi.org/10.2307/2404633>.
- Thompson, D.R., Furness, R.W., 1989. Comparison of the levels of total and organic mercury in seabird feathers. *Mar. Pollut. Bull.* 20, 577–579. [https://doi.org/10.1016/0025-326X\(89\)90361-5](https://doi.org/10.1016/0025-326X(89)90361-5).
- Thompson, D.R., Furness, R.W., Walsh, P.M., 1992. Historical changes in mercury concentrations in the marine ecosystem of the North and North-East Atlantic Ocean as indicated by seabird feathers. *J. Appl. Ecol.* 29, 79–84. <https://doi.org/10.2307/2404350>.
- Townhill, B.L., Couce, E., Bell, J., Reeves, S., Yates, O., 2021. Climate change impacts on Atlantic oceanic island tuna fisheries. *Front. Mar. Sci.* 8, 634280. <https://doi.org/10.3389/fmars.2021.634280>.
- UN Environment, 2019. *Global Mercury Assessment 2018*. UN Environment Programme. Chemicals and Health Branch, Geneva, Switzerland.
- Vizzini, S., Mazzola, A., 2003. Seasonal variations in the stable carbon and nitrogen isotope ratios ($^{13}\text{C}/^{12}\text{C}$ and $^{15}\text{N}/^{14}\text{N}$) of primary producers and consumers in a western Mediterranean coastal lagoon. *Mar. Biol.* 142, 1009–1018. <https://doi.org/10.1007/s00227-003-1027-6>.
- Vo, A.-T.E., Bank, M.S., Shine, J.P., Edwards, S.V., 2011. Temporal increase in organic mercury in an endangered pelagic seabird assessed by century-old museum specimens. *Proc. Natl. Acad. Sci. USA* 108, 7466–7471. <https://doi.org/10.1073/pnas.1013865108>.
- Wang, K., Munson, K.M., Beaupré-Laperrière, A., Mucci, A., Macdonald, R.W., Wang, F., 2018. Subsurface seawater methylmercury maximum explains biotic mercury concentrations in the Canadian Arctic. *Sci. Rep.* 8, 1–5. <https://doi.org/10.1038/s41598-018-32760-0>.
- Watson, A.J., 2016. Oceans on the edge of anoxia. *Science* 354, 1529–1530. <https://doi.org/10.1126/science.aaj2321>.
- Wood, S.N., 2011. Fast stable restricted maximum likelihood and marginal likelihood estimation of semiparametric generalized linear models. *J. R. Stat. Soc. Ser. B Stat. Methodol.* 73, 3–36. <https://doi.org/10.1111/j.1467-9868.2010.00749.x>.
- Zeileis, A., Hothorn, T., 2002. Diagnostic checking in regression relationships. *R. News* 2 (3), 7–10. <https://CRAN.R-project.org/doc/Rnews/>.
- Zhang, Y., Dutkiewicz, S., Sunderland, E.M., 2021. Impacts of climate change on methylmercury formation and bioaccumulation in the 21st Century ocean. *One Earth* 4, 279–288. <https://doi.org/10.1016/j.oneear.2021.01.005>.

SUPPLEMENTARY MATERIAL

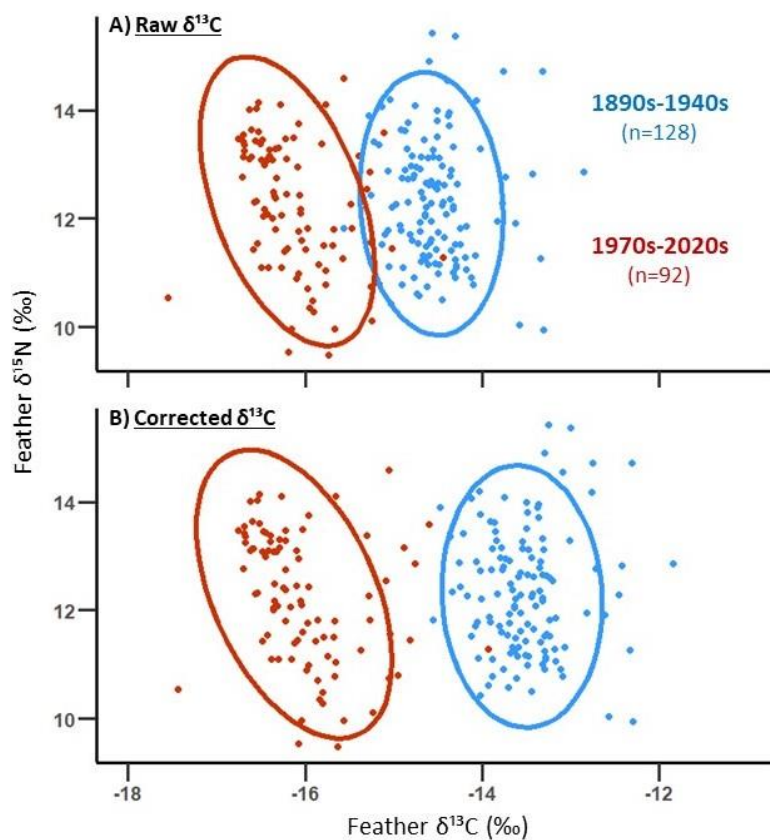
1) Supplementary figures

Figure S1. Isotopic niches of sooty terns (n=220) before (blue) and after (red) population collapse on Ascension Island (1960s-1990s), with (A) raw $\delta^{13}\text{C}$ and (B) $\delta^{13}\text{C}$ values corrected for the Suess Effect and phytoplankton fractionation (cf. details in Materials and Methods). Each ellipse includes 90% of the data.

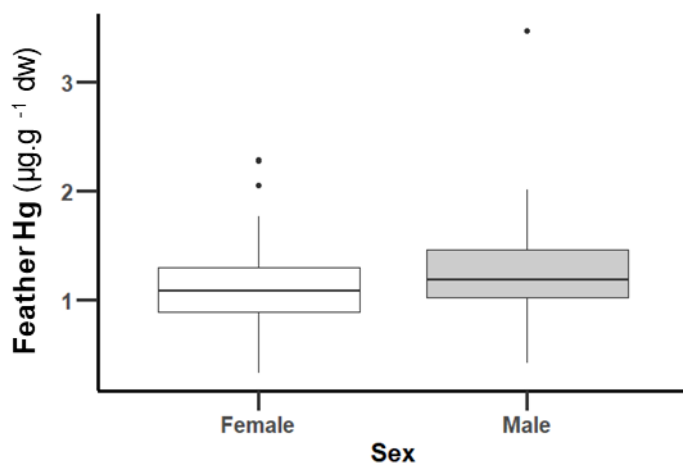


Figure S2. Mercury concentrations in male (grey; n=41) and female (white; n=43) sooty terns breeding on Ascension Island in 1925 (n=84). No statistical difference was detected between sexes ($F_{1,82}=2.82$, $p=0.10$). Boxplots indicate median values (midlines), errors bars (whiskers) and outliers (black dots).

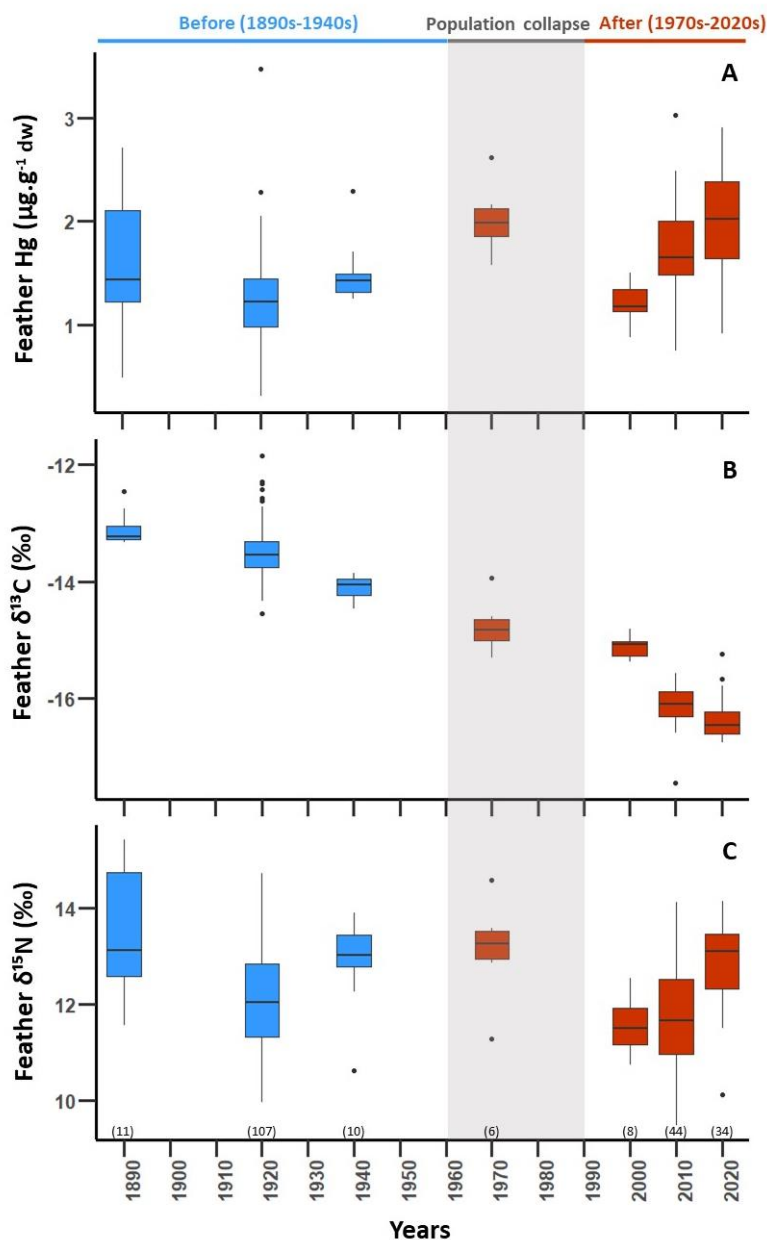


Figure S3. (A) Feather Hg concentrations and stable isotope values from sooty terns breeding on Ascension Island (South Atlantic Ocean) between the 1890s and the 2020s (i.e., over seven decades). (B) The $\delta^{13}\text{C}$ values were corrected for the Suess Effect and phytoplankton fractionation (see **Materials and Methods** section for further details) and represent a proxy for bird feeding habitat. (C) $\delta^{15}\text{N}$ is a proxy for bird's diet, and hence for its trophic position. Numbers in brackets represent sample sizes for each decade. The grey area represents the period where a marked population decline occurred (1960s–1990s). Birds were assigned to two main periods accordingly: before (blue) and after (red) population collapse. Boxplots indicate median values (midlines), errors bars (whiskers) and outliers (black dots).

2) Long-term Hg contamination in seabirds: A review

Table S1. Studies investigating long-term trends in Hg contamination in feathers of museum specimens. n indicates sample sizes for each species and study.

Reference, Species	n	Feather	Time range	Site, Region (Ocean)	Main findings	Isotopes
<u>Choy et al. (2022)</u>						
Glaucous-winged gull (<i>Larus glaucescens</i>)	65	Body	1887–1996	Salish Sea (Northeast Pacific Ocean)	No trend (stable)	Yes
<u>Bond and Lavers (2020)</u>						
Flesh-footed shearwater (<i>Puffinus carneipes</i>)	137	Body	1946–2011	Australia (Southeast Indian Ocean)	No significant trend (-0.3 % <i>per year</i>)	No
<u>Gilmour et al. (2019)</u>						
Gentoo penguin (<i>Pygoscelis papua</i>)	37		1950s–2003	Macquarie Island, (Southern Ocean; sub-Antarctic)	No trend	No
King penguin (<i>Aptenodytes patagonicus</i>)	30		1940s–2003		Decrease	
Rockhopper penguin (<i>Eudyptes sp.</i>)	34	Body	1940s–2003		Non-significant increase	
Royal penguin (<i>Eudyptes schlegeli</i>)	42		1930s–2003		Decrease	
<u>Gagné et al. (2019)</u>						
Laysan albatross (<i>Phoebastria immutabilis</i>)	-		1897–1992	Hawaiian Islands (North Pacific Ocean), American Samoa (South Pacific Ocean), Florida Keys (Atlantic Ocean)	Decreasing from the 1980s to 2015 for Hawaiian Islands only	No
Bulwer's petrel (<i>Bulweria bulweri</i>)	-		1891–2014			
Wedge-tailed shearwater (<i>Puffinus pacificus</i>)	-	Body/	1897–2014			
White-tailed tropicbird (<i>Phaethon lepturus</i>)	-	Primary	1892–2015			
Brown booby (<i>Sula leucogaster</i>)	-		1891–2015			
Brown noddy (<i>Anous stolidus</i>)	-		1939–1996			
White tern (<i>Gygis alba</i>)	-		1891–2013			

Sooty tern (<i>Onychoprion fuscatus</i>)	-		1896–2015			
<u>Carravieri et al. (2016)</u>						
Emperor penguin (<i>Aptenodytes forsteri</i>)	28	Body	1950s–2007	Adélie Land, Antarctica (Southern Ocean)	No change	Yes
Adelie penguin (<i>Pygoscelis adeliae</i>)	15		1950s–2007		Decrease (-77%)	
King penguin (<i>Aptenodytes patagonicus</i>)	38		1970s–2007	Crozet Islands	No significant change (+14%)	
Macaroni penguin (<i>Eudyptes chrysolophus</i>)	30		1970s–2007	(Southern Ocean; sub-Antarctic waters)	Increase (+32%)	
Gentoo penguin (<i>Pygoscelis papua</i>)	24		1970s–2007		Increase (+53%)	
<u>Bond et al. (2015)</u>						
Ivory gull (<i>Pagophila eburnea</i>)	80	Body	1877–2007	Canadian Arctic, Greenland and Eastern Canadian waters (Arctic Ocean)	45-fold increase (+1.6% <i>per year</i>)	Yes
<u>Vo et al. (2011)</u>						
Black-footed albatross (<i>Phoebastria nigripes</i>)	25	Body	1880–2002	Multiples sites (North Pacific Ocean)	Increase	Yes
<u>Scheifler et al. (2005)</u>						
King penguin (<i>Aptenodytes patagonicus</i>)	41	Body	1966–2001	Crozet Islands (Southern Ocean; sub-Antarctic waters)	Significant decrease (-34%)	No
<u>Monteiro and Furness (1997)</u>						
Cory's shearwater (<i>Calonectris borealis</i>)	267	Body	1886–1994	Azores, Madeira, Salvages (Northeast Atlantic Ocean)	Increase by 1.1 – 1.9% <i>per year</i>	No
Little shearwater (<i>Puffinus assimilis</i>)	49				-	
Common tern (<i>Sterna hirundo</i>)	37				-	
Bulwer's petrel (<i>Bulweria bulweri</i>)	85				Increase by 3.5 – 4.8% <i>per year</i>	
Madeiran storm petrel (<i>Oceanodroma castro</i>)	63				-	
<u>Furness et al. (1995)</u>						
Herring gull (<i>Larus argentatus</i>)	-	Body	1880–1990	German Bight, East Scotland, Shetland (North Sea, North Atlantic Ocean)	Increase	No
Common tern (<i>Sterna hirundo</i>)	-					
Kittiwakes (<i>Rissa sp.</i>)	-					
Guillemots (<i>Uria sp.</i>)	-					
<u>Thompson et al. (1993a)</u>						

Common tern (<i>Sterna hirundo</i>)	42	Body	1866–1990s	German North Sea coast, (Northeast Atlantic Ocean)	4-fold increase in adults (+377%), 2-fold in juveniles (+139%)	No
Herring gull (<i>Larus argentatus</i>)	140		1884–1990s		2-fold increase (adults: +75%, juveniles: +110%)	
Thompson et al. (1993b)						
Wandering albatross (<i>Diomedea exulans</i>)	35	Body	<1950–1980s	New Zealand, South Georgia, Gough Island, Marion Island (Southern Ocean; sub-Antarctic waters)	Significant increase in 3 species, but lack of widespread increase	No
Black-browed albatross (<i>Thalassarche melanorhynchus</i>)	20					
Grey-headed albatross (<i>Thalassarche chrysotoma</i>)	16					
Shy albatross (<i>Thalassarche cauta</i>)	9					
Northern giant petrel (<i>Macronectes halli</i>)	7					
Southern giant petrel (<i>Macronectes giganteus</i>)	42					
Thompson et al. (1992)						
Northern fulmar (<i>Fulmarus glacialis</i>)	57	Body	1850s–1980s	St Kilda, Foula, southern Ireland (Northeast Atlantic Ocean)	Decrease (-65% in Shetland, - 35% in St Kilda)	No
Manx shearwater (<i>Puffinus puffinus</i>)	96			Skomer, Wales (Northeast Atlantic Ocean)	Increase (+125%)	
North Atlantic gannet (<i>Morus bassanus</i>)	57			Bass Rock (North Atlantic Ocean)	Increase (+20%)	
Great skua (<i>Stercorarius skua</i>)	225			Foula, southern Ireland (Northeast Atlantic Ocean)	Increase (+53%)	
Atlantic puffin (<i>Fratercula arctica</i>)	110			St Kilda, Foula, Great Saltee, southern Ireland (Northeast Atlantic Ocean)	Increase (+120%)	
Appelquist et al. (1985)						
Black guillemot (<i>Cepphus grille</i>)	137	Primary	1830s–1979	Baltic Sea, Faroe Islands, Greenland (North Atlantic Ocean)	Substantial increase	No
Common, Brunnich guillemots (<i>Uria sp.</i>)	140					

-: Information not available in the original study

3) Museum sample collection

Table S2. Details of museums and their curators who assisted in initial enquiries about specimens of sooty tern skins collected from Ascension Island in the South Atlantic

Name of museums	Location	Name of curators
American Museum of Natural History (AMNH)	New York, NY, USA	Tom Trombone
Florida Museum of Natural History (Flor. Mus. Nat. Hist.)	Gainesville, FL, USA	Tom Webber
Peabody Museum of Natural History (Peabody)	Yale University, New Haven, CT, USA	Kristof Zyskowski
Smithsonian Institution – Division of Birds (Smithsonian)	Washington DC, USA	Chris Milensky
Great North Museum – Hancock Collection (Hancock)	Newcastle upon Tyne, UK	Dan Gordon
Museum of Natural Science (Mus. Nat. Sci. LSU)	Louisiana State University, Baton Rouge, LA, USA	Steve Cardiff, Nicholas Mason
National Museum of Natural History – Collection of Birds (NMNH Paris)	Paris, France	Jérôme Fuchs
National Museums Scotland (Nat. Mus. Scotland)	Edinburgh, UK	Bob McGowan
National Museum Liverpool (Nat. Mus. Liverpool)	Liverpool, UK	Tony Parker
Natural History Museum-Bird Group (NHM Tring)	Tring, UK	Mark Adams

Table S3. Details of body feathers of sooty terns breeding on Ascension Island in the South Atlantic, between the 1890s and the 2020s.

Sources: **AIG** – Ascension Island Government; **AMNH** – American Museum of Natural History, New York, NY, USA; **BJH** – B. John Hughes; **CPW** – Colin P. Wearn; **FC** – Fanny Cusset; **Flor. Mus. Nat. Hist.** – Florida Museum of Natural History, Gainesville, FL, USA; **Hancock** – Great North Museum-Hancock Collection, Newcastle upon Tyne, UK; **Mus. Nat. Sci. LSU** – Museum of Natural Science, Louisiana State University, Baton Rouge, LA, USA; **Nat. Mus. Liverpool** – National Museums Liverpool, Liverpool, UK; **Nat. Mus. Scotland** – National Museums Scotland, Edinburgh, UK; **NHM Tring** – Natural History Museum-Bird Group, Tring, UK; **NMNH Paris** – National Museum of Natural History-Collection of Birds, Paris, France; **Peabody** – Peabody Museum of Natural History, Yale University, New Haven, CT, USA; **SJR** – S. James Reynolds; and **Smithsonian** – Smithsonian Institution-Division of Birds, Washington DC, USA.

Sample ID	Source	Catalog number	Decade of collection
JR1	Hancock	B020.71	1890
JR2	Nat. Mus. Scotland	NMS.Z 1956.3 (3161)	1890
JR3	NHM Tring	2012.102.1	1890
JR4	NHM Tring	1880.11.18.707	1890
JR5	Smithonian	USNM 118379	1890
JR6	Smithonian	USNM 118380	1890
JR7	Smithonian	USNM 118381	1890
JR8	NHM Tring	1894.10.28.7	1890
JR9	NHM Tring	1899.1.4.19	1890
JR10	NHM Tring	1899.1.4.20	1890
JR11*	Nat. Mus. Liverpool	-	1920
JR12	NHM Tring	1922.12.6.49	1920
JR13	NHM Tring	1922.12.6.50	1920
JR14	Peabody	44863	1920
JR15	Peabody	44864	1920
JR16	Peabody	44865	1920
JR17	Peabody	44866	1920
JR18	Peabody	44868	1920
JR19	Peabody	44869	1920
JR20	Peabody	44870	1920
JR21	Peabody	44871	1920
JR22	Peabody	44872	1920
JR23	Peabody	44873	1920
JR24	Peabody	44874	1920
JR25	Peabody	44875	1920
JR26	Peabody	44876	1920
JR27	Peabody	44877	1920
JR28	Peabody	44878	1920
JR29	Peabody	44879	1920
JR30	Peabody	44888	1920
JR31	Peabody	44889	1920
JR32	Peabody	44890	1920

JR33	Peabody	44891	1920
JR34	Peabody	44892	1920
JR35	Peabody	44893	1920
JR36	Peabody	44894	1920
JR37	Peabody	44895	1920
JR38	Peabody	44896	1920
JR39	Peabody	44897	1920
JR40	Peabody	44898	1920
JR41	Peabody	44899	1920
JR42	Peabody	44901	1920
JR43	Peabody	44902	1920
JR44	Peabody	44903	1920
JR45	Peabody	44904	1920
JR46	Peabody	44905	1920
JR47	Peabody	44906	1920
JR48	Peabody	44907	1920
JR49	Peabody	44908	1920
JR50	Peabody	44909	1920
JR51	Peabody	44921	1920
JR52	Peabody	44922	1920
JR53	Peabody	44923	1920
JR54	Peabody	44924	1920
JR55	Peabody	44925	1920
JR56	Peabody	44934	1920
JR57	Peabody	44935	1920
JR58	Peabody	44936	1920
JR59	Peabody	44937	1920
JR60	Peabody	44938	1920
JR61	Peabody	44939	1920
JR62	Peabody	44940	1920
JR63	Peabody	44941	1920
JR64	Peabody	44942	1920
JR65	Peabody	44943	1920
JR66	Peabody	44944	1920
JR67	Peabody	44945	1920
JR68	Peabody	44946	1920
JR69	Peabody	44947	1920
JR70	Peabody	44948	1920
JR71	Peabody	44949	1920
JR72	Peabody	44950	1920
JR73	Peabody	44951	1920
JR74	Peabody	44952	1920
JR75	Peabody	44953	1920
JR76	Peabody	44954	1920
JR77	Peabody	44955	1920
JR78	Peabody	44956	1920

JR79	Peabody	44967	1920
JR80	Peabody	44968	1920
JR81	Peabody	44969	1920
JR82	Peabody	44970	1920
JR83	Peabody	44971	1920
JR84	Peabody	44972	1920
JR85	Peabody	44973	1920
JR86	Peabody	44974	1920
JR87	Peabody	44975	1920
JR88	Peabody	44976	1920
JR89	Peabody	44977	1920
JR90	Peabody	44978	1920
JR91	Peabody	44981	1920
JR92	Peabody	44982	1920
JR93	Peabody	44983	1920
JR94	Peabody	44984	1920
JR95	Peabody	44985	1920
JR96	AMNH	269206	1920
JR97	AMNH	269227	1920
JR98	AMNH	269226	1920
JR99	AMNH	269225	1920
JR100	AMNH	269224	1920
JR101	AMNH	269223	1920
JR102	AMNH	269222	1920
JR103	AMNH	269221	1920
JR104	AMNH	269220	1920
JR105	AMNH	269219	1920
JR106	AMNH	269218	1920
JR107	AMNH	269217	1920
JR108	AMNH	269216	1920
JR109	AMNH	269215	1920
JR110	AMNH	269214	1920
JR111	AMNH	269213	1920
JR112	AMNH	269212	1920
JR113	AMNH	269211	1920
JR114	AMNH	269210	1920
JR115	AMNH	269209	1920
JR116	AMNH	269208	1920
JR117	AMNH	269207	1920
JR118	AMNH	308427	1940
JR119	AMNH	308426	1940
JR120	AMNH	308425	1940
JR121	AMNH	308424	1940
JR122	AMNH	308423	1940
JR123	AMNH	308422	1940
JR124	AMNH	308421	1940

JR125	AMNH	308428	1940
JR126	AMNH	308429	1940
JR127	Nat. Sci. LSU	73125	1940
JR128	NHM Tring	1962.42.2	1970
JR129	Smithsonian	534287	1970
JR130	Smithsonian	534285	1970
JR131	Smithsonian	534286	1970
JR132	Smithsonian	534288	1970
JR133	BJH	-	2000
JR134	BJH	-	2000
JR135	BJH	-	2000
JR136	BJH	-	2000
JR137	BJH	-	2000
JR138	BJH	-	2000
JR139	BJH	-	2000
JR140	BJH	-	2000
JR141	NMNH Paris	CG 1973-286	1890
JR142	Flor. Mus. Nat. His.	UF 37533	1970
JR143	CPW/SJR	-	2010
JR144	CPW/SJR	-	2010
JR145	CPW/SJR	-	2010
JR146	CPW/SJR	-	2010
JR147	CPW/SJR	-	2010
JR148	CPW/SJR	-	2010
JR149	CPW/SJR	-	2010
JR150	CPW/SJR	-	2010
JR151	CPW/SJR	-	2010
JR152	CPW/SJR	-	2010
JR153	CPW/SJR	-	2010
JR154	CPW/SJR	-	2010
JR155	CPW/SJR	-	2010
JR156	CPW/SJR	-	2010
JR157	CPW/SJR	-	2010
JR158	CPW/SJR	-	2010
JR159	CPW/SJR	-	2010
JR160	CPW/SJR	-	2010
JR161	CPW/SJR	-	2010
JR162	CPW/SJR	-	2010
JR163	CPW/SJR	-	2010
JR164	CPW/SJR	-	2010
JR165	CPW/SJR	-	2010
JR166	CPW/SJR	-	2010
JR167	CPW/SJR	-	2010
JR168	CPW/SJR	-	2010
JR169	CPW/SJR	-	2010
JR170	CPW/SJR	-	2010

JR171	CPW/SJR	-	2010
JR172	CPW/SJR	-	2010
JR173	CPW/SJR	-	2010
JR174	CPW/SJR	-	2010
JR175	CPW/SJR	-	2010
JR176	CPW/SJR	-	2010
JR177	CPW/SJR	-	2010
JR178	CPW/SJR	-	2010
JR179	CPW/SJR	-	2010
JR180	CPW/SJR	-	2010
JR181	CPW/SJR	-	2010
JR182	CPW/SJR	-	2010
JR183	CPW/SJR	-	2010
JR185	CPW/SJR	-	2010
JR186	CPW/SJR	-	2010
JR187	CPW/SJR	-	2010
FCa31	FC/AIG	-	2020
FCa32	FC/AIG	-	2020
FCa33	FC/AIG	-	2020
FCa34	FC/AIG	-	2020
FCa35	FC/AIG	-	2020
FCb16	FC/AIG	-	2020
FCb17	FC/AIG	-	2020
FCb18	FC/AIG	-	2020
FCb19	FC/AIG	-	2020
FCb20	FC/AIG	-	2020
FCb21	FC/AIG	-	2020
FCb22	FC/AIG	-	2020
FCb23	FC/AIG	-	2020
FCb24	FC/AIG	-	2020
FCb25	FC/AIG	-	2020
FCb26	FC/AIG	-	2020
FCb27	FC/AIG	-	2020
FCb28	FC/AIG	-	2020
FCb29	FC/AIG	-	2020
FCb30	FC/AIG	-	2020
FCb31	FC/AIG	-	2020
FCb32	FC/AIG	-	2020
FCb33	FC/AIG	-	2020
FCb34	FC/AIG	-	2020
FCb36	FC/AIG	-	2020
FCb37	FC/AIG	-	2020
FCb38	FC/AIG	-	2020
FCb39	FC/AIG	-	2020
FCb40	FC/AIG	-	2020
FCb41	FC/AIG	-	2020

FCb42	FC/AIG	-	2020
FCb43	FC/AIG	-	2020
FCb44	FC/AIG	-	2020
FCb45	FC/AIG	-	2020

* Sample omitted from statistical analyses as it was identified as an outlier.

4) Museum inorganic contamination in old specimens

Context. Total-Hg (THg) includes two main forms: inorganic Hg (iHg) and methyl-Hg (MeHg). In bird feathers, the dominant form of THg is MeHg (>90%). For this reason, THg is routinely measured in bird feathers, as a proxy for bird MeHg burden.

Historically, iHg salts were used as preservatives in museum collections until approximately the 1970s and as a result represent a major bias in Hg quantification in older bird specimens. Measuring THg in old specimens is thus inappropriate. Therefore, analysing MeHg specifically is the best alternative to investigate Hg temporal trends in museum-archived bird specimens.

Methods- Hg speciation analyses. Mercury speciation analyses were performed following established methodology presented in Renedo et al. (2017). In this study, Hg species (iHg and MeHg) were extracted from feather homogenates by acid microwave digestion in 3 mL of suprapure grade nitric acid solution (HNO₃ 6N), characterized by 1 min of heating to 75°C and 4 min at 75°C (Discover SP-D, CEM Corporation, USA) in CEM Pyrex vessels, with magnetic agitation to homogenise samples and after a predigestion step overnight at room temperature. Sample mass fractions and HNO₃ 6N volumes were precisely weighted using a 10⁻⁵ analytical balance. Then, sample extracts underwent a derivatization step at pH 3.9 in order to allow liquid/liquid extraction of the Hg species in GC solvent and its subsequent chromatographic elution. Ethylation was thus achieved by adding to the sample extracts 5 mL of buffer solution (Acetic/Acetate, 0.1 M, pH 3.9) and small amounts of ultrapure grade NH₃ or HCl to reach pH=3.9 (3.85-4.05). GC solvent (isooctane, 300 µL) and NaBEt₄ (80 µL, 5%) were finally added before agitation (20 min, elliptic table) and centrifugation (2500 rpm, 3 min). The resulting organic phase was retrieved and transferred to GC vials. Final extracts were stored in the freezer (-20°C) prior GC analyses.

In order to achieve accurate and precise Hg speciation analyses on bird feather specimens, the Isotopic Dilution methodology was applied to correct efficiently the matrix effects and Hg artefacts during the sample preparation. Before the microwave extraction, samples were thus spiked with known amounts of two enriched isotope tracer solutions (ISC-Science, Spain), namely ¹⁹⁹iHg and ²⁰¹MeHg, to alter the natural isotopic abundance of the studied endogenous species (²⁰²iHg and ²⁰²MeHg). Mixed isotope ratios were then quantified, as explained elsewhere (Clémens et al., 2012; Rodríguez-González et al.,

2005). Mercury species analyses were carried out by GC-ICPMS Trace Ultra GC, equipped with a Triplus RSH autosampler coupled to an ICP-MS XSeries II (ThermoFisher Scientific, USA). The reported results of [THg] were calculated as the sum of [MeHg] and [iHg] determined by ID-GC-ICPMS and were compared to [THg] determined by AMA-254, to evaluate their similarity and verify the recovery of the extraction. Human hair certified reference material (NIES-13) was analysed during each analytical session to assess the robustness of the methodology. The certified values of NIES-13 were: [THg] = $4.42 \pm 0.20 \mu\text{g g}^{-1}$ and [MeHg] = $3.80 \pm 0.40 \mu\text{g g}^{-1}$.

Table S4. Tests for Hg speciation analyses of feathers from free-living birds (n=3) and museum specimens (n=3) specimens of sooty terns breeding on Ascension Island. Values are means \pm SD. Concentrations are expressed in $\mu\text{g g}^{-1}$ dw for methyl-Hg (MeHg), inorganic Hg (iHg), total-Hg obtained from Hg speciation analyses (Σ MeHg+iHg) and from AMA analyses (THg). Recovery is calculated as $(\Sigma \text{ MeHg} + \text{ iHg}) \times 100 / \text{ THg}$. Samples were analysed in duplicate/triplicates, with certified reference material (NIES-13). Further details are provided in the **Materials and Methods**.

Year	ID	MeHg	iHg	Σ MeHg+iHg	THg	Recovery (%)
2000	1A	1.24 ± 0.04	0.020 ± 0.001	1.26 ± 0.09	1.24	102
2000	1C	0.84 ± 0.03	0.002 ± 0.001	0.86 ± 0.09	0.93	92
2000	1F	1.31 ± 0.03	0.031 ± 0.002	1.34 ± 0.10	1.42	94
1877	JR3	0.49 ± 0.02	24.62 ± 0.34	25.11 ± 1.33	27.84	92
1890	JR5	0.69 ± 0.09	16.06 ± 0.07	16.75 ± 2.16	17.63	95
1925	JR74	0.57 ± 0.01	2.66 ± 0.05	3.24 ± 0.12	3.39	96
NIES-13	certified	3.80 ± 0.40	0.62 ± 0.60	4.42 ± 0.20	4.42	100
	measured	3.64 ± 0.02	0.89 ± 0.02	4.53 ± 0.11	4.42	103

Results. To test method validation on museum specimens, Hg speciation analyses were performed on three museum specimens (dating from 1877, 1890, 1925) and three free-living birds (from 2000) (Table S3).

Average recoveries (Σ MeHg + iHg determined by GC-ICPMS *versus* THg determined by AMA) were $96.13 \pm 4.88\%$ (range: 92–102%) for feathers from the 2000s and $94.11 \pm 1.99\%$ (range: 92–96%) for feathers from museum specimens, proving method robustness. Mercury species distribution in old specimens was $92.1 \pm 8.5\%$ (range: 82.3–98.1%) iHg and $7.9 \pm 8.5\%$ (1.9–17.7%) MeHg. In recent

specimens, iHg represented only $2.0 \pm 0.4\%$ (range: 1.6–2.3%) of the THg burden and MeHg $98.0 \pm 0.4\%$ (range: 97.7–98.4%), thus confirming the use of inorganic Hg salts as museum preservatives.

Overall, THg (AMA-254) concentrations ranged from 0.75 to $264.92 \mu\text{g g}^{-1}$ dw (Table 1), with highest values in old specimens (1890s: $70.12 \pm 87.34 \mu\text{g g}^{-1}$ dw, $n=11$). Figure S1 provides details of %iHg and %MeHg for all samples over time, highlighting that museum preservation processes used inorganic Hg salt for skin conservation. Table S4 provides details on Hg speciation analyses, with mean \pm SD (range) values for all Hg species and recoveries.

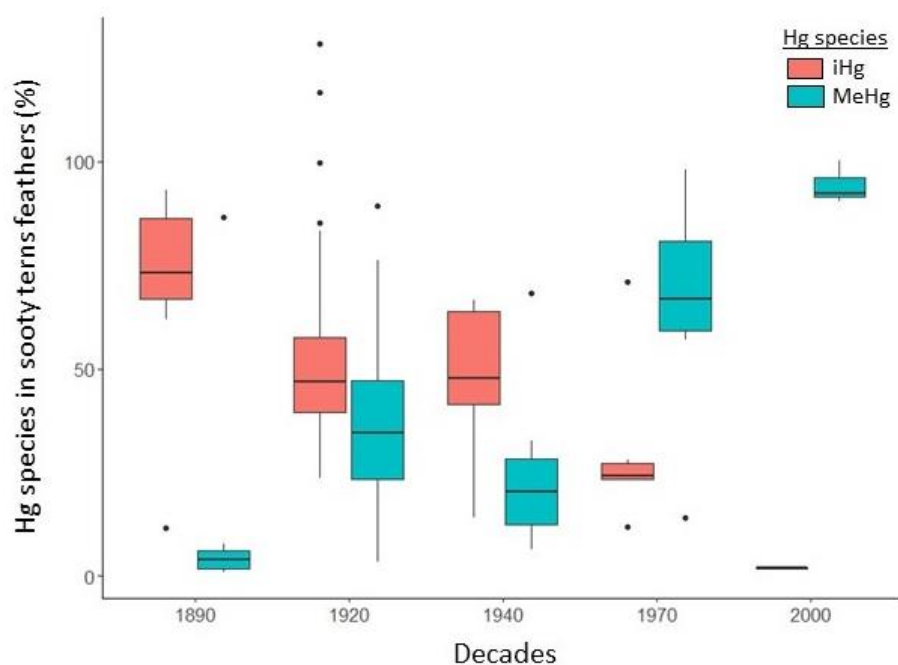


Figure S4. Percentage of different Hg species (inorganic Hg, iHg in red; methyl-Hg, MeHg in blue) in feathers of museum skins and free-living sooty terns breeding on Ascension Island, over 145 years. The sum of Hg (equivalent to total-Hg, THg) species is 100%.

Table S5. Summary of Hg speciation analyses of sooty tern feathers from Ascension Island (1876–2021): methyl-Hg (MeHg), inorganic Hg (iHg) and the sum of both (equivalent to total-Hg, THg). Values are means \pm SD (range). Concentrations ($\mu\text{g g}^{-1}$ dw) were quantified in all samples and in certified reference material (NIES-13). n indicates sample sizes. Individual recovery (%) is calculated as: $(\Sigma \text{MeHg} + \text{iHg}) \times 100 / \text{THg}$. Further details are provided in the **Materials and Methods**.

	MeHg	iHg	Σ MeHg + iHg	THg	Recovery (%)
Samples (n=131)	1.3 \pm 0.5 (0.3-3.5)	7.4 \pm 26.5 (0.2-246.4)	8.8 \pm 26.8 (1.2-249.1)	10.8 \pm 31.1 (1.7-264.9)	-*
NIES-13 (n=3)	3.6 \pm 0.1 (3.6-3.7)	0.7 \pm 0.2 (0.5-0.9)	4.3 \pm 0.3 (4.0-4.5)	4.42 \pm 0.01	97.7 \pm 5.8 (91.3-102.5)

*No recovery is provided for the samples, because of the high inorganic contamination in old specimens which completely biased the recovery percentage.

5) Empirical calculations of percentages of change

To enable trend comparison with published literature, we calculated the percentage of evolution (increase or decrease) between decades, for each evolution phase identified by GAM temporal trends and globally (i.e., between the 1920s and the 2020s). Negative and positive percentages correspond to a decrease and an increase, respectively. For example, between the 1920s and the 1970s, E.S1 applies as follows:

$$\% \text{change (increase)} = ([\text{Hg}]_{1970\text{s}} - [\text{Hg}]_{1920\text{s}}) / [\text{Hg}]_{1970\text{s}} \quad (\text{E.S1})$$

The overall percentage (for the entire period) was then converted into a % *per year* by dividing by the number of years (n=100).

Table S6. Percentage of change in temporal trends of Hg, $\delta^{13}\text{C}$ and $\delta^{15}\text{N}$ values between different focal periods of the study. Positive and negative values indicate increasing and decreasing metrics during each focal period, respectively. Following GAMs analyses, only periods in bold are scientifically appropriate (realistic) for interpretation.

Focal periods	Hg (%)	$\delta^{13}\text{C}$ (%)	$\delta^{15}\text{N}$ (%)
1890s – 1920s	- 23.9	- 3.0	- 10.4
1920s – 1970s	+ 62.9	- 4.4	-
1970s – 2000s	-	- 4.7	-
2000 – 2020s	+ 62.8	- 2.4	+ 11.5
Before <i>versus</i> after population collapse	+ 38.8	- 18.6	- 0.7
1920s <i>versus</i> 2020s	+ 37.1	- 17.4	+ 5.7

Example: Mean Hg concentrations decreased by 23.9% between the 1890s and the 1920s.

6) Statistics - Generalized Additive Models (GAMs)

Table S7. Outputs from GAM models explaining variation in feather Hg and stable isotope values between the 1890s and the 2020s in adult sooty terns breeding on Ascension Island in the South Atlantic Ocean. For the intercept, values are estimates and standard errors. For the smoother (year), values are effective degrees of freedom. K indicates the number of knots in temporal trends of each variable.

Response variable	Intercept	k	s(Year)	p-value	Deviance explained (%)
Hg	1.59 ± 0.04	5	3.61	<0.0001***	25.1
$\delta^{13}\text{C}$	-14.91 ± 0.03	5	3.39	<0.0001***	12.5
$\delta^{15}\text{N}$	12.38 ± 0.09	5	3.67	<0.0001***	91.0

Les oiseaux marins, bioindicateurs de la contamination passée et actuelle par le mercure : une approche globale

Résumé : Le mercure (Hg) est un métal toxique, qui constitue une menace majeure pour l'Homme et la biodiversité. Naturellement présent dans l'environnement, le Hg est aussi rejeté en quantité considérable par les activités humaines depuis la Révolution Industrielle et se dépose dans tous les écosystèmes, même les plus reculés. Les océans, qui recouvrent 70% de la surface de la Terre, sont très peu documentés dans les programmes internationaux de surveillance du Hg, notamment dans la région intertropicale et les régions polaires. Avec les changements climatiques, déterminer les tendances spatiales et temporelles de cette contamination dans ces régions inexplorées représente un enjeu capital. Les oiseaux marins constituent d'excellents bioindicateurs de la contamination des océans, à la fois à travers le temps et l'espace. En effet, ils reflètent la contamination du réseau trophique sur lequel ils reposent. Assimilé via l'alimentation, le Hg est majoritairement excrété lors de la mue et stocké dans leurs plumes de manière inerte. Ainsi, les plumes d'oiseaux marins représentent une archive précieuse, avec un potentiel de « machine à remonter le temps », grâce aux spécimens de musées. Dans ce contexte, ces travaux utilisent les oiseaux marins comme bioindicateurs des écosystèmes marins, dans trois grandes régions océaniques éloignées – l'Océan Arctique, la région intertropicale (Océans Pacifique, Atlantique et Indien) et l'Océan Austral – avec deux objectifs majeurs : (1) établir une cartographie contemporaine, à large échelle spatiale, de la contamination au Hg, et (2) déterminer rétrospectivement son évolution temporelle depuis le XIX^{ème} siècle, grâce aux spécimens de musée. Avec une couverture spatiale et temporelle uniques, ces travaux de thèse fournissent des données indispensables pour les programmes de surveillance internationaux, liés à la mise en application de la Convention de Minamata, qui vise à réguler les émissions anthropiques de Hg à échelle mondiale.

Mots clés : Hg, Oiseaux marins, Bioindicateurs, Océans éloignés, Spatial, Temporel

Seabirds as bioindicators of past and current mercury contamination: a global approach

Summary: Mercury (Hg) is a toxic metal, and its impacts on human and environmental health are a major concern. Globally, the amount of Hg released into the environment, through anthropogenic activities, has steadily increased since the Industrial Revolution. Both natural and anthropogenic Hg disperse globally and deposits in all ecosystems, including in remote oceans. Oceans, which cover 70% of the Earth's surface, are poorly documented in international monitoring programs of Hg, particularly in intertropical and polar regions. In the current context of global climate, determining spatial and temporal trends in Hg contamination in these underdocumented regions is crucial. Seabirds are excellent bioindicators of Hg contamination in the oceans, both across space and time, as they integrate and reflect Hg contamination of marine food webs on which they feed. After dietary assimilation, Hg is mainly excreted during moult and stored permanently in feathers. Therefore, seabird feathers represent valuable archives and act as a time-machine thanks to museum specimens. In this context, the present PhD thesis uses seabirds as bioindicators of Hg contamination in marine ecosystems, mainly from three remote oceanic regions – the Arctic Ocean, the intertropical region (Pacific, Atlantic and Indian Oceans) and the Southern Ocean – with two main objectives: (1) map contemporary Hg contamination at large spatial scale, and (2) document its temporal trends since the 19th century retrospectively, by using both museum-held and free-living seabirds. Thanks to unique spatial and temporal coverage, this work represents a valuable contribution to international monitoring programs that are fully involved in the implementation and effectiveness evaluation of the Minamata Convention, which aims to control and reduce anthropogenic Hg emissions at the global scale.

Keywords: Hg, Seabirds, Bioindicators, Remote oceans, Spatial monitoring, Temporal monitoring



LIENSs (Littoral, Environnement et Sociétés)
CEBC (Centre d'Études Biologiques de Chizé)

2 Rue Olympe de Gouges
17000 LA ROCHELLE
France

